FIELD GUIDE TO GEOLOGIC EXCURSIONS IN SOUTHWESTERN UTAH AND ADJACENT AREAS OF ARIZONA AND NEVADA

Prepared for the Geological Society of America, Rocky Mountain Section Meeting in Cedar City, Utah May 7-9, 2002

Field Trip Chairman
Peter D. Rowley
Geologic Mapping, Inc.
New Harmony, Utah

Field Guide Editor
William R. Lund
Utah Geological Survey
Cedar City, Utah

≈USGS
science for a changing world

Field Guide to Geologic Excursions In Southwestern Utah and Adjacent Areas of Arizona and Nevada

Field Trip Guide

Prepared for the Geological Society of America Rocky Mountain Section meeting in Cedar City, Utah, May 7-9, 2002

Edited By
William R. Lund
Utah Geological Survey

THE GEOLOGICAL SOCIETY OF AMERICA

Meeting Cosponsors

SOUTHERN UTAH UNIVERSITY
LEARNING LIVES FOREVER

UTAH GEOLOGICAL SURVEY

USGS
science for a changing world

Open-File Report 02-172

Field Guide to Geologic Excursions In Southwestern Utah and Adjacent Areas of Arizona and Nevada

Edited by William R. Lund

PREFACE

This field guide contains road logs for field trips planned in conjunction with the 2002 Rocky Mountain Section meeting of the Geological Society of America held at Southern Utah University in Cedar City, Utah. There are a total of eight field trips, covering various locations and topics in southwestern Utah and adjacent areas of Arizona and Nevada. In addition, the field guide contains a road log for a set of Geological Engineering Field Camp Exercises run annually by the University of Missouri at Rolla in and around Cedar City.

Two of the field trips address structural aspects of the geology in southwestern Utah and northwestern Arizona; two trips deal with ground water in the region; and along with the Field Camp Exercises, one trip, to the Grand Staircase, is designed specifically for educators. The remaining trips examine the volcanology and mineral resources of a large area in and around the Tusher Mountains in Utah; marine and brackish water strata in the Grand Staircase-Escalante National Monument; and the Pine Valley Mountains, which are cored by what may be the largest known laccolith in the world. The "Three Corners" area of Utah, Arizona, and Nevada is home to truly word-class geology, and I am confident that all of the 2002 Rocky Mountain Section meeting attendees will find a field trip suited to their interests.

As Field Guide editor, I express my appreciation to the road log authors who worked diligently not only to organize excellent field trips, but also to provide me with a "camera-ready" copy of their manuscripts for nearly seamless inclusion in this field guide. Without their hard work and forbearance, this publication would not be a reality. I thank Peter Rowley, Field Trip Chairman, for his help and encouragement with the field guide, and also Jane Ciener of the U.S. Geological Survey, who made publication of this field guide as a USGS Open-File Report possible.

William R. Lund
Field Guide Editor

CONTENTS

Premeeting

Postmeeting

2002 Rocky Mountain Section Meeting
Organizing Committee

Robert L. Eves	**Meeting Chair**
Robert E. Blackett	**Program Chair**
Peter D. Rowley	**Field Trip Chair**
William R. Lund	**Field Guide Editor**
Larry Davis	**Geoscience Education**
Robert L. Eves	**Local Treasurer**
Kenneth Kolm	**Section Treasurer**
Sue A. Finstick	**Exhibits Chair and Guest Activities**
Frederick C. Lohrengel	**A-V Supervision and Local Arrangements**
Mark Colberg	**Student Coordinator**
Fred Lohrengel and Robert Eves	**Special Activities**

STRUCTURAL DEVELOPMENT AND PALEOSEISMICITY OF THE HURRICANE FAULT, SOUTHWESTERN UTAH AND NORTHWESTERN ARIZONA

Geological Society of America
2002 Rocky Mountain Section Annual Meeting
Cedar City, Utah
May 5 and 6, 2002

View to the northwest of a lava cascade over the Hurricane Cliffs near the Utah – Arizona border.

FIELD TRIP LEADERS
William R. Lund, Utah Geological Survey
Wanda J. Taylor, University of Nevada at Las Vegas
Philip A. Pearthree, Arizona Geological Survey
Heidi Stenner, U.S. Geological Survey
Lee Amoroso, Arizona State University
Hugh Hurlow, Utah Geological Survey

STRUCTURAL DEVELOPMENT AND PALEOSEISMICITY OF THE HURRICANE FAULT, SOUTHWESTERN UTAH AND NORTHWESTERN ARIZONA

Geological Society of America
2002 Rocky Mountain Section Annual Meeting
Cedar City, Utah
May 5 and 6, 2002

William R. Lund, Utah Geological Survey
Wanda J. Taylor, University of Nevada at Las Vegas
Philip A. Pearthree, Arizona Geological Survey
Heidi Stenner, U.S. Geological Survey
Lee Amoroso, Arizona State University
Hugh Hurlow, Utah Geological Survey

INTRODUCTION

The Hurricane fault is one of the longest and most active of several large, late Cenozoic, west-dipping normal faults in southwestern Utah and northwestern Arizona. Quaternary activity of the fault is indicated by the geomorphology of the high, steep Hurricane Cliffs, the result of fault slip, and by displaced Quaternary basalt flows, alluvium, and colluvium at many locations along its length. Extending from Cedar City, Utah, to south of the Grand Canyon in Arizona (figure 1), the 250-kilometer-long fault almost certainly ruptures in segments, as observed historically for other long basin-and-range normal faults (Schwartz and Coppersmith, 1984; Schwartz and Crone, 1985; Machette and others, 1992). Previous workers (Stewart and Taylor, 1996; Stewart and others, 1997; Reber and others, 2001) have suggested that major convex fault bends and zones of structural complexity are likely candidates for boundaries between present-day seismogenic fault segments and also provide evidence of fault linkage and the long-term structural development of the fault. Initial paleoseismologic investigations along the fault have suggested that some parts of the fault have ruptured more recently than others (Stenner and others, 1999; Lund and others, 2001; Amoroso and others, 2002).

Assessing the seismic hazard presented by the active Hurricane fault is important because southwestern Utah and adjacent areas of Arizona and Nevada are experiencing a now decades-long population and construction boom. A proposed pipeline from Lake Powell to the St. George basin, which would cross the Hurricane fault, could provide water for an additional 300,000 residents in southwestern Utah within the next 10 to 15 years. We have integrated recent paleoseismologic and structural studies along the Hurricane fault (Stenner and others, 1999; Lund and others, 2001; Reber and others, 2001; Amoroso and others, 2002) to more completely describe the fault's behavior through time and evaluate potential earthquake hazards.

This trip focuses on the results of the recent studies that provide insight into the Hurricane fault's long-term development and paleoearthquake history, and covers that part of the Hurricane fault between Diamond Butte in Arizona and Cedar City, Utah.

GEOLOGIC OVERVIEW

The Hurricane fault lies within the ~150-kilometer-wide structural and seismic transition zone between the Colorado Plateau and Basin and Range physiographic provinces. Within this transition zone, generally subhorizontal Paleozoic and Mesozoic strata of the Colorado Plateau

are displaced down-to-the-west by a series of generally north-striking normal faults. Although the Hurricane fault also strikes generally north-south, it includes distinct sections that strike northeast or northwest. These variations in strike produce a sinuous fault trace that, in map view, suggests the Hurricane fault is geometrically segmented.

In southwestern Utah, from Cedar City to the Arizona border, the Hurricane fault zone is the tectonic boundary between the Colorado Plateau and Basin and Range (Arabasz and Julander, 1986). In northwest Arizona, the Hurricane fault is 50 kilometers east of the Grand Wash fault, which is considered the tectonic boundary (Mayer, 1985). Huntoon (1990) considers the normal faults in northwestern Arizona and southwestern Utah to be located along Precambrian normal faults that were later reactivated (in the reverse sense) during Laramide compression and uplift. These fault zones activated again, to a lesser degree, during late-Tertiary high-angle extension (Spencer and Reynolds, 1989), and to a greater degree during the Pliocene and Quaternary as normal faults (Menges and Pearthree, 1989).

The steep Hurricane Cliffs represent a fault-line scarp that closely follows the trace of the Hurricane fault and records the displacement across the structure. Total displacement varies along strike with the largest displacements in the north and the smallest in the south. The Hurricane fault's trend cutting across the Colorado Plateau – Basin and Range Province boundary near the border may explain a displacement of more than 2,500 meters in Utah as compared with 250-400 meters in Arizona (Stewart and others, 1997). Previous studies have documented displaced Quaternary basalt flows (hundreds of meters) and late Quaternary unconsolidated alluvial and colluvial deposits (meters to tens of meters) (Hamblin, 1963, 1965a, 1970a, 1970b, 1984; Anderson and Mehnert, 1979; Pearthree and others, 1983; Menges and Pearthree, 1983; Anderson and Christenson, 1989; Hecker, 1993; Stewart and Taylor, 1996). Estimates of displacement across the Hurricane fault have varied widely, ranging from a low of 1,400-4,000 feet (Kurie, 1966) to a high of 12,000-13,000 feet (Dutton, 1880). Kurie (1966) attributed the wide range in estimates to the failure of many workers to recognize the significance of major fold structures related to the Cretaceous to Eocene Sevier orogenic belt (Armstrong, 1968), which predate and parallel the trace of the Hurricane fault over much of its length in Utah. Anderson and Mehnert (1979) attribute the displacement discrepancies to the inclusion, or lack thereof, of near-fault deformation associated with the younger tectonics.

Figure 1. The Hurricane fault and proposed fault segments.

Along the route of this field trip, the Hurricane fault displaces strata ranging in age from Permian to Quaternary (figure 2). The Paleozoic and Mesozoic strata record depositional environments ranging from marine and marginal marine to terrestrial. Deposited by wind and
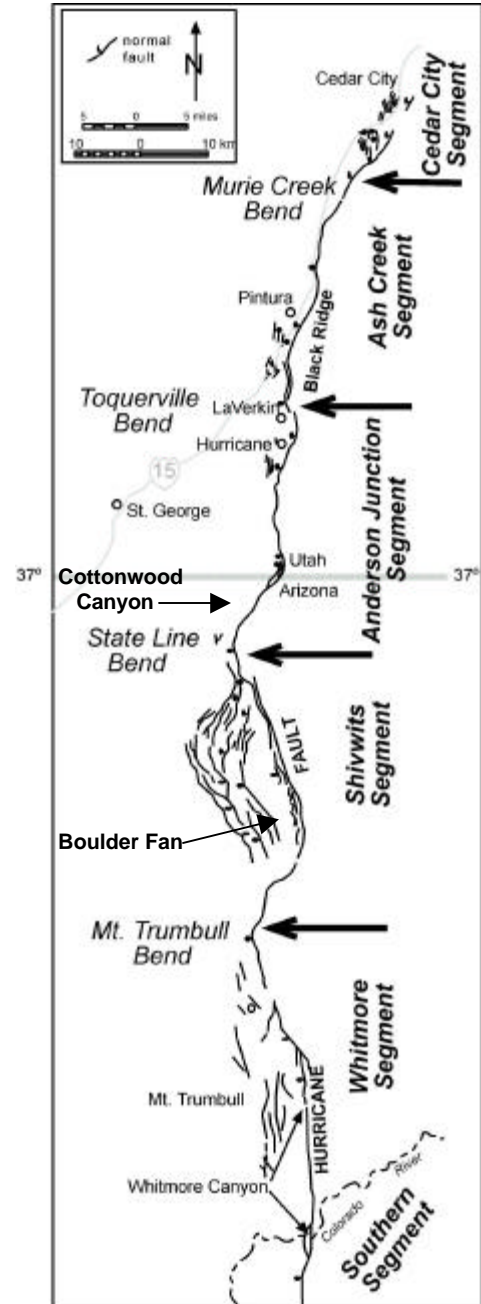
Age	Unit	Thickness (m)	Rock Type
Q	alluvium, colluvium & fluvial units	0-70	
Q	basalt	0-90	
Plio	Sevier River or Muddy Creek Fm. / unnamed sed unit.	0-90	
Miocene / Oligocene / Eocene	Tuffs & andesites - Page Ranch Volcs, Quichapa Gp., Isom tuffs, Needles Range Gp., Bullion Cyn, Osiris Tuff, Mt Dutton Fm., Brian Head, etc	0-1110	
Paleocene	Cedar Breaks / Wasatch / Claron Fms.	120-430	
Paleocene	+/-Pine Hollow Fm.	0-120	
	+/-Canaan Peak Fm.	0-305	
Cretaceous (Iron Springs Formation)	Kaiparowits Formation	80-215	
	Wahweap & Straight Cliffs Sandstones	165-495	
	Tropic (Mancos) Shale	190	
	Dakota SS	55	
	+/-Henrieville SS	0-90	
Jurassic	+/-Entrada Formation	0-155	
Carmel Frm	Wiggler Wash Mbr	0-20	
	Winsor Mbr	55-95	
	Paria River Gyp Mbr	20-50	
	Crystal Creek Mbr	0-55	
	Kolob LS Mbr	20-150	
	Temple Cap Mbr		
	Navajo Sandstone (main body)	520-700	
Triassic	+/-Kayenta SS - Tenney Canyon Tongue	0-40	
	+/-Navajo SS - Lamb Point Tongue	0-120	
	Kayenta Fm. (main body)	90-370	

Age	Unit	Thickness (m)	Rock Type
Triassic - Moenave Frm	Springdale SS Mbr	18-35	
	Whitemore Pt Mbr	0-20	
	Dinosaur Cyn Mbr	25-120	
Chinle Frm	Petrified Forest Member	80-120	
	Shinarump Member	0-50	
Moenkopi Frm	upper red member	~150	
	Shnabkaib Member	~100	
	middle red member	~90	
	Virgin Limestone	~40	
	lower red member +/- Timpoweap Mbr	~170	
Permian	Kaibab Limestone	75-260	
	+/- White Rim SS	0-60	
	Toroweap Formation	30-150	
	Hermit Shale	0-30	
	Queantoweap/ Esplanade / Coconino Sandstone	300-380	
	+/- Pakoon Fm.	0-90	
Penn	Callville Limestone	60-275	

Figure 2. Summarized and generalized stratigraphy for the entire Hurricane fault region, compiled and modified from Hintze (1980, 1988) and authors' data.

flowing water, the terrestrial sedimentary rocks along the field trip route are generally colored distinctive red tones and have been differentially eroded to form massive, near-vertical cliffs such as those seen in Zion National Park. The approximately 20-million-year-old Pine Valley laccolith crops out west of I-15 in the Pine Valley Mountains (Cook, 1953; McDuffie and Marsh, 1991), north of St. George, Utah, and late Cenozoic cinder cones and basalt flows are common along the fault. Quaternary deposits along the fault consist of steep colluvial deposits mantling the lower Hurricane Cliffs, steep alluvial fans emanating from smaller drainages along the cliffs, and fans, terraces and channels associated with the few larger drainages that breach the cliffs.

The Colorado Plateau/Basin and Range Transition Zone is coincident with part of the Intermountain seismic belt (Smith and Sbar, 1974; Smith and Arabasz, 1991; figure 3), although this belt of earthquake epicenters becomes broader and more poorly defined from north to south. Surface rupture has not occurred along the Hurricane fault historically, but the area does have a pronounced record of seismicity. At least 20 earthquakes greater than M 4 have occurred in southwestern Utah over the past century (Christenson and Nava, 1992; figure 4). The largest events were the M 6.3 Pine Valley earthquake in 1902 (Williams and Trapper, 1953) and the M 5.8 St. George earthquake in 1992 (Christenson, 1995). The Pine Valley earthquake is pre-instrumental and poorly located, and therefore not attributable to a recognized fault. However, the epicenter is west of the surface trace of the Hurricane fault, so the earthquake may have occurred on that fault at depth. Pechmann and others (1995) tentatively assigned the St. George earthquake to the Hurricane fault. The largest historical earthquake in northwestern Arizona was the 1959 M 5.7 Fredonia, Arizona earthquake (Dubois and others, 1982). Since 1987 northwestern Arizona has experienced more than 40 events with M ≥ 2.5, including the 1993 M 5.4 Cataract Canyon earthquake (Lay and others, 1994) between Flagstaff, Arizona, and the Grand Canyon (Arizona Earthquake Information Center, Arizona Earthquakes 1830 - 1998; http://vishnu.glg.nau.edu/aeic/azcat.txt).
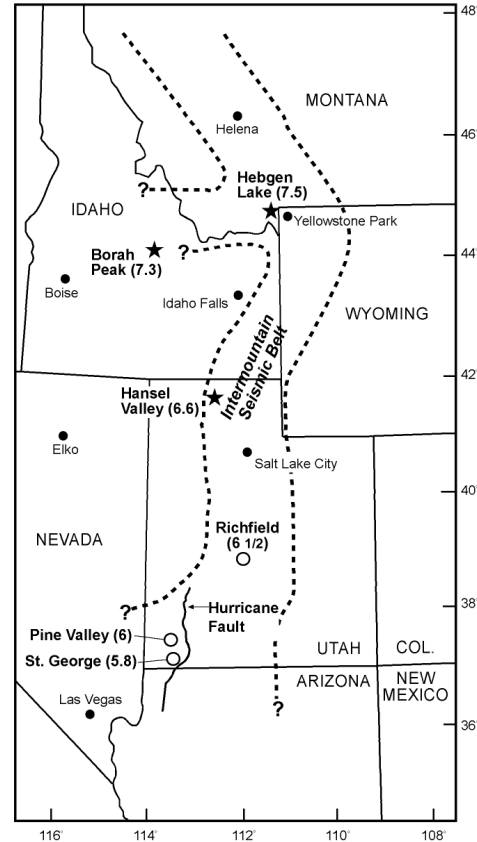

Figure 3. The Intermountain seismic belt showing major historical earthquakes and the Hurricane fault.

STRUCTURAL STUDIES

The sinuosity of the trace delineates the geometric segments along the Hurricane fault. A geometric segment is a portion of a fault that has a constant strike or a systematically and continually varying strike that results from a gently curved fault. Along normal faults, the curves of geometric segments are generally concave toward the hanging wall. From south to north, the geometric segments along the Hurricane fault are the Southern, Whitmore, Shivwitz, Anderson Junction, Ash Creek, and Cedar City segments (figure 1). We are currently investigating whether the Anderson Junction geometric segment should be divided into two geometric segments near Hurricane, Utah.

Geometric segments are separated by geometric segment boundary zones (GSBZ), which tend to have relatively sharp changes in strike. Along normal faults, GSBZ generally form bends, called salients, that are convex toward the hanging wall. In the area of this field trip, four GSBZ are present along the Hurricane fault: the Mt. Trumbull bend, the State line bend, the Toquerville bend, and the Murie Creek bend (figure 1). In addition, a possible GSBZ lies near the town of Hurricane, Utah. We interpret the GSBZ to be sites where fault segments linked.

Structural Linkage Models

In the first stage of the evolution of a segmented fault, originally isolated faults grow toward each other by radial propagation. Eventually, if the fault spacing is small enough, the stress fields in the fault tip regions interact causing the fault tips to curve toward each other (Burgmann and others, 1994; Willemse, 1997; Willemse and Pollard, 2000). In cases where the fault tips overlap,

5

a relay ramp forms between the propagating faults in the overlap zone (Larsen, 1988; Peacock and Sanderson, 1994; Trudgill and Cartwright, 1994; Childs and others, 1995; Walsh and others, 1999). In the second stage, the propagating fault segments can physically connect to form a through-going fault, which is called "hard" linkage (Trudgill and Cartwright, 1994; Young and others, 2001). A marked change in strike typically characterizes the linkage zone (figure 5). Fault growth by segment linkage implies that the length of the fault increases dramatically when the faults join (figure 5) (Segall and Pollard, 1980; Pollard and Aydin, 1984; Peacock and Sanderson, 1991; Cowie and Scholz, 1992a, 1992b; Dawers and others, 1993; Jackson and Leeder, 1994; Cartwright and others, 1995, 1996; Schlische and Anders, 1996). In the third stage, deformation is localized on the through-going fault (Cowie and others, 1995; Cowie, 1998; Gupta and others, 1998; Young and others, 2001). The Hurricane fault is completely hard linked in the area of this field trip.
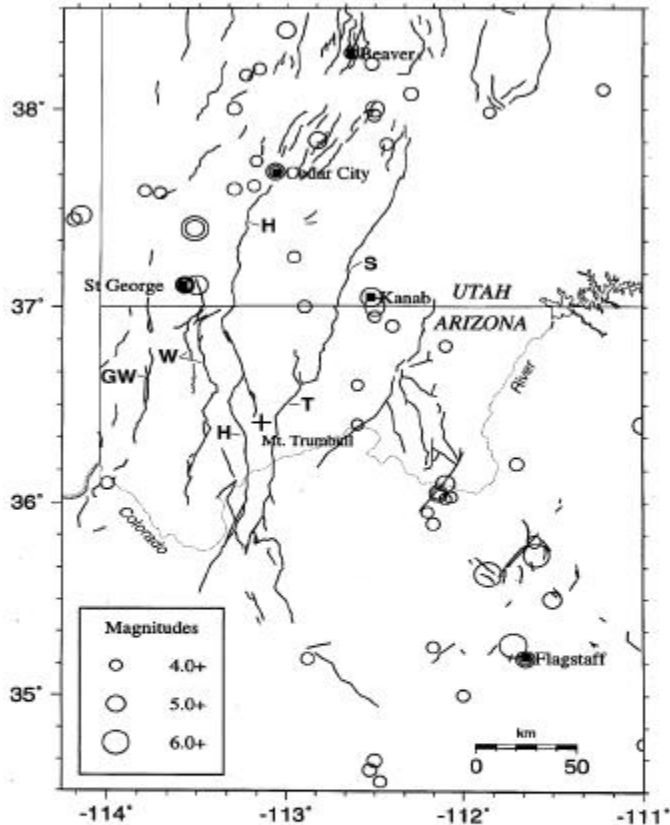

Figure 4. Historical earthquakes and Quaternary faults in southwestern Utah and northwestern Arizona. H = Hurricane fault, W = Washington fault, GW = Grand Wash fault, S = Sevier fault, and T = Toroweap fault.

The development of isolated or linked faults may be interpreted using displacement–distance profiles, graphs used to illustrate changes in displacement along a fault (Pollard and Segall, 1987; Walsh and Watterson, 1987; Peacock and Sanderson, 1991; Cowie and Scholz, 1992a; Burgmann and others, 1994; Peacock and Sanderson, 1996). Naturally occurring faults exhibit variations in displacement along strike that differ from predictions based on simple linear or power-law models (Peacock and Sanderson, 1996). This variability may result from fault interaction and linkage, fault bends, lithologic variations, and fault propagation rate variations (Peacock, 1991; Burgmann and others, 1994; Peacock and Sanderson, 1996). The average displacement gradient on a displacement–distance profile is steeper in a zone of interacting faults and the locus of maximum displacement of each fault shifts toward the interacting tip (Peacock and Sanderson, 1991, 1994; Willemse and others, 1996; Willemse, 1997).

If geometric bends are sites of segment linkage, then displacement gradients may be recorded near the bend on displacement - distance profiles providing that two assumptions apply: (1) slip on the original isolated faults was less near the ends than near the center, and (2) the linkage zones remain asperities at which slip is more difficult than elsewhere or the release of elastic strain concentrated around the original fault tips has not yet driven slip in the linkage zones to equalize with the rest of the fault. To illustrate displacement variations near linkage zones with geometric bends, Taylor and others (2001) generated synthetic displacement - distance profiles for three different styles of hard linkage: underlapping, overlapping, and fault

6

capture (figure 5). The profiles allow comparison of the observed total displacement at various positions along a fault to idealized map view examples of each type of linkage. The offsets across the faults are summed in areas of overlap. Where underlapping faults linked, displacement decreased at the bend because fault tip zones have less displacement than the middle regions of a fault (figure 5a). The minimum, which is at the center of the displacement decrease, is relatively sharp. Where overlapping faults linked at a bend relatively near both fault tips, displacement decreased, but a bench formed in the displacement-distance profile in the area of original overlap (figure 5b). The along-strike length of the bench is proportional to the length of fault overlap. Where faults linked by segment capture, either a decrease or increase could occur with a significant displacement gradient on one side of the site of linkage and little or no appreciable displacement gradient, or a plateau, on the opposite side (figure 5c). The significant gradient occurred in the area of overlap. The plateau occurred along the fault or segment that remained relatively static and that was captured. The plateau would be relatively constant (horizontal) if the linkage site is within the zone where fault slip is relatively constant, typically the central one-third of the fault. A slope in the plateau suggests a displacement gradient along the captured fault. The gradient may have existed prior to linkage. Alternatively, the gradient may have formed during post-linkage slip. Post-linkage slip is not illustrated in figure 5. The point of transition between the plateau and the gradient occurred near the site where the tip of the propagating fault intersected the relatively static fault.

Total displacement versus distance patterns around salients are consistent with at least four of the GSBZ in the Hurricane fault being sites of segment linkage. A through-going fault surface and displacement minima are present at these GSBZ (see Stop 1-3). Therefore, we suggest that the GSBZ at the Mt. Trumbull, State Line, Toquerville, and Murie Creek bends, are sites where fault tips (at which displacement is zero) linked. In addition, the post-linkage displacement history is not great enough to have erased the minima.

Post-linkage displacement can have a variety of effects on subsequent fault history. The elastic strain build up may drive additional slip in the linkage zone, which would cause an increase in post-linkage slip rates near the linkage zone. The modeled tendency for faults to maintain a constant length to displacement ratio that approaches a power law relationship could increase or decease slip rates at appropriate sites along the fault. In general, the step-wise length increase during linkage will increase slip without increasing fault length after linkage. In addition, the large bends created during linkage may prove unstable and new fault splays may be generated that effectively straighten the fault. Therefore, the presence of a geometric salient that is a site of segment linkage cannot be used as a simple predictor of subsequent fault history without data on post-linkage slip.

Reactivation of Older Structures

In structural studies, it is common to consider whether younger faults reactivate older structures. In the case of linked and segmented faults, such as the Hurricane fault, such a consideration is complicated by two factors: (1) the variations in strike along the length of the fault, and (2) the possibility that different older structures may have been reactivated by different segments (i.e., different original faults).

Much of the Ash Creek segment lies near subhorizontal to gently plunging upright open folds that formed during the Mesozoic Sevier orogeny. Two of these folds are most popularly called the Pintura anticline and the Kanarra anticline. The trend of these folds generally parallels the strike of much of the Ash Creek segment. However, the fault does not lie along the core of either fold or the likely location of the intervening syncline. The similarities in fault segment strike and dip and the fold axial surfaces suggests the possibility that along the Ash Creek segment the fault reactivated an axial planar cleavage or fracture. The Hurricane fault appears to depart from this trend at the Toquerville bend.

South of the Toquerville bend, the strike of the Anderson Junction geometric segment veers away from the trend of the Sevier-related folds, including the Virgin anticline. The trend of the Virgin anticline is more northeasterly than the strike of most of the fault segment. Whether this geometric segment reactivates another pre-existing structure is difficult to assess at this time, largely due to levels of exposure.

A. Linkage of Underlapping Fault Segments
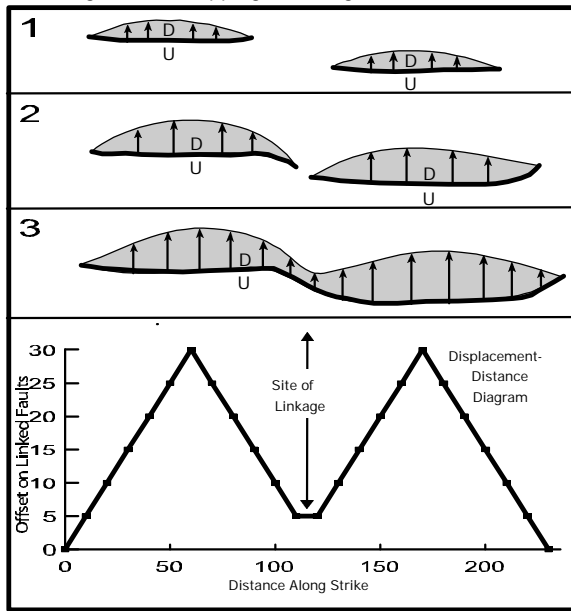
B. Linkage of Overlapping Fault Segments
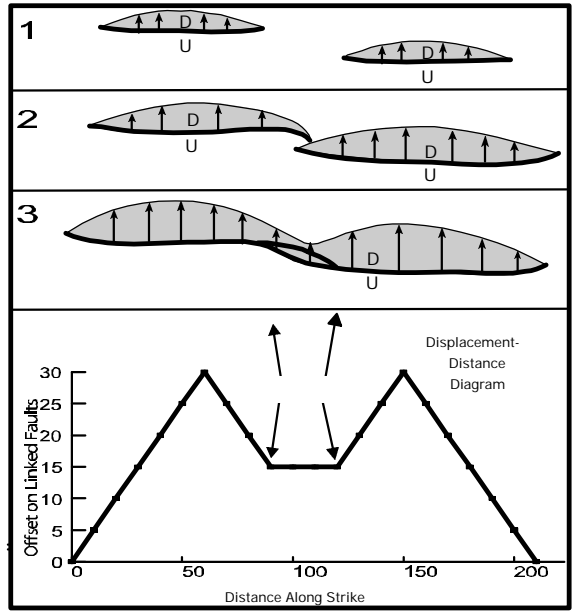
C. Fault Capture Along Connecting Faults
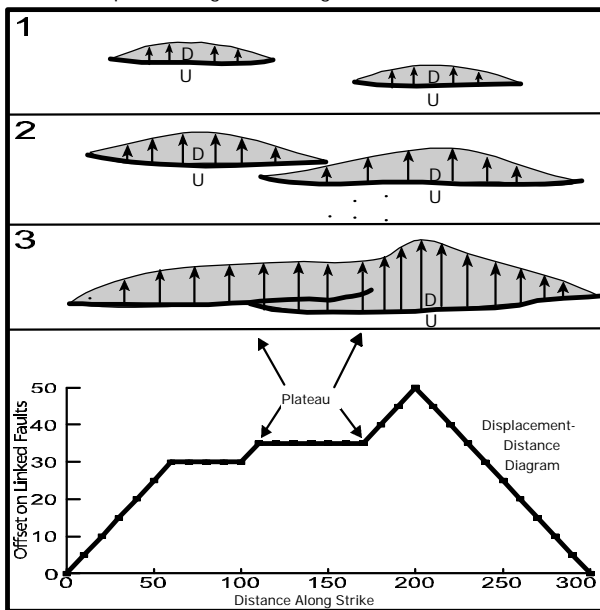
Figure 5. These conceptual models show map view patterns (upper) and displacement vs. distance graphs (lower) for idealized cases of (A) linkage of underlapping faults, (B) linkage of overlapping faults and (C) fault capture. The map patterns show three sequential stages in the development of linkage (1, 2 and 3). The heavyweight lines represent the fault traces. The lightweight line represents the slip distribution projected into map view. The arrows qualitatively show displacement vectors projected into map view. The displacement (offset) – distance diagrams show patterns of offset predicted around sites where different types of linkage took place. Underlapping fault linkage produces a sag in the diagram, while overlapping fault linkage produces a bench. Fault capture produces a plateau. These graphs represent situations where the post-linkage magnitude of slip around the linkage site is relatively small in comparison to the total displacement. Modified from Taylor and others (2001).

8

The long northern sections of both the Shivwitz and Southern geometric segments strike generally subparallel to Middle Proterozoic faults. Normal faults about 1.1 billion years in age exposed in the Grand Canyon strike northwest (Timmons and others, 2001). Some of these faults were reactivated during the Laramide orogeny. The parallelism suggests the possibility that sections of the Shivwitz and Southern geometric segments reactivated these older faults. However, additional data and analysis are needed to further evaluate this suggestion.

Linkage and Quaternary Displacements

Because of segment linkage, it is possible to form faults that are too long to rupture during a single earthquake. Thus, a question arises: Are post-linkage earthquakes confined to the original segments or do earthquake ruptures cross original segment boundaries? To date, various data sets and publications present conflicting alternatives. Walsh and Watterson (1991) suggested that structural linkage implies kinematic linkage. dePolo and others (1991) used empirical data to suggest that large magnitude earthquakes can rupture across GSBZ, but relatively small magnitude earthquakes are unlikely to do so. Mansfield and Cartwright (2001), using analog models, suggested that linked faults tend toward a long-term consistency in the displacement pattern along strike. However, on time scales that are short relative to the entire growth history of the fault, component segments may have independent activity and displacement, often for long time periods after hard linkage. Other studies show variations or other influences on the mechanics during and after linkage (Cowie and Roberts, 2001; Shipton and Cowie, 2001; Maerten and others, 2002). Given the paleoseismic data described below, we suggest that the Ash Creek and Anderson Junction geometric segments probably acted as independent rupture segments in the recent past. Whether the Shivwitz geometric segment is also an earthquake rupture segments is uncertain. Without further data we cannot exclude the possibility that recent ruptures have been located along segments of the fault defined by factors other than geometry.

Structural Conclusions

1. The sinuosity of the trace of the Hurricane fault indicates that the fault is geometrically segmented. It consists of at least six geometric segments from south to north: Southern, Whitmore, Shivwitz, Anderson Junction, Ash Creek, and Cedar City. The segments are separated by the Mt. Trumbull, State Line, Toquerville, and Murie Creek bends.
2. We suggest that fault linkage occurred at the bends. Along the State Line bend linkage occurred by fault capture. Along the Toquerville bend linkage of underlapping faults occurred.
3. The orientations of some sections of the geometric segments may be controlled by older structures that were reactivated. Much of the Ash Creek segment parallels nearby Sevier-age folds. Long sections of the Southern and Shivwitz geometric segments parallel Middle Proterozoic normal faults exposed near the Grand Canyon.
4. The available data suggest that the Toquerville and Murie Creek geometric bends may still be an earthquake rupture boundary. However, additional data are needed for greater certainty of this interpretation. Existing paleoseismic data do allow certain conclusion about whether the State Line geometric bend is still an earthquake rupture boundary.

PALEOSEISMIC STUDIES

The Hurricane fault has long been recognized as a potential source of large earthquakes in southwestern Utah and northwestern Arizona, but a general lack of definitive evidence for latest Pleistocene or Holocene surface rupture has made assessing the seismic hazard presented by the Hurricane fault problematic. Detailed paleoseismic investigations conducted over the past several years have begun to illuminate the recent history of surface-rupturing

earthquakes along the fault zone. We summarize the results of these investigations in this section.

Previous Workers

In addition to its structural characteristics, geologists have long been interested in the amount and timing of displacement on the Hurricane fault. Huntington and Goldthwait (1904, 1905) first introduced several important ideas regarding the Hurricane fault, including: (1) the fault partially follows an older fold and thrust belt, (2) displacement decreases from north to south, (3) much of the southern escarpment has retreated eastward from the trace of the fault, suggesting a long period of quiescence or long recurrence interval, and (4) offset has been episodic through time. Averitt (1964) prepared a chronology of post-Cretaceous geologic events on the Hurricane fault. Hamblin (1963, 1970a, 1987) studied late Cenozoic basalts along and near the fault in southwestern Utah and northwestern Arizona. His observations regarding displaced basalt flows resulted in several papers on the tectonics and rate of slip on the Hurricane fault (Hamblin, 1965a, 1965b, 1970b, 1984; Hamblin and Best, 1970; Hamblin and others, 1981). Anderson and Mehnert (1979) reinterpreted the history of the Hurricane fault, refuting several key elements of Averitt's (1964) fault chronology. They also provided a much smaller estimate of total net vertical displacement across the fault in Utah.

Several seismotectonic studies have been conducted along or near the Hurricane fault. Earth Sciences Associates (1982) mapped generalized surficial geology and photo lineaments along the fault and trenched scarps and sites of photo lineaments that cross U.S. Soil Conservation Service (now Natural Resources Conservation Service) flood-retention structures in southern Utah. Based on historical seismicity and existing geologic data, they estimated an average return period of 1,000-10,000 years for large, surface-faulting earthquakes (M 7.5) on the Hurricane fault. Menges and Pearthree (1983) conducted reconnaissance field investigations of the Hurricane fault in Arizona. They suggested that several portions of the fault ruptured as recently as the early Holocene or latest Pleistocene. Anderson and Christenson (1989) compiled a 1:250,000-scale map of Quaternary faults, folds, and selected volcanic features in the Cedar City 1°x2° quadrangle based on existing data and reconnaissance field work. The apparent absence of young fault scarps in unconsolidated deposits along the fault in Utah led them to conclude that a surface-faulting earthquake probably had not occurred there in the Holocene. They noted that a lack of Holocene activity on the fault seems inconsistent with the high Quaternary slip rate derived from displaced Quaternary basalts (Anderson and Mehnert, 1979; Hamblin and others, 1981). Hecker (1993) included the Hurricane fault in her 1:500,000-scale compilation of Quaternary tectonic features in Utah and assigned a probable age of late Pleistocene (10,000 - 130,000 years) to the time of most recent deformation. A structural analysis by Schramm (1994) of a complex portion of the Hurricane fault near the Toquerville, geometric bend, (figure 1) showed that movement on the fault there is predominantly dip-slip with a slight right-lateral component. Stewart and Taylor (1996), and Stewart and others (1997) defined a structural and possibly a seismogenic (earthquake) boundary at the large geometric bend in the Hurricane fault near Toquerville, which they called the Toquerville geometric bend. Fenton and others (2001) recently investigated basalt flows and alluvial landforms displaced by the Hurricane and Toroweap faults in the western Grand Canyon region. They concluded that both structures have been active through the Quaternary and that much of the development of the Inner Gorge of Grand Canyon can be attributed to relative uplift across these faults.

Christenson and Deen (1983) and Christenson (1992) reported on the engineering geology of the St. George, Utah area and discussed seismic hazards associated with the Hurricane and other Quaternary faults in the area. Christenson and others (1987) and Christenson and Nava (1992) included the Hurricane fault and other potentially active faults in southwestern Utah in their reports on Quaternary faults and seismic hazards in western Utah, and earthquake hazards in southwestern Utah, respectively. Williams and Tapper (1953) discussed the earthquake history of Utah including the 1902, M 6.3 Pine Valley earthquake. Christenson (1995) provided a comprehensive review of the 1992, M_L 5.8 St. George earthquake, which likely occurred on the Hurricane fault. Stewart and others (1997) included a review of seismicity and seismic hazards in southwestern Utah and northwestern Arizona in their review of the

10

neotectonics of the Hurricane fault. Pearthree and Bausch (1999) inferred that seismic hazard in northwestern Arizona is moderate based on historical seismic activity and the presence of many Quaternary faults.

Utah Geological Survey/Arizona Geological Survey
Cooperative Paleoseismic Study

To more accurately evaluate the seismic hazard presented by the Hurricane fault to southwestern Utah and northwestern Arizona, the Utah Geological Survey (UGS) and Arizona Geological Survey (AZGS) conducted two National Earthquake Hazard Reduction Program-funded cooperative studies (Pearthree and others, 1998; Lund and others, 2001) of the Hurricane fault to acquire data on long-term fault slip rates and on the magnitude, timing, and location of past surface-faulting earthquakes. The UGS investigated the paleoseismicity and long-term slip history of the northern portion of the fault (proposed Ash Creek and Anderson Junction segments) in Utah. The AZGS studied the southern part of the Anderson Junction segment and the adjacent Shivwitz segment to the south to better understand the geologic controls of earthquake rupture on the Hurricane fault in Arizona.

Utah Study

For approximately 80 kilometers the trace of the Hurricane fault trends generally north-south through southwestern Utah. Displaced Quaternary basalt flows and alluvial and colluvial deposits indicate a significant rate of Quaternary fault activity. The UGS proposed to excavate trenches across fault scarps formed on unconsolidated deposits to characterize the size, timing, and rate of late Quaternary faulting, and to calculate long-term slip rates from displaced basalt flows.

Fault scarps are formed on unconsolidated deposits at six sites along the Utah portion of the fault (figure 6). The preferred UGS trench site at Coyote Gulch is on private property and was unavailable for study. Trenching at Shurtz Creek, the best alternative site, encountered large boulders that prevented exposing the fault zone. The remaining sites had similar geologic constraints or access problems, so the UGS refocused on dating young alluvium along the fault at three locations along the Ash Creek segment. The alluvium at the two northern sites (Middleton and Bauer; figure 6) is not faulted, while the sediments at the southern site (Coyote Gulch) are displaced. Radiocarbon ages from detrital charcoal recovered from the unfaulted alluvium at the Bauer and Middleton sites were 330-525 cal yr. B.P. and 1,530-1,710 cal yr. B.P., respectively. Charcoal from the faulted alluvium at Coyote Gulch gave an age of 1,055-1,260 cal yr. B.P. The fact that the sediments at Coyote Gulch are faulted and those at the Bauer and Middleton sites are not, show that the most recent surface-faulting earthquake (MRE) at Coyote Gulch did not extend north to the other two sites, indicating the likely presence of a seismogenic boundary between Coyote Gulch and the Bauer and Middleton sites. The most likely location for a boundary is at a right bend in the fault north of Coyote Gulch at Murie Creek. The proposed new northern fault segment is named the Cedar City segment and is a minimum of 13 kilometers long. The redefined Ash Creek segment is about 32 kilometers long. If the segment boundary is indeed a consistently maintained seismologic boundary, then based on those lengths and on limited displacement-per-event data, rupture of the Cedar City segment could produce a M 6.5 earthquake and rupture of the Ash Creek segment could produce a M 6.9-7.1 event.

Displaced Quaternary basalt flows at several locations along the Hurricane fault in Utah provide good evidence for rates of long-term slip on the fault. Determining long-term slip rates using the displaced flows required correlating the flows across the fault using trace-element geochemistry and new geologic mapping, dating correlative flows using ^{40}Ar/^{39}Ar dating techniques, and evaluating near-fault deformation using a combination of paleomagnetic vector analysis and geologic mapping.

Geochemical data identified four locations in Utah where displaced basalts are correlative across the Hurricane fault: two on the Anderson Junction segment, one at the proposed boundary between the Anderson Junction and Ash Creek segments (Toquerville geometric bend), and one on the Ash Creek segment (figure 7). A fifth basalt site is 12 kilometers east of the fault in Cedar

11

Canyon and consists of a basalt remnant that occupies the ancestral channel of Coal Creek high on the north canyon wall. The basalt flow displaced Coal Creek, forcing the stream to incise a new channel and leaving the basalt remnant stranded high above the present stream. Coal Creek grades to Cedar Valley and crosses the Hurricane fault at the mouth of Cedar Canyon. Fault movement controls the stream base level and therefore, the stream-incision rate is a proxy for slip on the fault.

The new long-term slip rates for the Hurricane fault in Utah range from 0.21 to 0.57 mm/yr (table 1) and generally increase from south to north along the fault. Additionally, slip increases markedly to the north across the suspected Ash Creek/Anderson Junction segment boundary. Although little change in long-term slip rate is apparent across the proposed Ash Creek/Cedar City segment boundary, slip rates reported for segmented

Figure 6. Hurricane fault in southwestern Utah showing sites with scarps formed on unconsolidated alluvium. Ash Creek graben and the MP-35 cinder cone are also shown.

faults elsewhere in the western United States indicate that a seismogenic boundary could still be present (Machette and others, 1992). A comparison of the new long-term slip rates with late Quaternary rates determined for several locations in Utah shows that slip has slowed on the Hurricane fault in Utah over the past approximately one million years. We conclude that the average recurrence for surface-faulting earthquakes on the fault segments in Utah is now several thousand to more than ten thousand years.

Considering the three potential seismogenic segments in Utah, the newly proposed Cedar City segment has gone the longest without a surface-faulting earthquake. The proxy slip rate available for the Cedar City segment closely approaches that of the adjacent Ash Creek segment, which has had a Holocene surface-faulting earthquake. Given its long-term record of activity and the general absence of geologically young fault scarps indicative of recent surface faulting, the Cedar City segment is considered the most likely location for the next surface faulting on the Hurricane fault in Utah.

Arizona Study

Studies to characterize the late Quaternary rupture history of the southern Anderson Junction and Shivwitz segments of the Hurricane fault included: geologic and geomorphic mapping, scarp profiling, soil profile analysis, cosmogenic isotope dating, trenching, and geochemical correlation and dating of a displaced basalt flow. Detailed studies were conducted

12
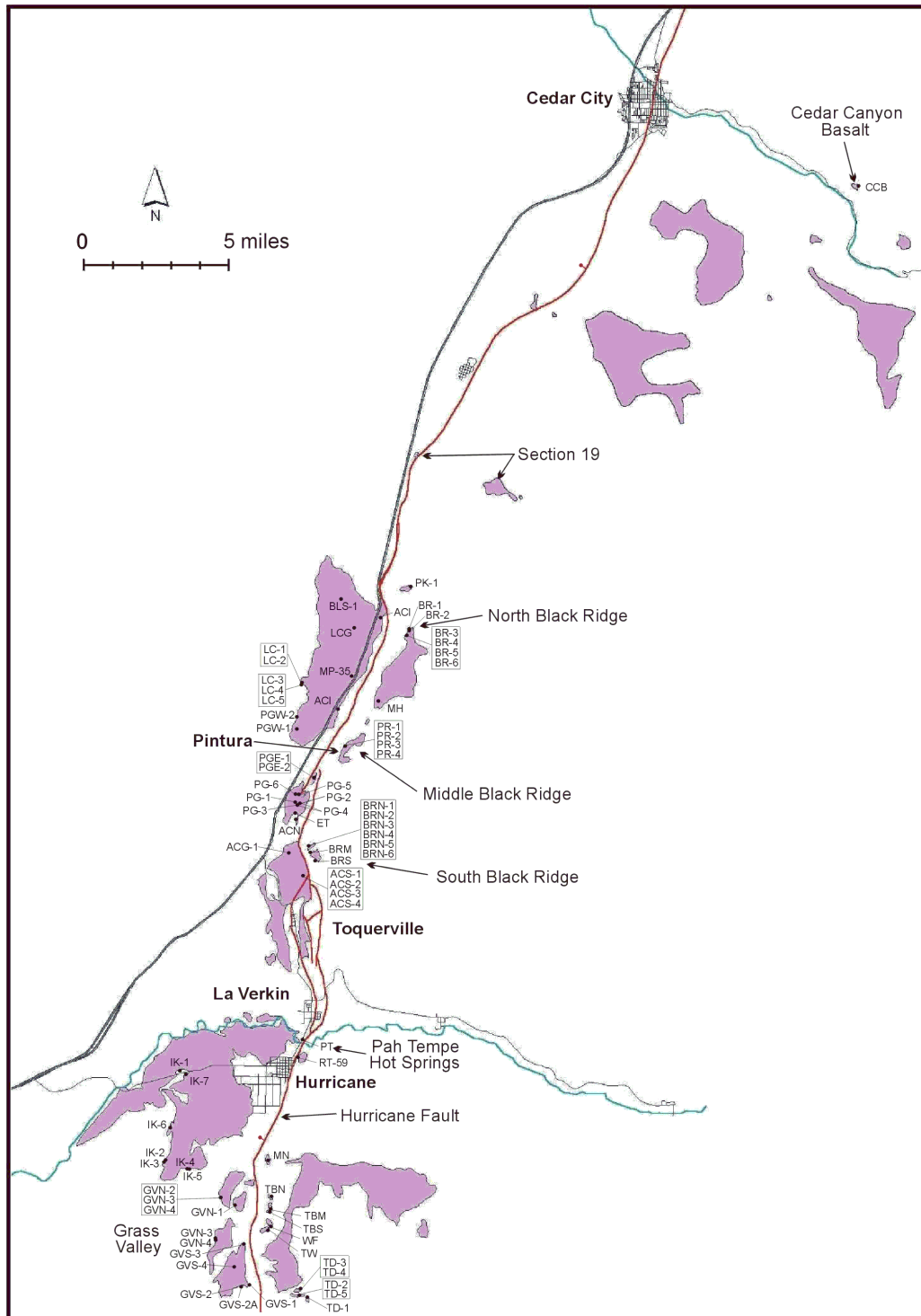
Figure 7. Quaternary basalts associated with the Hurricane fault in Utah and geochemical, paleomagnetic, and radiometric sample sites. Locations where displaced basalt could be geochemically correlated across the fault include: Grass Valley, Pah Tempe Hot Springs, South Black Ridge, and North Black Ridge. The Cedar Canyon basalt site is shown east of Cedar City.

13

Table 1. Slip rates derived from displaced basalt flows along the Utah portion of the Hurricane fault.

Location	Slip Rate mm/yr	Time Period Ma	Segment	Comments
Grass Valley	0.44	1.0	AJ	Higgins (2000) [40]Ar/[39]Ar ages
Pah Tempe Hot Springs	0.21	0.353	AJ	
S. Black Ridge	0.45	0.81	AJ/AC	Proposed segment boundary
N. Black Ridge	0.57	0.86	AC	
Section 19	0.37-0.51	1.08	CC	Ages from Anderson and Mehnert (1979)
Cedar Canyon	0.53	0.63	CC	Surrogate rate – from stream downcutting

on the Anderson Junction segment/section just north of the State Line geometric bend GSBZ and in the southern part of the Shivwitz segment/section. In both of these areas, there are obvious fault scarps formed in late Quaternary alluvium and colluvium along the base of the Hurricane Cliffs. Quaternary units displaced by the fault include the Moriah Knoll basalt and late Pleistocene to early Holocene (?) alluvial and colluvial deposits. Late Quaternary slip-rate estimates using soil analysis, cosmogenic isotope dating, and carbonate-rind-thickness to approximate surface-age, and scarp profile modeling vary from <0.1 to 0.6 mm/yr, but most fall in the range of 0.1 to 0.3 mm/yr (Stenner and others, 1999; Amoroso and others, 2002). Geochemical data and geologic mapping (Billingsley, 1994b) show that the Moriah Knoll basalt flow was erupted on top of the Hurricane Cliffs, flowed across a structurally complex part of the fault zone, and subsequently was displaced by faulting. A new [40]Ar/[39]Ar age estimate establishes the age of the basalt at 0.83± 0.06 Ma. There has been about 200 meters of cumulative displacement across several faults since the flow was extruded, resulting in a long-term slip rate for the Shivwitz segment of about 0.24 mm/yr.

The Arizona Geological Survey (AZGS) excavated trenches at two sites in Arizona, the Cottonwood Canyon site (two trenches) on the southernmost part of the Anderson Junction segment, and the Boulder Fan site (one trench) on the southern part of the Shivwitz segment (figure 1). At Cottonwood Canyon the AZGS excavated the Q1 trench across a low fault scarp with less than 1 meter of displacement formed on an early Holocene (?) alluvial terrace. The trench exposed a 2-meter-wide fault zone, and stratigraphic and structural relations showed that a single surface-faulting earthquake probably occurred 8-15 thousand years ago. A second trench excavated across a 5-meter-high scarp formed on a late Pleistocene terrace surface about 25 meters south of the Q1 trench did not reveal any further information about late Quaternary fault behavior, as burial of older fault-related sedimentary units in the fault hanging wall by younger alluvial deposits precluded direct observation of evidence for older surface-faulting earthquakes in the trench.

The possibly Holocene MRE for the southern Anderson Junction segment resulted in a 60- centimeter displacement at Cottonwood Canyon. The event was at least a M 6.5, and may have been small compared to previous events at the site. Based on a 30- to 35-kilometer-length, the proposed Anderson Junction segment could produce a M 6.8-6.9 event.

At the Boulder Fan site on the Shivwitz segment, the AZGS excavated a single trench across a scarp formed on a large, Pleistocene alluvial fan that is an estimated 15,000-33,000 years old. The fan surface there is displaced about 4.5 meters. The scarp shows little evidence of erosion and likely represents multiple surface-faulting events. Stratigraphy in the trench consisted of debris-flow deposits in the footwall, and fault-scarp colluvium, fissure-fill deposits,

slope-wash deposits, and a framework gravel deposit in the hanging wall. Two colluvial-wedge deposits are evidence of two surface-faulting earthquakes. Secondary geologic relations indicate that total slip for the two events is 4.3 to 4.7 meters. Retro-deformation analysis suggests that the MRE produced about 2.5 to 3 meters of vertical displacement. Detrital charcoal recovered from fissure-fill material at the base of the MRE colluvial wedge had an age of 9,300 +1,070, -430 cal B.P., which is considered close to the age for the MRE at this site.

A MRE single-event maximum surface displacement of 2.5 meters along the southern Shivwitz segment gives an estimated moment magnitude of 7-7.1. Using an estimated segment length of 57 kilometers, rupture of the Shivwitz segment is capable of producing M 6.8-7 events.

Summary and Conclusions

The UGS/AZGS studies of the Hurricane fault provide new information critical to earthquake hazard assessment in southwestern Utah and northwestern Arizona. In summary, their new results show:

1.   Long-term slip rates on the Hurricane fault in Utah and Arizona range from 0.21 to 0.57 mm/yr and generally increase from south to north indicating that for the past approximately one million years, the north end of the Hurricane fault has been its most active part.

2.   Differences in long-term slip rates appear to be incremental across previously suspected fault segment boundaries, lending support to the presence of a seismogenic boundary at the Toquerville GBBZ between the proposed Anderson Junction and Ash Creek segments and the State Line GBBZ between the Anderson Junction and Shivwitz segments. The data are also permissive, but not necessarily supportive, of another seismogenic boundary farther north at a right bend in the fault near Murie Creek.

3.   Slip rates determined from displaced late Pleistocene and Holocene alluvial and colluvial deposits along the fault in Utah are lower (<0.01 - 0.3 mm/yr) than the long-term rates (~0.4 - 0.6 mm/yr) and show that slip on the Hurricane fault has slowed there (generated fewer surface-faulting earthquakes) in more recent geologic time. This decrease in activity helps explain the sparse distribution of young fault scarps on unconsolidated deposits at the base of the high, steep Hurricane Cliffs in Utah. This slowing may have begun more than 350,000 years ago as evidenced by the 0.21 mm/yr slip rate for the Anderson Junction segment, determined from the displaced basalt flow at Pah Tempe Hot Springs. On the Shivwitz section of the Hurricane fault in Arizona, long-term (0.24 mm/year determined for the Moriah Knoll basalt) and late Quaternary slip rate estimates are not demonstrably different. Late Quaternary slip rate estimates for the Shivwitz, Anderson Junction, Ash Creek, and Cedar City segments are similar (0.1 to 0.3 mm/yr).

4.   Based on our trench investigations, the MRE on the southern part of the Shivwitz segment occurred about 8,900 to 10,400 cal B.P., and it involved at least 2 meters of surface displacement. The MRE on the southern part of the Anderson Junction segment probably occurred in the early Holocene and involved less than 1 meter of surface displacement. The MRE on the Ash Creek segment occurred in the late Holocene more recently than 1,260 cal. B.P. Timing of the MRE on the proposed Cedar City segment is prior to 1,530 cal B.P. How much prior is unknown, but the absence of young scarps on the Cedar City segment argues for a considerable period of time since the last surface-faulting earthquake.

5.   The most recent surface-faulting earthquakes on the Ash Creek and Anderson Junction segments are different in time, demonstrating that the two adjacent proposed segments last ruptured independently. Both segments must be considered active and capable of generating additional large earthquakes in the future. The rupture lengths of the MREs on the Anderson Junction and Shivwitz segments are poorly constrained at this time. The MRE on the Anderson Junction segment may have ruptured only the southern part of the segment with relatively little displacement. Alternatively, much or the entire segment may have ruptured, with evidence of the rupture only being clearly preserved at

the southern end. At least the southern part of the Shivwitz section ruptured about 10 thousand years ago. On the southern Shivwitz section, we found no evidence of rupture of mid- to late-Holocene deposits or landforms (including stream thalweg profiles). Because of the wide spacing between trenches and the uncertainty in the age estimates, we cannot rule out the possibility that the youngest faulting recorded on the Shivwitz and southern Anderson Junction segments occurred in one large earthquake.

6. The presence of faulted late Holocene alluvial-fan deposits at Coyote Gulch on the Ash Creek segment, and the absence of evidence for young faulting along the fault north of that point, argues for a third fault segment in Utah with a seismogenic segment boundary possible at the right bend in the fault at Murie Creek. We have named this proposed new northern segment the Cedar City segment.

7. The decrease in slip rates from early to late Quaternary time along the Hurricane fault in Utah translates into longer recurrence intervals between large surface-faulting earthquakes. The average recurrence interval for surface faulting on the Hurricane fault's Utah segments is probably several thousand to possibly more than 10,000 years.

8. Based on 2.75 meters of single-event displacement at Coyote Gulch, the MRE on the Ash Creek segment had an estimated moment magnitude of M 6.9-7.1. Based on an estimated segment length of 13 kilometers, the Cedar City segment is capable of producing up to M 6.5 events. Using ~0.6 meters of displacement recorded at Cottonwood Canyon, the most recent Anderson Junction rupture was likely at least M 6.5. Based on a 30-35 kilometer length, the Anderson Junction segment could produce M 6.8-6.9 events. Based on the ~2.5 meter single-event displacement at the Boulder Fan, the MRE estimated moment magnitude for the rupture on the Shivwitz section is M 7 – 7.1.

FIRST DAY ROAD LOG

The Shivwitz and Southern Anderson Junction Segments
Hurricane Fault Zone, Arizona and Utah
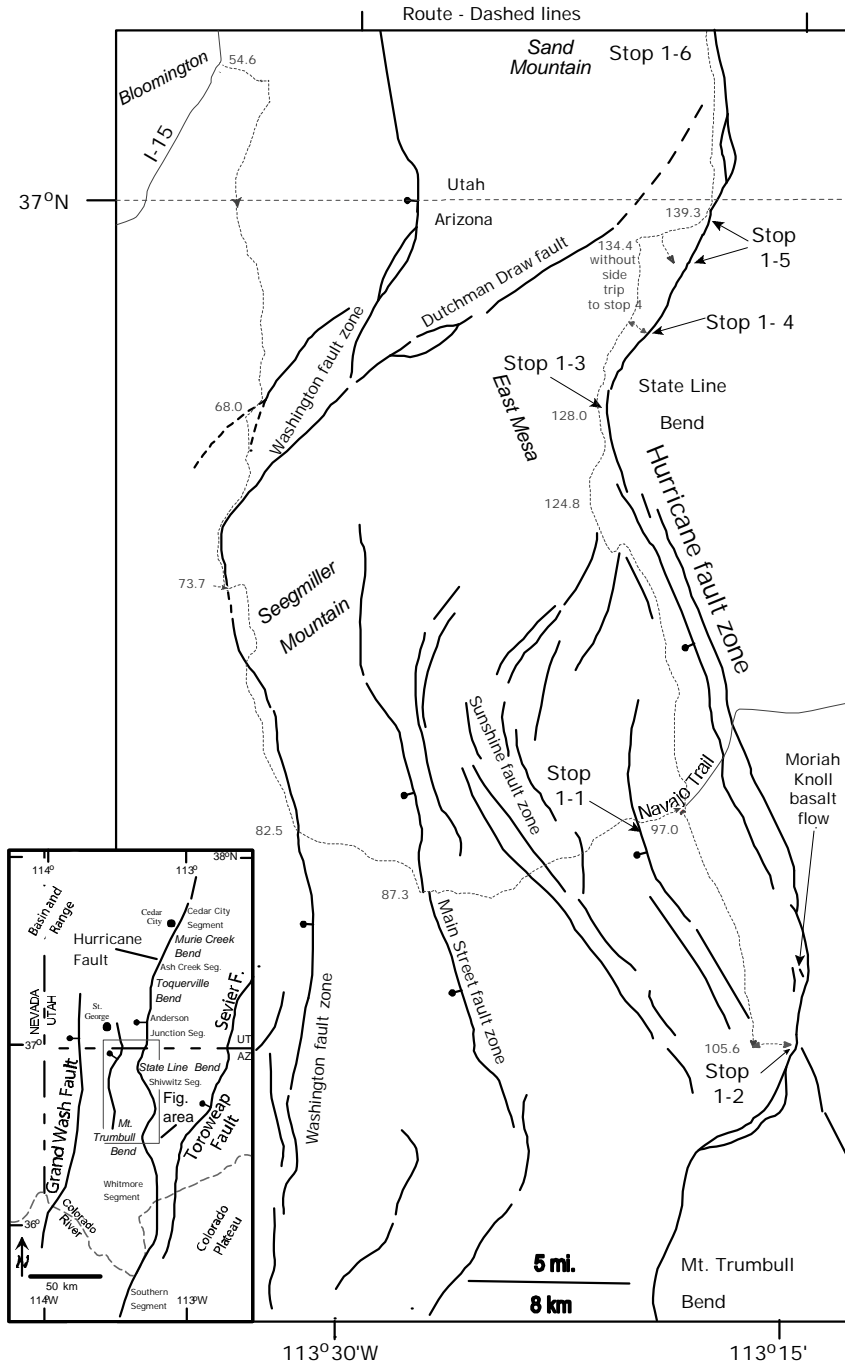
Day 1 Stop and Route Map

Figure 8. Day 1 Route Map. The dashed line shows the route of our trip on Day 1. Some key mileage values are shown along the route (note that the map begins at mileage 54.6 at Bloomington; I-15 exit #4). Heavy weight lines represent faults. Words in italics are geographic locations noted in the road log. Inset shows trip map in a regional context.

17

FIRST DAY ROAD LOG

The Shivwitz and Southern Anderson Junction Segments
Hurricane Fault Zone
Arizona and Utah

On the first day of this two-day field trip, we will examine the Shivwitz and the southern part of the Anderson Junction segments of the Hurricane fault in Arizona and Utah. The trip will depart from the Southern Utah University parking lot at 200 South and 1150 West Streets in Cedar City, Utah, and will proceed directly to the Utah/Arizona border south of St. George, Utah. From there we will continue via dirt roads into the Arizona Strip to our first stop along the Navajo Trail, which provides an overview of the Shivwitz segment. It is an approximately 2.5 hour drive from Cedar City to the first stop. We will next proceed to the Boulder Fan trench site and examine direct stratigraphic evidence for two paleo-earthquakes on the Shivwitz segment, the youngest probably being earliest Holocene in age. The remainder of the day will be spent traveling northward along the fault on the Temple and Honeymoon Trails, examining evidence of the Hurricane fault's long-term structural development, the proposed boundary between the Shivwitz and Anderson Junction segments at the State Line geometric bend, the Cottonwood Canyon trench site on the Anderson Junction segment, a proposed trench site at Rock Canyon, and basalt flows, some of which cascaded over the Hurricane Cliffs, and others of which are displaced hundreds of meters across the fault. We will end the first day in Hurricane, Utah.

The six stops today provide information that allowed us, at least in part, to draw six main conclusions. (1) The Hurricane fault is geometrically segmented. (2) Fault linkage occurred at the State Line bend. The linkage style was fault capture. (3) Long-term slip rates on the Hurricane fault range from 0.21 to 0.57 mm/yr. On the Shivwitz section in Arizona, long-term (0.24 mm/year determined for the Moriah Knoll basalt) and late Quaternary slip rate estimates are not demonstrably different. (4) Increases in long-term slip rates appear to be incremental across previously suspected fault segment boundaries, lending support to the presence of a seismogenic boundary at the State Line GBBZ between the Anderson Junction and Shivwitz segments. (5) Based on our trench investigations, the most recent surface-faulting earthquake (MRE) on the southern part of the Shivwitz segment occurred about 8,900 to 10,400 cal. B.P. Each faulting event involved at least 1.5 meters of surface displacement, suggesting that they were associated with large earthquakes that ruptured much or the entire Shivwitz segment of the Hurricane fault. The MRE on the southern part of the Anderson Junction segment probably occurred in the early Holocene, and may have been a smaller event.

Mileages
Inc. Cum.

0	0	Begin trip in parking lot at Southern Utah University near corner of 200 South and 1150 West streets. **Turn left (N)** onto 1150 West. Note that it will take about 2.5 hours to reach the first stop.
0.2	0.2	**Turn left (W)** at intersection of 1150 West and Center Streets. Proceed across freeway overpass.
0.3	0.5	**Turn right (N)** onto College Way (1650 West) at stop sign.
0.3	0.8	**Turn right (E)** onto 200 North at the stop light.
0.3	1.1	**Turn right (S)** onto I-15 on ramp.
0.8	1.9	At 11:00 the Green Hollow landslide is visible. It is a large late Pleistocene landslide extending from valley floor to ridge crest.

1.0	2.9	Providence Center Lighthouse on right (W). Constructed in 2000, this lighthouse has proven to be a major safety improvement for Cedar City, which has not experienced a single shipwreck since the lighthouse went into operation.
1.7	4.6	Another large, late Pleistocene landslide extending to the valley floor on the left (E).
0.1	4.7	Hurricane fault to left (E) near base of Hurricane Cliffs.
0.4	5.1	Quaternary basalt in road cut.
1.1	6.2	North Hills on left (E), which is a faulted anticline that deforms the Tertiary Claron Formation, Tertiary conglomerate, and Quaternary basalt.
4.2	10.4	At 9:00 (E) along the base of the Hurricane Cliffs is the active strand of the Hurricane fault. Here, the stratigraphic section in the footwall is overturned. The hanging wall is comprised of alluvium. We will visit this area tomorrow (STOP 2-6). For the next several miles I-15 will parallel the trace of the Hurricane fault. Also note the New Harmony Hills on the right (W) at about 1:00.
3.1	13.5	Great Basin drainage divide (near freeway overpass), leave the Great Basin and enter the Colorado River drainage.
1.0	14.5	To the left (E), the Hurricane Cliffs expose the grayish tan Permian Kaibab Formation. The Kaibab lies in the limb of an anticline that formed during the Sevier orogeny.
2.4	16.9	To the left (E), young fault scarps are generally absent along the Hurricane fault. The gravel quarry here is periodically monitored for fault exposures.
0.1	17.0	Nice exposures of the Hurricane fault at 9:00. The tan unit is the Permian Kaibab Formation (footwall) that is juxtaposed against the red Shnabkaib Member of the Triassic Moenkopi Formation (hanging wall).
1.0	18.0	To the left (E) the Hurricane Cliffs expose the Moenkopi Formation. The Pine Valley Mountains lie to the right (W) at 2:00.
1.4	19.4	Pass I-15 off ramp to the Kolob Canyons entrance to Zion National Park. Permian Kaibab Formation exposed in Hurricane Cliffs to the left (E).
1.8	21.2	At 2:00, Quaternary basalt of the informally named New Harmony basalt field.
1.0	22.2	At 3:00, Ash Creek Reservoir, I-15 forms the dam for this unused reservoir. At 11:00 along the skyline, Quaternary basalt crops out at the top of Black Ridge (Hurricane Cliffs).
0.6	22.8	Quaternary basalt in this road cut is geochemically and geochronologically the same as the basalt on the skyline in the footwall of the Hurricane fault. We will stop here tomorrow (STOP 2-5, I-15 Exit 36) to discuss the relation between the basalts and the Hurricane fault in more detail.
0.8	23.6	At 9:00, the hummocky topography of a landslide is visible on the flank of Black Ridge. The Triassic Chinle Formation is failing and carrying Quaternary basalt with it. Also, you are still looking at the east limb of a Mesozoic anticline.

2.9	26.5	At 9:00, large fault scarps are formed in unconsolidated deposits and bedrock near the base of the Hurricane Cliffs. Following cliffs to the south, more scarps are visible.

2.9   26.5   At 9:00, large fault scarps are formed in unconsolidated deposits and bedrock near the base of the Hurricane Cliffs. Following cliffs to the south, more scarps are visible.

1.5   28.0   Pass exit 31.

1.2   29.2   Look toward 10:00 to see a graben expressed topographically in Quaternary basalt.

0.6   29.8   The hill at 11:00 is comprised of Tertiary quartz monzonite of the Pine Valley laccolith.

0.7   30.5   To the right (W), at 3:00, the Tertiary Claron Formation (orange and white) crops out below more of the Pine Valley laccolith.

1.0   31.5   At 9:00 on the skyline are the radio towers where we will be about mid-day tomorrow (Stop 2-4). The towers are on the south end of Black Ridge.

1.0   32.5   Pass exit 27 to Toquerville. Here, I-15 diverges from the trace of the Hurricane fault. The fault bends east and the freeway continues generally south. This is Anderson Junction and the Toquerville geometric bend.

1.3   33.8   Red beds on the right (W) at 3:00 are Jurassic Navajo Sandstone. The Pine Valley laccolith crops out in the distance near the skyline.

0.6   34.4   At 11:00 is the nose of the north-plunging part of the doubly plunging Virgin anticline, a large fold related to the Mesozoic Sevier orogeny.

0.7   35.1   At 2:00 is the historic Silver Reef mining district with the reddish Kayenta Formation and Navajo Sandstone exposed in the near distance. The Silver Reef mining district is noted for its uncommon occurrence of ore-grade silver chloride (cerargyrite or horn silver) in sandstone, unaccompanied by obvious alteration or substantial base-metal ores. The principal mining activity in the district extended from 1876 to 1888 with lessee operations through 1909. The district produced about 8 million ounces of silver prior to 1910.

1.1   36.2   We are now driving parallel to the west flank of the Virgin anticline. The Shinarump Conglomerate Member of the Triassic Chinle Formation forms the resistant dip slope. The Triassic Moenkopi Formation crops out on the left (E). We are driving in a strike valley in the Petrified Forest Member of the Chinle Formation.

3.1   39.3   In the near distance at 3:00 the Moenkopi Formation crops out. In the background is the Jurassic Navajo Sandstone.

0.3   39.6   At 9:00, Quail Creek cuts through and forms a gap in the west limb of the Virgin anticline.

1.0   40.6   The Triassic Petrified Forest Member of the Chinle Formation crops out at 10:00.

0.9   41.5   Alluvial fans are visible in the low foothills at 3:00. This area is designated as desert tortoise habitat.

1.0   42.5   Conglomerate in road cut is a Tertiary deposit that contains mostly clasts of quartz monzonite from the Pine Valley laccolith. Hurlow (1998) interpreted this

deposit as debris-flow material derived from the steep southern and southeastern slopes of the Pine Valley Mountains.

2.2	44.7	At 12:00 is Washington Black Ridge. The road cut exposes the Washington basalt flow occupying the now inverted ancestral channel of Grapevine Wash. This is the most mafic of the flows in the St. George area. Best and others (1980) dated it at 1.7$\pm$0.1 Ma. The basalt is strongly jointed and has been quarried for building stone (Biek, 1997).
1.0	45.7	The hill at 11:00 is Shinob Kaib Butte, type section of the Shnabkaib Member of the Triassic Moenkopi Formation. The Shnabkaib Member is characterized by the "bacon slab" appearance of its alternating red and white strata. The Shinarump Member of the Chinle Formation, here a coarse, well-cemented pebbly sandstone, caps the butte.
0.8	46.5	Cross the Washington fault. The Washington fault is a 42-mile-long, down-to-the-west, high-angle normal fault that trends north-south through northern Arizona and southern Utah. Displacement on the Washington fault decreases to the north. It reaches a maximum of about 2,200 feet six miles south of the Utah/Arizona border, is approximately 1,600 feet at the border, and about 700 feet at this location, where the fault begins to bifurcate and quickly die out to the north (Higgins, 1998).
0.2	46.7	At 12:00 is the St. George basin. At 2:00, Quaternary basalt flows that were erupted from volcanoes located near the base of the Pine Valley Mountains.
2.3	49.0	At 2:00 is the doubly plunging Washington Dome, one of three such domes along the Virgin anticline.
0.8	49.8	At 12:00 is Middleton Black Ridge. The road cut exposes the Middleton basalt flow, which occupies a now inverted valley in the Jurassic Kayenta Formation (Willis and Higgins, 1995). The Middleton flow is about 200 feet above the Virgin River and has been dated at 1.5$\pm$0.1 Ma by Best and others (1980).
1.4	51.2	At 3:00, two levels of basalt flows are visible on West Black Ridge. The lower basalt flow is home to the St. George airport and is ^{40}Ar/^{39}Ar dated at approximately 1.23 Ma (Willis and Higgins, 1995). Below the flow, red siltstone outcrops of the Jurassic Dinosaur Canyon Member of the Moenave Formation dip northward on the mostly talus-covered hillside. The higher, and thus older, basalt flow that caps West Black Ridge is ^{40}Ar/^{39}Ar dated at 2.34 Ma. Note the well-formed columnar jointing. West Black Ridge is an outstanding example of inverted topography, wherein former stream channels tributary to the Virgin River now stand high above the surrounding landscape.
2.8	54.0	At 12:00, in the road cut the Triassic Shinarump Conglomerate overlies the upper red member of the Moenkopi Formation. This gap was cut by the Virgin River where it exits the St. George basin.
0.3	54.3	Cross the Virgin River.
0.3	54.6	**Take Exit 4 into Bloomington**.
0.3	54.9	Traffic circle. **Drivers exercise caution here, even the locals have trouble with this thing**. Follow around to the left and exit on Brigham Road, under the freeway.

0.2	55.1	Drive east on Brigham Road. At 9:00 is an excellent exposure of the Shnabkaib and upper red members of the Moenkopi Formation. The unit capping the ridge is the Shinarump Conglomerate Member of the Chinle Formation.

0.2   55.1   Drive east on Brigham Road. At 9:00 is an excellent exposure of the Shnabkaib and upper red members of the Moenkopi Formation. The unit capping the ridge is the Shinarump Conglomerate Member of the Chinle Formation.

1.7   56.8   **Turn right** at intersection with River Road. Proceed south toward Arizona and the Moenkopi Terrace.

3.7   60.5   Utah/Arizona state line. Beyond this point we will be entering the infamous Arizona Strip, note that in Utah, unlike Arizona, we mostly provide paved roads for field trips. You will come to appreciate that fact as today's trip bumps and grinds on and on. We are traveling through low relief terrain eroded into the Moenkopi Formation. This area is partially covered by Quaternary alluvial deposits, including young deposits along active washes and eroded remnants of terraces and alluvial fans (Billingsley, 1993a).

2.1   62.6   At 9:00, Pine Valley laccolith at the skyline.

0.4   63.0   The high ridge to the southwest is Mokaac Mountain, a large ridge composed of Moenkopi Formation capped by late Tertiary basalt (Hamblin, 1970a). Much of the slopes of Mokaac Mountain consist of large Quaternary landslides (Billingsley, 1993a).

0.6   63.6   A strand of the Washington fault zone, a major, down-to-the-west normal fault, is at the base of steep, linear cliffs formed in resistant beds of the Kaibab and Toroweap Formations at about 12:00. The Washington fault zone extends from the town of Washington, Utah, southward for about 60 kilometers into Arizona. In this area, the Washington fault zone consists of two generally northeast-trending strands. The western strand, which is most apparent from this vantage point, has been named the Mokaac fault (Billingsley, 1993a). Paleozoic rocks are displaced by about 200 to 400 meters across the Mokaac fault zone in this area, with displacement increasing to the northeast. Total displacement across the main strand of the Washington fault zone to the east is 100 to 600 meters, also generally increasing to the north through this area. Surface exposures of the Washington fault zone indicate that it is very high angle, and it has been interpreted as a reverse fault (Billingsley, 1993a) or high-angle normal fault (Billingsley and Workman, 2000). Quaternary activity on the Washington fault zone in Arizona has not been studied in detail, but late Quaternary alluvium and colluvium is displaced several meters at a number of localities (Billingsley, 1993a) and the linear, steep escarpments associated with portions of the fault zone suggest substantial Quaternary activity (Menges and Pearthree, 1983; Pearthree, 1998).

0.9   64.5   Where the West Stays Wild sign. You may well see no people on the field trip route in Arizona, and thus you should not venture out without plenty of gas, food, water, and good maps.

1.1   65.6   A low ridge of the Virgin Limestone Member of the Moenkopi Formation crops out at 11:00-12:00.

2.4   68.0   The road crosses the Mokaac fault in this area, although the fault zone is not exposed.

0.5   68.5   You are on a block between the two strands of the Washington fault zone. The main (eastern) strand of the fault zone is at the base of the large escarpment straight ahead.

1.2	69.7	The road roughly parallels the main strand of the Washington fault zone for a couple of miles. Kaibab Formation crops out in upper cliffs. The Harrisburg Member of the Kaibab Formation is eroded, whereas the Fossil Mountain Member is a resistant cliff-forming unit. Red and yellow units lower in the cliff are in the Toroweap Formation (Billingsley, 1993a).
0.7	70.4	We are driving mainly in the Harrisburg Member of the Kaibab Formation, and locally in the overlying Moenkopi Formation; equivalent units on the upthrown side of the fault are high above us. Total vertical displacement across the Washington fault zone here is about 300 meters (Hamblin and Best, 1970; Billingsley, 1993a).
1.4	71.8-71.9	Exposures of steeply dipping colluvial deposits in road cuts indicate we are quite close to the fault zone, but are probably still on the downthrown side of the fault.
0.7	72.6-72.9	The road probably crosses the Washington fault zone several times through this interval.
0.5	73.4	Exposure of the Fossil Mountain Member of the Kaibab Formation indicates that we are now driving on the upthrown side of the fault.
0.3	73.7	Top of the long uphill grade in a pass at the base of Quail Hill. The Washington fault zone continues southeastward from this point, and we will cross it several more times.
0.2	73.9	There is a radio tower on top of Seegmiller Mountain at 12:00. The mountain is capped by a basalt flow over the Moenkopi Formation. Reynolds and others (1986) dated the flow at 2 to 3 Ma (K-Ar), Wenrich and others (1995) dated it at 4 to 5 Ma (K-Ar), and Downing and others (2001) at 3.5 to 4.2 Ma (^{40}Ar/^{39}Ar).
0.6	74.3	Take right (main) fork at junction, left fork goes to Seegmiller Mountain.
0.9	75.2	Exposure of white and red Moenkopi Formation capped by Tertiary basalt at 8:00-9:00.
0.9	76.1	We are still roughly paralleling the Washington fault zone on the upthrown side of the fault.
0.9	77.0	We cross the Washington fault zone somewhere in this vicinity. The ridgeline to the left of the road is capped with the Seegmiller Mountain basalt, which is displaced about 100 meters here. Displacement of underlying Triassic strata is similar, implying that displacement on the Washington fault zone began less than 4 million years ago (Billingsley, 1993a; Downing and others, 2001).
0.8	77.8	The Shivwitz Plateau dominates this view to the south. The Shivwitz Plateau is the hanging-wall block of the Hurricane fault and the footwall block of the Grand Wash fault to the west. The Grand Wash fault and its associated cliffs form the western margin of the Colorado Plateau at this latitude. The Shivwitz Plateau is cut by a number of normal faults with much less displacement than either the Grand Wash or Hurricane faults, including the Washington fault zone.
0.5	78.3	To the northeast, several ridges are associated with multiple strands of the Washington fault.

4.9	79.2	BLM sign identifying Wolf Hole Valley. This tiny basin is on the downthrown side of the Washington fault. The low escarpment in the distance at 10:00-11:00 is the continuation of the upthrown side of the Washington fault. The high plateau to the west is Wolf Hole Mountain, which consists of Moenkopi Formation capped by late Tertiary basalt flows. Billingsley (1993a) obtained a K-Ar date of 3.1±0.4 Ma from a basalt atop Wolf Hole Mountain. Near this location, Wolf Hole, Arizona, now defunct, formerly consisted of a post office and general store to serve ranchers on the Arizona Strip. Edward Abbey listed Wolf Hole, Arizona as his home address.
0.4	79.6	Three small knobs (Mustang Knolls) at 2:00-3:00 are capped by basalts over the Moenkopi Formation.
0.6	80.2	Continue straight at T intersection with Black Mountain Road.
0.1	80.3	The upthrown block of the Washington fault is evident at 9:00, where there is about 60 meters of total displacement (Hamblin and Best, 1970; Billingsley and Workman, 2000).
2.3	82.6	Bear left at Y intersection and quickly cross the Washington fault.
0.7	83.3	High point in the road at Wolf Hole Pass with views to the east and south. The high escarpment in the distance at 12:00-1:30 is the Hurricane Cliffs. The plateau above the escarpment is the Uinkaret Plateau. The high, broad mountain on the Uinkaret Plateau in the far distance to the southeast is Mt. Trumbull, the remnant of an early Quaternary volcano. Left of Mt. Trumbull is Antelope Knoll, another Quaternary volcano. Diamond Butte at 1:00-1:30 is composed of Moenkopi Formation capped by basalt dated by Billingsley (1993b) at 4.3±0.6 (K-Ar). Extensive Pliocene basalts capping buttes and mountains on or around the margins of the Shivwitz imply that the land surface was generally formed on the Moenkopi Formation in the early Pliocene. In most places, Moenkopi deposits have been completely removed and the surface of the Shivwitz Plateau is now formed on the underlying Kaibab Formation. Erosion of the Moenkopi Formation must have provided abundant sediment to the Colorado River system over the past few million years. The road here is very close to the contact between the Permian Kaibab Formation to the north and the Triassic Moenkopi Formation to the south. In this area, the Moenkopi Formation filled a Triassic paleovalley carved into the Kaibab Formation (Billingsley, 1991).
2.1	85.4	We are driving through eroded Kaibab and Moenkopi rocks.
0.6	86.0	Bear right at Y intersection as you enter Main Street Valley. Main Street Valley is bounded on the east by an obvious escarpment associated with the principal strand of the Main Street fault. Total displacement across this eastern fault ranges from about 50 to 120 meters. Quaternary deposits and basalts are displaced in a few locations, but no detailed studies have been completed on this fault zone. Portions of the west side of the valley are also fault-bounded, and this part of the fault system has been labeled the Main Street graben (Menges and Pearthree, 1983; Billingsley, 1993c).
0.6	86.6	Cattle guard.
0.7	87.3	**Turn left onto Navajo Trail** and proceed east across the principal Main Street fault strand.

0.3	88.6	We are now driving on the Harrisburg Member of the Kaibab Formation. The knoll in the far distance at 12:00 is Antelope Knoll.
2.5	91.1	Hurricane Cliffs are visible in the distance at 12:00. The Fossil Mountain Member of the Kaibab Formation crops out in the lower parts of this valley. This is a prominent cliff-forming unit that you will see high up in the footwall of the Hurricane fault.
0.5	91.6	We cross the Sunshine fault as we emerge into a valley. The Sunshine fault has generated an escarpment at the southwestern margin of this valley; total displacement is about 110 to 130 meters, down-to-the-east (Billingsley, 1993c). The Sunshine fault is likely an east-dipping normal fault, antithetic to the Hurricane fault. It has the most linear and impressive escarpment of the secondary faults associated with the Hurricane fault. The road is on a young alluvial fan that is not displaced by the Sunshine fault. In the valley to the east there are several low scarps that are probably related to west-dipping normal faults.
0.7	92.3	Part of the Hurricane Cliffs escarpment is visible from 11:00-3:00. The Hurricane fault is at base of the escarpment. If the lighting is right, you may be able to see some low fault scarps formed in colluvium at the base of the cliffs that record late Quaternary displacement on the fault. The Pine Valley Mountains north of St. George, Utah, can be seen at 9:00-10:00.
0.4	92.7	A structurally complex portion of the Shivwitz section of the Hurricane fault, including the Navajo Trail crossing and the Grandstand, is visible from 11:00-1:00. We will discuss this area from Stop 1-1.
0.3	93.0	Keep straight on the Navajo Trail at the intersection with the Sunshine Trail.
0.2	93.2	This modest escarpment is associated with another minor, west-dipping fault strand. The road climbs across rocks of the Moenkopi Formation that filled a paleovalley in the Kaibab Formation; Kaibab Formation crops out at the top of the ridge.
0.6	93.8	A smaller west-dipping fault with a steep and linear scarp is visible in the near distance.
1.0	94.8	The ridgeline in the middle distance at 9:30-10:00 is capped with late Tertiary basalt dipping moderately towards the Hurricane fault.
0.5	95.3	Large stock tank and causeway at the crossing of Hurricane Wash.
0.2	95.5	Cross low escarpment associated with a west-dipping fault. Basalt-capped Diamond Butte is visible at 2:00.
0.2	95.7	Axis of the rollover Hurricane monocline is somewhere in this vicinity (Billingsley, 1993d). Park on the south side of the road; walk ~100 meters south of road to the top of a low hill (Stop 1-1). This hill is capped by a thin layer of alluvium (Billingsley, 1993d) that was probably part of an alluvial fan associated with a relict course of Hurricane Wash. It is likely that some combination of displacement on the fault zone immediately to our west and associated drainage capture altered the course of Hurricane Wash to its present position.

STOP 1-1. Overview of the Shivwitz segment of the Hurricane fault. (Grandstand 7.5' quadrangle, T38N, R10W, section 1)

From this vantage we can see much of the Shivwitz segment of the Hurricane fault. Down-to-the-west displacement across the Hurricane fault has resulted in the formation of the Hurricane Cliffs, the prominent escarpment that dominates our view to the east (figure 9). The Hurricane Cliffs separate the higher Uinkaret Plateau to the east from the Shivwitz Plateau on which we are standing. The obvious volcanic cone in the distance above the Hurricane Cliffs is Antelope Knoll, one of several Quaternary eruptive centers on the footwall of the Hurricane fault. Stop 1 is on the monocline in the hanging wall where strata on the downthrown side dip toward the fault. This increase in dip toward the fault likely results from reverse drag flexure due to decreasing fault dip at depth (Hamblin, 1965b; Billingsley and Workman, 2000).

The Hurricane Cliffs escarpment exposes Permian marine carbonates and marine to continental clastic rocks of the Toroweap and Kaibab Formations (Sorauf and Billingsley, 1991). The Harrisburg Member of the Kaibab Formation is at the top of the escarpment; in many places, it has retreated from the escarpment. The highest steep cliff is formed in the Fossil Mountain Member of the Kaibab Formation. Lower in the cliffs the Toroweap Formation consists of the slope-forming Woods Ranch member, the cliff-forming Brady Canyon member, and the slope-forming Seligman member (where exposed at the base of the cliffs). Coarse, very poorly sorted colluvium covers much of the slope-forming units, especially the Seligman Member. Because of the structural complexity of the Hurricane fault zone immediately across the valley from this vantage point, you may see all or parts of this sequence repeated several times.

Most of the Shivwitz segment is a large structural embayment between two prominent convex fault bends. On the hanging wall at the northern end of the Shivwitz segment you can see a prominent east-sloping
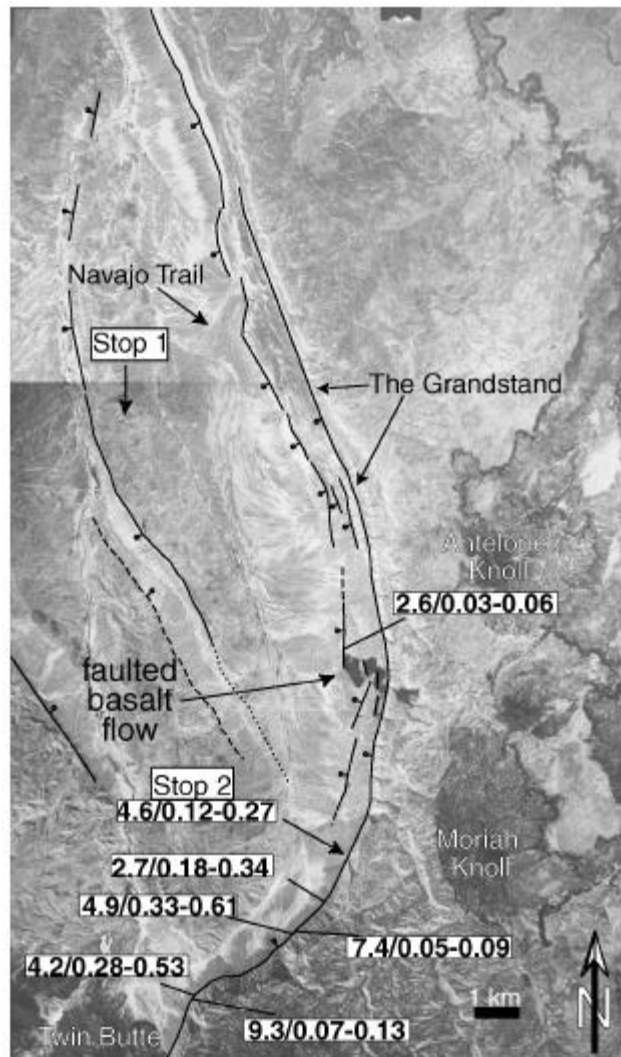

Figure 9. Mosaic of NASA high-altitude aerial photography of the Shivwitz section of the Hurricane fault zone showing fault traces and results of slip rate estimates. Faults are dashed where approximate or inferred, dotted where concealed. Field trip stops and features discussed in the text are labeled. Also shown is a compilation of the vertical surface displacement observations and slip rates estimated from scarp morphologies (surface offset in meters, slip rate range in mm/yr). We determined a slip rate of 0.1 to 0.3 mm/yr using similar methodology at Cottonwood Canyon 25 kilometers to the north of this portion of the Shivwitz section (Stenner and others, 1999). The basalt flow displaced by the Hurricane fault originated from Moriah Knoll.

26

butte, where beds of the Triassic Moenkopi Formation are capped with late Tertiary basalt and all are tilted toward the Hurricane fault. This butte is at a major convex bend in the trace of the Hurricane fault; this is the approximate location of the State Line geometric bend and the site of field trip Stop 1-3. Immediately northeast of our overlook, the gravel road of the Navajo Trail can be traced up to the Hurricane escarpment, where it ascends the surface of a ruptured relay ramp between overlapping strands of the Hurricane fault. The Grandstand, seen south of the Navajo Trail, is a zone of multiple fault strands associated with a left stepover.

To the southeast, we can see the Moriah Knoll basalt where it flowed across the escarpment (figure 10). The Moriah Knoll volcano erupted this basalt on top of the escarpment; the basalt then flowed down a valley cut into the early escarpment, across several fault strands,
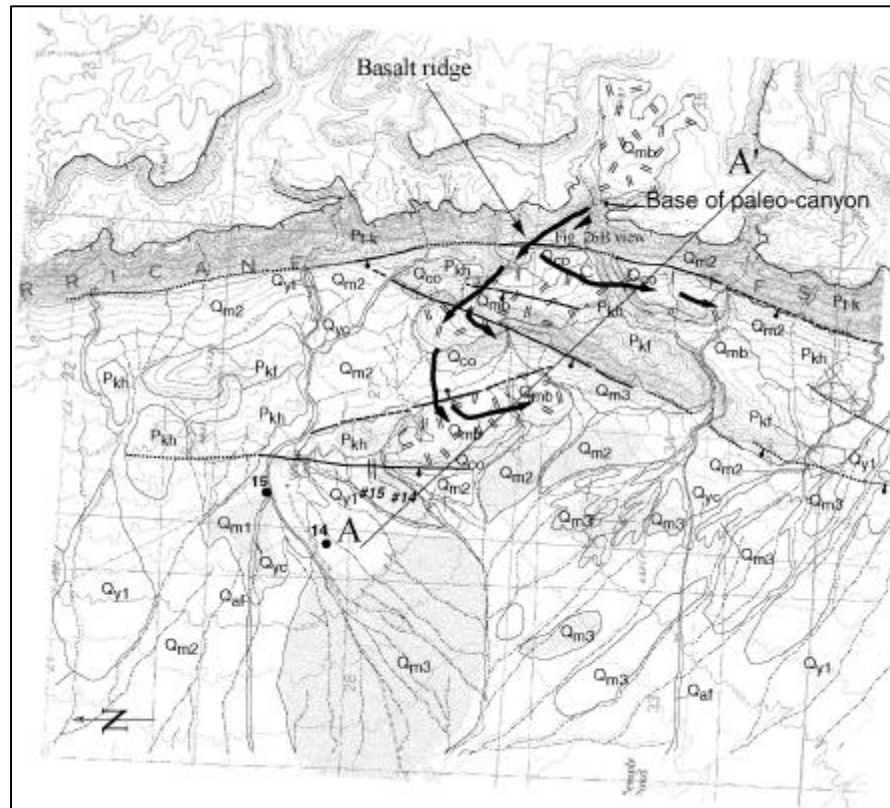

Figure 10. Geologic map showing the relation of the faults to the Moriah Knoll basalt flow (Amoroso and others, 2000). The basalt filled the space between the main escarpment and the Pkf ridge until the ridge was overtopped and the basalt flowed farther west. The basalt flow directions, estimated from flow thickness, are shown by heavy black arrows.

and onto the hanging wall. From map relations it appears that the basalt flowed south along a developing relay ramp, accumulated against the relay ramp ridge, over-topped the ramp to the west and flowed down onto the hanging wall (figure 11). Several fault strands have subsequently displaced the flow. We correlated various exposed remnants of the Moriah Knoll basalt across the fault using XRF geochemical correlation. A sample collected from the flow in a paleocanyon on the footwall gave a $^{40}Ar/^{39}Ar$ date of 0.83±0.06 Ma. Total displacement across the basalt is an estimated 200 meters, yielding a minimum long-term slip rate of about 0.24 mm/yr (Amoroso and others, 2002). We can see another convex portion of the fault far to the south at the basalt-capped mesas of Twin Butte, and to the west, Diamond Butte. These buttes preserve remnants of the easily eroded Moenkopi Formation on the hanging wall because of the resistant cap of late Tertiary basalt.
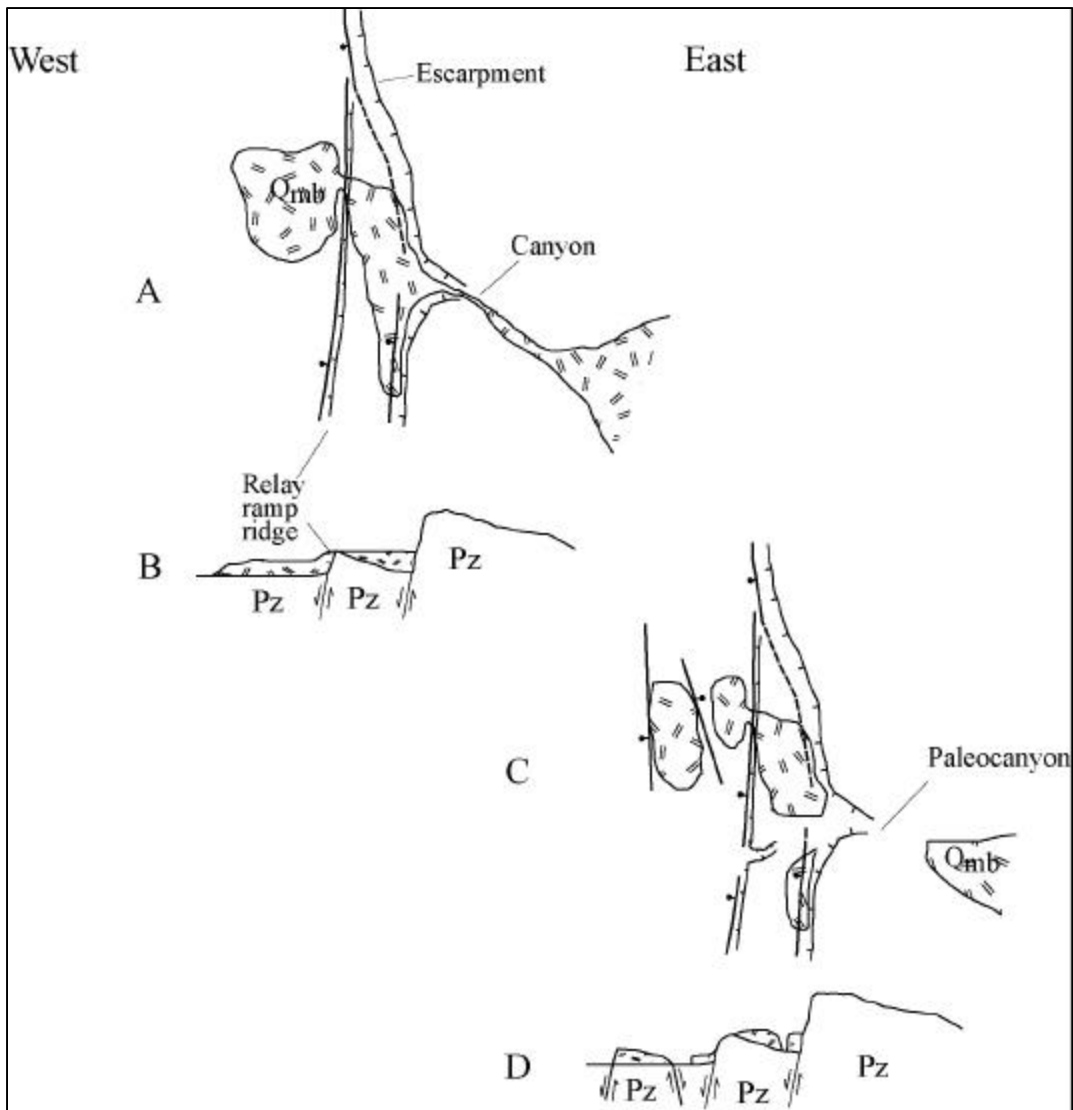
Figure 11. Sketches illustrating fault development history at the basalt flow. Faults are shown with stem and ball on downthrown side, dashed faults indicate possible lower displacement on the fault due to fault overlap. Teeth point down steep escarpment slopes. A) During emplacement of the basalt, the relay ramp must have dipped eastward to trap much of the basalt flow between the base of the escarpment and the relay ramp. B) East-west cross-section through A. Once sufficient basalt had been emplaced, the ridge was overtopped and the flow moved further west and ponded against the relay ramp. C) Basalt flow after being offset by several strands of the fault, and eroded from the paleocanyon. The western fault strands may have been present at time A/B but were not topographic barriers. D) The basalt between the ramp ridge and the escarpment has been incised by the present drainage, and both flow remnants west of the relay ramp are now tilted toward the east.

Changes in fault strike and escarpment height suggest that the Moriah Knoll basalt locale is another geometric boundary and might be a segment boundary. The fault strike changes from N20°E north of Twin Butte, to N15°W at the basalt locale; to N35°W south of the State Line geometric bend (figure 12). The escarpment is 470 meters high at the State Line geometric bend. To the south near Twin Butte, the escarpment is 450 meters high. The escarpment height is lowest (250 m) where the Moriah Knoll basalt crossed the fault zone. The faults seen in the fault development figure are rotational faults. The eastern fault shows increasing displacement to the north, and the fault to the west has increased displacement to the south (Billingsley, 1994a). We suggest that the minimum in escarpment height at the Moriah Knoll basalt is related to fault
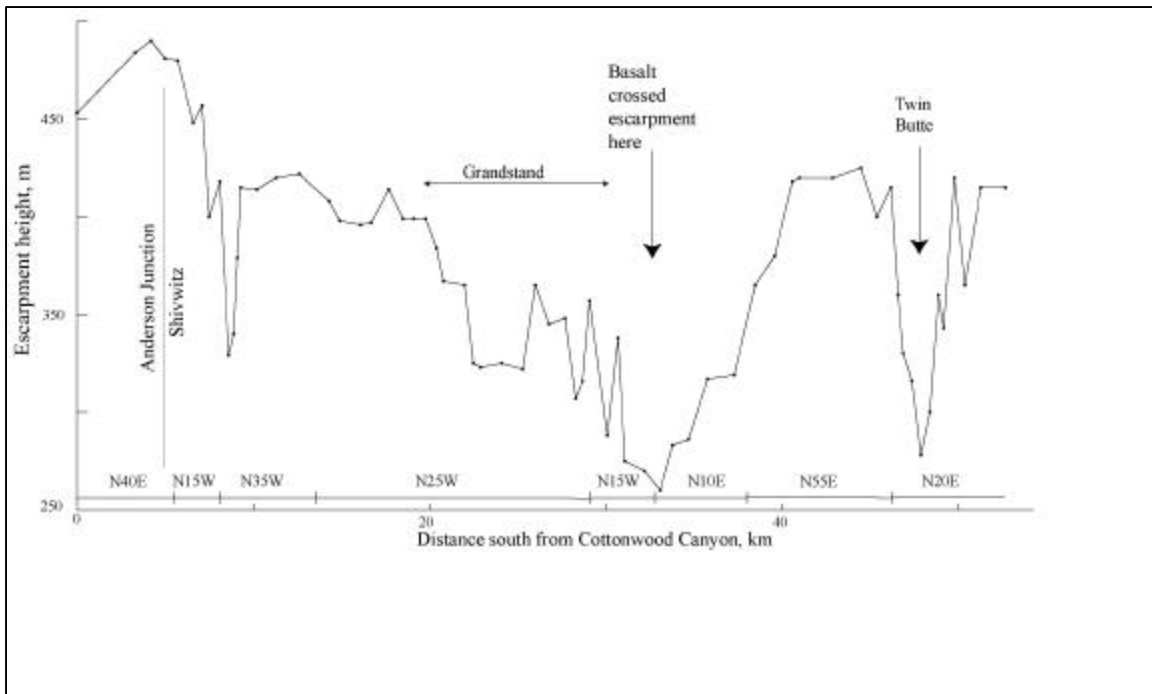

Figure 12. Variation in escarpment height along the Hurricane Cliffs for the Shivwitz section. The x-axis is the distance along the escarpment, and the strike of the Hurricane fault is shown at the bottom of the figure. The Shivwitz - Anderson Junction segment boundary is at kilometer 5, approximately where the fault strike changes 55 degrees. Note the broad decrease in elevation where the basalt crossed the escarpment is also where the fault strike changes 25 degrees. Differences in escarpment height reflect the general variation in total slip on the section.

geometry. The basalt flowed down the relay ramp between these faults where total displacement decreases and stress is distributed over several fault strands in the area (Zhang and others, 1991). The next stop, the Boulder Fan trench site, is another part of the fault where hard linking along the fault zone has isolated a smaller fault strand. Movement on this fault strand may have created a zone of weakness to form the embayment in the cliffs southeast of the Boulder Fan.

Return to the vehicles and proceed east on the Navajo Trail.

0.8 96.5 Rocks of the Moenkopi Formation crop out on the left side of the road here. These sediments filled a northeast-trending Triassic paleovalley (Billingsley, 1993d).

0.5	97.0	**Turn right** onto small dirt road. As we ascend a short incline, we are climbing onto older Quaternary fluvial deposits (Billingsley, 1993d) laid down by a stream that flowed northward in this valley along the Hurricane Cliffs.
0.4	97.4	The hummocky part of the Hurricane Cliffs at 11:00-12:00 is where the Moriah Knoll basalt flowed across the Hurricane fault zone. The Temple Trail traverses the Hurricane Cliffs on the Moriah Knoll basalt. Mormon pioneers constructed this trail to bring large Ponderosa pine logs from Mt. Trumbull to St. George, where they were used as roof beams in the construction of the Church of Latter Day Saints temple. The trail up the basalt flow is not passable by motor vehicles.
0.2	97.6	After we descend off of this low ridge to the south, we are driving on low terraces and the flood plain of a sizable, unnamed north-flowing tributary of Hurricane Wash.
0.9	98.7	Gate.
2.3	101.0	Another gate. Go right at Y intersection.
0.2	101.2	The Boulder Fan trench site is visible in the middle distance at 12:00. The large rockfall boulder on the fan is responsible for its name. Twin Butte is visible on the hanging wall of the Hurricane fault at 2:00.
0.3	101.5	A drilling rig is visible in the middle distance at 2:00. This is called the Dutchman Prospect, and it is being drilled into a surface anticline between the Hurricane and Sunshine fault zones. Potential source rocks are Paleozoic and Precambrian shales. Drilling began in 1998 using an old-fashioned cable tool rig. Because of hard drilling and lack of progress, the rig was converted to rotary drilling. As of mid-2001, the hole depth was about 3,200 feet.
1.0	102.5	Fault scarps along the base the Hurricane Cliffs are quite apparent at 11:00, especially when the sun is low in the sky. Alluvial fault scarps that record the past few faulting events are very common along the base of the cliffs from this area south to Twin Butte. These scarps are formed in steep late Quaternary alluvial fans or colluvial slope deposits composed of rather coarse, poorly sorted gravels. Morphologic analyses based on diffusion modeling suggest an early Holocene to late Pleistocene age for these fault scarps (Amoroso and others, 2002). The south-dipping Moriah Knoll basalt surface in the relay ramp is at 9:00. The basalt obviously flowed south along the relay ramp, but it also has likely been tilted southward because of increasing fault displacement to the south subsequent to its eruption.
0.5	103.0	Go through gate.
1.0	104.0	Boulder Fan and trench are in view at 11:00. The drainage cutting into the cliffs south of the Boulder Fan is the location of a secondary fault trace that continues for a few kilometers behind the main trace.
0.4	104.4	Proceed through gate at Merchant Tank. The U.S. Fish and Wildlife Service released a number of juvenile condors into the wild atop this section of the Hurricane Cliffs in 1999 as part of efforts to ensure the survival of this largest North American bird species. The birds remained in the area through most of 2000, but eventually flew off to join their colleagues in the eastern Grand Canyon area. It is rumored that they left either because the geology is more interesting or the pickings are better in Grand Canyon.

1.2	105.6	**Turn left** onto a dirt track, follow it toward Sheep Pockets Reservoir (a large stock tank), proceed around the tank to the left and follow the track up an increasingly steep alluvial fan to the base of the cliffs.
1.0	106.6	Park near the large boulder.

STOP 1-2. Boulder Fan trench. (Russell Spring 7.5' quadrangle, T37N, R9W, section 15).

This stop is near the apex of the Boulder Fan where we excavated a 70-meter-long trench across the Hurricane fault (figure 13). Topographic profiles across the fault scarp show 4 to 4.6 meters of far-field vertical surface displacement of the fan surface. Based on calibrated carbonate rind measurements, we estimate the age of the alluvial fan surface to be late
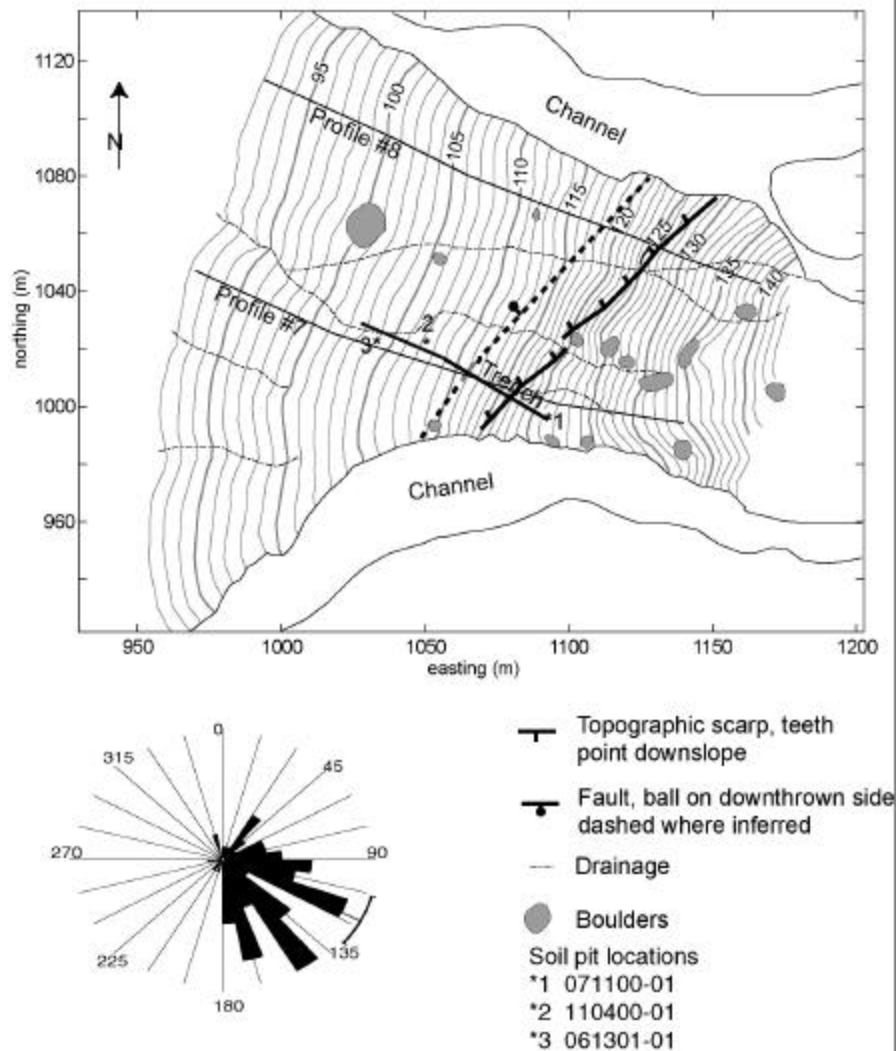

Figure 13. Detailed topographic map of the Boulder Fan, one-meter contour interval. The trench is on the southern part of the fan. The framework fluvial unit (Unit 5) seen in the trench was deposited in a back-tilted area on the hanging wall after the MRE. The results of 80 measurements of clast imbrication of Unit 5 indicate a source direction of 117° ±11° (95% confidence interval).

31

Pleistocene (15 to 75 ka; Amoroso and others, 2002). This trench revealed fairly complex stratigraphy in the hanging wall associated with fault deformation, rotation of strata adjacent to the fault, and erosion of the fault scarp. We believe there is solid evidence for two faulting events since deposition of the fan sediment; the youngest event occurred about 10 thousand years ago. Each faulting event involved at least 1.5 meters of surface displacement, suggesting that they were associated with large earthquakes that ruptured much or all of the Shivwitz segment of the Hurricane fault.

Trench Stratigraphy and Structure

     Deposits exposed in the trench record deformation in the past two faulting events and the erosion and deposition that occurred at the fault scarp in response to the faulting. Thus, we may use these deposits to interpret the recent history of the Hurricane fault at this site. The stratigraphy in the footwall consists of a series of ~0.5- to 3-meter-thick debris-flow deposits and minor framework gravels that are probably water-lain deposits (figure 14; see Amoroso and others [2002], for more complete discussion of the fault trench). The debris-flow materials are clayey to silty sand, pebbles, cobbles, and some boulders, primarily matrix supported. Stratigraphic relationships in the hanging wall are more complex. Beginning at the bottom, they consist of: (1) debris-flow deposits that we correlate with the uppermost strata exposed in the footwall (Unit 25), (2) a mystery unit against the fault zone (Unit 6) that probably is correlative with the debris-flow deposits of Unit 25, but might represent the oldest colluvial package derived from the fault scarp, (3) poorly sorted and weakly stratified colluvium derived from the fault scarp after the penultimate event (PUE; Unit 7), (4) a colluvial wedge derived from the scarp formed in the most-recent event (MRE; Unit 2), (5) a framework fluvial gravel also derived from the scarp after the MRE (Unit 5), and (6) a mantle of fine-grained slope colluvium that likely has a significant eolian component (Units 24 and 12).
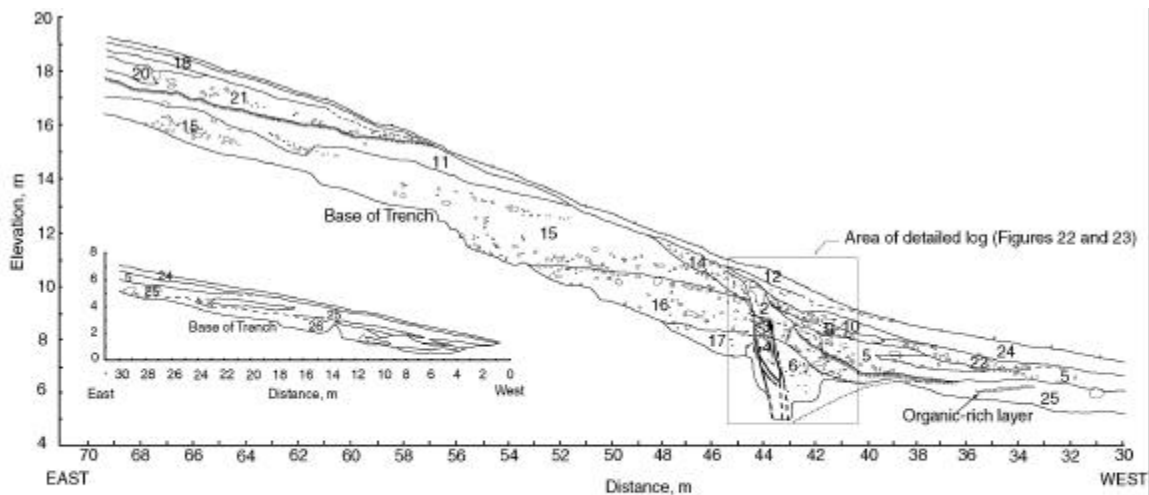
Figure 14. Log of the south wall of the Boulder fan trench. The lower portion of the trench is shown in the inset. Alluvial-fan deposits on the footwall consist of a series of debris flows with a thin veneer of slope-wash materials. Units adjacent to the fault in the hanging wall were derived from the degrading fault scarp; farther from the scarp, we observed pre-faulting fan deposits. Soil development on the surface of the penultimate wedge (Unit 7) appears to have obscured the basal contact with Unit 25. The buried soil zone in Unit 25 (between 34 and 36 m marks), and clast fabric of the eastern part of that unit (between 30 and 36 meter marks) show that these surfaces have tilted back toward the fault. We observed no antithetic faulting or tectonic fissures west of the fault zone.

     Structural relations of the fault zone shown in figure 15 are relatively subtle. The eastern fault is marked by weak shear fabric in Unit 17 against Unit 4 and by several rotated and broken

clasts. It appears to have experienced most of the movement during the MRE. The western bounding fault is clearly defined by shear fabric and an accumulation of additional soil carbonate low in the trench. The zone of cemented and sheared gravels between the faults may be a small graben that formed during the penultimate event. These faults were zones of preferential water infiltration suggested by the enhanced carbonate accumulation in Units 4 and 17, as well as roots of living plants that followed the fault zone to a depth of 4 meters below the ground surface. The western fault had an estimated 15-25 centimeters of movement in the MRE, based on the displacement of Unit 7A compared to Unit 7. Based on the limited upslope extent of the penultimate event (PUE) wedge (Units 7 and 7A), it is likely that most or all of the displacement in the PUE occurred on the western fault.
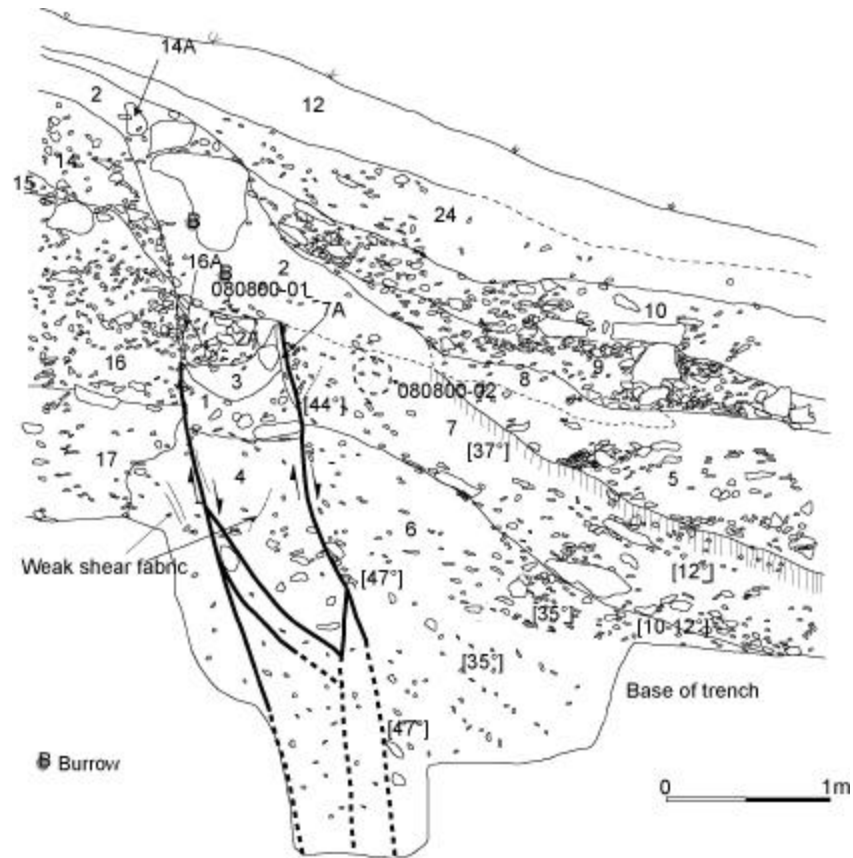
Figure 15. Detail of the fault zone in the Boulder Fan trench. We deepened the trench at the fault zone to further investigate the nature of the faulting and expose more of Unit 6. Unit 6 is depicted as a debris-flow unit that shows the effects of fault drag. Alternatively, Unit 6 may be evidence of a third event.

Most of the sediment exposed at the base of the scarp was deposited after the MRE (about 37 m^2 of the trench area; see table 2). The colluvial wedge associated with the MRE (Unit 2) was apparently deposited against an eroded free-face (Units 14 and 16 and on top of fissure-fill material (Units 2A and 3). The large boulder in Unit 2 probably fell during the MRE or was derived from degrading of the free-face immediately after the MRE. The basal contact of Unit 2 with the penultimate wedge (Unit 7) is locally indistinct, perhaps due to erosion of the top of the penultimate wedge. The upper stratigraphic units exposed in the hanging wall consist of framework gravels (Unit 5) that filled a trough along the base of the scarp, and a mantle of fine-grained material derived from the scarp. Closer to the scarp, Unit 5 appears to have been buried

33

below slope colluvium (Unit 24), a slump or debris flow (Unit 22), and fluvial deposits. Although the sedimentology of the framework gravels suggest that they might have been deposited by a stream flowing along the scarp, clast imbrication measurements show they were transported downslope across the fault (figure 13). A bulk sample from a fissure fill at the base of the most recent surface-faulting earthquake (MRE) colluvial wedge yielded 3 milligrams of unidentifiable charcoal and 2 milligrams of sagebrush charcoal. This sample was collected because such locations have been interpreted as providing the closest minimum limiting age of the rupture McCalpin and Nelson (1996). Lawrence Livermore National Laboratory (Center for Accelerator Mass Spectrometry, Livermore, CA) analyzed the organic material and reported a radiocarbon age of 9,910 ± 210 yr BP for the MRE. The corrected 2-σ calendar age of the sample is 8,870 to 10,370 cal B.P. This date is probably a reasonable age estimate for the MRE, as the dated material is rather delicate and it is likely that the fissure filled very soon after surface rupture.

Deposits associated with the PUE (Unit 7) are much less extensive than the MRE deposits. They consist primarily of matrix-supported, weakly stratified fault scarp colluvium that displays an increase in clast number and size downslope. McCalpin and others (1993) observed a similar change in the scarp derived colluvium fabric at the fault scarp produced by the 1983 Borah Peak earthquake, where they noted that proximal parts of the wedge are more matrix rich than the distal portion. Many of the larger clasts of Unit 7 are aligned with the long axis pointing downslope, and there is some imbrication of clasts in the medial and distal part of the wedge. Soil development at the top of Unit 7, manifested by enhanced soil carbonate and clay accumulation, implies a significant hiatus between the PUE and the MRE. The lower contact between Units 7 and 6 is clear, but the contact between Unit 7 and the pre-faulting fan surface (Unit 25) farther west is subtle and probably not completely exposed in the trench. A dark, slightly organic-rich horizon that may be a burned layer exists between the 34 and 36 meter marks (figures 14 and 16); it may be at the contact between Units 25 and 7, or it may be within Unit 25. Uncertainty regarding the base of Unit 7 leads to some uncertainty in the size of the colluvial wedge associated with the PUE (about 3.5 to 6 m^2 of the trench area).
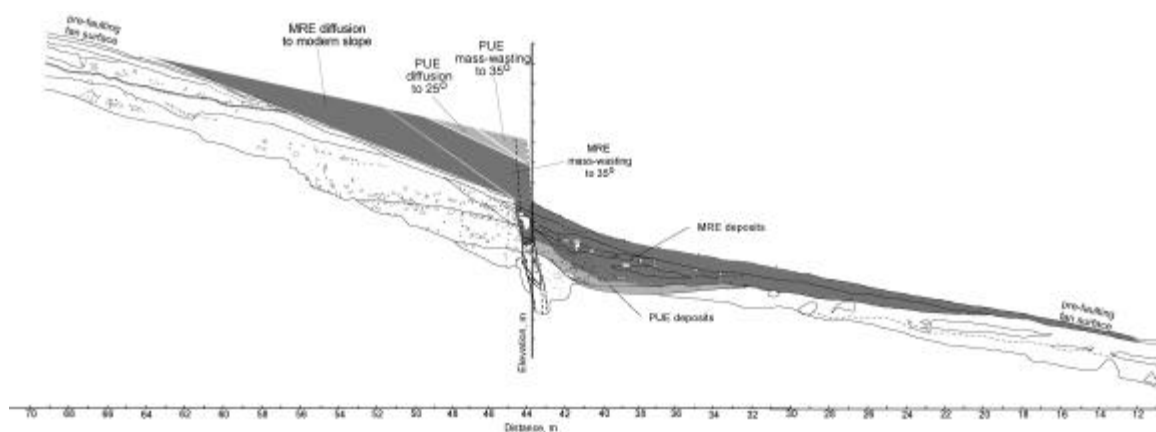
Figure 16. Trench log showing relations between scarp erosion and deposits observed in the Boulder Fan trench. Wedges on the footwall are approximations of the material eroded from the scarp after the PUE (light shading) and the MRE (dark shading). In this example, throw in the PUE and MRE was 2.5 and 3.5 meters, respectively. The same shading pattern shows the areas of deposits associated with the PUE and MRE interpreted from the trench log. The location of the base of the PUE wedge is uncertain and probably not completely exposed, and the near-surface horizon in the MRE wedge probably has a substantial eolian component. Nonetheless, there is a close correspondence between the areas eroded from the scarp and the actual observed deposits in this scenario.

Unit 6 is likely a debris-flow deposit that is correlative with Unit 25, but the possibility that it is a third colluvial wedge cannot be completely excluded. The clast fabric dip is somewhat less

34

than the penultimate wedge (Unit 7), which likely represents discordance between the dip of the original fan sediments and the overlying colluvial wedge as it accumulated. Support for correlation of Unit 6 with Unit 25 includes evidence of fewer clasts of 10 to 25 centimeters (long axis) in Unit 6 than in Unit 7. The depositional fabric of Unit 6 steepens from 35 degrees to 47 degrees near the fault; this is likely the result of normal fault drag. If Unit 6 is a colluvial wedge, it is at least 2 meters thick next to the fault as no obvious base to Unit 6 is exposed in the trench. Ostenaa (1984) observed in other trench investigations that colluvial wedge thickness was approximately half of the free-face height. The colluvial wedge interpretation for Unit 6 implies ~ 4 meters of throw across the fault zone in a possible third faulting event and at least 8 meters of cumulative throw at the fault zone since fan deposition. Rather sharp reverse-drag deformation of the hanging wall near the fault would be required to make space for the thick colluvial wedge. The principal problem with this interpretation is that the contact between Units 6 and 7 dips about 35 degrees to the west, and therefore cannot have been rotated to the east by any significant amount. Thus, all of the near-fault reverse drag occurred in the hypothetical first event, and none in the PUE or MRE. If Unit 6 is correlative with Unit 25, then this steep contact implies that fairly sharp normal drag exists immediately adjacent to the fault zone. This normal drag is superimposed on longer wavelength reverse drag to account for the decreasing dip of the top of Unit 25 between the 15- and 40-meter marks.

Paleoearthquake Scenarios

The fault-related stratigraphy in the trench provides some clues regarding the size and timing of the two surface ruptures that have occurred since deposition of the Boulder Fan. Immediately after a surface rupture, the fault scarp in alluvium erodes rapidly by processes of mass wasting until it reaches the angle of repose. Depending on the size of the scarp and the erodibility of scarp material, it might take decades to centuries to remove a scarp free-face (Wallace, 1977). The scarp subsequently erodes more slowly by diffusive slope processes (Nash, 1980; Hanks and others, 1984). We can estimate the amount of material eroded from the footwall by these processes in various displacement and scarp erosion scenarios using some simple graphical analyses. The fault zone marks the approximate transition between erosion and deposition on the scarp, so most or all of the material that is eroded from the footwall is deposited immediately downslope on the hanging wall, forming the fault-related deposits that we recognize in fault trenches. Using the trench log, we can compare predictions of the amount of material eroded from the footwall with the amount of material that has been deposited on the hanging wall.

We modeled several displacement scenarios to estimate the amount of material eroded from the upper half of the scarp in two faulting events (figure 16; see Amoroso and others, 2002, for more complete discussion of the modeling). All scenarios account for about 6 meters of total throw at the fault zone. In any reasonable scenario, erosion of the scarp to its modern form after the MRE generated a much larger wedge of colluvial deposits than erosion to a similar slope after the PUE. As the scarp crest migrates upslope on an existing fault scarp, a much larger slice of the footwall must be removed by erosion to decrease the scarp slope. This is consistent with our trench interpretation, in which the area of PUE deposits is 10 to 20 percent of the area of the MRE deposits (table 2). Moreover, the size of the PUE wedge indicates that displacement in the PUE could not have been any larger than the MRE. Something like 2.5 to 3 meters of throw in the PUE and subsequent erosion of the scarp to about 25 degrees predicts the size of Unit 7 quite well, and 3 to 3.5 meters of throw and erosion to the modern slope fits the size of post-Unit 7 deposits fairly well. There appears to be a modest excess of mass in the post-MRE deposits (~2 to 4 m^2), which may be the result of eolian input. The sizes of the PUE and MRE deposits can also be fit fairly well with a small PUE (2 meter throw) and a more eroded scarp (20°). In either case, it appears that the MRE was as large as or larger than the PUE.

Fairly large alluvial fault scarps are preserved intermittently along much of the Shivwitz segment, but this is the only locality where we have detailed information about the size and ages of young faulting events. The displacements we have inferred for paleoseismic events at the Boulder fan suggest that two large earthquakes occurred in the past few tens of thousands of years. Given the size of the surface displacements at the Boulder fan, it is reasonable that the earthquakes involved much of the entire Shivwitz segment. Morphologic analyses of fault scarps on the southern part of the Shivwitz segment suggest that this part of the segment ruptured in the

35

Table 2. Predicted and measured colluvial deposits for the Boulder Fan trench. All scenarios account for 6 meters of throw at the fault. "PUE erosion" refers to the scarp slope prior to the MRE. The amount of material eroded from the scarp after a faulting event is a function of throw in the event, the slope of the surface above the fault scarp, and how long the scarp is eroded. Measured wedge areas were determined from the trench log. The maximum area for the PUE was estimated using the dark organic layer as the base of the PUE colluvium and extrapolating beneath the floor of the trench. The maximum area for the MRE includes the fine-grained surface layer. Because the slope above the MRE scarp was greater than the original fan slope, much more material must have been eroded to achieve a 20 to 25 degree scarp slope. This resulted in the formation of a much larger colluvial package, which is consistent with what we observed in the trench. The amount of material deposited after the PUE (<6.5 m², excludes many of the displacement and erosion possibilities. Three displacement and erosion scenarios that fit the observed deposits in the trench are shown in bold font.

Modeled Erosion Scenarios					Measured Wedge Areas		
Scenario	PUE erosion	Event	Throw (m)	Wedge Area (m²)	Event	Min. Area (m²)	Max. Area (m²)
1	25°	**PUE**	**2.5**	**4.1**	PUE	3.5	6.5
		MRE	**3.5**	**36.1**			
2		**PUE**	**3.0**	**6.0**	MRE	22.5	37.9
		MRE	**3.0**	**34.5**			
3		PUE	3.5	7.9	Total	26.0	44.4
		MRE	2.5	32.1			
4	20°	PUE	3.5	13.9			
		MRE	2.5	27.0			
5		PUE	3.0	10.2			
		MRE	3.0	29.7			
6		PUE	2.5	7.3			
		MRE	3.5	33.0			
7		**PUE**	**2.0**	**4.5**			
		MRE	**4.0**	**35.5**			

latest Pleistocene or early Holocene, probably in the same event recorded in the trench (Amoroso and others, 2002). We know very little about the age of the MRE on the northern part of the Shivwitz segment, however. As we discussed at Stop 1-1, there is an extensive zone of fault complexity a few kilometers north of the Boulder Fan from the Moriah Knoll basalt to the Navajo Trail, and this is also an area of minimum escarpment height. These factors suggest that the Shivwitz segment could be further subdivided (see Menges and Pearthree, 1983) and that parts of the segment may rupture independently. At this time, the total length of the MRE on the Shivwitz segment is poorly constrained and we do not have sufficient evidence to evaluate the long-term seismologic behavior of the segment.

Return back the way you came in, turn right onto main track and retrace your path north to the Navajo Trail. We will now be driving along the Shivwitz segment of the Hurricane fault for about 15 miles.

3.3	109.9	Take main left road at small Y intersection.
0.3	110.2	Gate.
0.6	110.8	Bear right at road junction.
1.4	112.2	Bear left at road junction.
0.1	112.3	Gate. Continue straight ahead.
3.8	116.1	**Bear right at Y intersection** onto graded gravel road. You are now on the Navajo Trail.
0.3	116.4	**Turn left** off the Navajo Trail onto smaller road (Temple Trail). We are now on a thin Pleistocene alluvial deposit over the Moenkopi Formation. If the lighting is right, you should be able to see late Quaternary fault scarps along the base of the Hurricane Cliffs as we descend toward the valley bottom. Fault scarps are particularly apparent on steep alluvial fans below the prominent notch or wind gap in the top of the cliffs north of the Navajo Trail. Scarps just north of the small drainage that comes down from the wind gap are as much as 25 meters high, but because the fan slopes are so steep, surface displacements are more like 7 to 10 meters (figure 17).
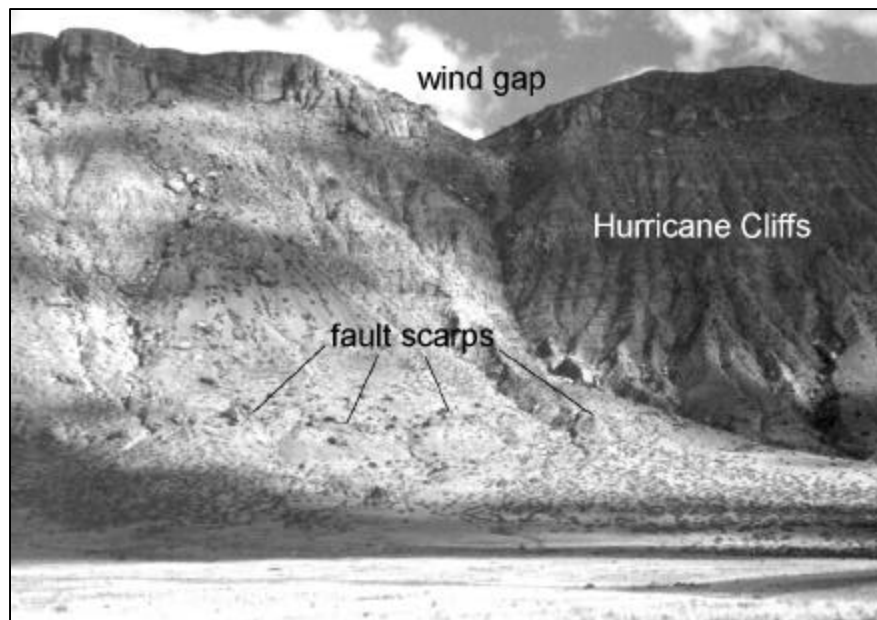
Figure 17. Photo showing fault scarps at the base of the Hurricane Cliffs north of the Navajo Trail. Scarps in the sunlight are as much as 25 meters high, but because of the steep far-field slopes, surface displacement is about 10 meters.

1.1	117.5	For the next few miles, we will chiefly be on Holocene valley bottom deposits and distal alluvial-fan deposits. Slightly higher areas are covered with relict valley-floor deposits that are likely Pleistocene in age. Bedrock exposures along the wash are the lower and middle members of the Moenkopi Formation, including

the relatively resistant Virgin Limestone Member (Billingsley, 1992a). The Toroweap and Kaibab Formations crop out in the Hurricane Cliffs to the east. The Kaibab Formation crops out in hills to the west. There is a nice view of some of the structural complexity of the Hurricane fault zone in the Navajo Trail area at 2:00.

1.0   118.5   Units dipping east into the Hurricane fault in a rollover monocline are evident at 1:00.

0.6   119.1   Pass through gate. At 12:00 we can see the apex of the State Line geometric bend; the back-tilted Hurricane Wash basalt is visible to the left (W).

1.4   120.5   Continue straight at Y intersection.

0.7   121.2   Fairly sharp east dip of beds of the Harrisburg Member of the Kaibab Formation in a rollover monocline is visible at 12:00-1:00.

0.7   121.9   Light-colored scars on the Hurricane Cliffs at 3:00-4:00 indicate locations of recent debris flows. Bouldery debris-flow lobes and levees are very common on Holocene fans along the Hurricane Cliffs, so debris flows are obviously a very important mechanism for moving material from the cliffs onto the adjacent piedmont.

0.2   122.1   At this point we begin to see deep arroyos that have formed along Hurricane Wash. Arroyos typically have fairly flat bottoms and nearly vertical sides as they initially develop. Arroyos propagate upstream through a series of headcuts (essentially waterfalls) where flow is concentrated and pours into the arroyos. During floods, headcuts may migrate hundreds of meters upstream. As arroyos mature, they become wider and eventually the sides become less steep. Similar arroyos have formed in many places in the Southwest in the past 120 years or so. As in the situation we see here, arroyos typically have formed where valley bottoms were covered with relatively fine sediment and channels were small and discontinuous. Concentration of flow in these areas by natural or anthropogenic causes, combined with floods, caused accelerated erosion of the fine valley bottom fill. The steep walls and headcuts in this system indicate that it is actively eroding upstream in the modern valley bottom. We will be following (and avoiding) this arroyo system for the next several kilometers.

0.2   122.3   As was noted earlier, strata of the Kaibab Formation are tilted unusually steeply toward the Hurricane fault in a rollover monocline at 9:00-10:00. Just to the north, this monocline is probably faulted (Billingsley, 1992b).

0.5   122.8   Coarse, fresh deposits on a tributary alluvial fan cross the road here. These deposits may represent the distal end of a debris flow that began on the Hurricane Cliffs.

0.1   122.9   Gate. The arroyo is about 30 meters to the west; to the east, steep alluvial/colluvial deposits are evident along the lower part of the Hurricane Cliffs.

0.5   123.4   Temple Trail sign. The Temple Trail followed the valley bottom from the Moriah Knoll basalt to Black Rock Canyon to the north.

1.4   124.8   **Keep right** and stay on Temple Trail. The left fork joins the Sunshine Trail, which may eventually be followed to St. George, Utah.

0.8   125.6   Headcut on a tributary wash is next to road. **Bear right**.

0.3	125.9	Numerous small arroyos to the right of the road. The road is migrating to the west to avoid the headcuts. At the base of the Hurricane Cliffs you can see steep alluvial fans and colluvial slopes with fairly large, eroded fault scarps developed on them.
0.2	126.1	Cross a sizable tributary wash.
0.2	126.3	Shinarump Conglomerate, at the base of the Triassic Chinle Formation, crops out on the left side of the road here.
0.2	126.5	The track formerly followed the left (west) bank of Hurricane Wash through this area, but it was washed out in the late 1980s. The track now crosses Hurricane Wash several times and circumvents the washed out stretch by traversing dissected alluvial fans on the east side of the wash. The next several kilometers of the route are rough and steep – 4-wheel drive is strongly recommended. See, you thought I was kidding about Arizona's rough roads.
0.5	127.0	Bear left at fork.
0.2	127.2	Cross Hurricane Wash. You are now back on the "road" that has existed for many decades. It climbs to a bench on the Hurricane Wash basalt, which has recently been dated at 5.2 ± 0.15 (Ar/Ar; Downing and others, 2001). The road has not been maintained very recently and is steep and rough.
3.3	128.3	Park just beyond the gate. Walk to top of knoll to the north.

STOP 1-3. State Line Bend. (Rock Canyon 7.5' quadrangle, T41N, R10W, section 34).

At this stop, we are standing on Quaternary basalt near the apex of the State Line geometric bend, a relatively abrupt bend in the trace of the Hurricane fault. This salient parallels the visible bend in the cliffs, which lie to the east and south. (figure 18). The State Line geometric bend lies between the Shivwits geometric segment to the south and the Anderson Junction geometric segment to the north. The Hurricane Cliffs form the fault-line scarp on the footwall of the fault. The butte to the northwest is East Mesa.

The Paleozoic units exposed in the cliff near here lie in the footwall. Recognition and identification of these units is critical in determining the total stratigraphic separation on the fault segments north and south of this bend as well as at the bend. The units are, from lowest to highest, the Permian Esplanade Sandstone, which is a red, white, or tan sandstone near the base of the cliffs; the Permian Hermit Shale, which is a red, brown, and white siltstone to sandstone; the Permian Toroweap Formation, which contains three members: a lower unit of interbedded gray, yellow, and brown sandstone, siltstone, and dolomite (Seligman Member); a middle gray limestone cliff (Brady Canyon Member); and an upper gypsiferous unit of gray siltstone and light-red siltstone to sandstone (Woods Ranch Member); and near the top of the cliffs, the Permian Kaibab Formation with a lower gray cherty limestone (Fossil Mountain Member) and an upper red and gray unit of interbedded limestone, sandstone, and siltstone with white gypsum. More complete descriptions of these units are available with the quadrangle map for this area (Billingsley and Workman, 2000) and in Sorauf and Billingsley (1991).

We interpret the State Line geometric bend as the zone of linkage between the Shivwits and Anderson Junction geometric segments for several reasons. (1) The general fault strike changes across the State Line geometric bend. Just south of the bend, the Shivwits segment strikes ~N30°W. Just to the north of the bend, the Anderson Junction segment strikes ~N25°E. (2) The number of fault strands in the two segments differs. The Shivwits segment, just to the south, contains several fault strands exposed in both the bedrock footwall and the Quaternary deposits. Several of these faults appear to link and form relay ramps, evidence of strain transfer.
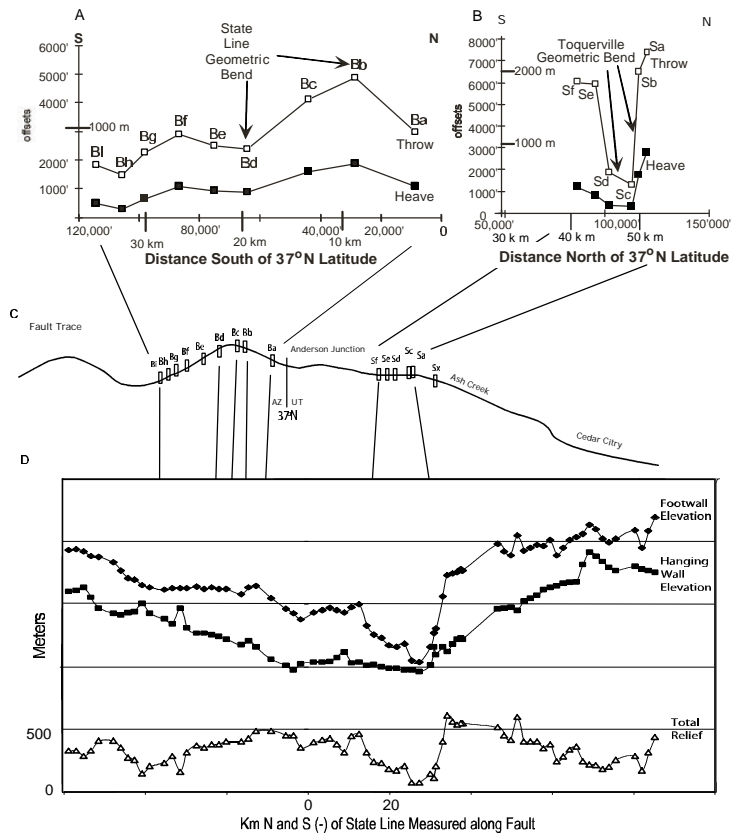
Figure 18. This figure summarizes the relations between changes in fault geometry, total displacement and elevation along the Hurricane fault from the Mt. Trumbull bend (salient) to the southern part of the Cedar City segment. (A) Displacement (offset) vs. distance graph along the State Line geometric bend. Note that the pattern most closely resembles that of fault capture (cf. Figure 5). (B) Displacement (offset) vs. distance graph along the Toquerville geometric bend. Note that the pattern most closely resembles that of linkage of underlapping faults (cf. Figure 5). (C) Map of the trace of the Hurricane fault. The salients at the State Line and Toquerville geometric bends are of different shapes and widths (measured normal to the general fault strike). The width probably reflects the original spacing between the linked faults. (D) Graph of distance vs. relief, footwall elevation and hanging wall elevation. Note that the changes in elevation mimic the changes in displacement at the State Line and Toquerville bends. Elevation may serve as a proxy for the total displacement pattern in locations where total offset cannot be determined.

In contrast, the Anderson Junction segment is more structurally simple. To the north, the Anderson Junction segment, contains one main strand near the Hurricane Cliffs with a few young scarps exposed in the Quaternary deposits. The few footwall faults present in the southern Anderson Junction segment have relatively minor offset and limited length. (3) The numbers and orientations of minor faults and folds also change at the bend (Billingsley and Workman, 2000). (4) The total displacement changes around the bend (figure 18). A minimum in total displacement exists slightly south of the bend apex. This pattern is consistent with that created by linked faults where the northern fault propagated more quickly than the southern fault and eventually captured the southern fault (figure 5). We can see an artifact of this displacement change in the elevation of the Triassic Chinle Formation in the hanging wall relative to the Paleozoic units in the footwall (described below). The elevation of the Chinle Formation is higher near the apex of the salient than along the fault sections to the north and south, which

40

corresponds to a decrease in stratigraphic separation at the bend. These multiple data sets allow us to interpret that the Anderson Junction and Shivwits segments linked by fault capture.

In cases where a large amount of the total slip occurred at a linkage zone after linkage, the fault may be driven by the release of elastic strain to increase slip rates at the bend. This process would effectively erase the displacement minimum near a linkage site. Because the displacement minimum still exists at the State Line geometric bend, it appears that the largest percentage of the slip at this bend took place prior to linkage. However, the Hurricane fault is a through-going fault in this area, which indicates that there was some post-linkage slip at the bend.

Another displacement minimum in the displacement-distance profile occurs along the Shivwits segment (figure 18) several miles south of the State Line geometric bend. Near this displacement minimum, the number of apparent fault strands and splays decreases and the displacement plateau slopes. A slope in the plateau suggests that a displacement gradient existed along the captured fault. However, it is also possible that the gradient formed during post-linkage slip. This minimum may reflect linkage of a smaller fault within the segment, displacement transfer via relay ramps containing folds, or post-linkage slip.

Various Quaternary deposits crop out along the base of the Hurricane Cliffs and in the fault's hanging wall. These deposits lack preserved fault scarps near the apex of the bend, but they, or similar deposits, are faulted north and south of the bend. These sedimentary deposits include small alluvial fans, talus, alluvium, landslide deposits, colluvium, and gravel terraces largely in the hanging wall. Many of these deposits are the debris-slope and wash-slope facies associated with the degradation of the Hurricane fault escarpment.

Quaternary igneous rocks include mafic lava flows and a small pluton that intrudes them. The hill to the west consists of mafic extrusive rocks and contains at least four distinct flows that are separated by agglomerates. The flows are fine grained and contain varying amounts of plagioclase and olivine phenocrysts.

Two flows from the basalt field in this area are dated. One sample is from East Mesa a few kilometers to the northwest at 36.9^{o}N, 113.363^{o}W. This flow cascaded over the boundary fault of a graben within the basalt field (Downing and others, 2001). The graben is in the hanging wall of the Hurricane fault. Based on ^{40}Ar/^{39}Ar dating, the basalt is 5.16 $\pm$ 0.14 Ma (Downing and others, 2001). However, this date represents a total gas age because the data lacked both a plateau and an isochron. Wenrich and others (1995) dated a second sample from East Mesa located at 36.902^{o}N, 113.417^{o}W. That sample yielded a date of 1.4 + 0.25 Ma using the K/Ar method.

Walk along the road to the south and then cross the wash on the east toward the mafic rocks that lie near the fault. The vertical columnar joints are associated with the pluton. This intrusion may plug a volcanic vent that was the source for some of the basalt flows in this region. The pluton or plug also has plagioclase and olivine phenocrysts, but is granular and coarser grained than the flows. Maureen Stuart (unpublished data from UNLV XRF laboratory, 1995) analyzed samples from the four flows and the plug for major and trace element contents; they are all subalkaline tholeiitic basalt. ^{40}Ar/^{39}Ar dating of this intrusion is in progress. Because of erosion along the east side of the intrusion, the timing of intrusion emplacement relative to movement along the Hurricane fault is equivocal. However, some flow directions in the basalt to the west are toward the east-southeast (and the Hurricane Cliffs) and no basalt crops out on the footwall directly to the east. This relationship suggests that at least some of the fault escarpment existed prior to eruption of the basalt flows and that the basalt flowed toward a topographic low along the fault.

Proceed north along dirt road.

0.7   129.0   Rocks of the Kaibab Formation crop out at 1:30-2:00 in front of the main escarpment across Hurricane Wash. The lower part of the main escarpment consists of the Toroweap Formation. This Kaibab block was probably displaced down-to-the-west by a minor fault or a landslide off of the cliffs.

1.0   130.0   We are driving over a fairly extensive, relatively young terrace of Hurricane Wash.

0.1	130.1	Drive up onto a Pleistocene terrace of Hurricane Wash.
0.1	130.2	Intersection with a power line road. Continue straight north.
0.4	130.6	We are driving near the interface between alluvial fans deposited by tributary drainages that head on the cliffs and a relict Pleistocene terrace of Hurricane Wash.
0.4	131.0	Gate.
0.2	131.2	Bear right.
0.5	131.7	Park on the side of the road and walk to left (west) of road ~35 meters to the top of a low hill. The hill is the eroded remnant of a Pleistocene terrace of Hurricane Wash. To the northeast along the Hurricane Cliffs, we can see a zone of multiple faults and structural complexity where the Honeymoon Trail ascends the cliffs. Farther to the north, we can see a relatively young Quaternary basalt that was erupted on the footwall and cascaded over the escarpment. The large canyon to the east-southeast is Cottonwood Canyon.
		Turnoff to right and follow rough, winding track if you want to drive up to the mouth of Cottonwood Canyon (0.7 miles each way).

STOP 1-4. Cottonwood Canyon Trench Site Overlook (Rock Canyon 7.5' quadrangle, T41N, R10W, section 14)

At this stop about 6 kilometers south of the Utah/Arizona border we will view the mouth of Cottonwood Canyon, where Cottonwood Wash has incised through the Hurricane Cliffs. Near the mouth of this canyon, the late Quaternary activity of the Hurricane fault is beautifully recorded in a stair-step sequence of fault scarps formed in different-aged alluvial fans and terraces (figure 19). The alluvial surfaces are each remnants of deposits that were graded to a unique base level during the late Quaternary period. The Hurricane fault displaces five of these surfaces by increasing amounts with increased surface age; the larger fault scarps record multiple rupture events during the late Quaternary. In addition to the larger fault scarps, there is a low fault scarp that records the displacement during the MRE along this part of the fault, which probably occurred between 8 and 15 thousand years ago. We calculated a preferred late Quaternary slip rate of 0.15-0.3 mm/yr (18.5-20 m in 70-125 kyr) for this area of the Hurricane fault. This slip rate is based on displacements measured from topographic profiles across the fault scarps and estimates of surface ages from the qualitative assessment of soil development (primarily assessing carbonate development) and geomorphic profile modeling of a fault scarp to estimate the time over which it formed.

Faulted and Unfaulted Alluvial Surfaces

We identified several young, unfaulted terraces at the mouth of Cottonwood Canyon and five faulted alluvial surfaces south of Cottonwood Wash. These units are differentiated by: (1) the relative elevation of the upthrown portion of the unit above adjacent active stream channels, (2) soil development, (3) the presence of undulations and degree of dissection into their surfaces, and (4) fault scarp height. The degree of soil development increases with increasing unit elevation. Figure 20 is a topographic map of the Cottonwood Canyon mouth area and displays the spatial relations between four of the units.

Soil-profile development provides the basis for estimating the ages of the faulted units in this area. We examined the soils developed on surfaces Q3, Q2, Q1, and Q0 (figure 20). We found that surface Q3 has stage III carbonate morphology (Birkeland, 1984), Q2 has stage II morphology, Q1 has stage I morphology, and Q0 also has stage I morphology, but shows less development than surface Q1. Based on these carbonate morphologies, and comparing them and other soil characteristics (soil structure, color) to soils of the Desert Project in New Mexico,
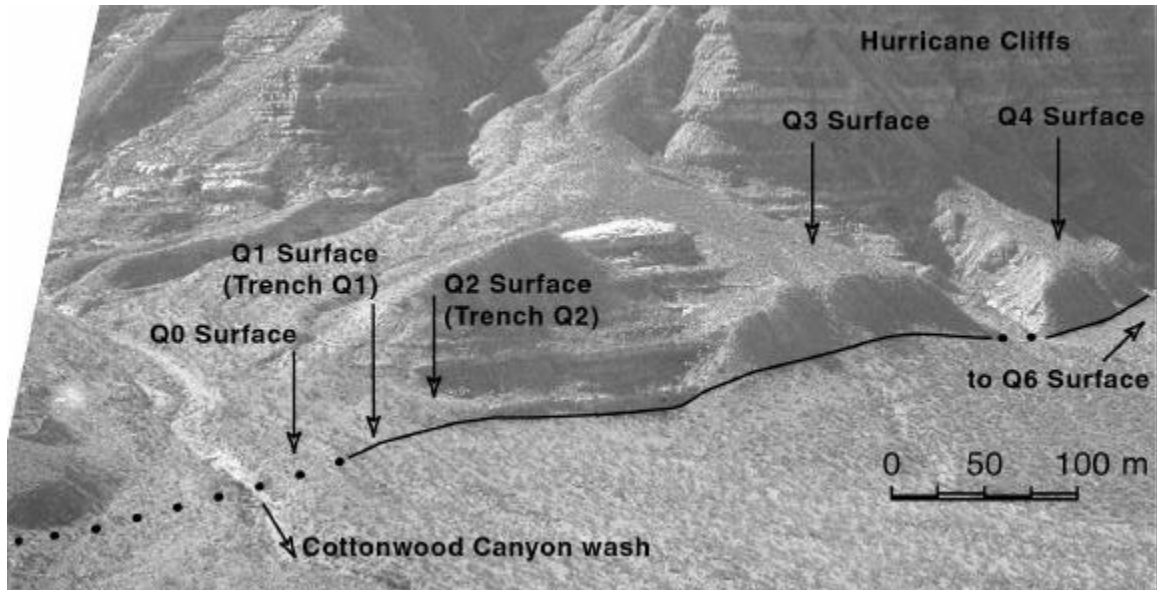
Figure 19. Oblique aerial photograph of the mouth of Cottonwood Canyon looking southeast.

where the soils have developed in a similar climate and have estimated numerical ages (Gile and Grossman, 1979; Gile, 1994), we estimate the surface ages as follows: Q3 at 70-125 ka, Q2 at 20-50 ka, Q1 at 8-15 ka, and Q0 at 2-6 ka. To the south of surface Q3 is another faulted alluvial fan, Q4. We interpret Q4 to be intermediate in age between Q2 and Q3 based on its relative elevation. Farther south along the fault, is a steep colluvial landform, surface Q6. The Q6 colluvial apron grades to about the same elevation as Q3 and has recorded the same displacement as Q3, so we interpret it to be of similar age as surface Q3. Geomorphic profile modeling of the Q6 landform, using the technique described in Hanks (2000), yields results consistent with a conservative formation age of 70-210 thousand years for the scarp.

We estimated the vertical displacement across the Hurricane fault for the five faulted alluvial surfaces near Cottonwood Canyon from topographic profiles and from trench exposures of two of the surfaces. Surface Q6 and Q3 record 18.5-20 meters of vertical displacement. The downthrown equivalent of the Q4 surface has been buried by younger material so the 10-meter displacement measured for it is a minimum. The downthrown equivalent of surface Q2 has also been buried by younger material (of ~Q1 age) by more than 2 meters, as observed in a trench exposure, yielding a minimum net displacement of 7 meters for the surface. Fault displacement of the Q1 terrace surface is less than 1 meter.

Fault Trenches

A 14-meter-long trench across surface Q1 exposed the deformation resulting from the MRE at Cottonwood Canyon (figure 21). Two fault strands reach to within 10-25 centimeters of the surface, displacing unconsolidated fluvial gravel and debris-flow deposits 37 centimeters down-to-the-west. Hanging-wall fault drag accommodates additional deformation, to yield a total of 58-60 centimeters of net vertical displacement across the 2-meter-wide fault and deformation zone.

A silt-dominated deposit of debris-flow, fluvial overbank, or eolian origin caps the Q1 terrace surface and is the youngest unit exposed in the trench (Unit 5) (see Stenner and others, 1999, for detailed descriptions of trench units). Unit 5, from 10- to 50-centimeters-thick, is about twice as thick on the hanging wall side of the fault zone. Unit 5 was either (1) deposited after MRE faulting and the increased hanging-wall thickness is a result of increased deposition at the base of the MRE scarp, (2) deposited before the MRE, faulted, and then reworked across the

43

UNITS:

Qac1   Holocene active channel deposit
Qac2   Holocene channel deposit, active during flood
Q0   Holocene stream and debris flow deposits of similar age, undifferentiated
Q1   Holocene-late Pleistocene stream and debris flow deposit,
          displaced 0.6 m by fault
Q1a   Holocene-late Pleistocene alluvium derived from Pz unit above
Qs   Fault scarp colluvium
Q2   Quaternary stream and debris flow deposit,
          displaced > 5-7 m by fault
Q2b   Quaternary stream and debris flow deposit
Q3   Quaternary alluvial fan deposit,
          displaced 18.5-20 m by fault
Q4   Older alluvial fan deposit
Qc   Hillslope colluvium
Pz   Paleozoic bedrock

×   soil pit
╲   trench
       normal fault.
       bar and ball on
       downthrown side,
       dotted where covered

Contour Interval one meter
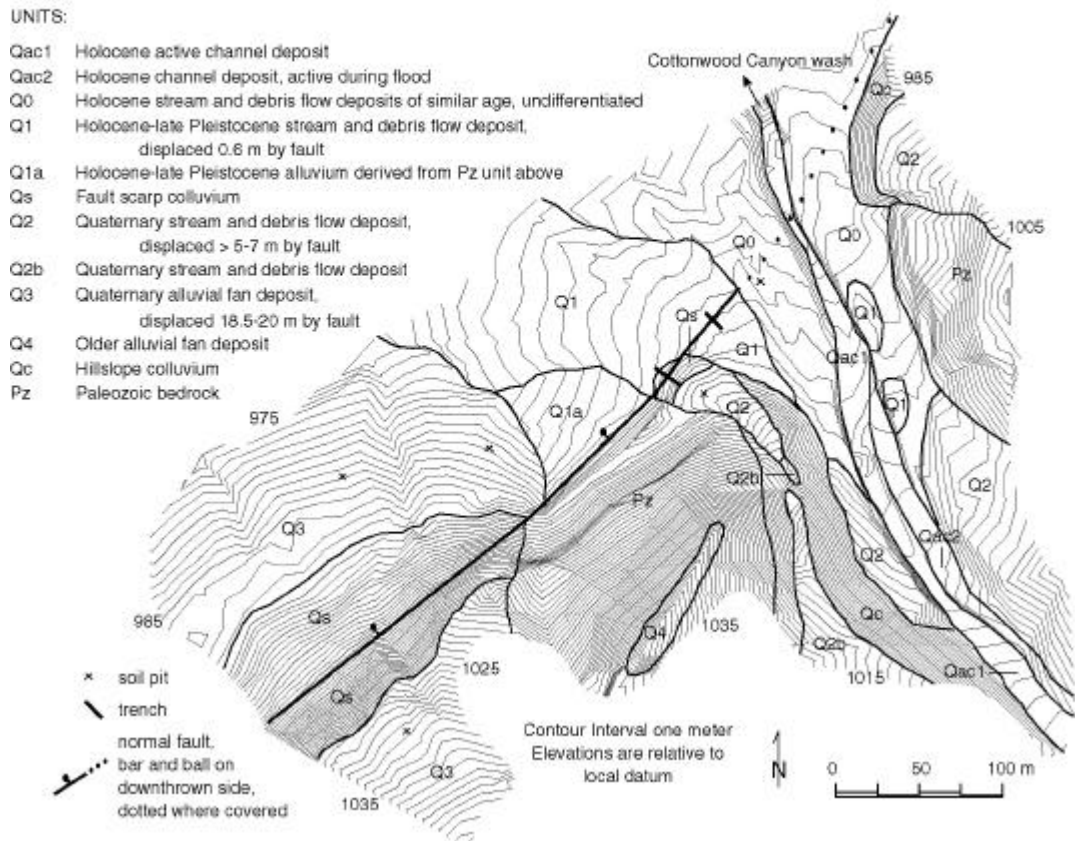Elevations are relative to
local datum

Figure 20. Detailed topographic and geologic map of the south side of Cottonwood Canyon. Increasing displacement of older surfaces is evident. Trenches are in units Q1 and Q2.

scarp to accumulate at the base, or (3) is eolian, and the oldest part of the unit is faulted with deposition continuing to accumulate more thickly in the swale formed against the scarp. The lower contact of Unit 5 does not have distinct displacement steps across the fault strands, suggesting that erosion began smoothing out the rupture topography before deposition of the uppermost unit. Alternatively, the lower contact of Unit 5 could be faulted, a possibility if displacement across the northwestern strand of the fault zone was distributed instead of discrete, and if the discrete displacement across the southeastern fault strand was obscured due to the presence of two large cobbles at the Unit 4/5 contact. A sub-vertical fabric observed in the lower part of Unit 5, above the fault strands, is consistent with the unit either being faulted or that post-event settling occurred above the fault zone subsequent to deposition. We believe that Unit 5 most likely post-dates the MRE.

Unit 4 is a poorly sorted, debris-flow gravel displaced by faulting. The 20- to 50-centimeter-thick, matrix-supported Unit 4 does not appear to have developed a significant soil before deposition of Unit 5, and we use the lack of a buried soil horizon to conclude that the time between deposition of Units 4 and 5 was possibly hundreds of years but not likely thousands of years. The three units underlying Unit 4 all show the same amount of vertical displacement across the fault zone, indicating that they have experienced the same faulting history.

44

Cottonwood Canyon Q1 Trench Log
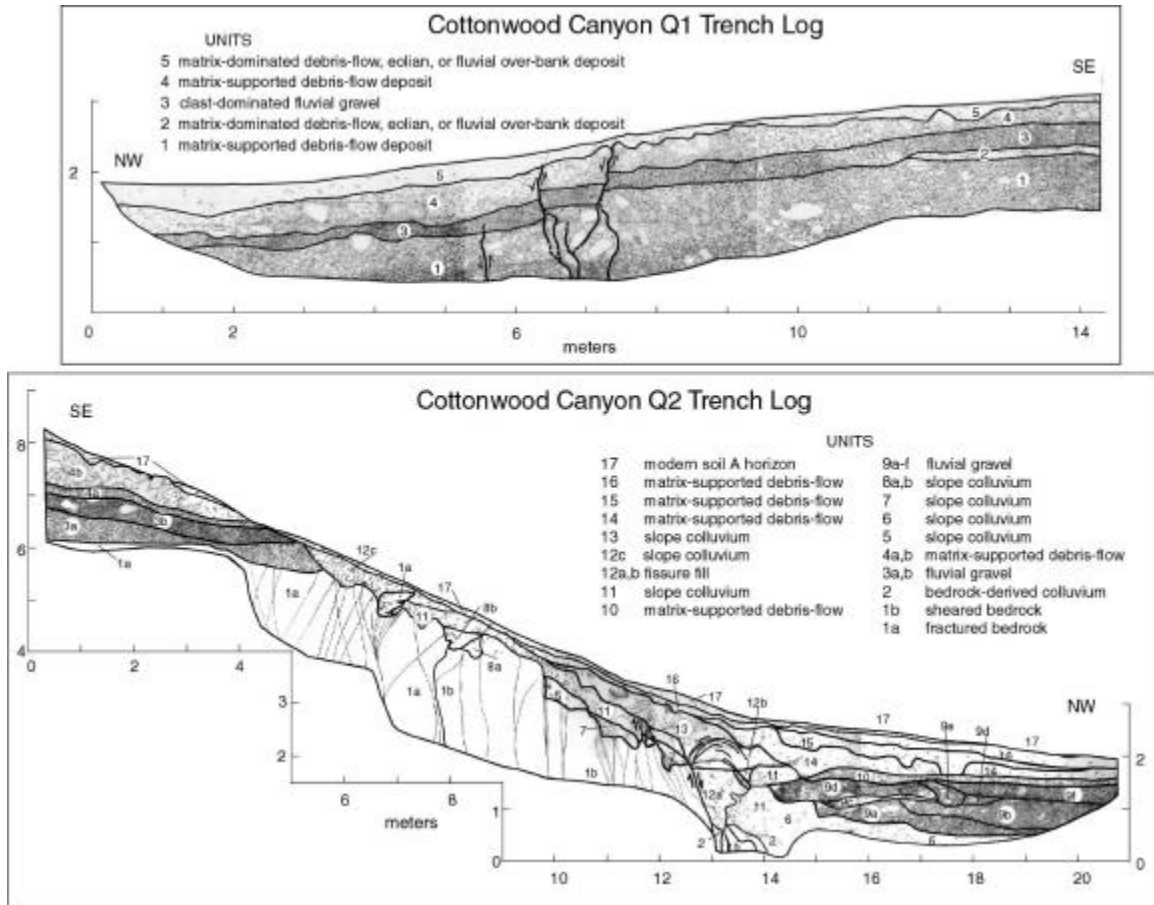
Cottonwood Canyon Q2 Trench Log

Figure 21. Logs for the trenches at Cottonwood Canyon. We found evidence for a single faulting event involving about 0.6 meters of vertical displacement in the Q1 trench. We concluded that the Q2 trench did not expose units in the hanging wall that are equivalent to the alluvial units in the footwall. The Q2 terrace surface has likely been buried on the hanging wall indicating a displacement of at least 7 meters.

A second trench exposed faulting through the 5-meter-high scarp in the Q2 surface, about 25 meters southwest of the Q1 trench (figure 20). The trench revealed a 9-meter-wide zone of faulting in Paleozoic bedrock and overlying fluvial and debris-flow alluvium and colluvial units (figure 21). Deformation from the MRE, as seen in the Q2 trench, produced a 1-meter-wide fissure at the interface between bedrock and alluvium. We believe the top of Unit 11 was likely the ground surface at the time of the MRE, based on a fault strand that terminates at the contact between Units 11 and 13 and stratigraphic relations above the fissure (figure 21). Unit 11 is a matrix-dominated deposit present only on the cumulative fault scarp, and is likely colluvium deposited as the scarp eroded. We correlated Unit 11 across the MRE fissure, but at that location the unit lies in a convex-down part of the scarp, which together with the unit's limited extent, makes measurement of net vertical displacement by projecting the unit across the fault imprecise. We believe the net displacement recorded in the Q1 trench to be more robust, but we estimate that the MRE resulted in approximately 0.35-1.15 meters of net displacement on the Q2 fault scarp. We established the Q2 measurement by projecting the lower contact of Unit 11 across the MRE fissure and across steps in the contact along the cumulative scarp to the east (figure 21). One such step in Unit 11 is 3-4 meters east of the fissure, with a maximum possible MRE vertical slip of 0.8 meters. Unit 13, a matrix-dominated sandy silt colluvium, lies down-

slope from this step. Unit 13 is similar in grain size and texture with the fissure-fill material (Unit 12a), and together they form a colluvial package of material eroded from the fault scarp and re-deposited in the fissure and across the lower scarp. Not all of the Unit 13 material necessarily came from MRE-formed scarp(s), but may also have come from other units higher in the cumulative scarp that eroded after the MRE in a continual process to smooth out the 5-meter-high fault scarp. Arcuate fractures within Unit 13 appear to originate at the main slip plane of the MRE fissure, and are possibly related to post-event compaction of the loose fissure-fill material.

The trench did not expose the down-faulted equivalent of the Q2 terrace surface, which is likely buried by alluvium of the Q1 alluvial fan/terrace (figure 20). Units 9, 10, and possibly 14 and 15 are part of the sediment package of Q1 age that buried the down-faulted Q2 surface. The Q2 trench was 2 meters deep across the 5 meter scarp, therefore unless erosion removed the Q2 surface from against the scarp before the Q1 material buried it, the minimum vertical displacement of the Q2 surface is 7 meters.

We dated one piece of charcoal from the Q2 trench at the lower contact of Unit 13 above the filled fissure, but we do not consider the resulting radiocarbon age of 870 14C yr B.P. as representative of Unit 13. There is significant deposition above the sample site, and the charcoal-bearing unit correlates laterally with units on which a soil has developed, suggesting more than 1 thousand years of elapsed time. More likely, the charcoal sample was emplaced by bioturbation. Without other datable material, we used soil development to estimate the age of the Q1 surface and to constrain the timing of the last ground-rupturing earthquake. We estimate that the faulted Q1 surface has an age of 8-15 thousand years and that this age of this soil approximates or slightly postdates the timing of the MRE given that Unit 5 in trench Q1 is unfaulted.

Paleoearthquake Scenarios

Cottonwood Canyon is near the southern end of the Anderson Junction segment of the Hurricane fault, a few kilometers north of the State Line geometric bend. Scarps with a height of about one meter or less in young fan deposits are present along the fault for 7 kilometers in either direction from Cottonwood Canyon, and likely formed in the same earthquake that displaced the Q1 surface at Cottonwood Canyon. As of yet, we have documented no clear evidence of similarly young scarps farther north along the Anderson Junction segment or immediately to the south on the Shivwitz segment. If the Anderson Junction geometric segment is also a seismologic rupture segment, then the MRE at Cottonwood Canyon may have been near the end of a segment rupture, increasing in slip to the north. Or, it could have been part of a rupture that 'spilled' around the boundary from an earthquake rupturing the Shivwitz segment. A third alternative is that the MRE may have been a small rupture limited to about 15 kilometers of the segment near the boundary zone. Perhaps the Anderson Junction geometric segment is not a seismological segment. In that case, the most recent rupture as recorded at Cottonwood Canyon need not have been constrained by the State Line segment boundary, and may have extended in both directions from the canyon mouth for some distance. It is likely that more small scarps existed beyond the 14 kilometers where we have observed them, but they have not been preserved. Using empirical relations from historical ruptures (Wells and Coppersmith, 1994), and assuming that the 60-centimeter-displacement was an average for the rupture, the earthquake may have been a M 6.3-7.0, and may have ruptured about 30 kilometers in length (Stenner and others, 1999).

From this stop we will continue driving north on the main road.

2.7   134.4   **Bear right**, cross Fort Pierce Wash. This is a major stream system that heads in Utah north of Colorado City and drains the western Vermillion Cliffs and much of the Uinkaret Plateau.

0.8   135.2   **Turn hard right** onto a small dirt track.

0.2   135.4   Take the left track. This track is rather rough, and 4-wheel drive is strongly recommended. Proceed south across two small hills.

0.6   136.0   Park on top of the third hill for a nice view of Rock Canyon.

STOP 1-5. Rock Canyon Site Overlook (Rock Canyon 7.5' quadrangle, T41N, R10W, section 1)

At this stop we can look to the east where Rock Canyon has incised through the Hurricane Cliffs, about 4 kilometers along the fault north of Cottonwood Canyon. The drainage that flows through Rock Canyon, known as Short Creek above the Hurricane Cliffs and Fort Pierce Wash through this area, is much larger than Cottonwood Wash. This drainage has had sufficient stream power to erode a large canyon through the Hurricane Cliffs and downcut extensively in the hanging wall as well (note the bouldery bedload deposited by the wash). We are currently standing on an eroded remnant of a Pleistocene terrace of Ft. Pierce Wash, and a higher terrace remnant is apparent immediately to the east of our position. Extensive exposures of the Triassic Petrified Forest Member of the Chinle Formation in this area clearly indicate that the thickness of Quaternary alluvium on the hanging wall is not great.

An alluvial fan on the north edge of the mouth of Rock Canyon is faulted, resulting in an approximately 30-meter-long fault scarp. Two profiles across this scarp reveal that the surface has probably been displaced at least 3-4.5 meters (figure 22). Based on surface character, we think it is possible that the hanging-wall side of the alluvial fan is preserved, and the 3-4.5 meters
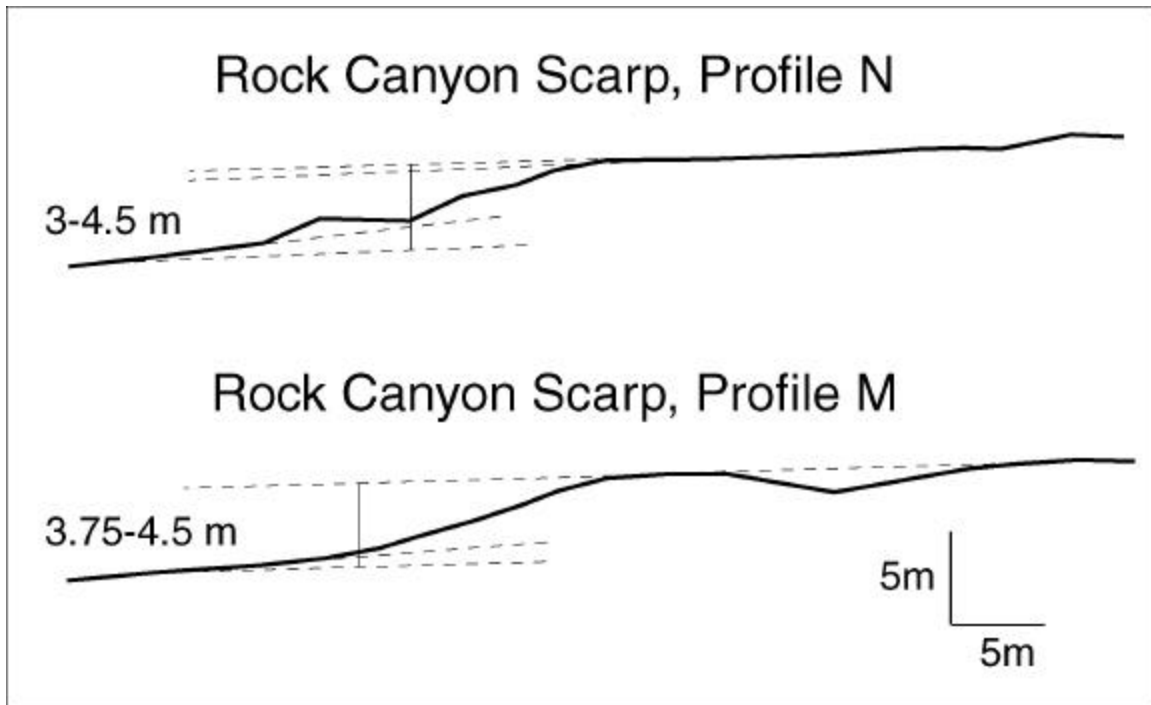

Figure 22. Topographic scarp profiles showing displacement of a tributary alluvial fan on the north side of Rock Canyon. Other evidence from this area indicates that displacement in the MRE may have been less than about 1 meter, this scarp likely formed in multiple faulting events.

may be the true vertical displacement. This displacement is likely the result of more than one earthquake, based on the smaller fault scarps we observed at Cottonwood Canyon and elsewhere along this part of the fault. We estimate the faulted fan is likely a latest Pleistocene surface, based on comparing the surface undulations, degree of dissection, and the relative elevation above the active stream channel to those investigated more thoroughly at Cottonwood Canyon.

We hope to trench this scarp in the spring of 2002 to address several questions about the recent faulting history along the southern part of the Anderson Junction segment. (1) Was the MRE at Rock Canyon part of the same rupture we found evidence for at Cottonwood Canyon? (2) If the timing was the same, can we refine the timing of that MRE? (3) How does the amount of slip during the MRE at Rock Canyon compare to the 60 centimeters observed at Cottonwood Canyon? (5) What does that displacement imply about the last event along the southern Anderson Junction section? For example, if Rock Canyon's MRE is the same event but with a larger slip than at Cottonwood Canyon, it could mean that the slip generally decreased toward the State Line bend and perhaps the event did not initiate within that geometric segment boundary or along the Shivwitz section to the south.

Exposures of the faulting within the Rock Canyon fan may also provide information about earthquakes previous to the MRE. If we can recognize the signature of previous events, we may be able to tell if the size of the MRE was typical for the fault at that location. If we can estimate the timing of the previous event(s), we can improve our understanding of the recurrence interval for this section of the fault.

Head back to the main road after this stop.

0.6   136.6   **Turn right** at T onto small track.

0.2   136.8   Merge right onto graded gravel road.

2.2   139.0   Two tracks turn off to the right, do not turn, continue straight on main road.

0.2   139.2   This is an area of multiple fault strands where the Hurricane Cliffs are less precipitous. The Mormon pioneers, who carved the Honeymoon Trail up and over the escarpment here, exploited this fact.

0.2   139.4   Arizona/Utah state line.

4.9   144.3   Pull off to the side of the road

STOP 1-6. Lava Cascade. (The Divide 7.5' quadrangle, T43S, R13 W, section 3)

To the east is a lava cascade where dark-colored lava of The Divide flow (Higgins, 2000) flowed down the upper part of the Hurricane Cliffs. The source of the basalt flow is a volcanic center on the plateau east of the Hurricane Cliffs (Sanchez, 1995). The rock is fine grained, black in color, contains small olivine phenocrysts, and is classified as a basanite with less than 46 percent silica (Sanchez, 1995). The flow still has a relatively fresh surface morphology. Higgins (2000) obtained a $^{40}Ar/^{39}Ar$ age of 0.41 $\pm$ 0.08 Ma from near the top of the cascade.

The Hurricane fault was active and the Hurricane Cliffs existed as essentially a fault escarpment, at least in part, prior to the eruption of the lava in the cascade because the flow conforms to the topography showing that it flowed down the cliff. The flow ends part way down the cliff. Primary structures within the flow suggest the present end of the flow is near the original terminus of the flow. The cliffs are about 300 meters high here and the flow ends about 150 meters down the cliff, which implies that at least one half of the total scarp height formed prior to eruption of the flow. However, more of the scarp may have existed and the flow was just not voluminous or liquid enough to flow to the bottom.

Higgins (2000) mapped the lava flows exposed in the hill west of the road as the Grass Valley flow, which is a very dark gray, fine- to medium-grained basalt. Based on surface morphology and position, this flow is considerably older than The Divide flow, and was erupted from a volcanic center located to the west (Sanchez, 1995; Higgins, 2000).

Remnants Flow in Grass Valley

Near the north end of Grass Valley approximately 4 kilometers north of the lava cascade, Higgins (2000) mapped the Remnants basalt flow on both the up- and downthrown sides of the

Hurricane fault. Geochemical data (Higgins, 2000; Lund and others, 2001) confirm that the flows are correlative across the fault. Higgins (2000) reported two whole-rock ^{40}Ar/^{39}Ar ages for the Remnants basalt, one from the footwall (0.94 $\pm$ 0.04 Ma) and one from the hanging wall (1.06 $\pm$ 0.03 Ma). Lund and others (2001) obtained a third ^{40}Ar/^{39}Ar age of 1.47 $\pm$ 0.34 Ma from a Remnants flow outcrop in the hanging wall. The two-sigma errors reported for the three ages do not overlap, indicating that they are discrete and non-correlative. Nevertheless, the two ages obtained by Higgins (2000) are relatively close in time and could represent a reasonable suite of ages from a single eruptive episode. Conversely, the Lund and others (2001) age from the Remnants flow on the hanging wall is approximately 500 thousand years older than the Higgins (2000) ages. The Lund and others (2001) age estimate came from the same basalt-capped hill as the Higgins (2000) 1.06 + 0.03 Ma age. The difference between the two age estimates remains unexplained.

The paleomagnetic data from the Remnants basalt flow are highly erratic, probably due to local remagnetization of the rock by lightning strikes (Lund and others, 2001, appendix C). As a result, those data were of no use in evaluating back-tilting of the hanging wall. Visual examination showed that the hanging-wall basalt is tilted toward the Hurricane fault, but the nearest Remnant flow outcrops are approximately 750 meters west of the fault (Higgins, 2000). Given those constraints, Lund and others (2001) used the elevation difference between the top of the Remnants flow on the footwall and the highest elevation on the least tilted basalt in the hanging wall as a best approximation of net slip. The elevation difference is 440 meters.

Because of the discrepancy in the radiometric ages, Lund and others (2001) calculated two slip rates for the Grass Valley site, the first using an average of the two Higgins (2000) ages and the second using their own older age estimate. The slip rates at Grass Valley are:

$$440,000 \text{ mm}/(0.94 + 1.06/2) \text{ Ma} = 0.44 \text{ mm/yr}$$

and

$$440,000 \text{mm}/1.47 \text{ Ma} = 0.30 \text{ mm/yr}$$

Because of the relatively close correspondence in time of the Higgins ages, Lund and others (2001) consider the 0.44 mm/yr slip rate to be the preferred long-term slip rate at Grass Valley.

Continue north on the main road after this stop.

1.5   145.8   Cross cattle guard and continue on pavement. Sky Ranch subdivision and airport on the left (W). This road generally parallels the Hurricane fault for a few miles.

3.8   149.6   Volcano Mountain (Stop 2-1) at 10:00.

0.5   159.1   **Turn left** (~NW) onto 700 West at T intersection and enter Hurricane, Utah. Note cluster of homes that are on or near the Hurricane fault and at the mouth of a canyon, which is subject to flash flooding. Optional stop, if time and light are available.

2.1   152.2   Stop light. **Turn right** (E) onto State Route (SR) 9.

0.3   152.5   Pass straight through light at 300 West and very shortly **turn left** (N) into the parking lot of the Lamplighter Motel.

End Day 1.

The Hurricane fault near Hurricane, Utah, with the Jurassic Moenkopi Formation (hanging wall) juxtaposed against the Permian Kaibab Formation (footwall).

SECOND DAY ROAD LOG

**The Northern Anderson Junction, Ash Creek, and Cedar City Segments
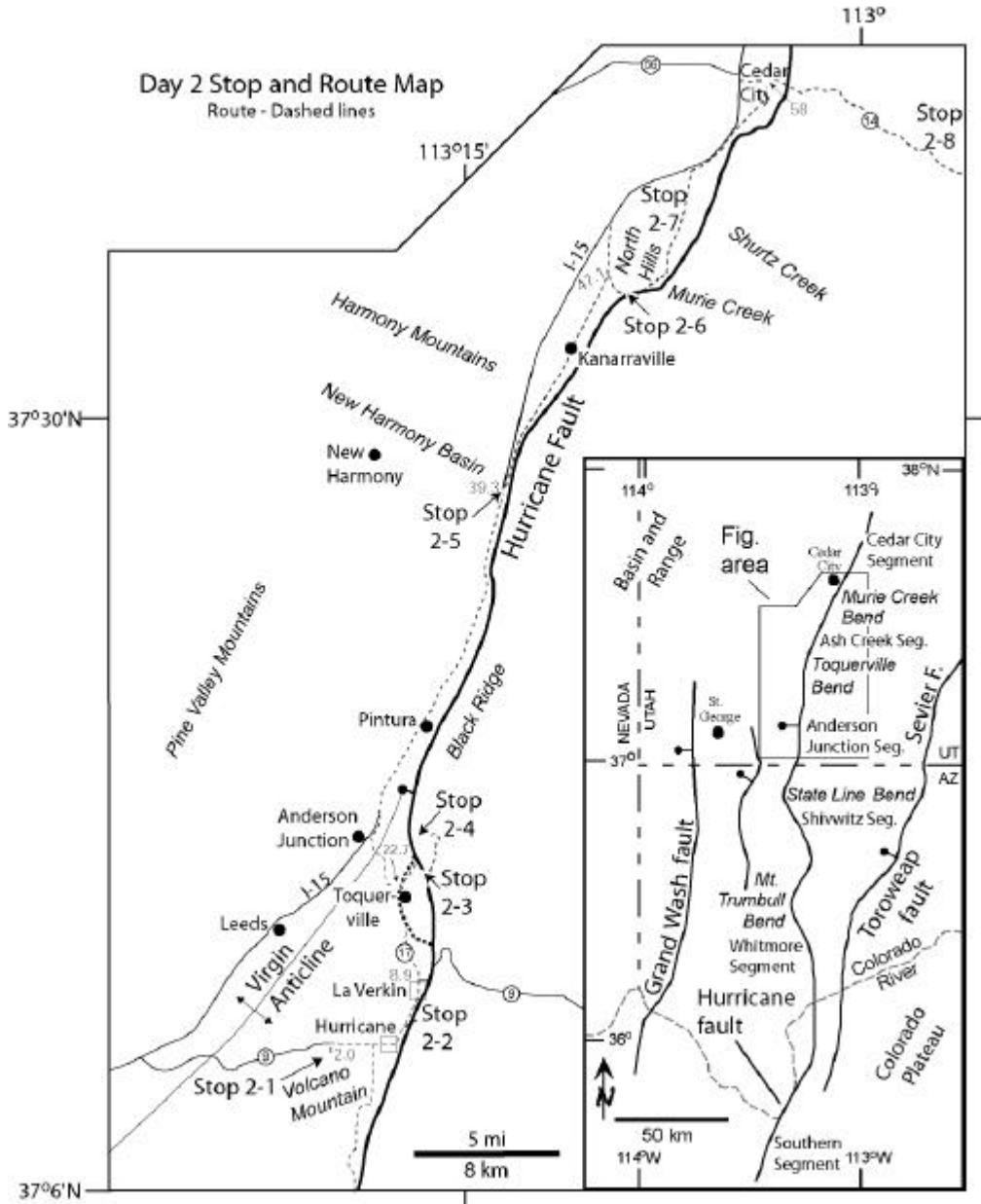Hurricane Fault Zone
Utah**

Figure 23. Day 2 Route Map. The dashed line shows the route of our trip on Day 2. Some key mileage values also are shown along the route. Words in italics are geographic locations noted in the road log. Inset shows trip map in a regional context.

SECOND DAY ROAD LOG

The Northern Anderson Junction, Ash Creek, and Cedar City Segments
Hurricane Fault Zone
Utah

The second day of this field trip begins in the parking lot of the Lamplighter Motel at the intersection of State Street and 300 West Street in Hurricane, Utah. We will spend today examining the northern part of the Anderson Junction segment and the Ash Creek and proposed Cedar City segments of the Hurricane fault in Utah. First we will proceed west from Hurricane to Volcano Mountain, which provides an overview of the northern part of the Anderson Junction segment. From Volcano Mountain, we will travel northward along the Anderson Junction segment, stopping to observe the fault in the walls of Timpoweap Canyon where the Virgin River cuts through the Hurricane Cliffs and also where a dated basalt flow is displaced across the fault, providing a good mid-Quaternary slip rate for the fault. Continuing north to the Toquerville geometric bend, we will examine structural evidence for the boundary between the Anderson Junction and Ash Creek segments and a dated basalt flow at the boundary that records nearly 370 meters of net slip across the fault and provides another long-tern Quaternary slip rate. Farther north we will observe more displaced basalt flows, visit the proposed boundary between the Ash Creek and Cedar City segments near Coyote Gulch and Murie Creek, and make an overview stop at the Shurtz Creek scarp and trench site. Finally, we will cross the Hurricane fault at Cedar City and drive up Cedar Canyon to observe a basalt flow stranded high on the canyon wall that provides a surrogate long-term slip rate for the Cedar City segment.

The eight stops today provide information that shows that: (1) long-term slip rates on the northern Anderson Junction and Ash Creek segments are higher than late Quaternary rates, (2) the long-term slip rate for the Ash Creek segment is higher than the long-term rate for the northern Anderson Junction segment and the increase is at or near the Toquerville geometric bend, (3) a difference in timing of the MRE north and south of the Murie Creek geometric bend between Kanarraville and Cedar City argues for the presence of a previously unrecognized seismogenic segment boundary, (4) the proposed Cedar City segment has a long-term slip rate generally comparable to the Ash Creek segment and higher than the Anderson Junction segment, but shows no comparable evidence of latest Pleistocene or Holocene surface faulting.

Mileage
Inc.   Cum.

0.0	0.0	Begin trip in parking lot of the Lamplighter Motel. Exit from northwest corner of lot. **Turn left (S)** onto 300 West.
0.1	0.1	Stop light. **Turn right (W)** at intersection with State Street.
0.3	0.4	Continue straight through stop light at State Street (SR-9) and 700 West. Volcano Mountain at 10:00.
0.5	0.9	Continue straight through stop light at SR-9 and 1150 West.
1.1	2.0	**Turn left (S)** into Painted Hills subdivision onto Rlington Parkway.
0.2	2.2	Continue straight at stop sign at Rlington and Ridge View Drive. Parallel rock wall to T intersection with Valley View Drive.
0.1	2.3	**Turn right (W)** onto Valley View Drive, just past end of rock wall.
0.1	2.4	**Turn left (S)** onto Ridge View Drive and proceed uphill.

0.1   2.5   **Turn right (S)** onto Panorama Drive, this road quickly turns to dirt.

0.2   2.7   Park by gate. Walk to rock promontory on spur to the northeast.

STOP 2-1. Volcano Mountain Overview (Hurricane 7.5' quadrangle, T42S, R13W, section 5)

Volcano Mountain is the largest of several volcanic vents in and near the town of Hurricane. Volcano Mountain still preserves its classic cinder cone shape and has moderately well developed rill weathering on its flanks (Biek, 1998) indicating a late Quaternary age. The cone is breached on its north side by a flow that rafted cinders associated with the breach downslope for a distance of at least a mile. The basaltic rocks here and visible from here are part of the western Grand Canyon basaltic field in southwestern Utah and adjacent northwestern Arizona (Hamblin, 1970a; Best and Brimhall, 1974). Although relatively small in volume when compared to other volcanic regions in the western United States, the flows of the Grand Canyon field provide important constraints on local tectonic and geomorphic development (Biek, 1998); we will examine several examples today.

Volcano Mountain provides a grand vista across a broad swath of southwestern Utah, and is an excellent location from which to orient ourselves for the morning portion of today's field trip. Looking to the southwest over our parked vehicles, in the far distance we can see the Beaver Dam Mountains, a metamorphic core complex flanked by Paleozoic sedimentary rocks. If we set the Beaver Dams at 9:00, we can begin a clockwise rotation through the vista before us. At 10:00 in the middle distance is the east limb of the Virgin anticline held up here by the resistant, east-dipping Shinarump Conglomerate Member of the Chinle Formation. Quail Creek reservoir occupies the breached core of the anticline. Beyond the anticline are the red-colored Jurassic Kayenta and Navajo Formations, which are capped by the lighter colored Cretaceous Iron Springs Formation. In the near distance along SR-9, we can see basalt flows associated with Volcano Mountain. At 11:00 are the Pine Valley Mountains, cored by the Tertiary Pine Valley laccolith, which intrudes the Clarion Formation, more about that at Stop 2-4 later today. At 12:00 we see craggy outcrops of the Navajo Sandstone in the east limb of the Virgin anticline. Black Ridge, the site of stops 2-3 and 2-4, is at 1:00. Black Ridge represents the east limb of the Kanarra anticline; the anticline's west limb has been displaced down-to-the-west and out of our view by the Hurricane fault. The Toquerville geometric bend and the proposed boundary between the Anderson Junction and Ash Creek segments of the Hurricane faults is near the south end of the ridge. In the far distance just east of Black Ridge, the Kolob Fingers (Navajo Sandstone) are visible in Zion National Park. At 2:00 in the near distance we can see the Cinder Pits and Radio Towers volcanic vents, which, along with Volcano Mountain, are the principal volcanic cones in the Hurricane volcanic field. The red cliffs in the middle distance expose nearly 470 meters of the Triassic Moenkopi Formation capped by the resistant Shinarump Conglomerate Member of the Chinle Formation, which we last saw behind us holding up the east limb of the Virgin anticline. Clearly a structure of major down-to-the-west displacement lies between our current vantage point and those cliffs. In the far distance are the white sandstone spires of Zion National Park.   The structure that separates the topographically high, nearly undeformed Shinarump capping the cliff to the east from the steeply east-dipping Shinarump outcrops behind and below us in the east limb of the Virgin anticline is the Hurricane fault, which lies at the base of the Hurricane Cliffs in the middle distance between about 12:00 and 3:00. The portion of the Hurricane Cliffs within our view represents the central part of the Anderson Junction segment of the Hurricane fault. The basalt flow stranded at about the midpoint of the cliffs originated from Ivans Knoll just to the south of us, and will be the topic of discussion at our next stop at the mouth of Timpoweap Canyon (2:00 low) where the Virgin River cuts through the Hurricane Cliffs.

Return to SR-9 via the same route.

0.6   3.3   **Turn right (E)** at intersection with SR-9, toward the town of Hurricane.

1.1   4.4   Continue straight through the stop light at 1150 West.

0.5	4.9	Continue straight through the stop light at 700 West.
0.4	5.3	Continue straight through the stop light at 300 West, near the Lamplighter Motel.
0.3	5.6	Continue straight through the stop light at Main Street. Follow SR-9 (Main Street), staying left ahead.
0.3	5.9	Main strand of the Hurricane fault lies to the left (E) near the base of the basalt cliffs.
0.8	6.7	**Turn right (E)** just before the bridge over the Virgin River onto Enchanted Way. Follow tree-lined road to the bottom of the hill.
0.4	7.1	Park near the small bridge across the Virgin River.

STOP 2-2. Exposures of the Hurricane fault in the walls of Timpoweap Canyon
(Hurricane 7.5' quadrangle, T41S, R13W, section 25)

At this stop, the Anderson Junction segment of the Hurricane fault consists of two easily visible fault strands and a third strand down the canyon to the west. At least two strands offset the Quaternary basalt at the top of the section, much of which contains well-developed columnar joints. On the south side of the canyon, the gray rocks on the left (E) are part of the Permian Kaibab and Toroweap Formations. These rocks lie in the footwall of the easternmost strand of the Hurricane fault. The eastern strand is in the steep side canyon. In the hanging wall of that strand (to the right), the brown, red, and green-gray layers are Triassic Moenkopi Formation that dips steeply (~60-80°W). This block of Moenkopi Formation is bounded on the right (W) by another fault strand that is exposed up the road and juxtaposes Chinle and Moenkopi Formations. These beds are overlain by Cenozoic basalt. The Moenkopi beds were steeply tilted prior to emplacement of the overlying basalt as evidenced by the strong angular unconformity between them and the overlying basalt. Thus, this site provides evidence that the Hurricane fault was active both before and after emplacement of the basalt.

The easternmost fault strand splays under the river and appears as two fault strands on the north side of the canyon. These splays lie just to the east of the north end of the bridge. The eastern splay, which is visible around the corner to the east from the end of the bridge, juxtaposes Permian Kaibab and Toroweap Formations. The western splay is apparent near the end of the bridge where it juxtaposes siliciclastic layers of the Moenkopi Formation (some of which is green-gray) in the hanging wall against the gray limestone of Permian Kaibab Formation in the footwall. The obvious gypsum is in the Moenkopi Formation.

To view the other two fault strands on the north side of the canyon, re-cross the bridge and look north. The middle strand juxtaposes the western part of the Moenkopi Formation against the purple-brown Triassic Chinle Formation on the west. The westernmost strand is evident where it places Quaternary basalt next to the western part of the Chinle exposure. As we continue to the north along the Anderson Junction segment, the number of strands increases. The increase in the number of strands stops at the Toquerville geometric bend.

Up stream of the bridge, hot springs feed into Virgin River from the river bottom and from the rocks along the edge of the stream. In 1981 the spring discharge was estimated to be 4,700 gpm (Cordova, 1981). The springs discharge directly from the Kaibab Formation. The water from these springs contains high concentrations of dissolved solids (2,270 ppm Na, 3,250 ppm Cl, 775 ppm Ca, 1,891 ppm SO_4, 907 ppm HCO_3; Yelken, 1996). Consequently, the water quality in the Virgin River degrades downstream from Pah Tempe hot springs. The spring area is presently privately owned and used a mineral-spa resort.

Mid-Quaternary Slip Rate from Displaced Basalt

The basalt flow displaced here occupies an intermediate position part way up the Hurricane Cliffs. The flow originated from Ivans Knoll to the southwest (Sanchez, 1995; Biek, 1998) and ponded along the base of the Hurricane Cliffs. Subsequent movement of the Hurricane fault displaced the basalt 73 meters down-to-the-west (Biek, 1998). Sanchez (1995) obtained a
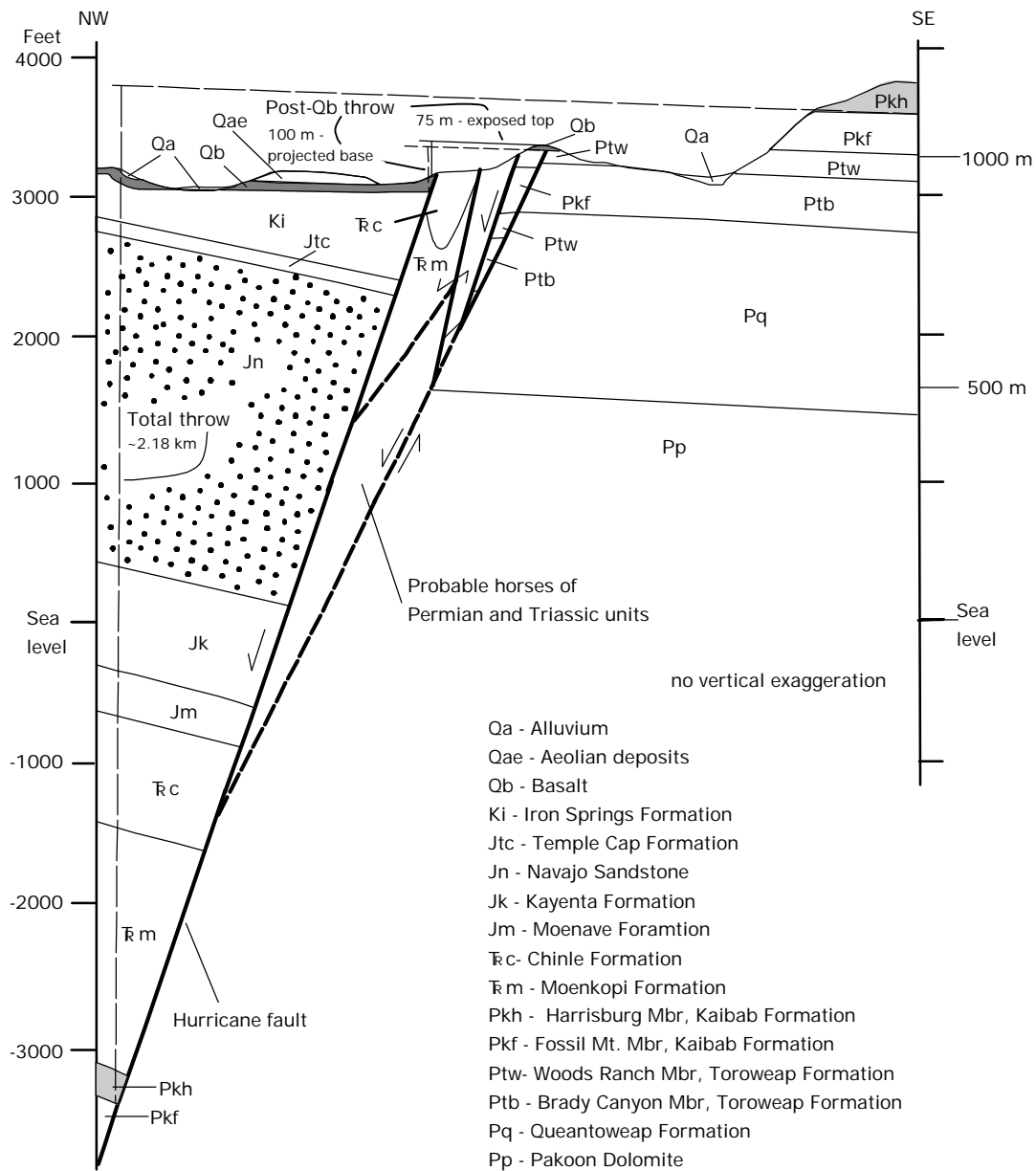
Figure 24. This cross section represents the geology just north of the bridge across the Virgin River at Stop 2-2. Total throw is ~ 7,770 feet (2,370 m). Post Quaternary basalt throw is ~240 feet (73 m).

^{40}Ar/^{39}Ar whole-rock age of 353 $\pm$ 45 ka for the basalt. Mapping and geochemical sampling by Biek (1998) shows that the basalts on either side of the fault are correlative. Paleomagnetic data from the basalt on both sides of the fault indicate that the basalt is normally magnetized and that the basalt in the hanging wall is tilted less than 10 degrees toward the fault, if it is tilted at all (Lund and others, 2001, appendix C). Visual examination confirms a lack of back tilting except in a very narrow zone immediately adjacent to the fault zone. The 73-meter difference in elevation (net slip) between the basalts in the footwall and hanging wall was measured outside of the deformation zone.

Using Sanchez's (1995) age estimate and a net slip of 73 meters (Biek, 1998), the slip rate at Pah Tempe Hot Springs for the past 353 thousand years is:

73,000 mm/353,000 yrs = 0.21 mm/yr

55

The Pah Tempe slip rate is approximately one-half the preferred slip rate at Grass Valley (0.44 mm/yr), which is also on the Anderson Junction segment. The difference between the two sites may represent a difference in long-term rates on two independent fault segments, with an as yet unrecognized segment boundary between them. However, based on new geologic mapping by Biek (1998), the presence of an unrecognized seismogenic boundary along this part of the fault is considered doubtful. Because the age of the displaced basalt flow at Pah Tempe Hot Springs is only about one-third the age of the basalt at Grass Valley, the lower slip rate at Pah Tempe more likely reflects a change in slip rate through time on a single seismogenic segment.

Return to main road at top of hill.

0.2	7.3	**Turn right (N)** onto SR-9 and proceed north crossing the Virgin River bridge.
0.1	7.4	Enter the town of LaVerkin. The road parallels the Hurricane Cliffs and the Hurricane fault.
0.3	7.7	A large landslide covered with basalt talus is visible at 9:00 along the canyon wall above the Virgin River. Quaternary basalt flows here are being undercut by slope failures in the underlying Cretaceous Iron Springs Formation, which locally contains abundant bentonitic mudstone.
0.5	8.2	School crossing, **drivers watch for flashing lights**. In LaVerkin SR-9 is also called State Street.
0.7	8.9	Stop light at intersection with SR-17. **Proceed straight ahead (N), which is along SR-17.** The Toquerville geometric bend is visible at 12:00.
0.3	9.2	Road cut through basin-fill sedimentary units.
0.4	9.6	Cross LaVerkin Creek. To the right (E), the Hurricane fault comprises several strands. In this area, a Quaternary conglomerate is offset by the Hurricane fault (Stewart and others, 1997).
0.2	9.8	Enter Toquerville. Quaternary basalt overlying the Shinarump Conglomerate crops out from 9:00 to 12:00.
0.5	10.3	Hurricane Mesa is at 9:00. The mesa consists of the red, brown and white Triassic Moenkopi Formation with the cliff-forming Shinarump Member of the Chinle Formation at the top. The water tower at the skyline is part of a former U.S. Air Force rocket sled research facility.
1.3	11.6	The northern end of the Virgin anticline, exposed in Jurassic Navajo Sandstone, lies at 10:00. Current thinking is that the Virgin anticline dies out northward as two different anticlines, the Pintura on the west and the Kanarra on the east, pick up.
0.2	11.8	Enter Toquerville, westernmost strand of the Hurricane fault parallels the basalt-covered ridge on the right.
0.6	12.4	**Turn right (~E)** onto Spring Drive, just before bridge crossing Ash Creek, the western strand of the fault makes a similar bend here, still paralleling the basalt-covered ridge.

0.5   12.9   Toquerville spring, to the left (~N), surfaces along the Hurricane fault and supplies culinary water to the town of Toquerville.

0.2   13.1   From the water tank, look toward 10:00, the Hurricane fault is easily visible where dark-colored basalt is juxtaposed against the gray Permian Kaibab Formation. We are in the Toquerville geometric bend at the boundary between the Anderson Junction and Ash Creek seismogenic segments. At the top of the footwall cliff, Quaternary basalt crops out where it fills former embayments in the Hurricane Cliffs. This basalt at the cliff top is geochemically equivalent to the basalt at 10:00.

0.3   13.4   Stay on main road as it curves to the right (~S).

0.2   13.6   Road parallels and lies between two strands of the Hurricane fault in the eastern part of the Toquerville bend. The eastern strand is exposed in several places a few meters to the left (~E). The hill of Triassic Moenkopi Formation to the right lies in the hanging wall of the western strand.

0.5   14.1   Pull out to left (~E) and park.

STOP 2-3. Toquerville Geometric Bend (Pintura, 7.5' quadrangle, T40S, R13W, section 36)

This stop is in the Toquerville geometric bend, which separates the Anderson Junction and Ash Creek geometric segments of the Hurricane fault (figure 25). To the north, the main trace of the Hurricane fault lies along the base of the Hurricane cliffs, concealed by Quaternary deposits; a secondary strand lies to the west. Just to the north of the visible part of the fault, a scarp cuts Quaternary alluvium. Along this dirt road to the north are slickenlines exposed on the Permian Kaibab Formation. South of the gravel quarry the main fault trace splits into at least three west-side-down normal faults displacing sandstone and mudstone of the Triassic Moenkopi and Chinle Formations. These rocks are also deformed by a complex array of normal faults subsidiary to the Hurricane fault. This complex zone lies within the salient in the fault zone.

The footwall of the Hurricane fault zone consists here of the Fossil Mountain and Harrisburg Members of the Permian Kaibab Limestone and the Timpoweap Member of the Moenkopi Formation. These units are folded in the Kanarra anticline, a Late Cretaceous-Paleocene (?) fold of the Cordilleran fold and thrust belt. Near the fault zone, these strata dip ~10-30 degrees west. About 0.5 kilometers and farther to the east of here, these units dip 30 to 80 degrees east in the eastern limb of the anticline. The Fossil Mountain Member forms a prominent cliff of cherty limestone that is repeated by a west-directed thrust fault in the eastern limb of the Kanarra anticline.

We suggest that the Toquerville bend is a zone where two faults linked for a number of reasons. The fault strike across the Toquerville geometric bend changes from approximately N15°W on the south side of the salient to N25°E on the north side. The number of fault strands changes from several south of the bend to one or few north of the bend. The basalt in the hanging wall contains a gentle anticline that trends nearly perpendicular to the strike of the fault, a classic geometry for extensional folds. Hanging wall anticlines with this geometry are common at or near fault segment boundaries (Schlische, 1993). Note that this gentle anticline is superimposed on a rollover anticline that also folds the basalt. The displacement-distance profile along the relatively symmetric Toquerville bend shows relatively smooth decreases in throw to a minimum just adjacent to the apex of the bend. This pattern resembles the expected pattern for linkage of underlapping faults (figure 5). The displacement-distance profile and strike change of 35-40 degrees around the bend are interpreted to result from originally underlapping faults that curved to link with each other. In addition, the map geometry of the fault at the bend is relatively symmetric, which is consistent with that expected at a site of symmetrical linkage as can occur with underlapping faults. The decrease in stratigraphic separation at this bend and then an
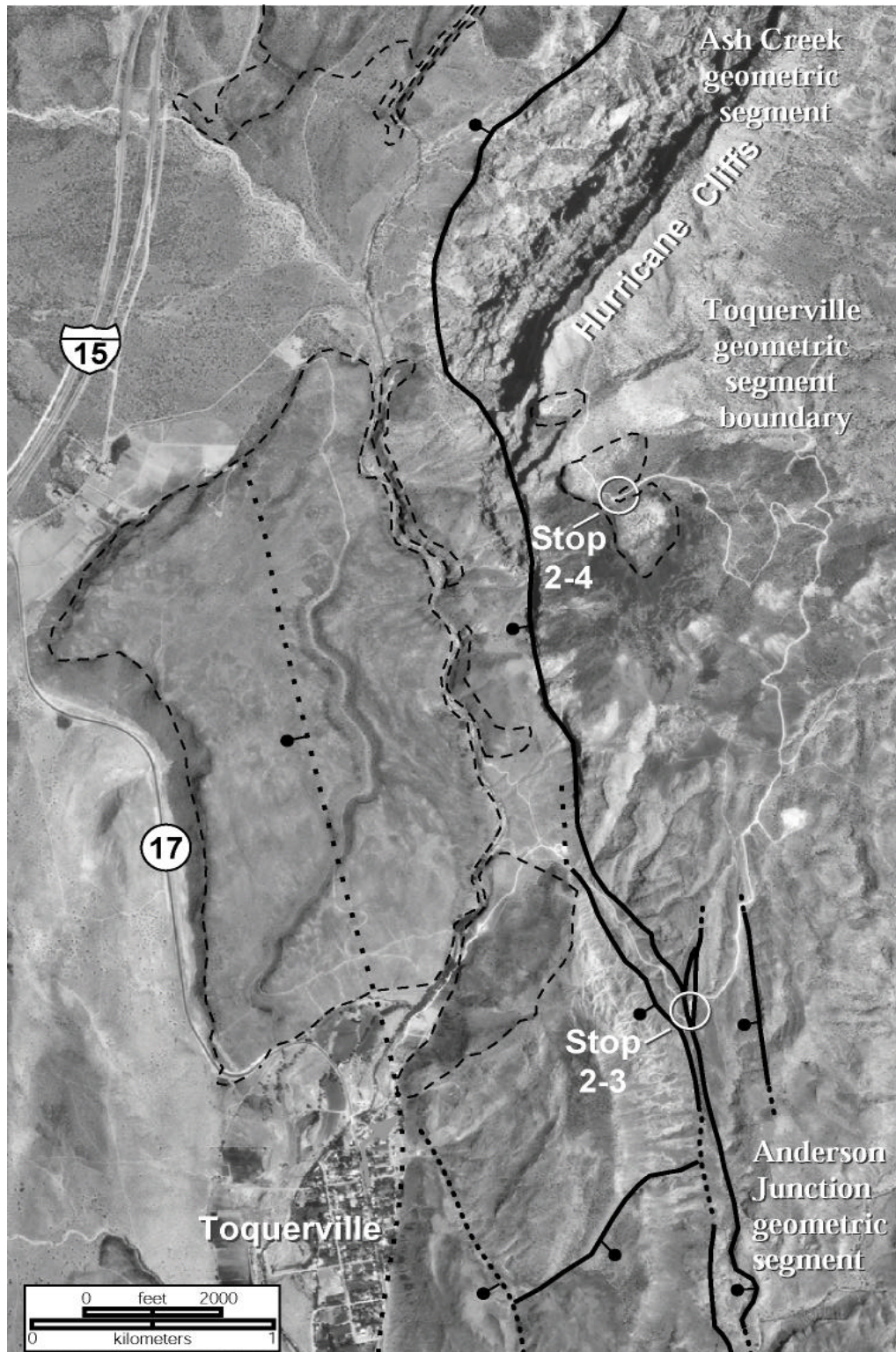
Figure 25 . Hurricane fault in the vicinity of the Toquerville bend between the Anderson Junction and Ask Creek geometric segments. Heavy-weight lines are faults; dotted where concealed. Light-weight lines outline Quaternary basalt fields. Modified from Reber and others (2001).

increase in displacement toward the south mimics relief profiles for the same section of the fault (Taylor and others, 2001), and also points to the probable linkage of two originally isolated faults (figure 5). The Ash Creek and Anderson Junction geometric segments are inferred to have propagated laterally and linked as underlapping faults forming the Toquerville geometric bend (figure 5; Taylor and others, 2001).

At the next stop we will discuss the problems posed by the spatial coincidence between the Hurricane fault and the Kanarra anticline for reconstructing both features.

Continue uphill along the dirt road.

0.8   14.9   Well drill pad at ~3:00 (~S). At 12:00, view of the Moenkopi Formation capped by the Shinarump Conglomerate. These nearly flat-lying rocks are in the footwall of the Hurricane fault. The red cliffs in the distance are composed of Jurassic Navajo Sandstone in Zion National Park.

0.8   15.7   Outcrops to the right (E) are the Moenkopi Formation, which is capped by the resistant, tan-colored Shinarump Conglomerate Member of the Triassic Chinle Formation.

0.3   16.0   Road to right (NE), continue on main road (left fork). Down the hill in the light-colored Virgin Limestone Member of the Moenkopi Formation, is a small thrust fault with 15 meters of stratigraphic separation. This is the southern exposure of the Taylor Creek thrust fault (Lovejoy, 1964). The average strike and dip is N15^{o}E, 30°E. Farther north in Zion National Park, this fault has more than 600 meters of vertical and 760 meters of horizontal displacement (Kurie, 1966).

0.1   16.1   To the right (~N) a high-angle fault is visible. Kaibab Limestone is in the footwall and Moenkopi Formation is in the hanging wall.

0.2   16.3   The red mudstone unit that we are driving across is the upper red member of the Moenkopi Formation.

0.4   16.7   Look down to the right (southeast), and see the Taylor Creek thrust fault again.

1.0   17.7   Radio towers at the south end of Black Ridge

.   **STOP 2-4. South Black Ridge Radio Towers** (Pintura 7.5' quadrangle, T40S, R13W, section 23)

The radio towers are on the southern end of Black Ridge, in the hanging wall of the Hurricane fault. The Ash Creek valley lies below us, and the Pine Valley Mountains, reaching elevations over 10,000 feet, form the western skyline. Pre-Quaternary features visible from this site formed along the southwestern margin of the Late Cretaceous-Paleocene Cordilleran fold and thrust belt, and during Tertiary normal faulting prior to initiation of the Hurricane fault (and/or on the Hurricane fault prior to eruption of the Quaternary basalts). Here we briefly describe these structures and their geometric relation to, and possible influences on, the structural development of the Hurricane fault.

Pre-Quaternary Structure and Stratigraphy

Southwest of the radio towers, hogbacks of the Shinarump Member of the Triassic Chinle Formation define the form of the Late Cretaceous-Paleocene Virgin anticline. Much of the Anderson Junction geometric segment, exposed to the south, parallels the trend of the Virgin anticline. However, the fault generally lies to the east of the axial surface. The parallelism between the fault strike and anticlinal trend along this segment suggests the possibility that the Hurricane fault formed along or reactivated a fracture that formed during the formation of the Virgin anticline. Northeast of these hogbacks the Virgin anticline plunges out and shortening

transfers northeastward to the Kanarra anticline and possibly northwestward to the Pintura anticline. The Hurricane Cliffs expose the eastern limb and, locally, the hinge zone of the north-trending Kanarra anticline from here to Cedar City, 45 kilometers to the north.

The Pintura anticline occupies the hanging wall of the Hurricane fault; the southern end of its 4-kilometer-long, north-striking hinge zone is just north of the Toquerville geometric segment boundary. Along the hinge zone of the Pintura anticline, the Maastrichtian-Paleocene Canaan Peak Formation and the Oligocene-Eocene Claron Formation depositionally overlie the Jurassic Navajo Sandstone (Goldstrand, 1994; Hurlow and Biek, 2000), indicating erosion of about 1,200 meters of stratigraphic section along a Late Cretaceous-early Tertiary structural culmination. The geometry of the Pintura anticline is, however, difficult to ascertain because it is mainly exposed in the trough-cross-bedded Navajo Sandstone and is overprinted by younger normal faults. Based on detailed mapping, Hurlow and Biek (2000) interpreted the Pintura anticline as a broad, poorly defined, composite fold that originally formed during Late Cretaceous-Paleocene time, and was modified by Tertiary normal faulting and folding in the axis of a large, reverse-drag fold related to displacement on the Hurricane fault and/or earlier west-side-down normal faults (figure 26).
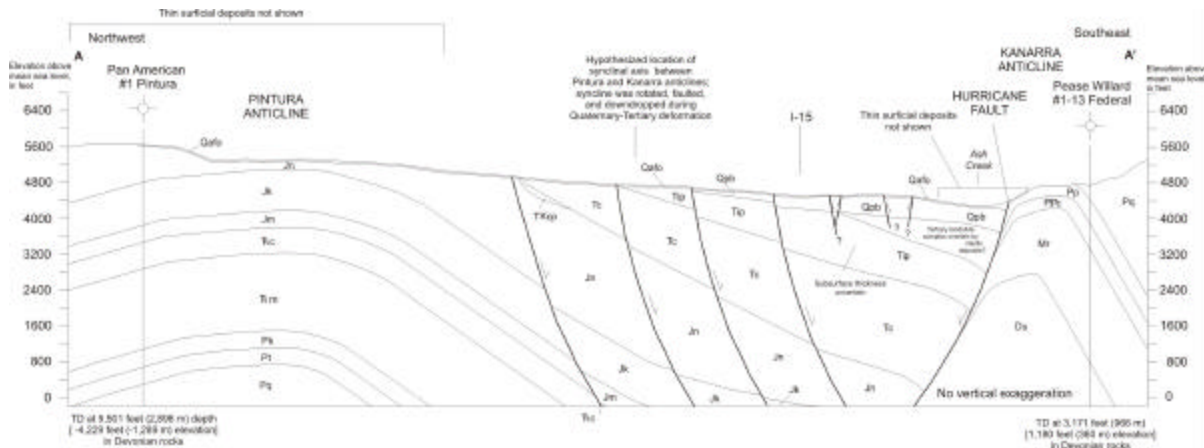

Figure 26. Cross section across the Ash Creek segment of the Hurricane fault modified from Hurlow and Biek (2000). Units from youngest to oldest: Qafo – early quaternary alluvial-fan deposits; Qpb – basalt flows of the Pintura field (about 830 ka); Tip – quartz monzonite porphyry of the Pine Valley Mountains (21 Ma); Tc – Clarion Formation (Oligocene-Eocene); TKcp – Canaan Peak Formation (Late Cretaceous-Paleocene); Jn – Navajo Sandstone (Jurassic); Jk – Kayenta Formation (Jurassic); Jm – Moenave Formation (Jurassic); TRc – Chinle Formation (Triassic); TRm – Moenkopi Formation (Triassic); Pk – Kaibab Formation (Permian); Pi – Toroweap Formation (Permian); Pq – Queantoweap Formation (Permian); Pp – Pakoon Formation (Permian); PPc – Callville Limestone (Permian-Pennsylvanian); Mr – Redwall Limestone (Mississippian); Du – Devonian rocks undivided.

The western limb and most of the hinge zone of the Kanarra anticline, the eastern limb of the Pintura anticline, and the intervening syncline are concealed below younger deposits in the hanging wall of the Hurricane fault, and few subsurface data are available for this area. Despite this lack of information, some preliminary interpretations on the possible role of structural inheritance on the development of the Hurricane fault can be made. The spatial coincidence between the Hurricane fault and the Kanarra anticline implies localization of the Hurricane fault by a pre-existing structure, perhaps a blind thrust ramp (Grant and others, 1995). Interpretation of seismic-reflection data from the Cedar City area (Stop 2-6) permits a similar conclusion. The Toquerville geometric segment boundary occupies the transfer zone between the Virgin and

Kanarra anticlines. This fold-transfer zone may have localized the Toquerville geometric segment boundary, although the subsurface geometry and localization mechanism are uncertain.

Quartz monzonite porphyry of the 21-million-year-old Pine Valley laccolith forms the precipitous cliffs of the southwestern front of the Pine Valley Mountains (figure 27). Several masses of the Pine Valley laccolith also crop out near Interstate 15 northwest of this stop. These outcrops are enigmatic because: (1) their basal contacts are about 915 meters lower than in the main laccolith body and are structurally discordant with bedding in underlying units, and (2) one of
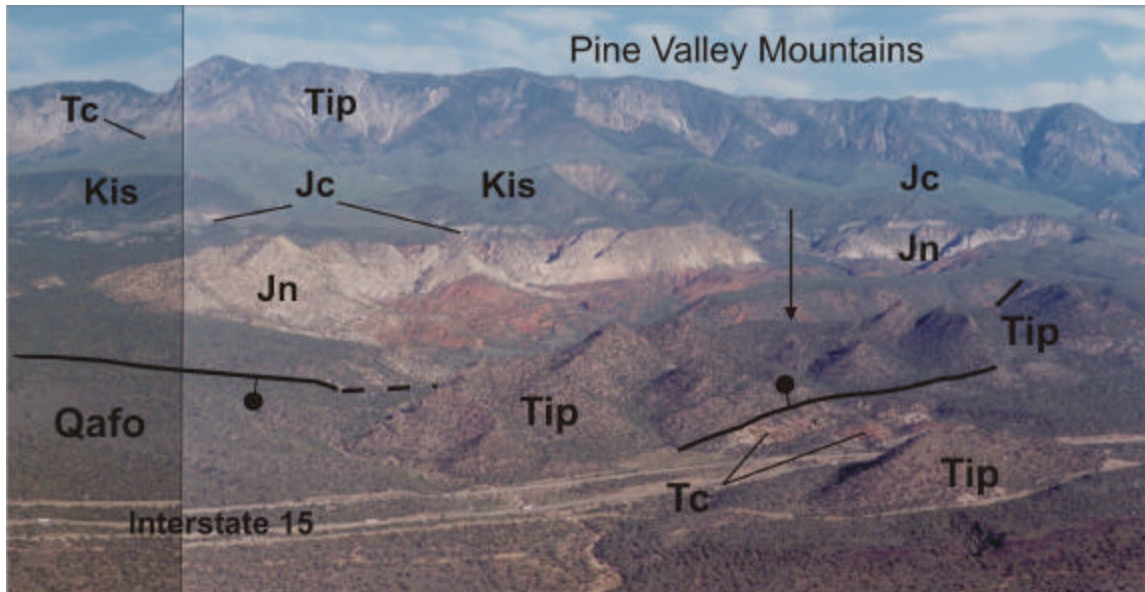

Figure 27. View to the northwest from southern Black Ridge near stop 2-4. The body of quartz monzonite porphyry of Pine Valley (Tip) west of Interstate 15 is about 915 meters below the main mass of the laccolith (visible in the background) and may be a satellitic intrusion or an erosional remnant of a once continuous sheet. The structurally low position of this body of quartz monzonite porphyry is due to the combined effects of: (1) normal faults bounding either side of the body (shown by solid lines where visible; the trace of the western fault is concealed behind the main body – the arrow shows its position), (2) reverse drag in the hanging wall of the Hurricane fault and/or other west-side-down normal faults. The base of the quartz monzonite porphyry here is discordant with bedding in the underlying Clarion Formation, indicating faulting during or prior to intrusion. Qafo = early Quaternary alluvial-fan deposits; Tip = quartz monzonite porphyry of Pine Valley; Tc = Clarion Formation (Oligocene-Eocene); Kis = Iron Springs Formation (Cretaceous); Jc = Carmel Formation (Jurassic); Jn = Navajo Sandstone (Jurassic). Photograph by Robert Biek, UGS.

these masses locally overlies the Cretaceous Iron Springs Formation. In contrast, the main mass of the Pine Valley laccolith consistently intrudes the middle part of the Claron Formation parallel to bedding, which dips gently toward the center of the laccolith (Cook, 1957, 1960; Hacker, 1998). These anomalous masses of quartz monzonite porphyry are either satellitic intrusions of the Pine Valley laccolith or erosional remnants of the once-continuous laccolith. The angular discordance between the intrusion base and bedding in the underlying Claron Formation and the local intrusion of the Iron Springs Formation reflect pre-intrusion faulting and related tilting. The masses owe their low structural position to the combined effects of pre-Quaternary normal faults and large-scale reverse drag in the hanging wall of the Hurricane fault. The largest body occupies a graben between two pre-Quaternary normal faults (figure 27), and covers a pre-intrusion, west-side-down normal fault that tilted and repeated section of the Claron Formation.

The western fault has stratigraphic separation of about 150 meters. A splay of this fault displaces early Quaternary alluvial-fan deposits by approximately 30 to 45 meters, indicating continued motion or reactivation during early Quaternary time (see discussion of Ash Creek graben above).

Structural Relations

To the north along much of the Ash Creek geometric segment, the strike of the Hurricane fault is ~N21°E. To the south along much of the Anderson Junction geometric segment, the fault strikes ~N12°W. Stratigraphic separation decreases markedly across this segment boundary (figure18), which is indicative of a boundary that has been a persistent barrier to slip (King, 1986).

Near the Toquerville bend (figure 25), it is clear that the Hurricane fault had significant offset prior to emplacement of the Quaternary basalt flows. In the footwall, the basalt occupies a paleochannel (visible here) in the (gray) Permian rocks. In the hanging wall (near the last stop), a section of basalt that is geochemically identical to that visible on the footwall overlies Triassic – Jurassic strata (Schramm, 1994; Stewart and Taylor, 1996). This stratigraphic difference indicates that the hanging-wall block was down-dropped relative to the footwall and that significant erosion of the footwall took place prior to basalt emplacement. The stratigraphic separation of the basalt across the fault is presently ~ 450 meters. The stratigraphic separation of the Navajo Sandstone is in the range of 1,740 – 2,070 meters (Stewart and Taylor, 1996). Therefore, only about one-quarter of the total stratigraphic separation in this area occurred since emplacement of the basalt.

The basalt can be used as a wide line to form a broad piercing point, because it had a limited original distribution. Using the geochemically identical basalt sections here and just to the SSW on the hanging wall, Stewart and Taylor (1996) determined a post-basalt slip vector ranging between 73°, N70°W and 75°, S18°W. This vector range is consistent with the limited number of slickenlines observed on the fault surface.

Long-Term Slip Rate Determined from Displaced Quaternary Basalt

The basalts flows here exhibit reverse magnetization, and paleomagnetic vector analysis shows the hanging-wall basalt tilts 25 degrees toward the fault around a northeasterly trending axis, with little or no tilting of the footwall basalt (Lund and others, 2001, appendix C). Visual examination and dip measurements of the basalts in the hanging wall showed a pronounced tilt toward the fault in a relatively narrow zone - a few hundred meters wide - adjacent to the fault. Basalts west of the zone of back-tilting dip as much as 7 degrees toward the fault, but those dips mimic the slope of the alluvial-fan surfaces on which the flows were extruded.

Lund and Everitt (1998) recognized a zone of relatively small-displacement synthetic and antithetic faults in the basalts and alluvial-fan units in the hanging wall of the Hurricane fault below the radio towers and extending north from the Toquerville geometric bend. Hurlow and Biek (2000) mapped these faults at 1:24,000-scale in the Pintura quadrangle, which includes the Radio Towers site. Pairs of antithetic and synthetic faults in the hanging wall form several small grabens that roughly parallel the main Hurricane fault and define a zone of extensional stress along the axis of an asymmetric anticline created by reverse-drag folding in the hanging wall. Dip measurements in the basalt confirm the presence of the anticline, the axis of which defines the western limit of pronounced back-tilting toward the Hurricane fault.

Lund and others (2001) sampled the uppermost basalt flow in the hanging wall at the base of the Hurricane Cliffs directly below the Radio Towers site. The basalt yielded an ^{40}Ar/^{39}Ar whole-rock age of 0.81 $\pm$ 0.1 Ma.

The highest elevation on basalt west of the zone of back-tilting in the hanging wall is approximately 1,217 meters. The highest elevation on top of the correlative basalt in the footwall is approximately 1,585 meters. For their slip-rate calculation, Lund and others (2001) used the difference between those two elevations (368 m) as their value for net slip.
.

The slip rate at South Black Ridge for the past 810 thousand years is:

368,000 mm/810,000 yr = 0.45 mm/yr

Because this slip rate is at a structural and possibly seismogenic fault boundary (Stewart and Taylor, 1996; Reber and others, 2001), it may or may not be typical of the long-term slip history of the proposed fault segments on either side of the boundary.
.
Turn around and return along same route to SR-17.

1.7	19.4	Pass fork on left (east) and continue along dirt road.

3.0   22.4   Cross cattle guard and continue southwest.

0.6   23.0   **Turn right (N)** off Spring Drive back onto SR-17 and immediately cross bridge over Ash Creek.

0.6   23.6   Road cut through the red Jurassic Navajo Sandstone. Near here dark-colored Quaternary basalt and bright orange-tan Quaternary dunes are visible.

1.8   25.4   **End SR-17, enter on ramp to I-15N.** Proceed north on I-15 paralleling the Hurricane Cliffs (Black Ridge). Hurricane fault is near the base of the cliffs, this is the Ash Creek segment of the Hurricane fault.

1.8   27.2   Quartz monzonite of the Pine Valley laccolith and orange and white Tertiary Claron Formation flank I-15 here. Both of these units are in the hanging wall of the Hurricane fault.

1.3   28.5   Hurricane fault at 2:00 between the dark-colored Quaternary basalt and the gray Permian rocks. This hanging wall basalt is geochemically distinct from Quaternary basalt in the footwall on the cliff top to the north. Because the basalts here are not correlative they were not used to calculate a long-term slip rate for the Hurricane fault.

4.3   32.8   Tree-covered hill at 9:00 is a cinder cone. Lund and Everitt (1998) designated this the MP-35 (milepost 35) cinder cone. This cone is the only known volcanic vent in the hanging wall of the Ash Creek segment, and is the likely source of much of the basalt in this area.

1.8   34.6   **Take Exit 36, Ranch Exit, to the right.**

0.1   34.7   Park near stop sign at bottom of off ramp.

   STOP 2-5. North Black Ridge (Kolob Arch 7.5' quadrangle, T39S, R12W, section 16)
   This stop is at about the midpoint of the proposed Ash Creek fault segment. Looking to the east, the Black Ridge (Hurricane Cliffs) in the Hurricane fault footwall consists of grayish tan Permian (Kaibab Formation) and reddish brown Mesozoic (Moenkopi and Chinle Formations) rocks capped by Quaternary basalt at the skyline. The sedimentary units and the Hurricane fault are covered by basalt talus, and in many places by hummocky topography that represents landslide deposits. The basalt exposed in road cuts here and in the walls of Ash Creek Gorge a few tens of meters west of this stop are in the fault hanging wall and are geochemically correlative with the basalt at the skyline (Lund and others, 2001, appendix B).
   Lund and Everitt (1998) sampled the basalts in the footwall and the hanging wall and obtained $^{40}Ar/^{39}Ar$ age estimates of 0.84 $\pm$ 0.03 Ma and 0.88 $\pm$ 0.05 Ma, respectively (figure 28). The two-sigma age uncertainties overlap and the two ages are considered analytically indistinguishable. Lund and others (2001) averaged the two age estimates for their slip rate calculation, and used 860 thousand years for the age of the basalts at this location.
   Magnetic vectors obtained from the basalts in the footwall and hanging wall document 10 degrees of back-tilt toward the fault in the hanging wall around a northeasterly trending axis (Lund
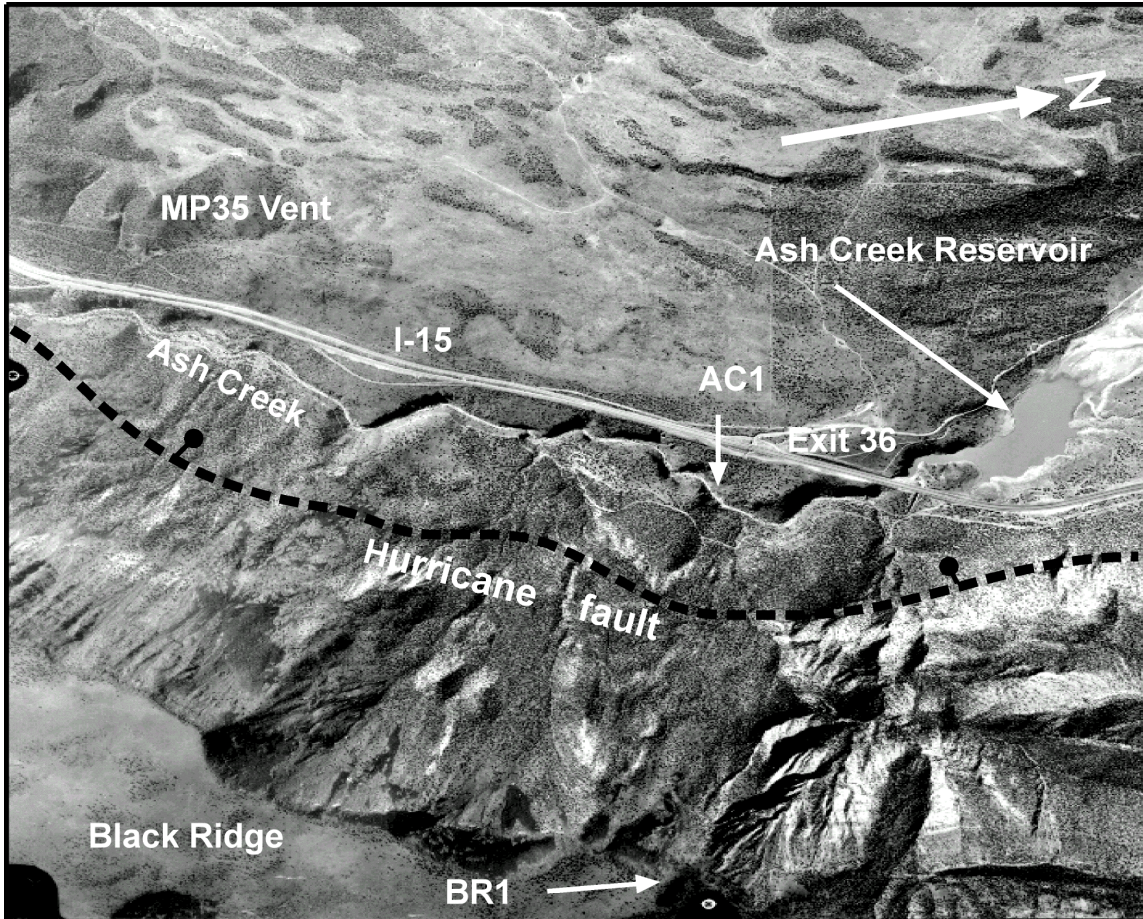
Figure 28. Oblique aerial view of North Black Ridge showing the location of the MP35 vent and 40Ar/39Ar isotopic age sample locations BR1 and AC1. Ages: BR1 = 0.84 myr; AC1 = 0.88 myr.

and others, 2001; appendix C). There is no indication of tilting in the footwall basalt. Visual examination of the basalts in the hanging wall showed that the zone of near-fault deformation is relatively narrow (a few hundred meters). Within a short distance west of the Exit 36 off ramp, the dip of the basalt toward the fault is generally less than 3 degrees, corresponding to the slope of the ground surface over which the basalt was extruded.

West of Exit 36 the basalt is displaced by a number of small synthetic and antithetic faults (Grant, 1995; Lund and Everitt, 1998). The displacement across these faults ranges from a few meters to possibly as much as ten meters. However, the faults are generally paired creating small graben; therefore, Lund and others (2001) consider the total net slip across this zone of secondary faulting minimal and of little net effect on slip-rate calculations.

Because the zone of near-fault deformation in the hanging wall is relatively narrow (a few hundred meters at most), Lund and others (2001) chose a basalt location at an elevation of 1,475 meters which, based on paleomagnetic analysis, visual observation, and dip measurements, is clearly west of the zone of near-fault deformation. They projected the basalt from that point at a dip of 3 degrees approximately 200 meters to the estimated location of the Hurricane fault, which at this site is buried by young landslide deposits. The resulting elevation of the basalt in the hanging wall at the Hurricane fault is 1,465 meters. Using that elevation and an elevation of 1,951 meters on top of the basalt in the footwall, results in a net slip across the fault at the north end of Black Ridge of 486 meters.

The slip rate at the north end of Black Ridge for the past 860 thousand years is:

64

<div align="center">486,000 mm/860,000 yr = 0.57 mm/yr</div>

This slip rate is substantially higher than those obtained for the Anderson Junction segment at Grass Valley and Pah Tempe Hot Springs, and at the proposed segment boundary at the Toquerville geometric bend (table 1). It is also higher than Lund and Everitt's (1998) estimated slip rate of 0.39 mm/yr, but is based on information that was not available to them at the time of their earlier estimate.

1.9	36.6	Rounded peak at ~11:00 is the Tertiary Stoddard Mountain stock/laccolith, one of a series of Miocene intrusions that continues from the Pine Valley laccolith ~NE into the Colorado Plateau. These Miocene intrusions form the "iron axis", named for the abundant hematite-magnetite replacement bodies and veins formed within and adjacent to the intrusions. The iron deposits comprise the Iron Springs mining district, which was exploited from 1923 until the late 1970s.
1.5	38.1	Pass exit to Kolob entrance to Zion National Park. A strand of the Ash Creek segment of the Hurricane fault lies near the base of the cliff to the right (E).
1.5	39.6	**Take Exit 42 to the right (E).**
0.5	40.1	**Turn right (E)** at bottom of off ramp. Follow signs to Kanarraville.
0.1	40.2	**Turn left (~N).**
2.0	42.2	The Hurricane Cliffs on the right are formed mostly by gray Permian carbonates.
1.9	44.1	Enter Kanarraville.
0.8	44.9	Leave Kanarraville. At 2:00, the stratigraphic section is overturned in the footwall of the Hurricane fault. The Triassic Moenkopi Formation (red and tan) lies beneath the gray Permian Kaibab Limestone.
2.5	47.4	**Turn right (~SE)** onto Murie Creek road (dirt).
1.0	48.4	Park on the right side of the road.

STOP 2-6. Coyote Gulch (Kanarraville 7.5' quadrangle, T37S, R12W, section 25)

Coyote Gulch is at the north end of the Ash Creek segment at the mouth of a small ephemeral drainage issuing from the Hurricane Cliffs about 1 kilometer southwest of Murie Creek. We will walk south along the Hurricane Cliffs to the best fault scarps formed on unconsolidated deposits on the Ash Creek segment. As we do, notice the rock units exposed in the cliff face in the fault footwall, the grayish tan Kaibab Formation and reddish brown Moenkopi Formation, which are overturned in the east limb of the Sevier-age Kanarra anticline.

The intermittent stream that flows from Coyote Gulch has deposited a young alluvial fan at the base of the Hurricane Cliffs (figure 29). The fan surface is displaced down-to-the-west across a partially buried approximately 3-meter-high, probable single-event fault scarp (Lund and Everitt, 1998). A few tens of meters north of the alluvial fan, a colluvial deposit at the base of the Hurricane Cliffs is also faulted and is displaced 10 meters down-to-the-west on a single fault strand. The two scarps at Coyote Gulch represent the best opportunity for developing detailed paleoseismic information at the north end of the Hurricane fault; however, the site is on private land and is not available for trenching.

Because they were unable to trench, Lund and others (2001) attempted to determine a maximum limiting age for the timing of the MRE at Coyote Gulch by dating the displaced alluvial-fan sediments. The fan is incised about 1.5 meters by the intermittent stream issuing from the gulch. The soil formed on the fan is very weakly developed, exhibiting minor rubification in a thin
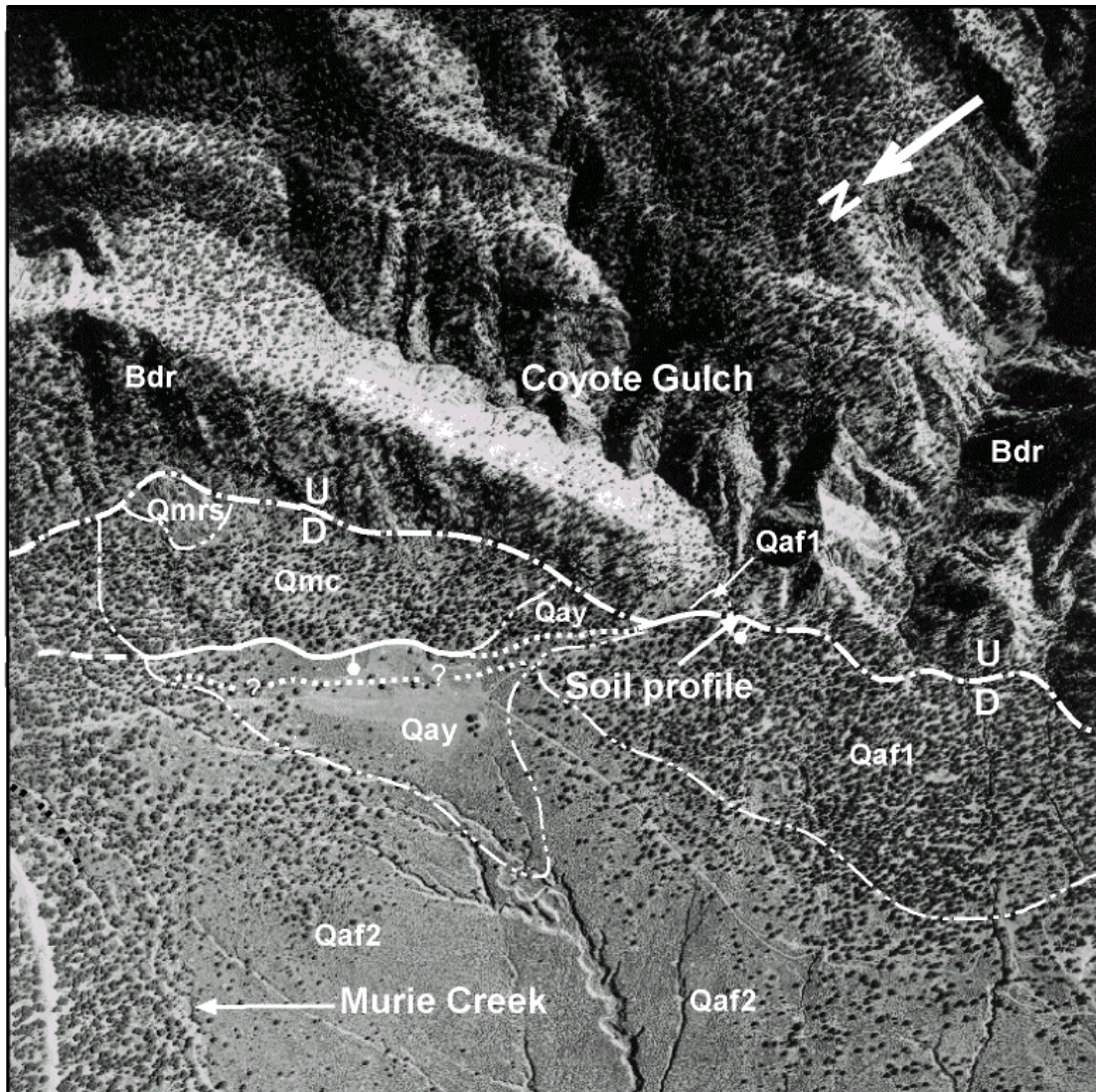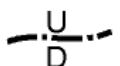
EXPLANATION

GEOLOGIC UNITS
Qay   Young alluvium
Qaf1 Young alluvial-fan deposits
Qaf2 Older alluvial-fan deposits
Qmc   Slope colluvium
Qmrs Rock slide deposit (?)
Bdr   Bedrock, undifferentiated

1/4 Mile

SYMBOLS

Geologic contact

Normal fault, bar and ball on downthrown side, dashed where approximately located, dotted where buried or inferred

U
D
Main trace Hurricane fault, approximately located ; U = upthrown side, D = down-thrown side of fault.

Figure 29. Photo-geologic map of the Coyote Gulch site on the Hurricane fault, Utah, showing soil profile location.

66

Btw horizon, a weak Bk horizon that shows Stage I or Stage I-minus carbonate development, and generally weak or absent soil structure (figure 30).

A bulk sediment sample collected from an interval 15 to 128 centimeters below the fan surface yielded three very small fragments of detrital charcoal. None of the fragments were individually large enough for accelerator mass spectrometer (AMS) radiocarbon dating, so they were combined for dating. The combined sample yielded a conventional AMS radiocarbon age of 1,220±40 yr B.P. (Beta-140468), which calendar calibrates to 1,260 to 1,055 cal B.P. (cal A.D. 690 to 895). The calibrated age represents a maximum limiting age on the timing of the MRE at Coyote Gulch. The MRE occurred after 1,055 to 1,260 cal B.P., but how long after is unknown, nor is the actual age of the fan known, other than it is younger than the detrital charcoal contained within it.
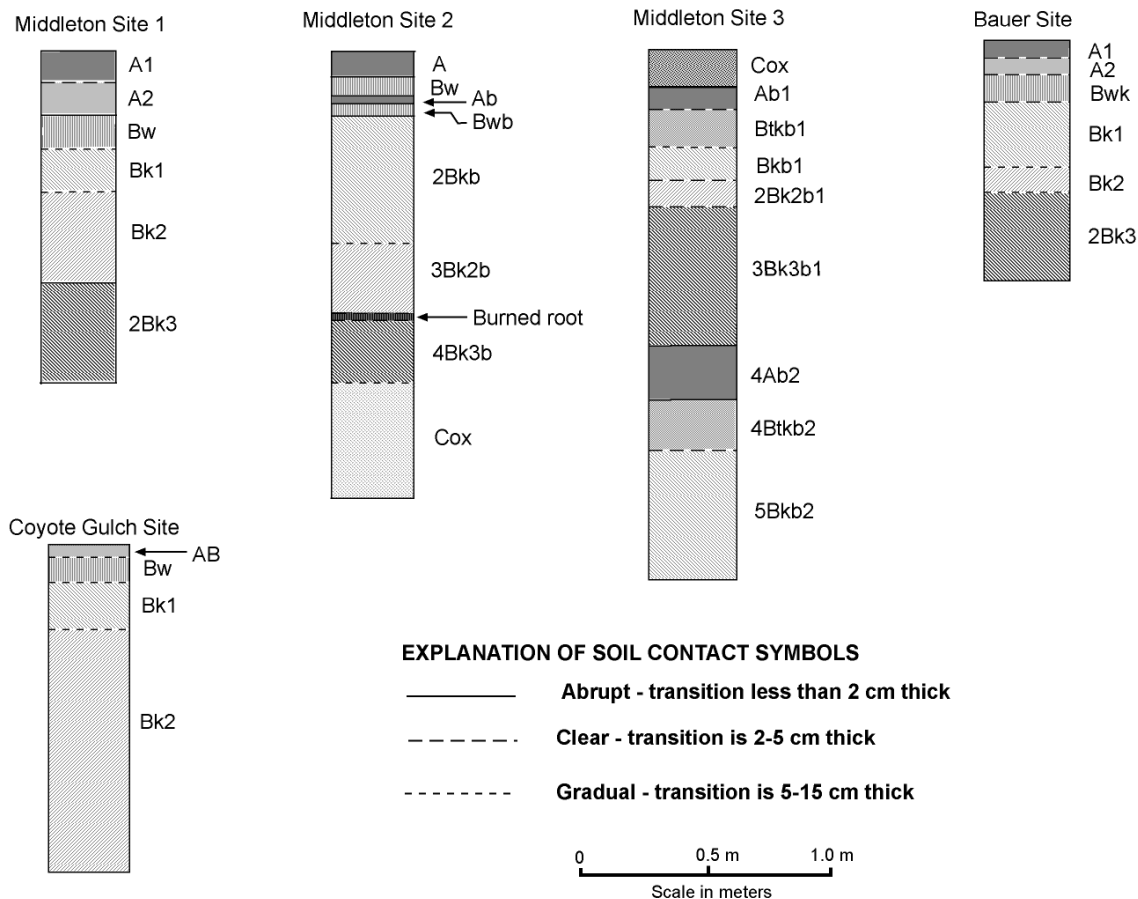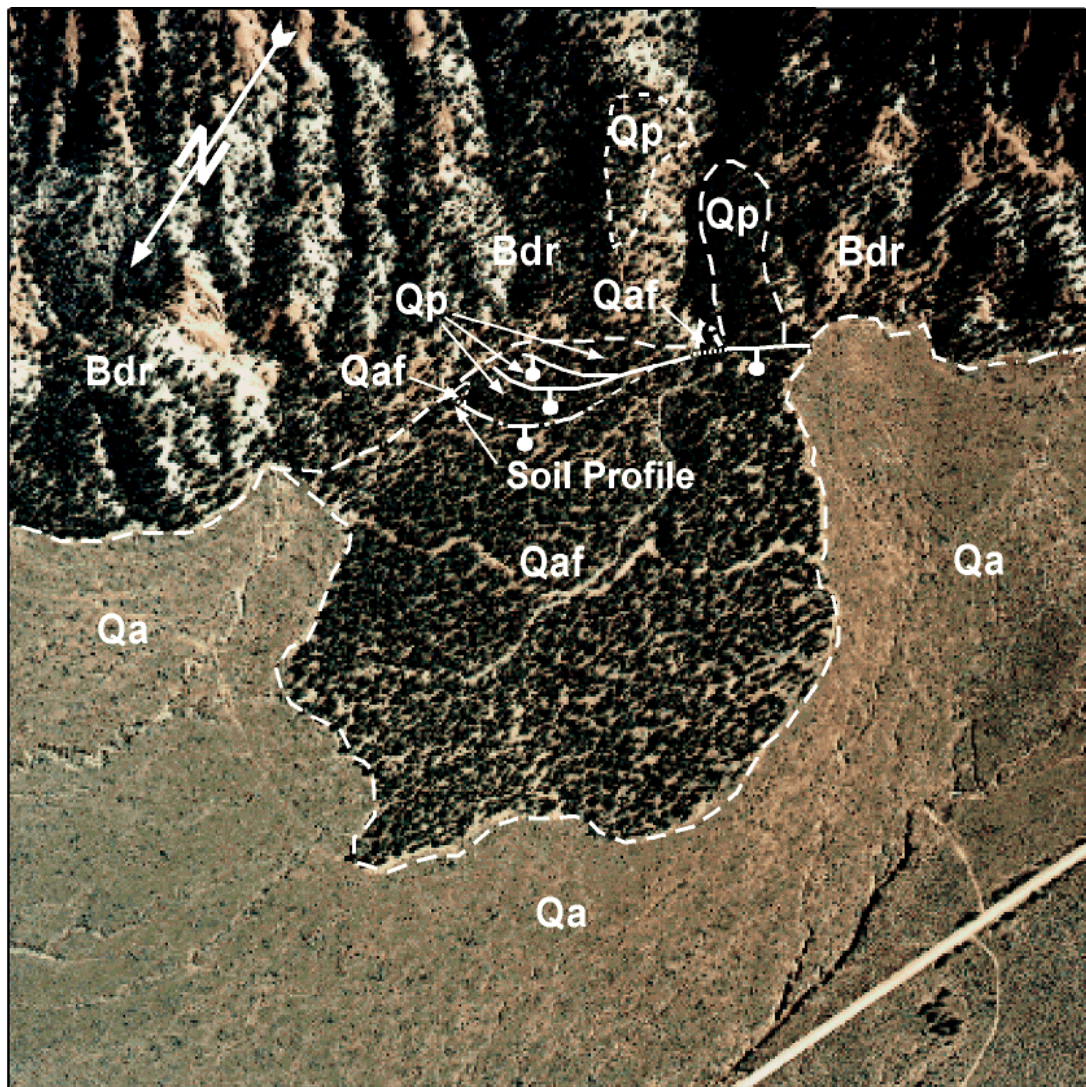

Figure 30. Soil profiles measured at the Coyote Gulch, Bauer, and Middleton sites, Hurricane fault, Utah.

A scarp profile recorded a net slip of 2.75 meters across the single-event scarp at Coyote Gulch (Lund and Everitt, 1998). Data on event displacement are limited for the Hurricane fault in Utah, but the 2.75 meters measured here is the largest observed on the proposed Ash Creek segment, and if not the maximum value, it is likely a close approximation. Employing Wells and Coppersmith's (1994) regression of displacement and moment magnitude for maximum displacement on a normal fault, and assuming that the 2.75 meters represents the maximum displacement during the MRE, Lund and others (2001) estimated a moment magnitude of M 6.9 for the event that displaced the fan surface. If the 2.75 meters represents the average

displacement, using the appropriate Wells and Coppersmith (1994) regression for average displacement on a normal fault produces a moment magnitude of M 7.1.

Return to cars and proceed approximately east along the Murie Creek road.

0.6   49.0   The Hurricane fault displaces Quaternary basalt at 2:00. Basalt in the footwall is found on the cliffs at 1:00. Source of the basalt is a cinder cone at the top of the cliffs. This is Lund and others (2001) Section 19 site. Anderson and Mehnert (1979) also studied this site. Lund and others (2001) best estimate for a slip rate here is 0.37-0.51 mm/yr (table 1), depending on which basalt in the footwall is selected as being "in place."

0.2   49.2   Stay left at fork in the road by corrals (~ straight).

0.3   49.5   T intersection with a road from the right (~SE). Stay left (~ straight).

0.4   49.9   Y intersection, take the right fork (~ E).

0.1   50.0   Continue straight (left) toward wooden structure that is part of an old coal tram and tipple. Coal mined on Cedar Mountain was trammed to the valley floor here during the 1930s and 1940s.

0.2   50.2   At base station for coal tram, stay left (~NW).

0.3   50.5   Bauer Site at 1:00 (Lund and others, 2001)
                The Bauer site is in section 17, T. 37 S., R. 11 W. (Cedar Mountain 7.5' quadrangle), at the mouth of two small unnamed ephemeral drainages issuing from the Hurricane Cliffs about 2.6 kilometers southwest of Shurtz Creek. The drainages dissect a late Quaternary alluvial fan. The pediment/fan surface is displaced 5.5 meters down-to-the-west across three strands of the Hurricane fault (figure 31). The unnamed ephemeral streams have combined to deposit a young alluvial fan at the base of the Hurricane Cliffs where they enter the valley. The fan apex extends up the northernmost drainage a short distance, burying the western fault strand where it crosses the stream channel.
                Lund and others (2001) described the soil formed on the young alluvial fan. The soil is poorly developed, exhibiting some rubification in a thin Btw horizon, a weak Bk horizon expressed as Stage I or Stage I-minus carbonate development, and generally weak soil structure (figure 30). A bulk sediment sample collected from the soil 13 to 60 centimeters below the ground surface yielded several small fragments of detrital charcoal. Only one charcoal fragment was large enough to permit AMS radiocarbon dating. The charcoal fragment provided a conventional AMS radiocarbon age of 420$\pm$40 yr B.P. (Beta-140469), which calendar calibrates to both cal A.D. 1425 to 1515 (cal B.P. 525 to 435) and cal A.D. 1590 to 1620 (cal B.P. 360 to 330). Because the alluvial-fan deposit is not displaced, the calibrated age represents a minimum limiting age on the timing of the MRE at the Bauer site. The MRE occurred sometime before ~360 to 525 cal B.P., but how much before is not known, and because the charcoal was detrital, the deposit is younger than the AMS age estimate.

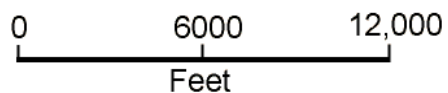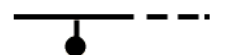1.6   52.1   Pull off on the right side of the road.

Figure 31. *Photo-geologic map of the Bauer site, Hurricane fault, Utah. Showing soil profile location (geology after Averitt, 1962).*

STOP 2-7. Shurtz Creek Overview (Cedar Mountain 7.5' quadrangle, T37S, R11W, section 9)

Shurtz Creek is on the newly proposed Cedar City seismogenic fault segment (figure 6). In the Hurricane Cliffs to the east, Mesozoic sedimentary rocks crop out in the Shurtz Creek drainage basin. Formations include the relatively soft Moenkopi and Chinle Formations with the more resistant Moenave, Kayenta, and Navajo Formations cropping out at higher elevations. The Sevier orogeny has deformed these units, and the axis of the Shurtz Creek (Kanarra) anticline (Averitt, 1962) is just east of and parallels the Hurricane fault, which lies at the base of the Hurricane Cliffs. Above these deformed units lie relatively undeformed Cretaceous and Cenozoic rocks including Quaternary basalt at the skyline. The Shurtz Creek pediment (Averitt, 1962) developed in the Shurtz Creek amphitheater, an area of relatively low elevation (middle distance) formed in the Hurricane Cliffs on the softer Mesozoic rock units.

The pediment is covered with large basalt boulders and is displaced across a 13-meter-high scarp (figure 32). Two ages of alluvial deposits are on the downthrown side of the fault; an active alluvial fan along Shurtz Creek, and an older alluvial deposit south of and a few meters higher than the young alluvial fan. This older alluvial surface is also covered with large basalt boulders. Lund and Everitt (1998) hypothesized that the older alluvial surface is correlative with the pediment surface in the footwall. Test pits showed that soils on both surfaces have moderate to well-developed argillic and calcic horizons, and gypsum is leached from both profiles confirming they are both older than Holocene. Soil colors are lighter (indicating more $CaCO_3$), moist consistence is firmer (indicating higher secondary clay content), and clay films are more abundant in the pediment soil. Additionally, pH is < 8 to a depth of 26 centimeters on the upthrown side, but < 8 only to a depth of 8 centimeters for the soil on the downthrown block, indicating that $CaCO_3$ removal has been more extensive on the upthrown side of the fault. The pediment soil exhibited Stage III carbonate development, while the soil on the downthrown block only reached Stage II. Based on these differences, the soil on the upthrown block is estimated to be up to twice as old as the soil on the downthrown block and therefore the surfaces are not correlative (Lund and Everitt, 1998).

Lund and Everitt (1998) sampled both surfaces at Shurtz Creek for [26]Al (sandstone) and [36]Cl (basalt) isotope abundances. The [26]Al abundances clustered around 15,000 to 18,000 years. The [36]Cl samples clustered at about 25,000 years. These young ages conflict with the soil-profile data, which argue for significantly older surface ages. Based on soil-profile development, the age of the upper surface is estimated at 80,000 to 100,000 years, and the age of the lower surface is estimated at about 50,000 years (Lund and Everitt, 1998). These estimates are in general agreement with ages assigned by Machette (1985a, 1985b) to soils with similar $CaCO_3$ accumulations in the Beaver Basin 90 kilometers north of Shurtz Creek. The difference between the estimated soil ages and the cosmogenic isotope data is difficult to explain, but likely reflects the effect of presently poorly understood ongoing geomorphic processes on the two surfaces.

The Shurtz Creek scarp has a maximum slope angle of 28 degrees, and a minimum net vertical tectonic displacement (NVTD) of 10.5 meters (Lund and Everitt, 1998). Because the surfaces on either side of the fault are not correlative, the scarp height and NVTD are minimum values, and a slip rate calculated using the NVTD data would also be a minimum value. Additionally, neither the time interval since the most recent surface-faulting earthquake, nor the interval between development of the pediment surface and the first surface-faulting earthquake are known. Together those two intervals could represent several thousand years, and combine to leave the pediment surface age open ended across two seismic cycles (the first and the most recent events). A slip rate calculated using the age of the pediment surface would therefore be a minimum value because the slip actually occurred over a shorter time interval than the age of the surface. Because both the net-slip data and the pediment surface age tend to produce minimum values, a slip rate calculated using the combination of those data would give a minimum "best

EXPLANATION

GEOLOGIC UNITS

Qa	Valley-fill alluvium
Qaf1	Young alluvial-fan deposit
Qaf2	Older alluvial-fan deposit
Qp	Pediment-mantle deposit
Bdr	Bedrock, undifferentiated

1/4 Mile

SYMBOLS

—··—··— Geologic contact

Shurtz Creek anticline

—•— — — Normal fault, bar and ball on downthrown side, dashed where approximately located

Figure 32. Photo-geologic map of the Shurtz Creek site, Hurricane fault, Utah, showing trench location (geology after Averitt, 1962).

approximation" of late Quaternary fault slip at Shurtz Creek. The wide variation in age estimates for the pediment surface (cosmogenic versus geomorphic and soils) makes it possible to significantly change the slip rate value obtained by changing the time interval selected for the age of the surface. Choosing a younger age would give a higher slip rate, while selecting an older age would give a slower slip rate. Based on geomorphic expression and a lack of young appearing scarps north and south of Shurtz Creek, Lund and others (2001) chose 100,000 years as a "best estimate" for the age of the pediment surface, resulting in a minimum late Quaternary slip rate at Shurtz Creek of 0.11 mm/yr.

Trenching at Shurtz Creek (see figure 32 for trench location) to better constrain the slip rate and determine other paleoseismic parameters for the proposed Cedar City segment was hampered by large basalt boulders in the subsurface that limited the trench depth to less than 1.5 meters, preventing exposure of the fault zone (Lund and others, 2001). Because basalt boulders are ubiquitous along the scarp, Lund and others (2001) concluded that the chances of successful trenching anywhere on the Shurtz Creek scarp were low and rejected further excavation there. The remaining scarps on the Cedar City segment were also rejected because of access problems and equally prohibitive geologic constraints.

Mobil Shurtz Creek Seismic Reflection Line

A seismic-reflection line by Mobil Exploration and Production Services U.S., Inc. (now part of ExxonMobil) crosses the Hurricane fault here (figure 33). Mobil collected this and several other seismic-reflection lines during a 1979-1981 data-acquisition program; the UGS recently obtained several of these lines as part of a hydrogeologic study of the Cedar City area (Hurlow, 2000; Hurlow, 2001).

Interpretation of the Mobil Shurtz Creek seismic-reflection line (figure 32) suggests that the Hurricane fault merges downward with a Late Cretaceous-Paleocene thrust ramp. The Hurricane fault may reactivate the listric thrust plane, or it may be relatively planar, departing from the thrust plane as its dip shallows to the northwest. This unresolved question has important implications for the seismic-hazard potential of the Hurricane fault in this area; the risk of a large earthquake is significantly greater in the planar-fault interpretation.

A Late Cretaceous-Paleocene anticline occupies the hanging wall of the Hurricane fault, as revealed by the geometry of reflectors and nearby outcrops and exploration wells. South of the Shurtz Creek line, the Oligocene-Eocene Claron Formation depositionally overlies the Jurassic Navajo Sandstone (Averitt, 1967; Anderson and Mehnert, 1979), as observed along the axis of the Pintura anticline to the south (Stop 2-3). The angular unconformity between the Claron Formation and underlying Mesozoic rocks shows that the anticline is at least in part pre-Tertiary. Normal displacement of the Permian-Triassic boundary is substantial. Refinement of the geologic interpretation of the Shurtz Creek seismic-reflection line and depth conversion would permit construction of a retrodeformable cross section, yielding substantial new information about the structural evolution of this area.

Continue north along the same road.

0.8   52.9   Bulldog fault expressed in basalt at 9:00 (Averitt, 1962).

0.5   53.4   Middleton site at ~ 1:00 (Lund and others, 2001).

             The Middleton site is in section 4, T37S, R11W (Cedar Mountain 7.5' quadrangle) at the mouth of an unnamed drainage issuing from the Hurricane Cliffs about 1.3 kilometers northeast of Shurtz Creek. The drainage dissects a late Quaternary surface mapped by Averitt (1962) as "pediment deposits in the Shurtz Creek amphitheater." The pediment surface is displaced 12.7 meters down-to-the-west across three strands of the Hurricane fault (Lund and Everitt, 1998; figure 34). The stream has deposited a young alluvial fan at the base of the cliffs where it enters the valley. The alluvial fan and an alluvial terrace that extends up the drainage from the fan apex combine to bury all three of the fault strands where they cross the stream and are not displaced.

Northwest   Southeast

A. Wave-migrated time section

B. Geologic interpretation
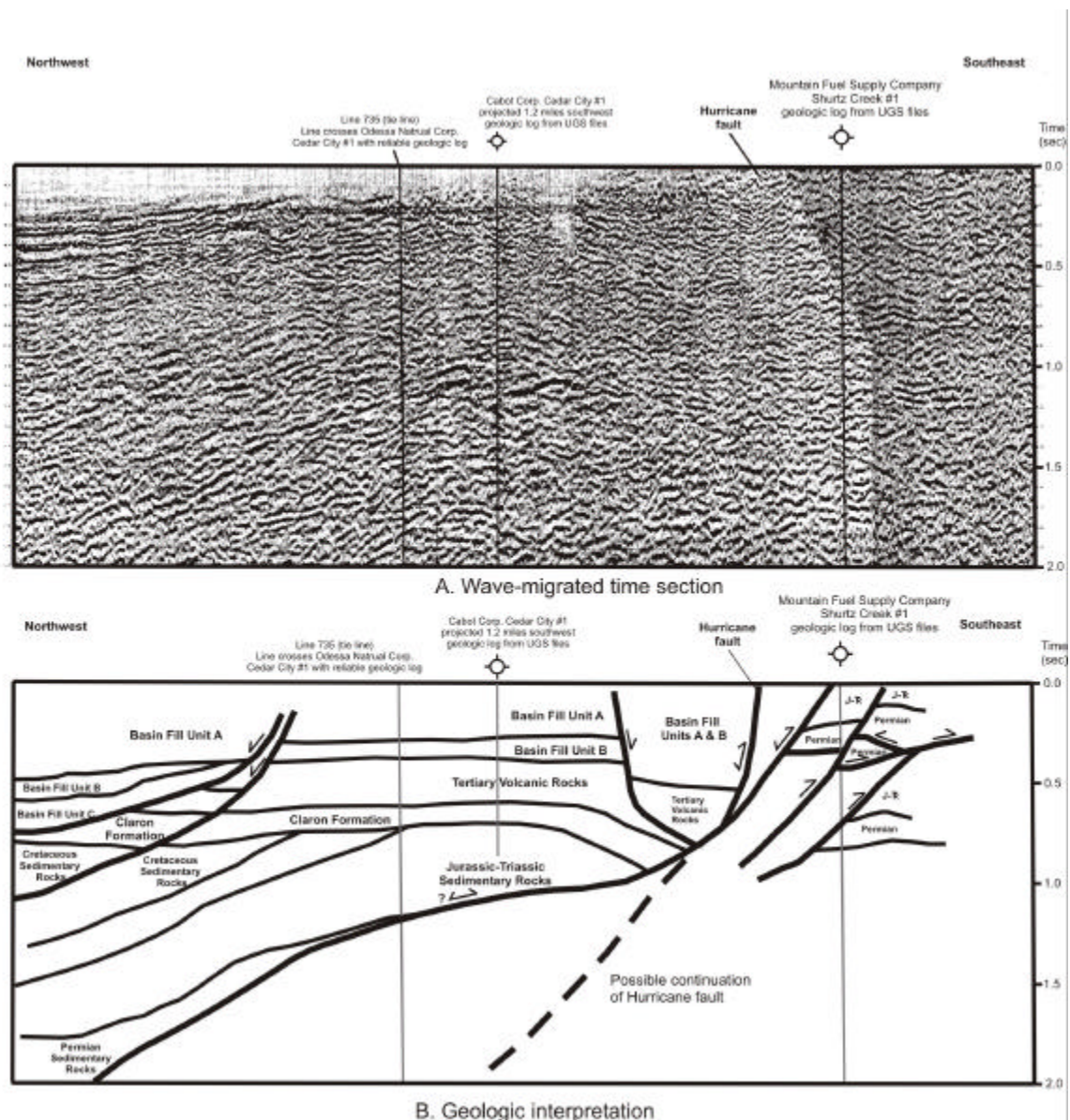
Figure 33. Wave-migrated time section(A) and geologic interpretation (B) of Mobil Shurtz Creek seismic-reflection line 81MM-738. The geologic interpretation was made on a 1:12,000-scale plot of the wave-migrated time section. The image shown in (A) is a scanned and reduced version of that plot, and is of considerably lower quality than the original plot.

Lund and others (2001) described three soil profiles at the Middleton site (figure 30), two on the young alluvial-fan deposit, and the third on the stream terrace. The profiles on alluvial-fan deposits consisted chiefly of coarse-grained debris-flow and debris-flood sediment. The stream terrace profile consisted chiefly of coarse fluvial and debris-flow material.

Lund and others (2001) submitted charcoal collected from the stream terrace profile for AMS radiocarbon dating. The charcoal came from the A horizon of a buried paleosol formed on a debris-flow/flood deposit at a depth of
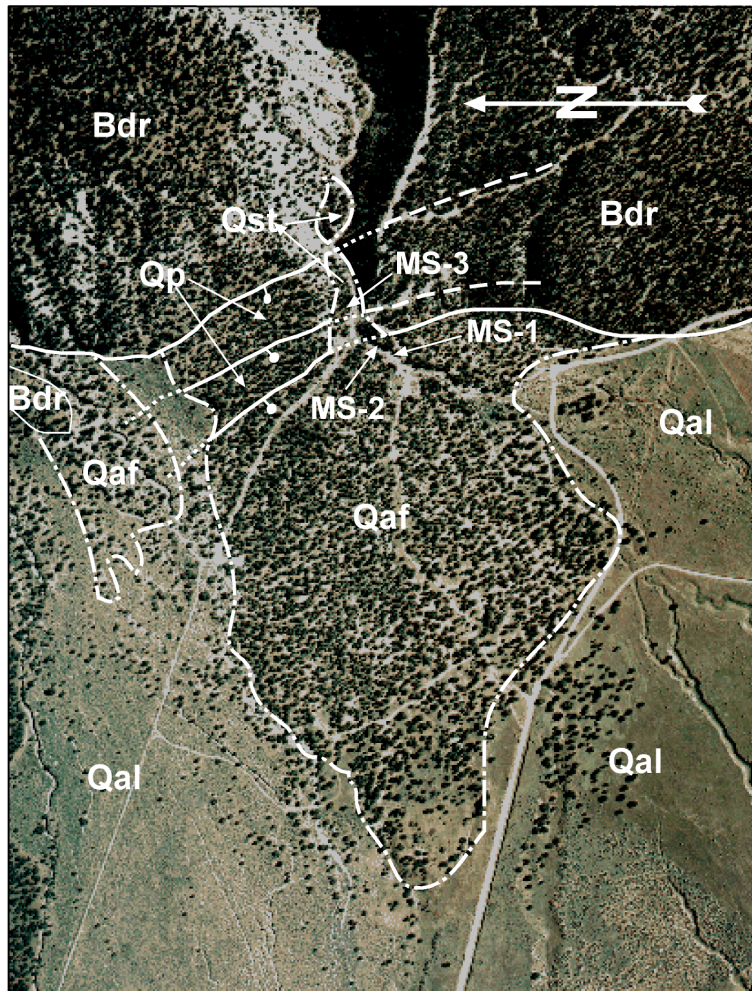
73

Figure 34. Photo-geologic map of the Middleton site, Hurricane fault, Utah showing the locations of soil profiles MS-1, Ms-2, and MS-3 (geology after Averitt, 1962).

117-139 centimeters. They selected this charcoal sample for dating because charcoal obtained from a soil A horizon is likely primary, accumulating during the soil-forming process, rather than detrital, having been entrained within a debris flow or flood and carried to the site from another location. The charcoal from the paleosol A horizon yielded a conventional AMS radiocarbon age of 1,710±40 yr B.P. (Beta-140470), which calendar calibrates to cal A.D. 240 to 420 (cal B.P. 1,710 to 1,530). This calibrated age represents a minimum limiting age for the timing of the MRE at Middleton.

The timing of the MRE at the Middleton site is older than the MRE at Coyote Gulch a few kilometers to the south. This difference in MRE timing is the principal evidence for the newly proposed Cedar City segment of the Hurricane fault.

1.0	54.4	**Turn right (N)** onto paved road at T intersection and proceed toward Cedar City.
2.1	56.5	Late Pleistocene Green Hollow landslide at 9:00.
0.3	56.8	**Turn right (~N)** at intersection with Main Street and proceed into Cedar City. After the turn, note the Cedar City-Parowan monocline at 12:00.
0.9	57.7	Continue straight on Main (N) through stop light at 800 South.
0.3	58.0	Continue straight on Main (N) through stop light at 600 South.
0.2	58.2	Lupita's Mexican restaurant is on the right (E). Highly recommended by Bill. I bought Wanda her lunch there when we did our dry run of this trip and I think she agrees.
0.4	58.6	Continue straight on Main (N) through stop light at 200 South.
0.2	58.8	**Turn right (E)** at the intersection of Main and Center Streets. Proceed toward the Hurricane Cliffs following SR-14 up Cedar Canyon. The close bluffs are formed on Triassic Moenkopi Formation and Jurassic Navajo Sandstone.
0.5	59.3	We are crossing the Hurricane fault and entering the structural transition zone between the Basin and Range and the Colorado Plateau physiographic provinces.
0.3	59.6	At 9:00, the steeply dipping red to brown Moenkopi Formation is in the east limb of the Kanarra anticline.
0.3	59.9	Tan-gray Shinarump Conglomerate is on the left (N) with the purple-brown Petrified Forest Member of the Triassic Chinle Formation just beyond.
0.3	60.2	Contact between the Navajo Sandstone and the underlying Kayenta Formation is visible here.
0.5	60.7	Deformed Jurassic Carmel Formation containing thick deposits of white gypsum on the left (N). Several high-grade gypsum claims have been staked in this area.
1.6	62.3	Anticline on the right (S).
1.0	63.3	Cliffs on the left (N) are composed of Cretaceous sandstone.
0.4	63.7	Continue up canyon past road to the right that leads to Right Hand Canyon.
1.9	65.6	On the right (S) is a fault in Cretaceous units, just before milepost 7. On the east side of the fault, green and red mudstones of the nonmarine middle member of the Dakota Formation are flat lying. On the west (down) side of the fault, sandstone with interbedded thin coal seams of the Tibbet Canyon Member of the Straight Cliffs Formation are dragged nearly vertical (Eaton and others, 2001). At 10:00 the orange-colored Tertiary Claron Formation can be seen up a side canyon.

0.8   66.4   Pull off in wide spot on left side of the road.

STOP 2-8. Cedar Canyon Basalt (Flanigan Arch 7.5' quadrangle, T36S, R10W, section 25)

At this site, 12 kilometers east of Cedar City in the footwall of the Hurricane fault, erosion on Coal Creek has left a basalt remnant isolated high on a cliff above the stream on the north side of Cedar Canyon (figure 35).   Coal Creek is graded to Cedar Valley and crosses the Hurricane fault at the mouth of Cedar Canyon. Lund and others (2001) believe that the rate of downcutting on Coal Creek is directly related to the rate of displacement on the Hurricane fault, which changes the stream's base level following each surface-faulting earthquake. Therefore, the rate of stream downcutting provides a surrogate slip rate for the Hurricane fault at Cedar City. However, because Cedar Valley is a closed basin, this slip rate is considered a minimum value due to the simultaneous filling of the valley, which slows the rate of downcutting from the maximum it would achieve if the sediment were carried away by a through-going drainage system.
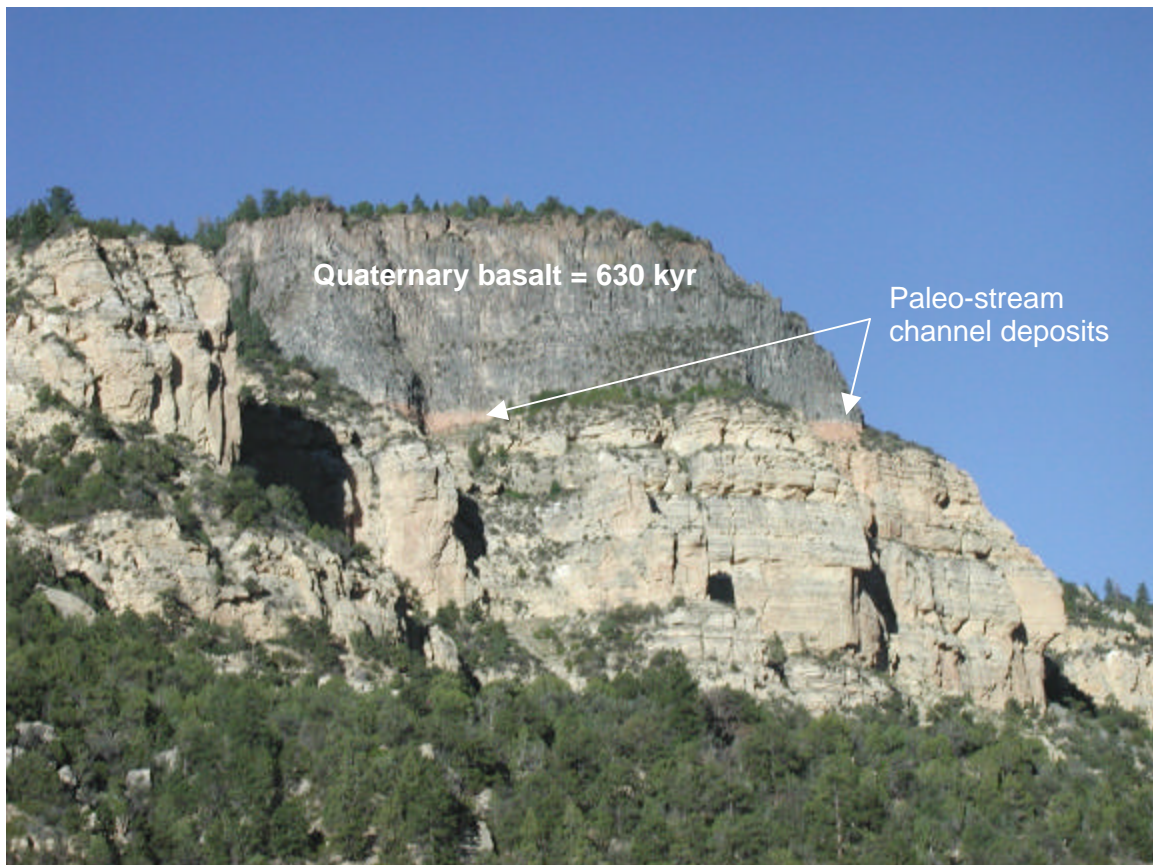
Figure 35.   Remnant of 0.63 Ma basalt flow occupying a paleo-stream channel high on the north side of Cedar Canyon near milepost 7 on SR-14 east of Cedar City, Utah.

Lund and others (2001) sampled the base of the basalt remnant in Cedar Canyon for both geochemistry and $^{40}Ar/^{39}Ar$ age analysis. Because the remnant is well outside the influence of near-fault deformation in the fault footwall, back-tilting is not an issue.   The basalt flow (possibly two stacked flows) occupies a narrow paleo-valley in Cretaceous bedrock and rests directly on paleo-channel deposits of Coal Creek. Diverted from its course by the basalt flow, Coal Creek eroded the soft Cretaceous sandstone adjacent to the basalt, and now occupies a new channel 335 meters below its former valley.   The geochemical data show that the basalt

remnant is unrelated to any of the other basalt flows analyzed along the Hurricane fault. The ^{40}Ar/^{39}Ar analysis yielded an age of 0.63 $\pm$ 0.10 Ma.

The rate of downcutting by Coal Creek, which provides a surrogate minimum slip rate for the Hurricane fault, is:

$$335,000 \text{ mm}/630,000 \text{ yr} = 0.53 \text{ mm/yr}$$

Although considered a minimum value, this slip rate is generally comparable with the other rates obtained from displaced basalts north of the proposed seismogenic boundary between the Anderson Junction and Ash Creek segments at the Toquerville geometric bend.

Turn around and return to Cedar City (W) on SR-14.

3.4	69.8	Fault at 1:00 in Moenkopi Formation (red next to yellow-tan)
3.6	73.4	Enter Cedar City on SR-14/Center Street.
0.6	74.0	Continue straight on Center Street (W) through stop light at intersection between Center and Main streets.
0.3	74.3	Continue straight on Center Street (W) through stop light at intersection with 300 West.
0.4	74.7	Continue straight on Center Street (W) through stop light at intersection with 800 West.
0.2	74.9	**Turn left (S)** onto 1150 West.
0.2	75.1	**Turn right (W)** into parking lot on SUU campus.

End trip.

REFERENCES

Amoroso, Lee, Pearthree, P.A., and Arrowsmith, J.R., 2002, Paleoseismology and neotectonics of the Shivwitz section of the Hurricane fault, Mohave County, northwestern Arizona: Arizona Geological Survey Open-File Report 02-05, 92 p., 1 sheet, scale 1:24,000.

Anderson, R.E., and Christenson, G.E., 1989, Quaternary faults, folds, and selected features in the Cedar City 1°x2° quadrangle, Utah: Utah Geological and Mineral Survey Miscellaneous Publication 89-6, 29 p.

Anderson, R.E., and Mehnert, H.H., 1979, Reinterpretation of the history of the Hurricane fault in Utah, *in* Newman, G. W., and Goode, H. D., editors, 1979 Basin and Range Symposium: Rocky Mountain Association of Geologists, p. 145-165.

Arabasz, W.J., and Julander, D.R., 1986, Geometry of seismically active faults and crustal deformation within the Basin and Range-Colorado Plateau transition in Utah, *in* Meyer, Larry, editor, Cenozoic Tectonics of the Basin and Range Province: A Perspective on Processes and Kinematics of an Extensional Origin: Boulder, Geological Society of America, Special Paper 208, p. 43-74.

Armstrong, R.L., 1968, Sevier orogenic belt in Nevada and Utah: Geological Society of America Bulletin, v. 79, p. 429-458.

Averitt, Paul, 1962, Geology and coal resources of the Cedar Mountain quadrangle, Iron County, Utah: U.S. Geological Survey Professional Paper 389, 71 p., 3 plates, scale 1:24,000.

_____, 1964, Table of post-Cretaceous geologic events along the Hurricane fault, near Cedar City, Iron County, Utah: Geological Society of America Bulletin, v. 75, p. 901-908.

    , 1967, Geology of the Kanarraville quadrangle, Iron County, Utah: U.S. Geological Survey Map GQ-694, 1 plate, scale 1:24,000.

Best, M.G., and Brimhall, W.H., 1974, Late Cenozoic alkalic basaltic magmas in the western Colorado Plateaus and Basin and Range transition zone, U.S.A., and their bearing on mantle dynamics: Geological Society of America Bulletin, v. 85, no. 11, p. 1677-1690.

Best, M.G., McKee, E.H., and Damon, P.E., 1980, Space-time composition patterns of late Cenozoic mafic volcanism, southwestern Utah and adjoining areas: American Journal of Science, v. 280, p. 1035-1050.

Biek, R.F., 1997, Interim geologic map of the Harrisburg Junction quadrangle, Washington County, Utah: Utah Geological Survey Open-file Report 353,123 p., scale 1:24,000.

    , 1998, Interim geologic map of the Hurricane quadrangle, Washington County, Utah: Utah Geological Survey Open-File Report, scale 1:24,000.

Billingsley, G.H., 1991, Geologic map of the Sullivan Draw North quadrangle, northern Mohave County, Arizona: U.S. Geological Survey Open-File Report 91-558, scale 1:24,000.

    , 1992a, Geologic map of the Gyp Pocket quadrangle, northern Mohave County, Arizona: U.S. Geological Survey Open-File Report 92-412, scale 1:24,000.

    , 1992b, Geologic map of the Rock Canyon quadrangle, northern Mohave County, Arizona: U.S. Geological Survey Open-File Report 92-449, scale 1:24,000.

    , 1993a, Geologic map of the Wolf Hole Mountain and vicinity, Mohave County, northwestern Arizona, U.S. Geological Survey Map I-2296, scale 1:31,680.

    ,, Geologic map of the Russell Spring quadrangle, northern Mohave County, Arizona: U.S. Geological Survey Open-File Report 93-717, scale 1:24,000.

    , 1993c, Geologic map of the Dutchman Draw quadrangle, northern Mohave County, Arizona: U.S. Geological Survey Open-File Report 93-587, scale 1:24,000.

    , 1993d, Geologic map of the Grandstand quadrangle, northern Mohave County, Arizona: U.S. Geological Survey Open-File Report 93-588, scale 1:24,000.

    , 1994a, Geologic map of the Antelope Knoll quadrangle, northern Mohave County, Arizona: U.S. Geological Survey Open-File Report 94-449, scale 1:24,000.

    , 1994b, Geologic map of the Moriah Knoll quadrangle, northern Mohave County, Arizona: U.S. Geologic Survey Open-File Report 94-634, scale 1:24,000.

Billingsley, G.H., and Workman, J.B., 2000, Geologic map of the Littlefield 30'x60' quadrangle, Mohave County, northwestern Arizona, with accompanying 25 page booklet: U.S. Geological Survey Miscellaneous Investigation Series Map I-2628, scale 1:100,000.

Birkeland, P.W., 1984, Soils and geomorphology: New York, Oxford University Press, 372 p.

Burgmann, R., Pollard, D.D., and Martel, S.J., 1994, Slip distributions on faults - Effects of stress gradients, inelastic deformation, heterogeneous host-rock stiffness, and fault interaction: Journal of Structural Geology, v. 16, p. 1675 -1690.

Cartwright, J.A., Mansfield, C.S., and Trudgill, B. D., 1996, The growth of normal faults by segment linkage, *in* Buchanan, P.G., and Nieuwland, D.A., editors, Modern developments in structural interpretation, validation, and modeling: Geological Society of America Special Publication, v. 99, p. 163-177.

Cartwright, J.A., Trudgill, B.D., and Mansfield, C.S., 1995, Fault growth by segment linkage; an explanation for scatter in maximum displacement and trace length data from the Canyonlands grabens of SE Utah: Journal of Structural Geology, v. 17, p. 1319-1326.

Childs, C., Watterson, J., and Walsh, J.J., 1995, Fault overlap zones within developing normal fault systems: Journal of the Geological Society of London, v. 152, pt. 3, p. 535-549.

Christenson, G.E., 1992, Geologic hazards of the St. George area, Washington County, Utah, *in* Harty, K.M., editor, Engineering and environmental geology of southwestern Utah: Utah Geological Association Publication 21, p. 99-107.

Christenson, G.E., editor, 1995, The September 2, 1992 M_L 5.8 St. George earthquake: Utah Geological Survey Circular 88, 41 p.

Christenson, G.E., and Deen, R.D., 1983, Engineering geology of the St. George area, Washington County, Utah: Utah Geological and Mineral Survey Special Studies 58, 32 p., 2 plates.

Christenson, G.E., Harty, K.M., and Hecker, Suzanne, 1987, Quaternary faults and seismic hazards in western Utah, *in* Kopp, R.S., and Cohenour, R.E., 1987, Cenozoic geology of

western Utah - Sites for precious metal and hydrocarbon accumulation: Utah Geological Association Publication 16, p. 389-400.

Christenson, G.E., and Nava, S.J., 1992, Earthquake hazards of southwestern Utah, *in* Harty, K.M., editor, Engineering and environmental geology of southwestern Utah: Utah Geological Association Publication 21, p. 123-137.

Cook, E.F., 1953, Pine Valley laccolith, Washington County, Utah: Geological Society of America Bulletin, v. 64, p.1543.

⸻, 1957, Geology of the Pine Valley Mountains, Utah: Utah Geological and Mineralogical Survey Bulletin, v. 58, 111 p.

⸻, 1960, Geologic atlas of Utah, Washington County: Utah Geological and Mineralogical Survey Bulletin, v. 70, 119 p., 1 plate, scale 1:125,000.

Cordova, R.M., 1981, Ground-water conditions in the upper Virgin River and Kanab Creek basins area, Utah, with emphasis on the Navajo Sandstone: State of Utah, Department of Natural Resources, Technical Publication No. 70, 87 p.

Cowie, P.A., 1998, A healing-reloading feedback control on the growth rate of seismogenic faults: Journal of Structural Geology, v. 20, p. 1075-1087.

Cowie, P.A., and Roberts, G.P., 2001, Constraining slip rates and spacings for active normal faults: Journal of Structural Geology, v. 23, p. 1901-1915.

Cowie, P.A., and Scholz, C.H., 1992a, Displacement-length scaling relationship for faults; data synthesis and discussion: Journal of Structural Geology, v. 14, p. 1149-1156.

⸻, 1992b, Growth of faults by accumulation of seismic slip: Journal of Geophysical Research, v. 97, p. 11,085-11,095.

Cowie, P.A., Sornette, D., and Vanneste, C., 1995, Multifractal scaling properties of a growing fault population: Geophysical Journal International, v. 122, p. 457-469.

Dawers, N.H., Anders, M.H., and Scholz, C.H., 1993, Growth of normal faults - Displacement-length scaling: Geology, v. 21, p. 1107-1110.

dePolo, C.M., Clark, D.G., Slemmons, D.B., and Ramallie, A., 1991, Historical Basin and Range Province surface faulting and fault segmentation: Journal of Structural Geology, v. 13, p. 123-136.

Downing, R.F., Smith, E.I., Orndorff, R.I., Spell, T.L., and Zanetti, K.A., 2001, Imaging the Colorado Plateau – Basin and Range transition zone using basalt geochemistry, geochronology and geographic information systems, *in* Erskine, M.C., Faults, J.E., Bartley, J.M., and Rowley, P.D., editors, The geologic transition, High Plateaus to Great Basin – A symposium and field guide (The Mackin Volume): Utah Geological Association Publication 30 and Pacific Section American Association of Petroleum Geologists Publication GB 78, p. 127-154.

DuBois, S.M., Smith, A.W., Nye, N.K. and Nowak, T.A., 1982, Arizona earthquakes, 1776-1980: Arizona Bureau of Geology and Mineral Technology Bulletin 193, 456 p.

Dutton, C.E., 1880, Report on the geology of the high plateaus of Utah: Washington D.C., Department of the Interior, U.S. Geographical and Geological Survey of the Rocky Mountain Region (Powell), 307 p., atlas.

Earth Sciences Associates, 1982, Seismic safety investigation of eight SCS dams in southwestern Utah: Portland, Oregon, unpublished consultant's report for the U.S. Soil Conservation Service, 2 vols.

Eaton, J.G., Laurin, J., Kirkland, J.I., Tibert, N.E., Leckie, R.M., Sageman, B.B.,   Goldstrand, P.M., Moore, D.W., Straub, A.W., Cobban, W.A., and Dalebout, J.D., 2001, Cretaceous and early Tertiary geology of Cedar and Parowan Canyons, western Markagunt Plateau, Utah, *in* Erskine, M.C., Faulds, J.E., Bartley, J.M., and Rowley, P.D., editors, The geologic transition, High Plateaus to Great Basin - A symposium and field guide (The Mackin Volume): Utah Geological Association Publication 30 and Pacific Section of the American Association of Petroleum Geologists Guidebook GB 78, p. 337-364.

Fenton, C.R., Webb, R.H., Pearthree, P.A., Cerling, T.E., and Poreda, R.J., 2001, Displacement rates on the Toroweap and Hurricane faults - Implications for Quaternary downcutting in the Grand Canyon, Arizona: Geology, v. 29, p. 1035-1038.

Gile, L.H., 1994, Soils, geomorphology, and multiple displacements along the Organ Mountains fault in southern New Mexico: New Mexico Bureau of Mines and Mineral Resources Bulletin 133, 91 p.

Gile, L.H., and Grossman, R.B., 1979. The Desert Project soil monograph - Soils and landscapes of a desert region astride the Rio Grande Valley near Las Cruces, New Mexico: Soil Conservation Service Monograph, Department of Agriculture, 984 p.

Goldstrand, P.M., 1994, Tectonic development of Upper Cretaceous to Eocene strata of southwestern Utah: Geological Society of America Bulletin, v. 106, p. 145-154.

Grant, S. K., 1995, Geologic map of the New Harmony quadrangle, Washington County, Utah: Utah Geological Survey Miscellaneous Publication 95-2, 2 plates, scale 1:24,000.

Grant, S.K., Fielding, L.W., and Noweir, M.A., 1994, Cenozoic fault patterns in southwestern Utah and their relationships to structures of the Sevier orogeny, *in* Blackett, R.E., and Moore, J.N., editors, Cenozoic geology and geothermal systems of southwestern Utah: Utah Geological Association Publication 23, p. 139-153.

Gupta, S., Cowie, P.A., Dawers, N.H., and Underhill, J.R., 1998, A mechanism to explain rift-basin subsidence and stratigraphic patterns through fault-array evolution: Geology, v. 26, p. 595-598.

Hacker, D.B. 1998, Catastrophic gravity sliding and volcanism associated with the growth of laccoliths - examples from early Miocene hypabyssal intrusions of the Iron Axis magmatic province, Pine Valley Mountains, southwestern Utah: Kent, Ohio, Kent State University, Ph.D. thesis, 258 p., 5 plates.

Hamblin, W.K., 1963, Late Cenozoic basalts of the St. George basin, Utah, *in* Heylmun, E.B., editor, Geology of the southwestern transition between the Basin-Range and Colorado Plateau, Utah: Intermountain Association of Petroleum Geologists, Guidebook to the Geology of Southwestern Utah, p. 84-89.

———, 1965a, Tectonics of the Hurricane fault zone, Arizona-Utah: Geological Society of America Special Paper 82, 83 p.

———, 1965b, Origin of "reverse drag" on the downthrown side of normal faults: Geological Society of America Bulletin, v. 76, p. 1145-1164.

———, 1970a, Late Cenozoic basalt flows of the western Grand Canyon, *in* Hamblin, W.K., and Best, M.G., editors, The western Grand Canyon region: Utah Geological Society Guidebook to the Geology of Utah, no. 23, p. 21-37.

———, 1970b, Structure of the western Grand Canyon region, *in* Hamblin, W.K., and Best, M.G., editors, The western Grand Canyon region: Utah Geological Society Guidebook to the Geology of Utah, no. 23, p. 3-20.

———, 1984, Direction of absolute movement along the boundary faults of the Basin and Range - Colorado Plateau margin: Geology, v. 12, p. 116-119.

———, 1987, Late Cenozoic volcanism in the St. George Basin, Utah: Geological Society of America Centennial Field Guide - Rocky Mountain Section, p. 291-294.

Hamblin, W.K., and Best, M.G., 1970, The western Grand Canyon District: Utah Geological Society, Guidebook to the Geology of Utah, no. 23, 156 p.

Hamblin, W.K., Damon, P.E., and Bull, W.B., 1981, Estimates of vertical crustal strain rates along the western margin of the Colorado Plateau: Geology, v. 9, p. 293-298.

Hanks, T.C., 2000, The age of scarp-like landforms from diffusion-equation analysis, *in* Noller, J. S., Sowers, J. M., and Lettis, W.R., editors, Quaternary geochronology: Methods and applications: Washington D.C., American Geophysical Union, p. 313-338.

Hanks, T.C., Bucknam, R.C., Lajoie, K.R., and Wallace, R.E., 1984, Modification of wave-cut and faulting-controlled landforms: Journal of Geophysical Research, v. 89, p. 5771-5790.

Hecker, Suzanne, 1993, Quaternary tectonics of Utah with emphasis on earthquake-hazard characterization: Utah Geological Survey Bulletin 127, 157 p., 2 plates.

Higgins, J.M., 1998, Interim geologic map of the Washington Dome quadrangle, Washington County, Utah: Utah Geological Survey Open-file Report 363, 106 p., scale 1:24,000.

———, 2000, Interim geologic map of The Divide 7.5' quadrangle, Washington County, Utah: Utah Geological Survey Open-File Report 378, 61 p., scale 1:24,000.

Huntington, Ellsworth, and Goldthwait, J.W., 1904, The Hurricane fault in southwestern Utah: Journal of Geology, v. 11, p. 45-63.

_____, 1905, The Hurricane fault in the Toquerville district, Utah: Harvard College, Bulletin of the Museum of Comparative Zoology, v. 42, p.199-259.

Huntoon, P., 1990, Phanerozoic structural geology of the Grand Canyon, *in* Beus, S. S., and Morales, M., editors, Grand Canyon Geology: New York, Oxford University Press/Museum of Northern Arizona, p. 261-309.

Hurlow, H.A., 1998, The geology of the central Virgin River basin, southwestern Utah, and its relation to ground-water conditions: Utah Geological Survey Water-Resources Bulletin 26, 53 p., 6 plates.

_____, 2000, Complex evolution of Neogene extensional faulting and basin subsidence in the eastern Basin and Range Province, Cedar Valley, southwestern Utah – Evidence from seismic reflection data [abs]: Geological Society of America Abstracts with Programs, v. 32, no. 7, p. A-506.

_____, 2001, Influence of Neogene extensional structure and stratigraphy on the hydrogeology of Cedar Valley, southwestern Utah [abs]: Geological Society of America Abstracts with Programs, v. 33, no. 5, p. A-16.

Hurlow, H.A., and Biek, R.F., 2000, Interim geologic map of the Pintura quadrangle, Washington County, Utah: Utah Geological Survey Open-File Report 375, 67 p., scale 1:24,000.

Jackson, J., and Leeder, M., 1994, Drainage systems and the development of normal faults - An example from Pleasant Valley, Nevada: Journal of Structural Geology, v. 16, p. 1041-1059.

King, G.C.P., 1986, Speculations on the geometry of the initiation and termination processes of earthquake rupture and its relation to morphology and geological structure: Pageoph, v. 124, p. 567–583.

Kurie, A. E., 1966, Recurrent structural disturbance of the Colorado Plateau margin near Zion National Park, Utah: Geological Society of America Bulletin, v. 77, p. 867-872.

Larsen, P.H., 1988, Relay structures in a Lower Permian basement-involved extension system, east Greenland: Journal of Structural Geology, v. 10, p. 3-8.

Lay, Thorne, Ritsema, J., Ammon, C.J., and Wallace, T.C., 1994, Rapid source mechanism analysis of the April 29, 1993 Cataract Creek (Mw 5.3), northern Arizona earthquake: Bulletin of the Seismological Society of America, v. 84, p. 451-457.

Lovejoy, E.M.P., 1964, The Hurricane fault zone and the Cedar Pocket-Shebit-Gunlock fault complex, southwestern Utah and northwestern Arizona: Tucson, Arizona, University of Arizona Ph.D. dissertation, 195 p., scale 1:125,000.

Lund, W.R., and Everitt, B.L., 1998, Reconnaissance paleoseismic investigation of the Hurricane fault in southwestern Utah, *in* Pearthree and others, 1998, Paleoseismic investigations of the Hurricane fault in southwestern Utah and northwestern Arizona - Final Project Report: Arizona Geological Survey (Tucson) and Utah Geological Survey (Salt Lake City), Final Technical Report to the U.S. Geological Survey National Earthquake Hazard Reduction Program, Award No. 1434-HQ-97-GR-03047, p. 8-48.

Lund, W.R., Pearthree, P.A., Amoroso, Lee, Hozik, M.J., and Hatfield, S.C., 2001, Paleoseismic investigation of earthquake hazard and long-term movement history of the Hurricane fault, southwestern Utah and northwestern Arizona: Utah Geological Survey (Salt Lake City) and Arizona Geological Survey (Tucson), Final Technical Report to the U.S. Geological Survey National Earthquake Hazard Reduction Program, Award No. 99HQGR0026, 71 p., 5 appendices.

Machette, M.N., 1985a, Calcic soils of the southwestern United States, *in* Weide, D.L., Farber, M.L., editors, Soils and Quaternary geology of the southwestern United States: Geological Society of America Special Paper 203, p. 1-21.

_____, 1985b, Late Cenozoic geology of the Beaver basin, southwestern Utah: Brigham Young University Geology Studies, v.32, pt. 1, p. 19-37.

Machette, M.N., Personius, S.F., and Nelson, A.R., 1992, Paleoseismology of the Wasatch fault zone – A summary of recent investigations, interpretations, and conclusions, *in* Gori, P.L., and Hays, W.W., editors, Assessment of regional earthquake hazard and risk along the Wasatch Front, Utah: U.S. Geological Survey Professional Paper 1500, p. A1-A59.

Maerten, L., Gillespie, P., and Pollard, D.D., 2002, Effects of local stress perturbation on secondary fault development: Journal of Structural Geology, v. 24, p. 145-153.

Mansfield, C., and Cartwright, J., 2001, Fault growth by linkage: Observations and implications from analogue models: Journal of Structural Geology, v. 23, p. 745 – 763.

Mayer, L., 1985, Tectonic geomorphology of the Basin and Range-Colorado Plateau boundary in Arizona, *in* Morisawa, M., and Hack, J.T., editors, Tectonic geomorphology - Proceedings of the 15th Annual Binghamton Geomorphology Symposium, September 1984: Boston, Allen and Unwin, p. 235-259.

McCalpin, J.P., and Nelson, A.R., 1996, Introduction to Paleoseismology, *in* McCalpin, J.P., editor, Paleoseismology: San Diego, Academic Press, p. 1-32.

McCalpin, J.P., Zuchiewicz, W., and Jones, L.C.A., 1993, Sedimentology of fault-scarp derived colluvium from the Borah Peak rupture, central Idaho: Journal of Sedimentary Petrology, v. 63, no. 1, p. 120-130.

McDuffie, S., and Marsh, B.D., 1991, Pine Valley Mountain laccolith; a thick, dacitic, phenocryst-rich body [abs]: Eos, Transactions, American Geophysical Union, v. 72, p. 316.

Menges, C.M., and Pearthree, P.A., 1983, Map of neotectonic (latest Pliocene-Quaternary) deformation in Arizona: Arizona Bureau of Geology and Mineral Technology Open-File Report 83-22, 48 p. booklet, 2 plates.

Nash, D. B., 1980, Morphologic dating of degraded normal fault scarps: Journal of Geology, v. 88, p. 353-360.

Ostenaa, Dean, 1984, Relationships affecting estimates of surface fault displacement based on scarp-derived colluvium deposits [abs]: Geological Society of America Abstracts with Programs, v. 16, no. 5, p. 327.

Peacock, D.C.P., 1991, Displacements and segment linkage in strike-slip fault zones: Journal of Structural Geology, v. 13, p. 1025-1035.

Peacock, D.C.P., and Sanderson, D.J., 1991, Displacements, segment linkage, and relay ramps in normal fault zones: Journal of Structural Geology, v. 13, p. 721-733.

_____, 1994, Geometry and development of relay ramps in normal fault zones: American Association of Petroleum Geologists Bulletin, v. 78, p. 147-165.

_____, 1996, Effects of propagation rate on displacement variations along faults: Journal of Structural Geology, v. 18, p. 311-320.

Pearthree, P.A., 1998, Quaternary fault data and map for Arizona: Arizona Geological Survey Open-File Report 98-24, 122 p., scale 750,000.

Pearthree, P.A., and Bausch, D.B., 1999, Earthquake hazards in Arizona: Arizona Geological Survey Map M-34, scale 1:1,000,000.

Pearthree, P.A., Lund, W.R., Stenner, H.D., and Everitt, B.L., 1998, Paleoseismic investigation of the Hurricane fault in southwestern Utah and northwestern Arizona - Final project report: Arizona Geological Survey (Tucson) and Utah Geological Survey (Salt Lake City), Final Technical Report to the U.S. Geological Survey National Earthquake Hazard Reduction Program, Award No. 1434-HQ-97-GR-03047, 131 p.

Pearthree, P.A., Menges, C.M., and Mayer, Larry, 1983, Distribution, recurrence, and possible tectonic implications of late Quaternary faulting in Arizona: Arizona Bureau of Geology and Mineral Technology Open-File Report 83-20, 36 p.

Pechmann, J.C., Arabasz, W.J., and Nava, S.J., 1995, Seismology, *in* Christenson, G.E., editor, The September 2, 1992 M_L 5.8 St. George earthquake, Washington County, Utah: Utah Geological Survey Circular 88, p. 1.

Pollard, D.D., and Aydin, A., 1984, Propagation and linkage of oceanic ridge segments: Journal of Geophysical Research, v. 89, p. 10,017-10,028.

Pollard, D.D., and Segall, P., 1987, Theoretical displacements and stresses near fractures in rock - With applications to faults, joints, veins, dikes, and solution surfaces, *in* Atkinson, B.K., editor, Fracture Mechanics of Rock: London, Academic Press, p. 277-349.

Reber, S., Taylor, W.J., Stewart, M., and Schiefelbein, I.M., 2001, Linkage and reactivation along the northern Hurricane and Sevier faults, southwestern Utah, *in* Erskine, M.C., Faults, J.E., Bartley, J.M., and Rowley, P.D., editors, The geologic transition, High Plateaus to Great Basin – A symposium and field guide (The Mackin Volume): Utah Geological Association Publication 30 and Pacific Section American Association of Petroleum Geologists Publication GB 78, p. 379-400.

Reynolds, S.J., Florence, F.P., Welty, J.W., Roddy, M.S., Currier, D.A., Anderson, A.V., and Keith, S.B., 1986, Compilation of radiometric age determinations in Arizona: Arizona Bureau of Geology and Mineral Technology Bulletin 197, 258 p., 2 sheets, scale 1:1,000,000.

Sanchez, Alexander, 1995, Mafic volcanism in the Colorado Plateau/Basin and Range transition zone, Hurricane, Utah: Las Vegas, Masters thesis, Department of Geoscience, University of Nevada, 92 p.

Schlische, R.W., 1993, Anatomy and evolution of the Triassic-Jurassic continental rift system, eastern North America: Tectonics, v. 12, p.1026-1042.

Schlische, R.W., and Anders, M.H., 1996, Stratigraphic effects and tectonic implications of the growth of normal faults and extensional basins, *in* Beratan, K.K., editor, Reconstructing the history of Basin and Range extension using sedimentology and stratigraphy: Geological Society of America Special Paper, v. 303, p. 183-203.

Schramm, M.E., 1994, Structural analysis of the Hurricane fault in the transition zone between the Basin and Range Province and the Colorado Plateau, Washington County, Utah: Las Vegas, Masters thesis, Department of Geosciences, University of Nevada, 90 p.

Schwartz, D.P., and Coppersmith, K.J., 1984, Fault behavior and characteristic earthquakes: Examples from the Wasatch and San Andreas fault zones: Journal of Geophysical Research, v. 89, p. 5681-5698.

Schwartz, D.P., and Crone, A.J., 1985, The 1983 Borah Peak earthquake: A calibration event for quantifying earthquake recurrence and fault behavior on Great Basin normal faults, *in* Stein, R.S. and Bucknam, R.C., editors, Proceedings of Workshop XXVIII on the Borah Peak, Idaho earthquake: U.S. Geological Survey Open-File Report 85-290, p. 153-160.

Segall, P., and Pollard, D.D., 1980, Mechanics of discontinuous faults: Journal of Geophysical Research, v. 85, p. 4337-4380.

Shipton, Z.K., and Cowie, P.A., 2001, Damage zone and slip-surface evolution over μm to km scales in high-porosity Navajo Sandstone, Utah: Journal of Structural Geology, v. 23, p. 1825-1844.

Smith, R.B., and Arabasz, W.J., 1991, Seismicity of the Intermountain seismic belt, *in* Slemmons, D.B., Engdahl, E.R., Zoback, M.D., and Blackwell, D.D., editors, Neotectonics of North America: Boulder, Colorado, Geological Society of America, Decade Map Volume, p. 185-228.

Smith, R.B., and Sbar, M.L., 1974, Contemporary seismicity in the Intermountain seismic belt: Geological Society of America Bulletin, v. 85, p. 1205-1218.

Sorauf, J.E., and Billingsley, G.H., 1991, Members of the Toroweap and Kaibab Formations, lower Permian, northern Arizona and southwestern Utah: The Mountain Geologist, v. 28, no. 1, p. 9-24.

Spencer, J.E., and Reynolds, S.J., 1989, Middle Tertiary tectonics of Arizona and adjacent areas, *in* Jenney, J. P., and Reynolds, S. J., editors, Geologic Evolution of Arizona: Tucson, Arizona Geological Society Digest 17, p. 539-574.

Stenner, H.D., Lund, W.R., Pearthree, P.A., and Everitt, B.L., 1999, Paleoseismologic investigations of the Hurricane fault in northwestern Arizona and southwestern Utah: Arizona Geological Survey Open-File Report. 99-8, 138 p.

Stewart, M.E., and Taylor, W.J., 1996, Structural analysis and fault segment boundary identification along the Hurricane fault in southwestern Utah: Journal of Structural Geology, v. 18, p. 1017-1029.

Stewart, M.E., Taylor, W.J., Pearthree, P.A., Solomon, B.J., and Hurlow, H.A., 1997, Neotectonics, fault segmentation, and seismic hazards along the Hurricane fault in Utah and Arizona: An overview of environmental factors in an actively extending region: Brigham Young University Geologic Studies 1997, v. 42, part II, p. 235-277.

Taylor, W.J., Stewart, M.E., and Orndorff, R.L., 2001, Definition of fault segments from bedrock data - Segmentation of the Hurricane fault, southwestern Utah and Northern Arizona: Utah Geological Association Publication 30, p. 113-126.

Timmons, J.M., Karlstrom, K.E., Dehler, C.M., Geissman, J.W., and Heizler, M.T., 2001, Proterozoic multistage (ca. 1.1 and 0.8 Ga) extension recorded in the Grand Canyon

Supergroup and establishment of northwest- and north-trending tectonic grains in the Southwestern United States: Geological Society of America Bulletin, v.113, p.163-180.

Trudgill, B., and Cartwright, J., 1994, Relay-ramp forms and normal-fault linkages, Canyonlands National Park, Utah: Geological Society of America Bulletin, v. 106, p. 1143-1157.

Wallace, R. E., 1977, Profiles and ages of young fault scarps, north-central Nevada: Geological Society of America Bulletin, v. 88, p. 1267-1281.

Walsh, J.J., and Watterson, J., 1987, Distributions of cumulative displacement and seismic slip on a single normal fault: Journal of Structural Geology, v. 9, p. 1039-1046.

_____, 1991, Geometric and kinematic coherence and scale effects in normal fault systems: Geological Society Special Publications, v. 56, p.193-203.

Walsh, J.J., Watterson, J., Bailey, W.R., and Childs, C., 1999, Fault relays, bends, and branch-lines: Journal of Structural Geology, v. 21, p. 1019-1026.

Wells, D.L., and Coppersmith, K.J., 1994, New empirical relationships between magnitude, rupture length, rupture width, rupture area, and surface displacement: Bulletin of the Seismological Society of America, v. 84, p. 974-1002.

Wenrich, K.J., Billingsley, G.H., Blackerby, B.A., 1995, Spatial migration and compositional changes of Miocene-Quaternary magmatism in the western Grand Canyon: Journal of Geophysical Research, v. 100, p.10,417-10,440.

Willemse, E.J.M., 1997, Segmented normal faults: Correspondence between three-dimensional mechanical models and field data: Journal of Geophysical Research, v. 102, p. 675-692.

Willemse, E.J.M, and Pollard, D.D., 2000, Normal fault growth; evolution of tipline shapes and slip distribution, in Lehner, F.K., and Urai, J.L., editors, Aspects of tectonic faulting: Springer,

Willemse, E.J.M., Pollard, D.D., Aydin, A., 1996, Three-dimensional analyses of slip distributions on normal fault arrays with consequences for fault scaling: Journal of Structural Geology, v. 18, p. 295-309.

Williams, J.S., and Trapper, M.L., 1953, Earthquake history of Utah: Bulletin of the Seismological Society of America, v. 43, p. 191-218.

Willis, G.C., and Higgins, J.M., 1995, Interim geologic map of the Washington quadrangle, Washington County, Utah: Utah Geological Survey Open-File Report 324, 2 plates, scale 1:24,000.

Yelken, M.A., 1996, Trace element analysis of selected springs in the Virgin River basin: M.S. thesis, University of Nevada, Las Vegas, 156 p.

Young, M.J., Gawthorpe, R.L., and Hardy, S., 2001, Growth and linkage of a segmented normal fault zone; the Late Jurassic Murchison-Statfjord North Fault, northern North Sea: Journal of Structural Geology, v. 23, p.1933-1952.

Zhang, P., Slemmons, D.B., and Mao, F., 1991, Geometric pattern, rupture termination, and fault segmentation of the Dixie Valley-Pleasant Valley active normal fault system, Nevada, U.S.A.: Journal of Structural Geology, v.13, no. 2, p. 165-176.

INFLUENCE OF PROTEROZOIC AND LARAMIDE STRUCTURES ON THE MIOCENE EXTENSIONAL STRAIN FIELD, NORTH VIRGIN MOUNTAINS, NEVADA / ARIZONA

2002 Geological Society of America Rocky Mountain Section Annual Meeting
Cedar City, Utah
May 4 to 6, 2002

Examining deformed North Virgin Mountain pillow basalts at the peak of Mount Bangs, 2.5 kilometers above sea level. Six kilometers to the west, equivalent Proterozoic rocks lie 5-6 kilometers below sea level in the Mesquite Basin of the Basin and Range Province. Two kilometers to the east, Proterozoic rocks lie one kilometer below sea level in the Colorado Plateau province. Development of this dramatic structural topography is one of the focuses of this trip.

Mark C. Quigley, University of New Mexico
Karl E. Karlstrom, University of New Mexico
Sue Beard, USGS Flagstaff
Bob Bohannon, USGS Denver

INFLUENCE OF PROTEROZOIC AND LARAMIDE STRUCTURES ON THE MIOCENE EXTENSIONAL STRAIN FIELD, NORTH VIRGIN MOUNTAINS, NEVADA / ARIZONA

**2002 Geological Society of America Rocky Mountain Section Annual Meeting
Cedar City, Utah
May 4 to 6, 2002**

**Mark C. Quigley, University of New Mexico
Karl E. Karlstrom, University of New Mexico
Sue Beard, USGS Flagstaff
Bob Bohannon, USGS Denver**

INTRODUCTION

This two-day field trip begins on the evening of May 4 and ends on the evening of May 6, 2002, in Cedar City, Utah. We will investigate the long-lived tectonic evolution of the North Virgin Mountains (NVM), approximately 5 kilometers east of Mesquite, Nevada, a northeast-trending basement-cored uplift straddling the Colorado Plateau – Basin and Range margin (figure 1). This trip will present the results of detailed structural mapping, U-Pb zircon and monazite geochronology, and Ar-Ar thermochronology, and examine how Proterozoic (circa 1,750 – 1,600 Ma) and Laramide (circa 70-55 Ma) – aged structures influenced the geometry of Miocene-aged extension and rapid exhumation of the North Virgin Mountains. We will examine a wide spectrum of rocks ranging from circa 1,700 Ma tectonic "mélanges" to middle Miocene conglomerates, in order to evaluate various aspects of the tectonic evolution of this region. We will spend two nights in Mesquite, Nevada, discussing the regional geologic and geochronologic context for the trip.

Figure 1. Location of the North Virgin Mountains, straddling the Arizona – Nevada border, and surrounding Proterozoic exposures (black) in the Beaverdam, Mormon, and South Virgin Mountains (Gold Butte Block).

The first day of the trip will begin in Cabin Canyon, in the core of a late Paleoproterozoic dextral-transpressive ductile shear zone. Here, we will investigate the complexly partitioned strain patterns in the context of regional Proterozoic tectonics. We will traverse the zone, discussing the shear sense and U-Pb monazite dating of the deformation events, and examine how the shear zone has been brittlely reactivated during Miocene deformation. We will conclude the morning with a brief look at syn-extensional Miocene conglomerates on the north flank of Bunkerville Ridge, and discuss how they provide time constraints on the exhumation of the Proterozoic core of the North Virgin Mountains (NVM), i.e. the Virgin Mountain anticline (VMA). This will be complemented by discussion of the apatite fission-track study conducted in the NVM in February 2001.

In the afternoon, we will drive to the north end of the NVM to examine Laramide contractional structures and various types of Miocene extensional structures. We will discuss the differences between "uplift" and "exhumation" of the VMA in terms of our structural, sedimentological, and thermochronological data, and look at how extensional deformation is partitioned throughout the Cambrian section. We will discuss the idea that the steep normal faults that sole into basal detachments in the Bright Angel Shale and at the Great Unconformity provide a small-scale analogue for a regional subhorizontal detachment at the Proterozoic – Phanerozoic interface. This concept of extensional slip along the Great Unconformity is important regionally for understanding Miocene extensional processes.

The second day of the trip will begin with a brief stop at the mouth of Elbow Canyon, where we will examine the Proterozoic ductile deformation history, especially the structural transition from high-temperature, syn-magmatic deformation to lower-temperature, mylonitic deformation. We will then drive west to begin our traverse through Paleoproterozoic "exotic" mélanges, including 2-pyroxene ultramafic rocks, calc-amphibolite gneisses, garnet-sillimanite paragneisses, and diopside-bearing marbles. We will discuss the petrologic and structural significance of these units in the context of the Paleoproterozoic tectonics of the region. We will also examine the structural overprinting of these units during Mesoproterozoic ductile shearing. At the 8,021 foot summit of Mount Bangs, we will discuss our findings within the Proterozoic rocks, than jump to a discussion of the Miocene extensional strain field over a spectacular panoramic view of the NVM, with the deepest basin in the Basin and Range (> 10 km) immediately juxtaposed with the highest peak on the western edge of the Colorado Plateau. We will present gravity and aeromagnetic data for the Mesquite Basin and discuss the tectonic development of this key region.

Major issues to be addressed by the field trip

1) **Proterozoic deformation and tectonic history – importance of late Paleoproterozoic ductile shear zones, and the question of whether they record a progressive deformation continuum or separate deformation events partitioned in time and space**
2) **The importance of a Laramide ancestry in forming the Virgin Mountain anticline – When did this structure form (Laramide, Miocene, or both) and when were the Proterozoic rocks unroofed?**
3) **How did older structural features affect the geometry of Laramide and Miocene deformation in the North Virgin Mountains?**
4) **What were the dominant processes during Miocene deformation: strike-slip faulting? Isostatic uplift? N-S shortening? Lower-crustal flow? Low-angle normal faulting?**
5) **What thermochronologic constraints can we place on deformation events, cooling events, and exhumation events? How robust are our interpretations?**

FIRST DAY ROAD LOG

Cabin Canyon, Bunkerville Ridge, and Hendricks Canyon, North Virgin Mountains

The first day will be divided into three parts: 1) structural analysis of a Proterozoic shear zone, 2) discussion of the tectonic significance of Miocene conglomerates, and 3) examination of the detachment at the Great Unconformity. We will examine structures ranging in age from circa 1,700 Ma to < 13 Ma, conceptually linked by our evidence that Proterozoic deformation fabrics were pervasively reactivated during Laramide and Miocene deformational events.

ROAD LOG

Increment Mileage	Cumulative Mileage	Description
91.0	91.0	Saturday, May 4: Drive from Cedar City, Utah to Casablanca Hotel, 950 W Mesquite Boulevard, Mesquite, Nevada via Interstate 15 S.

Increment Mileage	Cumulative Mileage	Description
0.0	0.0	Sunday, May 5: Casablanca Hotel, 950 W Mesquite Boulevard, Mesquite, Nevada. Assemble at front lobby by 7:45 am and depart for the Cabin Canyon shear zone at 8:00 am sharp. Proceed E on Mesquite Boulevard to Riverside Road. Head south on Riverside Road, take first left on dirt road immediately across bridge. Take this dirt road for 8 miles, bearing right at Y-junction at 2.5 miles. Park at entrance to Cabin Canyon, where we will be spending the entire morning.
9.5	9.5	Stop 1: The Cabin Canyon shear zone Stop 2: Miocene conglomeritic outcrops
25.5	35.5	Return to Mesquite via dirt road, go left on Mesquite Boulevard for roughly 0.5 miles, take Interstate 15 N on-ramp. Take Interstate N 12 miles to Farm Road exit, past Littlefield, Arizona. Take Farm Road south for 3 miles to Hendricks Canyon. Stop 3: Hendricks Canyon unconformity.
16.0	51.0	Return to Casablanca Hotel

Stop 1: The Cabin Canyon shear zone

Main points: 1) The Cabin Canyon shear zone segment forms part of the late Paleoproterozoic Virgin Mountains shear zone, a NE-trending dextral-transpressive deformation zone that is exposed throughout most of the length of the North Virgin Mountains
2) Deformation within this zone is strongly partitioned into pure shear dominated, simple shear dominated, and general shear dominated strain domains that operated synchronously during transpressional deformation (the space-time partitioning problem)
3) The strongly fissile mylonitic foliation that developed was brittlely reactivated during Miocene extension, and most likely during Laramide contraction, and thus helped control the uplift and current geometry of the Virgin Mountain anticline

Background Geology

The crystalline core of the NVM consists of Paleoproterozoic (circa 1,700 Ma) rocks that are part of the Mojave Precambrian province, an isotopically enriched, upper-amphibolite to granulite facies metamorphic terrain extending from west-central Arizona westward into the Basin and Range (figure 2). The proposed boundary between the Mojave and the juvenile Yavapai province (Karlstrom and Bowring, 1988) is at least 40 kilometers east of the NVM at the Gneiss Canyon shear zone, or perhaps lies farther east at the Crystal shear zone of the Grand Canyon.

The early tectonic history of the Virgin Mountain crystalline terrain (VMCT) likely involved burial to depths of 20-25 kilometers and complex bedding sub-parallel thrusting and contraction (S_1). This first-generation fabric has been intensely overprinted, with the only remaining structural evidence being northwest-trending inclusion trails in pre-D_2 porphyroblasts and weak fabrics in low strain domains south of the Big Springs
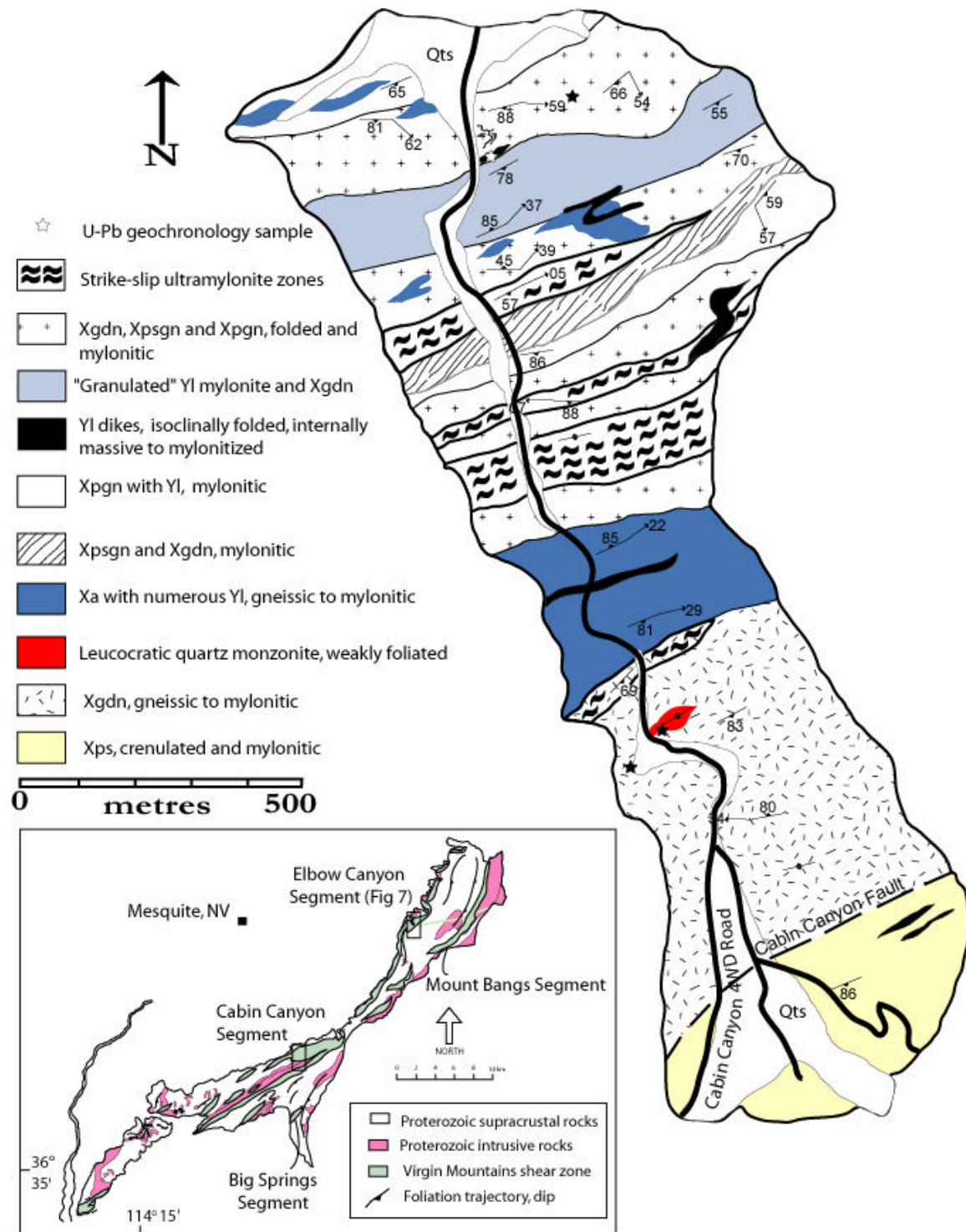
Figure 2. Geologic map of the Cabin Canyon segment, with location of U/Pb monazite and zircon samples. Inset. Virgin Mountain shear zone network, with location of Cabin Canyon segment (box)

89

segment (figure 2 inset). Throughout the rest of the VMCT, intense E-W contraction resulted in formation of a penetrative N-S fabric (S_{2a}), accompanied by high-temperature metamorphism and localized migmatization. This fabric was progressively reoriented into a NE-trend (S_{2b}) during synchronous NW-side-up thrusting, continuing peak temperature metamorphism (upper amphibolite facies), and granitic magmatism.

This NE-trending fabric was strongly reactivated during continual deformation at shallower crustal levels (D_3), resulting in formation of the Virgin Mountains shear zone network (VMSZ). The VMSZ is composed of structurally linked mylonitic shear zones displaying a wide variety of finite strain state geometries, including: 1) dextral strike-slip zones with spectacular structural asymmetry, 2) oblate (flattening) domains with conjugate shear bands and weakly developed vertical stretching lineations, 3) steeply lineated L>>S prolate (stretching) domains with poor asymmetry, and 4) obliquely lineated reverse and normal sense domains with excellent asymmetry. Deformation is most intense along pre-existing lithologic and structural heterogeneities, although almost all of the Proterozoic rocks have been overprinted by this event.

An overall kinematic analysis of the VMSZ suggests that deformation was primarily dextral-transpressive, with complexities arising due to variations in shear zone orientation and geometry, rheologic heterogeneities, and perhaps, timing of deformation. Regional deformation has been dated at circa 1,650-1,550 Ma using U-Pb monazite geochronology, a broad time range suggesting either multiple movement histories or a protracted deformation continuum lasting over 100 m.y. Seemingly incompatible structures can be easily created during heterogeneously partitioned transpressive deformation, and are correlated based on metamorphic conditions and deformation microstructures. The best-exposed, most intriguing evidence for this style of deformation is in the Cabin Canyon segment of the VMSZ, our first stop on the field trip.

VMSZ - Cabin Canyon Segment

The Cabin Canyon segment (figure 2) provides the best evidence for partitioned dextral-transpressive deformation in the VMSZ. Detailed mapping revealed strain patterns indicative of transpressional deformation; simple-shear dominated, dextral strike-slip domains (Stop 1D), flanked by pure-shear dominated domains (Stop 1B), and LS domains with oblique-reverse sense kinematics.

Stop 1A: Cross-cutting Leucopegmatite Dikes

The first outcrop reveals the complexity of the pre-mylonite, high-temperature S_{2a} and S_{2b} structural fabrics and associated plutonism of the VMCT. This biotite-hornblende granodiorite unit, interlayered with pelitic paragneiss and cross-cut by numerous leucopegmatite dikes and veins, preserves cross-cutting relationships that have been largely obliterated within the higher D_4 strain domains in the core of the Cabin Canyon shear zone. The chronology of events was as follows:

D_{2a}: High temperature metamorphism and development of compositional layering and strong S_2 foliation, defined here by alternating layers of granodiorite and isoclinally folded syn-D_2 migmatitic leucosomes (figure 3). This fabric was weakly crosscut by thicker late syn-D2 leucopegmatites (figure 3) that record slightly lesser degrees of D_2 isoclinal folding (although they are still strongly deformed in this fashion).

D_{2b}: Refolding of D_2 leucopegmatites orthogonal to their axial planes by open F3 folds, associated with the progressive re-orientation of the N-S fabric (S_2) into the NE-SW fabric (S_3) during NW-side-up thrusting. "Syn-D_3 leucopegmatites" (figure3) intruded axial planar to F_3 folds. The late-D2 leucopegmatites locally "bleed-into" the early-D3 pegmatites, and the formation of NW-side up shear fabrics associated with intrusion of these dikes and re-orientation of the S2 fabric. These dikes are relatively straight, although they have been folded locally. It is this generation of dike which we believe we have dated at Stop 1C (see below).

D_3: All fabrics and intrusions are overprinted by a lower temperature mylonitic foliation associated with dextral transpressive deformation in the VMSZ. The mylonitic fabric (S_3) weakly crosscuts the leucopegmatites, and likely records a retightening of the outcrop-scale F_3 open fold, which would account for the slight splaying in the D_{2b} pegmatites.

Stop 1B: Oblate (pure-shear dominated) Mylonites

Pure-shear domains contain mylonitic, conjugate shear planes at roughly 30 degrees from the mylonitic foliation on vertical rock faces. Foliation planes contain large (>12 centimeter) "pancake-like" K-feldspar porphyroclasts, likely derived via the mechanical dismemberment of leucopegmatite dikes during deformation. The same crystals appear as highly flattened and dismembered leucosomes on faces perpendicular to the mylonitic foliation, resulting in aspect ratios of roughly 30:30:1. The combination of these oblate flattening

strains, conjugate shear bands recording vertical extension parallel to the foliation planes, and development of a weak, vertical stretching lineation (figure 3) suggest that shortening in these domains was accommodated by intense vertical "extrusion", similar to that first predicted by the Sanderson and Marchini (1984) transpression model. While grain-sizes are coarser in these domains relative to the ultramylonitic strike-slip domains, the microstructures and metamorphic reactions are suggestive of similar tectonic conditions. The strike-slip domains are thus inferred to have recorded more intense finite strains than the oblate domains, as opposed to recording a different deformation event. Further evidence of increased strain in the strike-slip mylonites is that obliquely plunging fold axes in the wall rocks have been rotated into parallelism with the shallowly plunging lineation in the strike-slip domains.

Stop 1C: Folded Leucopegmatite Dike

This muscovite-biotite leucopegmatite dike is of early D_{2b} generation in that it crosscuts all other intrusions and the strong S_{2a} foliation, locally at high angles, but is tightly folded about an axis sub-parallel with those fabrics. It shows small domains of D_3 mylonitization and associated retrogression, but for the most part is internally unfoliated. This dike is currently being dated at the Massachusetts Institute of Technology (Samuel Bowring, personal communication) to constrain the minimum age of D_{2b} deformation and the maximum age of D_3 mylonitization.

☐ Syn-D2 migmatitic leucosomes with isoclinal D2 folds
▨ Late syn-D2 leucopegmatites with tight / isoclinal D2 folds
  and open D3 folds
☐ Syn-D3 leucopegmatites approximately axial planar to open
  F3 fold, cross-cut D2 pegmatites, and slightly obliquely cross-
  cut by mylonitic foliation
〰 Mylonitic foliation (S4)

Figure 3. Crosscutting leucopegmatite dikes at the opening to Cabin Canyon. These excellent cross-cutting relationships are obscured in higher strain zones within the Cabin Canyon shear zone, and record the transition from migmatization and foliation development associated with D2 to the reorientation of this fabric into a NE-trend (D3) and synchronous plutonism. Cross sectional view, looking northeast.

Stop 1D: Dextral Strike-Slip Mylonites

The narrow (~15 meters maximum) dextral strike-slip ultramylonite zones contain a variety of shear sense indicators on faces paralleling the lineation, including sigma and delta porphyroclasts (figure 4), antithetic bookshelf-type structures, asymmetric myrmekite fabrics in K-feldspars, C-S fabrics, and shear bands. The sub-horizontal lineation developed in these zones thus appears to represent the movement direction.   Quartz microstructures indicate deformation occurred predominantly by subgrain rotation and climb-accommodated dislocation creep, whereas feldspars deformed by internal kinking and development of mechanical twins, brittle fracturing, and recrystallization-accommodated dislocation creep, together are suggestive of lower amphibolite, upper greenschist deformation conditions. Garnet is retrogressed and locally psuedomorphed by plagioclase + epidote +/- actinolite, often resulting in a "disaggregation" of originally euhedral garnet porphyroclasts during progressive strain. Hornblende has broken down to form actinolite. The microstructures and metamorphic relations thus suggest that deformation and metamorphism occurred under upper greenschist facies conditions.
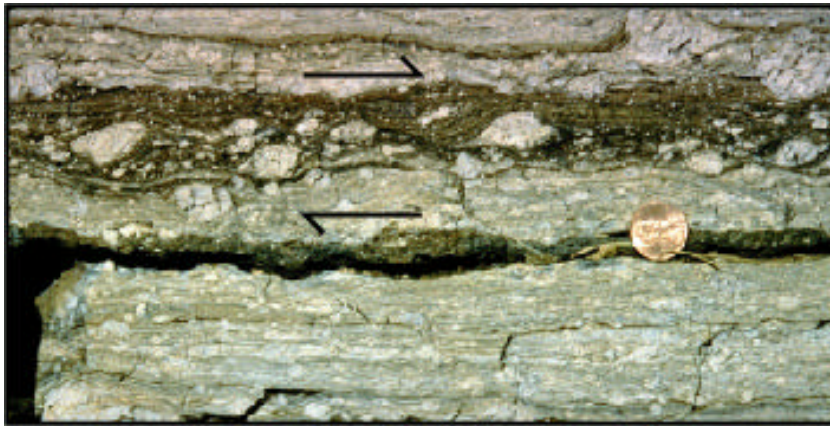

Figure 4. Sigma-porphyroclasts, and shear bands revealing dextral shear sense, ultramylonitic unit, Cabin Canyon shear zone. Plan view, NE is to the right.

As you walk up the canyon….

Interpreting the kinematic history in the strongly lineated, obliquely plunging domains is more complicated. Sinistral N-side-up indicators are present in some of the northern locations, although oblique-dextral deformation still predominates. Lower temperature shear sense indicators such as shear bands and sigma porphyroclasts are present on faces non-parallel to the strong lineation observed in these units. The apparent conflict between opposing senses of shear is reconciled with the interpretation of early, high-temperature NW-side up thrusting (D_{2b}) and development of the stretching lineation, overprinted by the upper greenschist facies dextral transpressive deformation (D_3), with some sinistral faults operating during D_4 shortening to accommodate space problems, structural anisotropies, and heterogeneous transpression. The steeply plunging lineation is interpreted to be the result of the earlier event based on: 1) the differing character between it and the strike-slip and vertical lineations observed in the simple shear and pure shear dominated domains, respectively, 2) the obliquity of lower temperature shear sense indicators to this lineation, and 3) the apparent overprinting and reorientation of this lineation proximal to the strike-slip domains.

To the east of Cabin Canyon in Lime Kiln Canyon, the mylonitic foliation is strongly folded and displays a combination of N and NE-trending, dextral-oblique strike-slip segments and N-trending, W-side-up reverse segments. This is interpreted as a partitioned, syn-mylonitic constraining bend in the Cabin Canyon segment (figure 2 inset), based on the presence of localized parasitic mylonitic folds with the same geometry, and lack of evidence that folding preceded the ductile deformation.

Stop 1E: Cabin Canyon Fault Trace

As you come southward out of Cabin Canyon, the trace of the sub-vertical Cabin Canyon fault is visible in the near saddle to the NE and the prominent valley and far saddle to the southwest. The fault separates granodioritic gneiss and semi-pelitic paragneiss to the north from a relatively thick package of pelitic schist to the

south. Kinematic indicators are rare, but where observed, slickenlines plunge shallowly (10-20°) to the east. This fault zone has had a long movement history, as a high-temperature D_2 deformation zone, a lower-temperature D_3 mylonitic shear zone, and most likely as a brittle Laramide reverse fault and Miocene oblique strike-slip fault.

The nature of basement-penetrating faults is enigmatic because their age (Miocene vs. Laramide) is largely unknown, and they rarely show slickenlines. They are often recognized as continuous chloritic breccia zones along Proterozoic lithologic contacts. Although Miocene left-slip is likely (Williams and others, 1995), reconstructions of fault separation using Proterozoic lithologies are unreliable due to the extremely heterogeneous nature of the Proterozoic basement. Furthermore, it is likely that most basement-penetrating faults had both a Laramide and Miocene component of slip. Aside from the Hen Spring fault, basement-penetrating faults predominantly follow the Proterozoic foliation, striking NE in S_{2b} dominated domains, and striking N-S in S_{2a} dominated domains. An important conclusion of our work is that the orientation of Proterozoic fabrics helped control the geometry of Miocene and Laramide faults, and uplift of the VMA.

Stop 2: Miocene conglomeritic outcrops on north flank of Bunkerville Ridge

Main points: 1) Bunkerville Ridge is a structurally complex package of steeply north-dipping to south-overturned Paleozoic limestones, and was created as a result of Miocene normal faulting modified by later, intense strike-slip deformation.
2) Miocene conglomeritic outcrops on the north flank of Bunkerville Ridge are assigned to the red sandstone unit (10-12 Ma) based on general appearance and presence of Proterozoic clasts. This section records a syn-extension middle Miocene unroofing sequence consistent with apatite-fission track ages of basement rocks ranging between 14-20 Ma.
3) The red sandstone conglomerates are vertical to overturned to the south, suggesting that intense strike-slip faulting occurred sometime during or after the 10-12 Ma deposition of this unit, post-dated uplift and exposure of the Proterozoic rocks, and thus post-dated formation of the VMA.

Geology of Bunkerville Ridge

From our lunch spot we can view the high-standing late Paleozoic limestones of Bunkerville Ridge, Miocene conglomerates at the foot of the ridge, and Pliocene and Quaternary alluvial strata of the Virgin River depression. Bunkerville Ridge is an east-northeast-trending section of Paleozoic strata that strike roughly parallel to the local trend of the physiographic high and dip northerly or are vertical to overturned to the south. The continuity of the ridge is broken by two prominent low areas through which northeast-striking faults pass.

The south side of the ridge is commonly marked by the depositional contact of the Tapeats Sandstone ($\in$ t) on various Proterozoic crystalline rock units or by the two northeast -trending faults that have Paleozoic rocks on their northwest sides and Proterozoic rocks on their southeast sides. South of the ridge the quadrangle is underlain by various Proterozoic crystalline rocks that are faulted by two regionally prominent faults that have northeast trends, the Hen Spring and Cabin Canyon faults. The Hen Spring fault marks the southern edge of Bunkerville Ridge where it separates Paleozoic rocks from crystalline basement, and is one of the few basement-penetrating faults that locally cut the Proterozoic foliation (Beal, 1965).

The basal Cambrian strata that form the southwestern ridge segment have moderate northwest dips. A broad, open fold pair, whose axial plunge parallels the stratal dips, is defined by changes in strike of the beds. The syncline is well displayed, but the anticlinal axis is buried by Quaternary and late Tertiary deposits and is cut by a fault with a northeast trend. This suggests a sequence of events in which a flat section of Cambrian rocks was folded gently, later to be tilted more steeply and cut by faults. Both the large east-bounding fault and the one cutting the anticline exhibit a well-developed left separation of the basal Proterozoic-Cambrian contact. The separation on the fault between the southwestern and central ridge segments is on the order of one kilometer.

The central ridge segment is primarily a moderately northeast-dipping homocline in Lower Cambrian to Mississippian rocks. Intermediate dips are common at high stratigraphic levels and steep dips are common near the base of the homocline. The Proterozoic-Cambrian contact is faulted in places and depositional in others, but it defines large open folds with northeast trends in the Proterozoic-Cambrian contact that are not obvious at higher levels in the homocline. Two large fault blocks rest tectonically above the homoclinal section

of rocks. The faults beneath each block form two convex-up, spoon-shaped surfaces, each of which appears to plunge to the southwest, perpendicular to the strikes in the underlying homocline and to the orientation parallel to the basement crenulations. Northeast-dipping homoclines of Cambrian to Pennsylvanian rocks form the hanging-wall blocks of each of the spoon faults. The stratigraphic separations suggest that each spoon was transported to the southwest relative to the underlying homoclinal block. The central part of the footwall homocline is offset with about 0.5 kilometers of left separation by a northeast-trending fault that merges with the fault that forms the west-northwest side of the eastern spoon.

The structural relations surrounding the two spoon-shaped fault surfaces suggest that they developed as a single normal fault surface that cut a flat-lying section of rocks. The original fault surface was probably gently crenulated and had a general northwest strike and a steep to intermediate southwest dip. Subsequent strong northeast-tilting of both the hanging wall and footwall blocks resulted in the gentle southwest dip of the modern spoon-shaped surface. Erosion of much of the hanging wall preserved only the cuspate crenulations in the original surface.

The strata in the eastern ridge segment form a deformed north-dipping homocline. The basement-basal Cambrian contact is depositional and gently dipping all along this part of the ridge. Two small left-separation faults with north-northeast trends cut the contact. Strata in the higher stratigraphic levels in the homocline dip steeply to the north. At no point is there a complete section exposed in this segment of the ridge. A complex pattern of low- to intermediate-angle, north dipping, normal faults disrupts the middle part of the homocline. Each of these faults locally eliminates part of the section, placing younger strata on older. At the eastern boundary of the quadrangle these faults merge into two, which in turn join with the Hen Spring fault to the east of the quadrangle. In map view the nearly continuous Tapeats Sandstone at the base of the homocline converges with Mississippian rocks in the homocline's upper part at the eastern border of the quadrangle, indicating that, at that location, a large amount of section is removed by the two faults.

Significance of the Miocene Conglomeritic Unit

Scattered outcrops of steeply dipping, middle Miocene red sandstone conglomerate cover an area of approximately 300 square meters on the north flank of Bunkerville Ridge, and provide key insights into the pre-tilting topography and structural evolution of the VMA. The conglomeritic unit is 50-100 meters thick, and contains angular clasts ranging in diameter from 1 to 100 centimeters. While the clast assemblage is dominated by middle to late Paleozoic limestones, nearby outcrops contain Proterozoic and lower Cambrian Tapeats clasts up to 5 percent. The presence of coarse clasts of Tapeats Sandstone and Proterozoic granite, amphibolite, biotite-garnet schist, pegmatite, and mylonite in the stratigraphically higher red sandstone units (figure 3), and absence in the stratigraphically lower units, suggests that this red sandstone conglomerate records a Miocene unroofing event, whereby the Proterozoic rocks were fully exhumed sometime during proximal red sandstone conglomerate deposition. This unroofing event was likely synchronous with basement-penetrating strike-slip and normal faulting, and development of the Mesquite Basin, after some structural relief was already present. The farthest west exposures of this unit lie disconformably on 74 degrees north-dipping Triassic Moenkopi Formation, middle-distance exposures dip between 60 degrees to the north and 74 degrees overturned to the south, and the closest outcrop dips 32 degrees to the east, at a high angle to adjacent, intensely overturned, south-dipping Kaibab Formation limestones. These complex geometries are likely a result of the syn-extensional strike-slip faulting that this area underwent probably during deposition of these units.

The Virgin River Depression

The Neogene Virgin River depression has a surface area that exceeds 1,500 square kilometers. The depression formed within the foreland of the Sevier orogenic zone, a region characterized in Paleogene time by a flat-lying section of Cambrian to Cretaceous platform strata about 5 kilometers thick and perhaps a small amplitude Laramide uplift to the east (VMA). Well data from Mobil Virgin 1A on Mormon Mesa reveal 2,000+ meters of Neogene basin fill that consists mostly of the Muddy Creek Formation (4-10 Ma), the red sandstone unit (10-12 Ma) of Bohannon (1984), and the Lovell Wash Member of the Horse Spring Formation (12-13 Ma). Seismic reflection data from six primacord and two vibroseis lines show that the Muddy Creek Formation uniformly fills Virgin River depression to a depth of 1-2 kilometers. Two older and less-extensive basins, the Mormon and Mesquite, lie beneath the Muddy Creek and are separated from one another by a complex buried ridge. The basins are mostly filled with rocks of the red sandstone unit and Lovell Wash Member to depths locally exceeding 6 kilometers. Two older members of the Horse Spring Formation, the Rainbow Gardens and Thumb, also are present in Mormon basin (the western one), where they rest disconformably on the pre-Tertiary

strata. The basins are east-tilted half grabens bound on the east and southeast by large listric normal fault systems. The Muddy Creek Formation buries the faults that bound Mormon basin, but the Piedmont fault, on the east side of Mesquite basin, cuts Quaternary alluvium.

The Virgin River depression formed in three stages. The period from 24-13 Ma is characterized by slow subsidence in Mormon basin and little noticeable deformation of the basin substrate. The Mormon and Mesquite basins became fully differentiated during the period from 13-10 Ma. This stage is associated with large displacements on the normal faults bounding both basins and the buried ridge. Proterozoic crystalline rocks were exposed locally, as determined from the unroofing sequence within the red sandstone unit and apatite-fission track data, which suggest rapid cooling through ~100°C between 20-14 Ma. Tectonic denudation during the 13-10 Ma stage locally removed large amounts of the pre-basin section. Pronounced strike-slip deformation affected the west limb of the VMA, and locally overturned red sandstone conglomerates, sometime after 12 Ma. Post 10 Ma, most of the fault activity had ceased, the ridge between the basins was overlapped, and the Virgin River depression began to subside uniformly over a wide area. This stage lasted until the commencement of the modern period of dissection associated with the Colorado River. Structural analysis suggests that upper crustal extension within the basin, mostly during the 13-10 Ma stage, might have exceeded 60 percent. The basin subsidence was partly due to extension in the upper crust and partly due to viscous flow in the deeper crust beneath the basin.

Stop 3: Hendricks Canyon Traverse

Main points: 1) Overturned monoclinal-style geometries in the lower Cambrian section at the NW end of the VMA suggest a component of Laramide deformation
2) Sub-horizontal fault surfaces in the Bright Angel Shale and at the Great Unconformity suggest detachment faulting and tectonic transport of allochtonous, tilted fault blocks above para-autochthonous Proterozoic basement

The Hendricks Canyon Area

Upon arrival at the north end of the NVM, we can view the only location where the Great Unconformity between the Proterozoic crystalline core of the NVM and the overlying Phanerozoic section runs east-west. It is the varying structural-rheological aspects of this Proterozoic-Phanerozoic surface that we will be focusing on during this stop.

The Proterozoic rocks in this area are predominantly garnet-biotite-sillimanite migmatitic paragneiss, pink monzogranitic pegmatite, and a thin (5-10 meters) quartzite layer that is concordant with the paragneiss. The Phanerozoic section north of the Great Unconformity consists of a variably thinned Cambrian section through to the Mississippian Monte Cristo Limestone, which forms the high peaks visible from this location. On the northeast flank of the NVM, not visible from here, the east-tilted section contains Cambrian through Middle Triassic units, capped by flat-lying Quaternary basalts and landslide deposits.

Visible in the section exposed before us is a complex array of east- and west-dipping conjugate normal faults, with offsets ranging from centimeters to >400 meters. We have focused mainly on fault geometry and deformation partitioning in the Cambrian section. The normal faults commonly dip 50-70 degrees in the Muav Limestone, and are associated with strong brecciation and formation of calcareous vein networks. These steep normal faults shallow to 40-50 degrees at the contact with the underlying Bright Angel Shale, resulting in moderately dipping horst and graben structures in the upper Bright Angel Shale. These faults sole out into sub-horizontal geometries throughout the highly fissile Bright Angel Shale, resulting in dramatic changes in stratigraphic thickness. The Tapeats Sandstone is also strongly attenuated due to segmentation by both steep and bedding parallel (basal) normal faults. These normal faults also obtain sub-horizontal geometries along the Great Unconformity, where the flat-lying Tapeats stratigraphy overlying the vertically foliated Proterozoic basement presents a dramatic rheological contrast. The best field example of lateral transport of allochtonous Cambrian section along low angle normal faults at the Great Unconformity in the NVM is at Stop 3B.

The strong rheologic contrasts between the competent overlying Paleozoic Limestones and the incompetent Bright Angel Shale, and the competent underlying Tapeats Sandstone and Bright Angel Shale, resulted in significant structural decoupling within the Phanerozoic section during crustal extension. The strong rheologic contrast between the Tapeats Sandstone and the underlying Proterozoic basement also resulted in this decoupling, suggesting that at least locally, the Phanerozoic cover may have moved independently from its

Proterozoic counterpart. Similar observations from the Gold Butte area in the South Virgin Mountains suggest this was a regionally important detachment surface.

Stop 3A: Evidence for Laramide-Style Deformation in the North Virgin Mountains

We investigated the possibility of a Laramide component to the finite strain field of the NVM based on the following: 1) The position of the VMA just east of the leading edge of the Sevier thrust belt, as documented in the Mormon Mountains (Axen, 1990), and west of the well documented high angle Laramide reverse faults and monoclines of the Grand Canyon (Huntoon, 1990), suggests that the VMA may occupy a "transition zone" between these two structural domains. Beard (1993) mapped Sevier-style thrust faults in the Phanerozoic section south of Virgin Peak, suggesting that contractional deformation did affect parts of the NVM. 2) The Laramide monoclinal uplifts of the Grand Canyon have a systematic spacing in map view, and are generally cored by basement-penetrating reverse faults. Just from the spacing, we suggest there were monoclines at the NVM, roughly 50 kilometers west of the Hurricane fault monocline; 3) Paleocurrent and stratigraphic relationships in the early Miocene (~26 Ma), pre-extensional Rainbow Gardens Member basal conglomerate suggest deposition in overall northest-flowing braided streams, with positive areas south of the Gold Butte block (figure 1) in the N-plunging Kingman highlands, and a "moderate to abrupt relief area" within the NVM, deemed the "Virgin positive area" (Beard, 1996). The shedding of sediments to the southeast off the Virgin positive area suggests some topography existed here before middle Miocene extension began.

Figure 5: Monoclinal west limb of the VMA, with dramatic angular relationships between the Cambrian Muav limestone (60° W-dipping) and Lower Cambrian Tapeats Sandstone (46° E-dipping) accommodated by spectacular tectonic thinning and splaying of the Bright Angel Shale. Monoclinal reverse fault dips at most 46 degrees to the E.

The outcrop before us (figure 5) consists of, from west to east, 1) moderately west-dipping Muav Limestone, 2) contact between the Muav and Bright Angel Shale (231/42°), 3) tectonically thinned Bright Angel Shale, which fans from moderately to steeply W-dipping (235/80°), 4) vertical contact between Bright Angel Shale and Tapeats Sandstone, and 5) overturned Tapeats Sandstone, which fans from near vertical to moderately E-dipping (240/46°); extrapolated reverse fault contact between Tapeats Sandstone and Proterozoic paragneiss. While the presence of overturned beds are not explicitly diagnostic of a Laramide structure, the geometry of the structure before us is similar to those commonly observed in the monoclines of the Grand Canyon, and not a feature as commonly observed in extensional or strike-slip faults within the Basin and Range. The lowest dip of the basal Tapeats Sandstone (240/46°), gives the maximum dip of the reverse fault, which in

this case must dip at most 46° to the east. The inward-verging, basement-penetrating nature of this fault, required to explain the observed geometry, is characteristic of the basement-cored Laramide uplifts of the Colorado Plateau.

As you walk up the arroyo…

Between stops 3A and 3B, examine the Paleozoic section outcropping to the north. Steep conjugate normal faults within the Paleozoic limestones sole into basal detachments within the Bright Angel Shale, Tapeats Sandstone, and at the Great Unconformity. It is the latter variety which we will observe at Stop 3B.

Stop 3B: Basal Detachment Fault at the Great Unconformity

The outcrop before us consists of W-tilted "domino blocks" of Tapeats Sandstone atop Proterozoic mafic schist and monzograntic pegmatite, separated by a chloritic–hematitic zone of fault gouge at the Great Unconformity.   The Tapeats Sandstone can be divided into three zones: 1) allochtonous W-tilted blocks separated by 50-60 degrees E-dipping normal faults, 2) quartz-cemented fault breccia, and 3) para-autochthonous fault slivers that appear to have glided along the Great Unconformity fault surface (figure 6). The allochthonous blocks dip roughly 50 degrees towards 335 degrees, and also contain some evidence of fault slip along bedding planes. The proposed extension direction related to tilting of these blocks is approximately 120 degrees, orthogonal to the trend of fault-block corners.

The Great Unconformity fault gouge is dominated by fine-grained, low-grade alteration minerals (chlorite, hematite, clay minerals), and exhibits chaos structure, whereby the fault breccia is thickest beneath the footwall at the normal fault, and thinnest beneath the hanging wall at the normal fault. The fault gouge is strongly layered and exhibits numerous conjugate horst and graben structures with small centimeter scale offsets. Measurements of these conjugate sets approximate 191/61 degrees and 346/49 degrees.
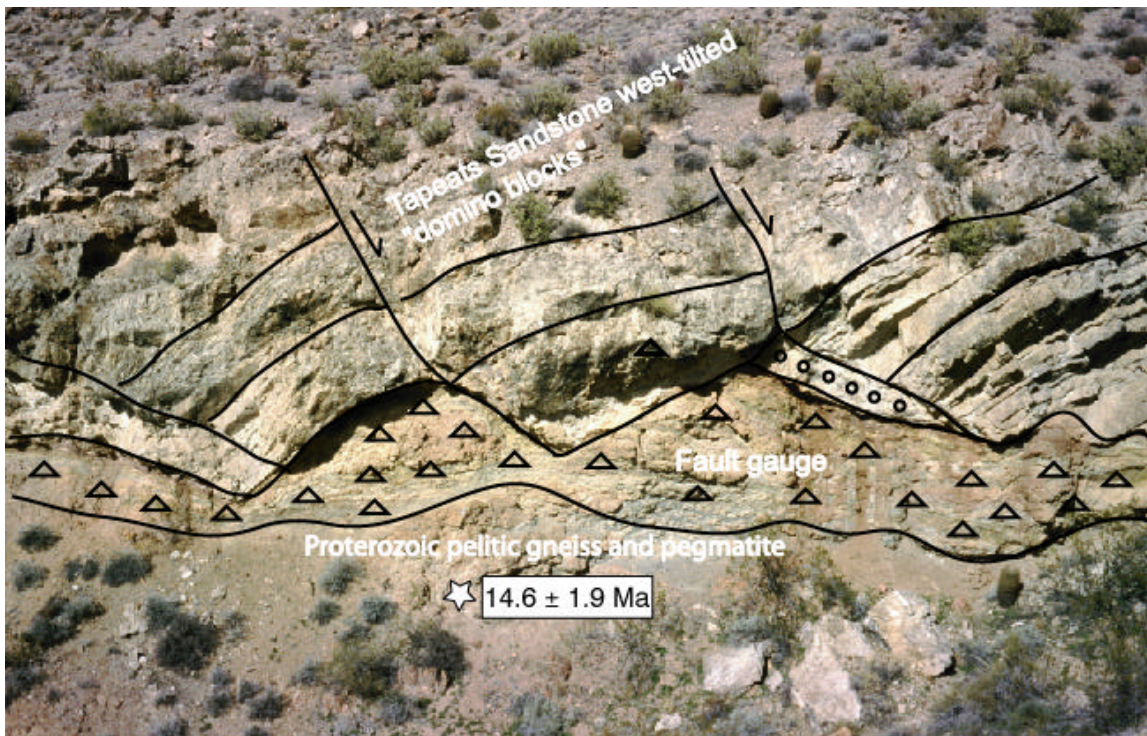
Figure 6: Allochtonous, W-tilted domino blocks of Cambrian Tapeats Sandstone overriding Proterozoic crystalline rocks (the Great Unconformity). The fault zone consists of para-autochtonous silvers of flat-lying Tapeats that have glided along the flat-lying fault zone (open circles), and ultrafine-grained fault gauge dominated by layers of low-grade alteration minerals and conjugate fault sets. Proterozoic pegmatite below the fault gauge yields an apatite fission-track age of 14.6± 1.9 Ma.

The Proterozoic rocks also show signs of localized alteration and faulting; however, they are not penetrated by the normal faults in the Tapeats Sandstone, confirming that these faults sole out into the basal fault zone at the Great Unconformity.

Three conclusions can be drawn from this outcrop; 1) this style of extensional block faulting was associated with extension towards 120°; 2) Proterozoic basement was structurally decoupled from the Phanerozoic section through soling of normal faults at the Great Unconformity; and 3) this style of deformation was likely early in the period of Miocene extension, and was proceeded by some component of "bowing up" and NW tilting of this once horizontal Great Unconformity fault surface.

SECOND DAY ROAD LOG

Elbow Canyon and Mount Bangs, North Virgin Mountains

On this second day, we will begin looking at the structural interplay between Proterozoic high temperature and lower temperature constriction-dominated strains in Elbow Canyon, and conclude with a traverse through a Paleoproterozoic mélange sequence leading up to the highest ridge in the NVM, Mount Bangs. At the summit, we will conclude the trip with a panoramic view of the NVM and surrounding region, looking east to the Colorado Plateau and west to the Basin and Range.

ROAD LOG

Increment Mileage	Cumulative Mileage	Description
0.0	0.0	Casablanca Hotel, 950 W. Mesquite Blvd., Mesquite, Nevada. Assemble at front lobby by 7:45 am and depart for the Elbow Canyon saddle at 8:00 am sharp. Proceed E on Mesquite Boulevard to Riverside Road. Head S on Riverside Road, take first left on dirt road immediately across bridge. Take this dirt road for 1 mile, take first left onto Elbow Canyon Road. Continue on Elbow Canyon Road E for 9 miles to opening of Elbow Canyon.
11.0	11.0	Stop 4: Stream wash W of Elbow Canyon Road, roughly 0.5 miles from opening of Elbow Canyon
4.5	15.5	Stop 5: Park at high saddle to execute Mt Bangs traverse.
15.5	31.0	After traverse is completed, return to Casablanca Hotel via Elbow Canyon Road. Pick up luggage at Casablanca Hotel.
91.0	122.0	Return to Cedar City, Utah via Interstate 15.

Stop 4: Mouth of Elbow Canyon

Main points: 1) High-temperature D_{2a}/D_{2b} structures (i.e. sheath folds, lineations, shear sense indicators) are overprinted by lower-temperature D_3 structures (mylonitic lineations, shear sense indicators) with similar lineation plunges and shear sense, suggesting that the Elbow Canyon segment may represent a long-lived northwest-side up contractional shear zone that continued during evolution of the crust from lower- to upper-middle crustal levels.
2) Preliminary U-Pb monazite dating of Elbow Canyon VMSZ tectonites reveals age groupings at ~1,700 Ma and between 1,650-1,550 Ma. These are correlative with tectonic fabrics and are tentatively interpreted to represent the high-temperature and lower

temperature tectonic events, respectively. **U-Pb apatite dates of 1420 Ma suggest that the crust was > 450C at this time, and shear zone reactivation is likely, but not documented at this time.**

VMSZ - Elbow Canyon Segment

This stop will provide an opportunity for further discussion of the Proterozoic deformational history of the crystalline basement of the VMA. The Proterozoic rocks of the Elbow Canyon area represent an excellent example of high temperature (upper amphibolite facies migmatitization [D_2]) and lower temperature (upper to middle greenschist facies [D_3]) constriction-dominated strains. These strains are interpreted within a tectonic and geochronologic context.

High Temperature Fabrics (S2,S3)

The roughly N-S trending foliation in Elbow Canyon is defined by metamorphically segregated garnet-biotite-sillimanite bearing paragneisses and leucosomes (Xpsgn), monzogranitic (Xmgn) and granodioritic (Xgdn) intrusions, pegmatites (Xl), and amphibolitic gneisses (Xa) (figure 7). Amphibolite pods are highly boudinaged, and wrapped by strongly foliated domains. The strong lineation, best developed in quartzofeldsapthic rocks, plunges dominantly to the NW, and is locally associated with the same NW-side-up shear sense as determined from the syn-pegmatitic shear bands at the mouth of Cabin Canyon.

The chronology of events is similar to Cabin Canyon; a north-striking foliation was variably reoriented into a northeast strike during northwest -side up thrusting and associated plutonism (pegmatites, granites). This event was related to strong constrictional strains, resulting in the strong, steeply plunging lineation and development of sheath folds, as F_1 and F_2 isoclines were variably rotated into the S_3 shear plane. An example of this is present within the exposure before us. This strongly anisotropic fabric was then progressively reactivated during dextral transpressive mylonitic deformation (D_3) at lower crustal levels (see below).

As you walk through the rocks exposed in the arroyo, attempt to differentiate the high-temperature foliation and associated structures (sheath folds, isoclinal folds) from lower-temperature mylonitic fabrics.

Mylonitic Fabrics (S$_3$)

The Elbow Canyon segment of the VMSZ (4A) contains two types of mylonitic deformation; L-tectonite mylonites with localized northwest-side-up shear sense, and a thin (3 meter) mylonite zone with sinistral E-side-up shear sense (figure 7).

The L-tectonite mylonites display an intense vertical stretching lineation at ~ 48 $\rightarrow$ 320°, with localized evidence (bookshelf structures, sigma K-feldspar porphyroclasts) for northwest-side-up (reverse) deformation, although much of the deformation appears to have been symmetric and a result of strongly prolate coaxial strain. This is an excellent location for participants to practice their shear sense interpretative skills. Mylonitic deformation utilizes pre-existing northeast-trending, high-temperature foliation planes (S_{2b}) as zones of weakness, creating complex structural geometries on the faces orthogonal to foliation planes. Intense, chaotic folding on these surfaces is interpreted as a composite fabric of pre-existing F_2 folds, which tightened during the intense vertical stretching (L_3) and northwest-southeast contraction. The mylonitic fabric is poorly developed on these foliation-orthogonal surfaces. The resultant geometry is shown in figure 4B.

The consistent constriction-dominated, northwest -side up kinematics of D_2 and D_3 events in this area suggest that these events may represent a progressive deformation, occurring as the crust cooled from upper amphibolite to greenschist facies conditions during contraction and exhumation.

A small shear zone with left-lateral, E-side-up sigma porphyroclasts wraps around amphibolite boudins to the south of the L-tectonite mylonites. This is interpreted as an accommodation zone enclosing the more competent amphibolite unit, resulting from the combination of heterogeneous mylonitic deformation and rheologic anisotropy.
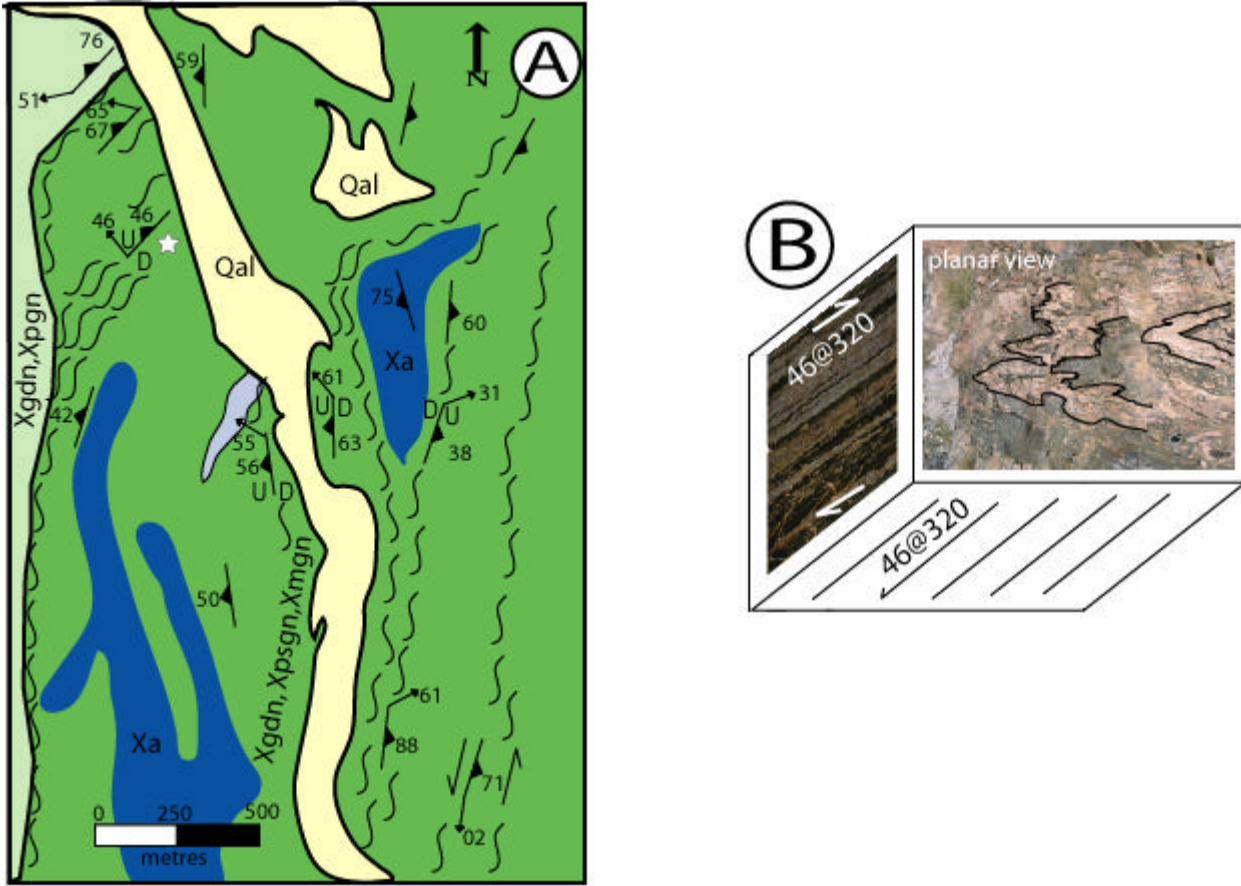
Figure 7: Geology of the Elbow Canyon segment of the Virgin Mountain shear zone. D$_3$ shear zones (~~) are NE-trending, L>>S constriction-dominated zones with strongly developed down-dip lineations and complexly folded YZ planes, and N-trending sinistral strike-slip zones, which may be weak conjugates to the dextral strike-slip domains in Cabin Canyon. Three-dimensional view of strained pelitic gneiss with monzogranite intrusions (B) shows strongly developed composite L3 / L4 lineation plunging 46° at 320° on XZ and XY planes, with strongly folded foliation striking 231°/46° in fold limbs (location of sample = star in map A), perpendicular to YZ plane (planar view).

Timing Constraints on Deformation

Preliminary U-Pb monazite ages from the L-tectonite mylonites of Elbow Canyon yield age clusters in at least three distinct intervals, correlative with multiple growth patterns and chemical U-Th-Pb zonations visible in backscatter images and compositional maps of the grains (figure 8). Earliest growth occurred circa 1,695 Ma, determined from core analyses of zoned monazites and consistent with preliminary zircon ages. This time frame appears to represent peak metamorphism (D$_2$), granitic plutonism, and formation of the penetrative NE-trending tectonic fabric (S$_{2b}$). This is also the time of peak tectonism (deformation at peak metamorphic grade) in the Lower and Upper Granite Gorge (1,700-1,680 Ma (Ilg and others, 1995), and in the Hualapai and Cerbat Mountains (Duebendorfer et al., 2001).

More puzzling, progressive monazite growth (rims) is recorded at 1,600 and 1,550 Ma. While these dates are preliminary and need to be checked using new methods for calculating background matrix values (Williams pers. comm., 2002) at present, we interpret them to record distinct monazite growth intervals that post-date 1,680 Ma. From regional consideration, we had thought they might be circa 1,400 Ma, but this remains unconstrained. If we interpret them to record distinct or progressive tectonothermal events, the VMSZ may provide evidence of recurrent mobilization of a partitioned, inboard crustal weak zone over a 200 m.y. time interval of tectonic convergence. Monazite structural asymmetry, and evidence that the growth of other
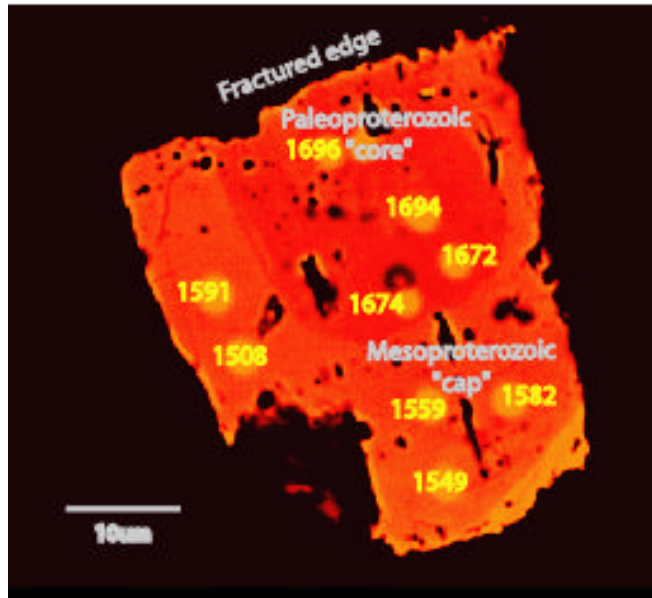
Figure 8: "Blackbody" backscatter image of monazite Q295A from L-tectonite mylonite in Elbow Canyon. U-Pb analysis yields Paleoproterozoic "core" ages (~1,696 Ma, ~1,673 Ma) and Mesoproterozoic "cap" ages (1,591 Ma – 1,508 Ma), suggesting multiple "zonation-type" monazite growth intervals. If these ages are interpreted to be tectonically significant, they may correspond to D_{2a} (1,696 Ma) and D_{2b} (1,675 Ma) high temperature metamorphism, and D_3 (1591 – 1508 Ma?) lower-temperature metamorphism, all of which are linked to tectonic fabric development.

metamorphic minerals was synchronous with the D_3 deformation, suggests that these dates may in fact be representative of the long-lived, complex history of the VMSZ. We note that other areas of 1,500 Ma deformation are known from eastern Australia (Betts and Giles, 2000), which may have been close by based on the Auswus reconsructions (Karlstrom et al, 1999). This is an important issue that we are trying to resolve with additional zircon and monazite geochronology.

Stop 5: Mount Bangs Traverse

Main points: 1) The formation of a tectonic mélange of "exotic" Paleoproterozoic lithologies from varying crustal levels suggests that this region may have been part of an accretionary boundary during Paleoproterozoic crustal assembly.

2) This ultramafic- and carbonate-dominated mélange belt has extreme competence contrasts relative to surrounding granitoids and other supracrustal rocks during subsequent deformation, and thus partitioned late Paleoproterozoic ductile shearing (D_3) and Tertiary brittle faulting of unknown age.

Introduction

This traverse has two objectives: 1) continued examination of the Proterozoic history—in this case, evidence for Paleoproterozoic mélange and discussion of the early accretionary history in this zone, and 2) visit a spectacular overlook of the surrounding geologic and physiographic terrain of the Colorado Plateau – Basin and Range transition to synthesize problems and issues surrounding understanding the Phanerozoic history of the VMA itself and the importance of Proterozoic ancestry on present structures. Although the final destination is the Vista Grande, some 1,240 feet above us, participants may progress as they see fit, based on both physical fitness and interest.

101

Stop 5A: Deformed Leucopegmatites and Pelitic Schists

We begin in a package of strongly foliated Paleoproterozoic garnet–biotite–sillimanite pelitic schist cross cut by a garnet-biotite-muscovite bearing leucopegmatite, of similar generation to the late D_3 leucopegmatites in Cabin Canyon (figure 9). The leucopegmatite here is strongly internally mylonitized, with large K-feldspar porphyroclasts in the dike displaying NW-side-down (normal) shear sense on faces parallel to the down-dip, NW-plunging lineation (practice your shear sense determinations and see if you agree). Shear bands in the pelitic schist record this same normal movement and down-dip lineation. The presence of the same lineation orientation and kinematics in the two lithologies present suggest that D_3 deformation was largely penetrative here, and was likely coeval with D_3 deformation in the Cabin Canyon and Elbow Canyon segments of the VMSZ. This deformation is thus part of the Mount Bangs segment of the VMSZ. Leucopegmatites to the S, outside of this D_3 high strain zone, are internally massive and show few signs of D_3 deformation.
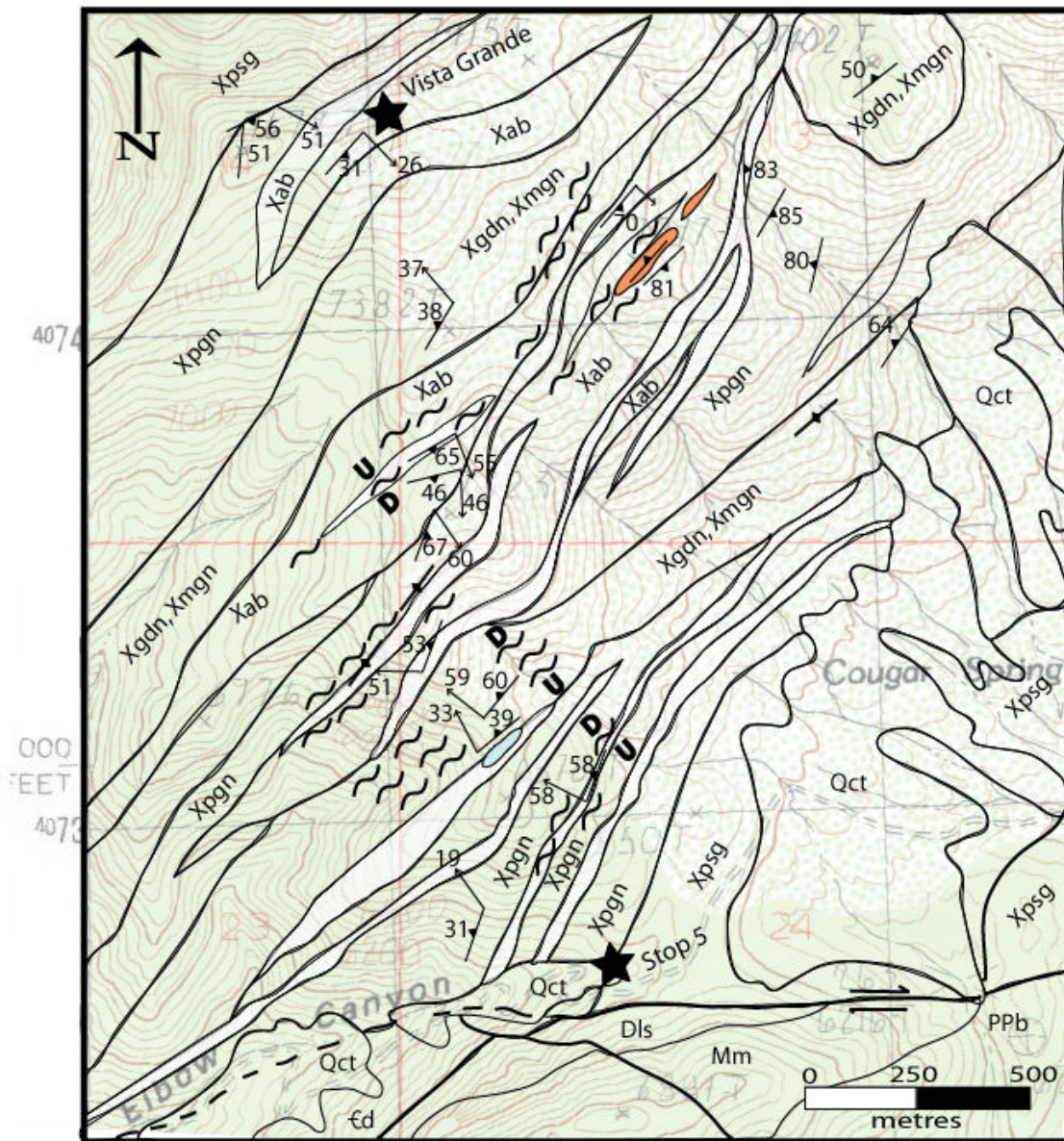
Stop 5B: Ultramafic Pods

After crossing through more deformed leucopegmatites and pelitic schist, we come to a pod of ultramafic rocks cut by leucopegmatites. The rock of interest is a clinopyroxene–orthopyroxene–hornblende ultramafic rock containing serpentinized pits that were formally olivine. This suggests that this rock was likely metamorphosed at granulite facies metamorphic conditions, and then hydrously altered during retrograde metamorphism. The pock-marked appearance is a likely result of the less resilient serpentine–brucite pits. The rock contains the high-temperature S_2 composite foliation, but shows little effect of the lower temperature mylonitic event, and probably remained a physically and chemically competent "lump" during D_3 deformation. We are unsure if these ultramafic rocks represent dismembered mantle rocks from an ophiolite complex or crustal cumulate from deep in an arc sequence, but as we proceed up the hill, think about the importance of juxtaposition of these deep crustal fragments with granitoids, pelitic schists, pillow basalts and marbles, the latter of which will be our last stop of the trip. This association can be thought of as a tectonic "mélange" and we suggest that this mélange represents tectonic mixing early during accretion (we favor the ophiolite idea) and progressive mixing at various crustal conditions (granulite to retrograde shear zone) during a long progressive deformational history.

Stop 5C: Sheared Leucopegmatite

One of the interesting puzzles of Proterozoic terrains throughout the southwestern United States is in unraveling the importance of various plutonic events in the overall crustal evolution. Like the Grand Canyon, the Mojave and adjacent regions (Cerbat Mountains) have evidence for 1,780-1,720 Ma arc (subduction-related) granodiorites, 1,710-1,680 Ma collisional granites and pegmatites that may represent crustal melting, and 1,400 Ma A-type granites. As we walk further up the hill you will see representatives of the first two - a package of granodioritic orthogneiss and pink monzogranite. Further up, we will come across a spectacularly sheared SW-dipping leucopegmatite dike with excellent SW-side-down (normal sense) shear sense indicators. Note that we are likely on the other limb of a NE-trending syncline of unknown generation, and that extensional slip, to this point, has dominated the kinematic analysis. On the underside of the saddle, note the presence of calc-amphibolite gneiss, with the calcareous layers dominated by a calcite-diopside-garnet-hornblende mineralogy (more components of the mélange). Again, the intense D_3 shearing had added an extra component of tectonic mixing of the earlier features, which makes understanding the early history difficult in this area. On our way down from the ridge, we may stop to have a look at an outcrop of tectonic mélange, characterized by a diopside-bearing marble unit juxtaposed with amphibolite layers and fragments of ultramafic rocks.

Stop 5D: Vista Grande

Here we stand along Mount Bangs ridge, with the rocky 8,021 foot summit of Mount Bangs to our immediate northeast; a complexly faulted, SW-dipping section of Cambrian through early Miocene strata to our immediate west and southwest; Sullivans Canyon and Front Faults to our immediate WNW; and the Elbow Canyon fault to our immediate south. Less than 5 kilometers to our west lies the flat-lying Phanerozoic section of the Colorado Plateau Province, capped by the Tertiary basalts of Black Rock Mountain. Less than 5 kilometers to our east lies the Mesquite Basin, one of the deepest basins in the Basin and Range Province, separated from the NVM by the Piedmont Fault. To the north we can view the north plunge of the Proterozoic core of the VMA

Figure 9. Geologic map of the Mount Bangs region, from "Stop 5" at the top of Elbow Canyon to "Vista Grande" along Mount Bangs ridge. See text for explanation.

103

beneath N-dipping strata, and to the south we can view the various faults and undulating basement topography, emphasizing the structural complexities of this region. Certainly a breath-taking spot for discussion of this complex structure!

The main ideas that we wish to discuss here are as follows. We present them as our favored interpretations in order to promote discussion and synthesize ideas presented throughout this field trip.

1) The Proterozoic history of the NVM involved an important early accretionary boundary within Mojave province.
2) The intrusive history and D_1, D_2 is similar to that documented in Grand Canyon and throughout the region.
3) D_3 shear zones are texturally similar to regional 1400 Ma shear zones, but monazite dates suggest deformation was late Paleoproterozoic and raises the intriguing idea that it is linked to a previously unrecognized 1,600-1,500 Ma event, similar to eastern Australia.
4) Proterozoic shear zones and foliation patterns controlled the geometry of Phanerozoic uplift.
5) The Sevier-Laramide history is more important than usually thought and probably marks the inititiation of a modest-sized VMA structural uplift bound by paired monoclines.
6) Miocene deformation involved slip of cover above para-autochthonous basement.
7) The importance of Miocene isostatic uplift as a driving force remains unresolved.
8) Importance of Miocene strike slip and NS shortening in generating the VMA remains unresolved.
9) By whatever combination of mechanisms, basement rocks were rapidly cooled through 100 degrees Celsius at 14 Ma – they were probable close to this temperature at end of Laramide, however there is no evidence for Laramide cooling here.

After discussion of these topics, please proceed back down to the vehicles for the drive back to Cedar City, Utah.

REFERENCES

Axen, G.J., Wernicke, B.P., Taylor, W.J., and Skelly, M.F., 1990, Mesozoic and Cenozoic tectonics of the Sevier thrust belt in the Virgin River Valley area, southern Nevada, *in* Wernicke, B.P., editor, Basin and Range extension near the latitude of Las Vegas, Nevada: Geological Society of America Memoir, v. 176, p. 123-154

Beal, L.H., 1965, Geology and mineral deposits of the Bunkerville mining district, Clark County, Nevada: Bulletin of the Nevada Bureau of Mines, v 63, 96 p.

Beard, L.S., 1993, Preliminary geologic map of the Whitney Pocket 7.5-minute quadrangle, Clark County, Nevada: United States Geological Survey Open-File Report 93-716, scale 1:24,000.

Beard, L.S., 1996, Paleogeography of the Horse Spring Formation in relation to the Lake Mead fault system, *in* Beratan, K.K., editor, Reconstructing the history of Basin and Range extension using sedimentology and stratigraphy: Geological Society of America Special Paper 303, p. 27-60.

Betts, P., and Giles, D., 2000, 1.8 Ga to 1.1 Ga evolution of the Australian continent: a northern, central, and eastern Australian perspective: Geological Society of Australia, v. 59, 34 p., 15th Geological Convention.

Bohannon, R.G., 1984, Nonmarine sedimentary rocks of Tertiary age in the Lake Mead region, southeastern Nevada and northwestern Arizona: U.S. Geological Survey Professional Paper 1259, 72 p.

Duebendorfer, E.M., Chamberlain, K.R., and Jones, C.S., 2001, Paleoproterozoic tectonic history of the Cerbat Mountains, northwest Arizona - Implications for crustal assembly in the southwestern United States: Geological Society of America Bulletin, v. 113, p. 575-590.

Ilg, B., Karlstrom, K.E., Hawkins, D., and Williams, M.L., 1996, Tectonic evolution of paleoproterozoic rocks in the Grand Canyon, insights into middle crustal processes: Geological Society of America Bulletin, v. 108, p. 1149-1166.

Huntoon, P.W., 1990, Phanerozoic structural geology of the Grand Canyon: Grand Canyon Geology, p.261-309.

Karlstrom, K.E., and Bowring, S.A., 1988, Early Proterozoic assembly of Tectonostratigraphic terrains in southwest North America: Journal of Geology, v.96, p. 561-576

Karlstrom, K.E., Harlan, S.S., William, M.L., McLelland, J., Geissman, J.W., and Ahall, K.I., 2001, Long-lived (1.8-0.8 Ga) Cordilleran – type orogen in southern Laurentia, its extensions to Australia and Baltica, and implications for refining Rodinia: Precambrian Research, v 111, p. 5-30

Sanderson, D.J., and Marchini, W.R.D., 1984, Transpression: Journal of Structural Geology, v.6, p. 449-458.

THE NAVAJO AQUIFER SYSTEM OF SOUTHWESTERN UTAH

Geological Society of America 2002 Rocky Mountain Section Annual Meeting
Cedar City, Utah
May 6, 2002

Outcrop of the Navajo Sandstone near Washington, Utah, in the foreground, with the Pine Valley Mountains in the background.

FIELD TRIP LEADERS

Victor M. Heilweil, U.S. Geological Survey
Dennis E. Watt, U.S. Bureau of Reclamation
D. Kip Solomon, University of Utah
Kimball E. Goddard, U.S. Geological Survey

THE NAVAJO AQUIFER SYSTEM OF SOUTHWESTERN UTAH

Geological Society of America 2002 Rocky Mountain Section Annual Meeting
Southern Utah University, Cedar City, Utah
May 6, 2002

Victor M. Heilweil, U.S. Geological Survey
Dennis E. Watt, U.S. Bureau of Reclamation
D. Kip Solomon, University of Utah
Kimball E. Goddard, U.S. Geological Survey

INTRODUCTION

This one-day field trip begins and ends in Cedar City, Utah. Field trip stops will focus on recharge to, movement within, and discharge from the Navajo aquifer system within the central Virgin River basin area (figure 1). The Navajo aquifer system, defined as the combination of the water-bearing parts of the Navajo Sandstone and the Kayenta Formation, provides the majority of municipal water to southwestern Utah. Rapid population growth in this warm and arid region is putting pressure on ground-water managers to further develop this resource in a sustainable manner. In order to do this, spatial and temporal variations in recharge to the aquifer, ground-water residence times, and points of discharge have been quantified during recent studies by the U.S. Geological Survey, the U.S. Bureau of Reclamation, and the University of Utah.

Deposition of the Navajo Sandstone occurred under eolian conditions. It is a well sorted, fine-grained sandstone, with a total thickness between 2,000 and 2,400 feet in the central Virgin River basin area (figure 2). The Kayenta Formation consists of laminar beds of sandstone, siltstone, and silty mudstone, with a total thickness varying between 400 and 900 feet. Located just west of the Colorado Plateau boundary (defined as the Hurricane fault), the formations generally dip toward the north, yet are offset by a series of normal faults, including the Washington Hollow fault, the Snow Canyon fault, and the Gunlock fault. Another prominent structural feature is the Virgin River anticline, which has resulted in uplift and erosion of the Navajo Sandstone and Kayenta Formation.

Most recharge to the Navajo aquifer occurs as diffuse infiltration of precipitation where the Navajo Sandstone crops out or is covered by a thin veneer of surficial soils. Precipitation along the outcrop ranges from 8 to 18 inches per year (figure 1). Detailed studies at Sand Hollow basin show that the amount of diffuse recharge from infiltrating precipitation varies widely and is primarily dependent on runoff from steeply dipping slickrock and the coarseness of surficial soil cover. Other sources of recharge include seepage from perennial and ephemeral streams, infiltration of unconsumed irrigation water, and seepage from underlying formations (figure 3). Recharge to the aquifer in Washington County (west of the Hurricane fault) is estimated at 14 to 59 cubic feet per second (table 1; Heilweil and others, 2000).

Table 1. Estimated ground-water budget for the Navajo aquifer, central Virgin River basin, Utah

	Flow component	Volume (cubic feet per second)
Recharge	Infiltration of precipitation	11 to 33
	Seepage from perennial streams and reservoirs	3 to 13
	Seepage from ephemeral streams	0.3 to 4
	Seepage from underlying formations	0 to 4
	Infiltration of unconsumed irrigation water	0 to 5
	Total Recharge (rounded)	**14 to 59**
Discharge	Well discharge	15 to 23
	Spring discharge	7 to 9
	Seepage to perennial streams (Virgin, Santa Clara Rivers)	7 to 9
	Seepage to underlying formations	0 to 8
	Total Discharge (rounded)	**29 to 49**
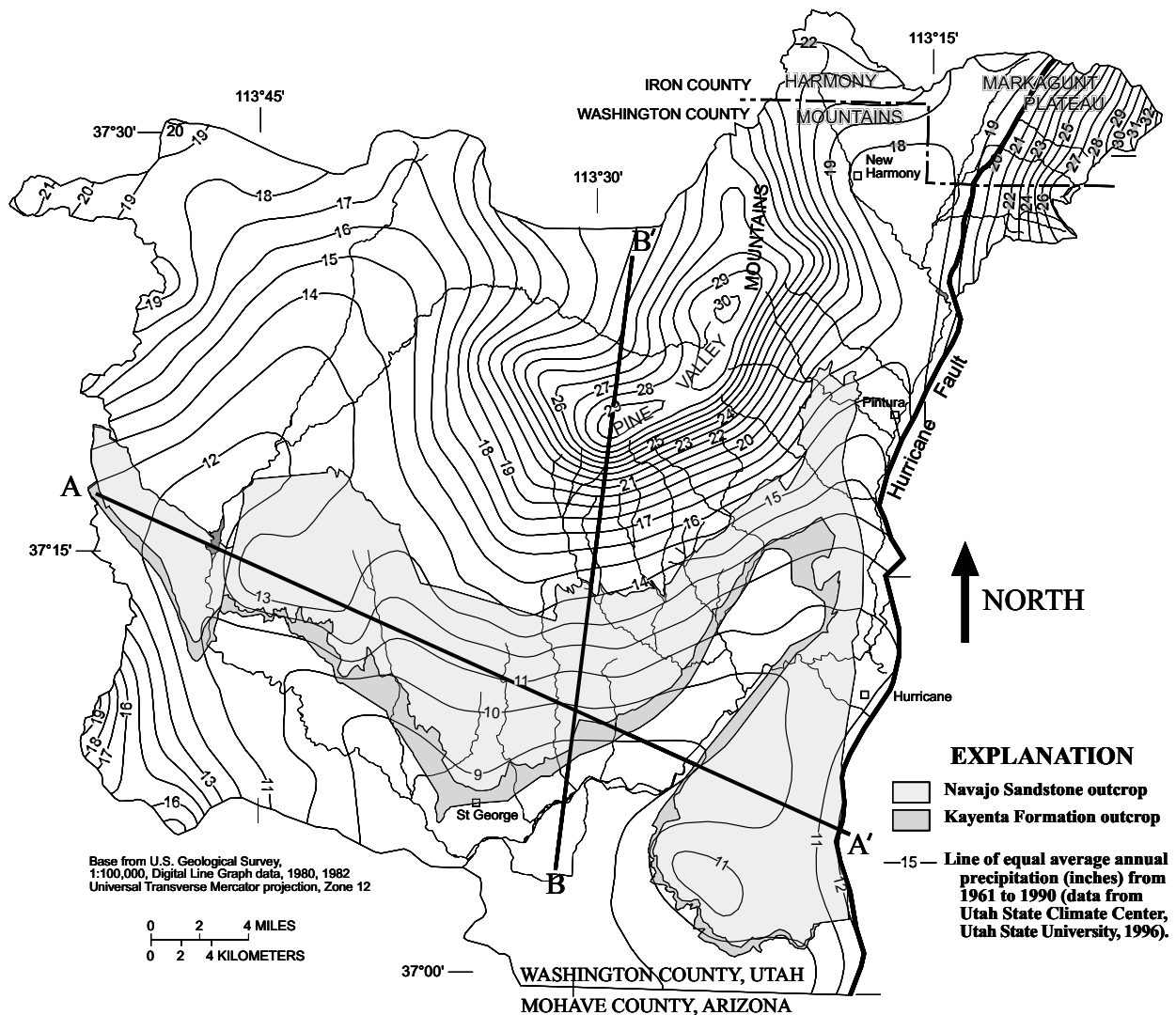
Figure 1. Average annual precipitation contours (1961-1990), location of the Navajo Sandstone and Kayenta Formation outcrops, and location of cross sections (see figure 1) for the central Virgin River basin area, Utah.
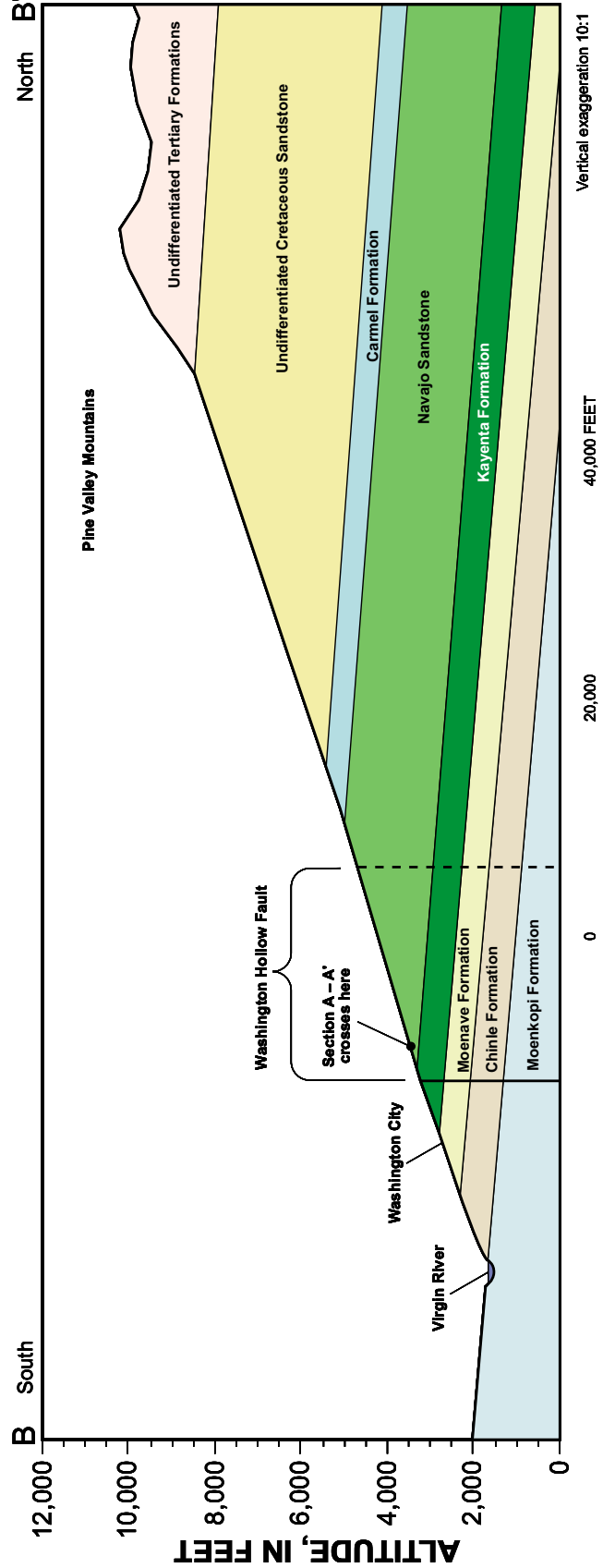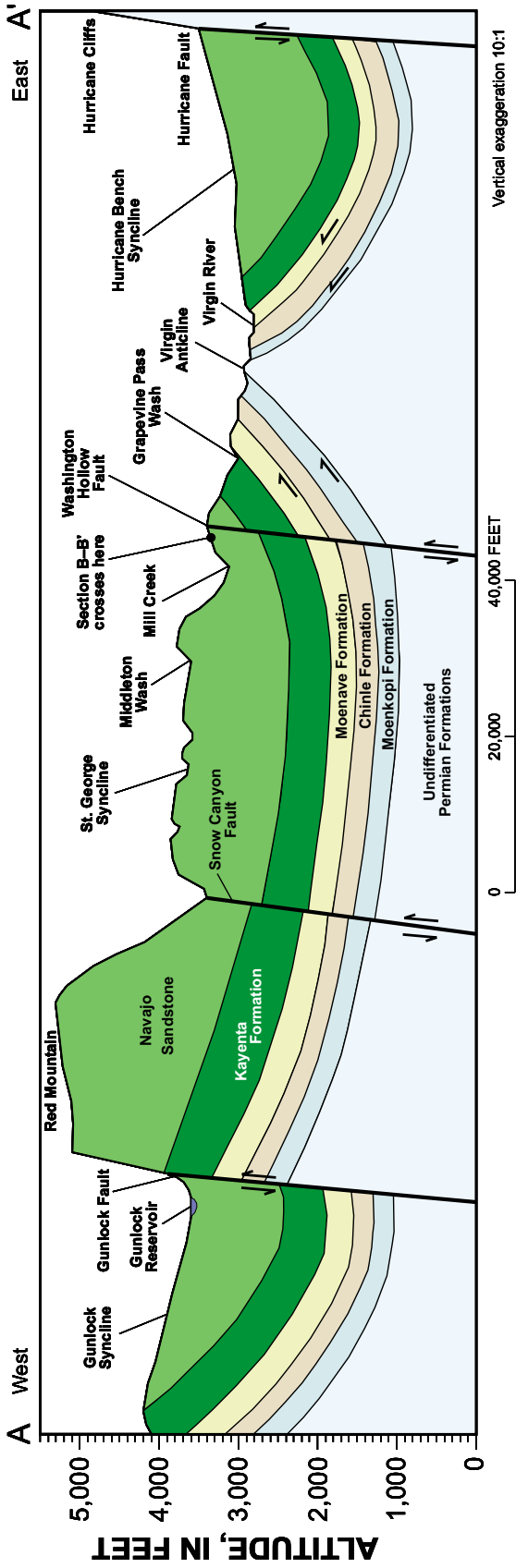
107

Figure 2. Generalized geologic cross sections of the Navajo Sandstone, Kayenta Formation, and surrounding formations within the central Virgin River basin study area, Utah. Cross-section locations shown in Figure 2.

108

Ground water within the Navajo aquifer generally moves from the northern higher-elevation recharge areas along the perimeter of the Pine Valley Mountains toward discharge points farther south. Based on ground-water age dating and modeling, residence times for travel through the aquifer range from tens to thousands of years (Heilweil and others, 1997). These flow rates depend on a combination of hydraulic gradient (steepness of the potentiometric surface) and hydraulic conductivity. While the primary permeability through the intergranular porosity of the sandstone is significant, secondary fracturing greatly enhances this permeability by more than an order of magnitude, as well as causing an anisotropic hydraulic conductivity tensor.

Well withdrawals are the main source of discharge from the aquifer. Other sources include spring discharge, seepage to the Virgin River, and seepage to underlying formations (figure 3). Total discharge from the aquifer in Washington County (west of the Hurricane fault) is estimated at 29 to 49 cubic feet per second (table 1; Heilweil and others, 2000). The recent increase in well withdrawals has intercepted ground-water flow from other natural discharge sources, such as springs and streams. An example of this is the Santa Clara River below Gunlock Reservoir, where increased ground-water pumping during the last three decades has changed this from a gaining to a losing stream reach. The increase in well withdrawals also has resulted in regional water-level declines within the aquifer on the order of tens of feet.
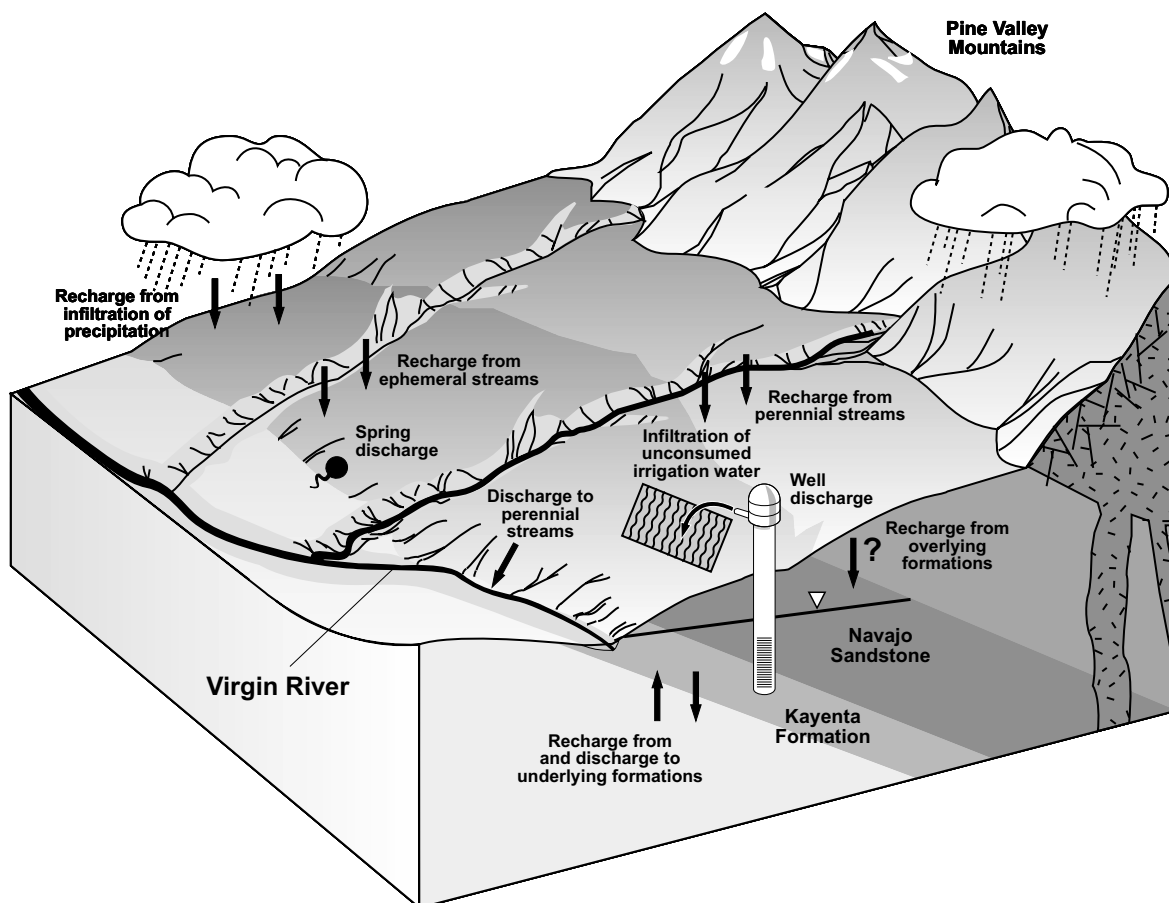
Figure 3. Generalized diagram showing sources of recharge to and discharge from the Navajo aquifer within the central Virgin River basin area, Utah.

Because of limited water resources and further projected growth, the Washington County Water Conservancy District (WCWCD) has been actively planning artificial recharge projects to enhance natural recharge to the Navajo aquifer. The nearly completed Sand Hollow Reservoir near Hurricane, Utah, will serve primarily as a ground-water recharge and recovery project to store Virgin River water during higher snowmelt runoff periods. Similarly, preliminary studies along Sand Cove Wash are underway to evaluate the potential for using excess snowmelt runoff in the Santa Clara River for enhancing recharge to the Navajo aquifer.
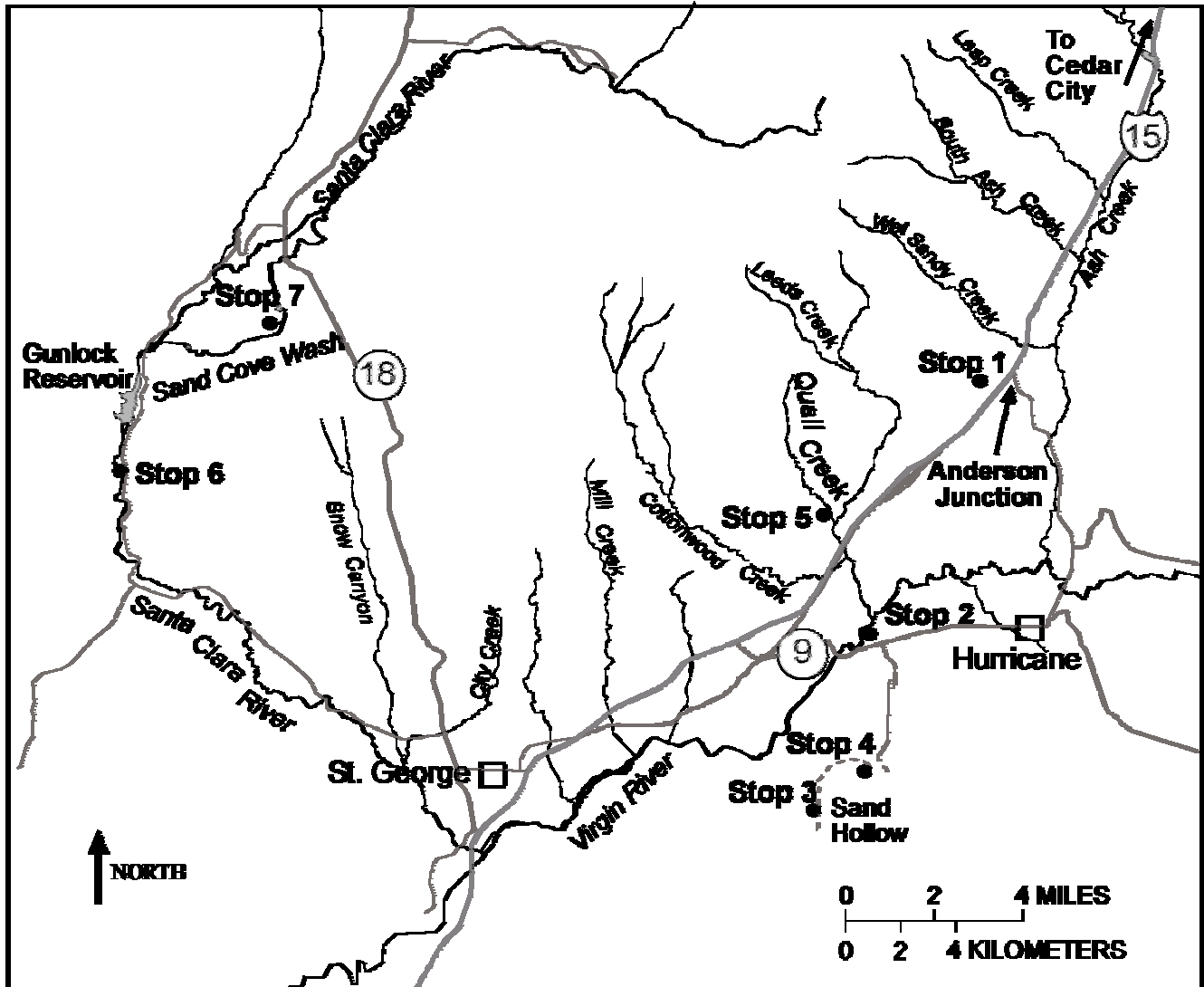
Figure 4. Map showing location of field trip stops.

ROAD LOG

Increment mileage	Cumulative mileage	Description
0.0	0.0	Begin trip at Southern Utah University parking lot near corner of 200 South and 1150 West. Left on 1150 West heading north.
0.2	0.2	Left on Center Street across freeway.
0.3	0.5	Right at stop sign on College Way (1650 West).
0.3	0.8	Right at stop light on 200 North.
0.3	1.1	Right onto southbound I-15 entrance ramp at exit 59.
31.0	32.1	Toquerville Exit, Route 17. South on frontage road.

1.0   33.1   **STOP NO. 1A.** INTRODUCTION AND OVERVIEW: Discussion leader: Kimball
                     Goddard, U.S. Geological Survey; **STOP NO. 1B.** ANDERSON JUNCTION WELL
                     FIELD: Discussion leaders: Hugh Hurlow, Utah Geological Survey; Vic Heilweil, U.S.
                     Geological Survey.

The Navajo Sandstone and Kayenta Formation are extensively fractured, resulting in enhanced secondary permeability of the aquifer. Large variations in hydraulic conductivity within the Navajo aquifer observed during four aquifer tests, conducted by the U.S. Geological Survey (figure 5), are attributed to this fracturing. Hydraulic-conductivity values determined from these tests ranged from 0.2 to 32 feet per day (table 2).
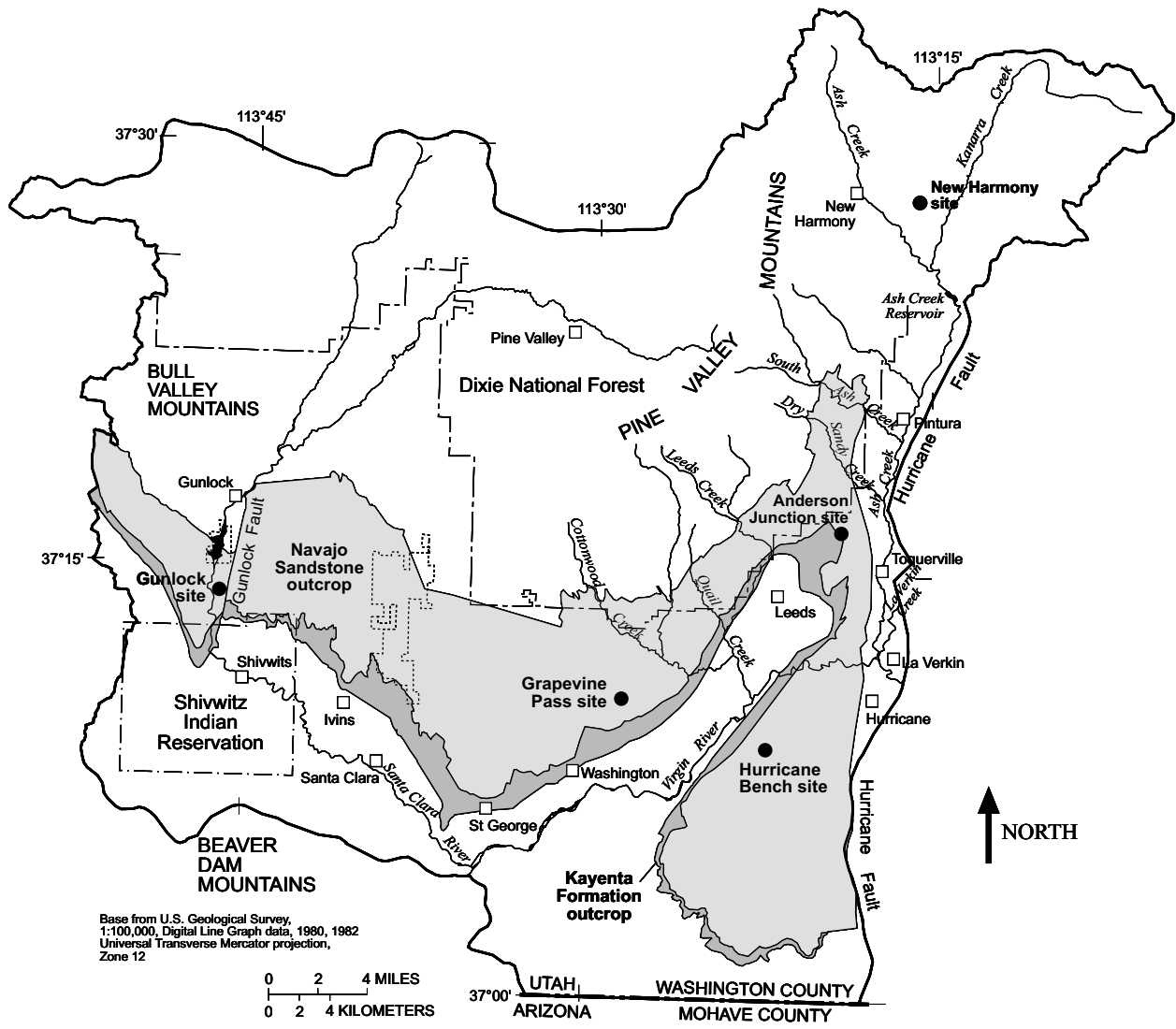
Figure 5. Location of the four Navajo aquifer test sites within the central Virgin River basin study area, Utah.

Table 2. Aquifer-test results from the Navajo aquifer, central Virgin River basin study area, Utah

Location	Number of observation wells	Pumping/ recovery period (days)	Horizontal hydraulic conductivity (feet/day)	Saturated thickness (feet)	Transmissivity (feet^2/day)	Storage coefficient
Anderson Junction	2	4	1.3 to 32	600	1,800 to 19,000	.0007 to .0025
Hurricane Bench	5	5	2.2	500	1,075	.002
Grapevine Pass	20	1	0.2	500	100	----
Gunlock well field	6	6	0.3 to 1.0	1,100	360 to 1,100	.001

The Anderson Junction aquifer test produced the largest hydraulic-conductivity values, corresponding to higher-than-average fracture density measurements taken along sandstone outcrops (Hurlow, 1998, table G.3). Based on these outcrop fracture density measurements, the WCWCD drilled two observation wells perpendicular to each other about 380 feet south and east of the production well (figure 6).
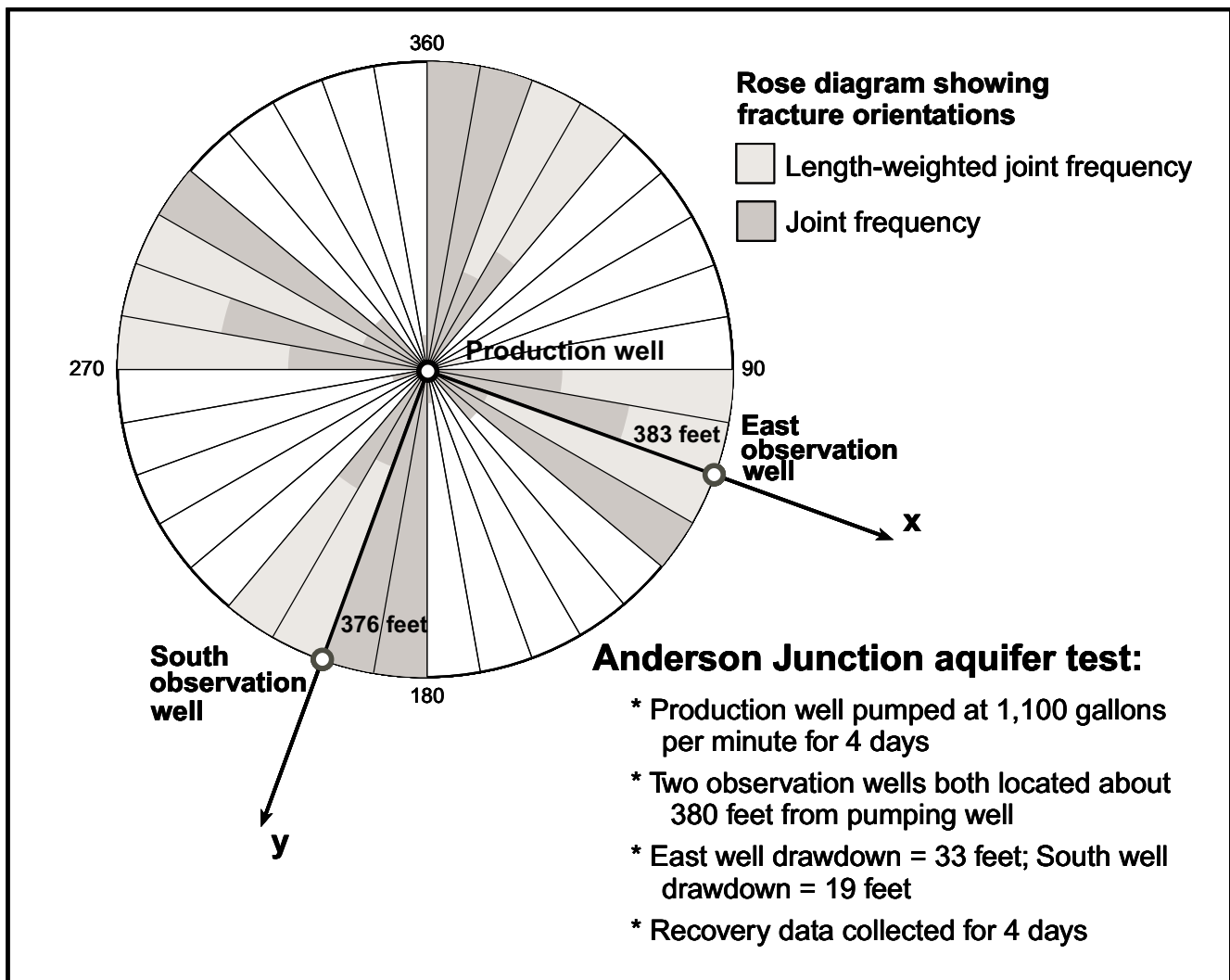
Figure 6. Location of production and observation wells for Anderson Junction aquifer test superimposed on a Rose diagram of outcrop fracture orientations, central Virgin River basin area, Utah.

Large differences in drawdown and recovery at the two wells indicated anisotropic conditions within the sandstone. Data interpretation using a modified version of the Papadopulos method (1965), indicates that hydraulic conductivity varies over 1.5 orders of magnitude because of secondary fracturing (Heilweil and Hseih, 1998). Calculated hydraulic-conductivity values ranged from 1.3 feet per day in the north-south direction to about 32 feet per day in the east-west direction (table 2).

1.0	34.1	Right on Route 17 toward Toquerville.
13.8	47.9	Right before Brentwood Bowling Alley on Hydro-plant road.
1.5	49.4	Left on gravel road.
0.5	49.9	**STOP NO. 2**. VIRGIN RIVER OVERLOOK: Discussion Leader: Vic Heilweil, U.S. Geological Survey.

The Virgin River acts as the primary natural drain for the Navajo Sandstone aquifer west of the Hurricane fault. A seepage study conducted in November 1994 (Herbert, 1995) determined that about 7.2 cubic feet per second directly discharged from the Navajo Sandstone aquifer into the Virgin River, and up to an additional 3.5 cubic feet per second discharged from the sandstone into alluvial deposits along the river (Heilweil and others, 2000). The sources of this discharging ground water include both flow from the north (Anderson Junction area) and flow from the south (Hurricane Bench).

0.5	50.4	Right on Hydro-plant road.
1.5	51.9	Left on Route 17.
0.1	52.0	Left on Floratech Road.
2.5	54.5	Right on gravel road at "Sand Dunes / Sand Hollow View Area" sign.
1.4	55.9	Left at "Y" intersection toward "View Area" (red sign).
0.5	56.4	**STOP NO. 3**. SAND HOLLOW RESERVOIR: Park at the south end of the viewing area. Discussion leaders: Ron Thompson, Washington County Water Conservancy District; Dennis Watt, U.S. Bureau of Reclamation; Vic Heilweil, U.S. Geological Survey.

This is the site of the WCWCD Sand Hollow ground-water recharge and recovery project. The North and West dams will impound surface water that should recharge the underlying Navajo aquifer. Average depth to ground water beneath the basin is about 100 feet. Surface water will be pumped to this off stream reservoir from the Virgin River during periods of high flow, such as spring snowmelt runoff. Infiltration from the conservation pool within the surface-water reservoir will likely be relatively low because of siltation and biofilm development along the reservoir bottom. Infiltration of water stored above the highest conservation pool elevation during higher inflows can be partially managed by scraping the upper margin of the reservoir bottom prior to these seasonal inflows. Scraping would enhance infiltration by breaking up the silt and biofilm deposited during the previous filling cycle. Infiltration rates also can be managed by pumping production wells around the reservoir perimeter to alter the slope of the underlying water table.

Construction of Sand Hollow Reservoir provided unique data-collection opportunities for investigating natural recharge to this basin. The WCWCD drilled more than a dozen observation wells in this small 40 square kilometer basin, which were also used for investigating movement through the unsaturated zone using environmental tracers. The WCWCD also excavated almost 10,000 feet of trenches to depths between 10 and 20 feet, allowing for detailed investigation of unsaturated-zone solutes on a basin-wide scale. The U.S. Geological Survey collected over 800 samples from the trench walls and prepared leachates (by mixing with deionized water). The specific conductance of these leachates revealed large variability in naturally accumulating, unsaturated-zone solutes (figure 7). Areas without large accumulations of solutes indicate regions where active recharge from infiltrating precipitation occurs. Conversely, areas with substantial solute accumulation indicate places where plant roots effectively capture most infiltration passing through the surficial soils. This evapotranspiration of pure water causes the concentration of solutes (from precipitation and atmospheric deposition) in the unsaturated zone.

The U.S. Geological Survey and the U.S. Bureau of Reclamation conducted a soil moisture survey adjacent to the trenches after a month of above-normal precipitation. The results indicate that areas where infiltrating precipitation is able to quickly reach the bedrock contact had correspondingly little solute accumulation in the underlying bedrock trench. Laboratory particle-size analysis of these surficial soils showed a similar correlation between grain size and accumulation of solutes in the underlying bedrock. Areas where surficial soils were coarser generally correspond to areas in the underlying trench with little or no accumulation of solutes in the unsaturated zone of the Navajo Sandstone. This indicates that infiltrating moisture can move more quickly past the root zone and into the underlying Navajo Sandstone in areas with coarser-grained soils, thus escaping interception by plant roots. In these active recharge areas, evapotranspiration and solute concentration are minimal. Conversely, areas with finer soils are able to store more water because of higher porosity and capillarity. In these regions, plant roots are able to use most of this infiltration, resulting in higher evapotranspiration rates and substantial solute accumulation in the underlying Navajo Sandstone (Heilweil and Solomon, 2001).
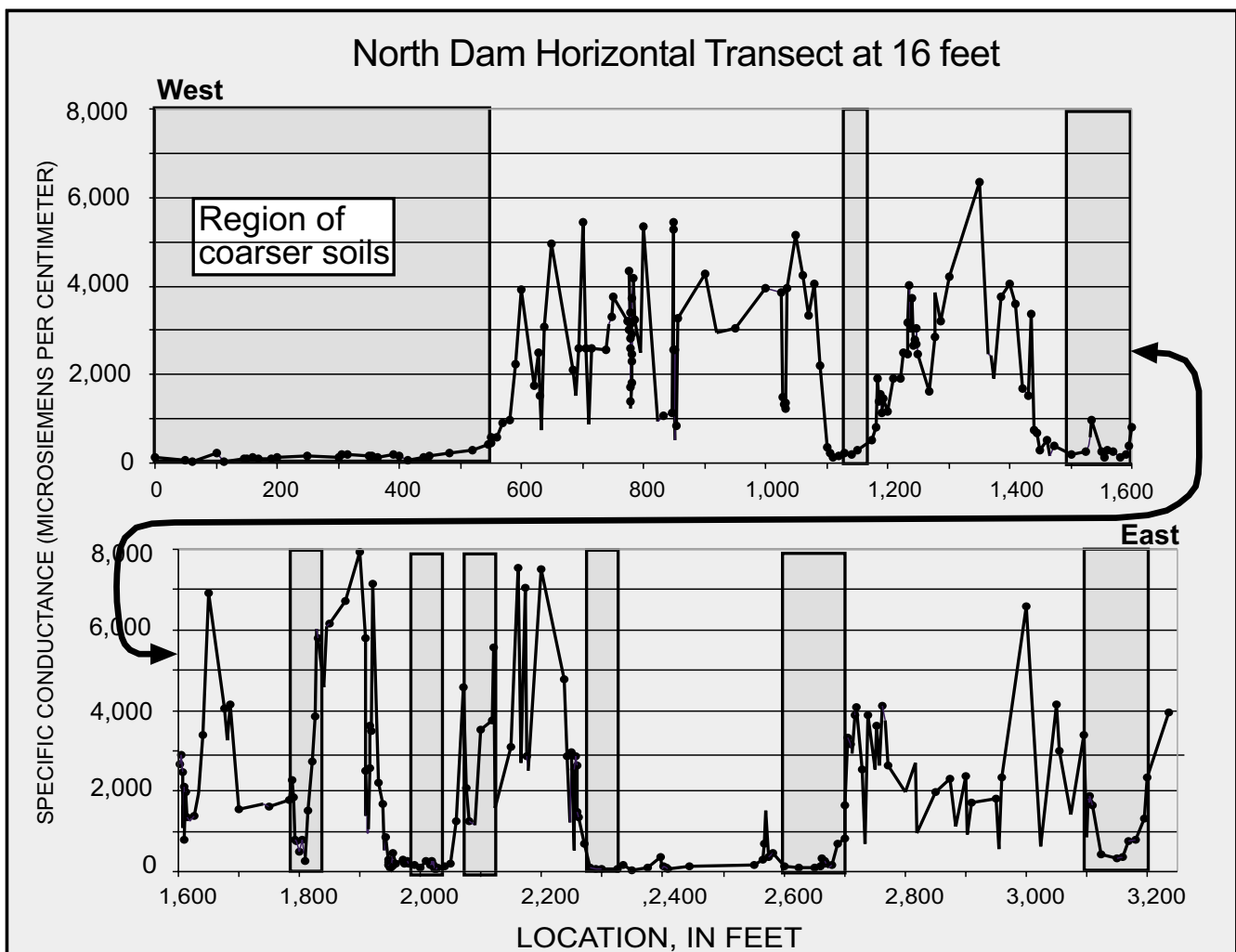
Figure 7. Solute concentrations of leachates along the bottom of the North Dam trench and relationship to coarseness of surficial soils, Sand Hollow basin, Utah.

The U.S. Geological Survey and the University of Utah analyzed chloride, tritium, and stable isotope (hydrogen and oxygen) concentrations of precipitation, unsaturated-zone pore water, and ground water to further evaluate recharge to Sand Hollow basin. The chloride mass balance method was used to estimate average recharge for the entire basin. This method compares average chloride concentration in precipitation to that of ground water. For Sand Hollow basin, that ratio is about 5 percent of precipitation, indicating about 0.4 inch of recharge annually. However, the variation in ground-water chloride concentrations from wells (from 3 to

60 mg/l) indicates considerable spatial variability throughout the basin. Chloride concentrations in unsaturated-zone pore waters are also elevated in many parts of the basin (up to 30,000 mg/l), indicating that solutes from precipitation have been accumulating for thousands of years. These accumulations are caused by plant evapotranspiration in areas with finer-grained soils, which can store more moisture. The large chloride accumulations show that plants can effectively utilize most of the infiltrating precipitation in these areas, resulting in little recharge. Therefore, large unsaturated-zone pore-water chloride concentrations in the underlying sandstone generally correlate with regions of higher ground-water chloride.
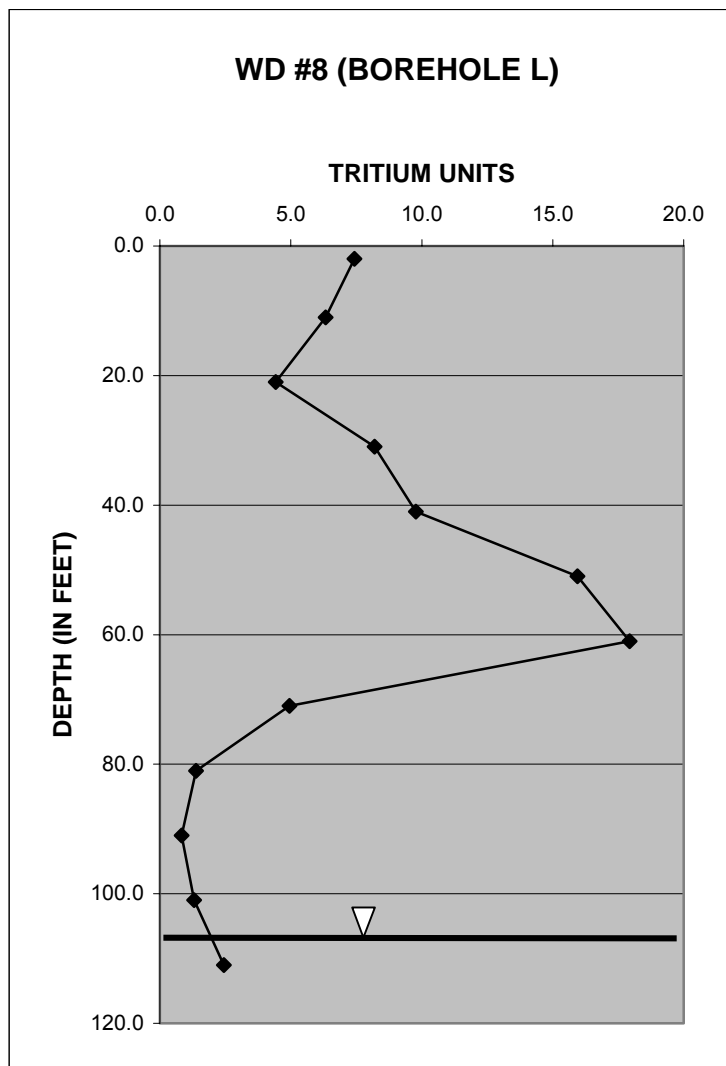
Figure 8. Profile of unsaturated-zone pore-water tritium from WD #8 well (borehole L), Sand Hollow basin, Utah.

Similar to the chloride mass balance method, the mass of anthropogenic tritium in the unsaturated zone can be compared to the amount of tritium in precipitation to estimate recharge rates. Figure 8 shows one unsaturated-zone tritium profile from a high recharge area at the base of a large exposure of sandstone outcrop. Note that the peak concentration (greater than 12 tritium units) at a depth of about 60 feet represents precipitation that fell during the early 1960's peak in above ground nuclear testing. On the basis of unsaturated-zone pore-water tritium profiles, recharge rates at Sand Hollow vary from around 0.5 to over 7 percent of precipitation. There is a strong correlation between areas with high recharge rates, based on unsaturated-zone tritium, and low unsaturated-zone solute accumulations. On the basis of trench and borehole core samples, the unshaded areas of figure 9 are regions within Sand Hollow basin with little solute accumulation in the unsaturated zone. Recharge rates in these areas, based on unsaturated-zone tritium, generally are greater than

1 percent of precipitation. Conversely, the shaded areas represent regions with substantial accumulation of unsaturated-zone solutes. Recharge rates in these areas generally are less than 1 percent of precipitation.
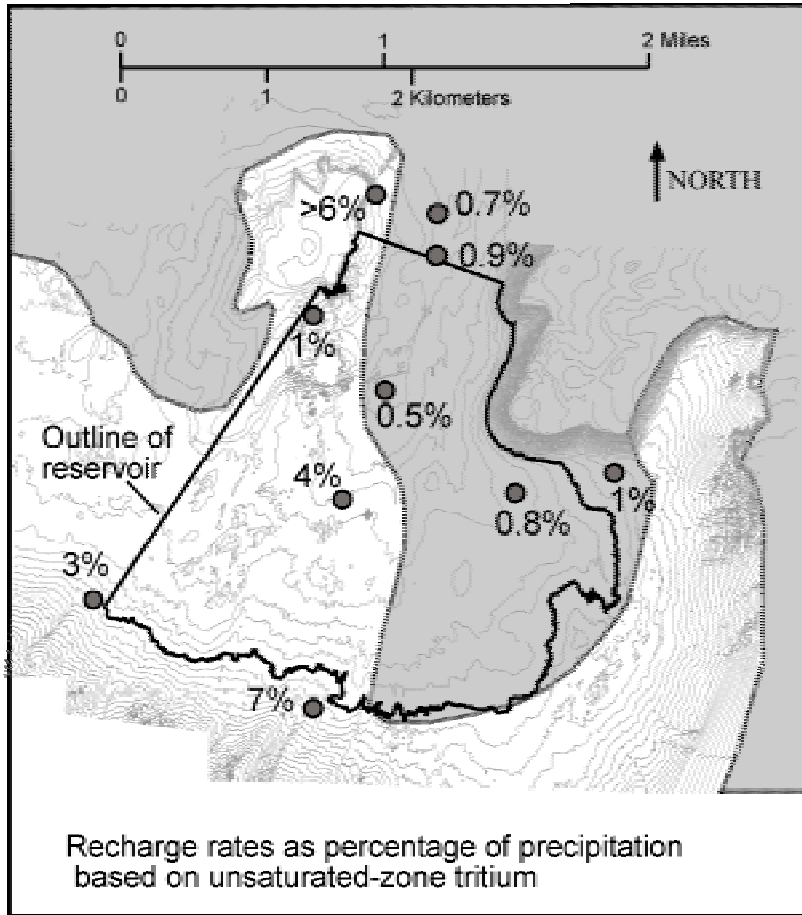
Figure 9. Relation between area of high unsaturated-zone solute accumulation (shown by gray shading) and higher recharge rates (based on unsaturated-zone tritium) at Sand Hollow basin, Utah.

2.3   58.7   Right on North Dam access road.

0.9   59.6   Right on dirt road before dam (then pass construction trailers on right).

0.2   59.8   **STOP NO. 4.** INFILTRATION POND EXPERIMENT SITE: Discussion leaders: D. Kip Solomon, University of Utah; Dennis Watt, U.S. Bureau of Reclamation; Vic Heilweil, U.S. Geological Survey.

This is the site of a 10-month infiltration experiment conducted by the U.S. Geological Survey, the U.S. Bureau of Reclamation, and the University of Utah to better estimate expected seepage rates beneath Sand Hollow Reservoir. After the first few days, net infiltration rates ranged from about 0.13 to 0.23 feet per day of water (fig. 10). These rates account for evaporation, which varied from 0.002 feet per day in the winter to 0.042 feet per day in the summer. It is likely that long-term seepage rates beneath Sand Hollow Reservoir will be much lower due to: (1) a decreasing hydraulic gradient once the ground-water mound connects with the saturated wetting front; and (2) siltation and biofilm development on the bottom of the reservoir. A feasibility study by EWP Engineering (1997) describes a Hantush calculation of 19 cubic feet per second of seepage beneath Sand Hollow Reservoir without considering reductions due to clogging. They estimated that siltation and biofilm development may reduce actual long-term seepage rates to about 10 cubic feet per second, or a rate of 0.04 feet per day, which is one quarter of the initial rates based on results from the infiltration pond experiment.

116
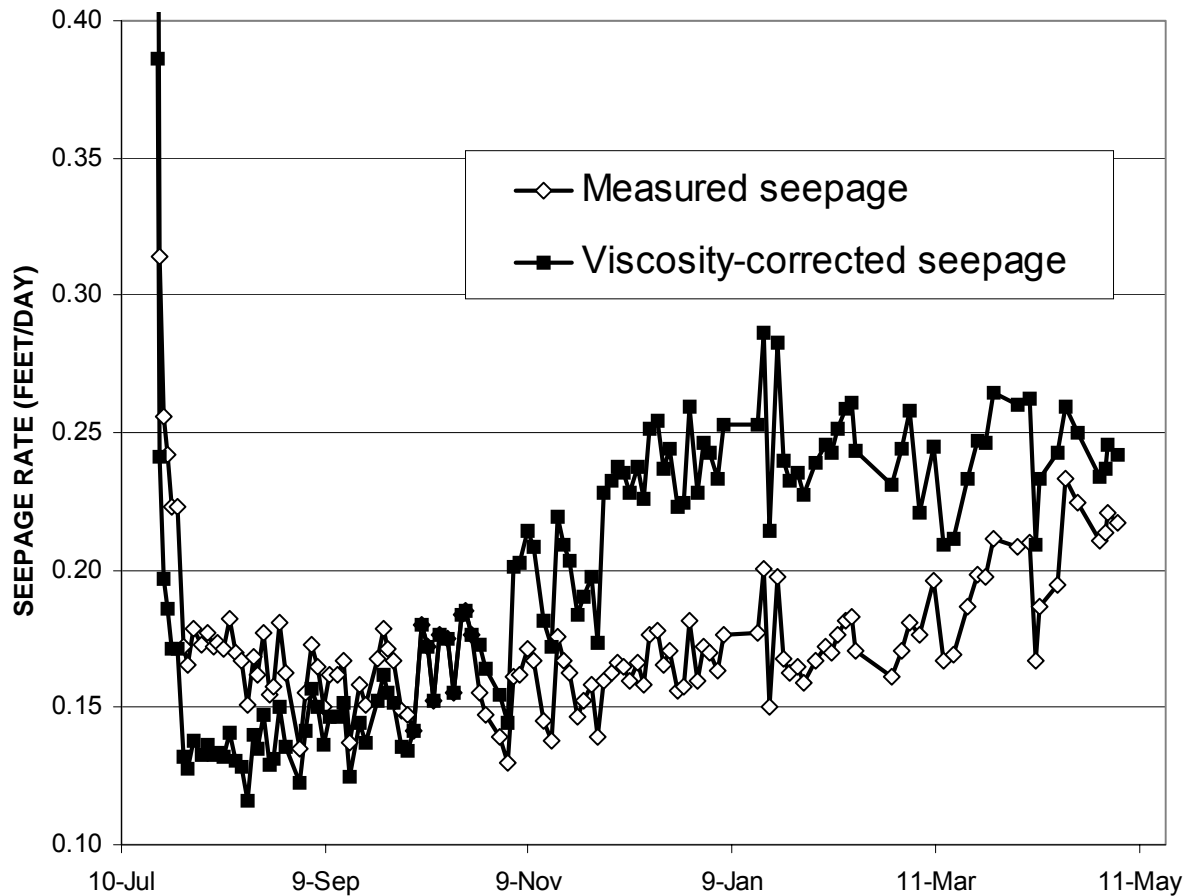
Figure 10. Seepage rates during the infiltration pond experiment at Sand Hollow basin, Utah.

The infiltration pond seepage rates were lower than expected based on laboratory permeability testing of the Navajo Sandstone and variably saturated flow modeling. It is thought that these lower rates were due to a combination of (1) trapped gas and/or biofilm development beneath the pond, and (2) a low-permeability layer of caliche along the top of the Navajo Sandstone contact. A dissolved-helium tracer was added to the pond to evaluate the percentage of trapped gas in the subsurface. Because of its low solubility, the helium readily partitioned into any trapped gas encountered. Its retardation, with respect to a conservative bromide tracer (figure 11), indicates that up to 8 percent of the total porosity was filled with trapped gas. Theoretically, this gas would exist mostly in the larger pore-throats and could result in a factor of 10 decrease in hydraulic conductivity. Figure 10 also shows seepage rates corrected for the variation in viscosity caused by changes water temperature. The increased viscosity-corrected seepage rates during the fall are likely caused by the dissolution of trapped gas.
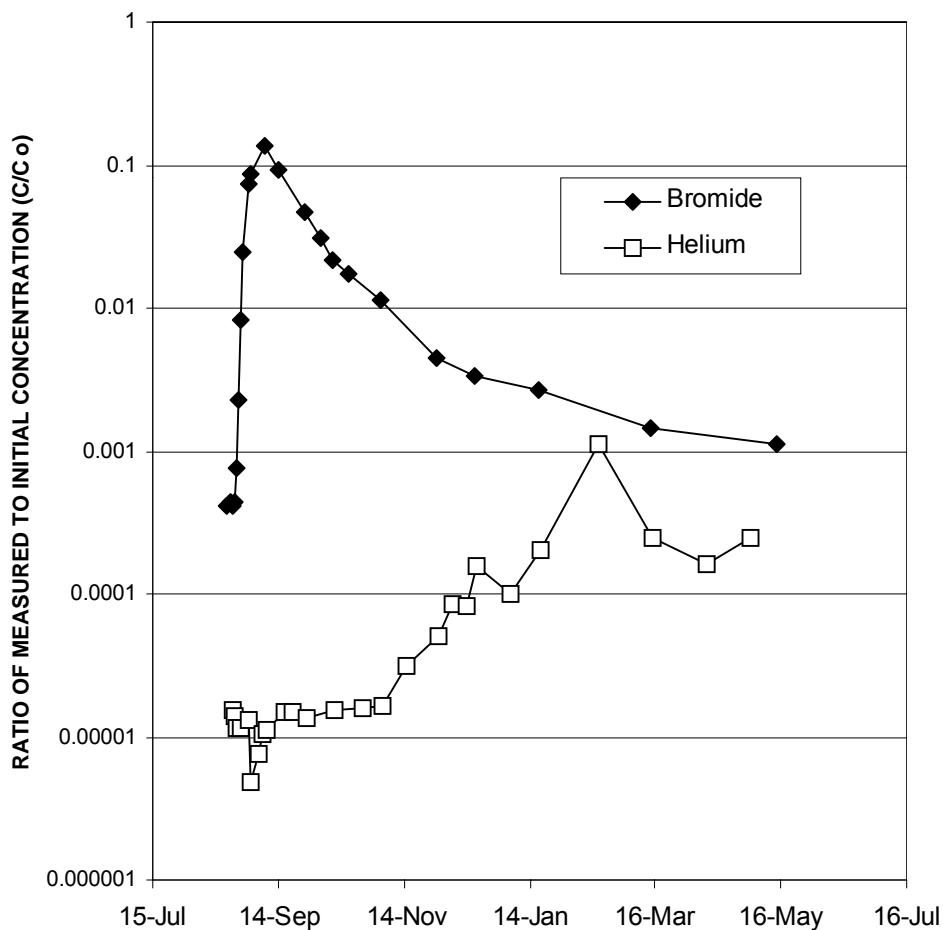
Figure 11. Retardation of helium with respect to bromide at a depth of 5.5 feet beneath the infiltration pond, Sand Hollow basin, Utah.

A previously unconsidered but potentially negative aspect of the infiltration pond experiment was the flushing of naturally accumulating unsaturated-zone salts down to the water table (figure 12). This caused dissolved-solids, nutrients, and arsenic concentrations in the ground water to temporarily exceed the State of Utah drinking water standards (Utah Department of Environmental Quality, 2001). Cross-sectional modeling indicates that these salts will rapidly be diluted in the underlying aquifer because of relatively high seepage rates and large aquifer thickness (Ludwig, 2002). However, such salt flushing from the unsaturated zone may cause substantial degradation of ground-water quality beneath arid-region artificial recharge basins with lower seepage rates and/or a thinner underlying aquifer.
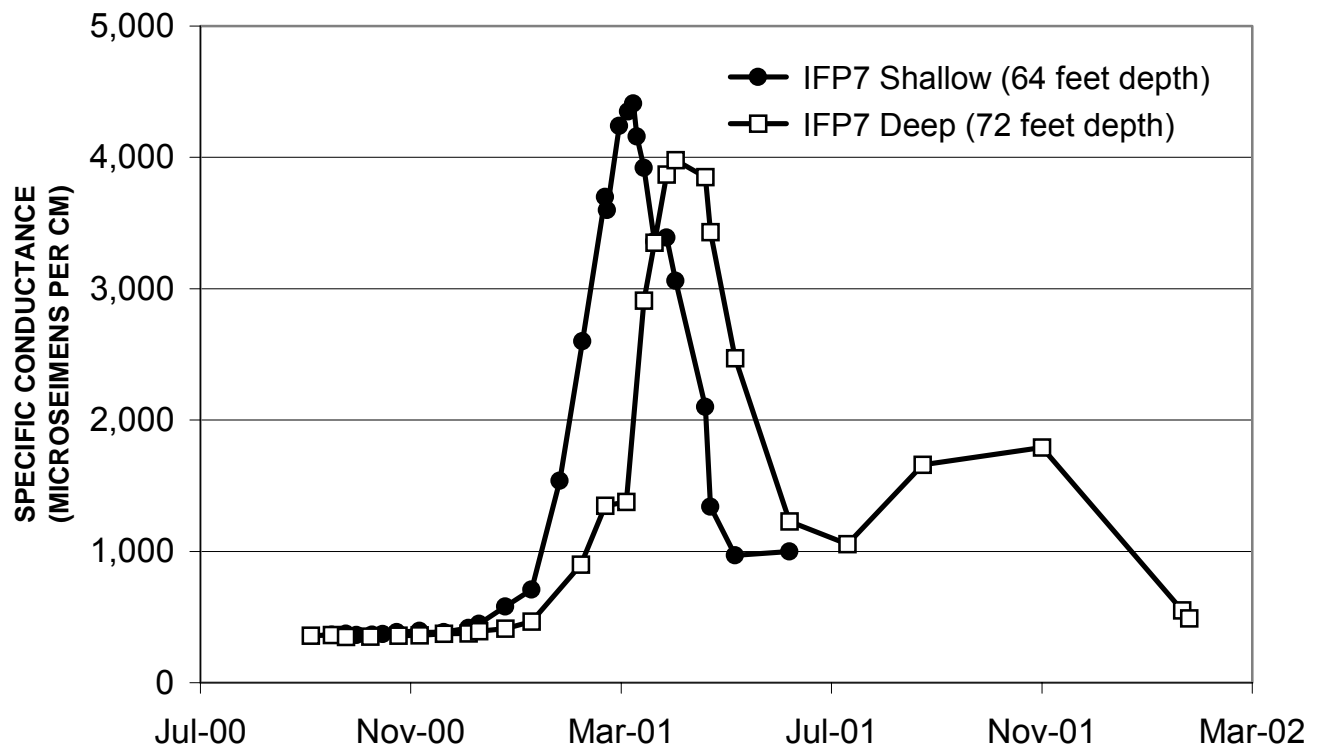
Figure 12. Increase in specific conductance of shallow ground water beneath the infiltration pond at Sand Hollow basin, Utah.

0.2	60.0	Left on North Dam access road.
3.4	63.4	Left on Highway 9.
2.3	65.7	Right on Quail Creek Reservoir road.
1.0	66.7	**Point of Interest**: Passing through axis of Virgin River anticline.
2.0	68.7	Right on I-15 frontage road.
0.3	69.0	Left under highway to Red Cliffs Recreation Area.
1.7	70.7	**STOP NO. 5**: RED CLIFFS RECREATION AREA: Lunch and optional hike along Quail Creek. Discussion Leader: Vic Heilweil, U.S. Geological Survey.

Quail Creek is one of six perennial streams within the central Virgin River basin that recharge the Navajo Sandstone aquifer as they traverse its outcrop. Seepage measurements during October 1995 indicated that about 0.2 cubic foot per second recharges the Navajo Sandstone aquifer from the creek. Figure 13 shows all potential sources of recharge to the aquifer, including the locations of these perennial streams and the amount of measured seepage loss to the underlying aquifer. Total recharge to the Navajo aquifer within the study area from perennial streams and reservoirs is estimated to be between 3 and 13 cubic feet per second (table 1, Heilweil and others, 2000).

<u>Lunch Discussion: Recharge from Underlying Formations</u>

Another source of recharge shown in figure 13, but not "visited" during a field trip stop is seepage from underlying formations. This form of recharge is thought to occur in two distinct areas within the central Virgin River basin: north of St. George and southwest of Hurricane (figure 13). These areas, characterized by the Utah Geological Survey as low-temperature geothermal areas (Budding and Sommer, 1986), have slightly elevated ground-water temperatures (20 to 35 degrees Centigrade) and dissolved-solids concentrations greater than 500 mg/L. The geochemical signature of these higher solute waters within the Navajo Sandstone aquifer, shown in figure 14, indicates that the source of this water is from underlying formations. Simple ground-water mixing models indicate that recharge to the aquifer from underlying formations is about 2.7 cubic feet per second north of St. George and 1.5 feet per second southwest of Hurricane (Heilweil and others, 2000).

1.7	72.4	Leave Red Cliffs Recreation Area and turn right on I-15 frontage road.
3.8	76.2	Right on Highway 9 (State St.).
1.0	77.2	Left on I-15 southbound entrance ramp.
7.3	84.5	Exit 8; Right on St. George Blvd.
2.0	86.5	Right on Bluff Street.
1.1	87.6	Left on Sunset Blvd. (old Highway 9).
11.0	98.6	Right on Gunlock Road.
4.2	102.8	Right on dirt road toward Gunlock Well #7 pump house. **STOP NO. 6A**: GUNLOCK WELL FIELD AQUIFER TEST: Discussion Leader: Vic Heilweil, U.S. Geological Survey.

During February 1996, The U.S. Geological Survey conducted a multiple-well aquifer test at St. George City Water and Power Well #7. St. George City pumped this well for 6 days at about 850 gallons per minute. The U.S. Geological Survey measured water levels at seven observation wells during the test (figure 15), but only two of these (#8 and #5) had measurable effects from the pumping (figure 16). Flumes installed in the Santa Clara River showed a decrease in flow by about 110 gallons per minute during the test. It is assumed that additional leakage to the Navajo aquifer came from the saturated fluvial sediments underlying the river. Because of this pumping-induced stream leakage and fracture-induced anisotropy, the aquifer-test data could not be analyzed with standard analytical techniques (figure 17). Rather, The U.S. Geological Survey constructed a three-dimensional ground-water flow model (figure 18) to evaluate hydraulic properties. The model indicates that the hydraulic conductivity of the Navajo Sandstone at this site is 0.3 feet per day in the east-west orientation and 1.0 feet per day in the north-south direction (Heilweil and others, 2000). Interestingly, this is perpendicular to the predominant direction of anisotropy found at the Anderson Junction aquifer test site (Stop No. 1). One limitation of the model is that the unconsolidated fluvial sediments were not included as a separate model layer.
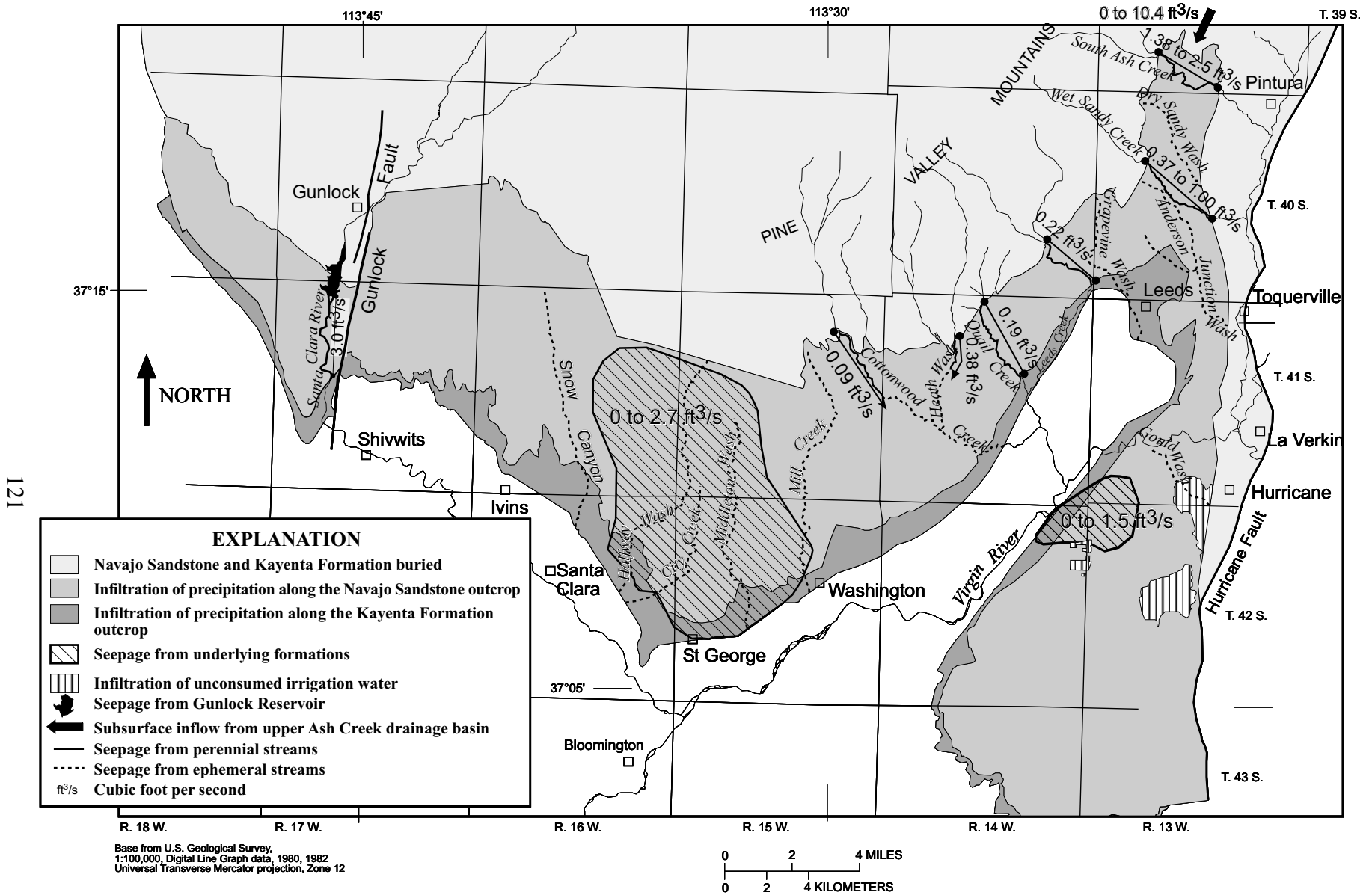
Figure 13. Potential sources of recharge to the Navajo Aquifer in the central Virgin River basin area, Utah

Figure 14. Relation of Navajo aquifer samples with high dissolved-solids concentration to the chemical composition of samples collected from overlying and underlying formations within the central Virgin River basin area, Utah.
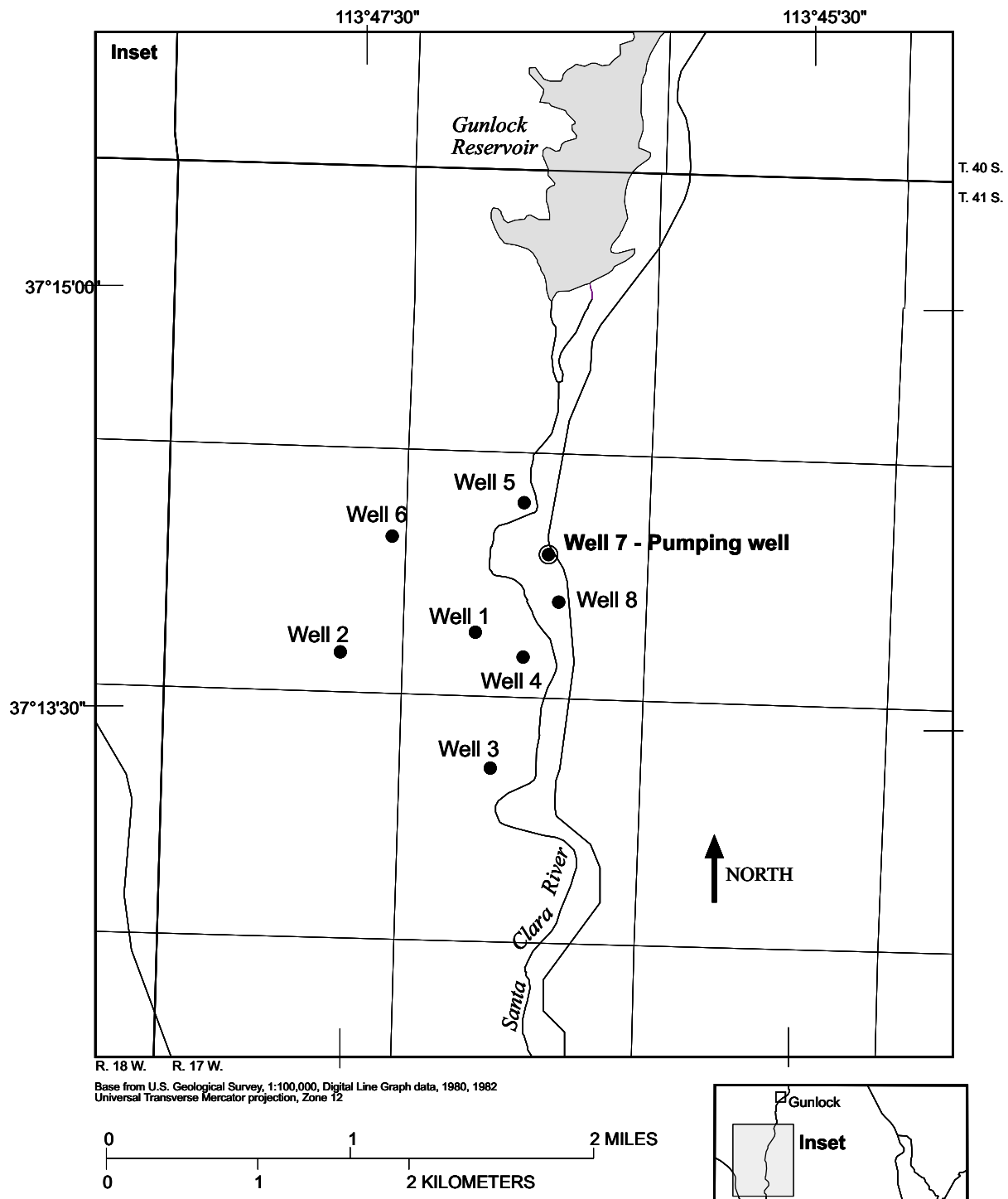
Figure 15. Location and identification of wells used for water-level measurements during the February 1996 Gunlock aquifer test, central Virgin River basin area, Utah.
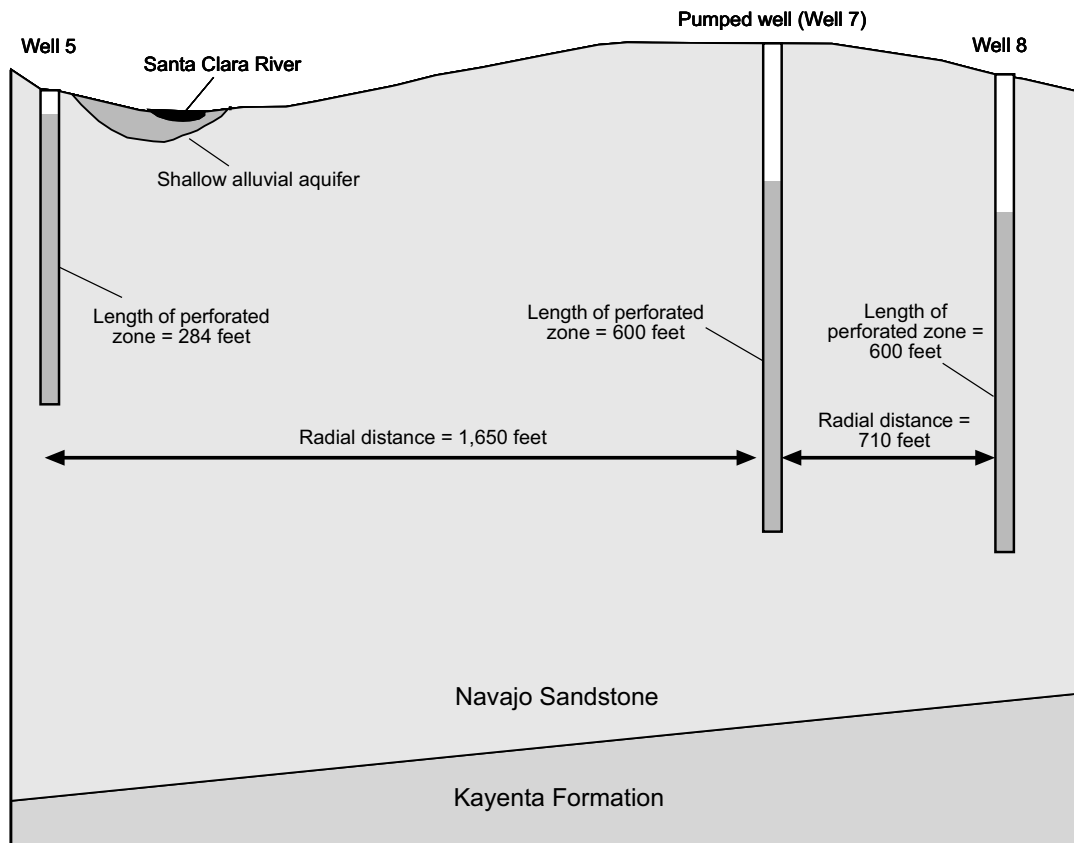
Figure 16. Generalized geologic cross section in the vicinity of the pumped well for the Gunlock aquifer test, central Virgin River basin area, Utah.
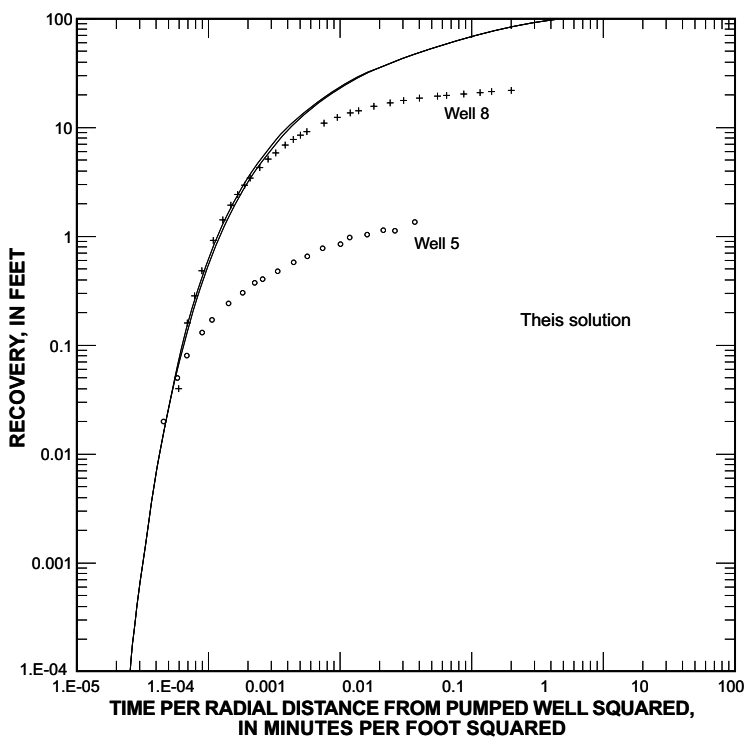
Figure 17. Theis solution fit to recovery data from two observation wells during the February 1996 Gunlock aquifer test, central Virgin River basin area, Utah.

124
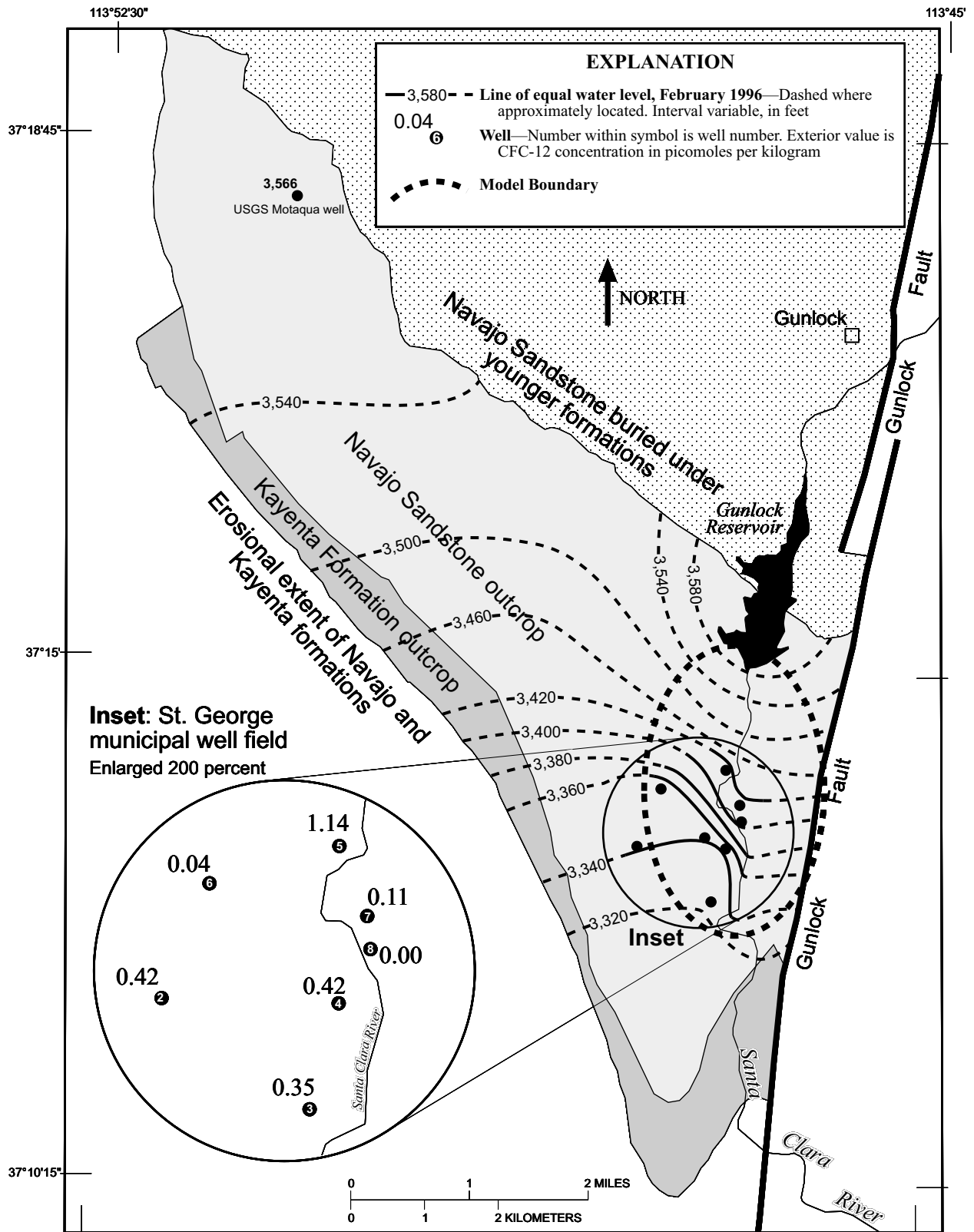
Figure 18. Aquifer-test ground-water model boundary, potentiometric contours, and chlorofluorocarbon concentrations in the Gunlock part of the Navajo aquifer, central Virgin River basin area, Utah.

125

0.0   102.8   **STOP NO. 6B**: SANTA CLARA RIVER: Cross road and walk down to Santa Clara River. Discussion leaders: Steve Meismer, Virgin River Recovery Program; Vic Heilweil, U.S. Geological Survey.

A seepage study along the part of the Santa Clara River traversing the Navajo Sandstone outcrop in 1974 (Cordova, 1978) found that 1.5 cubic feet per second of ground water discharged into the river, which acted as a regional drain for the aquifer. Subsequent ground-water development by the City of St. George has resulted in a reversal in hydraulic gradient, such that the Santa Clara River now loses water to the aquifer. Measurements in 1995 and 1996 indicate that between 4 and 5 cubic feet per second seeps from the river into the underlying aquifer (Heilweil and others, 2000). The amount of stream loss may increase as the amount of ground-water withdrawals continues to increase.

Comparison of ground water and Santa Clara River water chemistry also indicates that the river is the primary source of recharge for St. George City's well field. Figure 18 shows that wells downgradient of the river have fairly high CFC-12 concentrations, similar to Santa Clara River water. The presence of CFC-12 generally indicates a meteoric source of precipitation within the past 50 years (Busenberg and Plummer, 1992). Because these production wells are screened over hundreds of feet; however, the well water may be a mixture of both older and younger ground water. Except for Well No. 2, the general chemistry of the ground water is nearly identical to that of the Santa Clara River (figure 19). Well No. 2 has higher dissolved solids concentrations and a geochemical signature more similar to water from underlying formations (figure 14). This indicates that Well No. 2, which is perforated closer to the base of the Navajo Sandstone, derives some of its water from underlying formations (Heilweil and others, 2000).

To conserve surface water (protect it from seepage and evapotranspiration along the natural stream channel), a pipeline is being planned between the Gunlock Reservoir and the town of Ivins. This water savings should allow for at least 3 cubic feet per second to be released year round along the natural wash. The Virgin River Recovery Program, charged with protecting and enhancing native fish species in the Virgin River basin, is presently evaluating this amount of discharge from the reservoir to determine if it is sufficient to meet the in-stream needs of the native fish population. Part of this evaluation includes a release experiment from the Gunlock Reservoir along the Santa Clara River to determine the amount of water that needs to be released from the reservoir to maintain sufficient flow in the Santa Clara River below the Gunlock well field.

The array of piezometers at this location and two other downstream sites is part of this effort to evaluate instream flows. By monitoring water levels in the unconsolidated fluvial sediments during the release experiment, changes in storage can be evaluated for determining when seepage rates from the stream have reached steady-state conditions. The piezometers also will be used to evaluate the hydraulic connection between the river, the unconsolidated fluvial sediments, and the underlying Navajo Sandstone.
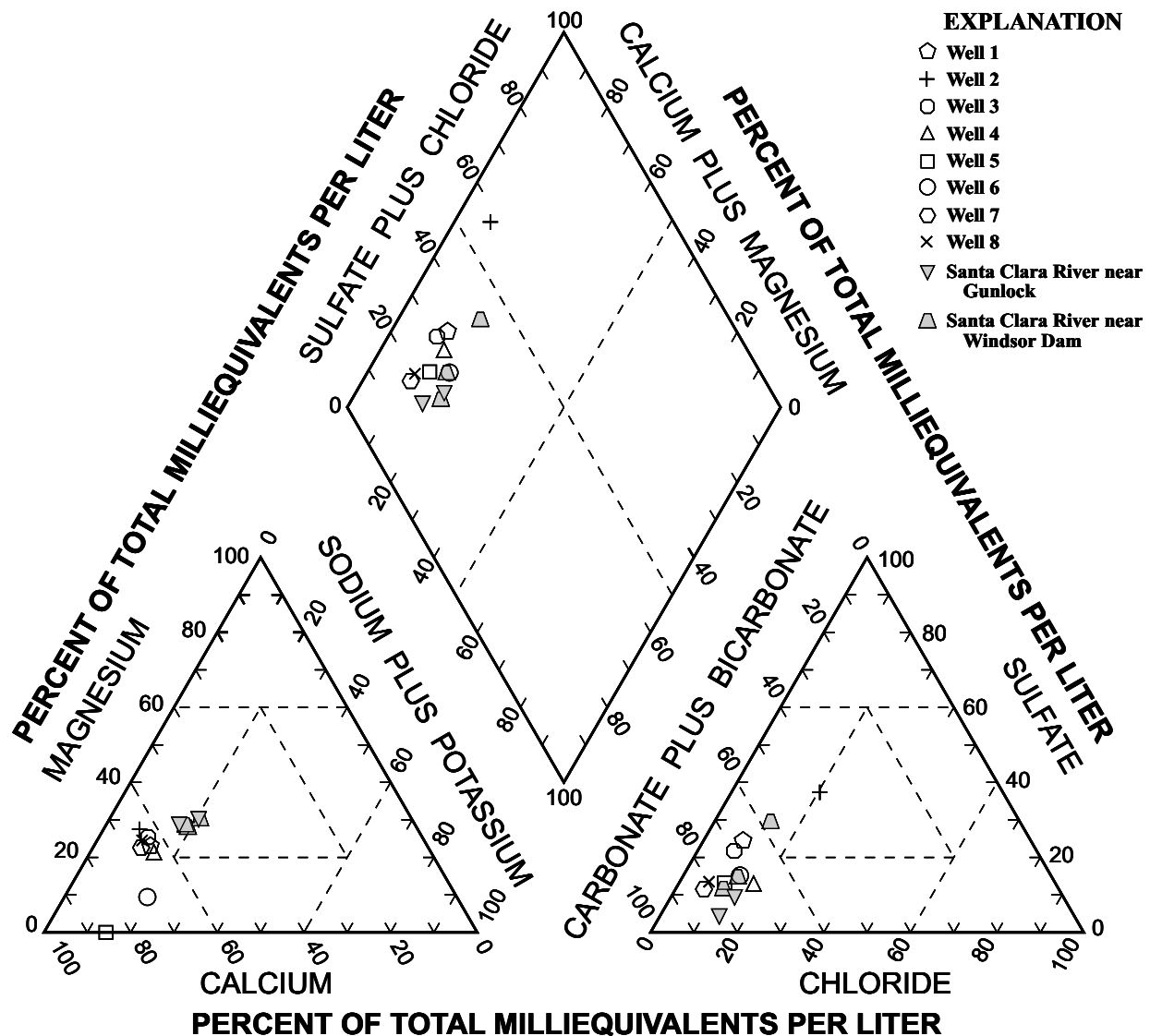
Figure 19. Geochemical comparison of Gunlock well-field ground water to Santa Clara River water, central Virgin River basin study area, Utah.

1.9	104.7	**Point of Interest**: Confluence of Sand Cove Wash with Gunlock Reservoir.
1.6	106.3	Right on gravel road at "Gunlock Town Limit" sign.
5.9	112.2	Right on dirt road toward Sand Cove.
1.0	113.2	**STOP NO. 7**: SAND COVE WASH: Discussion Leaders: David Susong, U.S. Geological Survey; Dennis Watt, U.S. Bureau of Reclamation. Note: Stop No. 7 is on private land and is not accessible to the public. An alternative spot to view Sand Cove Wash is behind the Utah Power and Light power plant on the south side of the road about 4 miles past Gunlock

Sand Cove Wash is an ephemeral wash that is presently being evaluated as a potential site for artificial recharge. About every third year, a substantial winter snow pack builds up in the Pine Valley Mountains. Spring snowmelt runoff in the Santa Clara River during these years often overflows the spillway at Gunlock Reservoir and is lost downstream. The Washington County Water Conservancy District is hoping to better utilize this snowmelt runoff by spreading some of this water into Sand Cove Wash. A series of aqueducts and pipelines

127

currently transport water from the Santa Clara River to two Utah Power and Light power plants nearby Sand Cove Wash. This same infrastructure could be used to transport a portion of the snowmelt runoff to the wash. The Washington County Water Conservancy District hopes that most of the water put in the wash would eventually reach the Gunlock Reservoir, but be delayed by at least a month. The U.S. Bureau of Reclamation and the U.S. Geological Survey are presently evaluating the artificial recharge potential of the site, including travel times to Gunlock Reservoir. These agencies will collect data and construct ground-water flow models to evaluate the amount of water that likely will seep into the underlying Navajo Sandstone, recharging the regional aquifer. Nearby wells indicate that the depth to the Navajo aquifer water table beneath the wash is around 1,000 feet, so unsaturated-zone travel times would likely be at least decades.

1.0	114.2	Left on gravel road toward Dameron Valley.
2.2	116.4	Right on Highway 18 toward St. George.
14.2	130.6	Left on Red Cliffs Road.
2.6	133.2	Left on Skyline Road.
1.0	134.2	Right on 1000 East.
0.1	134.3	Left on St. George Blvd.
0.3	134.6	Left on northbound I-15 entrance ramp.
50.0	184.6	Exit No. 59 (central Cedar City Exit); Right on 200 North.
0.1	184.7	Right on 1150 West.
0.4	185.1	Right at parking lot near corner of 200 South and 1150 West.

END OF ROAD LOG

REFERENCES

Budding, K.E., and Sommer, S.N., 1986, Low-temperature geothermal assessment of the Santa Clara and Virgin River valleys, Washington County, Utah: Utah Geological and Mineral Survey Special Studies No. 67, 34 p.

Busenberg, E., and Plummer, L.N., 1992, Use of chlorofluorocarbons as hydrologic tracers and age-dating tools: The alluvium and terrace system of central Oklahoma: Water Resources Research, v. 28, p. 2257-2883.

Cordova, R.M., 1978, Ground-water conditions in the Navajo Sandstone in the central Virgin River basin, Utah: State of Utah Department of Natural Resources Technical Publication No. 61, 66 p.

EWP Engineering, 1997, Sand Hollow artificial ground-water recharge and recovery project feasibility report: 45 p. and appendices.

Heilweil, V.M., Freethey, G.W., Stolp, B.J., Wilkowske, C.D., and Wilberg, D.E., 2000, Geohydrology and numerical simulation of ground-water flow in the central Virgin River basin of Iron and Washington Counties, Utah: State of Utah Department of Natural Resources Technical Publication No. 116, 139 p.

Heilweil, V.M., and Hseih, P.A., 1998, Simplification of the Papadopulos Method for determination of transmissivity and storage for a homogeneous and anisotropic aquifer: Eos, Transactions, American Geophysical Union 1998 Spring Meeting, v. 79, no. 17, p. S153.

Heilweil, V.M., and Solomon, D.K., 2001, Variability in basin-scale recharge to the Navajo Sandstone aquifer of the upper Mohave Desert, southwestern Utah: Eos, Transactions, American Geophysical Union 2001 Fall Meeting, v. 82, no. 17, p. F461.

Heilweil, V.M., Wilkowske, C.D., and Solomon, D.K., 1997, Use of aquifer testing and age tracers to understand ground-water flow in the Navajo aquifer in Washington County, Utah: Geological Society of America 1997 Annual Meeting, Abstracts with Programs, v. 29, no. 6, p. A-77.

Herbert, L.R., 1995, Seepage study of the Virgin River from Ash Creek to Harrisburg Dome, Washington County, Utah: State of Utah Department of Natural Resources Technical Publication No. 106, 8 p.

Hurlow, H.A., 1998, The geology of the central Virgin River basin, southwestern Utah, and its relation to ground-water conditions: Utah Geological Survey Water-Resources Bulletin 26, 53 p.

Ludwig, D.E., Solomon, D.K., and Heilweil, V.M., 2002, Cross-sectional computer model of ground-water flow and solute transport beneath the Sand Hollow reservoir near Hurricane, Utah: U.S. Geological Survey Administrative Report to the U.S. Bureau of Reclamation, 15 p. and figures.

Papadopulos, I.S., 1965, Nonsteady flow to a well in an infinite anisotropic aquifer, *in* Proceedings of the Dubrovnik Symposium on Hydrology of Fractured Rocks: Dubrovnik, Yugoslavia International Association of Scientific Hydrology, p. 21-31.

Utah Climate Center, 1996, 1961-90 normal precipitation contours: Utah State University, Logan, Utah.

Utah Department of Environmental Quality, Division of Drinking Water, 2001, Administrative rules for drinking water standards, R309-103, Water Quality maximum contaminant levels (MCLs).

Collecting core samples at Sand Hollow basin, Utah, for evaluating natural recharge.

GEOLOGY AND MINERAL RESOURCES OF THE MARYSVALE VOLCANIC FIELD, SOUTHWESTERN UTAH

Geological Society of America
2002 Rocky Mountain Section Annual Meeting, Cedar City, Utah
May 6, 2002

View southward of the hydrothermally altered rocks at Big Rock Candy Mountain, five miles north of Marysvale, Utah.

Peter D. Rowley, Geologic Mapping, Inc., New Harmony, UT 84757
Charles G. Cunningham, U.S. Geological Survey, Reston, VA 20192
John J. Anderson, New Harmony, UT 84757
Thomas A. Steven, Denver, CO 80227
Jeremiah B. Workman, U.S. Geological Survey, Denver, CO 80225
Lawrence W. Snee, U.S. Geological Survey, Denver, Co 80225

GEOLOGY AND MINERAL RESOURCES OF THE MARYSVALE VOLCANIC FIELD, SOUTHWESTERN UTAH

Peter D. Rowley, Geologic Mapping, Inc., New Harmony, UT 84757
Charles G. Cunningham, U.S. Geological Survey, Reston, VA 20192
John J. Anderson, New Harmony, UT 84757
Thomas A. Steven, Denver, CO 80227
Jeremiah B. Workman, U.S. Geological Survey, Denver, CO 80225
Lawrence W. Snee, U.S. Geological Survey, Denver, Co 80225

ABSTRACT

The Marysvale volcanic field, one of the largest such fields in the West, sits astride the Colorado Plateau-Great Basin transition zone. Most igneous rocks belong to a middle Cenozoic (32? to 22 million years old) calc-alkaline sequence, in which deposits from clustered stratovolcanoes dominate but ash-flow tuffs and their source calderas also are significant. About 5 percent of the igneous rocks belong to an upper Cenozoic (23 million years old to Holocene) bimodal (basalt and high-silica rhyolite) sequence, which was deposited as lava flows and ash-flow tuffs from calderas, volcanic domes, and cinder cones, and which was synchronous with major basin-range extension. Each of the two chemical rock sequences has its own distinctive mineral deposits, with gold in the older sequence and gold, molybdenum, uranium, and base metals in the younger.

INTRODUCTION

This field trip will visit the Marysvale volcanic field, one of the largest in the western United States, and one of significant mineral potential (fig. 1). We will begin the trip in Cedar City, Utah, at the border between the Great Basin and the Colorado Plateau, and just southwest of the volcanic field. From Cedar City, we will travel north on I-15 along those parts of the field (Black Mountains and Mineral Mountains) that are in the Great Basin, which is the area of greatest continental crustal extension in the world (fig. 2). Most of the volcanic field is in the High Plateaus subprovince of the Colorado Plateau, which is a geologic transition zone between the Great Basin and the main, unfaulted part of the Colorado Plateau to the east. So we will then travel east on I-70 into the center of the field, in the Tushar Mountains, Sevier Plateau, and northern Markagunt Plateau, where most eruptive centers and mineralized areas are located. On the trip, we will visit stratovolcano deposits, which dominate in the field, as well as ash-flow tuffs and their source calderas. Less significant vents that we will see are cinder cones, volcanic domes, and dikes. We will visit the uranium district, a mine for replacement alunite, and the only active mine in the area, which is developed in base and precious metal deposits.

The main part of the Marysvale volcanic field lies at the eastern end of the east-northeast-trending Pioche-Marysvale igneous belt, a site of extensive, mostly Oligocene and Miocene, volcanism and mineralization above a major batholith complex. The southern part of the field, containing deeper magmatic sources and less evolved rocks, lies at the eastern end of a second, generally younger belt of similar trend, the Delamar-Iron Springs igneous belt. Among structures that partly control vents, and thus mineral deposits, are two major east-west transverse zones. The northern one, the Cove Fort transverse zone, defines the northern side of the Pioche-
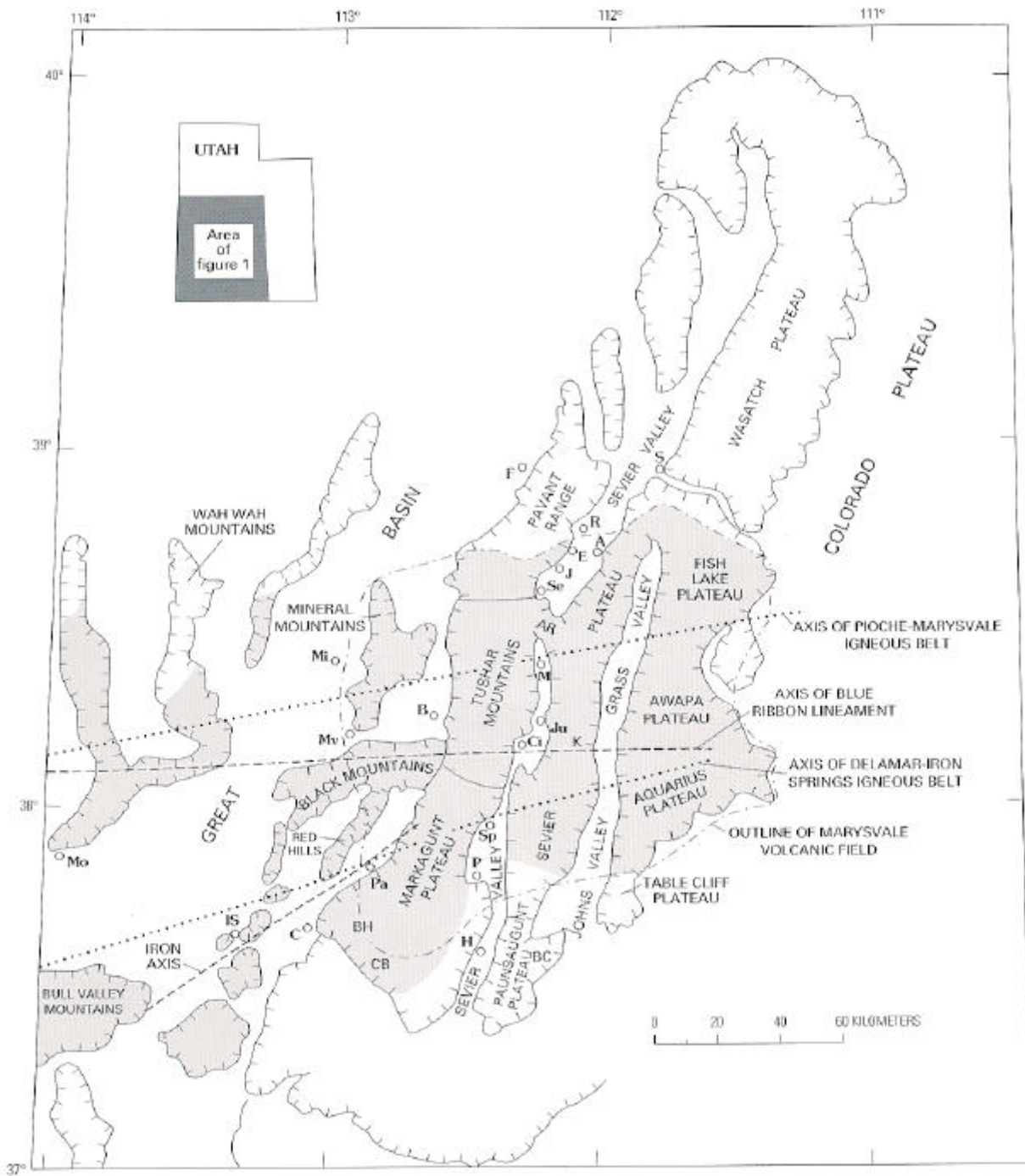
Figure 1. Index map showing location of the Marysvale volcanic field, plateaus and ranges of the High Plateaus, and adjacent areas in Utah, modified from Anderson and Rowley (1975, fig. 1) and Steven and others (1979, fig. 1). A, Annabella; AR, Antelope Range; B, Beaver; BC, Bryce Canyon National Park; BH, Brian Head; C, Cedar City; CB, Cedar Breaks National Monument; Ci, Circleville; E, Elsinore; F, Fillmore; H, Hatch; IS, Iron Springs; J, Joseph; Ju, Junction; K, Kingston Canyon; M, Marysvale; Mi, Milford; Mo, Modena; Mv, Minersville; P, Panguitch; Pa, Parowan; R, Richfield; S, Salina; Se, Sevier; Sp, Spry. Great Basin–Colorado Plateau boundary is just west of the towns of Fillmore, Beaver, Parowan, and Cedar City. Patterned areas are underlain largely by volcanic rocks.
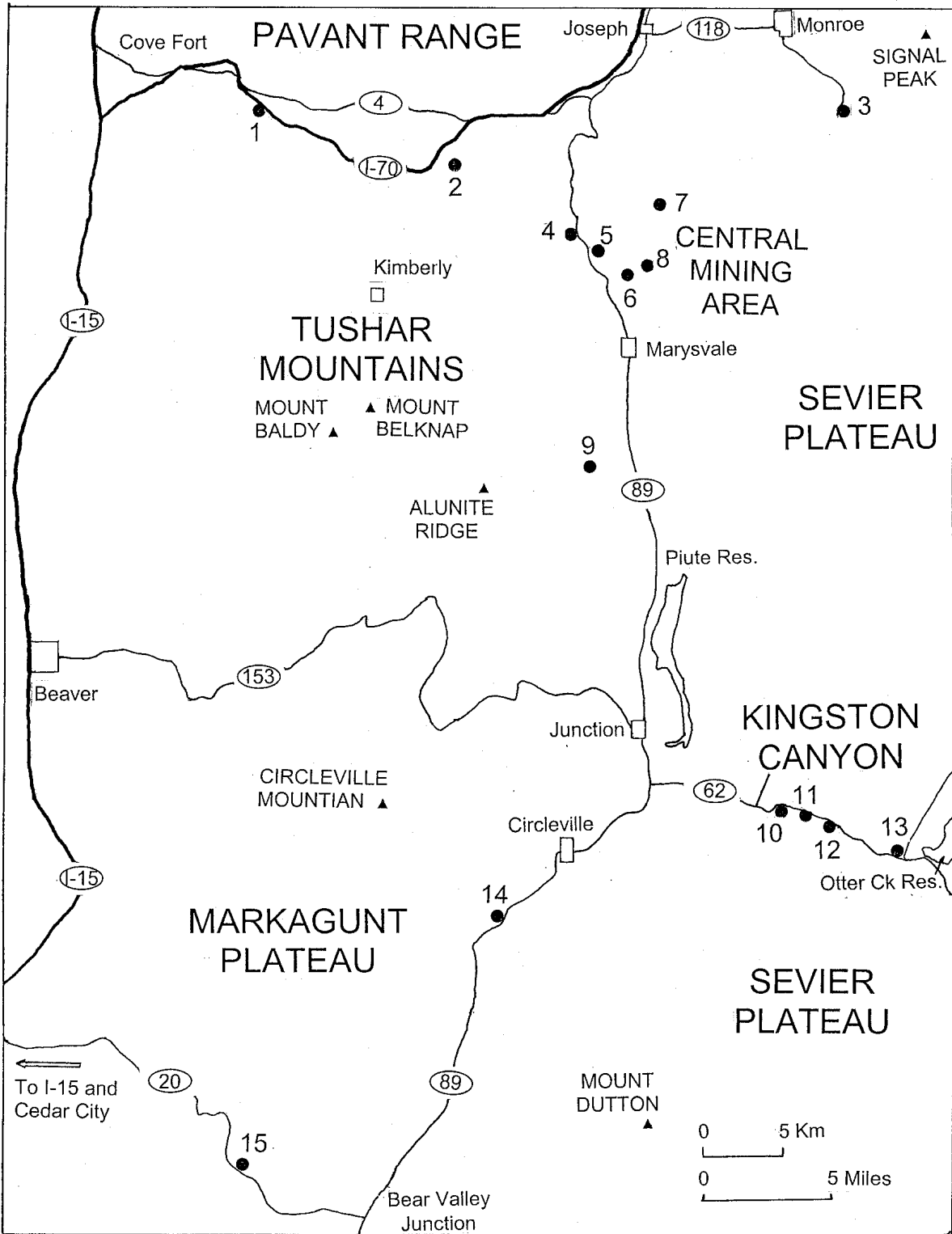
Figure 2. Index map showing major topographic features, roads, and stops (numbered dots) of the field trip

the southern vents in the field.

Cenozoic rocks in and adjacent to the Marysvale volcanic field consist of three main stratigraphic sequences: (1) lower Cenozoic (Paleocene to lower Oligocene) fluvial and lacustrine sedimentary rocks, exemplified by the Claron Formation; (2) voluminous middle Cenozoic (Oligocene and lower Miocene), 32- to 22-million-year-old intermediate-composition calc-alkaline igneous rocks; and (3) upper Cenozoic (middle Miocene, 23 million years old, to Holocene) compositionally bimodal (basaltic and high-silica rhyolite) igneous rocks, which intertongue with clastic sedimentary rocks resulting from erosion of landforms due mostly to regional extension. All of the igneous rocks were synchronous with extensional tectonics but, unlike many other parts of the Great Basin, faulting was relatively minor in the Marysvale area during the middle Cenozoic episode. During the upper Cenozoic episode, basin-range extension created most of the topography we will see today, although the most evident faulting did not begin until about 10 million years ago.

The geologic studies leading to this report began in 1963, when dissertation mapping was initiated in the southern Marysvale volcanic field by J.J. Anderson (1965) and P.D. Rowley (1968), supervised by J.H. Mackin at the University of Texas. Mapping continued as we became employed at Kent State University and the U.S. Geological Survey (USGS), respectively. This work concentrated in the southern and western parts of the field, with work in the northern Markagunt Plateau by Anderson, and the Black and southern Mineral Mountains and adjacent Iron Springs mining district by Rowley. In 1975, the USGS began mapping and related petrologic and mineral-resource studies in the Tushar Mountains and adjacent Sevier River valley, in the heart of the field where known mineral resources are located. T.A. Steven and C.G. Cunningham led this work, and both have continued with it off and on ever since. The work expanded into a broader study of the geology and mineral resources of the Richfield 1° by 2° quadrangle in 1978. The Marysvale field segment of the quadrangle was studied generally full time by Steven, Cunningham, and Rowley and part time by many others from the USGS and academia for more than a decade. H.T. Morris (USGS), J.J. Anderson (Kent State University and USGS), and M.G. Best (Brigham Young University and USGS) were prominent among the many participants of the Richfield work. K-Ar and fission-track dating by H.H. Mehnert and C.W. Naeser (both USGS) was an important part of the study early on, and others have continued this work to the present. Geophysics was likewise an important part of the work, and the recent publication of Campbell and others (1999) summarized these efforts at 1:100,000 scale.   The overall Richfield investigation resulted in more than 200 open-file and published reports and maps; many of these are cited in Steven and Morris (1987). Most project conclusions about the Marysvale field are based upon detailed geologic mapping. All the Marysvale field was covered except the eastern flank, which Williams and Hackman (1971) mapped earlier in reconnaissance fashion. Much of the detailed and reconnaissance field data from the project have been published in a series of geologic, geophysical, and mineral-resource maps. Cunningham and others (1983) compiled a detailed (1:50,000 scale) geologic map of the heart of the field, which was followed by geophysical and mineral-resource maps of the same area, only one of which (Cunningham and others, 1984b) is cited here. Steven and others (1990) released a summary map (1:250,000) of the Richfield quadrangle. A new revised geologic map (Rowley and others, 2001a), including access to the digital map data, of the same area covered by Cunningham and others (1983) and Campbell and others (1999), at 1:100,000 scale, is in press with the USGS and will be, we hope, available by the time of this field trip.

GEOLOGIC SETTING

We discuss the Marysvale volcanic field chronologically, first the middle Cenozoic rocks and structures, then the late Cenozoic rocks and structures (Cunningham and others, 2002). The middle Cenozoic igneous rocks are part of a magmatic arc in a plate-tectonic setting that resulted from subduction of Pacific plates beneath western North America (Lipman and others, 1972; Hamilton, 1989, 1995; Severinghaus and Atwater, 1990; Christiansen and Yeats, 1992). Voluminous calc-alkaline igneous rocks ranging in composition from andesite to low-silica rhyolite were emplaced (e.g., Lipman and others, 1972). In the Great Basin and the Colorado Plateau transition zone, most of the eruptive centers for these rocks were in east-west igneous belts, with

outflow in areas between the belts (e.g., Rowley, 1998). As is common above other subduction zones, extension prevailed (Hamilton, 1989, 1995), but in the Great Basin and the transition zone, it was expressed by north-northwest- and north-northeast-striking oblique-slip faults and normal faults (Zoback and others, 1981; Rowley and Dixon, 2001), whose presence has not been well recognized. Rowley (1998), Rowley and others (1998), and Rowley and Dixon (2001) proposed that extension was expressed by shallow plutons as well as by faults, and that in any one place extension would result in either or both mechanisms. The faults of this middle Cenozoic episode, when present, did not produce anything resembling the later basin-range structure that we are familiar with, in part because the extension direction (σ_3) for many areas of the West was oriented east-northeast (Zoback and others, 1981), and partly because the maximum principal stress direction (σ_1) appears to have been north or north-northwest rather than vertical (Anderson and Barnhard, 1993; Anderson and others, 1994; Rowley and Dixon, 2001). In the Marysvale area, faults of middle Cenozoic age generally are uncommon, probably because most extension was expressed by shallow plutonism. Transverse zones, which are parallel to extension directions (or, in the earlier Laramide, to compression directions), evolved in the late Mesozoic and the middle Cenozoic (e.g., Ekren and others, 1976; Rowley, 1998). They serve, as do transform faults of similar strike in the Pacific Ocean basin, to allow the crust north and south of them to extend by different amounts, styles, and rates of strain. Depending on the extension direction of the local area, middle Cenozoic transverse zones in the Great Basin generally strike east or east-northeast.

In the late Cenozoic (starting at about 25 to 20 million years ago, depending on the area), continental crust continued to extend, but the plate-tectonic setting changed radically. Except under the Cascade Range, the subducted slab beneath the western United States had given way to transform movement across a broad zone extending from the San Andreas fault zone to the Walker Lane belt (Severinghaus and Atwater, 1990; Christiansen and Yeats, 1992). As a result, the Great Basin area underwent oblique extension (Hamilton and Myers, 1966). At first, extension during the late Cenozoic seems to have been expressed by broad folding, but by about 10 million years ago, the present north-trending, basin-range topography started to form along normal faults (Gilbert, 1928; Mackin, 1960; Eaton and others, 1978; Zoback and others, 1981; Anderson and others, 1983; Anderson, 1989; Wernicke, 1992). This is referred to as the basin-range episode (Gilbert, 1928; Mackin, 1960). Contemporaneous magmatism in the western United States was largely bimodal in composition, consisting of basalts and high-silica rhyolites (Christiansen and Lipman, 1972). The volume of eruptive products in most areas of the West, however, was much less than that of the middle Cenozoic, being at Marysvale only about 5 percent that of the middle Cenozoic. In the Marysvale area, where high-angle normal faults dominate, most faults and topography represent the effect of basin-range extension. In two areas we will visit on this field trip, the age of the main phase of basin-range extension is particularly well constrained: (1) at Sevier, it postdates tephra in the Sevier River Formation of 7 Ma (Steven and others, 1979), and in Kingston Canyon, it took place between rhyolites dated at 8 and 5 Ma (Rowley and others, 1981). Transverse zones continued to be active in the late Cenozoic and, because the extension direction was in most places east-west (Zoback and others, 1981), so was the orientation of the transverse zones. It appears possible that a giant mantle plume underlay the entire Great Basin during this time (Eaton and others, 1978; Pierce and Morgan, 1992; Parsons and others, 1994; Zoback and others, 1994; Parsons, 1995; Saltus and Thompson, 1995; Thompson, 1998). For a more detailed discussion of these regional topics and their implications, see Rowley and Dixon (2001).

Middle Cenozoic Episode. The dominant middle Cenozoic rock types of the Marysvale volcanic field are volcanic mudflow breccia and subordinate lava flows, most from clustered stratovolcanoes (Rowley and others, 1979; Steven and others, 1979). These, as well as tuffs and other rock types of the middle Cenozoic episode, are compositionally calc-alkaline. Where the clasts in the mudflows and the lithologically similar flows are distinctive, the rock units made up of these rocks were mapped separately and given formal or informal names. Where such stratovolcano units were mapped, they commonly were separated into either vent facies or alluvial facies, following the concepts of Parsons (1969) and Smedes and Prostka (1973). The vent facies, as the name implies, consists of deposits that are concentrated near vents and high

136

on volcano flanks, whereas the alluvial facies is concentrated lower on the flanks and beyond the flanks, becoming a grain-supported conglomerate with distance from the source. Volcanic mudflow breccia is the main component of both facies but, in vent facies, these breccias tend to be monolithologic and they may be intertongued with lava flows, flow breccia, and dikes. In the Marysvale field, most of the stratovolcano sequences were mapped as two formations. The most voluminous (at least 5,000 km^3) of these is the Mount Dutton Formation (Anderson and Rowley, 1975), which is largely exposed in the southern half of the volcanic field (Rowley and others, 1998). Some stratigraphic sections, as along the western scarp of the Sevier Plateau at Mount Dutton, are at least 2,000 meters thick. Mapping in the southern Tushar Mountains and northern Markagunt Plateau suggests that many stratovolcano vents of the Mount Dutton Formation line up along the Blue Ribbon transverse zone. The formation has produced isotopic dates that range between 27 and 21 Ma (Fleck and others, 1975; Rowley and others, 1994), and stratigraphic relations indicate that some rocks predate regional ash-flow tuffs of 30 million years age. The clasts and flows of the Mount Dutton are largely andesite that contains sparse, small phenocrysts. Corresponding source intrusive rocks for the Mount Dutton Formation are rarely exposed in the southern half of the Marysvale field, and thus we interpret that Mount Dutton Formation magma chambers were very deep below their volcanic edifices (Cunningham and others, 1994, 1998a). An exception to these deep magma chambers in the southern part of the field (that is, in the Delamar-Iron Springs igneous belt) is a belt of shallow laccoliths. One of these is the large (50 km^3), 26-Ma Spry Intrusion in the Markagunt Plateau, which is a cupola on a batholith that produced other laccoliths (Blank and Kucks, 1989; Anderson, 1993). Another laccolith in the Markagunt Plateau, the Iron Peak (Anderson and Rowley, 1975), is at the northeastern end of the Iron Axis. Some of these shallow laccoliths vented, but their contribution to the volcanic field was minor.

The second most voluminous rock unit in the Marysvale field is the Bullion Canyon Volcanics (Callaghan, 1939; Steven and others, 1979). This unit consists largely of stratovolcano deposits mapped in the heart and northern half of the Marysvale volcanic field. Some sections of this map unit are at least 1,500 meters thick, not including intertongued ash-flow tuffs. The volume of the unit is conservatively estimated at 1,700 km^3. Isotopic dates and stratigraphic relations indicate a nearly identical age as the Mount Dutton Formation. Weathered basal parts have dates as old as 34 Ma (Willis, 1985; Kowallis and Best, 1990), and the Mount Dutton and Bullion Canyon sequences intertongue along the east-trending boundary between the Tushar Mountains and northern Markagunt Plateau. In contrast to the Mount Dutton, the dominant rock type in the Bullion Canyon is dacite that in most places contains 20 to 30 percent large phenocrysts. Source intrusive rocks are widely exposed throughout the sequence and it is thus clear that, for this unit and others in the heart of the field, the magma chambers were shallow and the rocks were more highly evolved (differentiated) (Cunningham and others, 1994, 1998a).

Ash-flow tuffs make up about only 10 percent of the volume of the calc-alkaline sequence, but their calderas are common (Rowley and others, 1979; Steven and others, 1979, 1984a). The most voluminous tuffs were derived from the northern half of the volcanic field, some as members of the Bullion Canyon Volcanics (Callaghan, 1939; Steven and others, 1979). Possibly the largest tuff in the field is the Three Creeks Tuff Member, derived from the Three Creeks caldera in the southern Pavant Range (Steven, 1981) about 27 million years ago. This moderately welded dacitic unit is crystal-rich, with nearly 50 percent large phenocrysts. It is widely distributed near the base of the Bullion Canyon and Mount Dutton sequences, but it is also commonly covered by other rocks so an estimate of its intracaldera and outflow volume is only 200 km^3. In hand specimen, it resembles another crystal-rich ash-flow sheet, the widespread 30-million-year-old Wah Wah Springs Formation of the Needles Range Group. In fact, the Three Creeks Tuff Member was originally included within the Needles Range Group until Best and others (1989a, b) did the regional correlations needed to work out the correct stratigraphy. Needles Range units were derived from the huge Indian Peak caldera complex that straddles the Utah-Nevada border (Best and others, 1989a, b). The Wah Wah Springs is below the Three Creeks Tuff Member, of course, and near the base of the stratovolcano sequences at Marysvale.

The 24-million-year old Delano Peak Tuff Member of the Bullion Canyon Volcanics (Callaghan, 1939; Steven and others, 1979) is a well welded dacitic ash-flow tuff that had an initial volume of at least 100 km^3. Its source is the Big John caldera in the central Tushar

Mountains (Steven and others, 1984b), but it is not widely exposed outside that mountain range. It is seen near the upper part of the Bullion Canyon section. Two thin, small-volume, densely welded, trachydacite ash-flow tuffs are members of the Mount Dutton Formation; these are the Kingston Tuff Member (26 Ma) and the Antimony Tuff Member (25 Ma). Named for exposures in Kingston Canyon of the southern Sevier Plateau (Anderson and Rowley, 1975), they are widely exposed throughout the southern and eastern Marysvale field. They are lithologically similar to each other and also resemble another small unit, the tuff of Albinus Canyon (Cunningham and others, 1983; Rowley and others, 1994), found in the northern part of the field. These three tuffs probably came from the same source, but its location is unknown. Based on the higher volume of these rocks, and their greater tendency for late rheomorphic flow in the mountains surrounding the town of Joseph, in the northern part of the field, we suggest that the source may be buried beneath a graben there.   High-temperature ash-flow tuffs such as this, including the Isom Formation of the Iron Springs mining district (Mackin, 1960; Anderson and Rowley, 2002) and some in southwestern Idaho (Ekren and others, 1984), appear to have been so hot that their sources are likely deep and not expressed as calderas (Ekren and others, 1984).

The largest caldera in the Marysvale field, and the youngest of the calc-alkaline sequence, is the Monroe Peak caldera in the northern part of the volcanic field (Steven and others, 1984a; Rowley and others, 1986a, b, 1988a, b). As with the source caldera for the other large ash-flow tuff (the Three Creeks Member), the Monroe Peak caldera is along and likely was controlled by the Cove Fort transverse zone. The Monroe Peak caldera was the source of the 23-million-year-old densely welded, trachydacitic Osiris Tuff (Williams and Hackman, 1971; Anderson and Rowley, 1975). This tuff spread widely throughout the volcanic field and, in places, outward across its flanks to form an isolated sheet. The initial volume of the Osiris is estimated at 250 km^3, including a thick intracaldera fill. Immediately after its eruption, the Monroe Peak caldera fill was capped by a series of lava flows that totaled another 100 km^3. Preliminary Ar-Ar dating by L.W. Snee of the USGS shows that all of the Osiris erupted between 22.92 and 22.81 Ma, and that the intracaldera post-Osiris lava flows are 22.48, 22.43, and 22.32 Ma. These data indicate that all volcanic activity of the Monroe Peak caldera took place in about 0.6 million years or less (unpublished data, 2001).

In addition to the stratigraphic units mentioned, many other calc-alkaline units formed during the middle Cenozoic eruptive episode. Few of these will be visited during the field trip, so many are not mentioned here; others are covered in passing in the road log. For details on these units, see other project maps and reports.

Late Cenozoic Episode. As in other volcanic fields in the western United States, the petrologic regime of the Marysvale volcanic field (Cunningham and others, 1998a) changed drastically from calc-alkaline to fundamentally bimodal somewhat before 20 million years ago (Christiansen and Lipman, 1978). This change is inferred to coincide with renewed crustal extension, but in a crust that was probably cooler and thicker overall than that of the calc-alkaline episode (Lucchitta, 1990; Wernicke, 1992). As a result, basaltic magmas rose along more deeply penetrating fractures to higher in the crust, raising the isotherms and forming alkali-rhyolite eutectic partial melts. Generally the first product of bimodal volcanism appears to have been rocks of small volume from local centers scattered around the field that were originally mapped as "older basalts" (Anderson and Rowley, 1975) or as "basalts" by previous workers. Later petrologic work (e.g., Best and others, 1980) showed that they are not true basalts, so we since have called them "potassium-rich mafic volcanic rocks." They have ages that range from 23 to 21 million years old, although some may be as old as 26 million years (Mattox, 1991a, b, 1992).

The largest volume of bimodal rocks in the Marysvale field formed the rhyolite of the Mount Belknap Vocanics (Callaghan, 1939; Cunningham and Steven, 1979a), which was erupted between 22 and 14 million years ago from two concurrently active eruptive centers, one in the central Tushar Mountains and the other in the Sevier River valley. Thus these rhyolite eruptive centers generally coincided with areas where the older intrusive and volcanic rocks of the calc-alkaline episode were deposited. The western and most voluminous of these two source areas subsided to form the large Mount Belknap caldera after its main ash-flow sheet, the Joe Lott Tuff Member of the Mount Belknap Volcanics, erupted 19 million years ago (Budding and others, 1987). The volume of rocks from this western source, including intracaldera and outflow Joe Lott

Tuff and associated lava flows, is at least 300 km^3. The volume of rocks in the eastern source, which is near Marysvale, is much less. It includes the Red Hills Tuff Member of the Mount Belknap Volcanics and its source, the Red Hills caldera, as well as a series of local volcanic domes and flows, all north of Marysvale. Both source areas include granite intrusions. In the eastern source area, these hosted the Central Mining Area, the main uranium district associated with the Marysvale volcanic field (Cunningham and Steven, 1979b). In the eastern Tushar Mountains about 10 km south-southwest of Marysvale, a 14-million-year-old intrusion domed the rocks at Alunite Ridge (Cunningham and Steven, 1979c), forming mineral deposits that have been mined for years (Cunningham and others, 1984a).

The Mineral Mountains, at the western margin of the Marysvale field, are underlain by a 25- to 9-million-year-old composite batholith, the largest exposed in Utah (Nielson and others, 1986; Steven and others, 1990; Coleman and Walker, 1992; Coleman and others, 2001). It is part of the huge batholith that underlies much of the Pioche-Marysvale igneous belt (Steven and Morris, 1987). Although minor early phases (those of 25 Ma) probably represent the calc-alkaline episode, the great majority of the batholith (22-11 Ma) is granitic and alkaline and interpreted to represent the bimodal episode; still later granites (9 Ma) are clearly bimodal. The granites were uplifted rapidly along listric faults and perhaps along detachment faults that are exposed on the western side of the range (Nielson and others, 1986). The uplift is interpreted to be the product of a metamorphic core complex (Price and Bartley, 1992; Coleman and others, 2001). Rhyolites accompanied the granites, although erosion has removed most of those except younger ones resting on the exposed batholith in the northern part of the Mineral Mountains. Ranging in age from 0.8 to 0.5 million years old, these consist of volcanic domes on the crest of the range, which shed ash-flow tuff and rhyolite flows down canyons on the western side of the range (Lipman and others, 1978). Some of these erupted volcanic rocks are obsidian flows that are devoid of phenocrysts and in prehistoric time were widely exported for use as points and tools by Indians.

Lava flows and cinder cones of true basalt began to be erupted in small volumes in the general area at about 14 million years ago (Best and others, 1980). These include many basalts in the Marysvale field, but basalts are not confined to the field, and their vents do not coincide with the older vent areas of calc-alkaline rocks or even of the older (23 to 16 million years old) rhyolites. Basalts are exposed, however, in association with many post-16-million-year-old rhyolite vents. Basalts continued to be erupted in the general area well into the Quaternary, and some on the Markagunt Plateau west of Cedar City are unvegetated and probably are Holocene (Hatfield and others, 2000). Beginning about 10 million years ago, basin-range faulting became widespread. Generally small rhyolite domes continued to be emplaced in the Marysvale field. These include the rhyolite of Gillies Hill and buried plutons at the Sheeprock Mine (9 to 8 Ma; Evans and Steven, 1982; Cunningham and others, 1984c) north of Beaver, rhyolites in Kingston Canyon (8 to 5 Ma; Rowley and others, 1981), rhyolites along the northern side of the Black Mountains (9 to 8 Ma; Anderson and others, 1990b) that continue westward along the Blue Ribbon transverse zone (Rowley and others, 1978), and the rhyolites of the Mineral Mountains (9 to 0.5 Ma; Lipman and others, 1978).

ECONOMIC GEOLOGY

Mineral deposits of the Marysvale field formed during three ages (Cunningham and others, 1994, 1998a). The first, at about 34 to 22 million years old, is associated with rocks of the calc-alkaline episode. The second (22-14 million years old) and third (9-5 million years old) are associated with rocks of the bimodal episode. Ore deposits of the calc-alkaline episode tend to be epithermal gold deposits, whereas those of the bimodal episode tend to be gold, molybdenum, uranium, and base metals. The many calc-alkaline plutons in the central to northern Tushar Mountains resulted in adjacent highly propylitized and argillic altered areas that contain pyrite-bearing quartz-carbonate veins (Cunningham and others, 1984b). In some areas these veins have gold and silver values, and this broad area has been widely prospected. The only area of significant production, however, was the Kimberly district, where mining produced several million dollars worth of gold and silver between 1892 and 1937 (Lindgren, 1906; Steven and Morris, 1987). Most ores came from the oxidized parts of two persistent vein zones cutting propylitized quartz monzonite intrusions. Metal values dropped off sharply in lower levels of the mines, where

the ores were unoxidized. Other areas where gold- and silver-bearing quartz-carbonate veins cut altered volcanic rocks are in lower Deer Creek, the Butler-Beck mine area in the headwaters of Deer Creek (5 kilometers east of Kimberly), a few kilometers south of Sulphurdale, the Rob Roy mine near the mouth of Indian Creek Canyon, and the Cork Ridge area south of the Mount Belknap caldera (Cunningham and others, 1984b, c; Steven and Morris, 1987).

Replacement alunite (for potash, alumina, and sulfuric acid) was mined in areas formed by alteration adjacent to shallow intracaldera plutons of the 23-million-year-old Monroe Peak caldera (Cunningham and others, 1984a, b; Steven and Morris, 1987). The hosts were volcanic rocks adjacent to and overlying these plutons, which were locally intensely altered to argillic and advanced-argillic mineral grades (Cunningham and others, 1984b). The Marysvale Peak and Manning Creek alunite deposits on the Sevier Plateau east to northeast of Marysvale, and the Box Creek kaolinite deposit farther east in the caldera are examples. One of the intracaldera plutons that is distinctive enough to be mapped separately is the Central Intrusion. Several geologists have studied the effects of sub-circular hydrothermal ground-water convection cells caused by and surrounding that intrusion (Podwysocki and Segal, 1983; Cunningham and others, 1994; Rockwell and others, 2002). Alunite formed in a near-surface environment from hydrothermal cells that reacted with evaporite-bearing strata at depth to supply sedimentary sulfur. Reaction with volcanic rocks at depth reduced some of the sulfur, and some sulfur may have been contributed by the magma. Near-surface reaction of this hydrogen sulfide with atmospheric oxygen formed a strongly acidic solution that altered the volcanic rocks and resulted in alunite and related products. The alunite at the Whitehorse and Yellow Jacket mines north and northeast of Marysvale are examples.

The best known mineral resources of the bimodal episode are the uranium deposits of the Central Mining Area northeast of Marysvale, which were mined between 1949 and 1967 (Cunningham and Steven, 1979b; Steven and others, 1981; Cunningham and others, 1982, 1994, 1998b, 1999; Rowley and others, 1988a, b). The uranium in the eastern source area of the Mount Belknap Volcanics is in veins formed about 19 million years ago that are associated with glassy rhyolite dikes widely exposed in the mines. The host rocks consist of the Central Intrusion and the fine-grained granite northeast of the Red Hills caldera. Molybdenum is associated with the uranium and becomes increasingly abundant with depth. Cunningham and others (1982) interpreted the uranium-molybdenum deposits to be derived from a hidden intrusion that possibly contains a porphyry-type disseminated molybdenum deposit. Extensive exploration drilling by industry encountered only low-grade uranium values east of the Central Mining Area. The western source area (Mount Belknap caldera) of the Mount Belknap Volcanics contains anomalous values of uranium, molybdenum, and beryllium but no deposits are yet known. In the Indian Creek area northeast of Beaver, anomalous fluorite and uranium in rocks of 16 million year old suggest a granite pluton at depth. The Sheep Rock alunite deposit, and the Sunday gold deposit in quartz-calcite veins are associated with granite source plutons of the 9- to 8-Ma rhyolite of Gillies Hill (Cunningham and others, 1984c).

Along the eastern margin of the central Tushar Mountains, hydrothermal mineral deposits dated at 14 Ma are exposed on two adjacent peaks that Cunningham and Steven (1979c) and Cunningham and others (1984a) interpreted to overlie cupolas on a hidden stock. On Alunite Ridge, alunite veins as wide as 20 meters filled open fissures in a structural dome cut by radial faults, and on Deer Trail Mountain, highly kaolinitized rocks mark another radial fracture pattern. An annular ring of base- and precious-metal deposits surround these altered areas. Quartz veins containing gold, silver, and minor base metals cut propylitized volcanic rocks in part of the ring, and the Deer Trail mine exploits a base-metal manto and associated precious-metal veins in carbonate strata along the eastern side of the ring (Beaty and others, 1986). Hidden igneous cupolas that may host porphyry-type disseminated copper and molybdenum deposits, and adjacent metal-bearing skarn deposits have been interpreted to underlie the altered areas (Cunningham and others, 1979c; Cunningham and others, 1984a; Beaty and others, 1986).

Other deposits associated with either the calc-alkaline or bimodal episodes are adjacent to intrusive rocks of the Mineral Mountains (Steven and Morris, 1987). The Bradshaw and Lincoln districts at the southern end of the range were mostly gold-silver-copper-lead-zinc-tungsten replacement deposits in Paleozoic limestones associated with east-striking fractures and with underlying and adjacent stocks associated with the Mineral Mountain batholith. At the northern

end of the range, the Antelope district shipped a little ore from small lead replacement bodies in limestone. East of the range, the Fortuna mine area at the northern end of the Beaver basin is adjacent to an extensive area of propylitically altered lava flows and consists of intensely altered rock and sparse gold-bearing quartz veins. At the southeastern end of the range, small ore deposits containing tungsten, and pegmatites with beryllium occur in skarn associated with the bimodal parts of the granite (Steven and Morris, 1987).

Hot springs are common in the area of the field trip. Although some of these, such as Monroe Hot Springs and spring deposits along the Dry Wash fault zone east of Joseph, are probably due to rapid upward movement of ground water along fault zones and thus reflect the geothermal gradient, others are likely due to heating of ground water by magma masses at depth. One of these is the Roosevelt Hot Springs geothermal area on the western side of the Mineral Mountains, which is heated by the same magma that fed young rhyolites on the crest of the range (Lipman and others, 1978) and which runs a power plant northeast of Milford, Utah (Blackett and Moore, 1994). Two others are the Sulphurdale geothermal area, along the western side of the Tushar Mountains south of Cove Fort, and the Cove Fort geothermal area along the western side of the Pavant Range east of Cove Fort (Blackett and others, 1994). The Sulphurdale area also was developed as a power plant. Both of these spring areas may have been heated by basaltic or rhyolitic magma at depth. Thus hydrothermal activity continues in the area, and mineral deposits continue to be formed.

ACKNOWLEDGMENTS

ROAD LOG

Increment Mileage	Cumulative Mileage	Description
0	0	BEGIN TRIP AT PARKING LOT at northwest corner of 200 South and 1150 West, Cedar City (west of Eccles Coliseum, at the southwest edge of the Southern Utah University campus). Drive north on 1150 West. On the left, west of I-15, the Cross Hollow Hills are made up of basin-fill and alluvial-fan deposits uplifted along faults and locally containing intertongued basalt lava flows of about 1 Ma (Averitt, 1967; Averitt and Threet, 1973; Fleck and others, 1975; Anderson and Mehnert, 1979; W.R. Lund, written communication, 2000). According to gravity data, the major normal faults of the Hurricane fault zone are west of the Cross Hollow Hills (Cook and Hardman, 1967).
0.4	0.4	AT SECOND STOP SIGN, TURN LEFT (WEST) ONTO 200 NORTH (STATE ROAD-56).
0.1	0.5	AT THE NORTHBOUND ENTRANCE RAMP TO I-15, TURN RIGHT (NORTH). As you enter I-15 from Exit 59 (the middle Cedar City exit), note at 9:00 the hills 10 km to the west, which make up the Iron Springs mining district, the largest U.S. iron

district west of the Great Lakes region but no longer being worked. The district is defined by a north-northeast-trending string (the Iron Axis) of quartz monzonite porphyry laccoliths of about 22-21.5 Ma (Mackin, 1947, 1960, 1968; Blank and Mackin, 1967; Mackin and others, 1976; Mackin and Rowley, 1976; Rowley and Barker, 1978; Barker, 1995). The iron deposits consist of huge hematite replacement bodies in the Homestake Limestone Member of the Jurassic Carmel Formation, adjacent to the concordant intrusive contacts. The southern part of the Iron Axis, especially the huge Pine Valley laccolith (Hacker, 1998), will be visited during a post-meeting field trip (Hacker and others, 2002) to see massive gravity slides that were shed off the flanks of the rising laccoliths and the volcanic products that erupted following the deroofing (Blank and others, 1992; Hacker, 1998; Rowley and others, 2001b). At 3:00, the red ridge on the northern side of Cedar Canyon, east of Cedar City, is the eastern flank (Triassic Moenkopi, Chinle, Moenave, and Kayenta formations, with Jurassic Navajo Sandstone and Carmel Formation east of the ridge) of a Sevier-age anticline whose western flank has been cut off and downthrown along the Hurricane fault zone (Averitt and Threet, 1973). The anticline is the leading edge above an eastward-verging blind Sevier thrust. Capping the Markagunt Plateau at the skyline is Brian Head, which is underlain by a ski resort and 26-Ma ash-flow tuffs of the Leach Canyon Formation and of the 27-Ma Isom Formation; Cedar Breaks National Monument is just southwest of Brian Head (Anderson, 1993; Hatfield and others, 2000).

2.7	3.2	The exit ramp to Exit 62, the north exit to Cedar City. At 2:30, the west limb of the Cedar City-Parowan monocline, probably a Sevier fold, is shown by the gray Cretaceous Straight Cliffs Formation. Ahead are the snow-capped peaks of the Tushar Mountains, the highest part of the Marysvale volcanic field. At 9:00 is a ring of hills making up The Three Peaks, the northeasternmost of the laccoliths of the Iron Springs district. An oil well spudded on the western flank of this laccolith drilled through the pluton into underlying sedimentary rocks (Van Kooten, 1988). The eastern side of the intrusion has been cut off by a fault that defines the western side of the Cedar Valley graben. The mostly brush-covered surface sloping toward us is a pediment cut on soft altered rock making up the interior phase of the intrusion. Geophysics indicates that the basin-fill deposits in the underlying basin-range graben west of the Hurricane fault zone are about 3 kilometers thick (Cook and Hardman, 1967).
4.1	7.3	Blue water tank on the left is on the northern side of Enoch, a suburb of Cedar City. Just north of Enoch and the water tank is the southern end of the Red Hills, a low range that is a horst defined by mostly Pliocene and Quaternary normal faults (Threet, 1952, 1963). The predominant red color of the range is from the Paleocene and Eocene Claron Formation, a fluvial and lacustrine sedimentary sequence that in some places is the basal Tertiary unit in southwestern Utah (Mackin, 1960), and is well known for its hoodoos and related landforms that characterize Bryce Canyon National Park (Davis and Pollock, 2000) and Cedar Breaks National Monument (Hatfield and

others, 2000). The northward continuation of the Hurricane fault zone likely defines the western side of the Red Hills. The Great Basin-Colorado Plateau boundary swings to the east of us and is defined by a series of north- to north-northeast-striking en echelon fault zones that die out southward into the Markagunt Plateau (Maldonado and Moore, 1995). The rocks to the right of us consist of huge landslides off these fault scarps (Averitt and Threet, 1973; Rowley and Threet, 1976).

| 3.4 | 10.7 | Hay barn on left (west). Farther west, basaltic lava flows of late Tertiary or Quaternary age are abundant in the southern Red Hills, where they rest on Claron Formation. An oil well, spudded in these basalts about 4 kilometers north of these rocks, was drilled on an aeromagnetic anomaly likely due to iron deposits. It encountered an intrusion of quartz monzonite porphyry at 1,060 meters depth, probably the continuation of the Iron Axis (Rowley and Threet, 1976). Enter Parowan Valley, a graben between the Red Hills and the Markagunt Plateau. |

| 5.7 | 16.4 | Exit 75, Parowan. At 8:00, Parowan Gap cuts through the Red Hills. The antecedent stream that flowed west and carved the canyon there was dammed by the latest movement (Quaternary) on the fault that defines the eastern side of the Red Hills, thus forming Little Salt Lake (Threet, 1963; Maldonado and Williams, 1993a, b). At 10:00, gray rocks farther north in the Red Hills are a series of huge Tertiary ash-flow sheets that overlie the Claron and were derived from caldera sources in the Great Basin (Maldonado and Williams, 1993b). The lowest of these is the 30-Ma Wah Wah Springs Formation of the Needles Range Group and the 27-Ma Isom Formation, both derived from the huge Indian Peak caldera complex that straddles the Utah-Nevada border (Best and others, 1989a, b).   These are overlain by additional ash-flow tuffs of the Quichapa Group (among them the Leach Canyon Formation), also derived from the Great Basin (Williams, 1967; Anderson and Rowley, 1975; Rowley and others, 2001b).   All these tuffs interfinger with locally derived volcanic rocks along the southwestern side of the Marysvale volcanic field.   At 3:00, these locally derived volcanics and intertongued Great Basin tuffs cap the Markagunt Plateau (Anderson, 1963, 1993; Anderson and Rowley, 1975; Maldonado and Moore, 1995; Hatfield and others, 2000). |

| 2.5 | 18.9 | Exit 78, Parowan and Paragonah. The easternmost fault zone of the en echelon assemblage, which continues north along the range front east of Parowan and Paragonah, is the Parowan fault zone (Maldonado and Williams, 1963b; Maldonado and Moore, 1995).   Red Claron rocks can be seen east of the fault zone, underlain by the light-gray Paleocene Grand Castle Formation, and in turn by the yellow and grayish-green Upper Cretaceous Iron Springs Formation (Maldonado and Moore, 1995). |

| 3.1 | 22.0 | Paragonah on the right, south of which are low ledges of basalt lava flows that flowed down the canyon into Parowan Valley and were in turn displaced by the latest movement on the Parowan fault zone (Anderson and Rowley, 1975; Maldonado and Williams, 1993b; Maldonado and Moore, 1995).   The basalts |

143

have K-Ar dates of about 450,000 years (Fleck and others, 1975). Northeast of Paragonah, the 20-Ma Iron Peak laccolith marks the northeast end of the Iron Axis, and like many of these laccoliths, it breached the surface and erupted volcanic rocks (Anderson and Rowley, 1975; Fleck and others, 1975; Rowley and others, 1994).

6.7	28.7	Exit to a Rest Area on I-15. The gray mountain at 2:00 consists of thick stratovolcano deposits, mostly volcanic mudflow breccia, of the Mount Dutton Formation, which overlies the Claron Formation here and to the north (Anderson and Rowley, 1975; Rowley and others, 1998). The dark-gray fault scarp at 10:00 is surmounted by Black Mountain, which also is made up of the Mount Dutton Formation. These outcrops look well bedded but consist entirely of volcanic mudflow breccia. Straight ahead, the lower hills consist of fault tilt blocks of mudflow breccia; those west of the highway belong to the southeastern Black Mountains, whereas those east of the highway belong to the Markagunt Plateau.
6.6	35.3	Exit 95, intersection with State Road (SR) 20, where we will return at the end of the day. Virtually all rocks you see to the west, north, and east consist of volcanic mudflow breccia of the Mount Dutton Formation. The high Tushar Mountains ahead are mostly rhyolites of the Mount Belknap Volcanics, within the Mount Belknap caldera (Callaghan, 1939; Cunningham and Steven, 1979a; Cunningham and others, 1983). The area west of this exit was mapped by Anderson (1965), some of which was published in Anderson and others (1990b). Just to the north, we enter the area of the Richfield 1:250,000 quadrangle (Steven and others, 1990).
5.2	40.5	Exit 100, ranch exit. Black Mountains to left; Markagunt Plateau to right. The east-trending scarp at 1:00 to 2:30 is a 30-kilometer-long, generally south-facing mountain front, with the Tushar Mountains making up both the scarp and the mountains north of it. The scarp follows an east-trending string of stratovolcanoes that shed part of the Mount Dutton Formation. The scarp is not linear, in part because it was controlled by these resistant but older and eroded vents and also by north-northwest-striking faults (Anderson, 2001). Most of the shallow intrusions, and thus most vents and mineral deposits, of the Marysvale field lie along and north of the scarp (Rowley and others, 1998). This east-west feature is part of a major structure called the Blue Ribbon transverse zone and interpreted to be about 25 km wide and 600 km long, spanning the entire Great Basin and Great Basin - High Plateaus transition zone. It and many others like it in the Great Basin are long lived and control the locations of many volcanic vents, plutons, mineral deposits, topographic features, and structures along them (Rowley and others, 1978; Rowley, 1998; Rowley and Dixon, 2001). Besides the southern margin of the Tushar Mountains, the transverse zone controls the northern side of the Black Mountains, which trends east-west for about 50 km, and Kingston Canyon, a 15-kilometer long east-west canyon that cuts through the Sevier Plateau to the east.

2.3	42.8	Roadcuts on the left and right expose scoria and airfall tuff from nearby basalt cinder cones. Continue north from this low summit through Nevershine Hollow (Anderson and others,1990a) into Beaver basin, a graben.

1.5 44.3 The high hill to the left and the roadcut coming up on the right are made up of thick dacitic lava flows of the 26-Ma Beaver Member of the Mount Dutton Formation (Anderson and Rowley, 1975; Fleck and others, 1975). The Mineral Mountains are at 11:00. The southern half of the crest is held up by light-gray granite pinnacles of the Mineral Mountains batholith, the largest exposed batholith in Utah. Despite its size and prominent expression, most of it is younger than 22 Ma (Nielson and others, 1986; Coleman and Walker, 1992; Coleman and others, 2001). The northern half of the crest is largely underlain by the batholith too, but these rocks are wooded and largely concealed by rounded rhyolite domes younger than 1 Ma (Lipman and others, 1978). The rhyolites are similar to the granite in composition and probably represent recurring upward invasion of magma from a common source area at depth. Their chambers provide geothermal heat for the Milford power plant, the largest geothermal power plant in Utah (Blackett and Moore, 1994).

4.0 48.3 On right, Quaternary fault scarps in basin-fill deposits of the Beaver basin. The basin-fill deposits here are at least 1.5 kilometers thick, the upper part of which has been well studied by Machette and others (1984) and Machette (1985). Dating of this upper part of the sequence is particularly complete, in part because of interbedded dated tephra beds and a basaltic lava flow, and in part by the study of calcrete soil deposits. This enabled mapping of a complicated series of Quaternary faults, which are clearly as young as late Pleistocene and perhaps early Holocene (Anderson and others, 1978; Machette, 1985). Basin formation began probably at about 12-9 Ma based on the oldest rhyolites on its northern margins (Evans and Steven, 1982), which were erupted along basin-range faults. Deposition was in a closed basin, which was breached at about 750,000 years ago. This was followed by formation of a series of pediments, the most prominent of which is Last Chance Bench that was cut about 500,000 years ago.

1.2 49.5 Exit 109, Beaver and Milford. The fault scarp just to the right has springs issuing from it, and it exposes on its east side basin-fill deposits of late Pliocene to early(?) Pleistocene age (Machette and others, 1984). Just to show you how we aim to please and give you choices, from about this point on, until we reach the town of Junction, we will be on two geologic maps with overlapping authorships, the more detailed (1:50,000) but older and thus slightly obsolete map by Cunningham and others (1983), and the less detailed (1:100,000) but new map by Rowley and others (2001a). Of course, we are also on the 1:250,000 geologic map of Steven and others (1990). The geology has not changed but its interpretation has evolved! We will not generally cite these maps along the way. The western

crest of the Tushar Mountains east of Beaver contains a ski area.

2.9	52.4	Exit 112, Beaver. White, snow-capped peak at 2:00 is rhyolite within the 19-Ma Mount Belknap caldera (Cunningham and Steven, 1979a).
3.1	55.5	Crest of Last Chance Bench, resistant because of a well developed calcrete soil beneath it (Machette, 1985). On the right, a major fault scarp underlies the base of the Tushar Mountains; most of the scarp is made up of stratovolcano deposits of the Bullion Canyon Volcanics (Steven and others, 1979).
5.3	60.8	Exit 120, Manderfield. The hill at 11:00 with the radio towers on it is Gillies Hill, and both it and Woodtick Hill north of it represent a large rhyolite dome complex (rhyolite of Gillies Hill) of about 9-8 Ma, interpreted to have formed at about the time the Beaver basin began to be blocked out (Evans and Steven, 1982; Cunningham and others, 1984c, 1994). At 2:30, low on the range front, the 24-23 Ma calc-alkaline Indian Creek stock probably was a local source for flows and mudflows in the Bullion Canyon Volcanics. Emplacement of the stock was the first in a series of events of hydrothermal alteration and mineralization in the area, which formed propylitic alteration and gold-bearing veins. This was followed by alteration and lithophile mineralization (uranium and molybdenum) associated with intrusions in the nearby wall of the 19-Ma Mount Belknap caldera. The later alteration and mineralization adjacent to the intrusions resulted in gold deposits and alunite at about 16 Ma and later during emplacement of the rhyolite of Gillies Hill in the same area (Cunningham and others, 1984c).
4.9	65.7	Exit 125, ranch exit, about a mile north of roadcuts in the rhyolite dome complex. Cross a low pass, leaving the Beaver basin.
1.4	67.1	Exit ramp to a Rest Area. High hill at 11:00 is a Pleistocene basaltic cinder cone, surrounded by smooth wooded slopes (basalt lava flows) (Steven and Morris, 1983). Dated by Best and others (1980) at 500,000 years old. Capping the Tushar Mountains to our right is the Mount Belknap caldera, part of the bimodal sequence with an age of about 20 Ma (Cunningham and Steven, 1979a).
2.8	69.9	Exit 129, Sulphurdale. Small rhyolite domes (rhyolite of Gillies Hill) to the left, about a mile from the Interstate and at the southern base of the cinder cone mentioned above, then another basaltic cinder cone a mile farther to the west. Western strands of the north-striking Sulphurdale fault zone (Cunningham and others, 1983) are a few hundred yards to our right. This zone lifts up the Tushar Mountains and controls hot springs and a broad area of hydrothermally altered rocks in the hills at 1:00-2:00 that have been mined for sulphur for many years. The geothermal resource is discussed in Blackett and Moore (1994), and a small geothermal power plant now is operating at the springs.

2.7	72.6	BEAR RIGHT AT EXIT 132, AND HEAD EAST ON I-70. Pleistocene basaltic flows to the left. Much of the Tushar flank to the right is made up of calc-alkaline intermediate composition intrusive rocks that were the local source for stratovolcanoes of the Bullion Canyon Volcanics (Steven and Morris, 1983). The flat top to the northwestern end of the range here, however, is the younger, nearly flat, 23-Ma Osiris Tuff (Anderson and Rowley, 1975). We will visit its source caldera, the Monroe Peak caldera, shortly. A patch of the 19-Ma Joe Lott Tuff Member of the Mount Belknap Volcanics (Callaghan, 1939; Cunningham and Steven, 1979a; Budding and others, 1987) rests on the Osiris there; the Joe Lott is the main product of the Mount Belknap caldera, and we will visit thicker sections of this unit shortly.
1.1	73.7	Exit 1. At about 10:00 is the small community of Cove Fort, named for a pioneer fort that now is a tourist attraction.
2.6	76.3	Cove Fort geothermal area is in highly faulted and deeply altered low hills to the left (Blackett and Moore, 1994). Native sulfur is exposed near its center, and a small fluorite deposit is along its northwestern side. This geothermal resource area has not been developed. The interstate here follows an east-striking fault, the Cove Creek fault (Steven and Morris, 1983), that is one expression of a major east-striking structural feature that is well expressed in geophysics, folds, topography, and an alignment of the edges of calderas and vents (Campbell and others, 1999; Rowley and others, 2001a). It is the Cove Fort transverse zone (Rowley, 1998; Rowley and others, 1998).
3.7	80.0	Top of the pass, following the Cove Creek fault (Steven and Morris, 1983); enter the Clear Creek drainage to the east. Pavant Range on the left; Tushar Mountains on the right. The Pavant Range is well known for its exposures of east-verging Sevier thrusts (Steven and Morris, 1983; Steven and others, 1990). The volcanics of the Maryvale field get into only the southern part of the range, so the thrusts and the Paleozoic and Mesozoic section are well exposed farther north.
0.2	80.2	BEAR RIGHT AT EXIT 8, RANCH EXIT.
0.4	80.6	Go through the stop sign and up the entrance ramp back toward I-70. **STOP NO. 1**, MOUNT BELKNAP CALDERA VIEWPOINT. Overview of the Marysvale volcanic field, Mount Belknap Volcanics, Cove Fort transverse zone, and the ghost town of Kimberly. The cream-colored rocks on the skyline to the south are within the Mount Belknap caldera. It formed 19 million years ago in response to the eruption of alkali rhyolite ash-flow tuffs of the Joe Lott Tuff Member of the Mount Belknap Volcanics, which we will see soon (Cunningham and Steven, 1979a; Budding and others, 1987). The caldera is filled with three major ash-flow units and associated lava flows and volcaniclastic rocks. Mt. Belknap is the high peak on the left and Mt. Baldy is on the right; both are capped by rhyolite flows. The light-colored ridge extending toward you is Gold Mountain, which is made up of the

147

middle tuff member of the intracaldera facies. The Kimberly mining district, located just north of the caldera wall, was discovered in 1888 and was a significant gold producer around the turn of the century. Gold was produced from quartz-pyrite-carbonate veins within and adjacent to a propylitically-altered 23-Ma quartz monzonite stock. The Annie Laurie and Sevier mines were the major producers (Lindgren, 1906). Entertaining popular accounts of life in the associated town of Kimberly are given by Herring (1989) and Utley (1992). The red outcrops in the middle distance are from a kaolinite mine developed in the Joe Lott Tuff. CONTINUE UP THE ENTRANCE RAMP AND BACK ON EAST-BOUND I-70.

1.5	82.1	At 2:00, views of the high Tushars, within the Mount Belknap caldera.
1.8	83.9	Start across a long bridge above Clear Creek Canyon. Cliffs on the left belong to the 27-Ma Three Creeks Tuff Member of the Bullion Canyon Volcanics, one of the most voluminous ash-flow sheets derived from the Marysvale field (Steven and others, 1979). These outcrops probably are within the Three Creeks caldera (Steven, 1981), but only parts of the walls of the caldera are exposed, just to the east of these cliffs.
1.6	85.5	Exit to Brake Test area. Kimberly is at about 2:00.
1.7	87.2	Start across a bridge that crosses Mill Creek, a tributary to Clear Creek. Upstream on Mill Creek, at about 4:00, is the site of the former stagecoach road to Kimberly, which was kept open even during the winter, although for this the stagecoach wheels were removed and sleigh runners installed instead (Utley, 1992). Joe Lott drove wagons up that road for many years (see preface of Budding and others, 1987).
0.5	87.7	Tan Sevier River Formation overlies the Joe Lott Tuff Member below and to the east. The Three Creeks Tuff Member on the left. All rocks are gently dipping into an east-striking syncline, the Clear Creek downwarp, and shorter flanking gentle anticlines. To the right, basalt flows dated at 9 and 7 Ma (Best and others, 1980) are interbedded with the Sevier River Formation. Two white tuff beds, dated at 14 (near the base) and 7 Ma (near the top) (Steven and others, 1979), can be seen in the formation. The unit resulted from erosion of highlands raised during initial phases of basin-range extension, but the basins in which the unit was deposited are not those of the main phase of basin-range extension, which are close to those we see today (Rowley and others, 2001a).
1.7	89.4	TAKE EXIT 17, FREMONT INDIAN STATE PARK. Outcrops of Joe Lott Tuff Member, characterized by cooling joints, on both sides of the road. Although we will not visit Fremont Indian State Park, we strongly recommend that you do so some day. It was established only a few years ago, when construction for the Interstate uncovered a major archeological site of pithouses, residences, and artifacts from Fremont Indians who lived here while farming this part of Clear Creek valley.

0.3	89.7	AT THE STOP SIGN AT THE TOP OF THE RAMP, TURN RIGHT. THEN IN 30 METERS TAKE ANOTHER RIGHT ONTO DIRT USFS ROAD-478. This road, in the canyon of Mill Creek, parallels the south side of the freeway.
0.6	90.3	The dirt road bears left (south) and enters the tributary canyon of Joe Lott Creek and the entrance to USFS Castle Rock Campground.
0.8	91.1	**STOP NO. 2**, CASTLE ROCK CAMPGROUND. Examine outcrops of the Joe Lott Tuff Member and the Sevier River Formation. These outcrops, of course, provided the type area of the Joe Lott Member (Callaghan, 1939). TURN AROUND AND RETURN TO THE ENTRANCE RAMP TO I-70.
1.4	92.5	AT THE TOP OF THE ENTRANCE RAMP, TURN RIGHT ONTO I-70. Off to the left, Mill Creek enters Clear Creek, near the location of the Lott family pioneer cabin. Joe Lott grew up here, one of 9 children; he in turn married, had a family, and ranched elsewhere in Clear Creek Canyon.
0.9	93.4	The sharp white hill on the right is where the main Fremont-age community was found and excavated. Fremont State Park headquarters at 10:00. Observe several cooling units of the unwelded Joe Lott Tuff Member. The tuff flowed north to this location, where it is at its thickest.
3.3	96.7	On left, good exposures of the Sevier River Formation. We are now in the Dry Wash fault zone, made up of several north-northeast-striking left-lateral strike-slip faults (Anderson and Barnhard, 1992). The zone can be thought of as accommodation faults created during east-west basin-range extension.
1.4	98.1	Exit 23, Sevier. At 10:00, along the southern edge of an older Quaternary pediment, Sevier River Formation is exposed. Tan clastic piedmont facies, interpreted to be a basin-margin facies, is on the west and partly underlies white to light-green lacustrine facies, on the east. These two facies of the Sevier River Formation are faulted against each other along a strand of the Dry Wash fault zone (Rowley and others, 1988b).
0.9	99.0	Adjacent to the lacustrine facies on the left. The flat-topped mountain at 2:00 is Monroe Peak, capping the Sevier Plateau. Because it caps a sequence of intracaldera tuffs related to the eruption of the Osiris Tuff, it gives its name to the Monroe Peak caldera, the largest in the Marysvale field (Steven and others, 1984a; Rowley and others, 1986a, b, 1988a, b). The Sevier Plateau was uplifted and tilted about 3° to the east along the Sevier fault zone, which runs along its western base.
1.5	100.5	TAKE EXIT 26, JOSEPH AND MONROE.
0.5	101.0	TURN RIGHT ON SR-118 AT THE BOTTOM OF THE RAMP.

0.4	101.4	Stop sign at intersection with US-89. Downtown Joseph. Continue straight on SR-118. A small tilt block straight ahead is uplifted by one strand of the Dry Wash fault zone, which passes along the western side (Rowley and others, 1988b). So here, the zone has a dip-slip component. Light-gray Three Creeks Tuff Member at the base of the block is overlain in turn by thin basaltic lava flows, the Osiris Tuff, and the Joe Lott Tuff Member. Cross the Sevier River about 2 kilometers east of the intersection.
1.9	103.3	Start to climb up over the small tilt block, going through faulted basin-fill deposits along its western side and an older uplifted pediment deposit on top. We use the term "basin-fill deposit" for sediments deposited in downthrown areas that are synchronous with the main episode of basin-range faulting (Rowley and others, 2001a). Hot springs and hot-spring deposits are exposed along the fault south of here. As we go over the top of the fault block, we see Monroe ahead, east of which is the Sevier fault zone and the uplifted northern Sevier Plateau. Monroe Canyon, where we are headed, is southeast of town.
3.5	106.8	Stop sign as SR-118 (100 South) intersects with Main Street, downtown Monroe. TURN RIGHT ON MAIN STREET. On left, the Three Creeks Tuff Member and the Bullion Canyon Volcanics in the mountain front behind Monroe are hydrothermally altered, and a popular recreation area at the base of the Sevier fault scarp is Monroe Hot Springs.
0.8	107.6	Road bends sharply left. At the base of the fault scarp at 12:00 to 2:00 is light-gray Three Creeks Tuff Member overlain by mudflows of the Bullion Canyon Volcanics.
1.3	108.9	House with duck pond on right, soon after entering Monroe Canyon.
1.3	110.2	Just past a narrowing of the canyon as it cuts through a thick andesitic lava flow of the Bullion Canyon Volcanics. The road becomes dirt.
0.3	110.5	Road forks. TAKE RIGHT FORK ACROSS THE BRIDGE. Left fork goes to Monrovian Park, a local picnic spot less than a kilometer away, at the contact of an intracaldera pluton in the Monroe Peak caldera.
1.6	112.1	**STOP NO. 3**, MONROE PEAK CALDERA MEGABRECCIA. Stop at the sharp switchback to the right, then hike several hundred meters up an old road along a stream that passes beneath the switchback. Pass along a lateral moraine and cross the concealed northern wall of the Monroe Peak caldera. Then climb up left (east) into propylitically altered megabreccia blocks adjacent to an intracaldera pluton that is farther to the east. Return to the vehicles. TURN AROUND AND RETRACE OUR STEPS TO THE STOP SIGN AT US-89 AT JOSEPH.
10.7	122.8	Intersection with US-89. Cross US-89 and continue on SR-118.

0.5	123.3	Pass beneath I-70 to the entrance ramp for westbound I-70. AT THE ENTRANCE RAMP, TURN LEFT AND ENTER FREEWAY.
1.8	125.1	TAKE EXIT 23, PANGUITCH AND KANAB.
1.6	126.7	US-89 (from the town of Sevier) enters on the left. Continue south on US-89. Low hill to the left, about 50 meters south of this intersection, contains a tuff bed in the Sevier River Formation that Steven and others (1979) dated at 7 Ma. The formation just predates main-phase basin-range deformation, which formed the present topography. Thus this date supplies evidence that basin-range faulting here is younger than 7 million years ago.
0.7	127.4	Cross the Sevier River and enter Marysvale Canyon, made up mostly of Bullion Canyon Volcanics, which here consists of volcanic mudflow breccia, subordinate lava flows, and minor ash-flow tuffs, all of dacitic composition.
0.8	128.2	On left, the upper, east-dipping unit is the Joe Lott Tuff Member.
2.2	130.4	Straight ahead, east of the Sevier River, is a monzonite stock of the calc-alkaline episode, synchronous with and a likely source of some parts of the Bullion Canyon Volcanics here. It is less than 1 kilometer in diameter and rises almost vertically about 200 meters above the canyon floor. Its fluted walls coincide with its intrusive contact. It was referred to as "The Plug" by Kerr and others (1957). About 400 meters above the floor of Marysvale Canyon, a subhorizontal surface beveled on the Bullion Canyon Volcanics is capped by poorly consolidated sandstone and conglomerate of the Sevier River Formation (Rowley and others, 1988a, b). This represents a higher level erosion surface, cut during an earlier episode of extension, probably when the Sevier River Formation was deposited but before the main episode of extension that led to the present canyon cutting.
2.3	132.7	View of Big Rock Candy Mountain, the same as shown in the photograph on the cover page of the field-trip log. This mountain is a well-known landmark for variegated altered volcanic rocks in west-central Utah. It consists of the eroded remnants of an alunite deposit that replaced intermediate-composition lava flows about 21 million years ago. The alunite formed in steam-heated conditions near the top of a hydrothermal plume that was one of at least six, spaced at 3- to 4-kilometer intervals, surrounding a monzonite stock (Cunningham and others, 1984a). Big Rock Candy Mountain is horizontally zoned outward from an alunite core to respective kaolinite, dickite, and propylite envelopes and is the lower part of a vertically zoned sequence from a lower pyrite-propylite assemblage upward through assemblages successively dominated by hypogene alunite, jarosite, and hematite, to a flooded silica cap. This hydrothermal assemblage is undergoing natural destruction in a steep canyon as a result of exposure owing to downcutting of the Sevier River in Marysvale Canyon. Integrated geologic, mineralogic, spectroscopic remote sensing using AVIRIS data, argon radiometric, and stable isotopic studies trace the hypogene origin and supergene

151

destruction of the deposit and permit distinction of primary and secondary processes. This destruction has led to the formation of widespread supergene gypsum in cross-cutting fractures and as surficial crusts, and of natrojarosite, which gives Big Rock Candy Mountain its buff color along ridges facing the canyon. A small spring, Lemonade Spring, with a pH of 2.6, containing Ca, Mg, Si, Al, Fe, Mn, Cl, and SO_4, is located near the back of the motel. A $^{40}Ar/^{39}Ar$ date (21.32$\pm$0.07 Ma) on the alunite is similar to that for other replacement alunites at Marysvale. However, the age sprectrum contains evidence of a 6.6-Ma thermal event that can be related to tectonic events (that is, main-phase basin-range extension) responsible for uplift that led to the downcutting of Big Rock Candy Mountain by the Sevier River. This 6.6-Ma event also is present in the age spectrum of supergene natrojarosite forming today and probably dates the beginning of supergene alteration of Big Rock Candy Mountain.

0.5	133.2	**STOP NO. 4**, BIG ROCK CANDY MOUNTAIN. PULL OVER TO THE RIGHT, at Big Rock Candy Mountain Resort. Made popular by a song of the same name by Burl Ives, the predecessor resort to this motel flourished in the 1940s and earlier as a dude ranch and place to hunt mountain lions; its inside is decorated with autographed pictures of movie actors, actresses, and other celebrities. Please do not break rocks or dig within view of the motel or climb to the alunite outcrops. Excellent samples and observations of altered rock relationships can be obtained by a short walk south along the cliff face. Be sure to visit, but do not drink from, Lemonade Spring behind the motel! RETURN TO THE VEHICLES AND CONTINUE SOUTHWARD ALONG US-89. Hoover pluton at 9:00 to 1:00, on the eastern side of the river.
0.9	134.1	**STOP NO. 5**, HOOVER'S TRUCK STOP. IF WE HAVE CALCULATED CORRECTLY, THIS WILL BE OUR LUNCH STOP. PULL OVER TO THE LEFT. For several years, USGS mapping of the Marysvale field was centered out of Hoover's, using government trailer homes. To the east of Hoover's Truck Stop is Hoover Peak, and the Hoover pluton, which is a large quartz monzonite stock of the calc-alkaline sequence. Steeply south-dipping ash-flow tuffs of the Mount Belknap Volcanics are on the right, including the gray Joe Lott Member and the overlying red Red Hills Member. The rhyolites are downdropped by a well-exposed east-striking basin-range fault.
1.3	135.4	Curve sharply to the right. Red rocks to the left belong to the Red Hills Tuff Member, within the Red Hills caldera. Flow foliations in this tuff are inclined steeply inward into the caldera, suggesting rheomorphic flowage back into the collapsing hole.
0.9	136.3	Black knob on the right is the basal glass of a lava flow in the Mount Belknap Volcanics. Enter Marysvale Valley, another graben between the Tushar fault zone on the west and the Sevier fault zone on the east.
0.8	137.1	Views of the Sevier Plateau to the left and the Tushar Mountains to the right. The Central Mining Area is at 8:00 (Cunningham

		and Steven, 1979b; Steven and others, 1981; Cunningham and others, 1982, 1998b).
0.9	138.0	Enter Marysvale, on Main Street.
0.4	138.4	AT THE INTERSECTION OF MAIN AND CENTER STREETS, TURN LEFT ON CENTER STREET (DIRT). "Our Bar" is on the southeastern corner of this intersection, and an Amoco gas station and convenience store is on the northeastern corner.
0.6	139.0	Cross the Sevier River. Then the dirt road bears left (north).
0.6	139.6	Maintaining "M" hill on the right has obviously kept a lot of high-school students occupied and thus more or less out of trouble. This hill is Bullion Canyon Volcanics, but a few hundred meters to the east it is intruded by intracaldera plutons at the western edge of the Monroe Peak caldera (Rowley and others, 1988a).
0.9	140.5	Hydrothermally altered intracaldera Osiris Tuff. The Monroe Peak caldera margin here is interpreted to be west of the road, and this margin continues north, through the middle of the Red Hills caldera. Thus the Monroe Peak caldera is interpreted to enclose the entire Central Mining Area.
0.3	140.8	The road forks. TAKE THE LEFT FORK. The flat-topped mountain at 1:00 is the high point of the Central Intrusion, an intracaldera intrusion within the Monroe Peak caldera and a host to some of the uranium deposits in the district. The Central Mining Area is from 11:00 to 1:00.
0.3	141.1	The road forks again. TAKE THE LEFT FORK.
0.2	141.3	The road forks a third time. AGAIN, TAKE THE LEFT FORK. At the fork is a Piute trail marker for all-terrain vehicles (ATVs).
0.6	141.9	Cross the wall of the Red Hills caldera. **STOP NO. 6**, RED HILLS CALDERA. Take a quick look at the Red Hills Tuff Member on the right. CONTINUE NORTH ON THE DIRT ROAD.
0.9	142.8	Electric substation on the right, in the middle of the Red Hills caldera. Highest flat-topped hill, with its many switchbacks, at 2:30 is horizontal Red Hills Member (19 Ma) sitting on the Central Intrusion (22 Ma) (Cunningham and Steven, 1979b; Cunningham and others, 1982, 1998b; Rowley and others, 1988b). Uranium veins occur in the Central Intrusion, fine-grained granite, and Red Hills Tuff Member.
0.6	143.4	The road forks. TAKE THE LEFT FORK. The heart of the Central Mining Area is on the right (Cunningham and Steven, 1979b; Cunningham and others, 1982, 1998b). Notice the flat-lying outflow Red Hills Tuff Member on the right. The highest hill at 3:00 is in the Central Intrusion, and the right fork would go into the Central Mining Area and the intrusion. The Central Intrusion is interpreted to be part of the calc-alkaline episode, but it is a host for many of the uranium deposits. A more important host is

the fine-grained silicic pluton, which makes up much of the rock containing the switchbacks and mines we can see. This pluton, with an age of is about 21 Ma, is interpreted to belong to the bimodal episode (Cunningham and Steven, 1979b; Rowley and others, 1988a, b). But the source and control for the uranium is a series of younger glassy rhyolite dikes of the Mount Belknap Volcanics that are dated at 19-18 Ma and cut the Central Intrusion and fine-grained silicic pluton (Cunningham and others, 1982). These dikes are interpreted to widen downward into an unexposed stock that provided the uranium to the district and that may host a porphyry molybdenum deposit (Cunningham and others, 1982).

1.3	144.7	Top of a hill, with outcrop of altered rhyolite to our right. We are now outside the Monroe Peak caldera, as are most rocks (Bullion Canyon Volcanics) surrounding Sage Flat, the valley ahead and below us (Rowley and others, 1988b). This valley is a shallow closed basin formed behind a young fault to the west. The caldera wall, however, passes through the eastern side of Sage Flat, then north. The red peak at 12:00 is made up of Monroe Peak intracaldera volcanic rocks that have been altered by one of the hydrothermal convection cells surrounding the Central Intrusion (Podwysocki and Segal, 1983). In these cells, a lower alunite zone passes upward into jarosite, hematite, and flooded silica zones (Cunningham and others, 1984a). When it breached the surface, the silica zone formed hot spring sinter at the surface and also silicified (replaced) the immediately underlying rocks. Surficial silica includes hydrothermal breccia ("blowouts") deposited under geyser conditions after pressure built up and was released explosively. The red peak is capped by a thick replacement silica zone, but slightly lower on the mountain, red hematite was mined at the Iron Cap mine from the underlying hematite zone. Quartz knobs that represent hot spring sinter and related hydrothermal breccia, as well as replacement silica are abundant in a 90° arc that ranges between north and east of our location (Rowley and others, 1988b).
1.2	145.9	Road forks after crossing Sage Flat and up a canyon in Bullion Canyon Volcanics. TAKE RIGHT FORK.
1.2	147.1	On right, entrance to Yellow Jacket mine. **STOP NO. 7**, YELLOW JACKET MINE. Discussion will focus on replacement alunite deposits that have been directly dated at about 23-22 Ma, the age of the Central Intrusion (Cunningham and others, 1984a). TURN AROUND AND RETRACE OUR STEPS TO THE FORK CONTAINING THE ATV TRAIL MARKER.
5.8	152.9	AT THE FORK CONTAINING THE PIUTE TRAIL MARKER, TAKE A SHARP LEFT (NORTH).
0.7	153.6	Approximate location of intrusive contact to the Central Intrusion, to the north. Enter the southern part of the Central Mining Area.
0.5	154.1	Intersection, on the left, with an old road that comes down from the VCA mine. **STOP NO. 8**, VCA MINE. Please stay away

from old mine workings! Hike up the old road, looking at mineralized Central Intrusion, the horizontal contact between the Central Intrusion and overlying Red Hills Tuff Member, and the VCA mine. The VCA mine, emplaced into the Central Intrusion at the southern edge of the Antelope Range quadrangle (Cunningham and Steven, 1979b; Cunningham and others, 1982, 1998b; Rowley and others, 1988b) was an important underground uranium mine. The glassy rhyolite dikes associated with uranium mineralization are exposed at depth, and molybdenum values increase in the veins downward (at 200 meters depth), suggesting that the dikes pass into a buried stock (Cunningham and others, 1982). RETURN TO THE VEHICLES AND RETRACE OUR TRACKS TO MARYSVALE. As we turn around the vehicles and head south, you will see roads, white outcrops, dumps, and mines at 12:30 to 1:30 that belong to the Whitehorse mine, which mined replacement alunite in another hydrothermal cell caused by emplacement of the Central Intrusion (Cunningham and others, 1984a, b).

4.1	158.2	AT INTERSECTION WITH US-89 IN DOWNTOWN MARYSVALE, TURN LEFT AND HEAD SOUTH ON US-89.
1.2	159.4	Dairy farm on left is on an older piedmont-slope (Pleistocene pediment and fan) deposit that in turn rests on Pliocene and Pleistocene basin-fill deposits that were deposited during basin-range extension. These deposits rest on Sevier River Formation, well exposed east of the Sevier River to our left (Rowley and others, 1988a). A western strand of the Sevier fault zone runs along the low scarp just east of the river, whereas an eastern strand runs along the base of the main scarp of the Sevier Plateau. Flat-topped mountain on the Sevier Plateau at 9:30 is Big Table, held up by basalt lava flows that cap outflow Osiris Tuff; below the Osiris are thick sequences of andesitic lava flows and volcanic mudflow breccia of a shield volcano that predates and lies just south of the Monroe Peak caldera. The rocks in the caldera just north of Big Table consist, from the base of the scarp to the top, of an intracaldera intrusion (lower 300 meters), intruded into heavily altered intracaldera Osiris Tuff that makes up the overlying 200 meters. This is overlain by fresh intracaldera lava flows that form the upper peaks and postdate the main intracaldera intrusion exposed at the base of the scarp.
2.3	161.7	Dirt road on right, with a sign on it "UNICO, Inc. Deer Trail mine." TURN RIGHT ONTO THAT ROAD. The Tushar fault zone, which runs along the base of the scarp, has raised the Tushar Mountains as a giant horst. The lower 1,000 meters of the scarp consist of sedimentary rocks, ranging from the Permian Queantoweap Sandstone at the base upward through the Jurassic Arapien Formation, in turn overlain unconformably by a thin unnamed lower Tertiary conglomerate less than 30 meters thick (Cunningham and Steven, 1979c). The Bullion Canyon Volcanics make up the rest of the rocks to the top of the Tushar Mountains.
2.0	163.7	Fork in road. BEAR RIGHT ON THE MAIN FORK.

0.2	163.9	Fork in road. TAKE RIGHT FORK TO THE LOCKED GATE. **STOP NO. 9**, DEER TRAIL MINE. The Deer Trail mine is an underground mine developed in a halo of gold-bearing veins and base- and precious-metal manto deposits adjacent to the easternmost of two cupolas on a blind intrusion (Cunningham and others, 1984a; Beaty and others, 1986). The western cupola has spectacularly domed up and split open its host rocks, then degassed (Cunningham and Steven, 1979c). These extension joints in the roof were filled by coarse-grained vein alunite at the crest of the dome, on Alunite Ridge. The alunite was dated at 14 Ma, the same age as the Deer Trail ore (Cunningham and others, 1984a). Details of the deposit will be discussed at the mine. The dump is a good place to collect samples of Deer Trail rocks and ore. TURN AROUND AND RETURN TO US-89.
2.2	166.1	STOP SIGN. TURN RIGHT AND HEAD SOUTH ON US-89. White outcrops on the eastern side of the river at 9:30 are made up of the Joe Lott Tuff Member, which underlies the tan Sevier River Formation well exposed north of it. These rocks are bounded by a fault at the base of the low scarp.
3.5	169.6	Dirt road on the left, with a large dirt stock tank along it. Hill at 9:30 is a tilt block. The strong ledge in the middle of the slope is outflow Osiris Tuff, overlain in turn by soft rocks of the Joe Lott Tuff Member and Sevier River Formation, then by a resistant caprock of basalt lava flows dated at 13 Ma (Best and others, 1980).
1.5	171.1	Paved road on left to Piute Lake State Park. The earthen dam to this lake, at the northern end of the lake but hidden from our view here, is old, has a late Quaternary fault through it, and may have to be replaced (D.B. Simon of Simon-Bymaster, Inc. and colleagues, written commun., 2001). The spectacular basin-range fault scarp east of the lake exposes the Three Creeks Tuff Member at the base, volcanic mudflow breccia of mostly the Mount Dutton Formation above, then at the top the same units as in the previously mentioned tilt block. Most of the black rocks in the hanging wall of the Sevier fault zone, including those west of the reservoir, are potassium rich mafic volcanic rocks that here and elsewhere have ages of between 25 and 21 Ma (Rowley and others, 1994). On the right, the Tushar Mountains flank we see is made up of the Bullion Canyon Volcanics, which intertongues southward with the Mount Dutton Formation, which in turn makes up most of the mountain flank another few kilometers to the south. The upper unit of the Bullion Canyon Volcanics to our right is the 23-Ma Delano Peak Tuff Member of the Bullion Canyon, a major ash-flow sheet derived from the Big John caldera just west of the crest of the Tushars 7 kilometers west of us (Steven and others, 1984b).
3.4	174.5	Former US-89 joins us on the left. The highest part of the Sevier Plateau on the horizon to our left is capped by a thick rhyolite lava flow that Rowley and others (1981) dated at about 8 Ma. It and the rocks below it dip gently eastward at about 3°, due to normal movement of at least 2.5 kilometers along the Sevier fault

zone. When we get to Kingston Canyon, we will stop at the rhyolite dome of Phonolite Hill that further constrains the movement of this fault zone. Ahead at 1:00, the highest point of the Sevier Plateau is called Mount Dutton and, to the left of it is Mount Pierson, named for Lynn Pierson, a Utah Highway Patrolman killed in the line of duty.

1.8	176.3	Piute County International Airport on the right, as we enter the town of Junction, the county seat.
0.9	177.2	Downtown Junction. The former courthouse is on the right, just south of which is a road that heads west across the Tushar Mountains to Beaver. Hills sticking out of the graben to the left and ahead are tilt blocks caught along the Sevier fault zone. We soon will leave the area shown by the maps of Cunningham and others (1983) and Rowley and others (2001a).
1.8	179.0	Intersection with SR-62 on the left. TURN LEFT TOWARD KINGSTON CANYON.
1.8	180.8	Enter the outskirts of Kingston.
0.4	181.2	Leave Kingston and enter Kingston Canyon. The canyon is an antecedent canyon formed when an east-flowing stream, the East Fork of the Sevier River, maintained its course as the Sevier Plateau was uplifted along the Sevier fault zone.
0.6	181.8	Purple Haze outside dance pavilion, its best days behind it, on the right. Most rocks we will see in the western part of Kingston Canyon are blocks of volcanic mudflow breccia of the Mount Dutton Formation, tilted by an intersecting series of parallel and en echelon normal faults of the Sevier fault zone. South of Kingston Canyon, most faults strike north-northeast, whereas north of Kingston Canyon, most strike north-northwest (Rowley, 1968). On the hill towering above the Purple Haze, two petrologically identical medium-brown, densely welded, crystal-poor, local ash-flow tuff cooling units filled a stream channel draining the stratovolcano that deposited the breccia. Although in most places these lenticular cooling units are in contact, they have a small wedge of breccia separating them in the center of the channel. This is the only place we have seen these cooling units, which probably differed in age by only a few minutes or a few years. We will get a better view of these rocks on our way back.
1.6	183.4	Osiris Tuff, a densely welded ash-flow unit, on the right. A north-northeast-striking fault passes across our path and displaces this tuff up on the east; it forms the caprock of the large hills at 1:00 and 10:00.
0.9	184.3	**STOP NO. 10**, KINGSTON CANYON MUDFLOWS. PULL OVER TO THE RIGHT. Look at volcanic mudflow breccias, the most voluminous rock type in the Maryvale volcanic field. We classify most breccias as alluvial facies, as opposed to near-source vent facies. A basaltic feeder dike stands up in bold relief on our left. RETURN TO THE VEHICLES AND CONTINUE

157

EAST. In about 200 meters, we will pass over another north-northeast-striking fault, also upthrown to the east, into pink rocks of the Three Creeks Tuff Member (Rowley, 1968).

1.4	185.7	**STOP NO. 11**, CRYSTAL-RICH TUFF. PULL OVER TO THE RIGHT. On our right, spectacular exposures on the northern wall of Kingston Canyon of, from base to top, 15 meters of resistant bedded sedimentary rocks that can be assigned to the Claron Formation; 15 meters of pink, crystal-rich ash-flow tuff of the 30-Ma Wah Wah Springs Formation of the Needles Range Group; 20 meters of bedded sedimentary rocks; and 200 meters of crystal-rich ash-flow tuff of the 27-Ma Three Creeks Member of the Bullion Canyon Volcanics. Cross the road to the north for a quick look at float samples of the Wah Wah and Three Creeks. RETURN TO THE VEHICLES AND CONTINUE EAST.
1.1	186.8	The hill at 10:00 is Phonolite Hill, mostly a rhyolite dome but with a tuff ring at its base. Observe the different geomorphology of the canyon exposures to our right versus those to our left: a classic function of erosion (notably freeze-thaw cycles) on south-facing versus north-facing slopes.
0.3	187.1	**STOP NO. 12**, PHONOLITE HILL. PULL OVER TO THE LEFT. The rhyolite of Phonolite Hill erupted at 5 Ma in the base of Kingston Canyon, which was cut following the main phase of basin-range faulting. This date, when combined with the east-dipping 8-Ma rhyolite flow that caps the Sevier Plateau north of us, provides one of the best constraints on basin-range faulting—between 8 and 5 Ma—yet reported (Rowley and others, 1981). Examine outcrops of tuff-ring sediments on the northern side of the road. The vertical contact of the dome with these sediments, containing a 1-meter thick vertical vitrophyre, is exposed on the slope above us, but we do not have the time to go there so will examine rhyolite float instead. RETURN TO THE VEHICLES AND CONTINUE EAST.
1.3	188.4	Several other domes are to the right. All of them are on a line with a northwest strike, probably erupted along a fracture.
1.4	189.8	On left and right, the gentle eastward dip (here it has steepened from its average of about 3°) of the Sevier Plateau is obvious. The Plateau rim to the left and right is held up by the Osiris Tuff and, locally, also by basalt lava flows. The next plateau to the east, the Awapa Plateau, is similarly uplifted along a fault zone (Paunsaugunt fault zone in Grass Valley to the east) and tilted eastward.
1.2	191.0	**STOP NO. 13**, OSIRIS TUFF. PULL OVER. Examine two densely welded ash-flow tuffs. The eastern (upper) of the two tuffs is the Osiris Tuff, derived from the Monroe Peak caldera at about 23 Ma. Three zones are clearly seen in its 20 meter stratigraphic section: a basal glass, the red devitrified stony zone, and the upper gray vapor-phase zone. The lower tuff is the 26-Ma Antimony Member of the Mount Dutton Formation, an even more densely welded ash-flow tuff and here about the same thickness as the Osiris (Rowley and others, 1994). Its

158

source is not known but probably is beneath the Sevier River Valley in the Joseph area, based on other cooling units in that area. It has the same zones as the Osiris. The type area of the Antimony is here, not far from the town of Antimony to the southeast (Anderson and Rowley, 1975); the type area of Osiris is near the ghost town of Osiris, south of Antimony (Williams and Hackman, 1971). At this stop, the Osiris rests directly on Antimony, but several kilometers to the east, about 300 meters of Mount Dutton mudflow deposits separate them. East of Antimony, the Mount Dutton Formation thins rapidly, at the flanks of the clustered stratovolcanoes and other volcanoes. Before they pinch out, however, the clasts become rounded and grain supported and instead of mudflow deposits, they have become reworked into conglomerate. A basalt flow overlies Osiris about 100 meters east of this stop; Rowley and others (1981) dated it at about 8 Ma. RETURN TO VEHICLES AND CONTINUE EAST.

0.3	191.3	SR-22 on the left intersects SR-62. We are in Grass Valley, north of the town of Antimony. The earthen dam of Otter Creek Reservoir is a few hundred meters to the east of us. TURN AROUND AND RETURN TO US-89.
12.3	203.6	Intersection with US-89. TURN LEFT (SOUTH) ON US-89. The rounded hills to the left and right are mostly faulted blocks of volcanic mudflow breccia of the Mount Dutton Formation, but some white conglomerate and sandstone of the Sevier River Formation are present. Enter Circle Valley.
2.1	205.7	Abandoned potato warehouse on the left. The Sevier fault zone on the left is complicated, so lots of small horst blocks can be seen sticking out of the basin fill. The large Tushar fault zone on the right exposes little more than volcanic mudflow breccia, with some lava flows, from the base to the top of the scarp. However, the scarp here creates a spectacular cross section through a stratovolcano, with a north-dipping northern flank and a south-dipping southern flank. The south faces of the highest peaks contain spectacular glacial cirques. These peaks are underlain by lava flows of the potassium-rich mafic volcanic rocks erupted about 23 to 22 Ma (Anderson and others, 1990b). This is the same south-facing scarp seen before, separating the Tushar Mountains from the Markagunt Plateau and largely controlled by the Blue Ribbon transverse zone.
1.4	207.1	Cross the Sevier River and enter Circleville.
1.5	208.6	Leave Circleville.
0.7	209.3	Spectacular outcrops of volcanic mudflow breccia adjacent to the highway on the right.
1.1	210.4	On the right, against the cottonwood trees, is the boyhood home of the infamous outlaw LeRoy Parker, better known as Butch Cassidy. Butch frequented the gold camp of Kimberly, but apparently he avoided trouble there and in other places when he was near home (Herring, 1989). Soon we will enter Circleville

Canyon, exposing mostly vent facies of the Mount Dutton Formation (Anderson and others, 1990b). Assigning vent versus alluvial facies is not a cut and dried procedure: we use vent facies when dikes, lava flows, and flow breccia are abundant, when initial dips are seen, and when the clasts in volcanic mudflow breccia masses are monolithologic.

1.1	211.5	**STOP NO. 14**, CIRCLEVILLE CANYON STRATOVOLCANO DEPOSITS. PULL OVER TO THE RIGHT JUST BEYOND THE VERTICAL ROADCUT ON A SHARP RIGHT CURVE. This roadcut on the right probably represents the throat of a stratovolcano, as suggested by the presence of dikes, a probable fault, lava flows, and volcanic mudflow breccia. CONTINUE SOUTH. Farther south, some of the breccias are well bedded, a feature that is more indicative of alluvial facies. Many of the breccias are tilted, but interpreting whether these are initial dips or fault tilt blocks is problematic.
2.4	213.9	**OPTIONAL STOP**, CIRCLEVILLE CANYON STRATOVOLCANO DEPOSITS. TIME PERMITTING, PULL OVER ON THE RIGHT JUST BEYOND THE ROADCUT, ALSO ON A RIGHT CURVE. This roadcut is best classified as vent facies, suggested by mostly flow breccia, lava flows, and volcanic mudflow breccia. CONTINUE SOUTH.
0.6	214.5	**OPTIONAL STOP**, CIRCLEVILLE CANYON STRATOVOLCANO DEPOSITS. TIME PERMITTING, PULL OVER ON THE LEFT, ACROSS THE ROAD FROM A VERTICAL ROADCUT. This is a possible throat or vent area, consisting of breccia dikes on top of each other as well as lava flows. CONTINUE SOUTH.
1.9	216.4	The outcrops to the left, across the Sevier River, consist mostly of scores of dikes emplaced into each other. Some of them are breccia dikes. The landform that was built up above them is assumed to have been a stratovolcano.
1.0	217.4	Roadcut on the right consists of basin-fill deposits plastered on the wall of this canyon.
1.5	218.9	**OPTIONAL STOP**, SPRY INTRUSION. PULL OVER ON THE RIGHT, TIME PERMITTING. The Spry Intrusion is a well exposed quartz monzonite porphyry laccolith of batholithic dimensions (Anderson, 1965, 1993; Anderson and Rowley, 1975). Furthermore, gravity and aeromagnetic data indicate that it extends in the subsurface at least 50 km south of these exposures (Blank and Kucks, 1989; Anderson, 1993; Rowley and others, 1998). It vented a local series of lava flows, dikes, and volcanic mudflow breccias, known collectively as the volcanic rocks of Bull Rush Creek (Anderson and others, 1990b) and it vented an ash-flow tuff called the Buckskin Breccia (Anderson, 1965; Anderson and Rowley, 1975). The Buckskin Breccia spread widely over the northern Markagunt Plateau and is distinctive because it contains abundant lithic clasts of the Spry Intrusion. All these volcanic and intrusive rocks have the same age, 26-25 Ma (Anderson and others, 1990b). The

Buckskin Breccia filled a series of grabens in the northern Markagunt Plateau, thereby partly providing proof of an early episode of west-northwest striking faults (Anderson, 2001). CONTINUE SOUTH. Note, as we continue along U.S.-89, that the Spry outcrops ahead and to the right have a flat top that is about 130 meters above road level; this surface is overlain by pediment deposits (Anderson and others, 1990b). This clearly represents an upper-level erosion surface. In addition, the top of Circleville Canyon north of us has subhorizontal to gently rolling topography at about 300 meters above the canyon bottom, further proof of older erosion surfaces at the same level as above Marysvale Canyon, noted above.

0.7	219.6	Cliffs of the Spry Intrusion on the right. Then, beyond this, we break out into the Sevier River valley, defined by the Sevier fault zone on the east and the generally east-tilted (but locally faulted) Markagunt Plateau on the west. Far to the south and the left, the red rocks on the lower part of the scarp of the Sevier Plateau are Claron Formation. This red member of the Claron is overlain by white sedimentary rocks, formerly considered the white member of the Claron (Rowley, 1968) but now perhaps part of the Brian Head Formation (Sable and Maldonado, 1997); the white rocks are in turn overlain by the southward thinning volcanic mudflow breccia (alluvial facies) of the Mount Dutton Formation.
5.1	224.7	Bear Valley Junction, where SR-20 intersects on the right with US-89. TURN RIGHT ON SR-20. As we make the turn, one of two crosses on the right is a tribute to Highway Patrolman Lynn Pierson.
1.3	226.0	North-dipping volcanic rocks on the hill to the right form the northern part of the Orton structural dome, which is probably caused by an underlying laccolith (Anderson, 1965; Anderson and Rowley, 1975, 1987). The oldest exposed rocks in the interior of the dome belong to the Claron Formation. The Claron is overlain by a local assemblage of volcanic rocks exposed to the left and low on the hill to the right. These volcanic rocks have a date of 32 Ma (Fleck and others, 1975) and predate ash-flow tuffs of the 30-Ma Wah Wah Springs Formation, which caps the hill to the right. The Wah Wah Springs is overlain by the 27-Ma Isom Formation, just north of the hill to the right, and in turn by the 26-25 Ma Bear Valley Formation (Anderson, 1971), a widespread eolian sandstone and intertongued local ash-flow tuffs.
1.3	227.3	Outcrops of gray, green, and yellow eolian sandstone of the Bear Valley Formation on both sides of the road. The Bear Valley accumulated to thicknesses of as much as 300 meters in parts of the northern Markagunt Plateau. Like the Buckskin Breccia, it is thickest along fault scarps and in grabens of west-northwest faults (Anderson, 1971, 2001). The Bear Valley is overlain by great thicknesses of volcanic mudflow breccia of the Mount Dutton Formation.
3.5	230.8	**STOP NO. 15**, BUCKSKIN BRECCIA. At the base of the ledge on the right, Wah Wah Springs Formation is overlain by Isom

161

Formation and in turn by Buckskin Breccia. Look at the unique ash-flow tuff of the Buckskin Breccia, which contains lithic clasts of the Spry Intrusion. These ash-flow tuffs, all 50 meters or less thick, are in turn overlain by thick masses of volcanic mudflow breccia of the Mount Dutton Formation (Anderson and Rowley, 1987). Then enter Bear Valley, a north-northeast trending graben. CONTINUE WEST ON SR-20.

3.6   234.4   **OPTIONAL STOP**, BEAR VALLEY. PULL OVER ON RIGHT, THEN WALK BACK TO AN OVERLOOK OF BEAR VALLEY. Discuss the origin of the northern Markagunt Plateau. CONTINUE WEST ON SR-20. From here, most of the outcrops are of the Mount Dutton Formation.

2.7   237.1   Enter Buckskin Valley, another north-northeast-trending graben (Anderson, 1965).

1.0   238.1   In the middle of Buckskin Valley, look right to see the high Tushar Mountains on the horizon; the white peaks are rhyolite intracaldera fill in the Mount Belknap caldera. The generally south-facing scarp between this range and the lower northern Markagunt Plateau is apparent.

6.9   245.0   In Parowan Valley, TURN LEFT (SOUTH) ONTO ENTRANCE RAMP TO I-15. RETRACE OUR ROUTE TO THE MIDDLE CEDAR CITY EXIT (EXIT 59), THEN TO THE PARKING LOT WEST OF ECCLES COLISEUM.

36.5   281.5   TURN INTO PARKING LOT WEST OF ECCLES COLISEUM. END OF FIELD TRIP.

REFERENCES

Anderson, J.J., 1965, Geology of northern Markagunt Plateau, Utah: Austin, unpublished Ph.D. thesis, University of Texas, 194 p.

_____, 1971, Geology of the southwestern High Plateaus of Utah—Bear Valley Formation, an Oligocene-Miocene volcanic arenite: Geological Society of America Bulletin, v. 82, p. 1179-1205.

_____, 1993, The Markagunt Megabreccia—Large Miocene gravity slides mantling the northern Markagunt Plateau, southwestern Utah: Utah Geological Survey Miscellaneous Publication 93-2, 37 p.

_____, 2001, Late Oligocene-early Miocene normal faulting along west-northwest strikes, northern Markagunt Plateau, Utah, *in* Erskine, M.C., Faulds, J.E., Bartley, J.M., and Rowley, P.D., eds., The geologic transition, High Plateaus to Great Basin—A symposium and field guide (The Mackin Volume): Utah Geological Association and Pacific Section of the American Association of Petroleum Geologists: Utah Geological Association Publication 30, p. 97-112.

Anderson, J.J., and Rowley, P.D., 1975, Cenozoic stratigraphy of the southwestern High Plateaus of Utah, *in* Anderson, J.J., Rowley, P.D., Fleck, R.J., and Nairn, A.E.M., Cenozoic geology of southwestern High Plateaus of Utah: Geological Society of America Special Paper 160, p. 1-52.

_____, 1987, Geologic map of the Panguitch NW quadrangle, Iron and Garfield Counties, Utah: Utah Geological and Mineral Survey Map 103, scale 1:24,000.

_____, 2002, The Oligocene Isom Formation, Utah-Nevada—A regional ash-flow tuff sheet containing fluidal features of a lava flow: Geological Society of America Abstracts with Programs, v. 34, no. 5, in press.

Anderson, J.J., Rowley, P.D., Machette, M.N., Decatur, S.H., and Mehnert, H.H., 1990a, Geologic map of the Nevershine Hollow area, eastern Black Mountains, southern Tushar Mountains, and northern Markagunt Plateau, Beaver and Iron Counties, Utah: U.S. Geological Survey Miscellaneous Investigations Series Map I-1999, scale 1:50,000.

Anderson, J.J., Rowley, P.D., Blackman, J.T., Mehnert, H.H., and Grant, T.C., 1990b, Geologic map of the Circleville Canyon area, southern Tushar Mountains and northern Markagunt Plateau, Beaver, Garfield, Iron, and Piute Counties, Utah: U.S. Geological Survey Miscellaneous Investigations Series Map I-2000, scale 1:50,000.

Anderson, R.E., 1989, Tectonic evolution of the Intermontane System, Basin and Range, Colorado Plateau, and High Lava Plains, Chapter 10, in Pakiser, L.C., and Mooney, W.D., eds., Geophysical framework of the continental United States: Geological Society of America Memoir 172, p. 163-176.

Anderson, R.E., and Barnhard, T.P., 1992, Neotectonic framework of the central Sevier Valley area, Utah, and its relationship to seismicity, in Gori, P.L., and Hays, W.W., eds., Assessment of regional earthquake hazards and risk along the Wasatch front, Utah: U.S. Geological Survey Professional Paper 1500-F, 47 p.

_____, 1993, Aspects of three-dimensional strain at the margin of the extensional orogen, Virgin River depression area, Nevada, Utah, and Arizona: Geological Association of America Bulletin, v. 105, p. 1019-1052.

Anderson, R.E., and Mehnert, H.H., 1979, Reinterpretation of the history of the Hurricane fault in Utah, in Newman, G.W., and Goode, H.D., eds., Basin and Range symposium: Rocky Mountain Association of Geologists and Utah Geological Association, p. 145-165.

Anderson, R.E., Barnhard, T.P., and Snee, L.W., 1994, Roles of plutonism, mid-crustal flow, tectonic rafting, and horizontal collapse in shaping the Miocene strain field of the Lake Mead area, Nevada and Arizona: Tectonics, v. 13, p. 1381-1410.

Anderson, R.E., Bucknam, R.C., and Hamblin, Kenneth, 1978, Road log to the Quaternary tectonics of the intermountain seismic belt between Provo and Cedar City, Utah: Geological Society of America Rocky Mountain Section Annual Meeting Field Trip #8, 50 p.

Anderson, R.E., Zoback, M.L., and Thompson, G.A., 1983, Implications of selected subsurface data on the structural form and evolution of some basins in the northern Basin and Range Province, Nevada and Utah: Geological Society of America Bulletin, v. 94, p. 1055-1072.

Averitt, Paul, 1967, Geologic map of the Kanarraville quadrangle, Iron County, Utah: U.S. Geological Survey Geologic Quadrangle Map GQ-694, scale 1;24,000.

Averitt, Paul, and Threet, R.L., 1973, Geologic map of the Cedar City quadrangle, Iron County, Utah: U.S. Geological Survey Geologic Quadrangle Map GQ-1120, scale 1:24,000.

Barker, D.S., 1995, Crystallization and alteration of quartz monzonite, Iron Springs mining district, Utah—Relation to associated iron deposits: Economic Geology, v. 90, p. 2197-2217.

Beaty, D.W., Cunningham, C.G., Rye, R.O., Steven, T.A., and Gonzalez-Urien, Eliseo, 1986, Geology and geochemistry of the Deer Trail Pb-Zn-Ag-Cu manto deposits, Marysvale district, west-central Utah: Economic Geology, v. 81, p. 1932-1952.

Best, M.G., McKee, E.H., and Damon, P.E., 1980, Space-time-composition patterns of late Cenozoic mafic volcanism, southwestern Utah and adjoining areas: American Journal of Science, v. 280, p. 1035-1050.

Best, M.G., Christiansen, E.H., and Blank, R.H., Jr., 1989a, Oligocene caldera complex and calc-alkaline tuffs and lavas of the Indian Peak volcanic field, Nevada and Utah: Geological Society of America Bulletin, v. 101, p. 1076-1090.

Best, M.G., Christiansen, E.H., Deino, A.L., Gromme, C.S., McKee, E.H., and Noble, D.C., 1989b, Excursion 3A—Eocene through Miocene volcanism in the Great Basin of the western United States: New Mexico Bureau of Mines and Mineral Resources Memoir 47, p. 91-133.

Blackett, R.E., and Moore, J.N., editors, 1994, Cenozoic geology and geothermal systems of southwestern Utah: Utah Geological Association Publication 23, 215 p.

163

Blank, H.R., and Kucks, R.P., 1989, Preliminary aeromagnetic, gravity, and generalized geologic maps of the USGS Basin and Range-Colorado Plateau transition zone study area in southwestern Utah, southeastern Nevada, and northwestern Arizona (the "BARCO" project): U.S. Geological Survey Open-File Report 89-432, 16 p.

Blank, H.R., Jr., and Mackin, J.H., 1967, Geologic interpretation of an aeromagnetic survey of the Iron Springs district, Utah: U.S. Geological Survey Professional Paper 516-B, 14 p.

Blank, H.R., Rowley, P.D, and Hacker, D.B., 1992, Miocene monzonite intrusions and associated megabreccias of the Iron Axis region, southwestern Utah, *in* Wilson, J.R., ed., Field guide to geologic excursions in Utah and adjacent areas of Nevada, Idaho, and Wyoming: Geological Society of America, Rocky Mountain section meeting: Utah Geological Survey Miscellaneous Publication 92-3, p. 399-420.

Budding, K.E., Cunningham, C.G., Zielinski, R.A., Steven, T.A., and Stern, C.R., 1987, Petrology and chemistry of the Joe Lott Tuff Member of the Mount Belknap Volcanics, Marysvale volcanic field, west-central Utah: U.S. Geological Survey Professional Paper 1354, 47 p.

Callaghan, Eugene, 1939, Volcanic sequence in the Marysvale region in southwest-central Utah: American Geophysical Union Transactions, 20th Annual Meeting, Washington, D.C., pt. 3, p. 438-452.

Campbell, D.L., Steven, T.A., Cunningham, C.G., and Rowley, P.D., 1999, Interpretation of aeromagnetic and gravity maps of the central Marysvale volcanic field, southwestern Utah: U.S. Geological Survey Investigation Series Map I-2645-B, scale 1:100,000.

Christiansen, R.L., and Lipman, P.W., 1972, Cenozoic volcanism and plate tectonic evolution of the western United States—II. Late Cenozoic: Royal Society of London Philosophical Transactions (A), v. 271, p. 249-284.

Christiansen, R.L., and Yeats, R.S., 1992, Post-Laramide geology of the U.S. Cordilleran region, *in* Burchfiel, B.C., Lipman, P.W., and Zoback, M.L., eds., The Cordilleran orogen—Conterminous U.S.: Boulder, Colorado, Geological Society of America, Geology of North America, v. G-3, p. 261-406.

Coleman, D.S., and Walker, J.D., 1992, Evidence for the generation of juvenile granitic crust during continental extension, Mineral Mountains batholith, Utah: Journal of Geophysical Research, v. 97, no. B7, p. 11,011-11,024.

Coleman, D.S., Walker, J.D., Bartley, J.M., and Hodges, K.V., 2001, Thermochronologic evidence for footwall deformation during extensional core complex development, Mineral Mountains, Utah, *in* Erskine, M.C., Faulds, J.E., Bartley, J.M., and Rowley, P.D., eds., The geologic transition, High Plateaus to Great Basin—A symposium and field guide (The Mackin Volume): Utah Geological Association and Pacific Section of the American Association of Petroleum Geologists: Utah Geological Association Publication 30, p. 155-168.

Cook, K.L., and Hardman, Elwood, 1967, Regional gravity survey of the Hurricane fault area and Iron Springs district, Utah: Geological Society of America Bulletin, v. 78, p. 1063-1076.

Cunningham, C.G., and Steven, T.A., 1979a, Mount Belknap and Red Hills calderas and associated rocks, Marysvale volcanic field, west-central Utah: U.S. Geological Survey Bulletin, 1468, 34 p.

_____, 1979b, Uranium in the Central Mining Area, Marysvale district, west central Utah: U.S. Geological Survey Miscellaneous Investigations Series Map I-1177, scale 1:24,000.

_____, 1979c, Geologic map of the Deer Trail Mountain--Alunite Ridge mining area, west-central Utah: U.S. Geological Survey Miscellaneous Investigations Series Map I-1230, scale 1:24,000.

Cunningham, C.G., Ludwig, K.R., Naeser, C.W., Weiland, E.K., Mehnert, H.H., Steven, T.A., and Rasmussen, J.D., 1982, Geochronology of hydrothermal uranium deposits and associated igneous rocks in the eastern source area of the Mount Belknap Volcanics, Marysvale, Utah: Economic Geology, v. 77, no. 2, p. 453-463.

Cunningham, C.G., Rasmussen, J.D., Steven, T.A., Rye, R.O., Rowley, P.D., Romberger, S.B., and Selverstone, Jane, 1998b, Hydrothermal uranium deposits containing molybdenum and fluorite in the Marysvale volcanic field, west-central Utah: Mineralium Deposita, v. 33, p. 477-494.

_____, 1999, Reply to the comment by Chuck Spirakis on "Hydrothermal uranium deposits containing molybdenum and fluorite in the Marysvale volcanic field, west-central Utah": Mineralium Deposita, v. 34, p. 725-726.

Cunningham, C.G., Rye, R.O., Steven, T.A., and Mehnert, H.H., 1984a, Origins and exploration significance of replacement and vein-type alunite deposits in the Marysvale volcanic field, west-central Utah: Economic Geology, v. 79, p. 50-71.

Cunningham, C.G., Steven, T.A., Campbell, D.L., Naeser, C.W., Pitkin, J.A., and Duval, J.S., 1984c, Multiple episodes of igneous activity, mineralization, and alteration in the western Tushar Mountains, Marysvale volcanic field, west-central Utah, *in* Steven, T.A., ed., Igneous activity and related ore deposits in the western and southern Tushar Mountains, Marysvale volcanic field, west-central Utah: U.S. Geological Survey Professional Paper 1299-A, 22 p.

Cunningham, C.G., Steven, T.A., and Rowley, P.D., 2002, Volcanic rocks and ore deposits of the Marysvale volcanic field, west-central Utah [abs.]: Geological Society of America Abstracts with Programs, v. 34, no. 5, in press.

Cunningham, C.G., Steven, T.A., Rowley, P.D., Glassgold, L.B., and Anderson, J.J., 1983, Geologic map of the Tushar Mountains and adjoining areas, Marysvale volcanic field, Utah: U.S. Geological Survey Miscellaneous Investigations Series Map I-1430-A, scale 1:50,000.

_____, 1984b, Map of argillic and advanced argillic alteration and principal hydrothermal quartz and alunite veins in the Tushar Mountains and adjoining areas, Marysvale volcanic field, Utah: U.S. Geological Survey Miscellaneous Investigations Series Map I-1430-B, scale 1:50,000.

Cunningham, C.G., Steven, T.A., Rowley, P.D., Naeser, C.W., Mehnert, H.H., Hedge, C.E., and Ludwig, K.R., 1994, Evolution of volcanic rocks and associated ore deposits in the Marysvale volcanic field, Utah: Economic Geology, v. 89, p. 2003-2005.

Cunningham, C.G., Unruh, D. M., Steven, T.A., Rowley, P.D., Naeser, C.W., Mehnert, H.H., Hedge, C.E., and Ludwig, K.R., 1998a, Geochemistry of volcanic rocks in the Marysvale volcanic field, west-central Utah, *in* Friedman, J.D., and Huffman, A.C., Jr., coordinators, Laccolith complexes of southeastern Utah—Time of emplacement and tectonic setting— Workshop proceedings: U.S. Geological Survey Bulletin 2158, p. 223-232.

Davis, G.H., and Pollock, G.L., 2000, Geology of Bryce Canyon National Park, Utah, *in* Sprinkel, D.A., Chidsey, T.C., Jr., and Anderson, P.B., eds., Geology of Utah's parks and monuments: Utah Geological Association Publication 28, p. 37-60.

Eaton, G.P., Wahl, R.R., Prostka, H.J., Mabey, D.R., and Kleinkopf, M.D., 1978, Regional gravity and tectonic patterns—their relation to late Cenozoic epeirogeny and lateral spreading in the western Cordillera, *in* Smith, R.B., and Eaton, G.P., eds., Cenozoic tectonics and regional geophysics of the western Cordillera: Geological Society of America Memoir, v. 152, p.51-91.

Ekren, E.B., Bucknam, R.C., Carr, W.J., Dixon, G.L., and Quinlivan, W.D., 1976, East-trending structural lineaments in central Nevada: U.S. Geological Survey Professional Paper 986, 16 p.

Ekren, E.B., McIntyre, D.H., and Bennett, E.H., 1984, High-temperature, large-volume, lavalike ash-flow tuffs without calderas in southwestern Idaho: U.S. Geological Survey Professional Paper 1272, 76 p.

Evans, S.H., Jr., and Steven, T.A., 1982, Rhyolites in the Gillies Hill-Woodtick Hill area, Beaver County, Utah: Geological Society of America Bulletin, v. 93, p. 1131-1141.

Fleck, R.J., Anderson, J.J., and Rowley, P.D., 1975, Chronology of mid-Tertiary volcanism in High Plateaus region of Utah, *in* Anderson, J.J., Rowley, P.D., Fleck, R.J., and Nairn, A.E.M., Cenozoic geology of southwestern High Plateaus of Utah: Geological Society of America Special Paper 160, p. 53-62.

Gilbert, G.K., 1928, Basin range faulting along the Oquirrh Range, Utah: Geological Society of America Bulletin, v. 39, p. 1103-1130.

Hacker, D.B., 1998, Catastrophic gravity sliding and volcanism associated with the growth of laccoliths—examples from early Miocene hypabyssal intrusions of the Iron Axis magmatic

province, Pine Valley Mountains, southwest Utah: Kent, Ohio, Kent State University, unpublished Ph.D. dissertation, 258 p.

Hacker, D.B., and Holm, D.K., 2002, Associated Miocene laccoliths, gravity slides, and volcanic rocks, Pine Valley Mountains and Iron Axis, southwestern Utah, *in* Lund, W.R., ed., Geological Society of America 2002 Rocky Mountain Section Annual Meeting, Field Trips, Cedar City, Utah: U.S. Geological Survey Open-Filer Report 02- , in press.

Hamilton, W.B., 1989, Crustal geologic processes of the United States, *in* Pakiser, L.C., and Mooney, W.D., eds., Geophysical framework of the continental United States: Geological Society of America Memoir 172, p. 743-781.

_____, 1995, Subduction systems and magmatism, *in* Smellie, J.L., ed., Volcanism associated with extension of consuming plate margins: Geological Society Special Publication 81, p. 3-28.

Hamilton, Warren, and Myers, W.B., 1966, Cenozoic tectonics of the Western United States: Reviews of Geophysics, v. 4, p. 509-549.

Hatfield, S.C., Rowley, P.D., Sable, E.G., Maxwell, D.J., Cox, B.V., McKell, M.D., and Kiel, D.E., 2000, Geology of Cedar Breaks National Monument, Utah, *in* Sprinkel, D.A., Chidsey, T.C., Jr., and Anderson, P.B., eds., Geology of Utah's parks and monuments: Utah Geological Association Publication 28, p. 139-154.

Herring, D.F., 1989, Kimberly, Utah—From lode to dust: Eugene, Oregon, Herring Publishers, 106 p.

Kerr, P.F., Brophy, G.P., Dahl, H.M., Green, Jack, and Woolard, L.E., 1957, Marysvale, Utah, uranium area--Geology, volcanic relations, and hydrothermal alteration: Geological Society of America Special Paper 64, 212 p.

Kowallis, B.J., and Best, M.G., 1990, Fission track ages from volcanic rocks in southwestern Utah and southeastern Nevada: Isochron/West, no. 55, p. 24-27.

Lindgren, Waldemar, 1906, The Annie Laurie mine, Piute County, Utah: U.S. Geological Survey Bulletin 285, p. 87-90.

Lipman, P.W., Prostka, H.J., and Christiansen, R.L., 1972, Cenozoic volcanism and evolution of the western United States—I. Early and middle Cenozoic: Royal Society of London, Philosophical Transactions (A), v. 271, p. 217-248.

Lipman, P.W., Rowley, P.D., Mehnert, H.H., Evans, S.H., Jr., Nash, W.P., and Brown, F.H., 1978, Pleistocene rhyolite of the Mineral Mountains, Utah—Geothermal and archeological significance, *with sections on* Fission-track dating, by G.A. Izett and C.W. Naeser, *and on* Obsidian-hydration dating, by Irving Friedman: U.S. Geological Survey Journal of Research, v. 6, no. 1, p. 133-147.

Lucchitta, Ivo, 1990, Role of heat and detachment in continental extension as viewed from the eastern Basin and Range Province in Arizona: Tectonophysics, v. 174, p. 77-114.

Machette, M.N., 1985, Late Cenozoic geology of the Beaver basin, southwestern Utah: Brigham Young University Studies in Geology, v. 32, pt. 1, p. 19-37.

Machette, M.N., Steven, T.A., Cunningham, C.G., and Anderson, J.J., 1984, Geologic map of the Beaver quadrangle, Beaver and Piute Counties, Utah: U.S. Geological Survey Miscellaneous Investigations Series Map I-1520, scale 1:50,000.

Mackin, J.H., 1947, Some structural features of the intrusions in the Iron Springs district: Utah Geological Society Guidebook 2, 62 p.

_____, 1960, Structural significance of Tertiary volcanic rocks in southwestern Utah: American Journal of Science, v. 258, no. 2, p. 81-131.

_____, 1968, Iron ore deposits of the Iron Springs district, southwestern Utah, *in* Ridge, J.D., ed., Ore deposits of the United States, 1933-1967 (Graton-Sales volume): New York, American Institute of Mining and Metallurgical Petroleum Engineers, v. 2, p. 992-1019.

Mackin, J.H., and Rowley, P.D., 1976, Geologic map of The Three Peaks quadrangle, Iron County, Utah: U.S. Geological Survey Geologic Quadrangle Map GQ-1297, scale 1:24,000.

Mackin, J.H., Nelson, W.H., and Rowley, P.D., 1976, Geologic map of the Cedar City NW quadrangle, Iron County, Utah: U.S. Geological Survey Geologic Quadrangle Map GQ-1295, scale 1:24,000.

Maldonado, Florian, and Moore, R.C., 1995, Geologic map of the Parowan quadrangle, Iron County, Utah: U.S. Geological Survey Geologic Quadrangle Map GQ-1762, scale 1:24.000.

Maldonado, Florian, and Williams, V.S., 1993a, Geologic map of the Parowan Gap quadrangle, Iron County, Utah: U.S. Geological Survey Geologic Quadrangle Map GQ-1712, scale 1:24,000.

_____, 1993b, Geologic map of the Paragonah quadrangle, Iron County, Utah: U.S. Geological Survey Geologic Quadrangle Map GQ-1713, scale 1:24,000.

Mattox, S.R., 1991a, Origin of potassium-rich mafic lava flows, Marysvale volcanic field, Utah [abs.]: Eos (American Geophysical Union) Program and Abstracts, v. 72, no. 44, p. 561.

Mattox, S.R., 1991b, Petrology, age, geochemistry, and correlation of the Tertiary volcanic rocks of the Awapa Plateau, Garfield, Piute, and Wayne Counties, Utah: Utah Geological Survey Miscellaneous Publication 91-5, 46 p.

Mattox, S.R., 1992, Geochemistry, origin, and tectonic implications of mid-Tertiary and late Tertiary and Quaternary volcanic rocks, southern Marysvale volcanic field, Utah: DeKalb, Illinois, Northern Illinois University, Ph.D. dissertation, 502 p.

Nielson, D.L., Evans, S.H., Jr., and Sibbett, B.S., 1986, Magmatic, structural, and hydrothermal evolution of the Mineral Mountains intrusive complex, Utah: Geological Society of America Bulletin, v. 97, p. 765-777.

Parsons, T., 1995, The Basin and Range Province, chapter 7, in Olsen, K.H., ed., Continental rifts—evolution, structure, tectonics: Developments in geotectonics 25, Amsterdam, Elsevier, p. 277-324.

Parsons, T., Thompson, G.A., and Sleep, N.H., 1994, Mantle plume influence on the Neogene uplift and extension of the U.S. western cordillera: Geology, v. 22, no. 1, p. 83-86.

Parsons, W.H., 1969, Criteria for the recognition of volcanic breccia--Review, in Igneous and metamorphic geology (Poldervaart volume): Geological Society of America Memoir 115, p. 263-304.

Pierce, K.L., and Morgan, L.A., 1992, The track of the Yellowstone hot spot—volcanism, faulting, and uplift, in Link, P.K., Kuntz, M.A., and Platt, L.B., ed., Regional geology of eastern Idaho and western Wyoming: Geological Society of America Memoir 179, p. 1-53.

Podwysocki, M.H., and Segal, D.B., 1983, Mapping of hydrothermally altered rocks using air-borne multispectral data, Marysvale, Utah, mining district: Economic Geology, v. 78, p. 675-687.

Price, D.E., and Bartley, J.M., 1992, Three-dimensional extensional structure of the southern Mineral Mountains, southwestern Utah [abs.]: Geological Society of America Abstracts with Programs, v. 24, no. 6, p. 58.

Rockwell, B.W., Cunningham, C.G., Clark, R.N., Sutley, S.J., Gent, C.A., and Rowley, P.D., 2002, Mapping of Miocene hydrothermal systems in the Marysvale volcanic field, west-central Utah, using AVIRIS high-resolution remote sensing data [abs.]: Geological Society of Americ Abstracts with Programs, v. 34, no. 5, in press.

Rowley, P.D., 1968, Geology of the southern Sevier Plateau, Utah: Austin, unpublished Ph.D. thesis, University of Texas, 385 p.

_____, 1998, Cenozoic transverse zones and igneous belts in the Great Basin, western United States--Their tectonic and economic implications, in Faulds, J.E., and Stewart, J.H., eds, Accommodation zones and transfer zones--The regional segmentation of the Basin and Range Province: Geological Society of America Special Paper 323, p. 195-228.

Rowley, P.D., and Barker, D.S., 1978, Geology of the Iron Springs mining district, Utah: Geological Association of Utah Publication 7, Guidebook to mineral deposits of southwestern Utah, p. 49-58.

Rowley, P.D., and Dixon, G.L., 2001, The Cenozoic evolution of the Great Basin area, U.S.A.—New interpretations based on regional geologic mapping, in Erskine, M.C., Faulds, J.E., Bartley, J.M., and Rowley, P.D., eds., The geologic transition, High Plateaus to Great Basin—A symposium and field guide (The Mackin Volume): Utah Geological Association and Pacific Section of the American Association of Petroleum Geologists: Utah Geological Association Publication 30, p. 169-188.

Rowley, P.D., and Threet, R.L., 1976, Geologic map of the Enoch quadrangle, Iron County, Utah: U.S. Geological Survey Geologic Quadrangle Map GQ-1296, scale 1:24,000.

Rowley, P.D., Cunningham, C.G., Steven, T.A., Mehnert, H.H., and Naeser, C.W., 1988a, Geologic map of the Marysvale quadrangle, Piute County, Utah: Utah Geological and Mineral Survey Map 105, scale 1:24,000.

_____, 1988b, Geologic map of the Antelope Range quadrangle, Sevier and Piute Counties, Utah: Utah Geological and Mineral Survey Map 106, scale 1:24,000.

_____, 1998, Cenozoic igneous and tectonic setting of the Marysvale volcanic field, and its relation to other igneous centers in Utah and Nevada, *in* Friedman, J.D., and Huffman, A.C., Jr., coordinators, Laccolith complexes of southeastern Utah—Time of emplacement and tectonic setting—Workshop proceedings: U.S. Geological Survey Bulletin 2158, p. 167-202.

Rowley, P.D., Cunningham, C.G., Steven, T.A., Workman, J.B., Anderson, J.J., and Theissen, K.M., 2001a, Geologic map of the central Marysvale volcanic field, southwestern Utah: U.S. Geological Survey Investigation Series Map I-2645-A, scale 1:100,000, in press.

Rowley, P.D., Snee, L.W., Anderson, R.E., Nealey, L.D., Unruh, D.M., and Ferris, D.E., 2001b, Field trip to the Caliente caldera complex, east-striking transverse zones, and nearby mining districts in Nevada-Utah--Implications for petroleum, ground-water, and mineral resources, *in* Erskine, M.C., Faulds, J.E., Bartley, J.M., and Rowley, P.D., eds., The geologic transition, High Plateaus to Great Basin—A symposium and field guide (The Mackin Volume): Utah Geological Association and Pacific Section of the American Association of Petroleum Geologists: Utah Geological Association Publication 30, p. 401-418.

Rowley, P.D., Lipman, P.W., Mehnert, H.H., Lindsey, D.A., and Anderson, J.J., 1978, Blue Ribbon lineament, an east-trending structural zone within the Pioche mineral belt of southwestern Utah and eastern Nevada: U.S. Geological Survey Journal of Research, v. 6, no. 2, p. 175-192.

Rowley, P.D., Mehnert, H.H., Naeser, C.W., Snee, L.W., Cunningham, C.G., Steven, T.A., Anderson, J.J., Sable, E.G., and Anderson, R.E., 1994, Isotopic ages and stratigraphy of Cenozoic rocks of the Marysvale volcanic field and adjacent areas, west-central Utah: U.S. Geological Survey Bulletin 2071, 35 p.

Rowley, P.D., Steven, T.A., and Mehnert, H.H., 1981, Origin and structural implications of upper Miocene rhyolites in Kingston Canyon, Piute County, Utah: Geological Society of America Bulletin, pt. I, v. 92, p. 590-602.

Rowley, P.D., Steven, T.A., Anderson, J.J., and Cunningham, C.G., 1979, Cenozoic stratigraphic and structural framework of southwestern Utah: U.S. Geological Survey Professional Paper 1149, 22 p.

Rowley, P.D., Williams, P.L., and Kaplan, A.M., 1986a, Geologic map of the Greenwich quadrangle, Piute County, Utah: U.S. Geological Survey Geologic Quadrangle Map GQ-1589, scale 1:24,000.

_____, 1986b, Geologic map of the Koosharem quadrangle, Sevier and Piute Counties, Utah: U.S. Geological Survey Geologic Quadrangle Map GQ-1590, scale 1:24,000.

Sable, E.G., and Maldonado, Florian, 1997, The Brian Head Formation (revised) and selected Tertiary sedimentary rock units, Markagunt Plateau and adjacent areas, southwestern Utah, *in* Maldonado, Florian, and Nealey, L.D., eds., Geologic studies in the Basin and Range-Colorado Plateau transition in southeastern Nevada, southwestern Utah, and northwestern Arizona, 1995: U.S. Geological Survey Bulletin 2153, p. 5-26.

Saltus, R.W., and Thompson, G.A., 1995, Why is it downhill from Tonopah to Las Vegas?—a case for mantle plume support of the high northern Basin and Range: Tectonics, v. 14, p. 1235-1244.

Severinghaus, J., and Atwater, T., 1990, Cenozoic geometry and thermal state of the subducting slabs beneath western North America, *in* Wernicke, B.P., ed., Basin and Range extensional tectonics near the latitude of Las Vegas, Nevada: Geological Society of America Memoir 176, p. 1-22.

Smedes, H.W., and Prostka, H.J., 1973, Stratigraphic framework of the Absaroka Volcanic Supergroup in the Yellowstone National Park region: U.S. Geological Survey Professional Paper 729-C, 33 p.

Steven, T.A., 1981, Three Creeks caldera, southern Pavant Range, Utah: Brigham Young University Geology Studies, v. 28, part 3, p. 1-7.

Steven, T.A., Cunningham, C.G., and Anderson, J.J., 1984b, Geologic history and uranium potential of the Big John caldera, southern Tushar Mountains, Utah, *in* Steven, T.A., ed., Igneous activity and related ore deposits in the western and southern Tushar Mountains, Marysvale volcanic field, west-central Utah: U.S. Geological Survey Professional Paper 1299-B, 33 p.

Steven, T.A., Cunningham, C.G., and Machette, M.N., 1981, Integrated uranium systems in the Marysvale volcanic field, west-central Utah, *in* Goodell, P.C., and Waters, A.C., ed., Uranium in volcanic and volcaniclastic rocks: American Association of Petroleum Geologists Studies in Geology, no. 13, p. 111-122.

Steven, T.A., Cunningham, C.G., Naeser, C.W., and Mehnert, H.H., 1979, Revised stratigraphy and radiometric ages of volcanic rocks and mineral deposits in the Marysvale area, west-central Utah: U.S. Geological Survey Bulletin 1469, 40 p.

Steven, T.A., and Morris, H.T., 1983, Geologic map of the Cove Fort quadrangle, west-central Utah: U.S. Geological Survey Miscellaneous Investigations Map I-1481, scale 1:50,000.

_____, 1987, Summary mineral resource appraisal of the Richfield 1° x 2° quadrangle, west-central Utah: U.S. Geological Survey Circular 916, 24 p.

Steven, T.A., Morris, H.T., and Rowley, P.D., 1990, Geologic map of the Richfield 1° x 2° quadrangle, west-central Utah: U.S. Geological Survey Miscellaneous Investigations Series Map I-1901, scale 1:250,000.

Steven, T.A., Rowley, P.D., and Cunningham, C.G., 1984a, Calderas of the Marysvale volcanic field, west central Utah: Journal of Geophysical Research, v. 89, no. B10, p. 8751-8764.

Thompson, G.A., 1998, Deep mantle plumes and geoscience vision: GSA Today, v. 8, no. 4, p. 17-25.

Threet, R.L., 1952, Geology of the Red Hills area, Iron County, Utah: Seattle, unpublished Ph.D. thesis, University of Washington, 107 p.

_____, 1963, Geology of the Parowan Gap area, Iron County, Utah, *in* Intermountain Association of Petroleum Geologists Guidebook, 12th Annual Field Conference, Geology of Southwestern Utah, 1963: Utah Geological and Mineralogical Survey, p. 136-145.

Utley, M.G., 1992, The ghosts of Gold Mountain—A history of the Gold Mountain mining district, Piute County, Utah: Sevier, Utah, M.G. Utley, 272 p.

Van Kooten, G.K., 1988, Structure and hydrocarbon potential beneath the Iron Springs laccolith, southwestern Utah: Geological Society of America Bulletin, v. 100, p. 1533-1540.

Wernicke, Brian, 1992, Cenozoic extensional tectonics of the U.S. Cordillera, *in* Burchfiel, B.C., Lipman, P.W., and Zoback, M.L., eds., The Cordilleran orogen—Conterminous U.S., The geology of North America: Geological Society of America, Vol. G-3, p. 553-581.

Williams, P.L., 1967, Stratigraphy and petrography of the Quichapa Group, southwestern Utah and southeastern Nevada: Seattle, University of Washington, Ph.D. dissertation, 182 p.

Williams, P.L., and Hackman, R.J., 1971, Geology, structure, and uranium deposits of the Salina quadrangle, Utah: U.S. Geological Survey Miscellaneous Geologic Investigations Map I-591, scale 1:250,000.

Willis, G.C., 1985, Revisions to the geochronology and source areas of early Tertiary formations in the Salina area of Sevier Valley, central Utah [abs.]: Geological Society of America Abstracts with Programs, v. 17, no. 4, p. 272.

Zoback, M.L., Anderson, R.E., and Thompson, G.A., 1981, Cainozoic evolution of the state of stress and style of tectonism in the Basin and Range Province of the western United States: Royal Society of London Philosophical Transactions, v. A300, p. 407-434.

Zoback, M.L., McKee, E.H., Blakely, R.J., and Thompson, G.A., 1994, The northern Nevada rift—regional tectono-magmatic relations and the middle Miocene stress direction: Geological Society of America Bulletin, v. 16, p. 371-382.

View to the west southwest into the Mount Belknap caldera from a point on its eastern topographic wall. Mount Belknap (elev. 12,139 ft) is the peak on the right. The smooth slopes and cliffs reflect the eruptve sequence of ash flow tuffs and cliff forming rhyolite lava flows.

UPPER CRETACEOUS MARINE AND BRACKISH WATER STRATA AT GRAND STAIRCASE-ESCALANTE NATIONAL MONUMENT, UTAH GEOLOGICAL SOCIETY OF AMERICA FIELD TRIP ROAD LOG, MAY 2002

Slick Rock Bench. This view north toward Wiggler Wash shows steep dip of Entrada through Straight Cliffs Formations in Kaibab anticline. Canaan Peak and Table Cliff Plateau can be seen on the far horizon

T.S. Dyman[1], W.A. Cobban[1], L.E. Davis[3], R.L. Eves[4], G.L. Pollock[2] J.D. Obradovich[1], A.L. Titus[5], K.I. Takahashi [1], T.C. Hester[1], and D. Cantu[2]

[1]U.S. Geological Survey, Denver, CO 80225 (e-mail: dyman@usgs.gov)
[2]Bryce Canyon National History Association, Bryce Canyon, UT 84717
[3]St. Johns University, Collegeville, MN 56321
[4]Southern Utah University, Cedar City, UT 84720
[5]Grand Staircase-Escalante National Monument, Kanab, UT 84741

UPPER CRETACEOUS MARINE AND BRACKISH WATER STRATA AT GRAND STAIRCASE-ESCALANTE NATIONAL MONUMENT, UTAH
GEOLOGICAL SOCIETY OF AMERICA FIELD TRIP ROAD LOG, MAY 2002

T.S. Dyman[1], W.A. Cobban[1], L.E. Davis[3], R.L. Eves[4], G.L. Pollock[2] J.D. Obradovich[1], A.L. Titus[5], K.I. Takahashi [1], T.C. Hester[1], and D. Cantu[2]

[1]U.S. Geological Survey, Denver, CO 80225 (e-mail: dyman@usgs.gov)
[2]Bryce Canyon National History Association, Bryce Canyon, UT 84717
[3]St. Johns University, Collegeville, MN 56321
[4]Southern Utah University, Cedar City, UT 84720
[5]Grand Staircase-Escalante National Monument, Kanab, UT 84741

INTRODUCTION

Mid-Cretaceous strata in southwestern Utah (figures 1 and 2) are transitional from shelf to nonmarine rocks in the foreland basin along the tectonically active western margin of the Western Interior basin. Predominantly nonmarine western sequences (Beaver Dam Mountains near Gunlock, Utah; Cedar Canyon near Cedar City, Utah; and at Parowan Gap near Parowan, Utah) are difficult to correlate with other rocks because they lack a representative suite of marine megafauna. Rocks in Grand Staircase-Escalante National Monument, are mostly marine, but have not been thoroughly sampled for datable fossils; thus correlations within the marine sequence are generally imprecise. Furthermore, correlations with key reference sections in the central part of the Western Interior basin are not well defined. Better correlations will help in establishing the timing of transgressive and regressive depositional events throughout the basin.

This field trip will familiarize geologists and non-geologists alike with the mid-Cretaceous sequence in Grand Staircase-Escalante National Monument, with emphasis on the fossiliferous marine units. We discuss the physical stratigraphy of key rock units, biostratigraphic correlations, and general environments of deposition. Characterization of the regional timing of transgressive and regressive stages of the Tropic sea will be made using new fossil collections of Cobban and others (2000) and Dyman and others (2000). We also include general explanations of other Mesozoic stratigraphic units along the field trip route. The field trip was designed as a one-day event in order to reduce participant costs and accommodate tight schedules. We have examined excellent marine sections farther to the east in the Monument, but have selected our stops as the best within existing logistical limitations.

Mid-Cretaceous strata in the Monument include the Cenomanian Dakota Formation, the Cenomanian to Turonian Tropic Shale, and the Turonian lower part of the Straight Cliffs Formation. At Tropic, Utah, and Cottonwood Wash, along the route of the trip, marine rocks associated with the Tropic transgression extend from near the upper part of the Dakota Formation through the Tibbet Canyon Member of the Straight Cliffs Formation (figure 2).
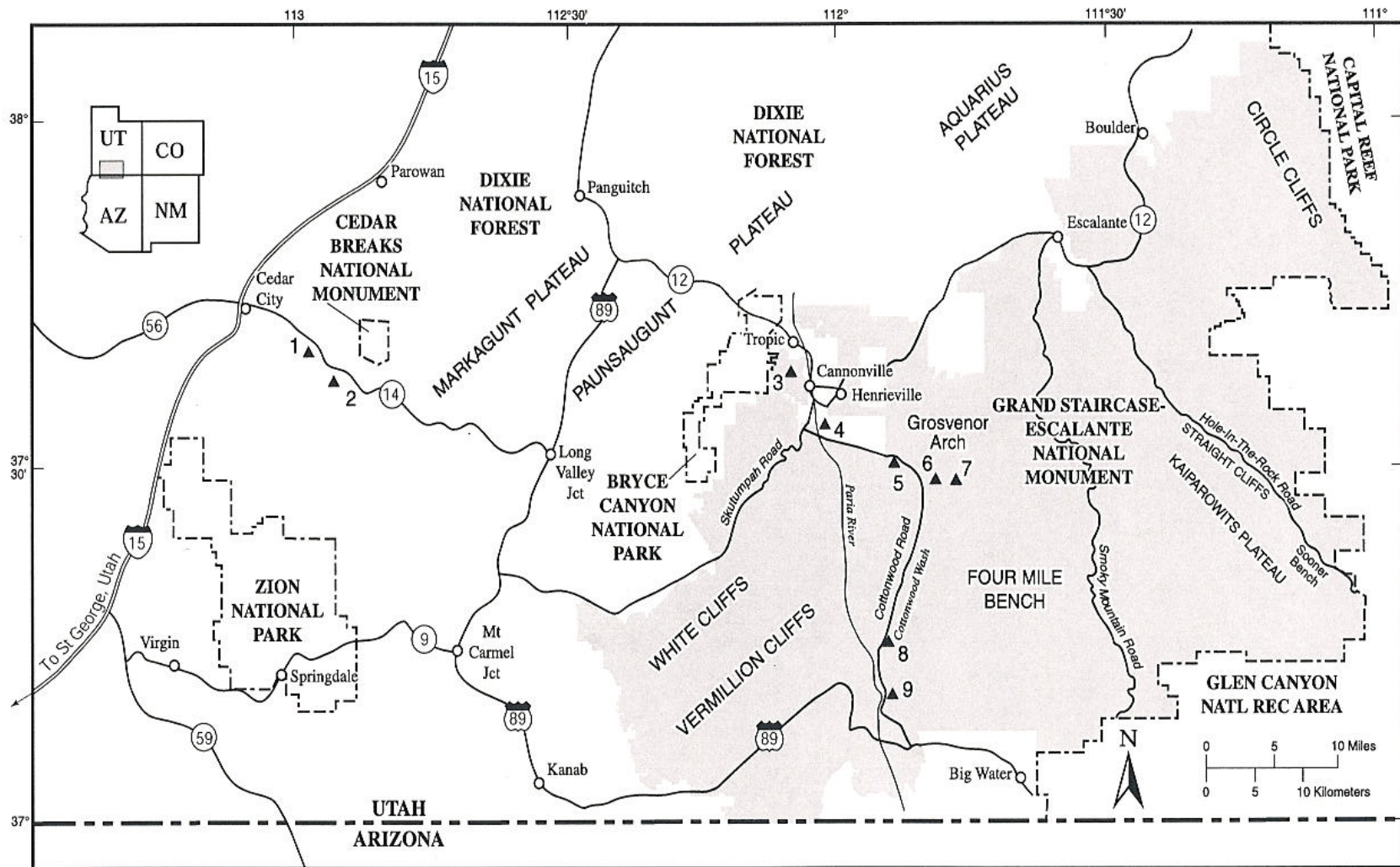
Figure 1. Index map of southwestern Utah, including the Cedar City area and Grand Staircase-Escalante National Monument, illustrating major geographic features, highways, and towns. Field trip stops 1-9 identified by numbered black triangles.

	STAGE	Cedar City, UT	Grand Staircase-Escalante Natl. Mon.	Capitol Reef National Park
UPPER CRETACEOUS (part)	Campanian (part)	Undifferentiated Straight Cliffs Formation	*Straight Cliffs Fm. (part):* Drip Tank Mbr. — John Henry Mbr. —Sh / —Cs — SH / Calico bed —Sv	*Mancos Shale (part):* Blue Gate Mbr. (part)
	Santonian			
	Coniacian			Ferron Ss. Mbr.
	Turonian	—Cw — Tropic Shale	TC — —Ph / Tropic Shale —Cw / —Es	Tununk Mbr.
	Cenomanian	Mk / Dakota Fm.	Dakota Fm. —Da	Dakota Fm.
LOWER CRET.	Albian (part)			Cedar Mt. Fm.

Figure 2. *Generalized stratigraphic correlation chart illustrating marine Cretaceous rock units of late Cenomanian through early Campanian age in Grand Staircase-Escalante National Monument, the Cedar City area, and the Capitol Reef National Park area. Hatchured pattern indicates unconformities. Abbreviations show the stratigraphic location of marine Cretaceous ammonite biozones, associated inoceramids, and stratigraphic units as follows: Cw, Collignoniceras woollgari; Cs, Clioscaphites vermiformis; Da, Dunveganoceras albertense; Es, Euomphaloceras septemseriatum; Ph, Prionocyclus hyatti; Sv, Scaphites ventricosus; SH, Smoky Hollow Member of Straight Cliffs Formation; TC, Tibbet Canyon Member of Straight Cliffs Formation.*

Farther east, near Escalante, Utah, marine rocks extend upward into the upper part (John Henry Member) of the Straight Cliffs Formation.

Fossil descriptions and supporting information for marine invertebrate collections from the Monument are available as a digital Microsoft EXCEL file in Dyman and others (2000) (Any use of trade, product, or firm names is for descriptive purposes only and does not imply endorsement by the U.S. Government). The fossil collections are stored at the U.S. Geological Survey in Denver, Colo. The authors wish to acknowledge Russell Tysdal and Carol Molnia, U.S. Geological Survey, Denver, Colo., and Bill Lund, Utah Geological Survey, Cedar City, Utah, for their critical reviews of the manuscript.

STRATIGRAPHY AND AGE

Figure 2 is a generalized correlation chart illustrating the stratigraphic position of Upper Cretaceous rocks in the Monument, adjacent to the eastern boundary of the Monument in Capitol Reef National Park, and in areas farther to the west in southwestern Utah. This chart presents a regional stratigraphic perspective. Within the Monument, as previously stated, marine rock units include the upper part of the Dakota Formation, the Tropic Shale, and the lower part of the Straight Cliffs Formation. At Capitol Reef National Park, marine rocks include most of the Dakota Formation and the overlying Mancos Shale Group. Figure 3 is a biostratigraphic chart showing Upper Cretaceous stages, formations and members in the Monument, informal stratigraphic units, Western Interior ammonite zones, and localities of biostratigraphically significant fossil collections from Cobban and others (2000) and Dyman and others (2000).

Dakota Formation

The upper part of the Dakota Formation contains the oldest marine rocks in the Monument. Near the town of Tropic (field trip stop 3), and southeastward at Grosvenor Arch and Cottonwood Wash (field trip stops 6, 8, 9), the Dakota is about 200-300 feet thick and is composed of sandstone, conglomerate, mudstone, siltstone, and coal. The Dakota thins in the eastern part of the Monument, where it averages less than 150 feet thick. The base of the Dakota consists of a coarse pebble and cobble conglomerate that persists throughout most of the region (figure 4). Clasts consist of quartzite, dark-gray chert, and various lithic fragments, including sandstone, conglomerate, and mudstone. Where the conglomerate is absent, the basal Dakota consists of carbonaceous mudstone, coal, and sandstone. The basal strata overlie a widespread regional unconformity above Jurassic rocks. The conglomeratic unit is time-equivalent to the Cedar Mountain Formation in central Utah (Doelling and others, 2000), based on an Early Cretaceous age of palynomorphs from interbedded siltstones.

The lower, middle, and upper parts of the Dakota contain several distinctive coally carbonaceous zones. Sandstones are generally fine to medium grained and lithic rich. The Dakota was deposited in coastal, floodplain, and shallow marine depositional environments at Cottonwood Wash. The Dakota Formation-Tropic Shale contact near the town of Tropic is sharp and marks an abrupt change in lithology from predominantly sandstone to shale.

The oldest marine fossils are in the uppermost beds of the Dakota, which are clearly of late Cenomanian age at the Monument (figure 3). Ammonites are scarce, but recent collecting has yielded specimens of *Dunveganoceras problematicum natronense*, *Dunveganoceras* cf. *D. albertense*, and *Metoicoceras* cf. *M. frontierense* from a channel-fill sandstone bed in the lower part of the upper sequence. *Inoceramus* cf. *I. prefragilis,* indicating the zone of *Calycoceras canitaurinum* (also ,zone of *Dunveganoceras pondi),* has also recently been collected from the lowermost marine shale, and the highest sandstones have yielded a *Vascoceras diartianum* assemblage, indicating that a nearly complete upper Cenomanian marine biostratigraphic sequence exists. At most localities, the top of the Dakota contains an extensive fauna of bivalves characterized by the oyster *Exogyra (Costagyra)*

CRETACEOUS STAGES		FORMATIONS AND MEMBERS	INFORMAL STRATIGRAPHIC UNITS	AMMONITE ZONES	FOSSIL LOCALITIES
Santo-nian	Upper	John Henry Member	Gss Fss — Coal zones; Ess, Dss — UMMT; Css, Bss — Coal zones; Ass — LMMT	Desmoscaphites bassleri / Desmoscaphites erdmanni / Clioscaphites choteauensis / Clioscaphites vermiformis / Clioscaphites saxitonianus	
	Middle				125, 141
	Lower				
Con-iacian	Upper		Calico bed	Scaphites depressus	106, 108, 109, 114, 120, 123, 129, 135, 150, 152, 159
	Middle			Scaphites ventricosus / Forresteria alluaudi	62, 113, 139, 158, 160
	Lower	Smoky Hollow Member	barren zone	Forresteria peruana / Prionocyclus germari / Scaphites nigricollensis / Scaphites whitfieldi / Scaphites ferronensis / Scaphites warreni	
Turonian	Upper				
			? coal zone	Prionocyclus macombi	140
	Tibbet Canyon Mbr		lower ss / noncalcareous shale	Prionocyclus hyatti / Collignoniceras praecox	5, 15, 16, 55, 56, 59, 60, 78, 96, 105, 107, 110, 126, 164
	Middle			Collignoniceras woollgari / Mammites nodosoides	4, 20, 54, 58, 77, 79, 83, 147, 155 / 28, 47-50
	Lower	Tropic Shale	calcareous shale	Vascoceras birchbyi / Pseudaspidoceras flexuosum / Watinoceras devonense	} 9, 10, 23, 30, 42-46, 52, 53 / 26
				Nigericeras scotti / Neocardioceras juddii / Burroceras clydense / Euomphaloceras septemseriatum	3, 131 / 2, 7, 8, 12, 19, 22, 25, 36, 38, 39, 51, 80, 85-86, 89-91, 93-95, 100-101, 148
Cenomanian (part)	Upper	Dakota Formation	upper member	Vascoceras diartianum / Dunveganoceras conditum / Dunveganoceras albertense / Dunveganoceras problematicum / Dunveganoceras pondi	6, 12, 17, 18, 21, 24, 27, 29, 31, 33, 34, 37, 70-72, 81, 82, 84, 87, 88, 92, 99, 134, 137, 161 / } 14, 32, 41
	Middle		? middle and lower members	Plesiacanthoceras wyomingense / Acanthoceras amphibolum / Acanthoceras bellense / Acanthoceras muldoonense / Acanthoceras granerosense / Conlinoceras tarrantense	

Figure 3. Biostratigraphic chart showing Upper Cretaceous stages, formations and members in the Grand Staircase-Escalante National Monument, informal stratigraphic units, Western Interior ammonite zones (modified from Cobban, in Obradovich, 1993), and localities of fossil collections in Dyman and others (2000). Upper part of informal stratigraphic units modified from Peterson (1969). LMMT and UMMT are lower and upper marine mudstone tongues, and A through G are sandstone tongues of the John Henry Member of Straight Cliffs Formation. Each number corresponds to the appropriate invertebrate fossil collection in Dyman and others (2000).

Figure 4. *Henrieville Sandstone-Dakota Formation contact in upper Henrieville Valley east of Henrieville, Utah. Hammer for scale.*

olisiponensis Sharpe and *Flemingostrea prudentia* (White). At one locality (Cobban and others, 2000; Dyman and others, 2000), we found *Metoicoceras mosbyense* with *E. olisiponensis,* which suggests that the *E. olisiponensis* assemblage lies at the top of the range of *M. mosbyense* (figure 5). Inasmuch as the highest specimens of *M. mosbyense* occur in the zone of *Vascoceras diartianum*, we assigned the highest beds of the Dakota to this zone. The presence of *M. mosbyense* lower in the upper part of the Dakota suggests assignment to one of the *Dunveganoceras* zones, such as *D. conditum* or *D. albertense*.

Using methods reported in Obradovich (1993), J.D. Obradovich recently obtained a new date for the middle part of the Dakota Formation in the Tropic area (field trip stop 3) by ^{40}Ar/^{39}Ar laser fusion dating of sanidine crystals. Several bentonite beds in the Dakota Formation contain sanidine. Obradovich took a sample from the middle part of the Dakota, 120 feet from the top of the unit, and isolated the sanidine by disaggregation and magnetic and heavy liquid separation, similar to methods used by Hicks and others (1995). Obradovich analyzed the samples using the GLM continuous laser system at the U.S. Geological Survey isotope facility at Menlo Park, California (Dalrymple, 1989) and presented the date as an unweighted mean as 95.97 +/-0.22 Ma which identifies the sample as early Cenomanian.

Tropic Shale

Gregory and Moore (1931) first described the Tropic Shale near the town of Tropic, Utah. It is about 700 to 900 feet thick in the Monument and composed of medium- to dark-gray fissile shale with local thin siltstone and sandstone lenses (figure 6). The lower part of the formation is generally calcareous and contains several distinctive concretionary zones. The lowermost limestone concretionary zone, which forms a distinct horizon about 15 to 20 feet above the base of the formation, contains the straight-shelled ammonite *Sciponoceras gracile* and associated fauna of the middle upper Cenomanian *Euomphaloceras septemseriatum* biozone (figure 3; field trip stops 8 and 9; Cobban and others, 2000; Dyman and others, 2000). A second horizon, not far above the first, contains a fauna characteristic of the *Neocardioceras juddii* biozone. A third horizon about 150 feet above the base of the formation contains fauna of the *Vascoceras birchbyi* biozone of early Turonian age. A fourth horizon has septarian concretions with large ammonites of the *Mammites nodosoides* biozone. A fifth horizon, containing the early middle Turonian ammonite *Collignoniceras woollgari* is located about 250 feet above the base of the Tropic. About 700 feet above the base, at a distinct color change from light gray calcareous to dark gray noncalcareous shale, is the approximate first appearance of the ammonite *Prionocyclus hyatti* of late middle Turonian age (field trip stop 8). This ammonite is also found in the overlying Tibbet Canyon Member of the Straight Cliffs Formation. A similar sharp color change has been recognized as far east as west-central Kansas, where it marks the contact of the stratigraphically equivalent Fairport and overlying Blue Hill Members of the Carlile Shale.

At the Cenomanian-Turonian boundary reference section near Pueblo, Colorado, we recognize the middle Turonian *Prionocyclus hyatti* biozone in the upper part of the Blue Hill Member of the Carlile Shale and in the overlying Codell Sandstone Member of the Carlile Shale. At Pueblo, these strata are unconformably overlain by upper Turonian and Coniacian limestones of the Fort Hays Limestone Member of the Niobrara Formation (Cobban and Scott, 1972).

The upper part of the Tropic Shale in the Monument is gradational with the overlying Tibbet Canyon Member of the Straight Cliffs Formation. Sandstones increase in abundance upward in the upper part of the Tropic until sandstone is the dominant lithology. The Tropic-Straight Cliffs contact is usually placed where sandstone becomes more abundant than shale (Peterson, 1969).

178

Figure 5. Upper part of Dakota Formation at field trip stop 6 (The Reservoir). The upper part of the Dakota Formation forms a coarsening upward cycle capped by sandstone and conglomeratic sandstone. Marine and brackish water invertebrates illustrated here include Inoceramus mesabiensis, Exogyra olisponensis, Ostrea sp., and the ammonite Metoicoceras mosbyense (see Dyman and others (2000) for a complete list of invertebrate fossils at this locality).

Figure 6. The Cockscomb along Cottonwood Wash (near field trip stop 8) looking south with views, from left to right, of the upper part of the Dakota Formation, Tropic Shale, and lower part of the Straight Cliffs Formation.

Bentonite beds are abundant throughout the Tropic. Four widely distributed beds of bentonite, lettered A to D, are present in the Bridge Creek Member of the chronostratigraphically equivalent Greenhorn Limestone at Pueblo, Colorado (Elder and Kirkland, 1985). Elder (1985) traced the four beds across the Western Interior basin from Pueblo to Black Mesa in northeastern Arizona. Obradovich (1993) dated bentonite A, which lies in the upper Cenomanian biozone of *Euomphaloceras septemseriatum*, at 93.49 +/- 0.89 Ma. Obradovich dated bentonite B, which lies higher in the upper Cenomanian biozone of *Neocardioceras juddii*, at 93.59 +/- 0.58 Ma. He dated bentonite C, which may lie in the lower Turonian biozone of *Pseudaspidoceras flexuosum*, at 93. 25 +/- 0.55 Ma. Bentonite D, in the lower Turonian biozone of *Vascoceras birchbyi*, was dated at 93.40 +/- 0.63 Ma. Elder (1991) described these bentonite beds from Black Mesa in Arizona to Wahweap Creek in the northern part of the Monument.

Refer to Obradovich (1993) for a detailed list of all dated bentonites within the middle Cretaceous of the Western Interior basin. Refer also to Zelt (1985) and Leithold (1994) for an alternative zonation for these bentonites and for bentonites higher in the stratigraphic section.

Straight Cliffs Formation
Gregory and Moore (1931) named the Straight Cliffs Formation for exposures along the eastern edge of the Kaiparowits Plateau near Fifty-Mile Mountain in the Monument. The formation represents the final regressive phase of the Tropic sea. Lithologic descriptions of drill core by Hettinger (1995) show the clastic-rich formation is lithologically diverse. It contains four named members designated by Peterson (1969). They are: the Tibbet Canyon, Smoky Hollow, John Henry, and Drip Tank Members (figures 2 and 3). Only the Tibbet Canyon and John Henry Members are known to contain marine invertebrate fauna (field trip stop 7).
Tibbet Canyon Member: The Tibbet Canyon, the lowest member of the Straight Cliffs Formation, is composed of gray-brown, fine- to medium-grained sandstone and interbedded mudstone and shale. Peterson (1969) identified the base of the Tibbet Canyon in the southeastern Kaiparowits Plateau, where sandstone becomes the dominant lithology above the Tropic Shale. The Tibbet Canyon Member is comprised of marine shoreface sandstone and contains the middle Turonian guide fossil *Prionocyclus hyatti*. At several localities, the Tibbet Canyon contains beds with abundant *Inoceramus howelli*, an inoceramid that occurs within the zone of *P. hyatti* (figure 7; field trip stop 7; Cobban and others, 2000; Dyman and others, 2000). The member ranges in thickness from about 70 to 200 feet in the Monument.
Smoky Hollow Member: The Smoky Hollow Member of the Straight Cliffs Formation is more lithologically and depositionally heterogeneous than the underlying Tibbet Canyon Member and is composed of interbedded sandstone, mudstone, carbonaceous mudstone, and coal. The base of the member consists of a zone of coal and carbonaceous mudstone that varies in thickness from 0 to 47 feet (Peterson, 1969) (field trip stop 7). The top of the member is composed of a yellow-brown iron-rich unit of quartz- and chert-rich sandstone and chert-pebble conglomerate. This unit is referred to as the Calico bed (Peterson, 1969) (figures 3 and 4) or the Calico sandstone or sequence (Hettinger, 1995). The Calico bed varies in thickness from 0 to about 50 feet and is in sharp contact with the overlying John Henry Shanley and others (1992) also placed the unconformity at the base of the Calico, and interpreted the sharp contact at the base of the overlying John Henry to represent a transgressive surface of erosion.

A late Turonian age is likely for most of the member (Peterson, 1969). Hettinger (1995, p. A6) noted the occurrence of an inoceramid bivalve identified as *Cremnoceramus deformis* (Meek) 12 feet below the top of the Smoky Hollow Member at a locality southwest of Escalante, just outside the Monument. The inoceramid is probably *Volviceramus involutus* (Sowerby) which is middle Coniacian in age. Cobban and others (2000) found middle

Figure 7. Sandstone slab taken near top of Tibbet Canyon Member of Straight Cliffs Formation from Alvey Wash about 3 miles south of Escalante, Utah, containing *Inoceramus howelli*. *Inoceramus howelli* is middle Turonian in age. Pen for scale.

Coniacian inoceramids at two localities in the Monument, but both are from the overlying John Henry Member.

John Henry Member: The John Henry Member varies in thickness from about 600 feet to more than 1,000 feet in the Monument and is composed of interbedded sandstone, siltstone, mudstone, carbonaceous mudstone, and coal (figure 8; field trip stop 7). Peterson (1969) placed the upper contact of the John Henry Member at the base of the lowest cliff-forming sandstone of the overlying Drip Tank Member. He also interpreted the John Henry-Drip Tank contact to be conformable, but Shanley and McCabe (1991) interpreted the contact to be unconformable.

In the southwestern third of the Monument, the John Henry Member seems to be entirely nonmarine, but in the central part of the Monument, thick marine sandstones intertongue with coal-bearing units, and farther east, two marine mudstone units intertongue with the sandstones. Peterson (1969) referred to the mudstone units as a "lower marine mudstone tongue" and an "upper marine mudstone tongue" (figure 3). The lower tongue commonly has pebbles at the base and rests on an unconformable surface above the Calico bed of the Smoky Hollow Member.

Ammonites and inoceramids date the lower tongue as late Coniacian. The upper tongue is not well dated, but has yielded a single fragment of an ammonite assigned to *Clioscaphites vermiformis* (Meek and Hayden) of middle Santonian age. Four major sandstone units separate the two mudstone tongues designated by Peterson (1969): A (lowest) to D (highest) (figure 3). Peterson collected an ammonite, *Baculites codyensis* Reeside, at the boundary of the B and C sandstones (Cobban and others, 2000; Dyman and others, 2000). It is a late Coniacian to middle Santonian species. Peterson collected the bivalve *Endocostea baltica* (Boehm) from the upper part of the upper mudstone tongue (Cobban and others, 2000; Dyman and others, 2000) as well as from the overlying G sandstone (Cobban and others, 2000; Dyman and others, 2000). This inoceramid has a range of late Santonian to early Campanian. Peterson also collected the late Santonian-early Campanian inoceramid *Sphenoceramus patootensiformis* (Seitz) from near the top of the G sandstone (Cobban and others, 2000; Dyman and others, 2000).

Another significant find by Peterson is a good collection of the inoceramids *Endocostea flexuosa* (Haenlein) and *E. flexibaltica* (Seitz) 350 feet below the top of the Straight Cliffs Formation just outside the Monument about 10 miles northwest of Escalante. According to Seitz (1967) *E. flexuosa* is found in rocks assigned to the lower Campanian in Germany, and *E. flexibaltica* has a range of late Santonian-early Campanian in Germany. Troeger (1987) shows *E. flexibaltica* as having a very narrow range straddling the late Santonian-early Campanian boundary. Until paleontologists discover diagnostic ammonites in the uppermost part of the Straight Cliffs, that part of the formation is herein regarded as of latest Santonian age, as also suggested by Eaton (1991, p. 52).

The Monument contains vast coal resources from the John Henry Member of the Straight Cliffs Formation. The original in-place coal resource for the entire Kaiparowits Plateau (figure 1) is more than 60 billion short tons, from coal zones primarily within the John Henry (Hettinger and others, 2000). The Utah Geological Survey (UGS) (in Petzet, 1997) estimated that the Kaiparowits coal field in the Monument contains nearly 12 billion tons of technically recoverable coal. The UGS assessment was in part derived from the U.S. Geological Survey assessment of Kirschbaum and others (2000).

Drip Tank Member: The Drip Tank is the uppermost member of the Straight Cliffs Formation and ranges from about 140 feet in thickness in the southern part of the Monument to more than 500 feet in the northern part. It is a cliff-forming, fine- to medium-grained, gray-brown, nonmarine sandstone with well-developed cross-stratification (figure 9).
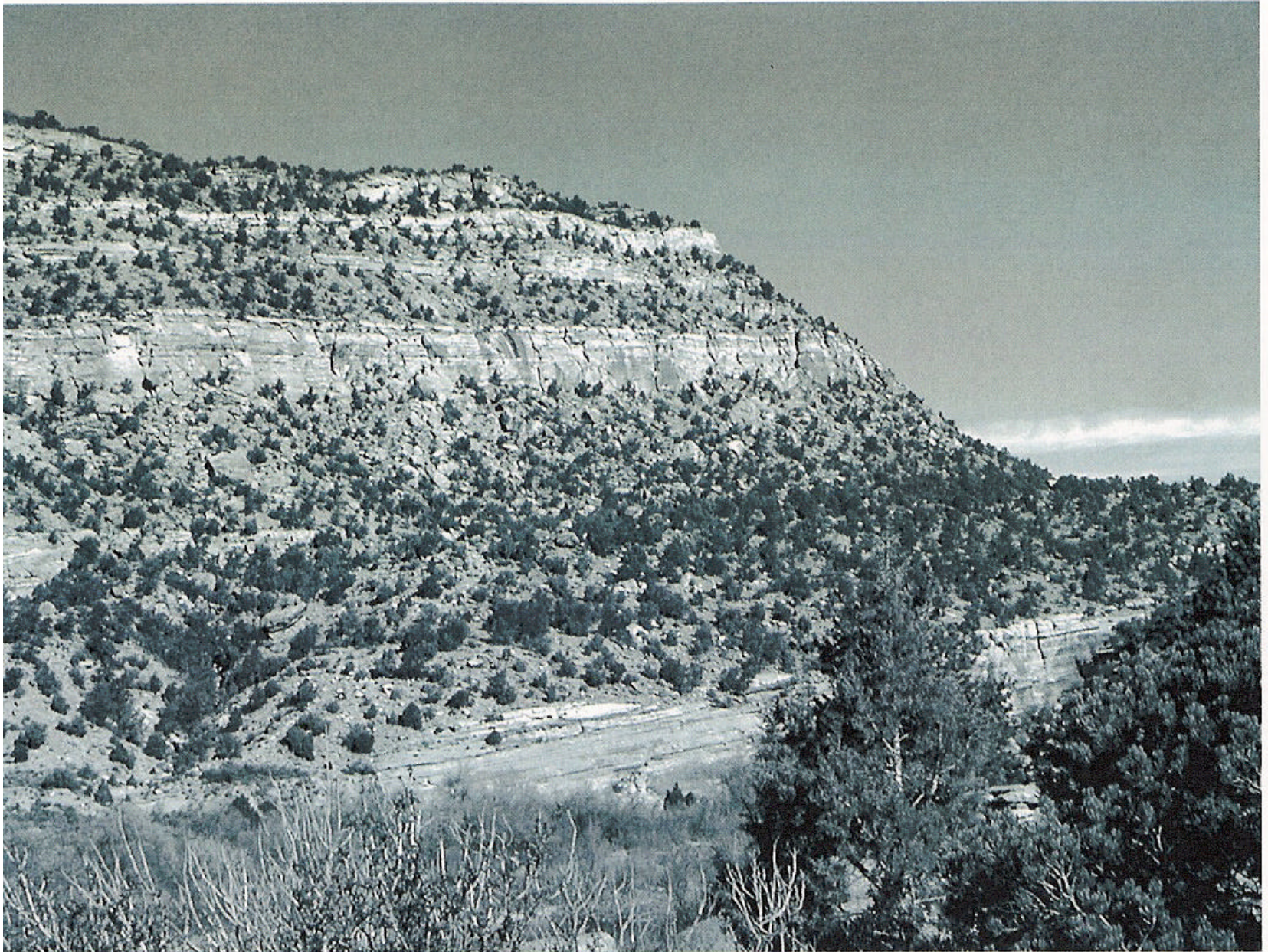
Figure 8. Smoky Hollow Member and lower part of John Henry Member of Straight Cliffs Formation in Alvey Wash, about 3 miles south of Escalante, Utah.

Figure 9. Upper part of John Henry Member and Drip Tank Member of Straight Cliffs Formation, looking north about 5 miles east of Henrieville, Utah.

MILEAGE

Int. Cum.   Description

0.0   0.0   Field trip starting point, westernmost parking lot of Southern Utah University, also known as the Motor Pool, west side of Eccles Coliseum, Cedar City, Utah. Drive north on 1150 W, 200 S to stop sign. Turn east on Center Street and drive toward mountains.

1.0   1.0   Stop light is intersection of Main and Center streets. Continue east toward mountains on State Route (SR) 14.

0.2   1.2   Lower red and gray cliffs at 12:00 are composed of Moenkopi Formation (Triassic) (figure 10). These rocks have been exposed along the Hurricane fault zone.

0.6   1.8   Complex structural relationships in Triassic Moenkopi and Chinle Formations (figure 10) within zone of Sevier orogenic overprint.

0.7   2.5   Gray beds at 9:00 are clinkers from the former Utah Power and Light coal-fired electric generating plant located in space now occupied by Utah Wildlife Sanctuary.

0.3   2.8   Jurassic Navajo Sandstone-Carmel Formation contact (figure 10) on both sides of road. The strata are dipping steeply to the east, and the Navajo Sandstone is probably tectonically thinned. The overlying Carmel Formation is thickened above the contact and may be repeated.

1.2   4.0   Thrust anticlines visible within limestone unit of Carmel Formation.

1.8   5.8   Right Hand-Kolob Canyon turnoff. Continue east on SR 14.

0.7   6.5   Lower part of Cretaceous Dakota Formation at road level overlying Jurassic Carmel Formation. Good exposures of flat-lying beds along road for next mile.

1.4   7.9   Unnamed fault at 3:00.

0.8   8.7   **STOP 1—**CEDAR CANYON. Westernmost facies of Cretaceous Dakota, Tropic, and Straight Cliffs Formations on field trip, exposed on both sides of road along Coal Creek in Cedar Canyon. Excellent views of fault along Coal Creek, landslides along highway, and paleovalley-filling basalts on north side of road. Park on north side of SR 14 away from traffic.

              This stop is a general overview of western facies of the marine Cretaceous than is exposed in Grand Staircase-Escalante National Monument. The approximate position of the Dakota-Tropic contact is on the south side of the highway, but landslides have covered most exposures. Marine rocks comprise the upper part of the Dakota, the Tropic, and lower part of the Straight Cliifs at Cedar Canyon. W.A. Cobban identified the oldest marine rocks in the lower part of the Tropic Shale as part of the lower Turonian

AGE	Formations, members, and thicknesses in feet		
TERTIARY	Mt Dutton volcanics		
	Claron Formation -1400		
	Pine Hollow Fm Grand Castle Fm Canaan Peak Fm 0-1300		
CRETACEOUS	Kaiparowits Formation 2000-3000		
	Wahweap Formation 1000-1500		
	Straight Cliffs Fm 900-1800	Drip Tank Mb	
		John Henry Mb	
		Smoky Hollow Mb	
		Tibbet Canyon Mb	
	Tropic Shale 500-750		
	Dakota & Cedar Mtn Fms 3-370		
JURASSIC	Morrison Fm / Henrieville Ss 0-950		
	Entrada Ss 0-1000	Escalante Mb	
		Cannonville Mb	
		Gunsight Butte Mb	
	Carmel-Page Fms 180-1040		
	Navajo Sandstone 1300-1500	main body	
		Tenney Canyon Tongue	
		Lamb Point Tongue	
	Kayenta Formation 150-350		
	Moenave Fm & Wingate Ss 100-350		
TRIASSIC	Chinle Fm 425-930	Petrified Forest Mb	
		Shinarump Mb	
	Moenkopi Fm 440-1150		
PERMIAN	Permian Fms 655+		

Figure 10. Generalized stratigraphic chart illustrating rock units along the field trip route. Modified from Doelling and others (2000).

187

Mytiloides kossmati biozone. The Tropic Shale is exposed for about 0.25 mi east along the highway and represents a Turonian-age western marine facies of the Tropic, although various other names have been used for these rocks. See Eaton and others (2001) for a detailed discussion of the various stratigraphic names used for Cretaceous rocks in Cedar Canyon and for a list of other fauna found in the area.

The overlying Straight Cliffs Formation forms the uppermost cliffs of the canyon and is at least 1,000 feet thick at this stop. It forms continuous ledges of fine- to medium-grained lithic-rich sandstone that can be attributed to a coastal origin. Marine fauna range up through the lower middle Turonain zone of *Collignoniceras woollgari*.

0.4   9.1   Exposures of marine Tropic Shale on right. Ashdown Canyon on left.

0.2   9.3   Massive coastal marine sandstones of the lower part of the Straight Cliffs Formation on both sides of road in middle lower Turonian zone of *Vascoceras birchbyi*.

0.3   9.6   Series of brackish-water coquina beds containing *Crassostrea soleniscus* in Straight Cliffs Formation. Alternating marine strata contain *Mytiloides mytiloides* and *M. labiatus.*

1.8   11.4   *C. soleniscus* and *Craginia coalvillensis* (gastropod) coquina beds in Straight Cliffs Formation on both sides of road.

0.4   11.8   Southern Utah University Mountain Center and field station.

0.3   12.1   Discontinuous exposures of nonmarine upper part of Straight Cliffs Formation.

0.3   12.4   Woods Ranch County Recreation Facility.

0.2   12.6   Dixie National Forest boundary.

0.4   13.0   Approximate contact of Straight Cliffs and overlying Wahweap Formations.

0.5   13.5   Sharp curves in road. **EXERCISE CAUTION**.

0.4   13.9   Beautiful exposures of concretionary sandstone in Cretaceous Wahweap and Kaiparowits Formations.

0.1   14.0   Exposures of nonmarine Paleocene-Eocene Claron Formation.

1.7   15.7   Websters Flat turnoff on right. Continue east on SR 14.

0.2   15.9   Excellent exposures of lacustrine facies of Claron Formation on left.

1.6   17.5   **STOP 2**—MARKAGUNT PLATEAU. Regional overview of structural and topographic features. Zion National Park, Kolob Terrace, and Pine Valley Mountains are visible to the south. Large southeast drainage is O'Neil Gulch. This overview parking area is on the western rim of the Markagunt Plateau. The Markagunt, which is bounded on the east by the Sevier fault and on the

west by the Hurricane fault, represents the farthest western influence of structures associated with the Colorado Plateau region. The Markagunt Plateau dips northeastward, exposing older strata to the southwest. The Pine Valley Mountains, composed primarily of monzonite porphyry, represent the exposed core of an eroded lacolith, which is part of the great Tertiary (20-25 m.y.) intrusive event in southwestern Utah. The Pine Valley Mountains are on the downthrown side of the Hurricane fault and rest on the Paleocene-Eocene Claron Formation. Exposures of the Paleocene-Eocene Claron Formation (figure 10) on the north side of the road.

0.5	18.0	Bristlecone pine viewing area on right. Continue east on SR 14.
0.9	18.9	Midway intersection. Turnoff for Cedar Breaks National Monument. Cedar Breaks National Monument contains spectacular erosional features in the Claron Formation. Continue east on SR 14.
2.2	21.1	Tree-covered cinder cone at 11:00.
0.5	21.6	Quaternary flow basalts at 10:00.
0.2	21.8	"Lava flows" interpretive sign.
1.7	23.5	Kane County line. Volcanic flows on both sides of road.
1.5	25.0	Navajo Lake overlook.
1.3	26.3	Navajo Lake turnoff on right. Continue east on SR 14.
2.4	28.7	Duck Creek Campground on left. Continue east on SR 14.
1.8	30.5	Duck Creek Village.
1.5	32.0	Mammoth Creek turnoff. Continue east on SR 14.
1.5	33.5	Junction of Uinta Flat (left) and Strawberry Point (right) roads.
1.3	34.8	Exposures of Claron Formation on left.
0.8	35.6	Swains Creek road.
3.5	39.1	Exiting Dixie National Forest.
0.5	39.6	Cretaceous Kaiparowits and Wahweap rocks on both sides of road. Sharp curves. **EXERCISE CAUTION.**
1.7	41.3	Junction SR 14 and U.S. Highway 89 (US 89). Long Valley Junction. Turn north on US 89.
0.9	42.2	Paleocene-Eocene Claron Formation on both sides of road.
3.2	45.4	Garfield County line.

3.0	48.4	Cross Asay Creek.
3.3	51.7	Cross Mammoth Creek.
0.5	52.2	Junction with Fish Hatchery Road. Continue north on US 89.
1.1	53.3	Town of Hatch, Utah.
1.7	55.0	Sevier River. Pleistocene and Holocene valley-fill gravels on both sides of road.
0.7	55.7	Valley-fill volcanic rocks cap ledges on left.
6.1	61.8	Junction SR 12. Turn east (right) toward Bryce Canyon National Park. Cross Sevier River.
2.5	64.3	Entrance to Red Canyon. Trace of Sevier fault visible at 9:00. Late Tertiary basalt, which has been dated as 12 Ma (Hintze, 1993), is on downthrown west side of fault. Claron Formation on both sides of road. Short photo stop.
0.9	65.2	Red Canyon Visitors Center. Continue east on SR 12.
3.9	69.1	Crest of Paunsaugunt Plateau. The name "Paunsaugunt" is a Paiute word meaning home of the beaver. Mt. Dutton volcanic rocks at 9:00. These volcanic rocks date from 23-26 Ma (Hintze, 1993). Highway on Claron Formation.
1.8	70.9	Leaving Dixie National Forest. Summit marker 7,619 feet.
2.5	73.4	Cross East Fork of Sevier River. Powell Point (elevation 10,188 feet) at 12:00 on Table Cliff Plateau.
2.1	75.5	Junction SR 63. Entrance to Bryce Canyon National Park on right. Continue east on SR 12.
0.8	76.3	Begin descent on east side of Paunsaugunt Plateau. Bryce Canyon National Park to the left.
0.5	76.8	Wahweap Sandstone block and Claron Formation on right side of road. This structural block is part of the Rubys Inn thrust fault, a Laramide structure.
2.3	79.1	Mossy Cave trailhead.
0.4	79.5	Sharp contact of Claron Formation on left and underlying Cretaceous John Henry Member of the Straight Cliffs Formation on right. Trace of Paunsaugunt fault.
0.5	80.0	Tropic, Utah, city limit. Exposures of Tibbet Canyon and Smoky Hollow Members of Straight Cliffs Formation on left.

0.5   80.5   Highway descends into Cretaceous Tropic Shale of Bryce Valley.

2.3   82.8   Dougs Place, Tropic, Utah. Short break.

1.3   84.1   Continue south on Utah Highway 12 through lower Tropic Shale and Dakota Formation. Bentonites of lower part of Tropic Shale exposed on low bench at 9:00.

0.4   84.5   Upper part of Dakota Formation including beds of sandstone and coal in roadcut on right.

0.7   85.2   **STOP 3--** STAN MECHAM PROPERTY. Turn right on private drive and park near fresh shale cut on Stan Mecham property. Fresh exposure of middle and upper part of Dakota Formation. Rubys Inn recently excavated this outcrop for a source of bentonite to line a sewage pond. The upper 135 feet of the Dakota crops out here as a series of alternating beds of sandstone, siltstone, shale, and bentonite. Approximately 5 miles to the east in Henrieville Valley, the entire Dakota is about 210 feet thick. Lower Dakota beds are nonmarine, but sandstones in the upper Dakota contain a marine assemblage including *Exogyra olisponensis, Flemingostrea prudentia*, *Inoceramus mesabiensis*, and *Metoicoceras mosbyense*. See Cobban and others (2000) and Dyman and others (2000) for a complete list of invertebrate fossils at this and nearby localities. The uppermost part of the Dakota here contains coal beds, which are in turn overlain by gray shales of the Tropic Shale. About 1 mile to the south along Yellow Creek, these upper Dakota coal beds contain tree trunks in their original upright position.

           J.D. Obradovich dated a bentonite in the middle part of the Dakota Formation in the Tropic area by $^{40}Ar/^{39}Ar$ laser fusion dating of sanidine crystals. The date is 96.06 +/- 0.30 Ma which identifies the sample as early middle Cenomanian according to Obradovich (1993). Refer to the text section in this report on the Dakota Formation for more details.

0.3   85.5   Return to SR 12 and continue south.

0.8   86.3   Cannonville Member of Jurassic Entrada Formation on right. Dakota Formation-Henrieville Sandstone contact on left across Paria River. The Henrieville Sandstone is a Morrison Formation equivalent unit (figure 10).

1.0   87.3   Cannonville, Utah, city limit.

0.4   87.7   Turn right on Main Street (Grand Staircase-Escalante National Monument Road No. 400). Continue south toward Kodachrome Basin State Park.

0.4   88.1   Views of contact between lower Gunsight Butte and upper Cannonville Members of Entrada Formation. Note large sweeping cross beds in Gunsight Butte Member.

1.2   89.3   Promise Rock on right in Gunsight Butte Member. According to local folklore, Promise Rock was a sacred Paiute marriage-ritual site.

0.5   89.8   Contact of upper Gunsight Butte Member of Entrada Formation and lower Wiggler Wash Member of Carmel Formation.

0.5   90.3   Intersection with Sheep Flat Road and Yellow Creek. Continue south.

0.3   90.6   Intersection with Skutumpah Road. Continue south.

0.4   91.0   Cross bridge over Paria River.

2.0   93.0   **STOP 4--** SHEPHARD POINT. Park on left or right side of road. Views of sedimentary pipes in the Winsor Member of the Carmel Formation. Evidence suggests that the clastic sedimentary pipes exposed here and at Kodachrome Basin State Park are liquefaction features related to paleoearthquake events. Note numerous normal faults cutting the pipes.

2.0   95.0   Entrance to Kodachrome Basin State Park on left.

1.0   96.0   Cliffs to north capped by Dakota Formation. Dakota-Henrieville contact well exposed below.

0.6   96.6   Cross Dry Valley-Rock Springs Creek.

3.8   100.4   Begin ascent of steep hill. Excellent view of north-plunging end of Kaibab anticline at 10:00.

0.3   100.7   **STOP 5--** SLICK ROCK BENCH. Stop on crest of hill for regional stratigraphic overview. The view north toward Wiggler Wash shows steep dip of Entrada through Straight Cliffs Formations (figure 10) in Kaibab anticline. Canaan Peak and Table Cliff Plateau on far horizon.

        The Upper Valley oil field is about 12 miles northeast of here, along the flank of the southeast-trending Upper Valley anticline. Hydrodynamic drive has forced hydrocarbons off the crest of the Upper Valley structure. Production occurs in dolomite reservoirs of the Permian Kaibab Formation and the Triassic Moenkopi Formation at depths ranging from about 6,300 to 7,600 feet. These reservoirs have produced more than 25 million barrels of oil since the field was discovered in 1964 (Petzet, 1997). The field is currently in a water-flood program in which reservoir water is re-injected to increase oil recovery. Because no long-distance pipelines exist in the area, produced oil is stored in local holding tanks and trucked to oil refineries in Salt Lake City. Potential new and deeper reservoirs in and near the Monument include the Mississippian Redwall Limestone, Cambrian Tapeats Sandstone, and Late Proterozoic Chuar Group.

        Conoco recently sought to drill several deep exploration wells in the southern part of the Monument about 45 miles south of Escalante, to test the Cambrian Tapeats Sandstone and the Late Proterozoic Chuar Group. Conoco completed the first of these wells, but detailed information about prospective targets is not available. Conoco holds leases on more than 140,000 acres within the Monument (Petzet, 1997).

        Other potential energy resources in the Monument include coal and coalbed gas from coal beds in the John Henry Member of the Straight Cliffs Formation. We will discuss these resources at STOP 7.

0.3   101.0   Distant views of Lower Jurassic Navajo Sandstone on right at 3:00. This section is part of the White Cliffs of the Grand Staircase.

0.7   101.7   Round Valley Draw. Cliffs on left in Upper Jurassic Henrieville Sandstone and capped by Cedar Mountain(?) and Dakota Formations.

0.4   102.1   Cliffs on left in Henrieville Sandstone.

0.5   102.6   Butler Valley.

1.9   104.5   Turn left on Monument Road No. 440 toward Grosvenor Arch. Road is in Carmel Formation.

1.0   105.5   Grosvenor Arch parking area. The base of this arch is in the Upper Jurassic Henrieville Sandstone. The upper part is in the Cretaceous Cedar Mountain(?) and Dakota Formations. **BATHROOM AND LUNCH STOP.**

0.3   105.8   Turn left on stock pond road.

0.1   105.9   **STOP 6--** DAKOTA FORMATION AT STOCK RESERVOIR. Park in open area to left of dam. The entire Dakota Formation crops out here along the east-dipping margin of the East Kaibab monocline. The Dakota is approximately 200 feet thick and is composed of three informal depositional units. The lower conglomeratic unit contains coarse sandstone and conglomerate clasts of quartzite, dark-gray chert, and limestone. The lower unit forms incised fluvial channels 1 to 3 feet thick with sharp scoured lower surfaces. This lower unit is equivalent in age to the Cedar Mountain Formation in central Utah, according to Doelling and others (2000), based on an Early Cretaceous age of palynomorphs from interbedded siltstones. The lower unit unconformably overlies the Jurassic Henrieville Sandstone. The middle unit is composed of carbonaceous mudstone, siltstone, sandstone, bentonite, and coal, and forms a coarsening upward depositional cycle with marine to coastal sandstones at the top. Thin sandstone beds in the middle of the unit contain iron-rich concretions up to 4 inches in diameter. A fine- to medium-grained lithic-rich sandstone bed forms the top of the unit and contains a marine invertebrate assemblage including *Metoicoceras mosbyense,* of late Cenomanian age. The upper unit forms another coarsening upward cycle of coal, carbonaceous mudstone, sandstone, and conglomeratic sandstone. Marine and brackish water invertebrates include *Inoceramus mesabiensis, Exogyra olisponensis, Ostrea* sp., and the ammonite *Metoicoceras mosbyense* (see Dyman and others (2000) for a complete list of invertebrate fossils at this locality).

       The Dakota Formation-Tropic Shale contact is not well exposed here but represents a transgressive surface of erosion in which gray marine shales of the Tropic overlie coastal beds of the Dakota. All but the upper part of the Tropic Shale is covered between this stop and STOP 7.

       Return to Monument Road No. 440 and turn left.

0.4   106.3   **STOP 7:** "THE GUT" AND STRAIGHT CLIFFS FORMATION. Park at crest of hill on left and right. Roadcuts continue for more than a half mile southeast. This stop provides an excellent opportunity to view the four named members of

the Straight Cliffs Formation originally described by Peterson (1969) at an equivalent sequence southeast of The Gut on the Kaiparowits Plateau. The Tibbet Canyon is the lowest member and crops out at the parking area and immediately east of the road. It is gradational with the underlying Tropic Shale and forms a regressive marine depositional system. The Tibbet Canyon contains *Inoceramus howelli* and *Prionocyclus hyatti* of middle Turonian age.

The Tibbet Canyon Member is conformably overlain by the nonmarine Smoky Hollow Member. Note the abundant coal and carbonaceous mudstone in the Smoky Hollow. The Smoky Hollow is in turn overlain by a distinctive white-weathering unconformity-bounded nonmarine sandstone called the Calico bed (Hettinger, 1995). The Calico bed is time-equivalent to a widespread Coniacian unconformity observed throughout the Western Interior basin. Sandstones in the Calico bed contain nodules that weather out on outcrop to form distinctive surfaces.

The Calico bed is unconformably overlain by the John Henry Member. Farther east in the Monument, in the Straight Cliffs region southeast of Escalante, Utah, the John Henry contains marine fossils as young as Santonian, within the zone of *Clioscaphites vermiformis* (Cobban and others, 2000). Equivalent rocks at this locality (field trip stop 7) in the upper part of the John Henry contain a nonmarine fossil assemblage including *Unio* sp., *Proparraysia*? sp., turtle shells, and reptilian bones. An intermediate locality along SR 12 east of Henrieville (Dyman and others, 2000) contains a brackish water assemblage of oysters and clams.

The John Henry Member of the Straight Cliffs Formation has the potential for significant resources of coalbed gas and coal. The Kaiparowits coal field in the Monument is estimated to contain 2.6-10.5 trillion cubic feet of coalbed gas in place at depths less than 6,000 feet and nearly 12 billion tons of technically recoverable coal (Utah Geological Survey, in Petzet, 1997). The original in-place coal resource for the entire Kaiparowits Plateau (figure 1) is more than 60 billion short tons, from coal zones primarily within the John Henry (Hettinger and others, 2000).

The uppermost Drip Tank Member is an entirely nonmarine sandstone sequence resting sharply on the John Henry (figure 9). The Drip Tank is readily identifiable by its lighter color and distinctive reticulate fracture pattern on outcrop. The Drip Tank is, in turn, overlain by the nonmarine Wahweap and Kaiparowits Formations. These uppermost Cretaceous units can be seen on Monument Road No. 440 east of The Gut in the drainages of Wahweap Creek.

0.4	106.7	Turn around and continue past the stock dam and Grosvenor Arch. Return to Monument Road 400.
1.3	108.0	Turn south (left) on Monument Road 400.
1.9	109.9	Entering The Cockscomb along the west-dipping East Kaibab monocline in the valley of Cottonwood Creek.
0.6	110.5	Henrieville Sandstone on left.
1.3	111.8	Steeply dipping Carmel and Entrada Formations. Santa Claus Rock on left.
4.3	116.1	Pump Canyon Spring on right.

2.9   119.0   Views of Dakota, Tropic, and Straight Cliffs Formations. Brief photo stop.

3.8   122.8   Series of deep washes along road. Views of compressed stratigraphy along East Kaibab monocline.

2.0   124.8   **STOP 8:** THE COCKSCOMB. Park along either side of road. **EXERCISE CAUTION**. Spectacular views of upper part of Dakota Formation, Tropic Shale and overlying Straight Cliffs Formation. The Tropic Shale is about 700 feet thick at this locality but may be structurally compressed due to folding. The lower part of the formation is calcareous and contains several distinctive fossiliferous concretionary zones and bentonite beds. Bentonite beds A-D in the lower part of the Tropic Shale are well exposed along this road cut. Bentonite A lies in the upper Cenomanian biozone of *Euomphaloceras septemseriatum* and has been dated at 93.49 +/- 0.89 Ma (Obradovich, 1993). Bentonite B, which lies higher in the upper Cenomanian biozone of *Neocardioceras juddii*, was dated at 93.59 +/- 0.58 Ma (Obradovich, 1993). Bentonite C, which may lie in the lower Turonian biozone of *Pseudaspidoceras flexuosum*, was dated at 93.25 +/- 0.55 Ma, and bentonite D, in the lower Turonian biozone of *Vascoceras birchbyi*, was dated at 93.40 +/- 0.63 Ma (Obradovich, 1993).

        The upper part of the lower Tropic calcareous unit contains *Collignoniceras woollgari* of early middle Turonian age. At the Cenomanian-Turonian boundary reference section near Pueblo, Colorado, *Collignoniceras woollgari* has been collected from the Fairport Member of the Carlile Shale (Cobban and Scott, 1972).

        Note the sharp color change in the upper part of the Tropic Shale from underlying medium gray to overlying dark gray color. This distinct color change, from calcareous to noncalcareous shale, represents the approximate first appearance of the ammonite *Prionocyclus hyatti* of middle Turonian age which is also found in the overlying Tibbet Canyon Member of the Straight Cliffs Formation. We recognize a similar sharp color change as far east as west-central Kansas, where it marks the contact of the underlying Fairport and Blue Hill Members of the Carlile Shale which are stratigraphically equivalent to the Tropic Shale.

        The Dakota-Tropic contact and the Tropic-Straight Cliffs contact are well exposed at this stop. Note the sharp transgressive surface separating the Dakota and Tropic, and the gradational upper Tropic-lower Straight Cliffs contact.

0.8   125.6   Cottonwood Wash begins to widen from here southward.

5.5   130.8   **STOP 9--** LOWER COTTONWOOD WASH. DAKOTA FORMATION-TROPIC SHALE CONTACT. Park along either side of the road. This stop offers an excellent opportunity to view the Dakota-Tropic contact and the various fossil horizons and bentonite horizons associated with this interval.

        The oldest marine fossils associated with the Tropic transgression are in these uppermost beds of the Dakota. Ammonites, although scarce, are represented by the presence of *Metoicoceras mosbyense* and *M. defordi.* This suggests an assignment to one of the zones of *Vascoceras diartianum*, *Dunveganoceras conditum*, or *D. albertense* and indicates an early late

195

Cenomanian age for the Dakota. The top of the Dakota at this locality contains several bivalve coquina zones characterized by the oyster *Exogyra (Costagyra) olisiponensis* Sharpe and *Flemingostrea prudentia* (White). Also, we found *Metoicoceras mosbyense* with *E. olisiponensis*, at this locality, which suggests that the *E. olisiponensis* assemblage lies at the top of the range of *M. mosbyense.* Inasmuch as the highest *M. mosbyense* occurs in the zone of *Vascoceras diartianum*, the highest beds of the Dakota here are assigned to this zone.

At the Cenomanian-Turonian boundary reference section near Pueblo, Colorado, the oldest marine fauna above the Dakota are in the lower middle Cenomanian *Conlinoceras terrantense* biozone in the Thatcher Limestone Member of the Graneros Shale. The lower upper Cenomanian *Metoicoceras mosbyense* biozone is in the lower part of the Hartland Shale Member of the Greenhorn Limestone (Cobban and Scott, 1972). Correlating these biozones provides valuable insight into the significant facies changes that occur within the mid-Cretaceous from the western to central parts of the Cretaceous Western Interior basin.

The lowermost concretionary zone of the overlying Tropic, which forms a distinct horizon about 15 to 20 feet above the base of the formation at this locality, contains the ammonite *Sciponoceras gracile* and associated fauna of the middle upper Cenomanian *Euomphaloceras septemseriatum* biozone.

This concludes our discussion of Cretaceous marine and brackish water strata of Grand Staircase-Escalante National Monument. The rocks and fossils along the fieldtrip route are a small but interesting part of the natural history of this unique and very scenic area.

1.1   131.9   Road continues south along Dakota-Tropic contact.

5.2   137.1   **END OF ROAD LOG.** Turn right on US 89 and continue west to Kanab and then north to Long Valley Junction (80 miles), and then west to Cedar City on Utah Highway 14 (41 miles).

REFERENCES

Cobban, W.A., Dyman, T.S., Pollock, G.L., Takahashi, K.I., Davis, L.E., and Riggin, D.B., 2000, Inventory of dominantly marine and brackish-water fossils from Late Cretaceous rocks in and near Grand Staircase-Escalante National Monument, Utah, *in* Sprinkel, D.A., Chidsey, T.C., and Anderson, P.B., editors, Geology of Utah's Parks and Monuments: Utah Geological Association Publication 28, p. 579-589.

Cobban, W.A., and Scott, G.R., 1972, Stratigraphy and ammonite fauna of the Graneros Shale and Greenhorn Limestone near Pueblo, Colorado: U.S. Geological Survey Professional Paper 645, 108 p.

Dalrymple, G.B., 1989, The GLM continuous laser system for ^{40}Ar/^{39}Ar dating--description and performance characteristics: U.S. Geological Survey Professional Paper 1176, 55 p.

Doelling, H.H., Blackett, R.E., Hamblin, A.H., Powell, J.D., and Pollock, G.L., 2000, Geologic guides to Grand Staircase-Escalante National Monument, Kane, and Garfield Counties, Utah, *in* Sprinkel, D.A., Chidsey, T.C., and Anderson, P.B., editors, Geology of Utah's Parks and Monuments: Utah Geological Association Publication 28, p. 1-70.

Dyman, T.S., Cobban, W.A., Pollock, G.L., Takahashi, K.I., Davis, L.E., and Riggin, D.B., 2000, Inventory of dominantly marine and brackish water fossils from Lower Cretaceous rocks in

and near the Grand Staircase National Monument, Utah, *in* Anderson, P.B., and Sprinkel, D.A., editors, Geologic road, trail, and lake guides to Utah's parks and monuments: Utah Geological Association Publication 29, one CD-ROM.

Eaton, J.G., 1991, Biostratigraphic framework for the Upper Cretaceous rocks of the Kaiparowits Plateau, southern Utah, *in* Nations, J.D., and Eaton, J.G., editors, Stratigraphy, depositional environments, and sedimentary tectonics of the western margin, Cretaceous Western Interior seaway: Geological Society of America Special Paper 260, p. 47-60.

Eaton, J.G., Laurin, J., Kirkland, J.I., Tibert, N.E., Leckie, R.M., Sageman, B.B., Goldstrand, P.M., Moore, D.W., Straub, A.W., Cobban, W.A., and Dalebout, J.D., 2001, Cretaceous and early Tertiary geology of Cedar and Parowan Canyons, western Markagunt Plateau, Utah, *in* Erskine, M.L., Faulds, J.E., Bartley, J.M., and Rowley, P.D., editors, The geologic transition, high plateaus to Great Basin- a symposium and field guide- the Mackin Volume: Utah Geological Association Publication 30, p. 337-364.

Elder, W.P., 1985, Biotic patterns across the Cenomanian-Turonian extinction boundary near Pueblo, Colorado, *in* Pratt, L.M., Kauffman, E.G., and Zelt, F.B., editors, Fine-grained deposits and biofacies of the Cretaceous Western Interior seaway--evidence of cyclic sedimentary processes: Society of Economic Paleontologists and Mineralogists Field Trip Guidebook No. 4, 1985 Midyear Meeting, p. 157-169.

_____ 1991, Molluscan paleoecology and sedimentation patterns of the Cenomanian-Turonian extinction interval in the southern Colorado Plateau region, *in* Nations, J.D., and Eaton, J.G., editors, Stratigraphy, depositional environments, and sedimentary tectonics of the western margin, Cretaceous Western Interior seaway: Geological Society of America Special Paper 260, p. 113-137.

Elder, W.P., and Kirkland, J.I., 1985, Stratigraphy and depositional environments of the Bridge Creek Limestone Member of the Greenhorn Limestone at Rock Canyon anticline near Pueblo, Colorado, *in* Pratt, L.M., Kauffman, E.G. and Zelt, F.B., editors, Fine-grained deposits and biofacies of the Cretaceous Western Interior seaway--evidence of cyclic processes: Society of Economic Paleontologists and Mineralogists Field Trip Guidebook No. 4, 1985 Midyear Meeting, p. 122-134.

Gregory, H.E., and Moore, R.C., 1931, The Kaiparowits region—A geographic and geologic reconnaissance of parts of Utah and Arizona: U.S. Geological Survey Professional Paper 164, p. 98-104.

Hettinger, R.D., 1995, Sedimentological descriptions and depositional interpretations, in sequence stratigraphic context, of two 300-meter cores from the Upper Cretaceous Straight Cliffs Formation, Kaiparowits Plateau, Kane County, Utah: U.S. Geological Survey Bulletin 2115-A, 32 p.

Hettinger, R.D., Roberts, L.N.R., Biewick, L.R.H., and Kirschbaum, M.A., 2000, Geologic Overview and Resource Assessment of Coal in the Kaiparowits Plateau, Southern Utah, chap. T of Kirschbaum, M.A., Roberts, L.N.R., and Biewick, L.R.H., editors, Geology and Resource Assessment of Coal in the Colorado Plateau: Arizona, Colorado, New Mexico, and Utah: U.S. Geological Survey Professional Paper 1625-B [available only on CD-ROM]; 68 p., 32 figs., 1 pl.

Hicks, F.H., Obradovich, J.D., and Tauxe, L., 1995. A new calibration for the Late Cretaceous time scale: The ^{40}Ar/^{39}Ar isotopic age of the C33r/C33n geomagnetic reversal from the Judith River Formation (Upper Cretaceous), Elk Basin, Wyoming, USA: The Journal of Geology, v. 103, 243-256.

Hintze, L.R., 1993, Geologic history of Utah: Brigham Young University Geology Studies Special Publication 7, 63 p.

Kirschbaum, M.A., Roberts, L.N.R., and Biewick, L.R.H., editors, 2000, Geologic assessment of

coal in the Colorado Plateau: Arizona, Colorado, New Mexico, and Utah: U.S. Geological Survey Professional Paper 1625-B, version 1.0, 2 CD-ROM set.

Leithold, E.L., 1994, Stratigraphical architecture of the muddy margin of the Cretaceous Western Interior seaway, southern Utah: Sedimentology, v. 41, p. 521-542.

Obradovich, J.D., 1993, A Cretaceous time scale, *in* Caldwell, W.G.E., and Kauffman, E.G., editors, Evolution of the Western Interior basin: Geological Association of Canada Special Paper 39, p. 379-396.

Peterson, Fred, 1969, Four members of the Straight Cliffs Formation in the southeastern Kaiparowits region, Kane County, Utah: U.S. Geological Survey Bulletin 1274-J, 28 p.

Petzet, G.A., 1997, Monument jeopardizes area of Utah's resources: Oil and Gas Journal, March 24, 1997, p. 69-72.

Seitz, Otto, 1967, Die Inoceramen des Santon und Unter-Campan von Nordwestdeutschland; II, Teil; biometrie, dimorphismus and stratigraphie der untergattung *Sphenoceramus* J. Boehm: Geologisches Jahrbuch Beihefte, no. 69, 194 p., 26 plates.

Shanley, K.W., and McCabe, P.J., 1991, Predicting facies architecture through sequence stratigraphy—an example from the Kaiparowits Plateau, Utah: Geology, v. 19, p. 742-745.

Shanley, K.W., McCabe, P.J., and Hettinger, R.D., 1992, Tidal influence in Cretaceous fluvial strata from Utah—a key to sequence stratigraphic interpretation: Sedimentology, v. 39, p. 905-930.

Troeger, K.A., 1987, Problems of Upper Cretaceous inoceramid biostratigraphy and paleogeography in Europe and western Asia, *in* Wiedmann, J., editor, Cretaceous of the western Tethys: Proceedings of the Third International Cretaceous Symposium, Tubingen, p. 911-930.

Zelt, F.B., 1985, Natural gamma-ray spectrometry, lithofacies, and depositional environments of selected Upper Cretaceous marine mudrocks, western United States, including Tropic Shale and Tununk Member of Mancos Shale: Princeton, New Jersey, Princeton University, Ph.D. Dissertation, 161 p.

THE GEOLOGY OF THE GRAND STAIRCASE IN SOUTHERN UTAH: A ROAD LOG AND GUIDE FOR PUBLIC SCHOOL TEACHERS

Larry E. Davis, Department of Geology, College of St. Benedict / St. John's University, Collegeville, MN 56321

Robert L. Eves, Division of Geosciences, Southern Utah University, Cedar City, UT 84720

THE GEOLOGY OF THE GRAND STAIRCASE IN SOUTHERN UTAH: A ROAD LOG AND GUIDE FOR PUBLIC SCHOOL TEACHERS

Larry E. Davis, Department of Geology, College of St. Benedict / St. John's University, Collegeville, MN 56321

Robert L. Eves, Division of Geosciences, Southern Utah University, Cedar City, UT 84720

As we started on, we left behind a long line of cliffs, many hundred feet high, composed of orange and vermilion sandstones. Have named them "Vermilion Cliffs". When we were out a few miles I looked back and saw the morning sun shining in splendor on their painted faces. The salient angles were on fire, and the retreating angles were buried in shade. I gazed and gazed until my vision dreamed, and the cliffs appeared a long bank of purple clouds piled high from the horizon high into the heaven.
John Wesley Powell, 1869

In many places, canyons have cut the terrace platform deeply, and open in magnificent gateways upon the broad desert plain in front. We look into them from afar, wonderingly and questioningly, with a fancy pleased to follow their windings until their sudden turns carry them into distant, unseen depths.
Clarence E. Dutton, Surveyor, Powell Expedition
Tertiary History of the Grand Canyon District, 1882

       The "Grand Staircase" is a majestic geological feature of unparalleled beauty and mystery. Many of the secrets of Earth's history are contained within the various rock formations exposed at each step. One might imagine each step as a book; each formation as a chapter in the book; and each rock layer as a page. The books are stacked and slightly offset with the spines facing northward. Each page records in the special hieroglyphics of geology the events of the past - the timeless currents of a tropical marine sea, the shifting sands of a vast desert, the meandering flow of rivers to the sea. As one climbs over the steps, interpreting the geological record, Earth's secrets are revealed. The "books" have been set aside for all to read and enjoy in Grand Canyon, Zion, and Bryce Canyon National Parks and the Grand Staircase-Escalante National Monument (GSENM).

General Overview of the Grand Staircase

       The term "Grand Staircase" was first applied to this region by Charles Keyes (1924). The series of topographic benches and cliffs, which form the "Grand Staircase", step progressively up in elevation from south to north (figure 1). The risers correspond to cliffs and the steps correspond to the broad benches, terraces, or plateaus in the staircase (figure 2). The bottom of the staircase commences at the top of the Kaibab Uplift, which correlates with, and is in the same stratigraphic position as, the highest bench of the Grand Canyon in Arizona. The first riser above the bench is the Chocolate Cliffs, which are not well developed and consist of the upper red member of the Lower Triassic Moenkopi Formation capped by the Upper Triassic Shinarump Conglomerate Member of the Chinle Formation. The next step is known as the Shinarump Flats. This bench is mostly developed on top of the resistant Shinarump Conglomerate Member and in the overlying, less resistant, Petrified Forest Member of the Chinle Formation. The Vermilion Cliffs form the next riser, which is well developed in the GSENM. The cliffs are composed of the resistant red sandstone beds of the Lower Jurassic Moenave and Kayenta Formations. The Wygaret Terrace forms the next step and includes the soft upper part of the Kayenta and the lower part of the Lower Jurassic Navajo Sandstone. The imposing White Cliffs form the next riser and consist of the upper part of the Navajo Sandstone and the Middle Jurassic Co-op Creek Limestone Member of the Carmel Formation. The bench on this riser is the Skutumpah Terrace built on the remaining soft parts of the Carmel Formation and the overlying Entrada Formation. The Gray Cliffs are a series
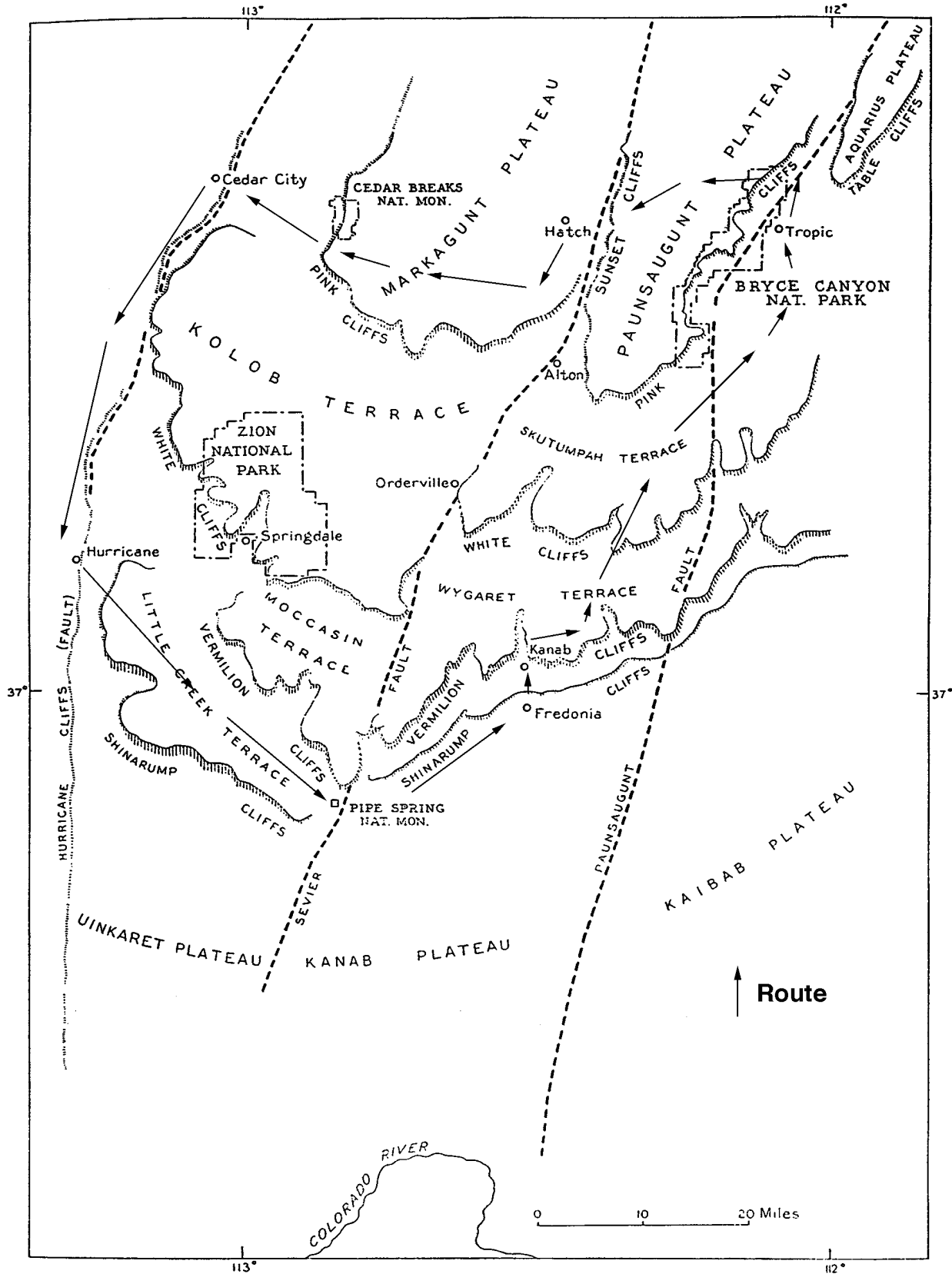
Figure 1. Sketch map showing the position of major plateaus, terraces, and cliffs in the Grand Staircase (after Gregory, 1950).

Formations, members, and thicknesses in feet		Map Symbol		Paunsaugunt Plateau
Claron Formation ~1,400	White mbr.	Tcw		
	Pink mbr.	Tcp		Pink Cliffs
Pine Hollow Fm. Grand Castle Fm. Canaan Peak Fm.	0-1,300	TKc	- K/T -	
Kaiparowits Formation 2,000-3,000		Kk		
Wahweap Formation 1,000-1,500		Kw		
Straight Cliffs Fm. 900-1,800	Drip Tank Mbr.	Ks		Grey Cliffs
	John Henry Mbr.			
	Smoky Mtn. Mbr.			
	Tibbet Cyn. Mbr.			
Tropic Shale 500-750		Kt		
Dakota & Cedar Mtn Fms. 3-370		Kd	- J/K -	
Morrison Formation 0-950		Jm	- J-5 -	
Entrada Ss. 0-1,000	Escalante Mbr.	Je		Skutumpah Terrace
	Cannonville Mbr.			
	Gunsight Butte Mbr.			
Carmel-Page Fms. 180-1,040	Upper	Jcu	Jc	
	Lower	Jcl	- J-1/J-2 -	
Navajo Sandstone 1,300-1,500	Main body	Jn		White Cliffs
	Tenney Cyn Tongue	Jkt		
	Lamb Pt. Tongue	Jnl		
Kayenta Formation 150-350		Jk		Vermilion cliffs
Moenave Fm & Wingate Ss 100-350		Jmo Jw	- J-0 -	
Chinle Fm. 425-930	Petrified Forest Mbr.	Trc		Wygaret Terrace
	Shinarump Mbr.		- Tr-3 -	Chocolate Cliffs
Moenkopi Fm. 440-1,150	Upper red mbr.	Trm		
	Shnabkaib Mbr.			
	Middle red mbr.			
	Virgin, lower red, & Timpoweap		- P/Tr -	
Permian Fms. 655+	Kaibab Fm.	P		Kaibab Plateau
	Toroweap-White Rim-Coconino			
	Hermit Fm.			

Figure 2. Grand Staircase Stratigraphy (adopted from Doelling and others, 2000, p. 201).

202

of low cliffs formed by hard Cretaceous sandstone and less resistant shale beds. Several benches have formed between these cliffs in the softer shale beds and sandstones of the Tropic, Straight Cliffs, Wahweap, and Kaiparowits Formations. The final riser, mostly north and west of the monument, in Dixie National Forest and Bryce Canyon National Park, is formed by the Pink Cliffs. The Pink Cliffs consist of lower Tertiary limestones and marls of the Claron Formation that are sculpted into the beautiful natural features found in Bryce Canyon. The cliffs culminate as the Paunsaugunt Plateau, which is the uppermost bench or step of the "Grand Staircase."

Geologic History

The Grand Canyon records the earliest history of the Colorado Plateau, albeit some chapters and pages are missing. Although the rocks exposed in the Grand Canyon are not part of this field trip, a brief discussion of the upper Grand Canyon sequence is provided.

The rocks of the Grand Staircase reveal nearly 275 million years of geologic history (Hintze, 1988). Permian age rocks are the base of the Grand Staircase. Deposition of these rocks occurred when the North American plate occupied an equatorial position, with the Colorado Plateau region located slightly south of the paleoequator (Levin, 1999). The environment was transitional consisting of lowland streams, flood plains, and marine tidal flats that deposited the sandstones and mudstones of the Hermit Shale and Toroweap Formation. To the east, dunes of wind blown sand in a vast desert formed the White Rim Sandstone exposed in Capitol Reef and Canyonlands National Parks. Further to the east in Colorado lay the Uncompahgre Uplift and adjacent fluvial and coastal plains (figure 3). The Kaibab Sea transgressed from the west far enough eastward to deposit the fossiliferous Kaibab Limestone on top of the Hermit Shale and Toroweap Formations. The Hermit Shale, Toroweap, and Kaibab Formations crop out in the upper Grand Canyon sequence, the Virgin River Gorge southwest of St. George, Utah, and in the Circle Cliffs in the GSENM. During this field trip we will observe the Kaibab Limestone in route to Stop 1.
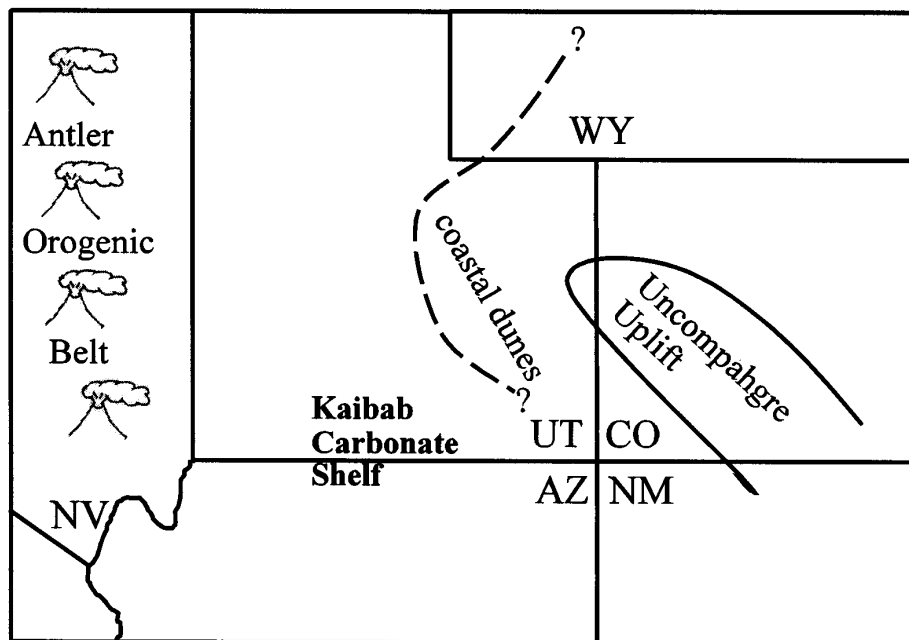
Figure 3. Permian paleogeography of the Four Corners area during deposition of the Kaibab Limestone (adopted from Condon, 1997).

The end of the Permian represents the largest extinction event recorded in the fossil record. A 10-million year unconformity, the Tr-1, separates Permian and Triassic rocks, and represents a period of subaerial exposure and erosion of the Kaibab Limestone. The early Triassic represents a continuation of the Permian paleogeography, with North America occupying an equatorial position. The Grand Staircase region formed a western interior basin with an Antler - Mogolion volcanic arc to the west-southwest and the Uncompahgre Uplift and ancestral Rocky Mountains to the east-northeast and the basin accumulated a thick sequence of marginal marine se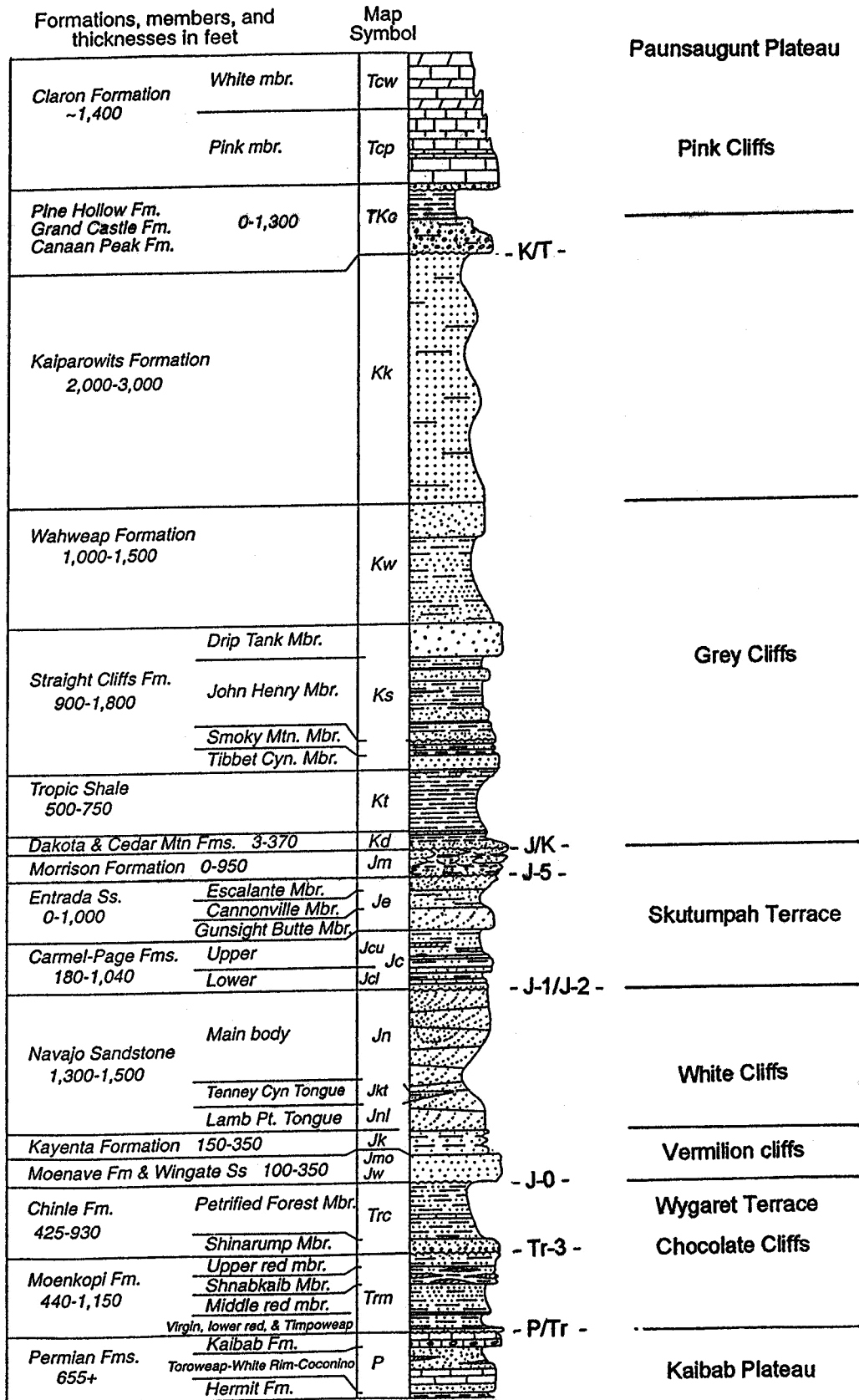diments (figure 4). The basal Rock Canyon Conglomerate Member, characterizing the beginning of Moenkopi deposition, is a chert pebble conglomerate. The resistant cherts came from the underlying Kaibab Limestone, while the Uncompahgre Uplift supplied finer-grained sediments. Blakely and others (1993) have

documented four major transgressive/regressive cycles in the Moenkopi. Minerals in the Moenkopi attest to the arid climate of southern Utah during early Triassic time. Poorly circulated, mineral-rich, waters of the western interior basin were evaporated, depositing beds of gypsum and gypsiferous siltstone, common components of the Moenkopi. Similar conditions exist today in the Persian Gulf region.
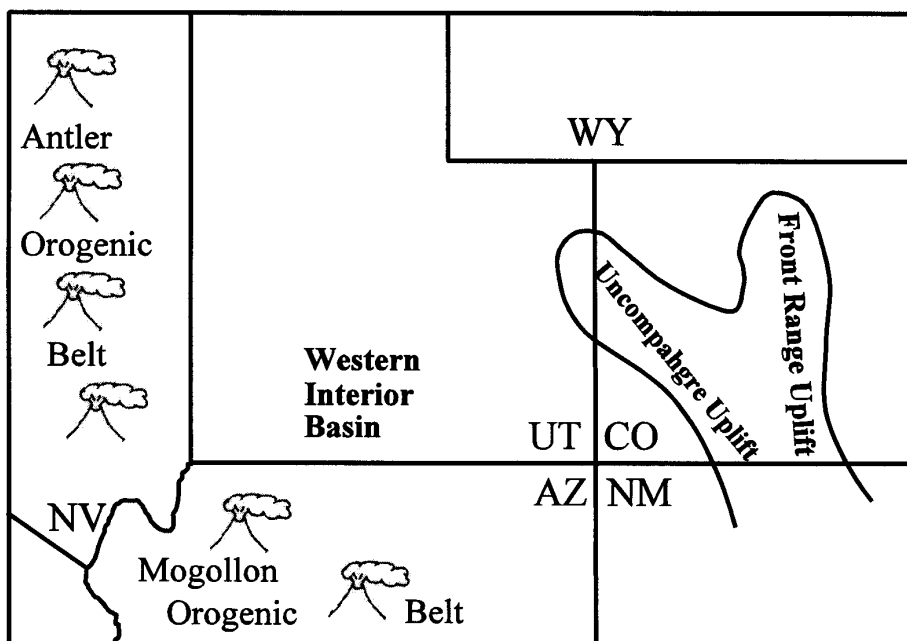
Figure 4. Triassic paleogeography of the Four Corners area during deposition of the Moenkopi and Chinle Formations (adopted from Dubiel, 1994).

Moenkopi deposition ceased by the end of the early Triassic and an interval of exposure and erosion lasting 20-million years ensued. Blakey and Gubitosa (1983) recognized deep channels cut into the Moenkopi. This unconformity is designed the Tr-3, and is overlain by the Shinarump Conglomerate, the basal member of the Chinle Formation, which marks the beginning of late Triassic deposition on the Colorado Plateau. The 500-foot-thick Chinle Formation consists of conglomerates, sandstones, siltstones, shales, and fresh-water limestones deposited in a variety of terrestrial environments, including broad fluvial flood plains, lakes, and marshes. The Chinle is easily recognized by its resistant, gray-brown basal conglomerate and the overlying finer sediments with a variegated pattern of purple, red, green, gray, and brown colors, which weather into rounded, low-lying hills and knobs. The highlands surrounding the extensive Chinle depositional basin supplied these sediments. The abundant volcanic ash associated with Chinle deposition, derived from a western volcanic arc, has altered to bentonite, which develops a popcorn-like surface texture following a rainfall. The Chinle and under lying upper red member of the Moenkopi constitute the Chocolate Cliffs of the Grand Staircase, and also provides the colorful backdrop for the Painted Desert of northern Arizona. The Chinle is perhaps most famous for its petrified wood found in the Petrified Forest Member.

Dubiel (1994) characterizes the Late Triassic climate of the North American western interior as tropical with seasonally high rainfall (monsoons). Evidence for this interpretation includes organic-rich lake and marsh deposits, as well as a fossil record of diverse vegetation. Fluctuating water tables produced alternating oxidizing (dry) and reducing (wet) conditions in the iron-rich sediments resulting in the variegated colors of these fine-grained, low-energy, deposits (Dubiel and others, 1987). Gradually the region became more arid as evidenced by eolian dune and playa lake deposits at the top of the formation. This pattern of aridity continues into the Jurassic Period.

A 5- to 10-million year period of non-deposition and erosion marks the Late Triassic and Early Jurassic transition and is termed the J-0 unconformity. The arid conditions initiated in the latest Triassic, which prevailed throughout the Jurassic, were brought about by changes in North American paleogeography due to the breakup of Pangaea. Tectonic activity to the west continued to produce periodic volcanic ash eruptions, as well as the initiation of a series of orogenic events, beginning with the Nevadan orogeny, which would continue sporadically for the next 150 million years.

During the Early Jurassic much of the Colorado Plateau experienced desert-like conditions and deposition of extensive eolian sands, exceeding 2,000 feet in thickness. Extensive tidal flat deposits form the lower Moenave Formation and consist of fine-grained sandstones and silty sandstones. These lithologies eventually give way to the stream-deposited, channeled sands and muddy overbank flood plain deposits of the upper Moenave and Kayenta Formations. The upper Moenave consists of mudstones and siltstones to fine-grained sandstones with thin, discontinuous lenses of intraformational conglomerates. The Kayenta Formation consists primarily of siltstones and fine-grained sandstones. The red-hued, resistant sandstones of the Moenave and Kayenta Formations make up the spectacular Vermilion Cliffs of the Grand Staircase. Both the Moenave and Kayenta Formations share a complex intertonguing relationship with the deposition of eolian sands to the north and east. Eventually, a gradual south-southwestern expansion of the Navajo Desert overtakes the Kayenta fluvial plain (figure 5), and by the Middle Jurassic, the Grand Staircase region is engulfed in desert-like conditions.

Figure 5. Early Jurassic paleogeography of the Four Corners area during deposition of the Navajo Sandstone (adopted from Peterson, 1994).

The high cliffs of spectacularly cross-bedded, white Navajo Sandstone represents the largest preserved coastal and inland eolian system in the geologic record of North America (Blakey and others, 1988; Peterson, 1988; Peterson and Turner-Peterson, 1989), and forms the distinctive White Cliffs of the Grand Staircase. The Navajo Sandstone is well known for its lithological uniformity, consisting of moderately well-cemented, well-rounded, frosted, fine- to medium-grained quartz grains. The sand was likely recycled from Paleozoic and Triassic sandstones to the north, possibly as far north as Alberta, and from local sources (Peterson, 1988). The large-scale cross-bedding of the Navajo is similar to the large, high relief dunes of the Sahara in North Africa. In Zion National Park, measurements of single cross-bed sets suggest a minimum dune relief of 60+ feet.

Toward the end of the Middle Jurassic, sea level began to rise once again and the Sundance Seaway transgressed southward from Idaho and Wyoming (figure 6), but arid terrestrial conditions continued in the region and deposition was dominated by eolian processes. The upper Navajo Sandstone underwent a period of erosion, known as the J-1 unconformity, marked by a discontinuous layer of chert pebbles. In southwestern Utah, the J-1 unconformity is capped by a west-thickening wedge of eolian-derived sandstone. The position of this sandstone atop the Navajo forms a cap on the many "temples" of Zion National Park, and hence the name Temple Cap Sandstone. Erosion of the Temple Cap Sandstone resulted in a patchy distribution and produced the J-2 unconformity. In places, the J-2 and lower J-1 unconformities merge (Brenner and Peterson, 1994**).**
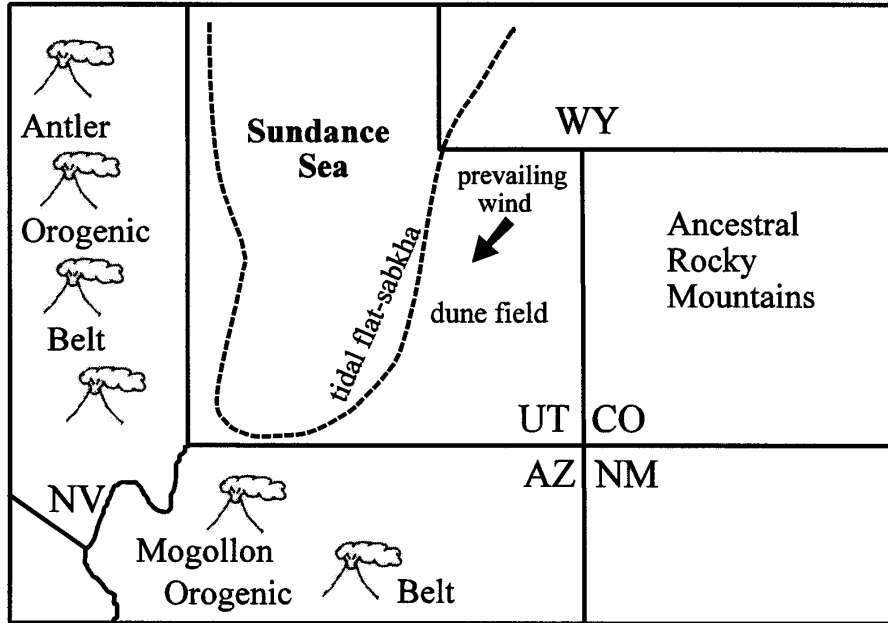
Figure 6. Middle Jurassic Paleogeography of the Four Corners area during deposition of the Carmel Formation and Page Sandstone (adopted from Peterson, 1994).

Continued rise of sea level eventually reached into the Grand Staircase region and signaled the return of marine deposition as evidenced by the Carmel Formation overlying the J-2 erosional surface. Eolian deposition continued in south central Utah with the deposition of the Page Sandstone. The Carmel Formation and Page Sandstone intertongue in the Paria River area, and reflect one of the complex interplays between marine, sabkha, fluvial, and eolian depositional systems typical of Carmel sedimentation (figure 7). The Carmel Formation even contains volcanic material, but the source area for these volcanics is disputed (Chapman, 1993, Riggs and Blakey, 1993). In the Grand Staircase region, the Carmel Formation consists of five members, including a tongue of the Page Sandstone called the Thousand Pockets Member. The Carmel Formation also contains several fossiliferous limestone and shale units. The presence of gypsum beds, such as those found in the Paria River Member, are indicative of highly evaporitic conditions in poorly circulating waters of the Sundance Seaway.
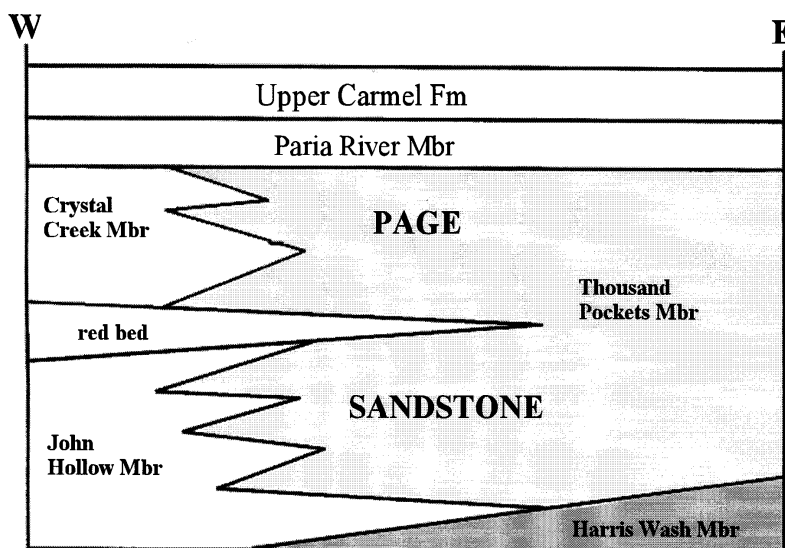
Figure 7. Intertonguing relationship of the Carmel Formation and the Page Sandstone (adopted from Blakely, 1994).

206

As the Sundance Sea withdrew northward near the end of the Middle Jurassic, another eolian system quickly advanced over the region and initiated deposition of the Entrada Formation (figure 8). Prior to Cenozoic erosion, the Entrada probably covered the entire Colorado Plateau region (Peterson, 1994). The Entrada is highly variable, but at most localities in the Grand Staircase region, the Entrada is a cross-bedded eolian sandstone (Peterson, 1994). In the GSENM, the Entrada Formation consists of three members (in ascending order) the Gunsight Butte Member, the Cannonville Member, and the Escalante Member. We will observe only the lower two members on this field trip.
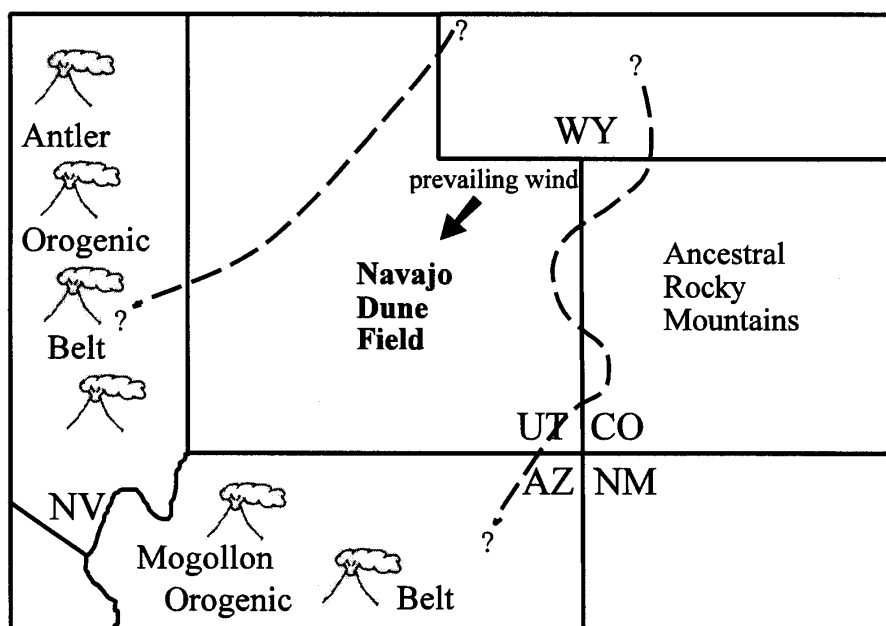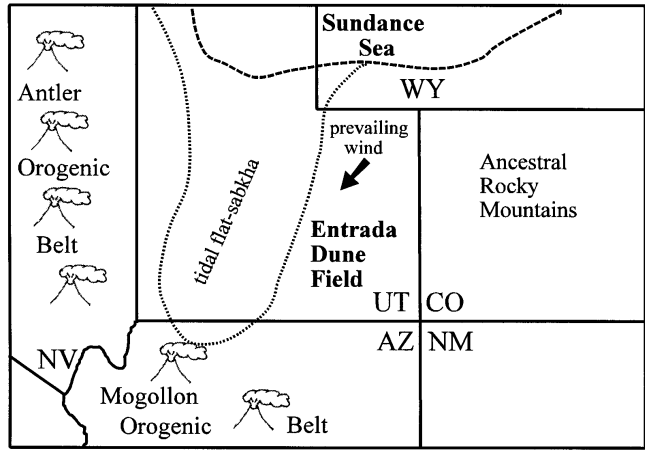

Figure 8. Late middle Jurassic paleogeography of the Four Corners area during deposition of the Entrada Sandstone (adopted from Peterson, 1994).

The Gunsight Butte Member weathers into sandstone cliffs and rounded, bare knobs. The sandstones are reddish-orange, silty to fine grained, with sparse medium to coarse, frosted, subrounded to rounded grains of pink and gray quartz (Doelling and others, 2000). The Cannonville Member generally forms steeper slopes of yellow-white sandstone with faint red bands. The Cannonville Member consists of interbedded, very fine-grained sandstones, silty sandstones, and siltstones (Doelling and others, 2000).

The Cretaceous Sevier orogeny represents a time of renewed mountain-building activity in western North America. At the same time, sea level began to rise to form the Cretaceous Western Interior Seaway, which eventually extended from the Gulf of Mexico northward into the Yukon and the Northwest Territories of Canada to connect with the Arctic Ocean (figure 9).

The Cretaceous rocks of the Colorado Plateau are dramatically different from the soft pastel and brilliant orange/red colored rocks lying below. Cretaceous rocks are more subdued shades of gray, brown, and yellow and form the Grey Cliffs of the Grand Staircase. Thick, resistant sandstones alternate with equally thick and less resistant shales to form a 3,000-4,000 foot thick sequence of cliffs and slopes.
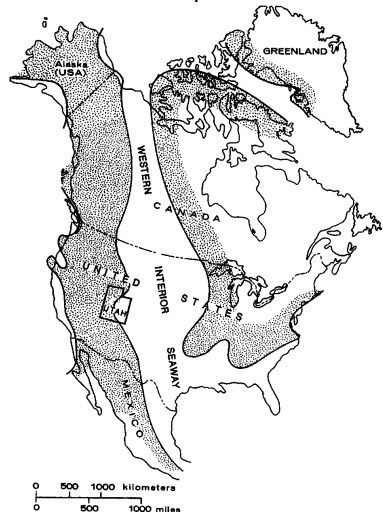
Figure 9. The Cretaceous Western Interior Seaway and emergent land areas in North America (stippled pattern) during the Late Cretaceous (from Peterson and Turner-Peterson, 1989).

207

The oldest stratum of the Grey Cliffs is the Dakota Sandstone. The Dakota Sandstone is composed of sandstone, conglomerate, mudstone, siltstone, and coal deposited in coastal, flood plain, and shallow marine environments. In the region of the Grand Staircase, the Dakota averages 200-300 feet thick, but thins to the east. The base of the formation is identified by a coarse pebble and cobble conglomerate that persists throughout most of the region (Cobban and others, 2000), and grades upward into finer sediments containing carbonaceous material and thin coal seams. The uppermost Dakota is marked by an oyster (*Exogyra olisiponensis* Sharpe) coquina horizon and organic-rich shale, which represents the first of four transgressive-regressive cycles during the Cretaceous.

The blue-gray Tropic Shale overlies the Dakota Formation in the Grand Staircase region and represents deposition of muds in the deeper waters of the Cretaceous Western Interior Seaway. In the GSENM, the Tropic Shale averages 700 to 900 feet thick and forms distinctive slopes prone to landslides and slumps. Bentonite beds are abundant throughout the Tropic and are correlated with well-established ammonite biozones (Cobban and others, 2000). The lower part of the Tropic contains several distinctive calcareous concretionary zones. The limestone concretions yield an extremely rich molluscan fauna, particularly ammonoids, which are useful in biostratigraphic correlations (Cobban and others, 2000). The upper Tropic becomes sandy as it grades into the overlying Straight Cliffs Formation.

The 900- to 1,800-foot-thick Straight Cliffs Formation represents the final regressive phase of the Cretaceous Western Interior Seaway and consists of four distinctive members. In ascending order, the basal Tibbet Canyon Member is a resistant, cliff-forming, shallow marine sandstone; the Smokey Hollow Member consists of ledge- and cliff-forming, lagoonal and flood plain shales and sandstones; the John Henry Member is a slope- and ledge-former of deltaic and fluvial shales, coals, and sandstones; and the upper, prominent cliff-forming, fluvial deposited, coarse-grained sandstones of the Drip Tank Member. The Tibbet Canyon and Smokey Hollow Members represent the regressive phase of the Cretaceous Western Interior Seaway (Doelling and others, 2000) and are the only members of the formation known to contain marine fossils (Cobban and others, 2000).

Two major coal seams in the John Henry Member represent significant economic deposits. These coal deposits were at the center of the initial controversy involving the GSENM. These coals have been studied (Hettinger and others, 1996) and several companies have expressed an interest in mining these them. Mining is bitterly opposed by environmental groups. Dutch-owned Andalex Resources was moving forward with plans for mining operations, but stopped when the GSENM was established by Presidential Proclamation on September 18, 1996.

Overlying the Straight Cliffs Formation are slope forming, finergrained sediments of the Wahweap Formation. More resistant, cliff-forming sandstones are present in the upper part of the Wahweap. The 1,000- to 1,500-foot-thick Wahweap is composed of interbedded, less-resistant mudstones and siltstones and resistant and non-resistant sandstones and conglomerates (Doelling and others, 2000). Wahweap sediments accumulated in fluvial, flood plain, and lacustrine environments, resulting in locally rich, fossil bearing deposits. Fossils include petrified wood, vertebrates (including dinosaurs), and gastropods.

The Kaiparowits Formation tops of the Grey Cliffs, and consists of over 2,000 feet of slope- and badlands-forming, drab gray to olive-gray shales and subarkosic sandstones. The Kaiparowits Formation cuts deeply into the eroded upper Wahweap Formation. Doelling and others (2000) describes the subarkosic sandstone as mostly very fine to fine grained, poorly sorted, and weakly cemented with calcite. The grains are mostly quartz, with orthoclase, albite, biotite, calcite, gypsum, clay, iron, and bits of coal or charcoal. Mudstones, siltstones, and sandy limestones and limey siltstones probably represent lacustrine deposits on a subsiding alluvial plain (Doelling and others, 2000). Vertebrate fossils, including dinosaurs, are common in the Kaiparowits Formation, particularly in the lower half of the formation (Eaton and others, 1999).

The close of the Cretaceous Period was punctuated by a global extinction event that obliterated 65 percent of the known species, including the 140-million year reign of the dinosaurs. Changes in depositional environments followed as the Cretaceous Western Interior Seaway receded. Sevier orogenic events had ended during the Cretaceous, and, to the west, the Sevier Highlands were gradually reduced by erosion during early Paleogene time. During the latest Cretaceous, and continuing into the early Paleogene, renewed mountain building (the Laramide orogeny) was initiated (Elston and Young, 1989). The Laramide resulted in the final stage of the formation of the North American Cordillera - the Rocky Mountains. The Laramide orogeny partitioned the Sevier foreland basin into a series of internally drained, non-marine, depositional basins bounded by basement-cored uplifts (Dickinson and others, 1986; Goldstrand, 1994). Large lakes began to occupy the inter basins, which extended from southwestern Wyoming to southwestern Utah. Uplifted areas produced by the Laramide orogeny became the main source of sediments, which filled the basins.

Stratigraphically, in the region of the Grand Staircase, the Canaan Peak, Grand Castle, and Claron Formations overly the Kaiparowits. The Canaan Peak Formation spans the K-T boundary. Both the Canaan Peak and Grand Castle Formations are conglomeratic, with the Canaan Peak being composed mainly of quartzite and felsic volcanic clasts, whereas, the Grand Castle Formation is composed mostly of quartzite and limestone clasts. The Claron Formation forms the Pink Cliffs, and uppermost step of the Grand Staircase.

The Claron Formation consists of two informal members, a lower pink limestone member and an upper white limestone member (Bowers, 1972). Ott (1999) recognized a cyclicity in deposition due to fluctuating lake levels. These two members are laterally continuous throughout the Markagunt, Paunsaugunt, Seiver, and Table Cliffs Plateaus. In the Bryce Canyon area, a discontinuous conglomerate unit found at the base of the lower pink member is less than 20 meters thick and contains well-rounded clasts of quartzite, chert, and limestone and is considered to be the Grand Castle Formation by Bowers (1972). Due to the lack of definitive age indicators, the Claron Formation is inferred by Bowers (1972) to be middle to late Eocene in age. At Bryce Canyon, a 35-meter thick conglomerate unit lies unconformably above the lower pink and upper white members of the Claron Formation and has been informally designated as the Conglomerate at Boat Mesa by Bowers (1990).

The timing and mechanism for the uplift of the Colorado Plateau and formation of the Grand Staircase is controversial. Baars and others (1988, p. 111) state that the Colorado Plateau is structurally unique in that it has been only moderately deformed compared to the more intensely deformed regions around it and appears to have behaved as a relatively stable structural unit during Laramide deformation. According to Peterson and Turner-Peterson (1989) regional uplift and volcanic activity were initiated by the Oligocene (late Paleocene). The resulting cinder cones and lava flows can be observed throughout the region, such as the volcanics from the Mount Dutton caldera, which cap the northern end of the Paunsaugunt Plateau. More recently, faulting brought on by crustal extension formed tilted fault blocks that result in the north-south-trending basins and ranges in western Utah and Nevada. The Grand Staircase is located to the east of the Basin and Range Province, and the Johnson Canyon and Paunsaugunt faults are the easternmost of the basin and range faults. The GSENM sits at the southern end of the dissected high plateau topography resulting from these faults. This movement continues to the present.

Following a period of aridity in the late Oligocene to middle Miocene, the Colorado River captured the flow of the Green River and the Green and Colorado river drainages were fully integrated by the early Pliocene (Peterson and Turner-Peterson, 1989; Elston and Young, 1989). By the end of the Pliocene, erosion of the Colorado River through the relatively soft Paleozoic strata had cut the Grand Canyon close to its present depth and most of the present character of the Colorado Plateau had been achieved (Peterson and Turner-Peterson, 1989).

Due to alpine and plateau glaciation, some landscape modification occurred during the Pleistocene. During the last phase of Pleistocene glaciation, the Clovis people (mammoth hunters) followed the Siberian mammoth herds across the Barrengia landmass (Bering land bridge) from Asia into southern Alaska and the Yukon Territory. These early hunters probably gave rise to the Folsom people (bison hunters). No direct evidence of Clovis or Folsom peoples exist on the Colorado Plateau; however, the region has yielded an assemblage of Late Pleistocene megafauna, including mammoths and mastodons, the giant ground sloth, musk and shrub oxen, camels, bison, several species of ancestral horses, and three species of bear (Nelson, 1990). Humans had arrived on the Colorado Plateau about 12,000 years B.P., during the waning stages of Pleistocene glaciation.

Holocene erosion has continued to deepen canyons, but only slightly. The nature of Holocene erosion and deposition have not changed since the Powell's explorations of the plateau country in the late 1800s.   The impact of modern humans on the landscape continues to be accessed and debated.

REFERENCES

Baars, D.L., and 15 others, 1988, Basins of the Rocky Mountain region, *in* Sloss, L.L., editor, Sedimentary cover-North American craton: U.S.: Geological Society of America, The Geology of North America, v. D-2, p. 109-220.

Best, M.G., McKee, E.H., and Damon, P.E., 1980, Space-time-composition patterns of late Cenozoic mafic volcanism, southwestern Utah and adjoining areas: American Journal of Science, v. 280, p. 1035-1050.

Blakey, R.C., and Gubitosa, R., 1983, Late Triassic paleogeography and depositional history of the Chinle Formation, *in* Reynolds, M.W. and Dolly, E.D., editors, Mesozoic paleogeography of the west-central United States: Rocky Mountain Section, Society of Economic Paleontologists and Mineralogists, p. 57-76.

Blakey, R.C., Peterson, F., and Kocurek, G., 1988, Synthesis of late Paleozoic and Mesozoic eolian deposits of the Western Interior of the United States: Sedimentary Geology, v. 56, p. 3-125.

Blakey, R.C., Basham, E.L., and Cook, M.L., 1993, Early and Middle Triassic paleogeography of the Colorado Plateau and vicinity, *in* Morales, M., editor, Aspects of Mesozoic geology and paleontology of the Colorado Plateau: Museum of Northern Arizona Bulletin 59, p. 13-26.

Blakey, R.C., 1994. Paleogeographic and tectonic controls on some Lower and Middle Jurassic erg deposits, Colorado Plateau, *in* Caputo, M.V., Peterson, J.A., and Franczyk, K.J., editors, Mesozoic systems of the Rocky Mountain region, USA, p. 273-298.

Bowers, W.E., 1972, The Canaan Peak, Pine Hollow, and Wasatch Formations in the Table Cliffs region, Garfield County, Utah: U.S. Geological Survey Bulletin 1331-B, 39 p.

Bowers, W.E., 1990, Geologic map of Bryce Canyon National Park and vicinity, southwestern Utah: U.S. Geological Survey Miscellaneous Investigations Series Map I-2108, scale 1:24,000.

Brenner, R.L., and Peterson, J. A., 1994, Jurassic sedimentary history of the northern portion of the western interior seaway, USA, *in* Caputto, M.V., Peterson, J.A., and Franczyk, K.J., editors, Mesozoic systems of the Rocky Mountain region, USA: Rocky Mountain Section, Society for Sedimentary Geology, p. 217-232.

Chapman, M.G., 1993, Catastrophic floods during the Middle Jurassic: Evidence in the upper member and the Crystal Creek Member of the Carmel Formation, southern Utah, *in* Dunne, G.C. and McDouglall, K.A., editors, Mesozoic paleogeography of the western United States II: Pacific Section, Society of Economic Paleontologists and Mineralogists, p. 407-416.

Christenson, G.E., editor, 1995, The September 2, 1992 ML 5.8 St. George earthquake, Washington County, Utah: Utah Geological Survey Circular 88, 41 p.

Cobban, W.A., Dyman, T.S., Pollock, G.L., Takahashi, K.I., Davis, L.E., and Riggin, D.B., 2000, Inventory of dominantly marine and brackish-water fossils from Late Cretaceous rocks in and near Grand Staircase-Escalante National Monument, Utah, *in* Sprinkel, D.A., Chidsey, T.C., and Anderson, P.B., editors, Geology of Utah's Parks and Monuments: Utah Geological Association Publication 28, p. 579-589.

Condon, S.M., 1997, Geology of the Pennsylvanian and Permian Cutler Group and Permian Kaibab Limestone in the Paradox basin southeastern Utah and southwestern Colorado: U.S. Geological Survey Bulletin 2000-P, P1-P46.

Dickenson, W.R., Lawton, T.F., and Inman, K.F., 1986, Sandstone detrital modes, central Utah and foreland regions - Stratigraphic record of Cretaceous-Paleocene tectonic evolution: Journal of Sedimentary Petrology, v. 56, p. 276-293.

Doelling, H.H., and Davis, F.D., 1989, The geology of Kane County, Utah - Geology, mineral resources, geologic hazards: Utah Geological and Mineral Survey Bulletin 124, 192 p.

Doelling, H.H., Blackett, R.E., Hamblin, A.H., Powell, J.D., and Pollock, G.L., 2000, Geology of Grand Staircase-Escalante National Monument, Utah, *in* Sprinkel, D.A., Chidsey, T.C., and Anderson, P.B., editors, Geology of Utah's Parks and Monuments: Utah Geological Association Publication 28, p. 189-231.

Dubiel, R.F., 1994, Triassic deposystems, paleogeography, and paleoclimate of the Western Interior, *in* Caputto, M.V., Peterson, J.A., and Franczyk, K.J., editors, Mesozoic Systems of the Rocky Mountain Region, USA: Rocky Mountain Section, Society for Sedimentary Geology, p. 133-168.

Dubiel, R.F., Blodgett, R.H., and Bown, T.M., 1987, Lungfish burrows in the Upper Triassic Chinle and Dolores Formations, Colorado Plateau: Journal of Sedimentary Petrology, v. 57, p. 512-521.

Eaton, J.G., Cifelli, R.L., Hutchison, J.H., Kirkland, J.I., and Parrish, J.M., 1999, Cretaceous vertebrate faunas from the Kaiparowits Plateau, south-central Utah, *in* Gillette, D.D., editor, Vertebrate paleontology in Utah: Utah Geological Survey Miscellaneous Publication 99-1, p. 345-354.

Elston, D.P., and Young. R.A., 1989, Development of Cenozoic landscape of central and northern Arizona: Cutting of Grand Canyon, *in* Elston, D.P, Billingsley, G.H., and Young, R.A., editors, Geology of Grand Canyon, Northern Arizona (with Colorado River Guides): American Geophysical Union, Field Trip Guidebook T115/315, p. 145-153.

Goldstrand, P.M., 1994, Tectonic development of Upper Cretaceous to Eocene strata of southwestern Utah: Geological Society of America Bulletin, v. 106, p. 145-154.

Grant, S.K., 1987, Kolob Canyons, Utah: structure and stratigraphy, *in* Beus, S.S., editor, Rocky Mountain Section of the Geological Society of America Centennial Field Guide Volume 2: p. 287-290.

Gregory, H.E., 1950, Geology and geography of the Zion Park region Utah and Arizona: U.S. Geological Survey Professional Paper 220, 200 p.

Gregory, H.E., 1951, The geology and geography of the Paunsaugunt region, Utah: U.S. Geological Survey Professional Paper 226, 161 p.

Harris, A.G., Tuttle, E., and Tuttle, S.D., 1997, Geology of national parks, 5e: Dubuque, Iowa, Kendall/Hunt Publishing, 758 p.

Hettinger, R.D., Roberts, L.N., Biewick, L.R., and Kirschbaum, M.A., 1996, Preliminary investigations of the distribution and resources of coal in the Kaiparowits Plateau, southern Utah: U.S. Geological Survey Open-File Report 95-539, 72 p.

Hintze, L.F., 1988 (revised 1993), Geologic history of Utah: Brigham Young University Geology Studies Special Publication 7, 202 p.

Keyes, C., 1924, Grand Staircase of Utah: The Pan-American Geologist, v. XLI, p. 33-68.

Levin, H.L., 1999, The Earth through time, 6e: Ft. Worth, Saunders College Publishing, 673 p.

Lund, W.R., Pearthree, P.A., Amoroso, Lee, Hozik, M.J., and Hatfield, S.C., 2001, Paleoseismic investigation of earthquake hazard and long-term movement history of the Hurricane fault, southwestern Utah and northwestern Arizona: Final Technical Report to the U.S. Geological Survey, National Earthquake Hazards Reduction Program External Research Award No. 99HQGR0026, p.15.

Nelson, L., 1990, Ice age mammals of the Colorado Plateau: Northern Arizona University Press, Flagstaff, 24 p.

Ott, A.L., 1999, Detailed stratigraphy and stable isotope analysis of the Claron Formation, Bryce Canyon National Park, southwestern Utah: Pullman, unpublished MS thesis, Washington State University, 130 p.

Peterson, F., 1988, Pennsylvanian to Jurassic eolian transportation systems in the western United States, *in* Kocurek, G., editor, Late Paleozoic and Mesozoic eolian deposits of the western interior of the United States: Sedimentary Geology, v. 56, p. 207-260.

Peterson, F., 1994, Sand dunes, sabkhas, streams, and shallow seas: Jurassic paleogeography in the southern part of the Western Interior Basin, *in* Caputto, M.V., Peterson, J.A., and Franczyk, K.J., editors, Mesozoic Systems of the Rocky Mountain Region, USA: Rocky Mountain Section, Society for Sedimentary Geology, p. 233-272.

Peterson, F., and Turner-Peterson, C., 1989, Geology of the Colorado Plateau: Field Trip Guidebook T130, 28th International Geological Congress, American Geophysical Union, Washington D.C., 65 p.

Reber, S., Taylor, W.J., Stewart, M., Sciefelbein, I.M., 2001, Linkage and reactivation along the northern Hurricane and Sevier faults, southwestern Utah, *in* Erskine, M.C., editor, The geologic transition, High Plateaus to Great Basin-A symposium and field guide, The Mackin Volume: Utah Geological Association Guidebook 30, p. 379-400.

Riggs, N.R., and Blakey, R.C., 1993, Early and Middle Jurassic paleogeography and volcanology of Arizona and adjacent areas, *in* Dunne, G.C., and McDougall, K.A., editors, Mesozoic paleogeography of the western United States II: Pacific Section, Society of Economic Paleontologists and Mineralogists, p. 347-375.

Stewart, M.E., Taylor, W.J., Pearthree, P.A., Solomon, B.J., and Hurlow, H.A., 1997, Neotectonics, fault segmentation, and seismic hazards along the Hurricane fault in Utah and Arizona: An overview of environmental factors in an actively extending region, *in* Link, P.K. and Kowallis, B.J., editors, Geological Society of America Field Trip Guide Book, 1997 Annual Meeting, Salt Lake City, Utah: Brigham Young University, Geology Studies, v. 42, part 2, p. 235-252.

Warner, T., editor, 1995, The Dominguez-Escalante journal (translated by Fray Angelico Chavez): University of Utah Press, Salt Lake City, 153 p.

Looking south over the Skutumpah and Wygaret terraces from Yovimpa Point.

ROAD LOG

Note: Directions for viewing from the vehicle are given as clock hour, where the front of the vehicle is always 12 o'clock. A feature directly to the right of the vehicle is then 3:00; to the left at 9:00. A feature at 1:00 or 2:00 is only slightly to the right of the front of the vehicle.
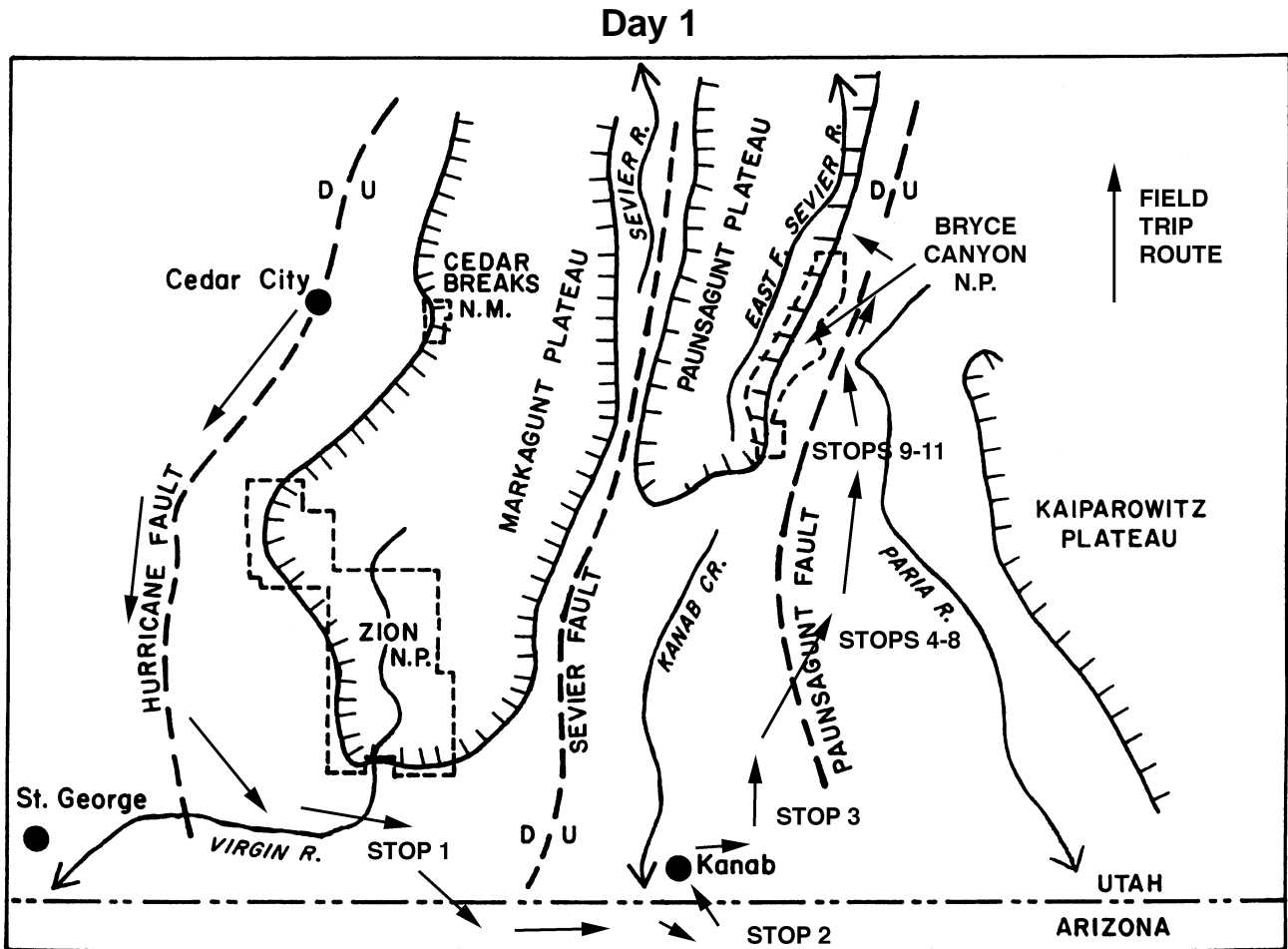
Day 1

Figure 10. Sketch map of Day 1 field trip route (from Harris and others, 1997)

We will drive south via I-15, along the Hurricane Fault scarp. We will leave the interstate at the Toquerville, Utah, exit and proceed generally south-southeast through La Verkin and Hurricane, Utah; Colorado City, Pipe Spring, Fredonia and LeFevre Point, Arizona; and then drive north-northeast through Kanab, Johnson Canyon, to Tropic, Utah. This circuitous route provides excellent views of the Chocolate, Vermillion and White Cliffs of the Grand Staircase. In Johnson Canyon we will view the White, Gray and Pink Cliffs and travel on the Skutumpah Terrace. In the course of our travels, we will familiarize ourselves with the geologic history, sedimentology, and stratigraphy of the region.

MILEAGE

Interval	Cum	Description
0.0	0.0	Motor Pool Parking Lot, the western-most SUU parking lot, located at 200 South 1150 West, in Cedar City, Utah. Turn right out of SUU Motor Pool Parking Lot.
0.1	0.1	Turn left on 200 South Street, and proceed east.

213

0.6	0.7	Stop sign at the junction of 200 South and 300 West Streets. Turn right (south) on 300 West.
0.3	1.0	Stop sign at junction of 300 West and 400 South Streets. Continue south on 300 West.
0.2	1.2	Stop sign at junction of 300 West and 600 South. Continue south on 300 West.
0.1	1.3	Stop sign at junction of 300 West and south Main Streets. Turn right (south) on Main.
0.1	1.4	Signal, continue south on Main Street.
0.9	2.3	Signal, continue south onto southbound I-15 freeway on-ramp.
2.3	4.6	Pleistocene lava flow in road cut at 9:00 and 3:00.
10.0	14.6	Rest area, I-15.
2.9	17.5	Cliffs at 9:00 are Triassic Moenkopi Formation.
1.4	18.9	Exit 40. Kolob Canyon, Zion National Park. See Grant (1987) for a discussion of the geology of Kolob Canyons. Located at 2:00-3:00, the Pine Valley Mountains. This laccolithic to extrusive complex is approximately 23 million years old. At the base of the mountains (1:00 -2:00) are a series of basalt flows that create a prominent, tree-covered, ridge. We will drive across the toe of the ridge, west of its truncation by Ash Creek Canyon.
4.1	23.0	Hurricane fault scarp at 9:00. Most of what you see is Kaibab Limestone (base), Triassic Moenkopi Formation, with a recent basalt cap. The basalts in this area have recently been dated in order to constrain slip rates on this segment of the Hurricane fault, see Lund and others, 2001.
2.7	25.7	Located on the east side of I-15 at Exit 33, is the San Daniel Campsite used by the Escalante–Dominguez party on the night of October 14, 1776. These Dominican Fathers traveled from Santa Fe, New Mexico in search of an overland route to Monterey, California. They had many adventures, which are chronicled in *The Dominguez–Escalante Journal*, edited by Ted Warner, and translated by Fray Angelico Chavez (University of Utah Press, 1995, 153 pages). The party camped at the San Daniel Campsite after being abandoned by two native American guides they had found along Ash Creek on the north side of the Black Ridge. From here, the party continued south through Toquerville, along the Hurricane Cliffs, and across the Arizona Strip to eventually cross the Colorado River and return to Santa Fe, New Mexico.
3.3	29.0	Pine Valley laccolith outliers along I-15 viewed at 11:00, 1:00, 2:00 and 3:00.
2.7	31.7	Exit 27 of I-15 to Toquerville / Hurricane, proceed to stop sign, then turn left (south) on SR-17.
0.7	32.4	Cenozoic lavas fill paleo-valleys high on the cliff at 9:00.
0.1	32.5	Navajo Sandstone at 3:00. Slivers of this rock have here been caught in the Hurricane fault zone and are sporadically capped on by Quaternary volcanics.
1.3	33.8	Toquerville city limits.
0.1	33.9	Cross Ash Creek.

0.6	34.5	J. Conrad Naile (Naegle) Home and Dixie Mission Winery. The Naegle Big House, known as the Naegle winery, or the Naile House. Constructed in 1866-68 by John Conrad Naile (Naegle), a Mormon polygamist, rancher, farmer, and colonist. The house served several purposes - a home for several wives and family; headquarters for Naegle's widespread ranching and business enterprises; and as a winery. The Naegle family relocated to Mexico in the late 1880s.
1.2	35.7	Road on right leads to Toquerville Cemetary.
0.4	36.1	Quaternary basalts and capping Quaternary alluvium.
0.3	36.4	La Verkin city limits.
0.2	36.6	Crossing La Verkin Creek.
0.2	36.8	Smith Mesa at 9:00.
0.4	37.2	Junction of SR-17 and SR-9, SR-17 ends. Continue south on SR-9.
1.4	38.6	Crossing Virgin River. The canyon walls are comprised of Quaternary basalts and show columnar jointing. Just beneath the Virgin River bridge and upstream is the small commercial spa called Pah Tempe Hot Springs, which has welcomed visitors from around the world for over a century. There are seven hot mineral pools (100°F), a swimming pool, a campground, and a bed-and-breakfast. These heated waters flow upward along fractures associated with the Hurricane fault, the scarp of which is visible at 3:00.
0.1	38.7	Road on left leads to Pah Tempe Hot Springs.
0.1	38.8	Hurricane city limits.
0.8	39.6	Turn left on 100 East Street in Hurricane. Continue to the stop sign and turn left on SR-59. Drive up scarp of Hurricane fault through Quaternary basalts and alluvium. The Hurricane fault is commonly used to draw the western margin of the Colorado Plateau in southwest Utah. The 160-mile long fault runs from south of the Grand Canyon northward past Cedar City, Utah, where it forms the precipitous west boundary of the Markagunt Plateau. The lack of erosional degradation of the escarpment suggests some recent movement. Toquerville, Utah, sits on the west side of the Hurricane fault which has over 8,000 feet of stratigraphic separation. About 1,500 feet of this displacement has occurred since the eruption of a Quaternary basalt flow across the fault. Offsets of up to 20 feet in unconsolidated gravel at the base of the fault (Steward and others, 1997) suggest even more recent movement. A magnitude 5.8 earthquake near St. George on September 2, 1992 has been attributed to movement on the Hurricane fault (Christenson, 1995).
0.6	40.2	View at 9:00 of several cinder cones and Pine Valley Mountains.
0.3	40.5	View at 11:00 of Smith Mesa site of U.S. Air Force ejection seat testing in 1950s and 60s.
0.5	41.0	Permian Kaibab Formation on both sides of the road.
1.2	42.2	Riding on top of the Timpoweap Member of the Moenkopi Formation. View at 11:00 is a butte composed of other Moenkopi Formation members. Lower red member forms the slope that rises from valley floor, and is capped in low ridge by cliff-forming Virgin Limestone Member. Middle red slope is comprised of the middle red, Shnabkaib, and

upper red Members and is capped by the basal Shinarump Conglomerate Member of the Triassic Chinle Formation.

0.6   42.8   **STOP 1.** Turn left off of SR 59 to the petroleum seeps in the Timpoweap Member, Moenkopi Formation. Return to SR-59.

Mile 42.8 Petroleum seep in the Timpoweap Member, Moenkopki Formation.

1.8   44.6   At 12:00 is a recent cinder cone and valley-fill lava flow extending to your right.

2.3   46.9   View at 3:00 is of a cinder cone being mined for road metal.

2.5   49.4   At 12:00 is our first view of J. W. Powell's Vermillion Cliffs, exposed here along the western edge of the Moccasin Terrace (Gregory, 1950). The Vermillion Cliffs are composed of the Jurassic Moenave and Kayenta Formations.

0.5   49.9   View at 9:00 is the Temples of Zion in Zion National Park. "Temples" are composed of the Jurassic Navajo Sandstone and Temple Cap Formations.

1.0   50.9   View at 3:00 of a cinder cone, called Cinder Mountain, on the east facing dip slope of Little Creek Mesa.

9.8   60.7   Entering Hilldale, Utah. In the early days of Mormon history, polygamy was openly practiced. Believing participation to be commandment, from 1852 until 1890, the LDS (Mormon) Church leaders preached and encouraged members, especially those in leadership positions, to marry additional wives. A majority of the Latter-day Saints, however, never lived the principle. Reactions from outside the church to participation in polygamy were immediate and negative. In 1862 the United States Congress passed the Morrill Act, which prohibited plural marriage in the territories, disincorporated the LDS Church, and restricted the church's ownership of property. The nation was in the midst of the Civil War, however, and the law was not enforced. The Latter-day Saints continued to practice polygamy despite these laws, since they believed that the practice was protected by the freedom of religion clause in the Bill of Rights. Wilford Woodruff, then president of the LDS Church, initially supported the continued practice of polygamy; however, as pressure increased, he began to change the church's policy. On 26 September 1890 he issued a press release, the Manifesto, which read, "I publicly declare that my advice to the Latter-day Saints is to refrain from contracting any marriages forbidden by the law of the land." The Manifesto was approved at the

216

church's general conference on 6 October 1890. Fundamentalist groups who believe that the church discontinued polygamy only because of government pressure continued the practice. As these groups were discovered by the LDS Church, their participants were excommunicated. Some of these polygamists have appointed their own leaders and continue to live in groups, including those in Colorado City (formerly Short Creek), Arizona, and Hilldale, Utah.

0.6	61.3	Arizona-Utah border.
0.1	61.4	Entering Colorado City, Arizona. Road changes to Arizona Highway 389 East. The region to the south is called the Arizona Strip, and lies north of the Colorado River and Grand Canyon. The Arizona Strip encompasses five million acres of the far northwestern corner of Arizona north of the Colorado River and south of the Utah border. An arid, isolated, and sparse landscape, the region nonetheless has sustained a rich human history, from the 8,000 year-old remains of paleo Indians to the creation of the million-acre Grand Canyon-Parashant National Monument in January of 2000. The Arizona Strip has been an important regional ranching area since the late 19th century.
3.6	65.0	View at 2:00 is of Mount Trumble and the new Grand Canyon-Parashant National Monument. From an environmental history perspective the region records climate change, human use, and paleoecological transformations over the past 50,000 years. It has been an important site for ecological restoration of forests, springs, and wildlife such as desert bighorn, pronghorn antelope, and California condor. The new monument essentially doubles the area of Grand Canyon National Park, protecting a vast area of northern Arizona from development.
6.3	71.3	View at 11:00 of the upper Moenave, Kayenta, Navajo transition, the southern exposure of Powell's Vermillion Cliffs.
3.2	74.5	View at 12:00 of the Kaibab Uplift (East Kaibab monocline).
0.1	74.6	Entering Kaibab Paiute Indian Reservation.
5.0	79.6	Road on left to Pipe Spring National Monument. Pipe Spring, and near by Moccasin Spring, are the only perennial water sources on the high desert plain between the North Rim of the Grand Canyon and the Vermilion Cliffs. Water flows from the subsurface along the Sevier fault. For countless centuries the native peoples of the region, the Kaibab Paiute, relied on the springs for their existence. Later, in the mid-1800s, Mormon families moved into the region and struggled to build self-reliant communities. In 1870, Mormon settlers built a fortified ranch at Pipe Spring and raised tithe cattle owned by the LDS Church. The purpose of the ranch was to provide meat and dairy products for workers on church projects in St. George, Utah. The old Mormon ranch at the spring was purchased by the National Park Service in 1923.
1.7	81.3	View at 10:00 of the Chocolate (lower) and Vermillion Cliffs.
3.2	84.5	Road on the right is the Toroweap turn off which leads to the Toroweap section of the Grand Canyon where one can view Vulcan's Throne and Anvil and Lava Falls, the highest navigable falls in North America. The features formed when late Tertiary lavas flowed into the Grand Canyon to form a temporary dam.
6.1	90.6	Road to the left leads to Six Mile Village. Leaving Kaibab Paiute Indian Reservation.
1.5	92.1	Crossing Kanab Creek and entering Fredonia, Arizona.
0.5	92.6	Junction of Arizona Highway 389 East and US 89A. Turn right and travel south on US 89A.

7.5	100.1	View at 9:00 of the Grand Staircase that includes the Chocolate, Vermillion, White, and Pink Cliffs.
8.4	108.5	Exposures of the Kaibab Limestone dipping west off the flanks of the Kaibab Uplift (East Kaibab monocline).
2.5	111.0	**STOP 2.** LeFevre Overlook, Kaibab National Forest, elevation 6,700 feet. Complete view to the north of the Grand Staircase. **LUNCH STOP.** Return to US 89A and travel north, back toward Fredonia, Arizona and Kanab, Utah.
13.9	124.9	Low cliff at 2:00 is the middle red member of the Moenkopi Formation with Chocolate Cliffs behind it.
2.1	127.0	Chocolate / Vermillion Cliffs in the middle distance.
4.3	131.3	Junction of Arizona Highway 389 and US 89A. Continue north on US 89A.
1.6	132.9	Paramont Petroleum Asphalt Terminal on the right. View at 11:00 of the Chocolate Cliffs. Upper red Moenkopi, and Shinarump Conglomerate, Chinle Formation, and in background the Vermillion Cliffs composed of Moenave and Kayenta Formations.
0.6	133.5	Chocolate Cliffs.
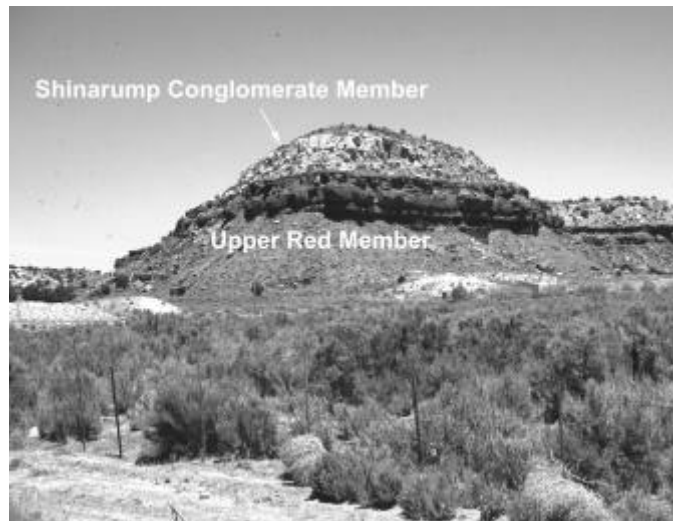
Mile 133.5 Exposure of the Chocolate Cliffs north of Fredonia, Arizona.

1.3	134.8	Utah / Arizona border.
0.1	134.9	Entering Kanab, Utah city limits (Kanab is the Paiute word for "willows"). Vermillion Cliffs visible in all directions.
0.2	135.1	Kanab Fort historical marker on left. Kanab Fort construction begun in 1864 by Jacob Hamblin as protection from Indians and as a base of exploration. Severe and frequent Indian attacks made it impractical to maintain. The fort was abandoned in 1866 and reoccupied in 1870, by Levi Stewart and others sent to do missionary work and establish peace with local Indians. In December of 1870, a fire in the fort killed Levi's wife and five sons. Restored fort used as a movie prop in "Fury at Furnace Creek" and "The Apple Dumpling Gang."

2.5	137.6	Junction of US 89A and US 89. Turn right at stop light on US 89 and drive east toward Page, Arizona.

2.0	139.6	Vermillion Cliffs.
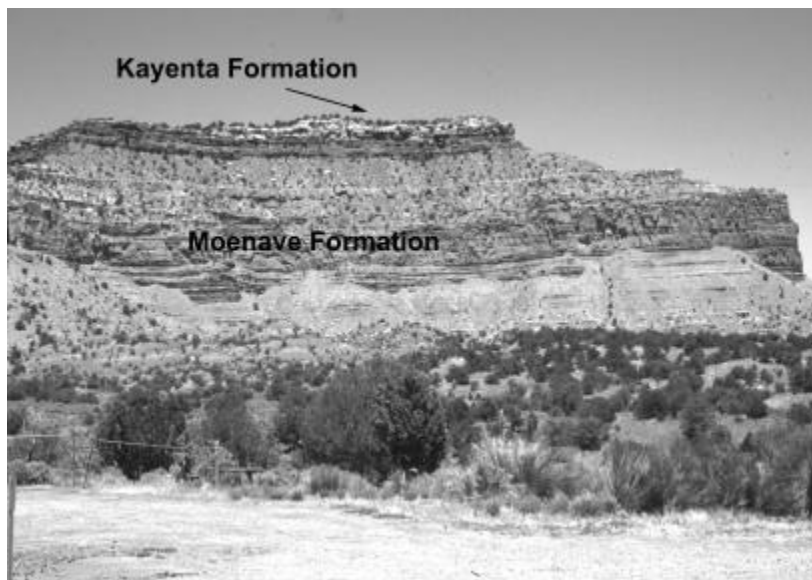
Mile 139.6 Exposures of the Vermillion Cliffs east of Kanab, Utah.

7.2	146.8	Turn left (north) on Johnson Canyon Road.
0.3	147.1	View at 1:00 of the Vermillion Cliffs in the foreground and White Cliffs in the background.
1.3	148.4	**STOP 3**. Look at upper Moenave Formation of the Vermillion Cliffs. This area provides exposures of an interfingering zone between strata of the Jurassic Kayenta Formation and the overlying Navajo Sandstone. According to Hintze (1988), the Kayenta Formation in this area is split by the Lamb Point Tongue of the Navajo Sandstone. The strata below the Lamb Point Tongue is still the Kayenta Formation, but the strata above the Lamb Point Tongue and below the Navajo Sandstone is referred to as the Tenney Canyon Tongue of the Kayenta Formation. This interfingering suggests that this area represents the margins of the Navajo and Kayenta depositional basins.
1.8	150.2	Cross bridge.
0.1	150.3	View at 3:00 is "biscuit" weathering in the lower Kayenta Formation.
1.8	152.1	Movie set on the right was used for the Gunsmoke TV series.
0.5	152.6	**STOP 4**. View at 10:00 of the Lamb's Point Tongue of the Navajo Sandstone and the overlying Kayenta. Faulting can be observed on the west side of the road in a fault zone that parallels Johnson Canyon. Named the Johnson Canyon fault zone, the faults are considered active (Doelling and Davis, 1989).

Mile 152.6 Weathering features in the Kayenta Formation, Johnson Canyon, Utah.

1.5	154.1	More displaced strata at 10:00, exposures of White Cliffs of the Navajo Sandstone at 11:00.
1.1	155.2	View at 2:00 "biscuit" weathering and soft sediment/slump features. View at 1:00, an excellent example of the Lamb Point Tongue of the Navajo Sandstone.
1.4	156.6	**STOP 5**. View of Pink Cliffs at 11:00. Road to Lock Ridge, Flood Canyon, Nephi Pasture, and Buckskin Wash on right. In this region of the Monument, the stratigraphic interval can be divided into a series of formal (upper case names) and informal (lower case names) units. Starting form the exposed base, in ascending order: Lamb Point Tongue of Navajo Sandstone, Tenney Canyon Tongue of Kayenta Formation, brown Navajo Sandstone, pink Navajo Sandstone, and white Navajo Sandstone (Doelling and others, 2000). The brown and white Navajo Sandstone units are resistant and form cliffs, while the pink Navajo Sandstone is softer and forms benches and low hills.
0.9	157.5	Cross Johnson Wash, then a cattle guard.
1.0	158.5	Entering the Grand Staircase–Escalante National Monument (GSENM), sign on right. GSENM, administered by the Bureau of Land Management (BLM), was established by Presidential Proclamation on September 18, 1996, to protect an array of geological, paleontological, historical, archaeological, and biological resources. The Monument covers about 1.9 million acres of land in south-central Utah. About 68 percent of the Monument is in Kane County, while the remaining 32 percent is in Garfield County. The Monument is surrounded on three sides primarily by national forest and national park lands, and by other BLM administered lands to the south and west. Kodachrome State Park also adjoins the monument near Cannonville.
1.5	160.0	View at 12:00 of the Navajo Sandstone–Carmel Formation (Co-op Creek Member) contact.

Co-op Creek Member, Carmel Formation
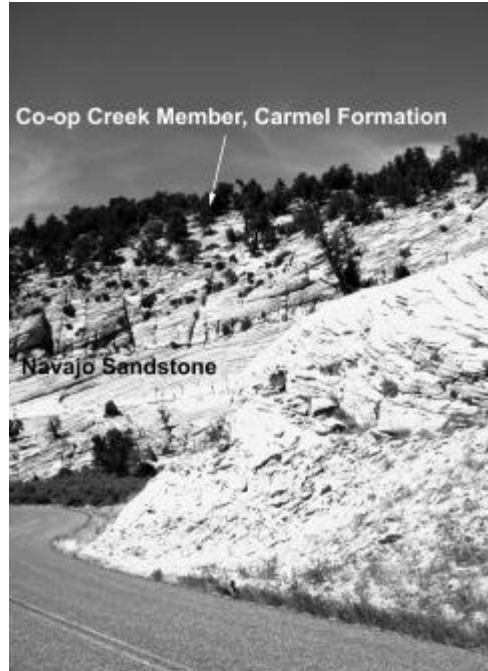
Navajo Sandstone

Mile 160.0 Navajo Sandstone - Carmel Formation contact.

2.1   162.1   Cross wash, pull off on right shoulder. **STOP 6**. The outcrop at road level is the Navajo Sandstone. Note the large scale, high-angle cross-beds and truncated dune tops. The drainage on the right is Skutumpah Canyon, and the road continues up Johnson Canyon. The Co-op Creek Member of the Carmel Formation sits on the white Navajo Sandstone. This erosional surface forms the Skutumpah Terrace. The olivine lava flow visible up Johnson Canyon, and upon which the road lies, is a disconnected flow from Bald Knoll, located approximately seven miles to the north.

Co-op Creek Member, Carmel Formation
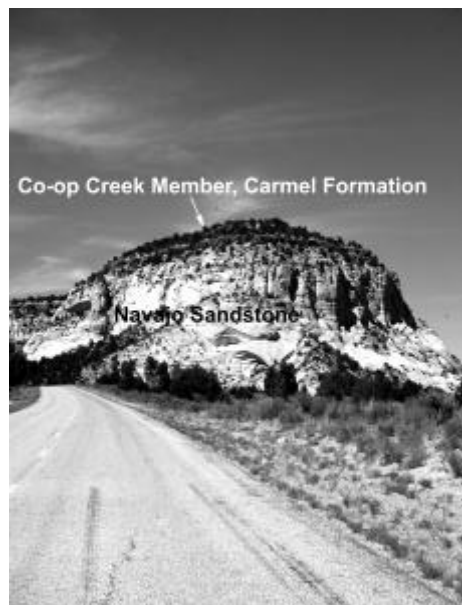
Navajo Sandstone

Mile 162.1 Navajo Sandstone - Co-op Creek Member, Carmel Formation contact.

221

1.9	164.0	**STOP 7**. See the information kiosk at the junction of Johnson Canyon, Glendale Bench (left fork) and Skutumpah (right fork) Roads. The lava flow at 12:00 is part of the Bald Knoll flow. View the Gray Cliffs at 12:00. Examine the yellow to gray thin beds of the Co-op Creek Member of the Carmel Formation. Bear right on the Skutumpah Road toward Cannonville.
0.6	164.6	View at 9:00 to 11:00, Gray Cliffs composed of Dakota, Tropic Shale, and Straight Cliffs Formations. The valley is comprised of the Carmel Formation.
0.8	165.4	Take the right fork, toward Deer Springs Ranch.
1.2	166.6	Sand and gravel pit located adjacent to road in Quaternary alluvium is visible at 9:00. Also visible at 9:00, in the distance, are the Gray Cliffs. In this area, the Cretaceous Dakota Formation immediately overlies the Middle Jurassic Carmel Formation because the Middle Jurassic Entrada Formation, Upper Jurassic Morrison Formation, and the Upper Jurassic to Lower Cretaceous Cedar Mountain Formation have been removed by erosion. This gap in geological time is locally referred to as the sub-Dakota unconformity.
0.4	167.0	Junction Mill Creek Road on left. Continue on Skutumpah Road.
0.2	167.2	Paria River Member of the Carmel Formation at 10:00. This unit forms a series of light-gray knobs on the left side of the road. It contains both pink and white gypsum.
1.1	168.3	At 9:00, view a limestone bed in the upper Paria River Member of the Carmel Formation.
1.5	169.8	Junction Skutumpah Pasture and Timber Mountain roads.
4.0	173.8	Road cut in upper Carmel Formation.

Mile 173.8 Road cut in the upper Carmel Formation, Skutumpah Road.

0.4	174.2	View at 9:00 the upper Carmel (Winsor Member) to Dakota transition. At 1:00 view the Navajo Sandstone elevated here by a fault. Cross cattle guard, entering Deer Springs Ranch.
0.1	174.3	Cross Dunham Wash.
0.6	174.9	Junction. Keep left on main road, which passes through a cut in the Carmel Formation. The road to the right provides access to private property along Deer Springs Wash and to the Ranch.
0.3	175.2	Junction. Stay on main road. Gray Cliffs visible at 9:00.
0.6	175.8	Road cut in pediment gravels. The gravels here have been eroded from Upper Cretaceous sandstone formations and the basal Claron Formation, which makes up the hoodoos and spires of Bryce Canyon National Park.
0.1	175.9	Cross Meadow Creek. Pink Cliffs (Claron Formation) visible in the left distance.
0.8	176.7	Road proceeds up Dry Valley.
1.1	177.8	Road drops into Lick Wash and Podunk Creek.
0.4	178.2	**STOP 8**. Lick Wash. After crossing Lick Wash, an infrequently used road extends south (right). White to light-gray outcrops of the Navajo Sandstone are visible to the south. These are bounded by a northeast-trending fault with the downthrown block to the northwest (Doelling and others, 2000). The hill to the east of where we are parked shows yellow-gray, thin-bedded Co-op Creek limestone covered by red- and white-banded beds of the Crystal Creek Member of the Carmel Formation. The Crystal Creek Member is overlain by the buff to tan colored Thousand Pockets Tongue of the Page Sandstone. This is the western most exposure of the Thousand Pockets Tongue. Gypsum of the Paria River Member of the Carmel Formation directly overlies the Thousand Pockets Tongue, wherever the Thousand Pocket Tongue is present. The Paria River Member is overlain by the yellowish and reddish Winsor Member. Looking north from this location the Gray Cliffs, primarily composed of Dakota Formation rocks, are visible. Some pinkish coloration is present in these cliffs due to the natural burning and oxidation of thin coal beds in the Dakota. Under the gray is a harder yellow layer that is difficult to distinguish from the underlying Winsor Member beds. This hardened yellow layer is an erosional remnant of the Entrada Formation. The unconformity at the base of the Dakota cuts out the Entrada west of this location, so up until now, we have seen Dakota resting directly on the Winsor Member of the Carmel Formation. From this point eastward, the Dakota rests on the Entrada Formation. We will walk the upper portions of Lick Wash, a small slot canyon to the south. After the stop, the road log continues eastward on the main road.
1.0	179.2	On the right, outcrops of the Thousand Pockets Tongue rest on the Crystal Creek Member of the Carmel Formation. Gypsum of the Paria River Member overlies the yellow Thousand Pockets Tongue. Gray Cliffs continue on the left.
2.8	182.0	Cross Bullrush Hollow. Pink Cliffs visible at 9:00.
1.0	183.0	More gypsum of the Paria River Member exposed at 11:00.
1.2	184.2	**STOP 9**. Paria River Amphitheater Overlook at turn in road. In the middle ground to the north we see the Winsor Member of the Carmel Formation (a white to pink siltstone), which overlies the Paria River Member of the Carmel Formation, which in turn overlies the yellow Thousand Pockets Tongue of the Page Sandstone. The Thousand Pockets Tongue overlies red beds of the Crystal Creek Member of the

Carmel Formation, which overlies the Co-op Creek Member here in Indian Hollow. The Pink Cliffs exposed in the distance across the amphitheater are part of the Table Cliffs Plateau. The hill south of Table Cliff Plateau is Canaan Peak in the northern Kaiparowits Plateau. The flat benches ahead in the valley are various Carmel members capped with pediment gravels. After a brief stop we will continue driving down Indian Hollow, which starts in the Winsor Member of the Carmel Formation and stratigraphically descends to the Co-op Creek Member of the Carmel Formation.

1.0	185.2	Cross wash in the Co-op Creek Member. The road will be in this member for the next few miles.
1.0	186.2	Cross wash. The yellow Thousand Pockets Tongue is visible ahead at 1:00 overlying the reddish or brownish Crystal Creek Member of the Carmel Formation.
0.9	187.1	The road joins the Bull Run drainage, affording more views of the various members of the Carmel Formation. The road continues in the Co-op Creek Member.
0.5	187.6	Note the thin gypsum beds in the Co-op Creek Member in the road cut at 9:00.
0.4	188.0	**STOP 10**. Cross Bull Valley Gorge, an impressive slot canyon in the top of the Navajo Sandstone. Park another 0.1 mile up the road. The Co-op Creek Member is at road level, overlain by the Crystal Creek Member of the Carmel and the Thousand Pockets Tongue of the Page Sandstone. After stop, continue on main road.
0.4	188.4	View at 12:00, Powell Point in the Pink Cliffs (composed of Claron Formation) and the underlying Gray Cliffs (composed of [descending stratigraphic order] the Kaiparowits, Wahweap, Straight Cliffs, Tropic Shale, Dakota, Entrada, and Carmel Formations).
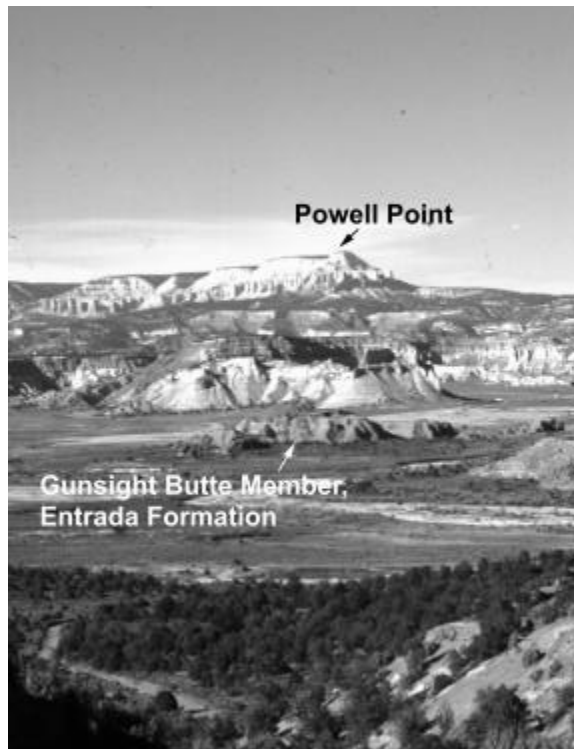
Mile 188.4 Looking northeast at the Pink Cliffs and Powell Point.

224

1.3	189.7	Drop into Willis Creek drainage through the Thousand Pockets Tongue, Crystal Creek, and Co-op Members. Cross Willis Creek at Carmel Navajo Contact. Willis Creek cuts some modest (about half a mile long) narrows in the Navajo Sandstone just east of the crossing.
1.7	191.4	Climb out of the wash to **STOP 11**. We are parked on gypsum of the Paria River Member of the Carmel Formation. Walk to the canyon edge and view the Thousand Pockets Tongue across the canyon.
1.4	192.8	Road crosses Sheep Creek (concrete spillway), which lies in the lower members of the Carmel Formation. Thousand Pockets Tongue is visible above the drainage.
1.9	194.7	View at 12:00 of Powell Point. Looking into the Paria River Valley with the Carmel to Entrada transition visible at 12:00.
0.8	195.5	Grand Staircase - Escalante National Monument boundary.
0.1	195.6	Carmel to Entrada transition visible at 1:00 across Yellow Creek.
0.1	195.7	Cross Yellow Creek.
0.1	195.8	Turn left at stop sign toward Cannonville, Utah on asphalt.
0.3	196.1	Junction, stay on pavement toward Cannonville.
0.5	196.6	View at 3:00, half way up ledge of the contact between the Carmel Formation and the Gunsight Butte Member of the Entrada Formation.

Mile 196.6 Looking east at the Carmel Formation - Gunsight Butte Member, Entrada Formation contact.

0.6	197.2	Orange-brown slickrock at 3:00 is Gunsight Butte Member of the Entrada Formation, and is locally called Promise Rock. According to local folklore, it served as the site for many pioneer marriage proposals.
1.7	198.9	Entering Cannonville, Utah.
0.4	199.3	Junction with SR 12. Turn left toward Tropic, Utah. View at 12:00 is the Cannonville Member of the Entrada Formation and the overlying Escalante Member, Cedar Mountain and Dakota Formations.

Mile 199.3 Looking east at (in ascending stratigraphic order) the Cannonville and Escalante Members, Entrada Formation, and the Cedar Mountain and Dakota Formations.

2.2	201.5	View at 9:00 is the contact of the Dakota Formation and the overlying Tropic Shale. The Grey Cliffs occupy the view.
1.0	202.5	Entering Tropic, Utah.
1.2	203.7	View at 1:00 is the contact of the Tropic Shale and the overlying Straight Cliffs Formation. In the distance is Powell Point where the pinkish colored Claron Formation sits on the Kaiparowits Formation. Claron Formation at Powell Point shows the division of the lower pink and upper white members.
1.5	205.2	View at 3:00 of the contact between the Tropic Shale and overlying Tibbet Canyon Member of the Straight Cliffs Formation.
0.7	205.9	Trace of the Paunsaugunt fault at 3:00. Claron Formation on the left is on the downthrown block. The Paunsaugunt fault separates the Tropic Valley to the east from the sculpted buttress of the Paunsaugunt Plateau to the west. The fault passes through the center of Bryce Canyon National Park, which owes much of its existence to this fault. The spectacular hoodoos and fins carved into the pastel limestone and siltstones of the Claron Formation are preserved on the downthrown west side of the fault. The topographically low Tropic Valley on the upthrown east side of the fault seems illogical but its existence is due to the relative differences in erosion rates of the rocks on either side of the fault. On the upthrown block, the soft limestones and siltstones of capping Claron Formation and less resistant shales and sandstones of the underlying Cretaceous age rocks were quickly eroded and removed to form Tropic Valley. The Claron on the downthrown side of the fault is partially volcanic capped and has only experienced lateral erosion and gullying along the edge of the Paunsaugunt Plateau.
0.4	206.3	Pink member of the Claron Formation visible on both sides of the road. The Claron is a lacustrine (freshwater lake) limestone deposit.
2.1	208.4	View at 9:00 of Claron Formation hoodoos in the Bryce Canyon amphitheater.
0.7	209.1	View at 1:00 is the top of the Paunsaugunt Plateau with volcanics of the Mount Dutton caldera acting as a cap.
0.7	209.8	Junction of SR-62 with SR-12. Turn left to Bryce Canyon National Park.

2.4 212.2 Ruby's Inn at 3:00. Driving along the top of the Paunsaugunt Plateau, on top of the Claron Formation. We will spend the night here, at Ruby's Inn, and continue the road log tomorrow from this point.

End of Day 1 Road Log

Bryce Point overlook with the Table Cliffs plateau in the background.

Day 2
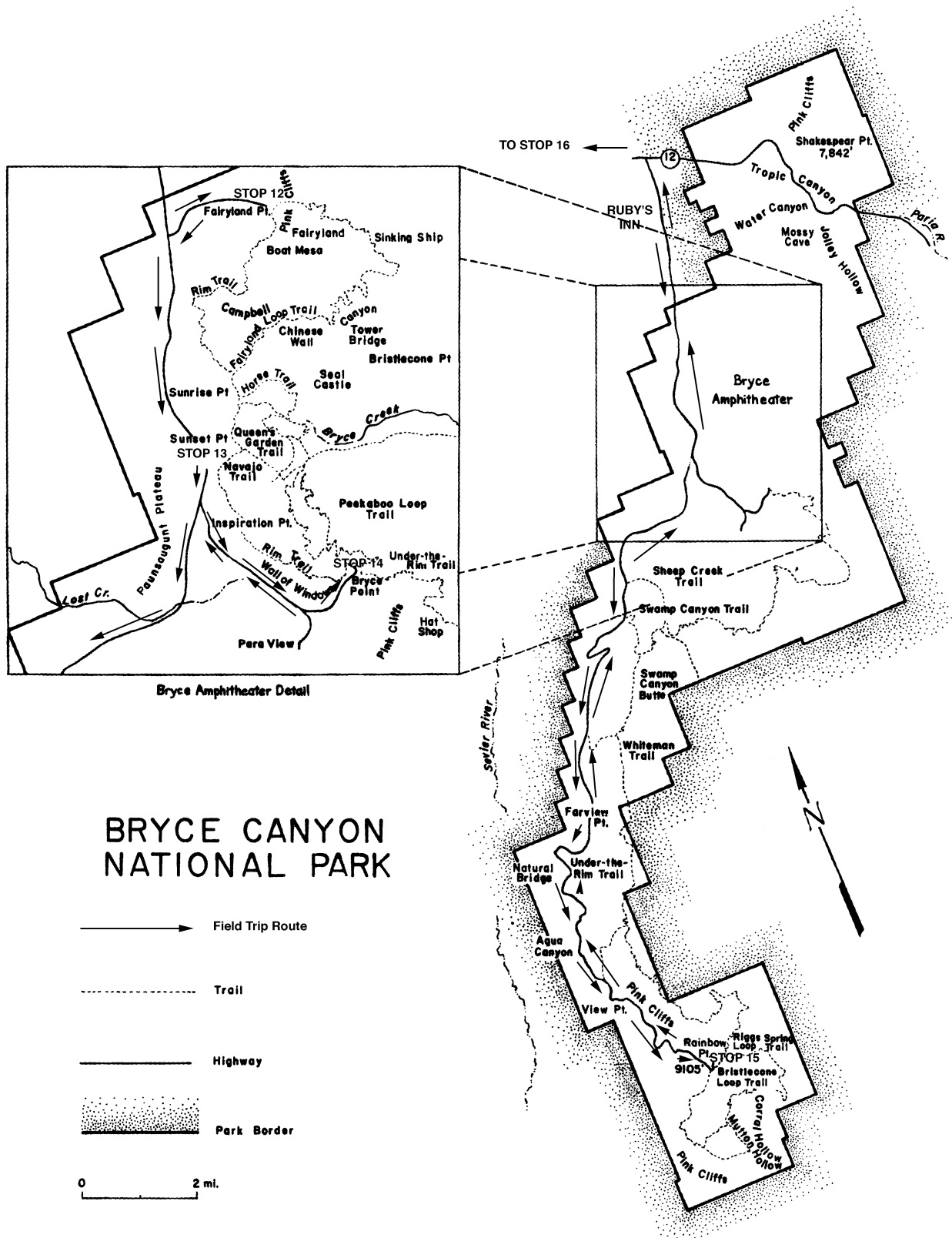
Figure 11. Sketch map of the field trip route for Day 2 (from Harris and others, 1997).

We will spend most of the day in Bryce Canyon National Park. The field trip will proceed south along the scenic drive to the Fairyland, Sunset Point, Bryce Point, Rainbow Point, and Yovimpa overlooks. These viewpoints will allow us to view the hoodoos and spires of the Claron Formation, and overlook much of the Skutumpah Terrace, the area we drove through yesterday. Once we leave Bryce Canyon, we will proceed west on SR-12, through Red Canyon to the Sevier fault scarp, and return to Cedar City via US 89 south and SR-14 west.

MILAGE

Interval	Cum	Description
0.0	0.0	Leave Ruby's Inn parking lot, turn left (south) toward Bryce Canyon National Park.
1.3	1.3	Entering Bryce Canyon National Park. Bryce Canyon National Park (BCNP) lies along the high eastern escarpment of the Paunsaugunt Plateau. Its special geological features include the rock chimneys (hoodoos), fins, and windows all carved by nature into the pink and white Claron Formation. BCNP is 56.2 mi^2 in area and has an elevation range of 7,600 to 9,100 feet. The earliest people in the area arrived approximately 12,000 years ago, but left little record of their existence. Paiutes were living throughout the region when the first Europeans arrived. Paiute legend refers to Bryce Canyon as "the ruins of a great city, buried in red mud and now partly excavated, the work of Shin-away, a Paiute demigod of great power. Before there were any Indians, the To-whon-an-ung-wa lived in that place. There were many of them. They were of many kinds - birds, animals, lizards, and such things - but they looked like people. They were not people; they had power to make themselves look that way. Because they were bad, Shin-away turned them all into rocks; some standing in rows, some sitting down, some holding on to others. You can see their faces, with paint on them just as they were before they became rocks. The name of that place is Angka-ku-wass-a-wits ['red-painted faces']" (Gregory, 1951, p. 17). Other Paiutes have called Bryce "Unka-timpe-was-wince-pock-ich", meaning 'red rock standing like men in a bowl-shaped recess.'
0.3	1.6	Turn left to Fairyland Point.
1.0	2.6	**STOP 12**. Fairyland Point parking, elevation 7,758 ft. Walk down the Fairyland Trail to observe cycles in the lower pink member limestone member of the Claron Formation.
1.0	3.6	Junction of Fairyland Point road and main park road. Turn left.
0.8	4.4	Entrance Station and Visitor's Center, Bryce Canyon National Park.
0.9	5.3	Entrance to Bryce Canyon lodge.
0.2	5.5	Entrance to Sunset Point. Turn left.
0.2	5.7	**STOP 13**. Sunset Point parking area. Good views of the upper, white member of the Claron Formation.
0.3	6.0	Junction of Sunset Point road and main park road. Turn left.
0.4	6.4	Entrance to Bryce Point. Turn left.
0.1	6.5	Road forks, turn right toward Bryce Point.
0.3	6.8	Road forks, turn left toward Bryce Point.
1.6	8.4	**STOP 14.** Bryce Point parking lot. Exit Bryce Point parking lot and return.

0.6	9.0	Bear right at Paria View fork.
1.2	10.2	Bear left at junction to Inspiration Point.
0.1	10.3	Stop sign. Bear left toward Rainbow Point.
0.1	10.4	Bear left to Rainbow Point. Stop at main park road and turn left. Driving on top of Claron Formation.
7.7	18.1	Turn for Farview Point. Do not turn. Continue 8 miles to Rainbow Point.
7.3	25.4	**STOP 15**. Rainbow Point parking lot. Take trail to Yovimpa Point. Overlook of Grey and White Cliffs to the south and the Skutumpah and Wygaret Terraces, over which we have just driven.
20.3	45.7	Return to Bryce Canyon Park entrance by same route. Junction of SR-63 and SR-12. Turn left on SR-12 west.
0.5	46.2	View at 3:00 of Tertiary Mt. Dutton volcanics. Another splay of the Sevier fault is apparent and expressed by the cliffs of the lower pink member of the Claron Formation at 11:00.
6.1	52.3	Entering Red Canyon, administered by the U.S. Forest Service. Lower pink member of the Claron Formation exposed on west side of Paunsaugunt Plateau.
1.6	53.9	Passing through two sharp ridges in the lower pink member of the Claron Formation.
1.7	55.6	View at 2:00, Claron Formation capped by Quaternary volcanics.
0.5	56.1	**STOP 16**. Looking north you can see an exposure of the Sevier fault on the west side of the Paunsaugunt Plateau. The fault is dipping steeply to the west and is normal. This segment of the Sevier fault has up to 3,000 feet of offset (Reber and others, 2001). The gray volcanics are andesite, and they dominate the visible hanging wall portion. The footwall is composed of Tertiary Claron Formation. Best and others (1980) date the volcanics in this road cut at 560,000 years.
2.5	58.6	Cross the Sevier River.
0.4	59.0	Junction of SR-12 and US 89. **END OF ROAD LOG**. Turn left to return to Cedar City, Utah.

GLOSSARY

Albite	A sodium-rich member of the plagioclase feldspar mineral group.
Alluvial	Of or pertaining to all deposits resulting from the operations of modern streams; including sediments laid down in riverbeds, flood plains, lakes and fans at the foot of mountain ranges.
Ammonite	One of a large, extinct, group of Mollusks (Class Cephalopoda) related to the living chambered nautilus.
Ammonoid	An inclusive term for all ammonite-like organisms (Goniatites, Ceratites, and Ammonites).
Bentonite	A clay formed from the decomposition of volcanic ash. The mineral has a great ability to absorb water and swell accordingly.
Biostratigraphic	Bodies of strata containing recognizably distinct fossils.
Biotite	A mineral, a dark brown, to green, member of the mica group.
Biozone	The fundamental biostratgraphic unit: defined by its fossil content.
Calcareous	Containing calcium carbonate (calcite).
Calcite	A mineral, calcium carbonate, $CaCO_3$.
Carbonaceous	Pertaining to, or composed largely of, carbon.
Caldera	A large depression typically caused by the collapse or ejection of the summit area of a volcano.
Chert	A compact, siliceous rock formed from cryptocrystalline varieties of silica (quartz).
Concretion	A nodular or irregular concentration of mineral constituents in sedimentary rocks; developed by localized deposition of material from solution, generally about a central nucleus.
Coquina	A coarse-grained, porous, variety of limestone chiefly made up of cemented shell fragments.
Cyclicity	Tendency of some sedimentary processes to repeat over time, resulting in repetitive, stacked strata.
Eolian	A term applied to the erosive action of the wind, and to deposits which are due to the transporting action of the wind.
Evaporitic	Climatic conditions leading to the formation of evaporates; sedimentary rocks formed by material deposited form solution during the evaporation of water.
Felsic	A general term applied to light-colored igneous rocks containing an abundance of feldspar and quartz.
Fluvial	A term referring to streams, stream action, and the deposits of streams.

232

Formation	The basic litho(rock)stratigraphic unit; a unit of strata that is mappable and that has distinctive upper and lower boundaries.
Intraformational conglomerate	A conglomerate developed by the breaking up of a partially consolidated bed and the incorporation of the fragments in new strata nearly contemporaneous with the original beds.
Intertonguing	A series of jagged pinchouts between laterally adjacent rock bodies; form in response to rapid changes in the shoreline.
Lacustrine	Produced by, or belonging to, lakes.
Lithology	The physical characteristics of rocks.
Marine	Of or belonging to, or caused by, the sea.
Marl	A calcareous clay, or intimate mixture of clay and particles of calcite or dolomite, usually fragments of shells.
Member	A subunit of the lithostratigraphic formation; multiple members make up a formation.
Molluscan	Of, or pertaining to, the phylum Mollusca.
Orogeny	The process of forming mountains, especially by folding and thrust faulting; an episode of mountain building, e.g., the Laramide orogeny.
Orthoclase	A potassium-rich member of the feldspar mineral group.
Oxidation	The loss of electrons by an element or ion, due to chemical interaction (weathering). So named because the elements commonly combine with oxygen.
Pangaea	The name proposed by Alfred Wegener for a supercontinent that existed at the end of the Paleozoic Era and consisted of all of Earth's landmasses.
Playa	The flat central area of an undrained desert basin.
Quartzite	A coarsely crystalline metamorphic rock consisting essentially of the mineral quartz.
Reduction	The gain of electrons by an element or ion, due to chemical weathering: contrasted with oxidation.
Regression	The opposite of marine transgression; the withdrawal of the sea from a continent or coastal area resulting in the emergence of land as sea level falls or the land rises with respect to sea level.
Resistant	Less susceptible to the forces of weathering and erosion. Resistant strata tend to form cliffs and rock faces.
Sabkha	A tidally produced salt flat.
Subaerial	Formed, existing, or taking place on the land surface; contrasted with subaqueous.

Subarkosic	A clastic sedimentary rock containing abundant quartz and lesser amounts of feldspar.
Topography	The physical features of a district or region, such as are represented on maps; the relief and contour of the land.
Transgression	Refers to the migration of a marine shoreline. The invasion of coastal areas or much of a continent by the sea resulting from a rise in sea level or subsidence of the land.
Unconformity	An erosion surface that separates younger strata from older rocks.
Volcanic arc	Mountains formed in part by igneous activity associated with the subduction of oceanic lithosphere beneath a continent. Modern examples include the Andes and Cascade Mountains.

ASSOCIATED MIOCENE LACCOLITHS, GRAVITY SLIDES, AND VOLCANIC ROCKS, PINE VALLEY MOUNTAINS AND IRON AXIS REGION, SOUTHWESTERN UTAH

Geological Society of America 2002 Rocky Mountain Section Annual Meeting
Cedar City, Utah
May 10, 2002
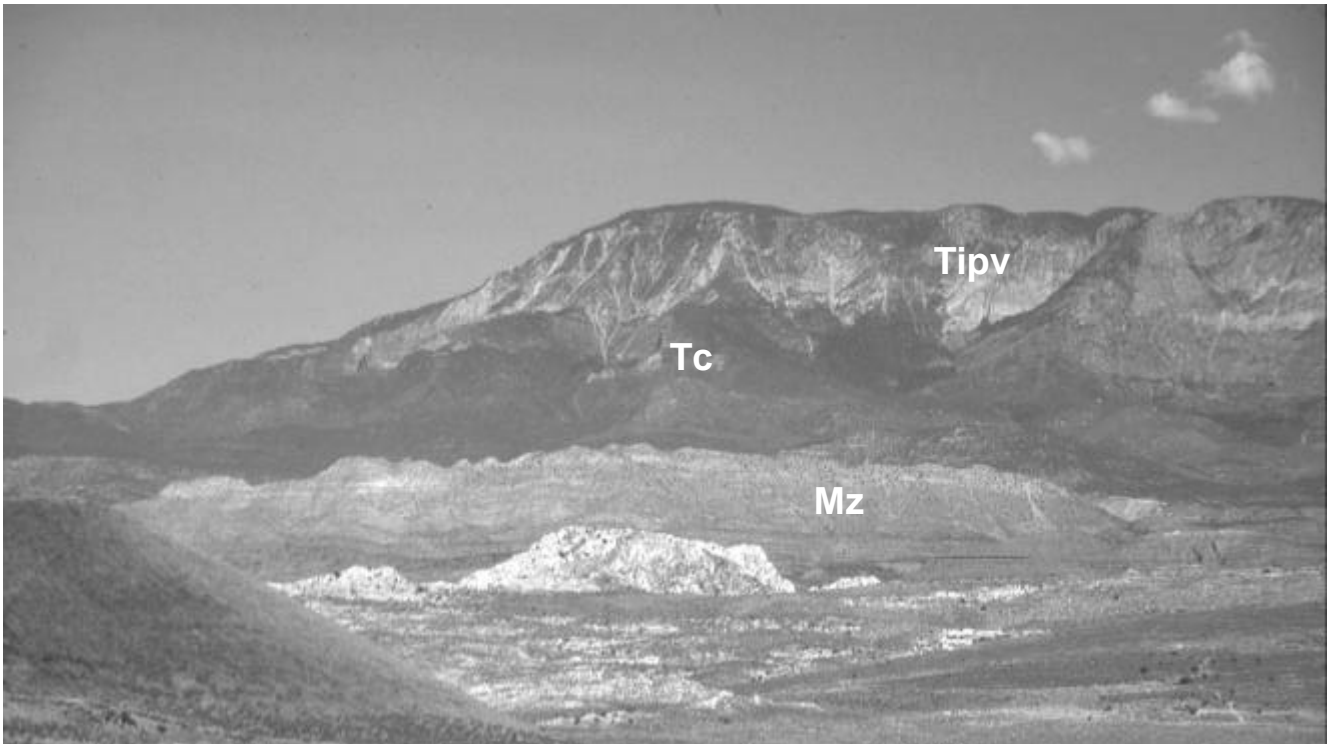
The unroofed Pine Valley laccolith (Tipv) capping the south side of the Pine Valley Mountains looking northwest from the Hurricane Cliffs. The light colored Mesozoic (Mz) rocks at the base of the mountains form the Virgin anticline, and they are overlain by Tertiary sedimentary rocks of the Claron Formation (Tc), into which the laccolith intruded and overlies.

FIELD TRIP LEADERS
David B. Hacker, Kent State University
Daniel K. Holm, Kent State University
Peter D. Rowley, Geologic Mapping, Inc.
H. Richard Blank, U.S. Geological Survey

ASSOCIATED MIOCENE LACCOLITHS, GRAVITY SLIDES, AND VOLCANIC ROCKS, PINE VALLEY MOUNTAINS AND IRON AXIS REGION, SOUTHWESTERN UTAH

Geological Society of America 2002 Rocky Mountain Section Annual Meeting
Cedar City, Utah
May 10, 2002

David B. Hacker
Daniel K. Holm
Department of Geology, Kent State University
Kent, Ohio 44242

Peter D. Rowley
Geologic Mapping, Inc., P.O. Box 651
New Harmony, Utah 84757

H. Richard Blank
U.S. Geological Survey, 904 W. Riverside
Spokane, Washington 99201

ABSTRACT

Detailed mapping in the Pine Valley Mountains and adjacent Bull Valley Mountains and Iron Springs mining district of southwestern Utah has delineated large allochthonous masses consisting of Tertiary volcanic and sedimentary strata laterally bounded by tear faults and soled on low-angle detachments. These masses are interpreted to be gravity slides resulting from catastrophic slope failure on oversteepened topography produced by rapidly inflating, early Miocene quartz monzonite intrusions (Pinto Peak, Iron Mountain, Bull Valley-Big Mountain, Stoddard Mountain, and Pine Valley laccoliths) of the so called "Iron Axis" magmatic province. The largest slide mass covers >150 km^2, is more than 550 m thick, and extends more than 20 km from its parent laccolithic dome. Mappable rock units within slide masses are typically broken and rotated and some are pervasively brecciated and sheared; internal folds and faults as well as disconnection and omission of rock units are common. However, the overall stratigraphic order in many instances is perseved. Deformation is confined to the allochthons, with structures terminating abruptly downward at bounding low-angle faults. These slides have resulted in emplacement both of younger rocks on older rocks and of older rocks on younger rocks.

During or closely following each sliding event, probably due at least in part to concomitant sudden release of overburden pressure, each intrusion (except Iron Mountain) erupted ash flows and (or) lava flows that partly or totally covered the associated slide mass. These deposits help date and separate the slides and identify their sources. The age of all this activity is constrained by $^{40}Ar/^{39}Ar$ ages of 21.93$\pm$0.07 Ma on the oldest volcanic unit of Iron Axis affinity (from the Pinto Peak intrusion) and 20.54$\pm$0.07 Ma on the youngest unit (from the Pine Valley intrusion), ages that are nearly indistinguishable from the ages of the quartz monzonite sources. On this one-day field trip we will visit and examine several of these representative allochthons and examine structural and volcanic features that bear on their mode of origin.

Evidence from recent studies supports current models of laccolith development, with initial emplacement as sills before the main phase of intrusion and doming. Laccoliths of the study area show continuous growth stages including: (1) initial sill emplacement, (2) vertical growth, (3) gravity sliding of portions of the roof, and (4) eruption. Field relationships show that the large (>200 km^2) Pine Valley laccolith is an intrusive feature (not extrusive as suggested by some earlier investigators) that was emplaced as a very shallow (<200 m) concordant intrusion.

INTRODUCTION

The purpose of this one-day field trip is to examine gravity-slide structures and volcanic deposits in the northern Pine Valley Mountains and adjacent areas of southwestern Utah (figure 1), and to evaluate field evidence bearing on their relations to laccolithic quartz monzonite intrusions. Rocks of the Pine Valley Mountains consist mostly of volcanic and intrusive rocks that range in age from Oligocene to Quaternary that were erupted upon or intruded into Mesozoic and Tertiary sedimentary rocks (figure 2). The laccolithic bodies belong to a group of more than a dozen closely related, early Miocene intrusions that constitute a magmatic province trending northeasterly across the structural transition zone between the Basin and Range and Colorado Plateau in this region, generally along the trend of the Sevier orogenic front. Because laccoliths of the Iron Springs district and eastern Bull Valley Mountains are well aligned within the belt and have produced sizable iron deposits, the belt has known informally as the "Iron Axis" (Toby, 1976; Blank and others, 1992; Rowley and others, 1995; Hacker, 1998) (figure 3). Intrusions of Iron Axis affinity were forcibly emplaced within 3.0 to 0.25 km of the surface as bulbous laccoliths, sills, and other partly concordant bodies, and were emplaced within the axial zones of some of the older, southeast-vergent Sevier thrusts and folds (Mackin, 1960).

The largest Iron Axis intrusion forms the gigantic (>200 km^2) igneous mass capping the Pine Valley Mountains. Previous studies have placed its origin either as an extrusive volcanic dome (Mattison, 1976; Grant, 1991) or as an intrusive laccolith of world-class size areal extent and volume (Cook, 1957, 1960). Recent work has aimed at resolving differences of interpretation of this unique feature. A fruitful approach has proved to be detailed mapping directed towards delineation of and identification of the sources of far-traveled slide masses that involve roof rocks of the several quartz monzonite-cored uplifts in the vicinity, including the Pine Valley Mountains body (Hacker, 1998). Similar slide masses were earlier recognized and mapped in the Iron Springs mining district (Mackin, 1947, Blank and Mackin, 1967) and in the Bull Valley Mountains (Blank, 1959, 1993); more recent work focused on gravity slides in the northern Pine Valley Mountains (Hacker, 1998). It can be inferred from field relations that slides are the result of slope failure on oversteepened topography produced by the rapid rise of laccolithic intrusions. This slide-laccolith association was the focus of an earlier Geological Society of America field trip in the Iron Axis region (Blank and others, 1992). Moreover, sliding was often synchronous with or immediately followed by volcanic eruption from the flank of the associated intrusion, doubtless triggered at least in part by the sudden release of overburden pressure and accompanied by earthquakes. As a result, the slide masses are typically blanketed by ash-flow tuffs, tuff breccias, and lava flows that post-date volcanics of the cover rock succession. This sequence of events (1-doming, 2-gravity sliding, 3-volcanism) has been documented elsewhere for initiating violent eruptions by release of confining pressure on magma chambers within large volcanic cones (e.g., see Lipman and Mullineaux, 1981). The association of gravity sliding and volcanism on the flanks of laccoliths is less well known; therefore, a summary of new evidence pertaining to the geometry, scale, and timing of gravity faulting and their relationships to the growth and eruptive history of laccoliths is presented here. We also discuss a model for the growth of the Iron Axis laccoliths.

Gravity slides are recognized in the field as highly sheared, allochthonous rock masses soled on low-angle faults and laterally bounded by tear faults. A typical mass is pervasively faulted, fractured and locally pulverized, with much internal rotation and interpenetration of constituent formations. Duplication and omission of strata are common although in most places the overall stratigraphic order is preserved. Internal faults terminate downward at the sole fault, which may juxtapose younger over older rocks or vice versa. The slide sole faults of the study area are distinctly different from well known other low-angle fault systems such as the Sevier thrust faults of Cretaceous age and Neogene basin-range detachment faults (see figure 4). They do resemble soles of gravity slides associated with collapse of regional high-angle fault scarps (e.g., Swadley and others, 1994), but candidate fault scarps that pre-date basin-range faults, yet are not laccolith-related, are lacking in the Pine Valley Mountains area. Mapping of the stratigraphy and structures of the displaced slide masses confirms their relation to intrusive doming.

GEOLOGIC SETTING

The Pine Valley Mountains are situated in a structural and stratigraphic transition zone between the Colorado Plateau and the Basin and Range physiographic provinces (figure 5). During the Paleozoic and early Mesozoic, this area occupied the edge of the shelf of the North American continent, and it accumulated a thick wedge of westerly thickening shelf sediments that represented deeper water farther to the west. In the late Cretaceous and Paleocene, the area was affected by the Sevier orogeny where deformation consisted manly of
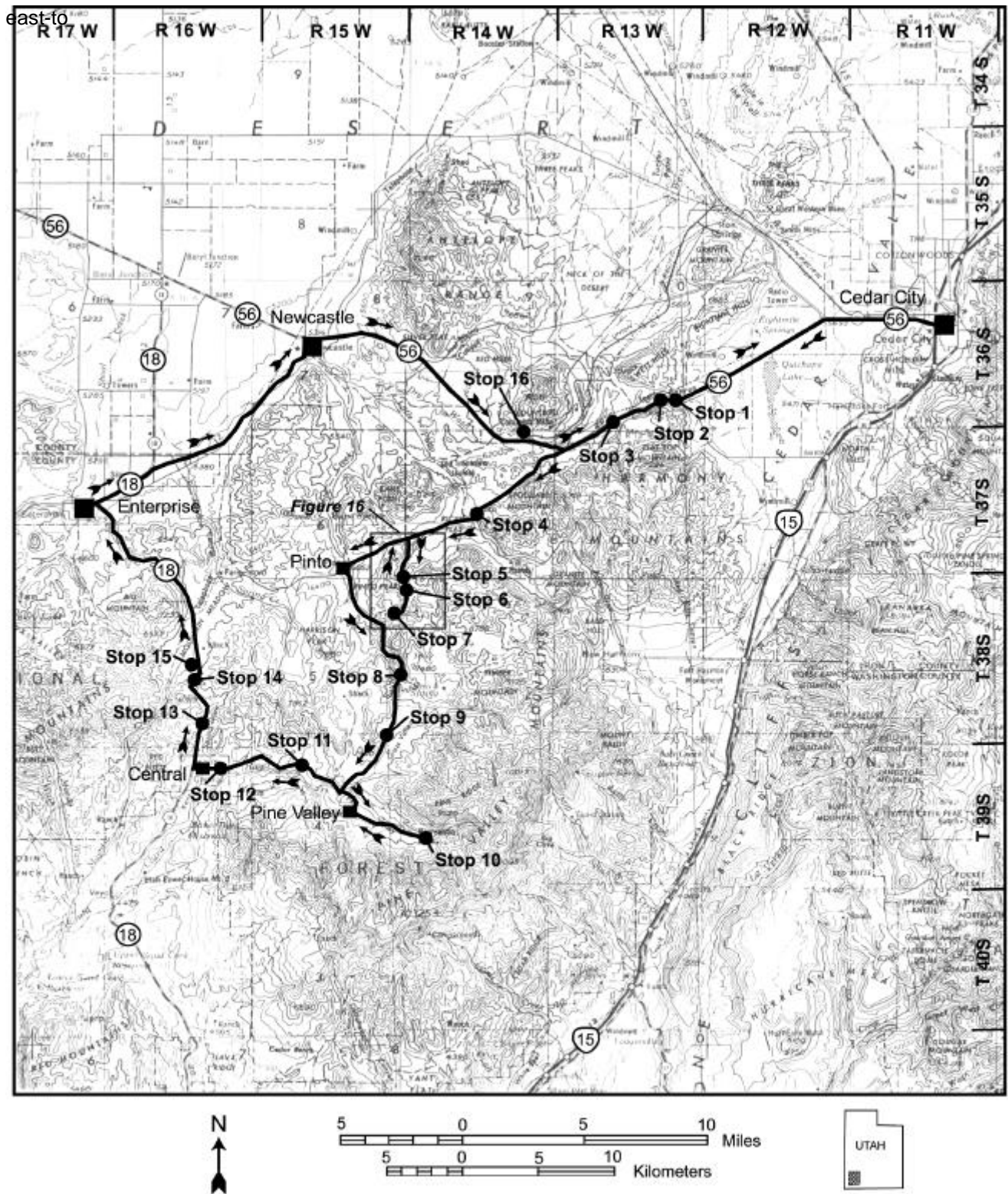
Figure 1. Map of the Pine Valley Mountains area showing location of stops. Based on U.S.G.S. Cedar City 1:250,000 topographic map NJ 12-7, 1971 (revised)

LEGEND

	Quaternary and Tertiary sediments
	Quaternary and Tertiary basalts
	Tertiary volcanic rocks
	Tertiary intrusive rocks
	Tertiary and Cretaceous sedimentary rocks
	Jurassic and Triassic sedimentary rocks
	Paleozoic sedimentary rocks
	Precambrian metamorphic rocks
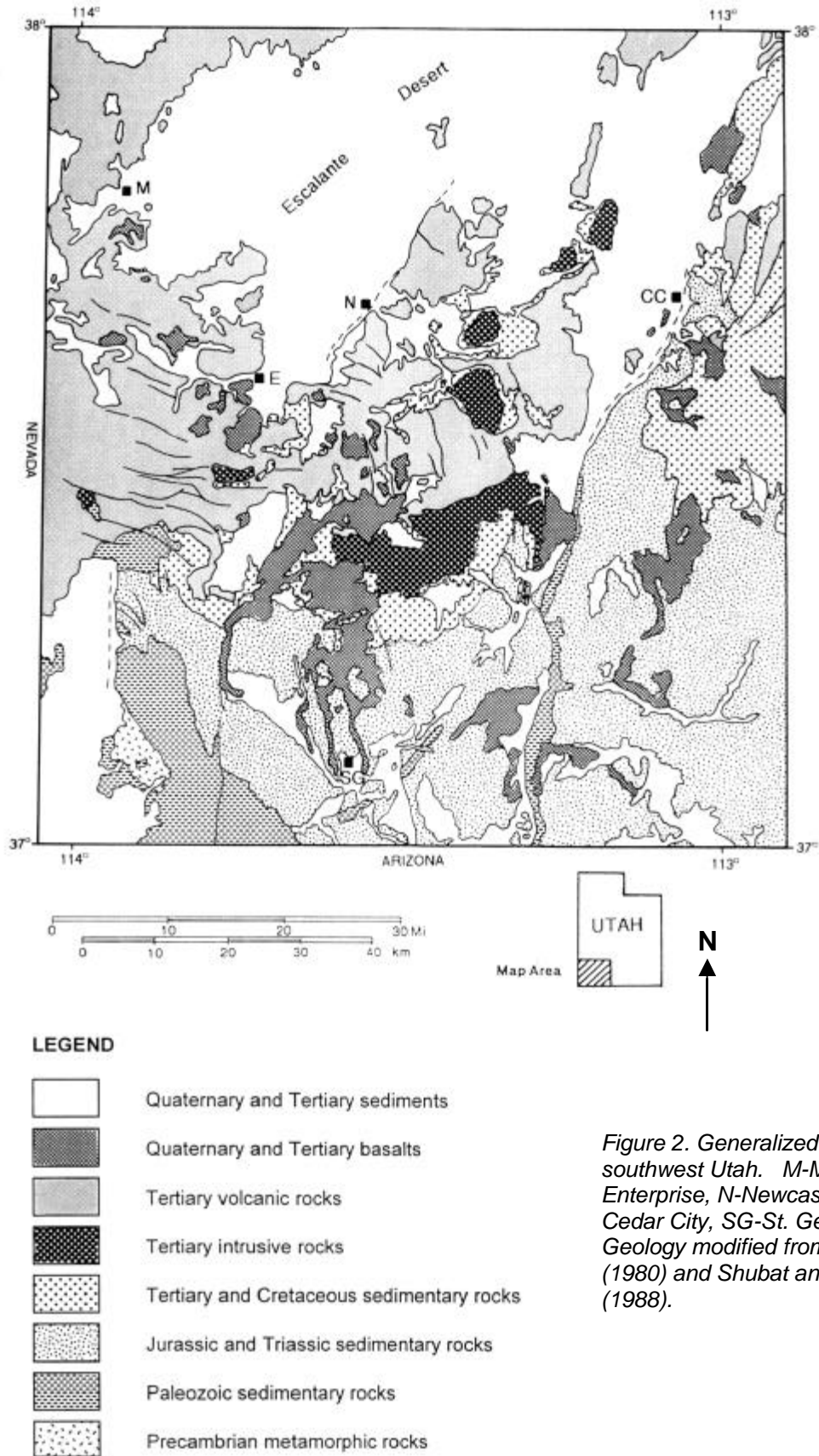
Figure 2. Generalized geology of southwest Utah. M-Modena, E-Enterprise, N-Newcastle, CC-Cedar City, SG-St. George. Geology modified from Hintze (1980) and Shubat and Siders (1988).
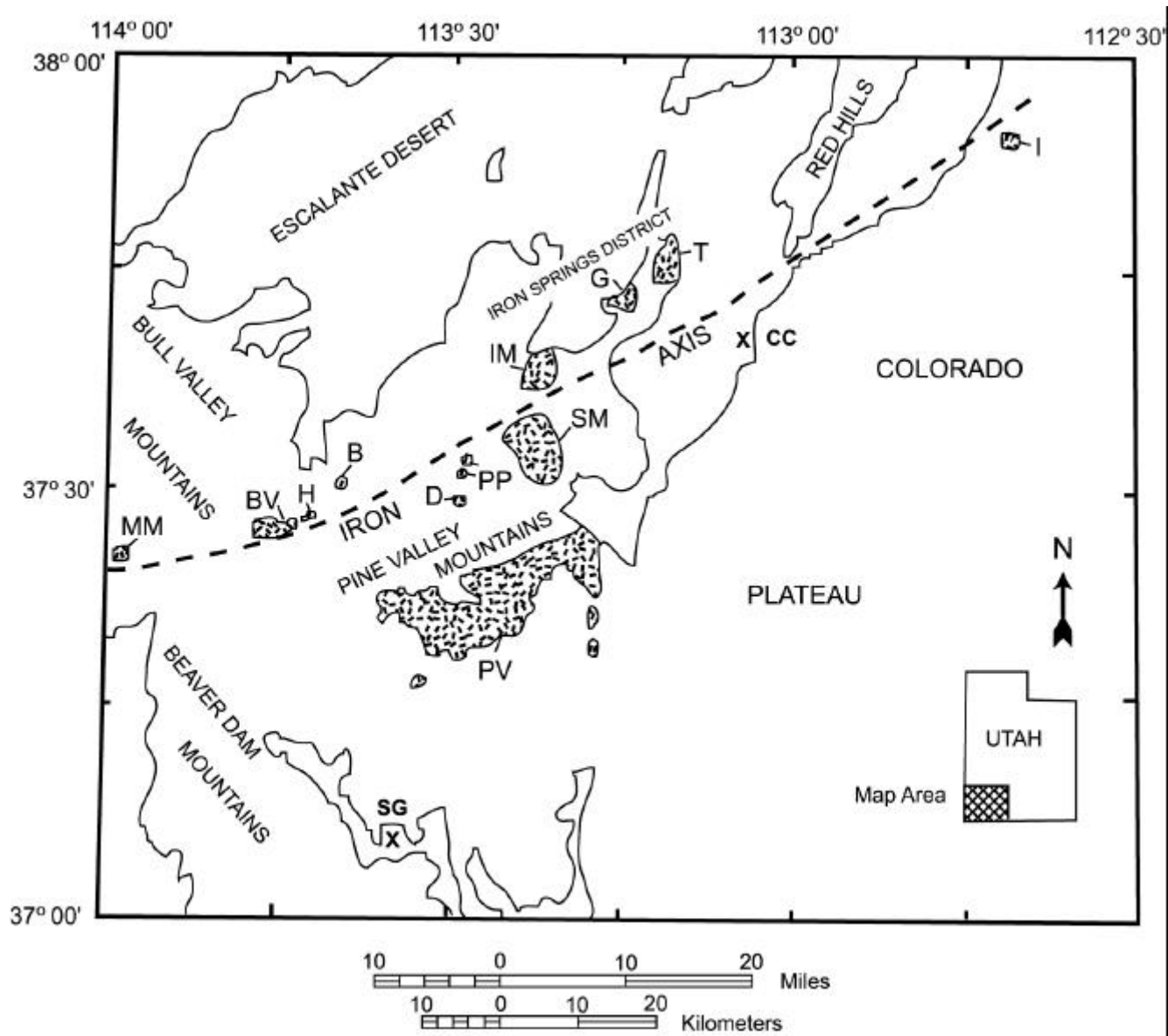
Figure 3. Index map of the Iron Axis region of southwest Utah, showing area of study. Intrusions of and near the Iron Axis are stippled and have the following name symbols: B - Big Mountain; BV - Bull Valley; D - The Dairy; G - Granite Mountain; H -Hardscrabble Hollow; I - Iron Peak; IM - Iron Mountain; LP - Lookout Point; MM - Mineral Mountain; PP - Pinto Peak; PV - Pine Valley; SM - Stoddard Mountain; T - Three Peaks. Towns: CC - Cedar City; SG - St. George.

A

Extension   Shortening

10 Km

B

Brittle Shear   Ductile Shear

10 Km

C

Shortening

10 Km

Figure 4. Diagrammatic sketches of three types of low-angle faults found in the Basin and Range. A-Gravity-slides, B-Detachment faults, and C-Thrust faults. Modified from Wernicke (1981) and Van Kooten (1988).

241
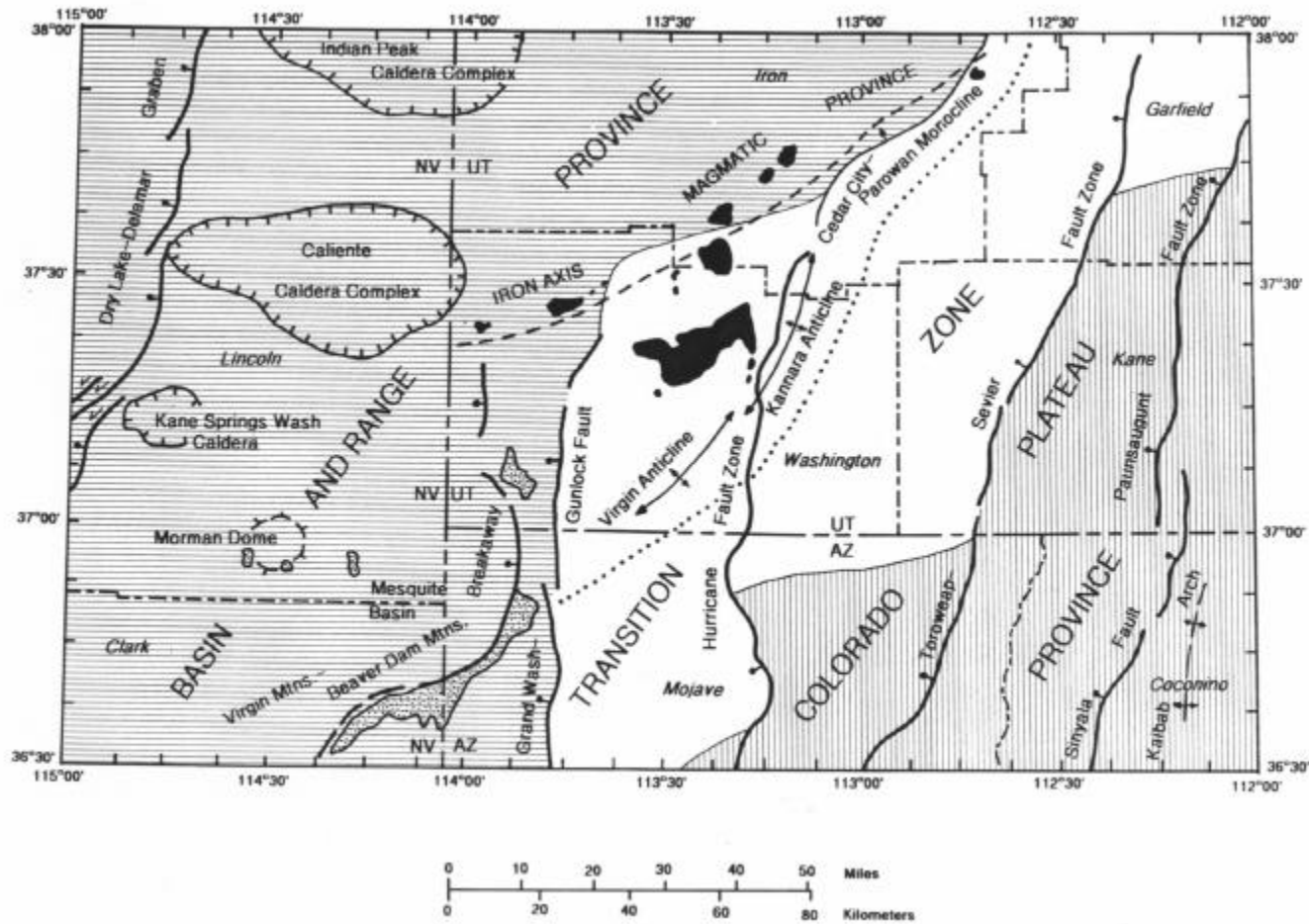
Figure 5. Tectonic map of southwest Utah, southeast Nevada, and northwest Arizona showing trends of major structures (modified from Blank and Kucks [1989] and Scott and Swadley [1995]).

southeast-directed, thin-skinned ramp-decollement style thrusting. Not coincidentally, the easternmost extent of Mesozoic thrusting and folding in Utah corresponds closely to the structural shelf hinge that marks the eastward change from thick "miogeoclinal" shelf strata to thinner strata of cratonic platform facies (Hintze, 1986).   In southwestern Utah, the easternmost extent of major exposed Sevier thrusting is represented by the Square Top Mountain thrust fault, located in the northern Beaver Dam Mountains to the west of the Pine Valley Mountains. East of the Square Top Mountain thrust, a Sevier-age northeast-trending anticlinal structure extends mostly in the subsurface from the Bull Valley Mountains through the Iron Springs district to the Red Hills. The Iron Springs thrust, also known as the Iron Springs Gap thrust of Mackin (1947) and the Calumet fault of Lewis (1958), locally displaces the fault. This fault shows about 5.6 km of southeastward displacement and places strata of the Jurassic Carmel Formation over units of the Cretaceous Iron Springs Formation (Van Kooten, 1988). Other related folds include the Virgin anticline-Kanarra fold system, which is east-southeast of the Pine Valley Mountains and extends from southeast of St. George northeast past Cedar City (Threet, 1963; Kurie, 1966).

Following the Sevier orogeny, erosion reduced the structural and topographic forms in the Pine Valley Mountains area during the Late Cretaceous and early Paleocene. A broad basin later developed in the region, beginning in the late Paleocene (Goldstrand, 1994), into which interbedded conglomerate, sandstone, and limestone were deposited within alternating fluvial, deltaic, and lacustrine environments.   Conditions in southwest Utah changed dramatically in early Oligocene time with the onset of calc-alkalic igneous activity at about 34 to 33 Ma (Anderson and Rowley, 1975; Best and others, 1989; Rowley and others, 1994; Rowley, 1998; Rowley and Dixon, 2001) and continuing into the early Miocene. The Pine Valley Mountains area was a relatively flat plain during this time, across which regional calc-alkaline ash-flow tuff sheets were deposited from sources outside the area. These sources included the Oligocene Indian Peak calde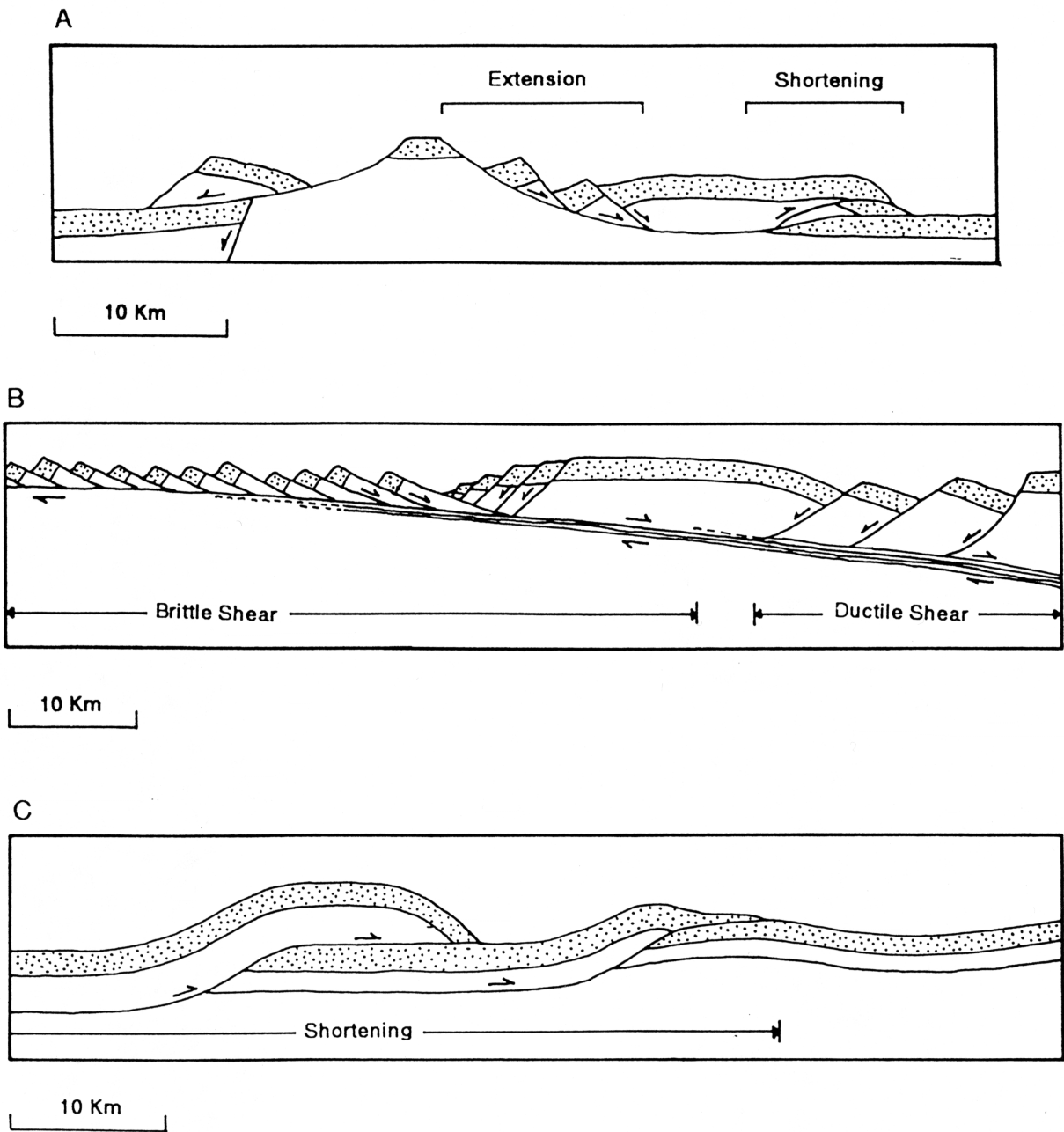ra complex (Best and others, 1989) to the northwest, and the Caliente caldera complex (Williams, 1967; Noble and McKee, 1972; Ekren and others, 1977; Rowley and others, 1995, 2001) to the west (figure 5). Both caldera complexes consist of numerous nested and partially overlapping calderas produced during catastrophic eruption cycles. Locally the tuffs intertongue with lava flows and laharic breccia from andesitic volcanoes and fissure eruptions.

Structural and topographic relief returned to the Pine Valley Mountains area again during an episode of early Miocene magmatic activity, starting at about 22 Ma, which produced the series of shallow, calc-alkaline laccolithic intrusions of the Iron Axis magmatic province (figure 3 and 5). Other intrusions in the province are known in the subsurface through drilling or have been inferred from their roof rock structures and aeromagnetic signatures. Geophysical data suggest that many of the intrusions are interconnected at depth and are inferred to be underlain and fed by a larger batholith complex (Mackin, 1947; Blank and Mackin, 1967; Blank and Kucks, 1989; Blank and others, 1992; Rowley and others, 1994, 1998, 2001). Most of the Iron Axis intrusions are quartz monzonite to granodiorite porphyries (Blank and others, 1992). However, the Mineral Mountain intrusion at the southwest end of the belt is a granite porphyry (Morris, 1980; Adair, 1986), and the Iron Peak intrusion, at the northeast end, is a gabbro-diorite porphyry (Spurney, 1984). The intrusions were forcibly emplaced into Paleozoic, Mesozoic, and Tertiary sedimentary rocks to form laccoliths, sills, and other partly concordant bodies that strongly deformed their roofs by folding and faulting. The alignment of the intrusions closely coincides with the northeast trend of earlier Sevier orogenic structures (Mackin, 1954, 1960; Blank, 1959; Van Kooten, 1988). The intrusions in the eastern Bull Valley Mountains (Bull Valley, Hardscrabble Hollow, and Big Mountain) and Iron Springs district (Iron Mountain, Granite Mountain, and Three Peaks) intruded into limestone strata of the Jurassic Carmel Formation and produced major replacement iron ore bodies (Mackin, 1968) that led to the term "Iron Axis" (Tobey, 1976). At least four intrusions (Pinto Peak, Bull Valley, Stoddard Mountain, and Pine Valley) broke through their roofs and erupted ash-flow tuffs and (or) lava flows (Blank, 1959; Hacker, 1995, 1998; Hacker and others, 1996). Most of the major structures within the Pine Valley Mountains are associated with the laccolithic intrusions emplaced during the Iron Axis magmatic episode.

Following Iron Axis magmatic activity (post-22 Ma), the area once again received additional regional calc-alkaline ash-flow deposits from the Caliente caldera complex to the west. Beginning at about 14-15 Ma, a change from calc-alkaline to bimodal (basalt and high silica rhyolite) magmatism began in the region and has persisted sporadically throughout the late Cenozoic and was accompanied by regional basin-range extensional faulting. Bimodal magmatism produced the extensive basaltic lava flows and associated cinder cones found in southwest Utah (see figure 2), but their total volume is much less than that of the earlier calc-alkaline volcanic rocks (Rowley and Dixon, 2001). The basin-range style tectonic extension imprinted a dominantly northerly striking fault pattern upon previously formed structures. Regional crustal extension in the Basin and Range occurred through a complex combination of displacements along low-angle normal, high-angle normal, and strike-slip fault systems (Moores and others, 1968; Anderson, 1971; Armstrong, 1972; Wernicke and others, 1988; Anderson and Barnhard, 1993; Rowley and Dixon, 2001). Extension in the region occurred principally

during the last 20 Ma (Anderson and Mehnert, 1979; Wernicke and others, 1988; Rowley and Dixon, 2001) and appears to have taken place in two episodes with two slightly different extension directions.

The present topographic relief of this eastern part of the Basin and Range Province is primarily the result of high-angle, basin-range block faulting (horst and graben style) that began in the late Miocene, at about 10 to 8 Ma (Anderson and Mehnert, 1979; Rowley and others, 1979; 1981; Shubat and Siders, 1988; Rowley and Dixon, 2001). Steep, north-to-northeast-trending, high-angle normal faults are abundant. Synextensional sediments eroded from the uplifted blocks were deposited in the adjacent developing basins, and now generally occupy more area than the ranges. Many basins have accumulated very thick sections of basin fill, such as the Newcastle graben west of the Antelope Range in the southern Escalante desert. In contrast, the Colorado Plateau to the east remained an undeformed stable highland. The boundary between the Basin and Range Province and Colorado Plateau is not sharp in southwest Utah; instead they are separated by a structural transition zone that varies in width from about 30 to 100 km (figure 5). The area of transition is characterized by high-angle faults similar to those in the Basin and Range but generally they are less abundant and have less displacement (Anderson and Rowley, 1975; Rowley and others, 1979, 1998; Scott and Swadley, 1995; Rowley 1998; Rowley and Dixon, 2001), and the intervening basins occupy less area than the ranges and are filled with a thinner sequence of alluvial fill or do not receive erosional fill at all.

STRATIGRAPHIC AND IGNEOUS UNITS

The rock section of the Pine Valley Mountains can be divided into four distinct sequences based on their associated origin before, with, or following Iron Axis magmatic activity (figure 6). Pre-Iron Axis rocks include a lower sequence of in-place sedimentary rocks, which hosted the Iron Axis intrusions, and an upper sequence of mostly regionally deposited volcanic rocks that later became part of the allochthonous gravity-slide masses derived from the roofs of the intrusions. The Iron Axis rocks include a sequence of volcanic and intrusive igneous rocks related to magmas that formed laccolithic structures. The post-Iron Axis rocks include regionally and locally derived volcanic rocks and local sedimentary rocks that formed contemporaneously with post-Iron Axis extensional structures.

Pre-Iron Axis Sedimentary Rocks

The pre-Iron Axis sedimentary rocks consist of 2,700 m of Mesozoic and Cenozoic strata, belonging to seven well-known and regionally extensive formations (figure 7). The pre-Iron Axis sedimentary rocks are exposed mostly in the southern part of the range and also in the eroded cores and flanks of intrusive anticlines and gravity-slide masses. The Mesozoic section consists of clastic sedimentary rocks of continental origin along with minor shallow-marine carbonates and evaporates of the Jurassic Kayenta Formation, Navajo Sandstone, Temple Cap Formation, and Carmel Formation, and the Cretaceous Dakota Conglomerate and Iron Springs Formation (Hintze, 1986). The sedimentary sequence is interrupted by at least two regional unconformities, one at the base of the Temple Cap Formation, and the other at the base of the Dakota Conglomerate. The Cretaceous section represents conglomeratic to shaly clastic material shed eastward from the Sevier orogenic belt in eastern Nevada and western Utah into a foreland basin (Hintze, 1986).

The Jurassic to Cretaceous sequence was thrusted and folded in the Late Cretaceous to form subaerial topographic features later planed down by erosion and overlain unconformably by Paleocene to Oligocene fluvial and lacustrine sedimentary rocks of the Claron Formation (Cook, 1960). The Claron forms the basal Tertiary unit throughout the Pine Valley Mountains as well as over much of southwestern Utah. The Claron and Iron Springs Formations were the host rocks for Iron Axis intrusions in the Pine Valley Mountains (Cook, 1957; Hacker, 1998) while in the Iron Springs district and Bull Valley Mountains, the Temple Cap and Carmel Formations were the host rocks for intrusions (Blank, 1959, 1993; Blank and Mackin, 1967).

Pre-Iron Axis Volcanic Rocks

The pre-Iron Axis volcanic rocks (figure 8) consist of late Oligocene to early Miocene (30 to 22 Ma) regional ash-flow tuff deposits derived from distant sources to the northwest and west. Their ages are known from several published isotopic and fission track dates (see Anderson and Rowley, 1975; Best and others, 1989; Rowley and others, 1995). They include ash-flow tuffs of the Wah Wah Springs Formation (of the Needles Range Group) and the Isom Formation, both derived from the Indian Peak caldera complex to the north; ash-flow tuffs of the Leach Canyon Formation and Condor Canyon Formation (of the Quichipa Group) derived from the Caliente caldera complex to the northwest; and the Harmony Hills Tuff (of the Quichapa Group) from the Bull Valley Mountains (see figure 5 for caldera locations). This volcanic sequence shows an overall thinning from

AGE (Ma)	FORMATION			MEMBER	Thickness (m)	
HOLOCENE-PLEISTOCENE	Surficial deposits-alluvial, mass wasting				0-46	**Post-Iron Axis Volcanic and Sedimentary Rocks**
	Basaltic lava flows				0-61	
1.6	Boulder deposits				0-61	
PLEISTOCENE-PLIOCENE	Eight Mile Dacite				0-152	
	Older piedmont-slope deposits				0-91	
PLIOCENE	Older basaltic lava flows				0-61	
MIOCENE	Alluvial deposits of Spring Creek				0-91	
19	Racer Canyon Tuff				0-91	
20.5	Pine Valley intrusion	Pine Valley Latite		Timber Mountain member	0-610	**Iron Axis Rocks**
				Rencher Peak member	0-457	
	Page Ranch Formation				0-122	
	The Dairy intrusion	Stoddard Mountain intrusion	Volcanic rocks of Comanche Canyon	Lava flow member	0-152	
				Ash-flow tuff member	0-61	
21.5	Rencher Formation (Derived from Bull Valley Intrusion)			Upper ash-flow tuff member	0-46	
				Lower ash-flow tuff member	0-107	
21.9	Pinto Peak intrusion	Rocks of Paradise		Sandstone member	0-7.6	
				Upper lava flow member	0-183	
				Lower lava flow member	0-122	
				Ash-flow tuff Member	0-91	
	Local volcanic rocks				0-24	**Pre-Iron Axis Volcanic Rocks**
22.5	Quichapa Group	Harmony Hills Tuff			30-99	
		Little Creek andesite -allochthonous only in Pine Valley Mountains			0-183	
		Local volcanic mudflow breccia			4.5	
23		Condor Canyon Formation		Bauers Tuff Member	24-61	
				Swett Tuff Member	0-9	
		Local sedimentary rocks			2	
24		Leach Canyon Formation			46-152	
OLIGOCENE	27-26	Isom Formation		Hole-in-the-Wall Tuff Mbr	12	
			Baldhills Tuff Member	Associated lava flows and sedimentary rocks	15-30	
	30	Wah Wah Springs Fm., Needles Range Group			0-9	
OLIGOCENE-PALEOCENE	Claron Formation				137-213	**Pre-Iron Axis Sedimentary Rocks**
CRETACEOUS	Iron Springs Formation				1067-1280	
	Dakota Conglomerate				0-15	
JURASSIC	Carmel Formation			Upper Co-Op Creek Limestone Member	15-46	
				Lower Co-Op Creek Limestone Member	76-91	
	Temple Cap Formation				61	
	Navajo Sandstone				610	
	Kayenta Formation			Upper member	122	
				Middle member	122	

Figure 6. Composite table of stratigraphic (sedimentary and volcanic) and lithodemic (igneous intrusive) units mapped in the Pine Valley Mountains. Thicknesses relate to stratigraphic units only.

AGE	FORMATION	MEMBER	Thickness (m)	LITHOLOGY
OLIGOCENE-PALEOCENE	Claron Formation		137-213	
CRETACEOUS	Iron Springs Formation		1067-1280	
	Dakota Conglomerate		0-15	
JURASSIC	Carmel Formation	Upper Co-Op Creek Limestone Member	15-46	
		Lower Co-Op Creek Limestone Member	76-91	
	Temple Cap Formation		61	
	Navajo Sandstone		610	
	Kayenta Formation	Upper member	122	
		Middle member	122	

Figure 7. Generalized stratigraphic column of pre-Iron Axis sedimentary rocks.

246

AGE	FORMATION		MEMBER	Thickness (m)	LITHOLOGY
MIOCENE	Local volcanic rocks			0-24	
	Quichapa Group	Harmony Hills Tuff		30-99	
		Little Creek andesite -allochthonous only		0-183	
		Local volcanic mudflow breccia		4.5	
		Condor Canyon Formation	Bauers Tuff Member	24-61	
			Swett Tuff Member	0-9	
		Local sedimentary rocks		2	
		Leach Canyon Formation		46-152	
OLIGOCENE	Isom Formation		Hole-in-the-Wall Tuff Mbr	27-42	
			Baldhills Tuff Member		
	Wah Wah Springs Fm., Needles Range Group			0-9	

Figure 8. Generalized stratigraphic column of pre-Iron Axis volcanic rocks.

north to south within the Pine Valley Mountains that is reflective of their source areas being located to the north. The lower ash-flow tuffs (Wah Wah Springs, Isom, and Leach Canyon Formations) were deposited in a still-active Claron depositional basin where the tuffs became intercalated with lacustrine limestone and volcaniclastic sedimentary rocks. The sequence also contains some local lava flows that proved to be very valuable in determining the source areas of various gravity-slide masses derived from the Iron Axis intrusions. Some flows mapped within the gravity-slides proved to be totally allochthonous and could be correlated to autochthonous units located within the Bull Valley Mountains (e.g., Little Creek andesite unit). The pre-Iron Axis volcanic rocks crop out throughout the northern part of the study area within the eroded flanks of laccoliths or in parts of their preserved roof sequence, in erosional valleys, and in remnants of gravity-slides. The original southern extent of the pre-Iron Axis volcanic rocks is unknown due to extensive erosion, but are believed to have been present south of the Pine Valley intrusion based on outcrops found adjacent to the intrusion on its south side.

Iron Axis Rocks

The Iron Axis rocks (figure 9) exposed in the Pine Valley Mountains consist of early Miocene (22 to 20 Ma) hypabyssal, quartz monzonite, porphyry intrusive rocks and associated extrusive volcanics produced as part of the regional Iron Axis magmatic episode. The Pine Valley intrusion caps a large portion of the range. It crops

AGE	FORMATION	MEMBER	Thickness (m)	LITHOLOGY
MIOCENE	Pine Valley Latite	Timber Mountain member	0-610	
		Rencher Peak member	0-457	
	Page Ranch Formation		0-122	
	Volcanic rocks of Comanche Canyon	Lava flow member	0-152	
		Ash-flow tuff member	0-61	
	Rencher Formation	Upper ash-flow tuff mbr	0-46	
		Lower ash-flow tuff member	0-107	
	Rocks of Paradise	Sandstone member	0-8	
		Upper lava flow member	0-183	
		Lower lava flow member	0-122	
		Ash-flow tuff Member	0-91	

Figure 9. Generalized stratigraphic column of Iron-Axis rocks.

out over a 240 km^2 area and has a remaining thickness of over 900 m. The Iron Axis rocks crop out in the central core of anticlines, where erosion has breached the pre-Iron Axis roof rocks to expose intrusive rocks, or in the preserved paleo-lowlands between the laccoliths where the volcanic rocks were deposited. Volcanic activity during this magmatic episode was previously thought to be represented by ash-flow tuff and lava flow deposits of the Rencher Formation and lava flows of the younger Pine Valley Latite. Cook (1957) defined both formations from exposures in the Pine Valley Mountains, but did not document their source areas. Blank (1959) later documented that the volcanic rocks of the Rencher Formation erupted from the Bull Valley Intrusion. Cook (1957) believed the Pine Valley Latite covered its vent area and was later intruded by the Pine Valley intrusion (Cook, 1957).

Detailed mapping by Hacker (1998) and Rowley (unpublished data) has revealed that volcanic units of Rencher lithology have more than one source area. Field evidence shows that the Pinto Peak and Stoddard Mountain intrusions in the northern Pine Valley Mountains both erupted a sequence of ash-flow tuffs and lava flows distinct from the Rencher Formation. These are named the "rocks of Paradise" and the "volcanic rocks of Comanche Canyon" respectively. Field evidence also shows that the previously defined Paradise intrusion of Cook (1957) is in fact a large lava flow derived from the Pinto Peak intrusion, and was included as a member of the rocks of Paradise (Hacker, 1998). The name "Rencher Formation" is retained, but restricted to volcanic rocks derived only from the Bull Valley intrusion. Finally, mapping indicates that the Pine Valley Latite erupted from two source areas: (1) at Rencher Peak, possibly from an early episode of the Pine Valley intrusion, and (2) directly from the main Pine Valley intrusion. Figure 10 shows the inferred areal distribution of the volcanic units erupted from Iron Axis intrusions. Locally derived volcaniclastic rocks of the Page Ranch Formation are genetically related to erosion of the intrusive uplifts and provide a marker unit that aided in deciphering the structural history of the intrusions.
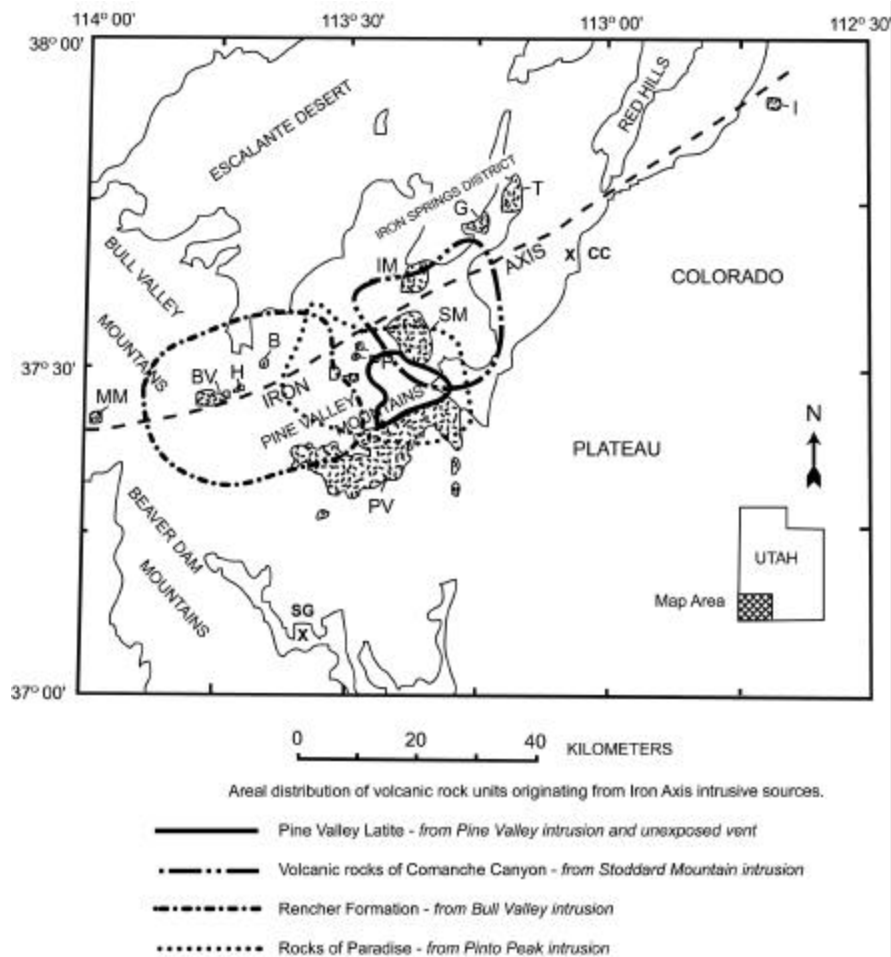
Figure 10. Generalized map of southwest Utah showing areal distribution of volcanic rocks erupted from laccoliths.

Post-Iron Axis Rocks

The post-Iron Axis rocks (figure 11) consist of upper Tertiary and Quaternary (19 Ma to recent) regional and local volcanic rocks deposited over a rugged topographic area developed by earlier Iron Axis intrusions and later by their erosion. The last regional ash-flow tuff to enter the area was the Racer Canyon Tuff derived from the Caliente caldera complex. Topographic barriers raised by the earlier intrusive structures to the south probably resulted in the thick Racer Canyon Tuff being restricted to the very northern part of the study area. Erosion of the remaining highlands in the late Miocene resulted in the deposition of alluvial deposits in the north that are now capped by late Tertiary (Miocene and Pliocene to Pleistocene) basaltic lava flows. Many stream valleys were dammed by lava flows and subsequently filled in with clastic sediment to form broad fertile plains (Pine Valley, Grass Valley, Grassy Flat, Diamond Valley, and the unnamed area south of the town of Central). Large aprons of Pliocene (?) and Pleistocene boulder alluvium, formed mostly by debris flows, are located on the flanks of the Pine Valley intrusion and represent the only other major sedimentary deposits.

AGE	FORMATION	MEMBER	Thickness (m)	LITHOLOGY
HOLOCENE-PLEISTOCENE	Surficial deposits-alluvial, mass wasting		0-46	
	Basaltic lava flows		0-61	
	Boulder deposits		0-61	
PLEISTOCENE-PLIOCENE	Eight Mile Dacite		0-152	
	Old alluvial-fan deposits		0-91	
PLIOCENE	Older basaltic lava flows		0-61	
MIOCENE	Alluvial deposits of Spring Creek		0-91	
	Racer Canyon Tuff		0-91	

Figure 11. Generalized stratigraphic column of post-Iron Axis rocks.

250

STRUCTURES - EARLY MIOCENE (IRON AXIS INTRUSIVE TYPE)

The major deformation in the Pine Valley Mountains occurred during early Miocene magmatism related to the forcible intrusion of quartz monzonite, as it formed laccolithic structures. Most successive intrusions deformed earlier structures formed by adjacent intrusions, thus complicating yet aiding in deciphering age relations. The intrusions made room for themselves by forcibly deforming the country rock by: (1) upflexing, producing domed or arched roofs containing extensional faults and attenuated bedding, and (2) shouldering aside the confining rocks, producing overturned monoclinal flexures, thrust faults, reverse faults, and fault-propagation folds. These structures are directly associated with the processes of intrusion and are familiar features of many laccoliths. Less familiar to the emplacement of laccoliths are structures formed indirectly by detachment faulting of large slabs of roof rock from the growing flanks of the intrusions. These low-angle, detached fault masses constitute a large allochthonous complex of gravity slides (figure 12). Although these are secondary structural features, they owe their existence to the doming of cover strata as the laccoliths intruded and made room for themselves at depth. The recognition of the detached masses as gravity slides formed from the flanks of rapidly growing laccoliths greatly aided in defining the structural history of the intrusions.

Gravity Slide Complex

Within the study area are numerous large allochthonous masses (sheets or blocks) of fractured, brecciated, sheared, and attenuated Tertiary volcanic and sedimentary rocks resting on low-angle faults. Faulting placed both younger rocks over older and older rocks over younger. Some of these anomalous structural relations within the Pine Valley Mountains were first hinted at by Cook (1954, 1957), who recognized a similarity between Tertiary rock units that he defined as the Grass Valley and Atchinson Formations and the older rock units underlying them. Cook suggested that the different formations could be the same rock units brought together tectonically by thrust faulting. Cook (1960) later abandoned the two formations and mapped some of the rocks on the north side of Grass Valley and in Grassy Flat Canyon as allochthonous faulted "slide masses," and suggested that they were emplaced by gravity sliding along low-angle normal faults off the up-arched roof of an intrusive body exposed 5.6 km south-southeast of Pinto. This location corresponds to Cook's (1957) Paradise intrusion that is now interpreted to be an extrusive lava flow (upper lava member of the rocks of Paradise), and therefore the lava flow could not have been an area of structural relief necessary for sliding.

Allochthonous rock masses were earlier recognized in the adjacent Bull Valley Mountains (Blank, 1959) and Iron Springs District (Mackin, 1960), and interpreted as slide masses related to gravitational unroofing of nearby intrusions (Blank, 1959, 1993; Mackin, 1960; Rowley and others, 1989, 2001). Recently, allochthonous rock masses have also been recently recognized in the northeastern end of the Iron Axis in both the Basin and Range sector (Red Hills area), and on the western Colorado Plateau sector (Markagunt Plateau area). These features have been interpreted to result from general gravity-sliding events initiated by different mechanisms at different times (Maldonado and others, 1997; Davis, 1999; Hatfield and others, 2000). The emplacement of the masses have been variously related to plateau uplift (Sable and Anderson, 1985), fault scarp collapse (Anderson, 1985), tilting above a batholith (Anderson, 1993), or tilting by crustal extension and associated block faulting (Maldonado, 1995; Maldonado and others, 1997). These allochthonous rock masses were emplaced during the Miocene (Maldonado and others, 1997; Hatfield and others, 2000).

Mapping for this study shows that the allochthonous rock masses within the Pine Valley Mountains are more extensive and more numerous than previously thought (e.g., Cook, 1960). A detailed study of the allochthonous stratigraphy, when compared with surrounding autochthonous units, also indicates that the allochthonous masses have more than one source area. Comparison of these allochthonous masses with others in the nearby eastern Bull Valley Mountains and Iron Springs district also strongly suggests that they have a common origin as detached masses derived from the growing uplifted flanks of nearby intrusive domes and were emplaced by gravitational sliding (Blank and others, 1992; Hacker and others, 1996). At least six major sliding episodes in this part of the Iron Axis can be attributed to the rapid emplacement of the Pinto Peak, Bull Valley-Big Mountain, Iron Mountain, Stoddard Mountain, and Pine Valley intrusions (Hacker, 1998). Individually, each sliding event was immediately followed by volcanic eruptions from their respective intrusions (except for the Iron Mountain intrusion) that broke through the uplifted cover rocks and erupted ash flows and/or lava flows that partly or totally covered the slide masses. Individual slide masses from different intrusions can be distinguished from one another by their position beneath or upon these newly discovered volcanic rock units, as well as the incorporation of these units in subsequent slide masses.

Distribution and Composition of Slide Masses: The general structural relations and distribution of displaced slide masses within the entire slide complex (i.e., the areas of the Pine Valley Mountains, eastern Bull

Stratigraphy of Bull Valley Slide Masses

| Harmony Hills Tuff |
| Andesite of Little Creek |
| Condor Canyon Formation |
| Leach Canyon Formation |
| Isom Formation |
| Claron Formation |

Stratigraphy of Big Mountain Slide Masses

| Lower Tuff Mbr of Rencher Fm |
| Harmony Hills Tuff |
| Andesite of Little Creek |
| Condor Canyon Formation |
| Leach Canyon Formation |
| Isom Formation |
| Claron Formation |

Stratigraphy of Pinto Peak Slide Masses

| Harmony Hills Tuff |
| Condor Canyon Formation |
| Leach Canyon Formation |
| Isom Formation |
| Claron Formation |

Stratigraphy of Iron Mountain Slide Masses

| Harmony Hills Tuff |
| Condor Canyon Formation |
| Leach Canyon Formation |
| Isom Formation |
| Claron Formation |
| Iron Springs Formation |

Stratigraphy of Stoddard Mountain Slide Masses

| Tuff Mbr of the Rocks Paradise |
| Harmony Hills Tuff |
| Condor Canyon Formation |
| Leach Canyon Formation |
| Claron Formation |

Stratigraphy of Pine Valley Slide Masses

| Page Ranch Formation |
| Bull Valley or Big Mountain Slide Masses |
| Tuff Mbr of the Rocks Paradise |
| Harmony Hills Tuff |
| Condor Canyon Formation |
| Leach Canyon Formation |
| Isom Formation |
| Claron Formation |

COLORADO

PLATEAU

UTAH
Map Area

0   20   40 KILOMETERS

N

LEGEND

QTs Quaternary and Tertiary sedimentary rocks

QTb Quaternary and Tertiary basalts, includes minor dacites

Tv3 Tertiary post - Iron Axis regional volcanic rocks, includes minor rhyolites

Tv2 Tertiary Iron Axis volcanic rocks and minor volcaniclastics

Ti   Tertiary Iron Axis intrusive rocks

Tv1 Tertiary pre - Iron Axis regional volcanic rocks, mostly Quichapa Gp

Ts   Tertiary sedimentary rocks, mostly Claron Fm

Mz   Mesozoic sedimentary rocks, mostly Iron Springs and Carmel Fms

Pz   Paleozoic sedimentary rocks

Allochthonous Slide Masses

Pine Valley Slide Masses   Youngest
Stoddard Mountain Slide Masses
Iron Mountain Slide Masses
Big Mountain Slide Masses
Bull Valley Slide Masses
Pinto Peak Slide Mass   Oldest

High - angle fault

Low - angle fault at base of gravity slide mass, sawteeth on upper plate

Transport direction of gravity slide mass

Contact

Anticline and syncline, dotted where covered, Sevier age

1 ● Field trip stops #1 - 16

0   5 MILES

0   5 KILOMETERS

N

113° 45'

113° 45'

113° 30'

113° 30'

37° 30'

37° 15'

37° 15'

Figure 12. Generalized geologic map of Pine Valley Mountains and adjacent Iron Axis regions showing areal distribution of gravity slide masses and Iron Axis rocks. Stratigraphic boxes show allochthonous rock units exposed in slide masses that match autochthonous stratigraphy in the source areas. Landmarks include: A - Atchinson Mountain; BM - Big Mountain; GV - Grass Valley; RF - Richie Flat; C - Central; E - Enterprise; NH - New Harmony; P - Pinto; PV - Pine Valley.

Valley Mountains, and southwestern Iron Springs district) are displayed on a generalized geologic map (figure 12). Field relations strongly suggest that the present distribution of the scattered masses over the more than 600 km^2 area is not the result of subsequent erosion of a once continuous sheet. Instead, the distribution is the result of separate sliding events that displaced rock masses away from source areas occupied by intrusions. The slide structures are therefore grouped on figure 12 according to their inferred intrusive source. Arrows shown on the geologic map (figure 12) show the interpreted emplacement-direction of the individual slide masses. Opposing directions of transport and variable internal stratigraphy indicate the slide masses were not part of a single continuous slide sheet.

Displaced rocks that compose individual slide masses originated from nearby recognizable autochthonous formations and include volcanic and sedimentary rocks that range in age from Cretaceous (Iron Springs Formation) through early Miocene (Page Ranch Formation) (see figure 12). It should be noted that not every slide mass contains the same stratigraphy. This is due to: (1) the original lateral lithologic variations in the stratigraphic sequence at the different source areas, and (2) the timing of sliding events in relation to volcanic eruptions from different intrusions. Most slide masses can be distinguished from one another in the field by their lithology.

General Internal Structures of Slide Masses: The formations within the slide masses show attenuation and exhibit various internal structural complexities; however, normal internal stratigraphic succession is commonly maintained that allows individual rock units to be mapped. Typically, the formations exhibit pervasive internal fracturing and shattering but are well indurated. Some formations are brecciated and consist of pebble-to-boulder-sized, angular to subangular rock fragments with a crushed matrix of the same composition as the fragments. The brecciated zones are commonly matrix-poor, with the fragments commonly tightly packed in a jigsaw-puzzle mosaic separated by a cataclastically generated sand-to-granule-size matrix (figure 13). Most

Figure 13. Outcrop of allochthonous Harmony Hills Tuff showing rotated angular rock fragments in a comminuted matrix of the same composition as the fragments. In other areas where the matrix is sparse, the shattered rock resembles a three-dimensional jigsaw puzzle. The rocks shown in this photo are in Grass Valley and are part of the Big Mountain slide mass.

fragments have moved slightly relative to their neighbors, while others show some rotation. Rocks from adjacent formations are usually not mixed, but locally are chaotically juxtaposed along close-spaced shear domains. Omission or smearing out of stratigraphic units takes place along low-angle shear zones or bedding-plane faults. In fact, many of the formation contacts are actually fault contacts, but are mapped with a formation contact symbol due to the scale of mapping. Mechanically, the character of the internal deformation varies with rock lithology. The softer, moderately welded ash-flow tuffs (e.g., lower tuff member of the Rencher Formation and tuff member of the rock of Paradise) deformed along sheared zones as much as 3 cm thick containing pulverized rock flour material (cataclasite) with the consistency of clay, formed by the mechanical breakdown by crushing and grinding of the ash-flow tuff. In contrast, the more competent highly welded ash-flow tuffs (e.g., Leach Canyon Formation, Bauers Tuff Member of Condor Canyon Formation, and locally the Harmony Hills Tuff) deformed along brittle intersecting or anastomosing sets of shear fractures, which result in brecciation of the rocks.

In addition to internal deformation of the rock units, many structurally complex areas within the slide masses that contain extensively faulted and folded strata. Faulting occurs along: (1) local tear faults oriented parallel to transport direction, and (2) high-to low-angle normal and reverse faults oriented mostly perpendicular to transport direction.

Nature of Basal Fault Contacts: Overall, the slide masses closely resemble remnants of "erosional thrust sheets" in form. All deformation is confined to the slide masses themselves and abruptly terminates downward at low-angle, basal bounding detachment faults (referred to here as gravity-slide faults). The basal gravity-slide faults are a composite of four types of fault surfaces. They include: (1) a subhorizontal "bedding fault" (decollement) within sedimentary rocks of the Tertiary Claron or Upper Cretaceous Iron Springs Formation, in which younger rocks overlie older rocks, (2) subvertical "flanking faults," which are lateral bounding tear faults with strike-slip movement, (3) a transgressive "ramp fault" that cuts upward across bedding, and (4) a subhorizontal "land surface fault," which is a fault between the slide mass and the pre-existing land surface of that time, in which older rocks overlie younger rocks. All four fault components are not necessarily preserved beneath every slide mass due to differential erosion, especially at the proximal ends of the slide masses where the bedding and ramp structures were mostly located at higher elevations on the intrusive domes and therefore were more susceptible to erosion, or they were destroyed by subsequent extrusion of magma. The Big Mountain slide is the most complete structure that retains a set of all four bounding faults, as illustrated diagrammatically in figure 14. The contacts between individual slide masses and the underlying autochthonous rocks appear to be smooth and sharp. However, most contacts are covered and can only be located within the nearest meter or two.

Age of Sliding Events: The timing of all sliding is tightly constrained between 22 and 20.5 Ma. The Harmony Hills Tuff, a key pre-Iron Axis unit involved in all of the slide masses, yields a 22.03 ± 0.15 Ma $^{40}Ar/^{39}Ar$ plateau age (Cornell and others, 2001). The Pine Valley Latite, which overlies the youngest slide mass, yields a 20.54 ± 0.07 Ma $^{40}Ar/^{39}Ar$ plateau age (L.W. Snee, U.S. Geological Survey, written communication, 1995; Hacker and others, 1996). Gravity sliding was initiated abruptly after deposition of the Harmony Hills Tuff, as the oldest slide mass (the Pinto Peak slide) is overlain by the 21.93 ± 0.07 Ma rocks of Paradise (lower lava flow member; L.W. Snee, U.S. Geological Survey, written communication, 1995; Hacker and others, 1996). Importantly, this 1.5 m.y. time interval of gravity sliding corresponds to the age of Iron Axis intrusions within the Iron Axis region.

Speed of Emplacement: The velocity of the gravity slides is a matter of speculation, but has special implications in the origin of the intrusions. The speed is estimated to be rapid and most likely catastrophic. The absence of field evidence for continued thrusting and gouging and the internal structure (e.g., brecciation, extensional faulting) suggest movement by a body force (i.e. gravity). Very rapid to catastrophic movement of the gravity slides seems necessary to explain the following observations:

(1) There are no sedimentary deposits immediately beneath the slide masses indicative of erosion along an elevated area (i.e., laccolithic domes in this case) prior to sliding.

(2) No erosion material exists between the slide and the overlying volcanic rocks that erupted from the same source area following sliding. This indicates that volcanism was synchronous with or immediately followed sliding. Most of the volcanic material overlying the slides consists of ash-flow tuffs erupted from the laccoliths. The tuffs indicate violent eruptions and catastrophic emplacement.

254

(3) Extremely thin but stratigraphically preserved rock units that traveled at least 12 km over the former land surface.

(4) Internal brecciation and shattering of rock units within slide masses precludes a push from the rear and requires a "one-shot" emplacement mechanism, especially for such thin layers of rock.
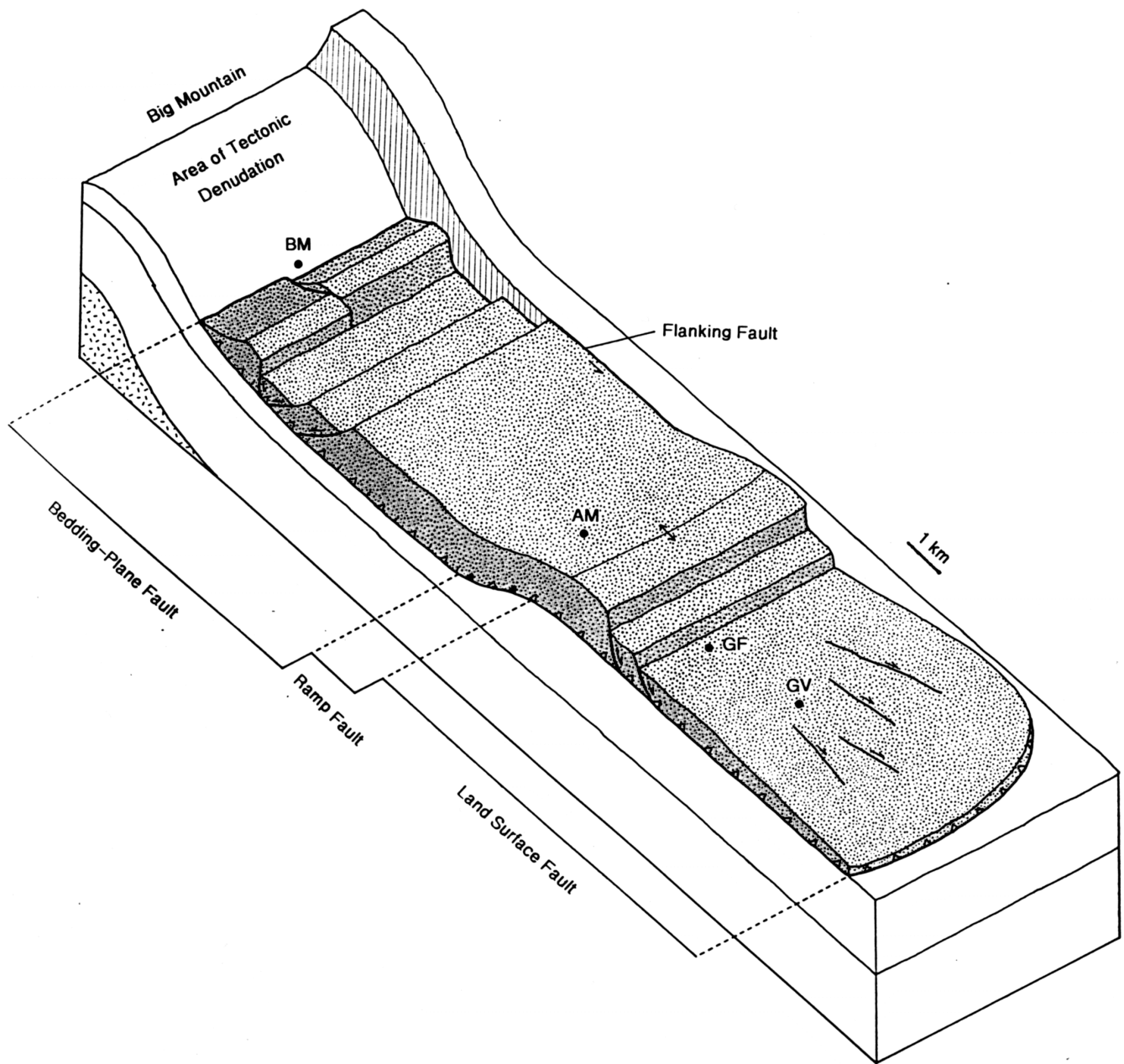

Figure 14. Sketch block diagram of Big Mountain slide showing four types of bounding faults.

Structural Interpretation: From the preceding descriptions and review of cross sections it is difficult to avoid the interpretation that the allochthonous masses originated by downslope sliding of large bodies of detached strata pulled by the force of gravity. A necessary prerequisite for downslope gravity sliding is the creation of tectonic elevations. The timing of formation of the gravity slide complex corresponds very well to the time of emplacement of intrusions that formed laccolithic structures with elevated domal roofs. Therefore, the interpretation that detachment and displacement of large rock masses were related to the dynamics of formation of the intrusions seems clear.

However, as pointed out by J. Hoover Mackin (1960), the concept of gravity sliding from igneous intrusive domes is not well known due in part to: (1) only a small percentage of intrusions form topographic features steep enough to cause sliding, (2) many intrusions of pre-Tertiary age are deeply eroded so that any slides that might have developed have been removed, and (3) slides from intrusive domes have been interpreted as thrusts due directly to the intrusive room-making process. However, timing of deformation was also contemporaneous with the extrusion of large volumes of volcanic material from the intrusions, which, when thick enough, can independently create abnormal stress on adjacent strata. A brief examination, therefore, of possible alternative mechanisms related to the formation of the intrusions and their associated volcanics seems warranted.

The emplacement of older rocks upon younger rocks along low-angle surfaces usually brings to mind deformation by compressional forces that produce thrust faults. Grant (1991) suggested that such a compressional force during growth of the Pine Valley intrusion was responsible for the shouldering aside of large volumes of volcanic rock to create the flat floor within sedimentary units of the Claron Formation. However, Grant's interpretation is not supported by field data that shows that the Pine Valley intrusion formed by uplifting its cover rocks (see section on laccoliths below). Some compressive forces were generated during growth of the Pine Valley intrusion, which produced minor thrusting of the peripheral country rocks with as much as 600 m of displacement (Hacker, 1995,1998). These features, however, post-date the slide structures.

The largest and best-preserved slide in the study area, the Big Mountain slide, has many structural characteristics comparable to the Heart Mountain fault in northwest Wyoming. The Heart Mountain fault covers 3,400 km^2 and has transported a thin (~750 m) allochthon tens of kilometers over a nearly horizontal detachment surface (Pierce, 1973, 1991; Hague, 1985, 1990). The Heart Mountain fault is similar to the Big Mountain fault in that it evolved progressively from a bedding fault, to a ramp fault, and finally to a land-surface fault. It is also similar in being partially buried by volcanic rocks, but is dissimilar in that it contains a breakaway fault. Moreover, the upper plate of the Heart Mountain fault broke into numerous blocks that became separated during detachment and transported individually over the fault surface. The Big Mountain slide apparently moved as a single mass, (although it became internally broken). It also probably contained a breakaway-type of fault that either has been eroded or is covered by volcanic rocks.

Two models have been proposed for the development of the Heart Mountain fault: (1) a tectonic-denudation model (Pierce, 1973), and (2) a continuous allochthon model (Hauge, 1985). The tectonic denudation model suggests that the discrete blocks of Paleozoic rocks moved at catastrophic rates along the detachment surface due to gravity and aided by earthquake oscillations. The slide area was blanketed immediately after faulting by catastrophic volcanism. In the continuous allochthon model, a continuous plate of thick volcanic and Paleozoic rocks moved over millions of years by the slow process of gravity spreading. In the Big Mountain slide, there are several lines of evidence that suggest the structure was not produced by gravity spreading or any compression from the rear: (1) the internal deformation of the displaced masses show extensive attenuation by internal extensional faulting and brecciation rather than compressional thickening, (2) the overlying volcanic rocks are very thin and show no signs of being deformed, (3) the preserved denudation surfaces at the proximal end of the slide are covered with volcanic rocks that are not deformed, and 4) volcanic rocks did not cover the entire structure and therefore spreading would be only from the proximal end and form compressional structures at the slide's toe. However, the toe is thin (<100 m) and could not have transmitted compressional stresses for any acceptable distance. Sliding in the Pine Valley Mountains is interpreted to be similar to the tectonic-denudation model of catastrophic emplacement of the allochthonous masses prior to burial by volcanic rocks. Catastrophic emplacement best fits the observation of a thin allochthonous sheet over the former land-surface fault segment that could not have sustained compression from the rear. Since the Big Mountain slide, as well as most slides of the study area, is overlain by explosive volcanic deposits, earthquake oscillations from the eruptions could also have aided in their emplacement as suggested by Pierce (1973) for the Heart Mountain fault.

Laccoliths

The intrusions within the Pine Valley Mountains area are variably eroded. Some of the intrusions are completely concealed beneath their cover so that the shape (anticlines or domes) reflects the general shape of

the underlying intrusion (e.g., Pinto, Ritchie Flat, and Grass Valley areas). In other intrusions the cover has been partly removed so that the upper crests and flanks are exposed (e.g., The Dairy, Pinto Peak, Stoddard Mountain). Only the Pine Valley and Iron Peak (at the northeast end of the Iron Axis) intrusions have been eroded so that the floor is exposed. Between the intrusions are intervening synclines or basins formed of sedimentary and volcanic rocks and gravity slide masses. Local compression between the Stoddard Mountain and Iron Mountain intrusions formed an out-of-syncline thrust. The nature of the igneous intrusions in the Iron Axis province has been a controversial issue for some time. Workers in the Iron Springs district have suggested that the exposed intrusive bodies are parts of either laccoliths (Leith and Harder, 1908; Mackin, 1947, 1954, 1960; Blank and Mackin, 1967) or stocks (Butler, 1920; Ratte, 1963; Bullock, 1973). The present erosional level of the intrusions makes it difficult to distinguish stocks from laccoliths. Recent exploratory seismic reflection and exploratory drilling data clearly show that the Three Peaks intrusive body is a laccolith (Van Kooten, 1988). The laccolith floor was penetrated at a depth of 1,498 m in the ARCO Three Peaks No. 1 well while exploring the petroleum potential of the anticlinal structure located below the laccolith. The laccolith has a thickness of 788 m at the well location, and is both overlain and floored by units of the Jurassic Carmel Formation. Drilling and seismic data do not indicate the presence of additional stacked laccoliths below the Three Peaks laccolith, or the presence of a central stock that would have acted as a central feeder system for satellite laccoliths as envisioned by Hunt (1953) for the laccolithic centers in the Henry Mountains of the Colorado Plateau.

The laccolith interpretation best fits the observed field relations of all of the intrusions within the Pine Valley Mountains. Cross-sections show that most intrusions have a somewhat typical plano-convex shape (Gilbert, 1877), but are not circular when viewed in plan. The Pine Valley intrusion is more tabular in shape and resembles a large sill, although its cover has been entirely removed by erosion and therefore the curvature of its roof at the time of emplacement is unknown. Attempts to arbitrarily distinguish laccoliths from sills on the basis of diameter/thickness ratios (e.g., Billings, 1972) have not been followed in the literature due to the continuous transition between the two and differential erosion. A recent compilation of laccoliths by Corry (1988) led him to suggest that laccoliths be distinguished from a sill when the thickness is $\geq$ 30 m. Corry (1988) also referred to laccoliths in the generic sense as intrusions of any final form that domed the country rock above or below them through a forcible intrusive and thickening process. Later publications incorporate this usage (e.g., Henry and others, 1997) and is followed here.

Pine Valley Intrusion - Laccolith or Lava Flow?

The Pine Valley intrusion is the largest and most controversial intrusion within the Iron Axis region. The exposed body has a preserved maximum thickness of 900 m and a maximum horizontal dimension of over 32 km in a northeast-southwest direction. The original extent is unknown, but must have been much larger than its present areal extent of over 240 km^2 based on erosional remnants found on the south side where erosion was greatest. Its northern and western limits are still mostly preserved. Its eastern limit is also unknown due to burial beneath younger sediments (Grant, 1991). The igneous body exhibits an overall irregular shape in plan view as shown by separate lobes that extend from the main mass (e.g., north side of Pine Valley).

Early workers (Dobbin, 1939; Gardner, 1941) believed the igneous body was the product of lava flows, based on their observations on the south side of the mass where it has a layered appearance and on the aphanitic groundmass of the porphyry. Subsequently Cook (1954, 1957, 1960) made the first comprehensive study of the entire igneous body and interpreted the mass to be part of possibly the largest laccolith in the world. Cook based his intrusive interpretation on field evidence that included: (1) the intrusive nature of the contact on the north side of the mass, and (2) the lack of evidence that showed that the layering was due to separate volcanic lava flows. Cook's interpretation was that a single shot of magma intruded beneath at least 900 m of cover rocks. The petrographically identical Pine Valley Latite was interpreted by Cook to be pre-intrusive and part of the cover strata that was deformed by intrusive faulting. In a more detailed study of the nature of the layering, Mattison (1972) came to the same conclusion as Cook that the layering was not due to separate lava flows. However, Mattison believed the mass was extrusive in origin, probably formed as an "extrusion ridge," and not as a laccolith. The lack of any roof rocks remaining on top of the mass and the glassy groundmass of a great portion of the mass were cited as some of the reasons for rejecting Cook's intrusive concept. Mattison made no mention of the relationship between the extrusive Pine Valley Latite and intrusive rocks. Mattison's study was based only on transects through the igneous body and did not include field studies of the surrounding areas. Grant (1991) later adopted a similar interpretation as Mattison after a field study of the eastern side of the Pine Valley Mountains conducted during mapping of the New Harmony quadrangle. Grant interpreted the upper 305 m of the mass to be extrusive and made up of a lava flow dome that was subsequently intruded from below. Grant mapped the upper purple layer as the Pine Valley Latite and thus extended the Pine Valley Latite over the entire intrusion. Grant explained the missing pre-Iron Axis volcanic rocks above the Claron Formation

by shouldering aside the rocks during the initial lava flow dome formation, allowing the Pine Valley Latite to rest temporarily on the Claron Formation, before magma later intruded between the Claron and the latite. Grant suggested that the folded rocks in Comanche Canyon were part of the bulldozed rocks and that the rest were buried below parts of the dome.

A variation of Cook's laccolith interpretation best fits the overall field relations, with the addition of widespread eruptive phases as well. In short, field data show that magma was intruded first beneath a thin cover (<250 m), and uplifted its roof to form a laccolithic structure that broke through to the surface and extruded lava over the country rock. This lava forms part of the Pine Valley Latite (i.e. the Timber Mountain flow unit of the Pine Valley Latite). The upper layer of igneous rock, interpreted as extrusive by Grant, is envisioned here to be the upper glassy zone of the intrusion just below the cover rocks that have been removed. Thus, field relations from this study support Cook's interpretation that the igneous mass was an intrusive laccolith, although there is also evidence of extrusive activity resulting from the laccolith breaking through its roof and erupting latite lava.

Evidence of intrusion: The evidence of forcible intrusive activity is demonstrated in: 1) the lack of extrusive layering, (2) the intrusive character of the basal contact, (3) the intrusive character of the peripheral contact, and (4) the presence of gravity-slide structures.

(1) Field evidence from this study supports the conclusions of Cook (1957) and Mattison (1972) that the colored layers or zones that are so prominent in the south side of the intrusion are not the products of separate lava flows or even due to separate intrusions. The contact between the zones is gradational and irregular and shows no visible changes in phenocryst size from one layer to the next. The contact between the upper purple and middle white zones was examined closely for evidence of an intrusive contact, as envisioned by Grant (1991). This contact should be sharp or show signs of a basal vitrophyre in the purple zone, which is prominent everywhere at the base of the Timber Mountain flow member of the Pine Valley Latite. However, no physical difference was found at this contact to support two separate events.

(2) Along the south side of the intrusion the igneous mass rests upon units of the Claron Formation. The only exception is at Cedar Knoll, where the intrusion appears to rest on the Iron Springs Formation displaced along a high-angle fault that strikes northeast. North of the intrusion the Claron Formation is overlain by a thick section of pre-Iron Axis volcanic rocks. There is no evidence that the volcanics were removed by erosion to expose the Claron prior to emplacement of the intrusion. There are no sedimentary units found beneath the intrusion that are indicative of erosion of the volcanics. The contact between the Claron and intrusive rocks is mostly sharp to irregular and the layer below the contact is fractured and sheared and slightly baked or bleached. The basal glass clearly visible in outcrops becomes highly sheared near the peripheral areas of the intrusion and suggests continued movement of the mass.

(3) Compelling evidence of intrusive contacts are found on the preserved northern and western flanks of the intrusion where upturned to overturned strata are highly attenuated adjacent to intrusive rock. The overturned strata include rocks of the Claron Formation and units of the Quichapa Group, as well as parts of the Bull Valley and Big Mountain slide masses. North of Pine Valley, the intrusion compressionally deformed the flanking country rocks forming a small thrust fault and a fault-propagation-fold. The thrust fault dips 20 degrees toward and under the intrusion and has a maximum displacement of over 300 m. Country rocks adjacent to the intrusion are overturned indicating that thrusting occurred after the intrusion grew vertically by upturning its roof rocks.

Cook (1957) interpreted the intrusion's northern extent, from Water Canyon eastward to New Harmony, to be in intrusive fault contact with members of the volcanic sequence and the Pine Valley Latite. Detailed examination of the exposed contact did not reveal a high-angle fault contact surface. Instead, upturned and overturned units of the Claron and overlying volcanic units (but not the Pine Valley Latite) were observed. These host units are highly attenuated and could very easily be missed in a reconnaissance study such as Cook's (1954, 1957). At Water Canyon the intrusive and extrusive rocks are in contact with each other and, due to lack of fault indicators, are separated in mapping with a gradational intrusive-extrusive contact instead of the intrusive fault envisioned by Cook (1957). The Timber Mountain flow overlies the eastern Pine Valley gravity slide mass (which was contemporaneous with the intrusive rocks), so the extrusive rock appears to postdate the initial growth of the intrusion and was not intrusively faulted at this contact. Evidence can be found in a stream cut on the south side of the Bench (in Water Canyon), where intrusive rock appears to be in direct fault contact with the eastern Pine Valley slide mass, but upon close examination it is separated by a few meters of brecciated Claron and smeared-out Quichapa units. These rocks represent part of the upturned country rock sequence that is attenuated (by brecciation and shearing) vertically as the intrusion grew. The intrusive rock in contact with this "crush breccia" is a black glass that is also locally highly sheared. The crush breccia ends

abruptly upward where the intrusive and extrusive rocks (i.e., Timber Mountain flow) come in contact with each other. No Claron or Quichapa units are between the two rocks that would be expected if the Timber Mountain flow pre-dated the intrusion. The extrusive rocks show more horizontal flow layering than the intrusive rocks, but are not upturned or faulted as observed by Cook (1957). Glass flow breccias appear to be more common closer to the intrusion, and in one location (at First Water), a red and black flow breccia overlies steeply dipping foliated intrusive rock. These relationships suggest that the intrusion pre-dated the Timber Mountain flow and was the source of some of the extrusive rocks.

(4) As just discussed in the "Gravity Slide Complex" section, the presence of allochthonous rock masses interpreted as gravity slides (i.e., the Pine Valley slides) demonstrates indirectly, yet compellingly, the need for an elevated area. The structural and stratigraphic indicators of slide masses on the north side of the intrusion, in the Grass Valley and Mahogany Creek area (Pine Valley slide system), show their source area to be to the south in the area now occupied by the Pine Valley igneous mass. The presence of gravity slides related to the Pine Valley intrusion is evidence against the igneous mass being extrusive in nature since extrusive lava does not have the strength to lift large areas of the landscape.

Evidence of extrusions: The Timber Mountain flow member of the Pine Valley Latite partially covers the gravity slide masses that originated from the elevated roof of the Pine Valley intrusion. This critical relationship indicates that the intrusion occurred before the latite flow formed, contrary to the ideas of Cook (1957) and Grant (1991), who both suggested the latite formed first and was part of the cover rocks that deformed during subsequent intrusive activity. However, the latite is not deformed where it is in contact with the intrusive rocks. The contact between the two rock units is hard to distinguish in the field because of the identical textures of the two units. An intrusive-extrusive contact is even hard to distinguish on air photos. If the intrusive rock formed first and was exposed by erosion at the time of latite emplacement, then a prominent contact should have formed as a result of the flowing lava butting up against the elevated intrusion as is found with the Stoddard Mountain intrusion. Instead, the contact in most places appears to be gradational as flow layered latite grades into massive layered latite and then into structureless intrusive rock. The latite flow layers strike parallel to the inferred contact but have various dips into or away from the intrusion. The varying dips reflect flow folding in the latite and are not deformational folds from later intrusive activity.

It is proposed here that the Timber Mountain flow originated from the intrusion and flowed northward onto country rocks and parts of the Rencher Peak flow that originated at a vent in the Rencher Peak area. It cannot be ruled out however, that the Timber Mountain flow also originated from a separate vent in the Timber Mountain area and flowed south and commingled with contemporaneously forming latite flows erupting from the intrusion.

Depth of emplacement: Field evidence shows that the Pine Valley intrusion intuded laterally within the sedimentary units of the Claron Formation. The Claron beneath the intrusion ranges in thickness from 120 to 150 m. Stratigraphic study of the Claron north of the intrusion indicates that the Claron is 180 m thick and that the intrusion was therefore emplaced into the upper part of the formation.

The maximum total thickness of the cover is estimated to be only 150 to 200 m at the time of intrusion. This includes ~40 m of upper Claron units, ~120 m of various volcanic units (see units listed in stratigraphic boxes of the Pine Valley slide masses in figure 12, which represents the detached parts of the roof), and ~20 m of previous slide masses (i.e. Big Mountain and Bull Valley slides), which did not cover the entire intrusion area. This maximum thickness is from the measured thicknesses of the rock sequence found just north of the intrusion. The thickness of the cover was most likely thinner on the south side due to southward depositional thinning of the volcanics and the absence of the Bull Valley or Big Mountain slide masses. The actual thickness to the south is unknown, but could have been as little as 100 m based on thinning of the Quichapa volcanics observed from north to south.

The Pine Valley intrusion is therefore estimated to have been emplaced at a maximum depth of <200 m based on field measurements of the thickness of the proposed cover rock stratigraphy, and it is inferred to have had a structural relief of at least 900 m based on the maximum remaining thickness of the intrusion. The estimated cover rock thickness (from approximately 150 to 200 m) is considerably less than the 1,219-1,523 m estimated by Cook (1957). The discrepancy is based mostly on the involvement of the Pine Valley Latite which Cook included as part of the cover but which field relations presented here show was formed shortly after or during the intrusion and therefore should not be included as part of the cover.

DISCUSSION

Relationship of Gravity Sliding to Volcanic Eruptions

The areas of structural and topographic relief that were necessary for the formation of gravity slide structures were formed by the forceful intrusion of quartz monzonite magma into sedimentary rocks and structurally uplifting their host rocks and forming laccoliths. Field evidence shows that volcanic activity closely followed gravity sliding events. This close relationship suggests that eruptions from the laccoliths could not take place until the initiation of gravity sliding. It is proposed that catastrophic gravity sliding initiated volcanism from growing laccoliths by sloughing off part of the roof and thus reducing the overburden pressure on the magma which led to violent magma frothing (vesiculation) and catastrophic eruptions of some of the intrusions. Most initial volcanic activity was of the violent ash-flow tuff type, giving support to gravity slides being the "initiators" of volcanism.

The initiation of volcanism by gravity sliding is not new to volcanic terrains. One of the best-known slides in recent times was the spectacular one initiating the devastating Mount St. Helens eruption of May 1980 (Lipman and Mullineaux, 1981). The growth of magma within the core of the stratovolcano caused gradual oversteepening of its flank, which collapsed and caused a huge landslide. The landslide unroofed the magma chamber, releasing the confining pressure, and thus initiating a simultaneous pyroclastic eruption.

Rate of Emplacement and Growth of the Laccoliths

It has been shown through experimental studies and observations that sill emplacement is rapid, on the order of 7 years or less in some areas (Corry, 1988), during which magma can migrate over several kilometers without crystallization taking place. The rate of emplacement of sills and the growth of laccoliths have been modeled experimentally and suggest rapid rates of emplacement ranging from 1 to 20 m/sec (e.g., Spera and others, 1985). It seems reasonable that the large Pine Valley laccolith also grew within a relatively short period of time, notwithstanding its large size. McDuffie and Marsh (1991) calculated the crystallization time for the Pine Valley intrusion to be approximately 2,500 years based on crystal setting rates. The emplacement and vertical growth of the Pine Valley laccolith had to be less than 2,500 years and could conceivably have been less than the general 100-year laccolith growth time frame suggested by Corry (1988). Certain field observations support the rapid rate of emplacement and growth time of the Pine Valley laccolith. These include:

(1) No evidence of erosion before gravity-slide emplacement. No sedimentary deposits were found below the slide that could be attributed to erosion of the dome prior to gravity sliding. Sedimentary rocks of the Page Ranch Formation are the only erosional products below and within some of the gravity slides, but they were formed by partial erosion of the Big Mountain slide, which formed an elevated area to the northwest. Fanglomerates of the Page Ranch Formation thicken to the northwest and overlap the edges of the Big Mountain slide mass and thin to the southeast toward the Pine Valley Mountains. Therefore the Page Ranch Formation was not derived from the initial Pine Valley dome.

(2) No evidence of erosion after gravity sliding and prior to eruption. No sedimentary deposits were found between the Pine Valley gravity slide masses and the overlying Pine Valley Latite that would indicate a pause in laccolith growth prior to its eruption.

(3) The porphyry. The glassy nature of the quartz monzonite porphyry and its overall thickness indicates rapid intrusion of magma. Otherwise the mass would cool too quickly and show brittle deformation during any subsequent internal pulses.

(4) The thin cover. The extremely thin cover rock (<250 m thick) would allow more rapid cooling of the porphyry by not supplying a sufficient "blanket" against rapid heat loss. Therefore, the magma intruded rapidly to avoid rapid congealing.

Genesis of the Iron Axis Laccoliths

The field observations presented here have major implications on the intrusive evolution of the laccoliths of the Iron Axis. Based on the new field evidence pertaining to the structure of the large Pine Valley laccolith, a new model of emplacement and growth of the intrusion is presented below (figure 15). This model can be used to view the growth of the other Iron Axis laccoliths. The model is broken down into sequential stages of growth, culminating in the eruption to the surface of the Pine Valley latite lava. The progression of stages is viewed here as a continuum as suggested by Corry (1988) for the genesis of most laccoliths in general.

Stage 1 -- Initial Lateral Sill Emplacement: The magma that formed the laccolith was a half-crystallized mush at the time of emplacement (as evidenced by the large percentage of phenocysts in the porphyritic rock) and spread laterally as a thin sill within the sedimentary strata of the Claron Formation at a depth of
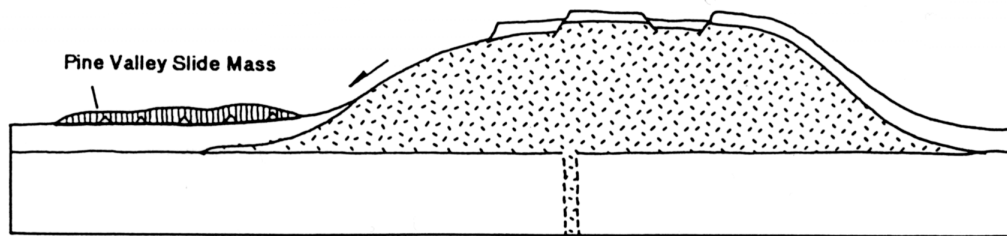
A) Lateral Sill Migration

200 m

B) Vertical Growth

Extension Reduces Lateral Support

Future Slide
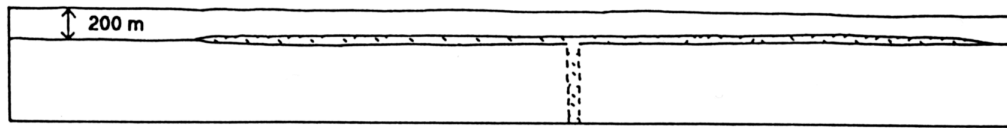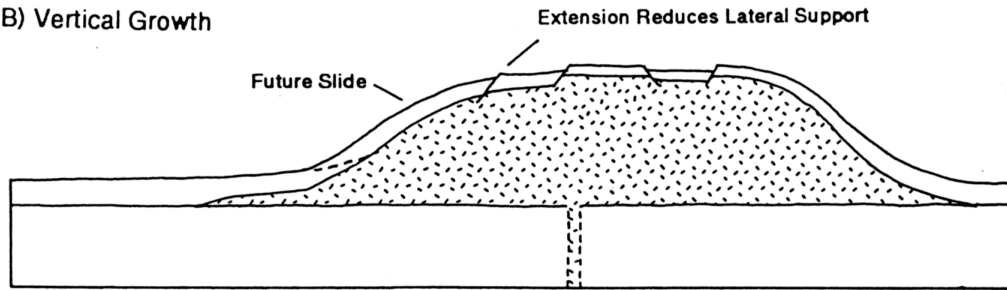
C) Gravity Sliding From Flanks

Pine Valley Slide Mass

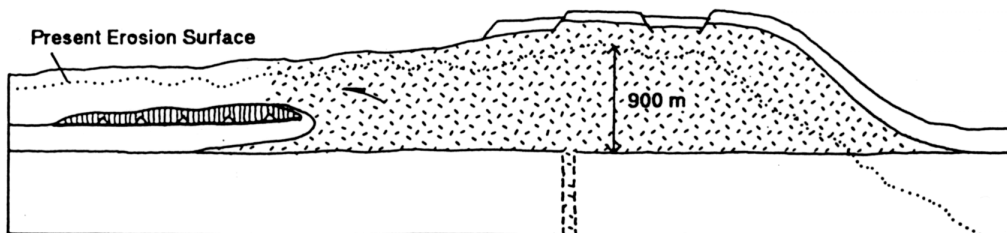D) Volcanism and Lateral Growth

Present Erosion Surface

900 m

Figure 15. Proposed model of Pine Valley intrusive growth based on field evidence. Growth is envisioned to be a continuum from one stage to the next. (A) Initial lateral migration of the sill to its fullest extent, followed by (B) vertical growth of laccolith, (C) gravity sliding of flanks, and (D) lateral growth by overturning the remaining peripheral flanks and extruding onto surface.

261

approximately 200 m (figure 15A). The actual thickness of the sill is unknown but Corry (1988) suggests that the sills (or protolaccoliths) in most laccoliths were less than 30 m thick regardless of the overall diameter of the laccolith. The magma is assumed to have spread to its full length as a sill prior to vertical growth of the laccolith (based on studies by Corry, 1988), and was fed from below by a feeder dike system. Although feeder dikes are not exposed beneath the Pine Valley laccolith (even though its floor is exposed over its entire southern flank), a dike system with a northeast-southwest trend would explain the anomalous length of the laccolith along this line. Also, the natural cross-section of its western side shows that the lowest elevation of the intrusive floor occurs in the middle of the laccolith where the Claron is thinnest. This is the assumed location of the dike system as the intrusion steps up through the Claron toward the intrusive periphery. Feeder dikes are present below the Iron Peak intrusion (figure 3), which is the only other laccolith in the Iron Axis group with an exposed floor. The Iron Peak intrusion also intruded into the Claron Formation and erosion has exposed a tightly clustered swarm of feeder dikes that average approximately 2 m thick and cut up through the nearly horizontal Claron beds at an angle of 40 to 90 degrees (Spurney, 1984). Evidence of lateral spreading as a sill is lacking due to the absence of shattered rock structures that should form in the country rock if the magma bulldozed its way through them at its full vertical thickness. Spreading as a sill explains the pattern of intrusion for the Dairy and Stoddard Mountain laccoliths. Both intrusions apparently emanated from a common conduit north of Pinto Peak (most likely the same conduit that fed the Pinto Peak intrusion). Finding the area to the south blocked by the already congealed Pinto Peak intrusion, the magma migrated to the east (for Stoddard Mountain intrusion) and west (for the Dairy intrusion). The thick lava flows from the Pinto Peak intrusion provided greater lithostatic pressure and also acted as a barrier to sill migration. Therefore, the sills migrated east and west (Richie Flat and Pinto anticlines) before migrating to the south to their fullest extent. By analogy, the Pine Valley laccolith also began as a sill and a remnant sill-like structure is interpreted to connect with the intrusion beneath Grass Valley (see cross section in figure 21).

Stage 2 -- Vertical Growth and Roof Deformation: Following emplacement of the sill to its full lateral extent, bending of the entire 200 m of overburden began as magma was continually added to the now vertically thickening laccolith (figure 15B). As the intrusion inflated, the overlying host rock was gently rotated and arched into doubly hinged flexures around the periphery, but was probably flat-roofed over most of its center due to its large lateral extent. Due to the shallow emplacement (thin overburden), extension over the upflexed area was accommodated by brittle fracturing and high-angle normal faulting of the roof. Although the peripheral flexures of the Pine Valley intrusion are only partially preserved and the crestal extensional faults have presumably been eroded, the described features are consistent with those found preserved in the crest of Dairy and Stoddard Mountain intrusion east of Pinto. The shape is consistent with experimental results of the bending of a circular plate driven upward by a thickening laccolith (Jackson and Pollard, 1988).

This stage of growth is in contrast to the concept of Cook (1957), who envisioned the periphery of the laccolith to be marked by high-angle intrusion faults similar to a bysmalith. These peripheral faults would occur if initial failure of the roof was by shearing at the periphery as suggested by Corry (1988) for what he termed punched laccoliths (bysmalith type). However, the structural geometry of this interpretation does not fit the requirements needed for gravity sliding and extrusive activity described in Stage 3.

Stage 3 -- Gravity Sliding from Peripheral Flexures: As the intrusion continued its vertical growth, the limb of the overlying peripheral flexure steepened as the hinges tightened. The extensional faulting at the hinge crest reduced the lateral support of the limb on an otherwise already steepened and unstable slope. The resulting slabs of roof rock detached within the sedimentary beds of the Claron Formation and slid intact onto the former land surface below (figure 15C). Detachment of large slabs of the roof rock greatly reduced the effective thickness of the peripheral overburden to only about 20 m of Claron strata on the remaining part of the flexure.

Stage 4 -- Vertical and Lateral Thickening and Magma Extrusion: The sudden loss of peripheral overburden greatly reduced the lithostatic pressure that was essentially holding the roof "down" in advance of the upward loading forces applied by the thickening magma. The now thin Claron units of the peripheral flexure left behind by the gravity slides were not strong enough to hold back the magma, which continued to undergo vertical thickening in conjunction with lateral growing. The magma was able to overturn the remaining peripheral roof rocks and extrude onto the surface, burying the previous gravity slide masses with lava flows (figure 15D). Subsequent removal of the roof by erosion left the present erosional profile shown in figure 15D. In areas where gravity sliding did not take place, the intrusive porphyry exerted enough lateral compression to form small displacement, low-angle thrust faults, or completely overturned the adjacent strata and broke out

onto the former land surface. At this stage, the loss of lateral support resulted in total breakdown of the flanking strata by thrust faulting, flexure overturning, and compartmental high-angle faulting due to lateral growth. In the other intrusions that vented more violent ash-flows prior to lava eruptions (e.g., Pinto Peak, Stoddard Mountain, and Bull Valley intrusions) the sudden release of overburden by gravity sliding most likely resulted in immediate frothing of the magma due to massive pressure release, as with the 1980 Mount St. Helens eruption (Lipman and Mullineaux, 1981).

ACKNOWLEDGMENTS

FIELD TRIP ROAD LOG

Mileage Increment	Cumulative	Description
0.0	0.0	Mileage for this road log begins at the traffic light at the intersection of 200 North and Main Street in Cedar City, Utah. All stops during the trip are shown on figures 1 and 12. Proceed west from this intersection on SR-56 (200 North).
0.9	0.9	Overpass of I-15. Continue west on SR-56.
4.5	5.4	The "Y" intersection where SR-56 bends to the left and a paved road that goes to Iron Springs and Desert Mound intersects on the right. Continue west on SR-56. The Three Peaks intrusion with visible mine dumps on its flanks can be seen to the north (at right) at 3:00 to 4:00. The Three Peaks, Granite Mountain, and Iron Mountain intrusions make up the Iron Springs mining district, which contains the largest iron deposits in the western United States (Mackin, 1947, 1960; Mackin and Ingerson, 1960; Blank and Mackin, 1967; Mackin and others, 1976; Mackin and Rowley, 1976; Rowley and Barker, 1978; Blank and others, 1992; Barker, 1995; Rowley and others, 2001). These three laccoliths consist of porphyritic quartz monzonite emplaced concordantly at the base of, or within the middle of, the Middle Jurassic Temple Cap Formation that was displaced along one or more Late Cretaceous to early Tertiary Sevier thrust faults. The iron deposits consist of huge hematite and magnetite replacement ore bodies in the Homestake Limestone Member of the Jurassic Carmel Formation, overlying the thin Temple Cap Formation (Mackin 1947, 1968; Barker 1995). The ore forming fluids resulted from deuteric breakdown of ferromagnesian minerals in the outer parts of the crystallizing porphyritic mush of the intrusions (Mackin and Ingerson, 1960; Barker, 1995). Floors of the intrusions are not exposed, but an exploratory petroleum well was drilled on the southwest side of the Three Peaks body and intersected the bottom contact of the pluton at 1,500 m depth, proving that the intrusion is a laccolith (Van Kooten, 1988). Additional seismic reflection profiles show that the buried part of this intrusion connects with Granite Mountain and together they have a nearly planar floor and an irregular but concordant roof. The near hills on the right (2:00) are the Eightmile Hills made up of Tertiary ash-flow tuffs dipping southeast off the flank of Granite Mountain intrusion, which is partially visible above the hills. Large abandoned open-pit iron mines surround Granite Mountain.
2.9	8.3	Low area on left is Quichapa Lake, normally a dry playa on the valley floor in Holocene and Pleistocene valley bottom alluvial deposits (Mackin and others, 1976). Harmony Mountains (10:00 to 12:00) consist mostly of faulted Tertiary ash-flow tuffs. Swett Hills

263

are visible at 1:00 to 2:00 and consist of east-dipping Tertiary ash-flow tuffs as found in Eightmile Hills to the right.

3.2 11.5 Crest of low hill formed in older, poorly consolidated Miocene to Pleistocene fanglomerates.

0.7 12.2 Enter Leach Canyon with outcrop of east-dipping Harmony Hills Tuff on right.

0.1 12.3 Bureau of Land Management sign on right.

0.1 12.4 Bauers Tuff Member of Condor Canyon Formation on right.

0.1 12.5 **STOP 1.** LEACH CANYON – EXAMINATION OF AUTOCHTHONOUS ASH-FLOW TUFFS. Pull off to the right to view three regional Tertiary ash-flow tuffs belonging to the Quichapa Group, on the north side of road. The first unit is the pink, crystal-poor Leach Canyon Formation (24 Ma) located where we park. Walk up the hill to the northeast to the overlying crystal-poor Bauers Tuff Member (22.8 Ma) of the Condor Canyon Formation. The contact is marked by a black basal glass zone of the Bauers Tuff that is overlain by a stony red devitrified zone, then an upper gray vapor-phase zone. Above the Bauers is the brown and tan, crystal-rich Harmony Hills Tuff (22.5 Ma). These unfractured ash-flow tuffs represent autochthonous rocks tilted eastward by the Iron Mountain Intrusion to the west. Return to vehicles and continue west on SR-56.

0.1 12.6 Highly fractured Leach Canyon Formation on the right. We just crossed over the frontal fault of the Iron Mountain slide. From here to mile 18.9 we will be traveling over allochthonous rocks of the Iron Mountain slide.

0.4 13.0 **STOP 2.** LEACH CANYON – EXAMINATION OF ALLOCHTHONOUS ASH–FLOW TUFFS. Pull off to the right and park to view highly fractured, steeply east-dipping, ash-flow tuffs above a low-angle detachment of the Iron Mountain slide. The roadcut on the north side of the road contains the light-pink Leach Canyon Formation on the right (east), underlain by purple and brown ash-flow tuffs of the Isom Formation (27-26 Ma) to the left (west). Sedimentary rocks of the Eocene to Oligocene Claron Formation farther to the west underlie the Isom Formation. These allochthonous rocks were highly fractured and steeply tilted during sliding eastward from Iron Mountain, but the stratigraphic order of the units is preserved. Return to vehicles and continue west on SR-56.

0.5 13.5 Roadcut on right of highly fractured red and yellow allochthonous Claron Formation within the Iron Mountain slide.

0.6 14.1 Old Woolsey Ranch and Duncan Creek on left (south) and Mount Claron on right (north). Mount Claron is the type locality of the Claron Formation and is made up of faulted and fractured red and white limestone, sandstone, and mudstone above red and tan sandstone and mudstone of the Upper Cretaceous Iron Springs Formation exposed at the base of the hill. The basal low-angle gravity slide plane formed in the incompetent rocks of the Iron Springs Formation. To the left (south), the large hills on the near horizon (Flat Top Mountain) consist of allochthonous Quichapa rocks and represent the farthest reaching (about 6 km) of the slides from the Iron Mountain intrusion (Rowley and others, 2001).

0.8 14.9 **STOP 3.** ALLOCHTHONOUS CLARON ROCKS. Pull off to the left to view highly fractured and pulverized outcrop of red Claron Formation on north side of road. These steeply dipping allochthonous rocks, along with others viewed from this vantage point, are formed of resistant narrow ribs of Claron beds that form an arcuate pattern around the Iron Mountain intrusion. Beyond Mount Claron (now behind us at 5:00 to 6:00) is a view of the Swett Hills bounded by a south-facing cliff. At the base of the high cliff is the

Woolsey Ranch fault, a northwest-striking, left-lateral tear fault (bounding slide fault) that offsets to the east the allochthonous rocks that we have been driving on relative to the autochthonous rocks of the Swett Hills. Overall, the Iron Mountain slide covered an area of at least 30 km^2 (10 mi^2) (Rowley and others, 2001). Return to vehicles and continue west on SR-56.

|		
1.2	16.1	Diamond Z Ranch driveway on left. Ribs of resistant Claron beds to the left and right of the road. Duncan Mountain to the south (at 10:00) consists of allochthonous Quichapa rocks. Continue on SR-56.
1.0	17.1	Comstock Road (gravel) on the right leads to abandoned Comstock Mine on the northeast flank of Iron Mountain. Mount Stoddard of the Stoddard Mountain intrusion at 10:00. Continue on SR-56.
0.3	17.4	Junction of SR-56 and road to Pinto (Dixie National Forest road 009) on left. **Turn left onto gravel surfaced Pinto road and proceed southwest.**
0.4	17.8	Highly fractured Claron in hills to right and left.
1.1	18.9	Cross over approximate western edge of Iron Mountain slide complex. On the left are Claron and Iron Springs rocks that are overturned to the north by the Stoddard Mountain intrusion, which forms the high gray cliffs directly to the south (left). The laccolith intruded into the Iron Springs Formation at a shallower level than the other intrusions of the Iron Springs mining district and did not form any strata-bound iron deposits.
0.8	19.7	Near-vertical units of Claron on right (north) and Iron Springs on left (south). Quartz monzonite of the Stoddard Mountain intrusion exposed in cliff to the south. Hill to the north consists of Quichapa rocks that have been thrust to the north over the Harmony Hills Tuff by the shouldering action of the Stoddard Mountain intrusion.
1.0	20.7	Hill to the right is capped by a small slide mass from the Stoddard Mountain intrusion (see cross section in figure16) composed of Claron, Leach Canyon, Bauers, and Harmony Hills units transported northward. The mass rests on the former land surface consisting of Harmony Hills Tuff and a local andesitic lava flow (local volcanic rocks of Hacker, 1998) derived from fissures and deposited above the Harmony Hills before Iron Axis magmatic activity. Iron Springs country rocks on the left, adjacent to Stoddard Mountain intrusion.
1.2	21.9	**STOP 4.** STODDARD MOUNTAIN INTRUSION. Pull off to right and view roadcut in Stoddard Mountain intrusion on south side of road. The intrusion consists of two recognizable zones of quartz monzonite porphyry. The outermost zone is a 20 to 60 m thick chilled margin known as the "peripheral shell phase" in the intrusions of the Iron Springs district (Mackin and Rowley, 1976; Mackin and others, 1976). This zone, exposed here in the roadcut, consists of resistant, light-gray, unaltered porphyritic rock with medium-to coarse-grained phenocrysts set in an aphanitic groundmass. Note the fresh appearance of the plagioclase, biotite, and ferromagnesian phenocrysts of this peripheral phase. The inner zone, which makes up the majority of the intrusion, consists of an "interior phase" (Mackin and Rowley, 1976) of crumbly, light-grayish-green and pink, deuterically altered porphyritic rock. McKee and others (1997) determined a K-Ar date on biotite of 21.5 ± 0.9 Ma from peripheral shell samples taken from this roadcut. Return to vehicles and continue southwest on Pinto road, crossing Little Pinto Creek.
0.1	22.0	Historic Page Ranch on right. Junction with gravel road on left (Dixie National Forest road 029) that leads southeast to New Harmony. Continue southwest on Pinto road.
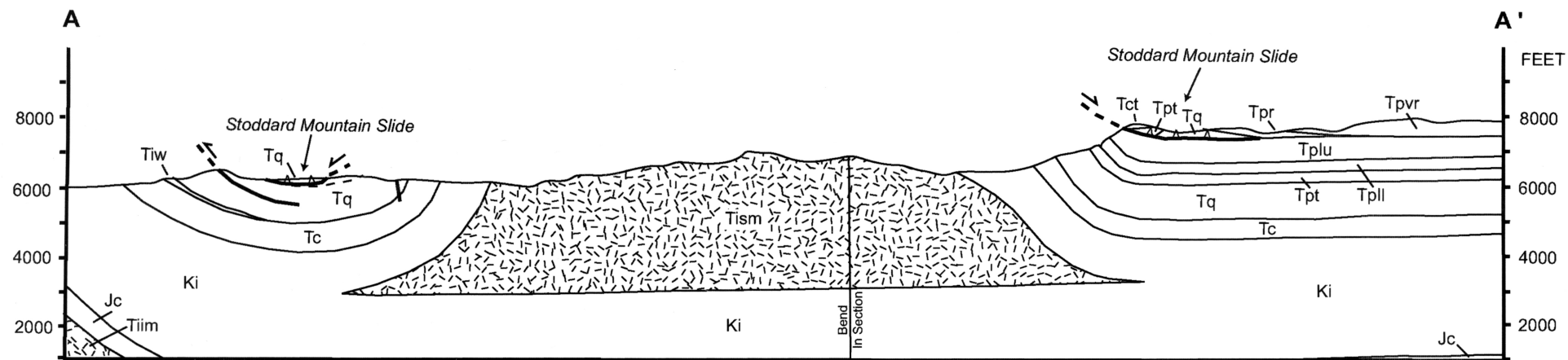
Figure 16. Geologic cross section A-A' (north-south with A to the north) through the Stoddard Mountain intrusion (see figure 12 for location of section). No vertical exaggeration.

Key (For figures 16, 17, & 18)

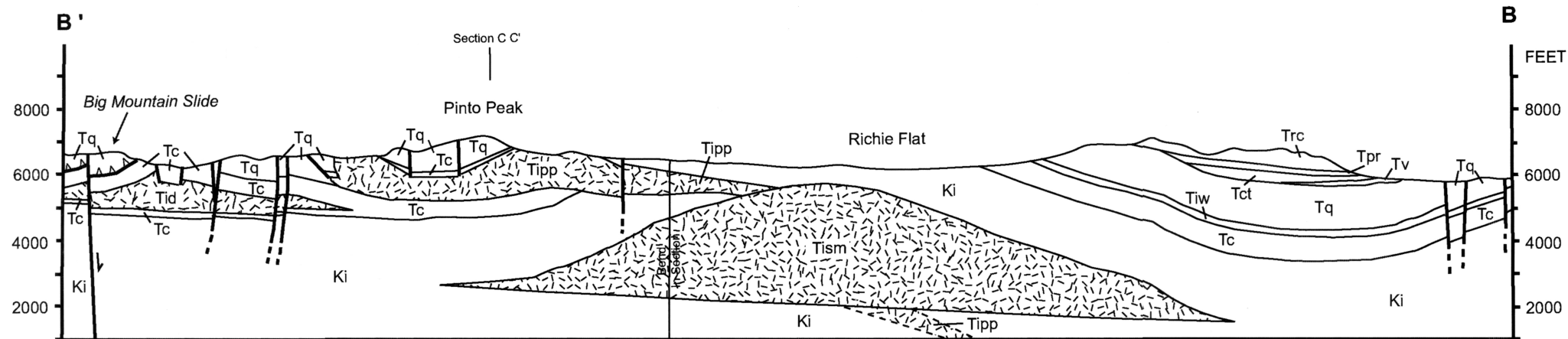|		
Tertiary	Trc	Racer Canyon Tuff
	Tpvr	Rencher Peak flow member of Pine Valley Latite
	Tpr	Page Ranch Formation
	Tct	Ash-flow tuff member of volvanic rocks of Comanche Canyon
	Tism	Stoddard Mountain intrusion
	Tid	The Dairy intrusion
	Tiim	Iron Mountain intrusion
	Tplu	Upper lava flow member of rocks of Paradise
	Tpll	Lower lava flow member of rocks of Paradise
	Tpt	Ash-flow tuff member of the rocks of Paradise
	Tpv	Vent Unit of the rocks of Paradise
	Tipp	Pinto Peak intrusion
	Tv	Local volcanic rocks
	Tq	Quichapa Group - includes: Harmony Hills Tuff, Little Creek andesite, Condor Canyon Fm, Leach Canyon Fm, and local sedimentary rocks
	Tiw	Isom and Wah Wah Springs Formations
	Tc	Claron Formation - includes thin units of Isom Fm and Wah Wah Springs Fm
Cretaceous	Ki	Iron Springs Formation
Jurassic	Jc	Carmel Formation

Figure 17. Geologic cross section B-B' (north-south with B' to the north) through Richie Flat and Pinto Peak (see figure 12 for location of section). No vertical exaggeration.
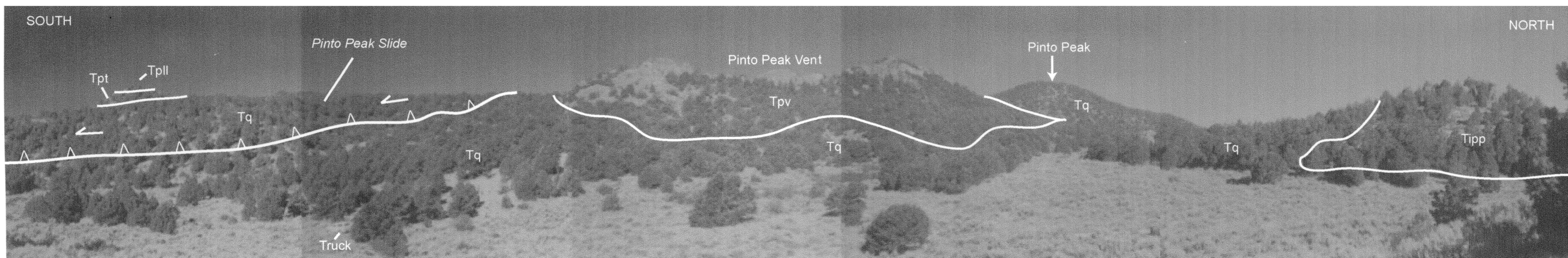
Figure 18. View looking west at vent area of the Pinto Peak intrusion at stop 6. Truck in foreground for scale. See figure 20 for closeup of vent sequence rocks.

266

0.1   22.1   Crest of low rise, entering Richie Flat straight ahead. Richie Flat is floored by the Iron Springs Formation that has been arched upward by the unexposed part of the Stoddard Mountain intrusion (figure 17) to form a northeast-southwest trending anticline, which the Pinto road follows. This anticlinal valley is due to the brittle nature of the overlying roof rocks that were extensionally broken along crestal faults and fractures during uplift that made them more susceptible to erosion.

0.2   22.3   Paradise ridge on left contains tilted (by Stoddard Mountain intrusion) units of the Claron Formation, Quichapa Group, and volcanic "rocks of Paradise." The rocks of Paradise (Hacker, 1998) consist of an ash-flow tuff unit (white layer toward the top) overlain by two lava flow units (capping the ridge) that vented from the Pinto Peak intrusion. The lava flow units were originally mapped as the Paradise intrusion by Cook (1957), who believed it connected with the Stoddard Mountain intrusion. As we will see at stop 6, the lavas can be followed into the vent of the Pinto intrusion.

0.7   23.0   Kane Point ridge on right contains northward tilted (also by Stoddard Mountain intrusion) units of the Claron Formation and Quichapa Group, capped by nearly flat lying Racer Canyon Tuff (not visible from here). Hill on near right (2:00) is a Quaternary (?) slide mass made up of pink and white Claron rocks and darker colored Quichapa units that slumped southward from the cliff. Detachment occurred in the Iron Springs Formation.

0.5   23.5   Iron Springs Formation on right involved in Quaternary landslide.

1.4   24.9   Junction with road on left (Dixie National Forest road 014) leading south to Pinto Spring. **Turn left and proceed south on dirt road after crossing cattle guard.** To the left is a good view of the intrusive anticline in Richie Flat looking east along the axis of the anticline, with the Stoddard Mountain intrusion in the distance. Kane Point ridge to the north, with visible Racer Canyon Tuff cliff on top, and Paradise ridge on the south help define the scale of the anticline.

1.5   26.4   **STOP 5.** PINTO PEAK INTRUSION. Pull off into small dirt road trail on right to examine outcrop of Pinto Peak intrusion on the left (east) side of the road. The quartz monzonite is typically a resistant to crumbly, light gray to light-purplish-gray porphyry with an aphanitic to glassy groundmass. The rock is partly to highly deuterically altered with the mafic phenocrysts having a visible red halo of hematite. The more altered rock is less resistant to weathering and forms lowland areas covered in grass. Locally the intrusion has a chilled margin as thick as 2 m, consisting of a black vitrophyre with abundant white plagioclase phenocrysts. The porphyry intruded from the north into the Iron Springs Formation, then stepped up section into the Claron Formation to the south (see map of intrusion in figure 19). Hike directly west about 50 yards to a small tree-covered hill where the intrusion is in contact with the Claron Formation. The Claron here consists of a resistant basal quartzite conglomerate, which could be correlative with the Grand Castle Formation (Goldstrand and Mullet, 1997) on the Colorado Plateau to the east. The ash-flow tuff unit of the rocks of Paradise contains abundant broken quartzite clasts from this conglomerate Which originated when the intrusion vesiculated and exploded within this unit. Return to vehicles and continue south on dirt road. Pinto Peak is at 2:00 and is made of Harmony Hill Tuff.

0.8   27.2   **STOP 6.** PINTO PEAK VENT. Pull off into the sagebrush to view the vent area for the extrusive rocks mapped as the "rocks of Paradise." Hike up hill to the east a short distance and turn around to face west to view the west part of the vent area as shown in figure 18 (see map of vent in figure 19). The dark-colored rocks at the top of the hills consist of an intra-vent sequence of ash-flow tuff intruded by dikes of dark-gray, glassy porphyritic dikes (see figure 20) with various textures ranging from dense glass to highly vesicular. The dike rocks show faint vertical flow foliation and grade down into intrusive

quartz monzonite. Harmony Hills Tuff (at Pinto Peak in the background) forms the vent wall and is in fault contact with sheared Claron rocks. To the left in the trees is the Pinto Peak slide mass consisting of Quichapa and Claron units that once covered the vent area overlying the Harmony Hills Tuff. The small knoll capping the slide mass on top consists of outflow ash-flow tuff and lava from the vent area. Hike over to and examine the vent rocks, then return to vehicles and continue south on dirt road.

KEY OF SIGNIFICANT UNITS

Tpvr   Rencher Peak flow mbr of Pine Valley Latite
Tpr   Page Ranch Fm
Tpv   Vent sequence of rocks of Paradise
Tplu   Upper lava flow mbr of rocks of Paradise
Tpll   Lower lava flow mbr of rocks of Paradise
Tpt   Ash-flow tuff mbr of rocks of Paradise
Tar   Allochthonous rocks of gravity slide mass
Tipp   Pinto Peak intrusion
Th   Harmony Hills Tuff
Tccb   Bauers Tuff Mbr of Condor Canyon Fm
Tl   Leach Canyon Fm
Tc   Claron Fm
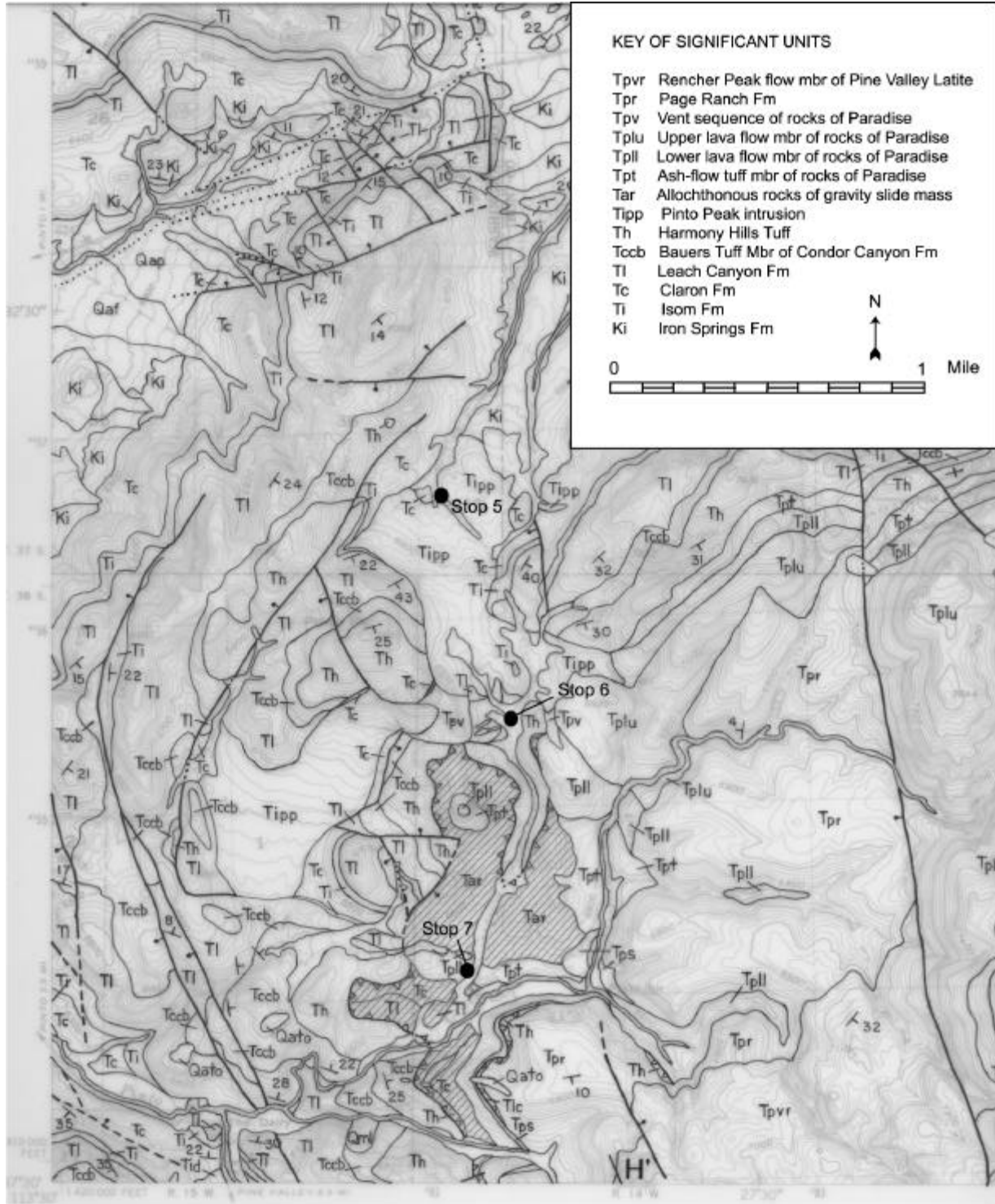Ti   Isom Fm
Ki   Iron Springs Fm

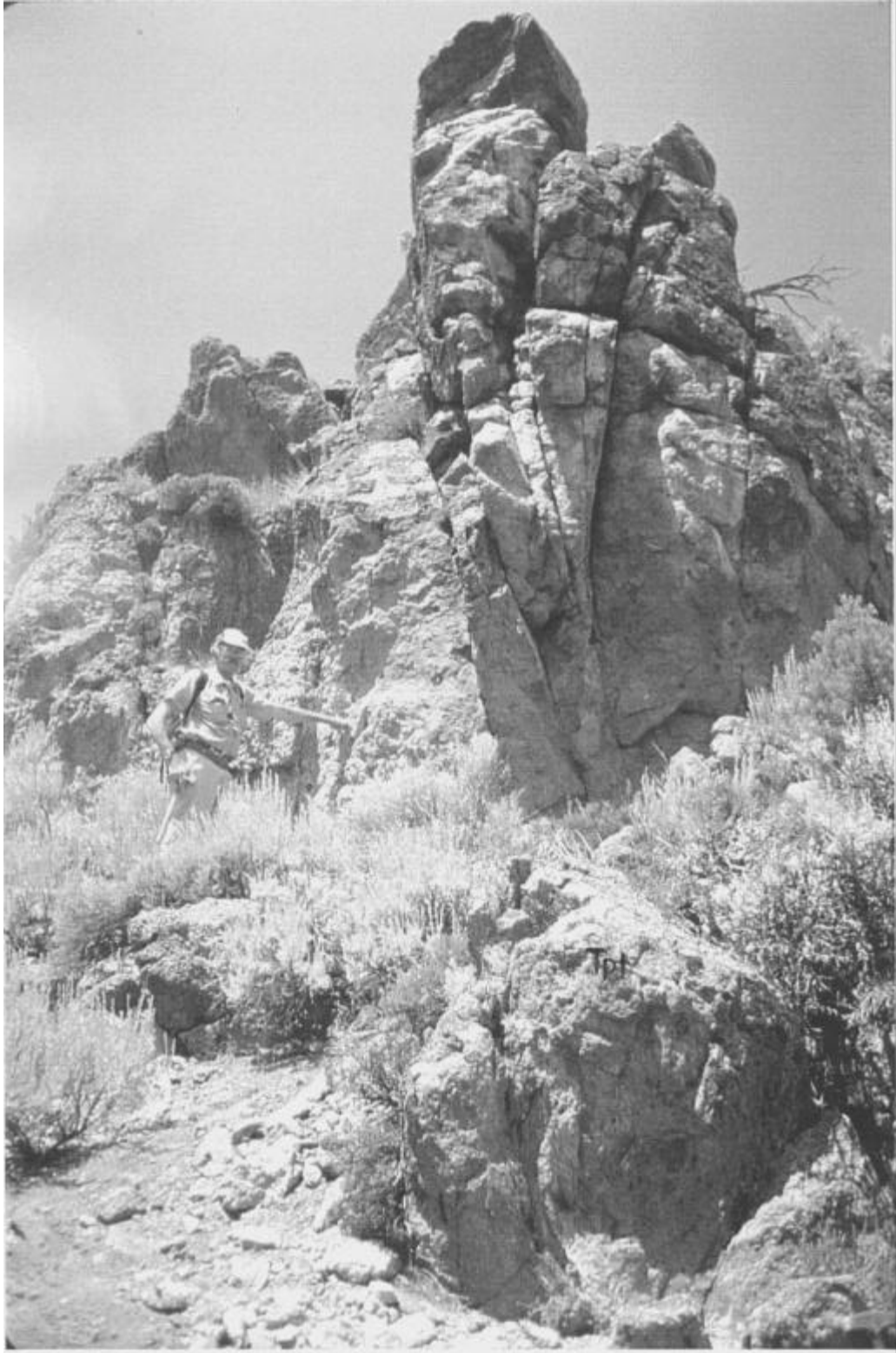*Figure 19. Geologic map of the Pinto Peak intrusion area. Based on unpublished mapping of 1:24,000 Page Ranch Quadrangle.*

268

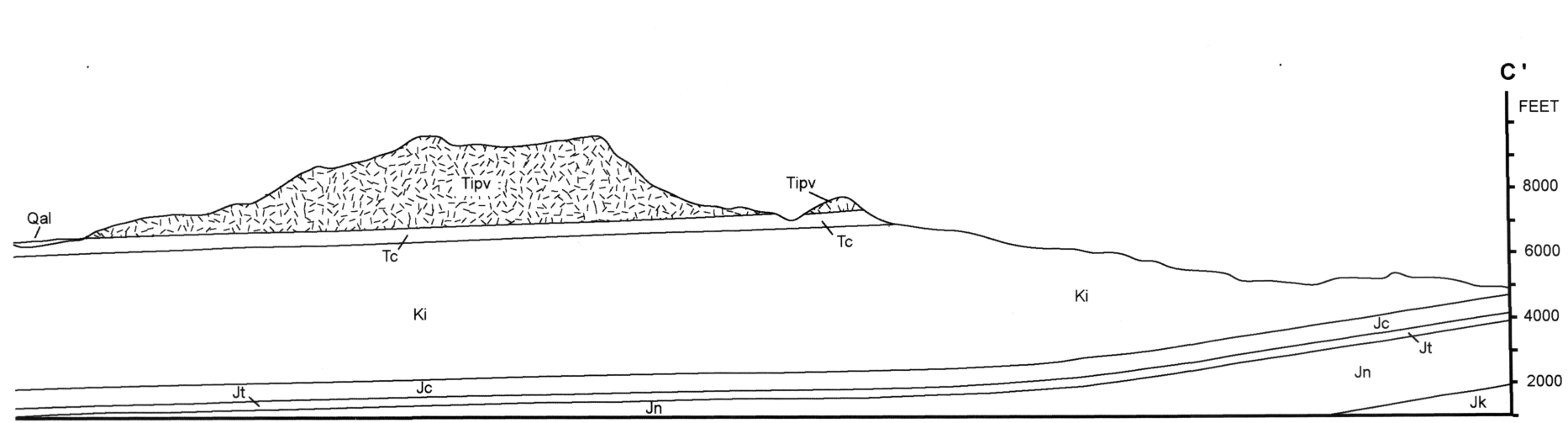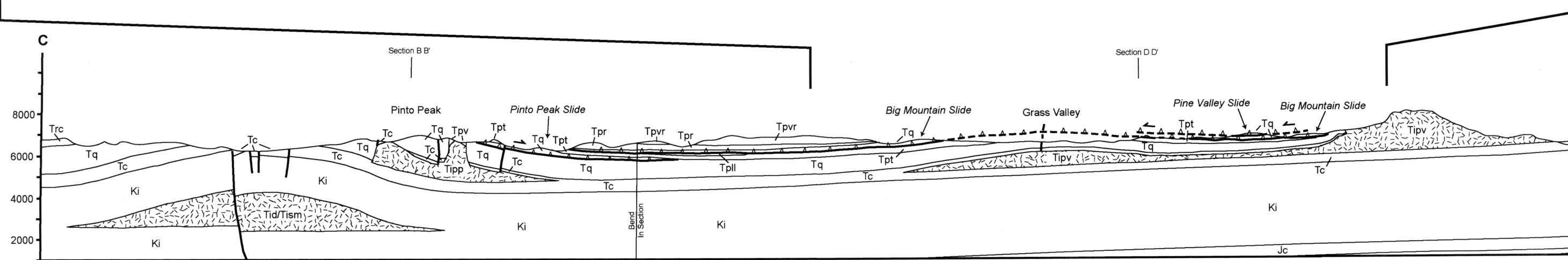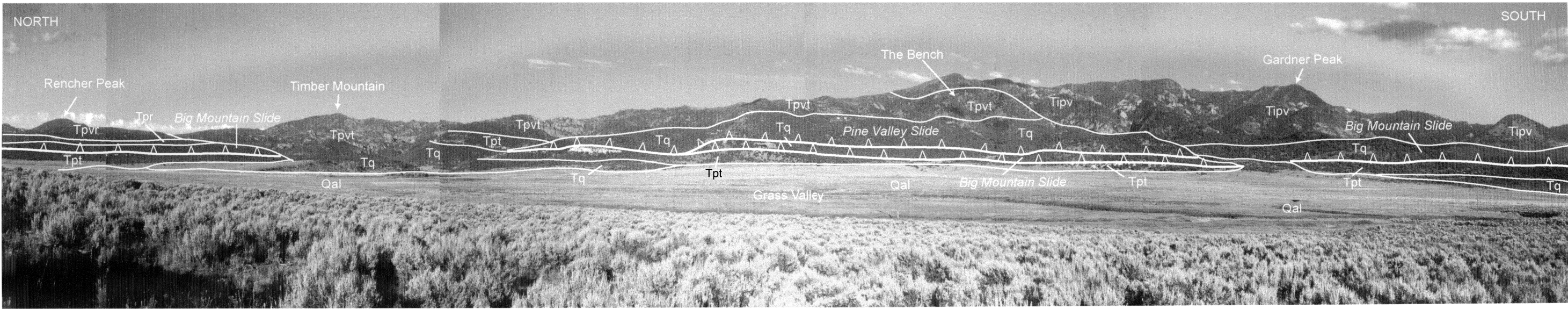*Figure 20. Photo of vent sequence with ash-flow tuff (next to Dick Blank's hand) cut by vertical dike* systems of glassy lava.

0.9	28.1	Crossroads. Pinto Springs road bends to the left. Continue straight on dirt road (Dixie National Forest road 346) that then bends to the right.
0.2	28.3	**STOP 7.** ASH-FLOW TUFF MEMBER OF THE ROCKS OF PARADISE. Pull off to right on small trail road. South of the road are broken units of the Claron and Leach Canyon in the Pinto Peak slide mass. On the north side of the road are good outcrops of ash-flow tuff member that vented from the Pinto Peak intrusion. This member overlies rock units of the Pinto Peak slide mass. Note the large pumice holes and the quartzite clasts derived from the Claron Formation, which we examined previously at Stop 5. Cook (1957) initially mapped this unit as the "pebble tuff" member of the Rencher Formation because of the abundant quartzite clasts. In the field, the presence of these quartzite clasts distinguishes this tuff from similar tuff of the Rencher Formation (derived from the Bull Valley intrusion emplced into the Jurassic Carmel Formation) and volcanic rocks of Comanche Canyon (derived from the Stoddard Mountain intrusion emplaced into the Iron Springs Formation). Return to vehicles and turn around and return to Pinto road in Richie Flat.
3.3	31.6	Junction with Pinto road (Dixie National Forest road 009). **Turn left and proceed west on Pinto road.**
0.4	32.0	Crest of hill in intrusively faulted Claron and Quichipa units.
2.2	34.2	Pinto settlement. Junction of Pinto road and gravel road on right (Dixie National Forest road 011) leading north to the town of Newcastle. Continue west on Pinto road.
0.2	34.4	Junction of Pinto road and gravel road on left (Dixie National Forest road 011) leading south to Grass Valley and Pine Valley. **Turn left and proceed south on Grass Valley road.**
0.4	34.8	Houses in valley on left are located on Iron Springs Formation. Red and white Claron and brown Quichapa rocks cap the surrounding hills. Pinto is in a domal valley created by an unexposed intrusion that connects with The Dairy intrusion to the south and probably with the Stoddard Mountain intrusion to the west.
2.9	37.7	The Dairy intrusion. Quartz monzonite intruded into upper white Claron rocks that can be seen dipping north and south off the laccolith. The Dairy did not vent any volcanic units, but it deformed the rocks of Paradise and the Pinto Peak slide mass (both derived from the Pinto Peak intrusion), as well as Big Mountain slide mass (from the Bull Valley-Big Mountain arch).
0.2	37.9	Claron and the Wah Wah Springs Formation of the Needles Range Group on the right. In the northern Pine Valley Mountains and eastern Bull Valley Mountains (Blank, 1993) the ash-flow tuffs of the Wah Wah Springs Formation and members of the Isom Formation are intercalated with lacustine carbonates in the top of the Claron indicating persistence of the Claron lake in this area of Utah before succumbing to the ash-flow sheets of the Quichapa Group.
0.1	38.0	Tilted Leach Canyon Formation on right above Claron Formation.
0.1	38.1	Harmony Hills Tuff on right.
0.1	38.2	Ash-flow tuff member of the rocks of Paradise on right, overlying Harmony Hills Tuff. Lower lava flow member of the rocks of Paradise (Hacker, 1998) on left, across South Fork of Pinto Creek. This volcanic flow breccia was initially mapped by Cook (1957) as the "blue breccia" member of the Rencher Formation. This lava flow originated from the

Pinto Peak intrusion from the vent at Stop 6.

0.2	38.4	Bridge over South Fork of Pinto Creek. Lower lava flow member of the rocks of Paradise on right.

0.2   38.6   Less brecciated zone of lower lava flow member of the rocks of Paradise on left. Samples from this exposure yielded a preliminary $^{40}Ar/^{39}Ar$ date on biotite of 21.93 $\pm$ 0.07 Ma (L.W. Snee, U.S. Geological Survey, written communication, 1995; Hacker and others, 1999).

0.5   39.1   Rencher Peak flow member of the Pine Valley Latite forms high cliffs at 11:00. This part of the Pine Valley Latite is slightly older than the comagmatic Pine Valley intrusion and extruded as a large lava dome and coulée type flow from the Rencher Peak area north of Grass Valley.

0.6   39.7   Outcrop on left of allochthonous Little Creek andesite, within the Big Mountain slide.

0.5   40.2   **STOP 8.** RENCHER FORMATION AND BIG MOUNTAIN SLIDE. Pull off on right by large Ponderosa pine tree. Roadcuts on left (east) side of road is of the lower ash-flow tuff member of Rencher Formation (Blank, 1993), overlain by fractured and brecciated allochthonous rocks within the Big Mountain slide. The lower ash-flow tuff member of Rencher Formation is white to light-gray, poorly to moderately indurated, crystal-rich ash-flow tuff with subrounded cognate inclusions that are darker or lighter than the host matrix and resemble pumice clasts but without vesiculation. Angular lithic fragments consist of mostly Quichapa rocks and porpyritic quartz monzonite. The lithics and cognate inclusions decrease in size and abundance eastward from the vent area in the Bull Valley Mountains and are almost nonexistent here in the Grass Valley area. Walking a short distance southward along the road, you will see exposures of Isom, Leach Canyon, and Little Creek andesite within the Big Mountain slide mass. This portion of the slide is on the former land surface composed of the lower ash-flow tuff member of Rencher Formation. Return to vehicles and continue south on Grass Valley road.

0.5   40.7   Roadcut on left of allochthonous Leach Canyon Formation.

0.1   40.8   Roadcut on left of allochthonous white and pink Claron, and a thin unit of Wah Wah Springs Formation.

0.2   41.0   Outcrops on left and right of allochthonous Little Creek andesite. The Little Creek andesite is an autochthonous unit present between the Bauers and Harmony Hills units in the Bull Valley Mountains, but in the Pine Valley Mountains appears in allochthonous rocks within slide masses only (Bull Valley slide and Big Mountain slide). Crest of hill (at cattle-guard in road) is the drainage divide of South Fork of Pinto Creek (draining north into the Escalante basin) and Grass Valley Creek (part of the Colorado River drainage basin).

0.3   41.3   Road on left to Mill Canyon trailhead and Broken Arrow Ranch (formerly Rencher Ranch, which is the type locality of the Rencher Formation). Continue south on Grass Valley road.

1.2   42.5   **STOP 9.** GRASS VALLEY. Pull off at crest of hill to view geologic features on east side of Grass Valley (see figure 21). Grass Valley is another eroded anticline produced by an unexposed intrusion that is interpreted to be an extension of the Pine Valley intrusion exposed in the hills to the right. The white cliffs just above the valley floor are exposures of the ash-flow tuff member of the rocks of Paradise overlain by the Big Mountain slide mass. The Rencher Formation was not deposited this far east. The Big Mountain slide is overlain by fanglomerates of the Page Ranch Formation and the Pine

Valley slide mass. Overlying the Pine Valley slide is the Timber Mountain flow member of the Pine Valley Latite that extruded northward from the Pine Valley laccolith following the collapse of its flank by gravity sliding. Rencher Peak (source area for the slightly older Rencher Peak flow member of the Pine Valley Latite) is the high peak visible on the north side of Grass Valley. Return to vehicles and continue south on Grass Valley road.

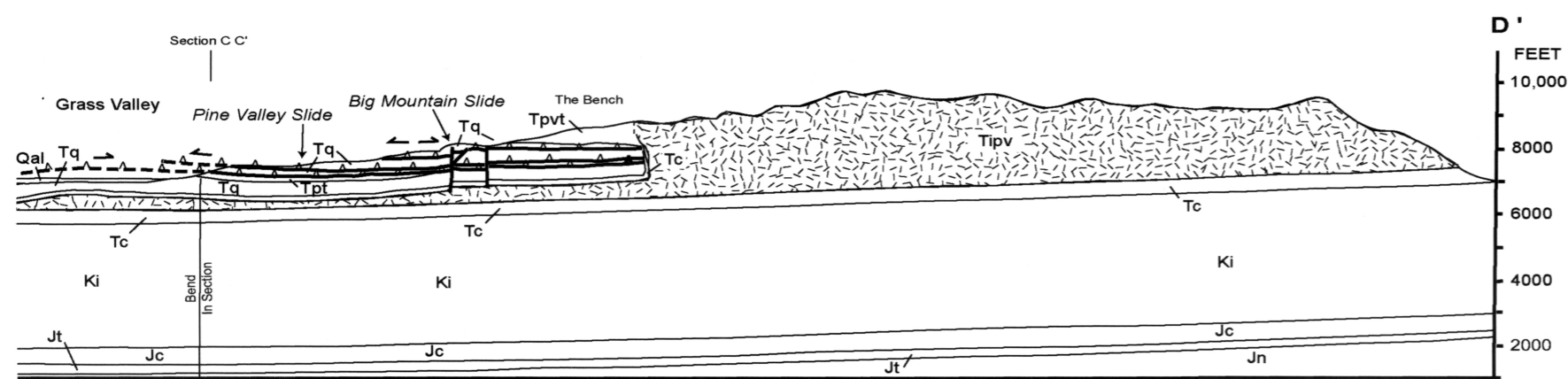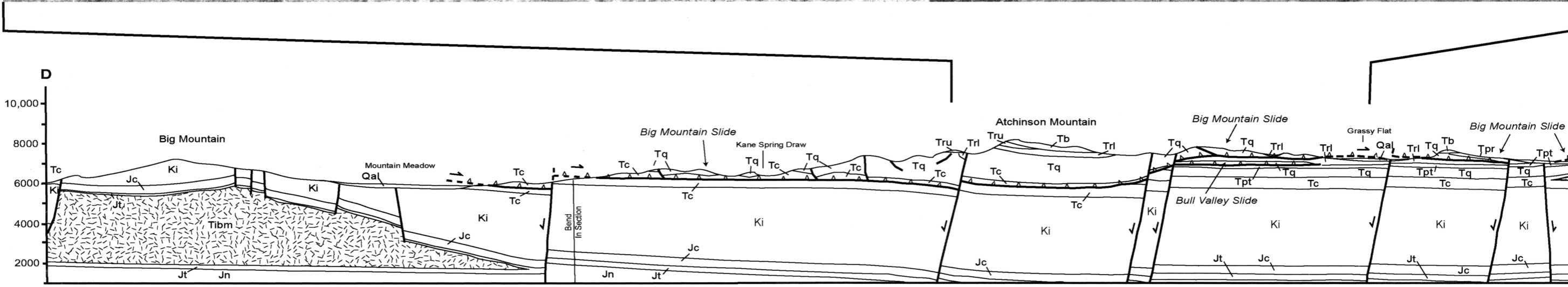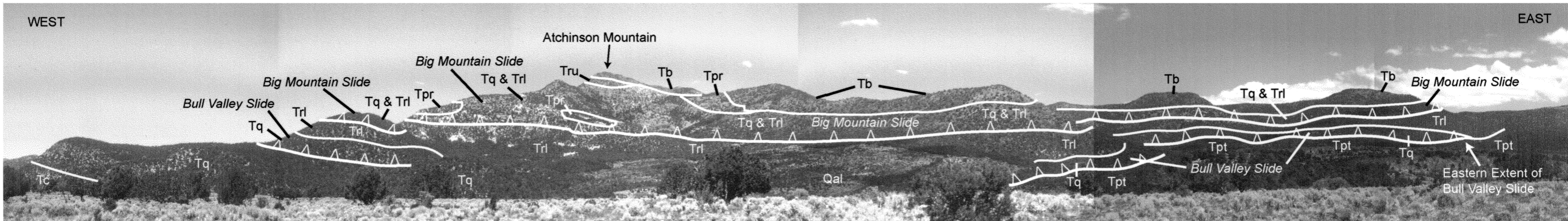|		
1.0	43.5	Cinder cone of quartz-bearing basalt on right. Lava from this and other vents dammed Grass Valley, which then filled in with fluvial sediments and minor lacustrine deposits to form the relatively broad valley floor. Many fertile valleys in this area formed in this manner, including Pine Valley, Grassy Flat, and Diamond Valley.
1.7	45.2	Road turns to the southeast, with a view of Pine Valley and rugged topography of the Pine Valley laccolith. The Pine Valley laccolith intruded into the middle to upper part of the Claron Formation.
0.4	45.6	Junction with Central-Pine Valley road (paved). **Turn left (east) at stop sign and proceed to town of Pine Valley.**
0.5	46.1	Descend hill of basalt into Pine Valley, which is drained by the Santa Clara River. Hills to left are made of autochthonous units of the Claron Formation (tree covered red and white rocks at base of hill) and Quichipa Group rocks. Gardner Peak is on the left at 11:00 and is part of a westward extending lobe of the Pine Valley laccolith. Mapping of the peripheral structures of the laccolith indicates that this lobe did not extend across Pine Valley and connect with the main part of the intrusion to the south. The Santa Clara River and Pine Valley therefore occupy a natural, easily erodable V-shaped discontinuity in the laccolith.
0.2	46.3	Cross Santa Clara River.
0.5	46.8	Junction with Main Street in town of Pine Valley. **Turn left (east) at stop sign and proceed through town.**
0.1	46.9	Dixie National Forest Pine Valley visitor center and workstation on right.
1.4	48.3	Pine Valley Recreation Area sign on right.
0.7	49.0	Red soil on left belongs to the Claron Formation, which is capped by quartz monzonite porphyry of the Pine Valley intrusion.
0.2	49.2	Pine Valley Reservoir on right.
0.5	49.7	**STOP 10.** PONDEROSA PICNIC AREA. Turn right into picnic parking area for lunch stop. We are now within the eroded part of the laccolith and about level with its base. Alluvial boulders of quartz monzonite porphyry litter the picnic area. Samples taken from the campground area yielded a K-Ar date on biotite of 20.9 ± 0.6 Ma (Mckee and others, 1997). After lunch return to vehicles and turn left out of parking area and retrace route back to the town of Pine Valley.
2.9	52.6	Junction with road to Central. **Turn right (north).**
1.2	53.8	Junction with Grass Valley road to Pinto on right. Continue westward on paved Central-Pine Valley road.
0.5	54.3	Junction with road to Grassy Flat on right. Continue westward on paved main road that is on basalt that erupted from a buried northeast striking basin-range fault or fissure that is lined with cinder cones (to the left and right).

Figure 21. Geologic cross section C-C' (north-south with C to the north) through the Pine Valley Mountains (see figure 12 for location of section) and photo view of Grass Valley area (looking east) at stop 9. No vertical exaggeration.

Key

Quaternary	Qal	Fluvial and alluvial units
Tertiary	Tb	Older basalt
	Trc	Racer Canyon Tuff
	Tpvt	Timber Mountain flow member of Pine Valley Latite
	Tpvr	Rencher Peak flow member of Pine Valley Latite
	Tipv	Pine Valley intrusion
	Tpr	Page Ranch Formation
	Tism	Stoddard Mountain intrusion
	Tid	The Dairy intrusion
	Tpll	Lower lava flow member of rocks of Paradise
	Tpt	Ash-flow tuff member of the rocks of Paradise
	Tpv	Vent unit of the rocks of Paradise
	Tipp	Pinto Peak intrusion
	Tq	Quichapa Group - includes: Harmony Hills Tuff, Little Creek andesite, Condor Canyon Fm, Leach Canyon Fm, and local sedimentary rocks
	Tc	Claron Formation - includes thin units of Isom Fm and Wah Wah Springs Fm
Cretaceous	Ki	Iron Springs Formation
Jurassic	Jc	Carmel Formation
	Jt	Temple Cap Formation
	Jn	Navajo Sandstone
	Jk	Kayenta Formation

273

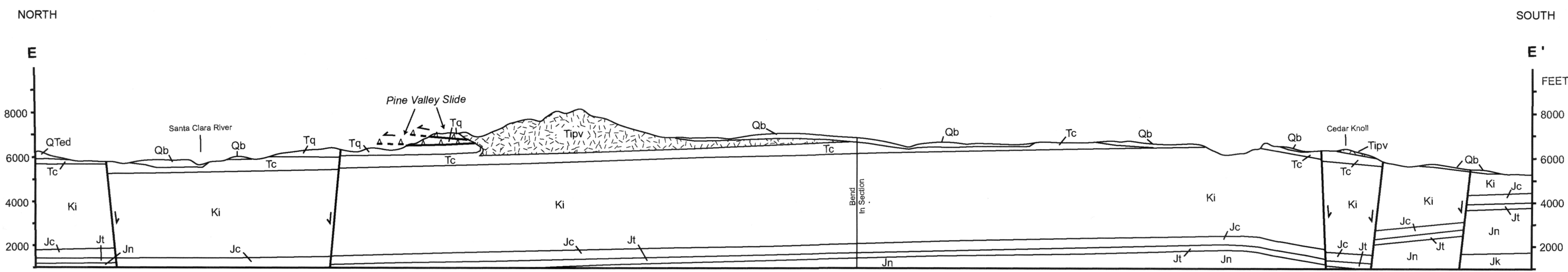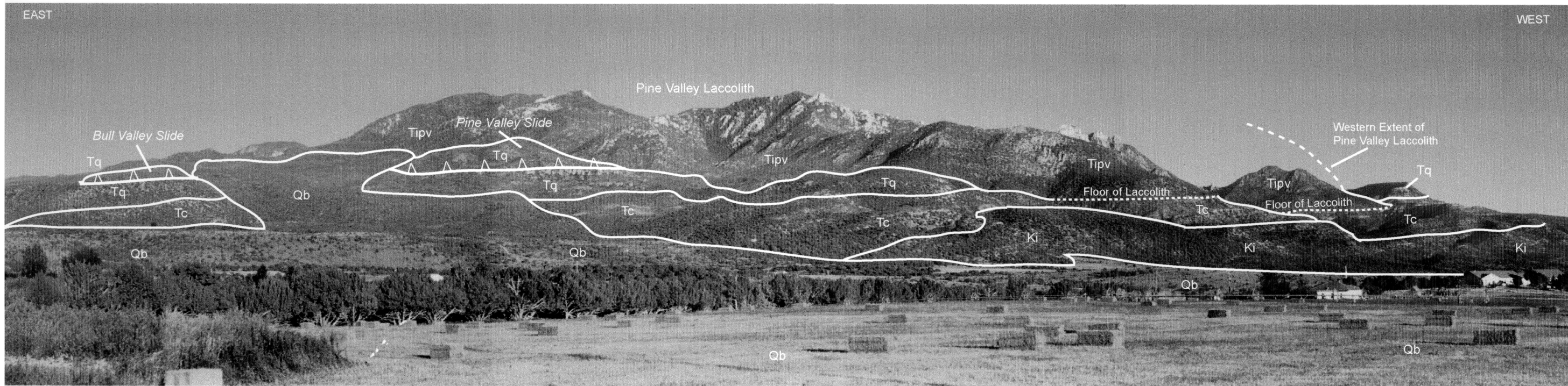| 0.8	55.1	View of Square Top Mountain in the far distance at 10:00 and the Bull Valley Mountains to its right (north) at 11:00 to 12:00. The white rocks visible in the Bull Valley Mountains consist of ash-flow tuffs of the Rencher Formation located very near their vent from the Bull Valley intrusion. Square Top Mountain consists of subhorizontal Pennsylvanian and Permian rocks thrusted eastward over rocks as young as the Upper Cretaceous Iron Springs Formation during the Sevier orogeny (Hintze, 1986). Atchinson Mountain at 2:00.
1.1	56.2	**STOP 11.** ATCHINSON MOUNTAIN. Pull off to right into driveway of Forest Service dump station to view geologic features of Atchinson Mountain (see figure 22). Both the Bull Valley and Big Mountain slides are present here. Return to vehicles and continue westward on Central-Pine Valley road.
1.0	57.2	Red and white autochthonous Claron to right (north of road) overlain by autochthonous Quichapa rocks that lack the Little Creek andesite between the Bauers and Harmony Hills.
0.9	58.1	Junction with jeep trail (Dixie National Forest road 823) to right that leads to Eight Mile Spring. The Big Mountain slide forming the rugged topography west of Atchinson Mountain contains allochthonous Little Creek andesite rocks within the Qichapa Group and rests upon a low-angle bedding detachment fault within the Claron Formation. The near hill at 2:00 is made of Pliocene (?) to Pleistocene Eight Mile Dacite of Cook (1957) that forms a series of northeast trending volcanic domes erupted along a basin-range fault similar to the basalt flows at mile 54.3. Continue westward on Central-Pine Valley road.
0.2	58.3	Older alluvial-fan deposits of Pliocene to Pleistocene age overlain by Pleistocene lava flows. Apparent dike of basalt cuts the alluvium on right.
0.2	58.5	View of Eight Mile Dacite on right showing conspicuous flow layering and folding within the volcanic domes. Basalt flows on south side of road (left).
0.6	59.1	Dixie National Forest boundary. Hill at 2:00 above the town of Central is composed of autochthonous Claron and Quichapa (without Little Creek andesite). At the top are remnants of the Bull Valley slide forming klippes of allochthonous Claron and Quichapa resting on the former land surface of Harmony Hill Tuff and ash-flow tuff member of the rocks of Paradise. Behind the hill to the north is the high-angle southern bounding fault of the Big Mountain slide. The far hill is composed of a thick section of allochthonous Little Creek andesite faulted against autochthonous rocks exposed in the hill just described above the town of Central.
0.8	59.9	**STOP 12.** GRAVITY-SLIDE MASS OF PINE VALLEY LACCOLITH. Pull off on left opposite the Saucer Ranch (on right) to view geologic features of the Pine Valley laccolith to the south (see figure 23). This marks the western extent of the Pine Valley laccolith. The floor of the laccolith can be observed where the dark quartz monzonite of the intrusion overlies red Claron rocks. The small hill to the right contains a full Claron section and a partial Quichapa section (see figure 23). Return to vehicles and continue westward on Central-Pine Valley road.
0.2	60.1	Basin-range faulted autochthonous Claron and Isom (across from 300 East Street) rocks in roadcuts on right.
0.5	60.6	Intersection with SR-18. **Turn right at stop sign and proceed north toward the town of Enterprise.**

0.6	61.2	Hills from 1:00 to 3:00 are capped with klippes of the Bull Valley slide composed of Quichapa and Claron rocks overlying the former land surface fault. Hills on the left are composed of the autochthonous lower ash-flow tuff member of the Rencher Formation, capped by younger basalts. The Rencher here overlies the Bull Valley slide.
1.7	62.9	**STOP 13.** SOUTHERN FLANKING FAULT OF THE BIG MOUNTAIN SLIDE. Pull off road to right (0.1 mile before Kane Spring). We just crossed over the southern strike-slip bounding fault of the Big Mountain slide. This fault can be seen in the notch between the two hills on the left (east) side of road. Looking east, the hill on the left (north) is capped with a thick section of Little Creek andesite underlain by Bauers and Leach Canyon rocks. These allochthonous units are part of the Big Mountain slide and have traveled eastward away from the viewer. The hill on the right consists of a thinner section of autochthonous Bauers and Harmony Hills Tuff (with no intercalated Little Creek andesite) capped by klippes of the Bull Valley slide. Return to vehicles and continue north on SR-18.
0.2	63.1	SR-18 bends to the left (west). Hills to the right are composed of mostly Bauers, Little Creek andesite, and Harmony Hills Tuff of the Big Mountain slide above a bedding detachment fault.
0.7	63.8	Hill at 2:00 to 3:00 consists of white rocks of the lower ash-flow tuff member of the Rencher Formation, capped by darker red rocks of the upper ash-flow tuff member of the Rencher Formation. The lower Rencher here is allochthonous and part of the Big Mountain slide and capped by the autochthonous upper Rencher , which immediately followed the Big Mountain sliding episode.
0.5	64.3	Roadcut of allochthonous white, lower ash-flow tuff member of the Rencher Formation on left and right. The lower Rencher here contains larger lithic clasts and cognate inclusions than found in Grass Valley, indicating a closer proximity to the vent (Bull Valley intrusion). Road bends to the right (north).
0.5	64.8	**STOP 14.** BIG MOUNTAIN SLIDE IN ROADCUT. Pull off road to the right and park near the "Mountain Meadow ½ Mile" sign. Roadcut on right consists of highly fractured and brecciated rocks of Little Creek andesite and Harmony Hills Tuff in the Big Mountain slide mass. These and lower units override the bedding detachment fault segment of the slide. Detachment is within the lower Claron and/or upper Iron Springs. Return to vehicles and continue north on SR-18.
0.5	65.3	Entrance road to Mountain Meadow monument of left. **Turn left on the monument road** and proceed to the overlook parking area on Dan Sill Hill. You will pass a gravel road on the left that leads to the gravesite in Mountain Meadow. This is the site of the infamous 1857 massacre of about 120 emigrants while they were traveling the Old Spanish Trail that traverses Mountain Meadow.
0.1	65.4	**STOP 15.** MOUNTAIN MEADOW OVERLOOK. Park in monument parking lot and take short paved trail to monument overlook on Dan Sill Hill. The hill is made of the upper ash-flow tuff member of the Rencher Formation overlying allochthonous Claron rocks of the Big Mountain slide. Northwest of Mountain Meadow is Big Mountain (with radio towers on top) at the northern end of the Bull Valley-Big Mountain arch. The Big Mountain dome consists of Iron Springs rocks and locally some Carmel limestone and intrusive quartz monzonite. In this denuded area of the arch, the Iron Springs and/or Claron are overlain by the upper ash-flow tuff of the Rencher Formation. The hills on the east side of Mountain Meadow (east of SR-18 behind you) consist of the Big Mountain slide that originated on Big Mountain. These hills contain a thick section of the conspicuous allochthonous white lower Rencher, which has slid eastward from the

275

Figure 22. Geologic cross section D-D' (east-west with D to the west) through the Pine Valley Mountains (see figure 12 for location of section) and photo view of Atchinson Mountain area (looking north) at stop 11. No Vertical exaggeration.

Key

Quaternary	Qal	Fluvial and alluvial units
Tertiary	Tb	Older basalt
	Tpvt	Timber Mountain flow member of Pine Valley Latite
	Tipv	Pine Valley intrusion
	Tpr	Page Ranch Formation
	Tru	Upper ash-flow tuff member of Rencher Formation
	Trl	Lower ash-flow tuff member of Rencher Formation
	Tibm	Big Mountain intrusion
	Tpt	Ash-flow tuff member of the rocks of Paradise
	Tq	Quichapa Group - includes: Harmony Hills Tuff, Little Creek andesite, Condor Canyon Fm, Leach Canyon Fm, and local sedimentary rocks
	Tc	Claron Formation - includes thin units of Isom Fm and Wah Wah Springs Fm
Cretaceous	Ki	Iron Springs Formation
Jurassic	Jc	Carmel Formation
	Jt	Temple Cap Formation
	Jn	Navajo Sandstone

276

EAST / WEST

Pine Valley Laccolith

Bull Valley Slide

Pine Valley Slide

Tq

Tq

Tc

Qb

Tipv

Tq

Tc

Qb

Tipv

Tq

Tc

Ki

Qb

Western Extent of
Pine Valley Laccolith

Floor of Laccolith

Tipv

Tc

Floor of Laccolith

Ki

Qb

Tipv

Tq

Tc

Ki

Qb

NORTH / SOUTH

E / E'

FEET

Pine Valley Slide

8000

Santa Clara River

QTed

Qb

Tc

Ki

Jc

Jt

Jn

Tq

Qb

Tc

Jc

Tq

Tc

Tq

Ki

Jc

Jt

Tipv

Jn

Qb

Tc

Ki

Jt

Bend In Section

Qb

Tc

Ki

Jn

Qb

Tc

Ki

Jc

Jt

Jn

Cedar Knoll

Qb

Tc

Tipv

Tc

Qb

Ki

Ki

Jc

Jt

Jn

Ki

Jc

Jt

Jn

Jk

8000

6000

4000

2000

Key

Quaternary	Qb	Basalt
	QTed	Eight Mile Dacite
Tertiary	Tipv	Pine Valley intrusion
	Tq	Quichapa Group - includes: Harmony Hills Tuff, Little Creek andesite, Condor Canyon Fm, Leach Canyon Fm, and local sedimentary rocks
	Tc	Claron Formation - includes thin units of Isom Fm and Wah Wah Springs Fm
Cretaceous	Ki	Iron Springs Formation
Jurassic	Jc	Carmel Formation
	Jt	Temple Cap Formation
	Jn	Navajo Sandstone
	Jk	Kayenta Formation

Figure 23. Geologic cross section E-E' (north-south with E to the north) through west end of Pine Valley laccolith (see figure 12 for location of section) and photo view of Pine Valley laccolith (looking south) at stop 12 near the town of Central. No vertical exaggeration.

277

crest or flank of the Bull Valley – Big Mountain arch prior to the eruption of the upper Rencher. Return to vehicles and return to SR-18 via the overlook access road.

0.1	65.5	Intersection with SR-18. **Turn left at stop sign and continue north on SR-18.**
2.2	67.7	Junction with gravel road on right leading to Pinto. Continue northward on SR-18. Iron Springs Formation to the left, on flank of Big Mountain.
1.2	68.9	Roadcuts of Iron Springs Formation on north flank of Big Mountain dome.
1.5	70.4	Road crosses Big Mountain normal fault on the west flank of Big Mountain that strikes north and is down-to-the-west. Big Mountain formed by arching of the laccolith (Blank, 1993). Here Claron (exposed in the roadcuts) is juxtaposed against Iron Springs on the west, and farther south on the arch, Claron is juxtaposed against Carmel.
1.0	71.4	Roadcut through red ash flow-tuff (Bald Hills Member) of the Isom Formation.
1.4	72.8	Dixie National Forest boundary sign. Road is cutting through Piocene/Pleistocene valley-fill deposits of Blank (1993).
1.3	74.1	T-Junction (at stop sign) with road to left leading to the town of Enterprise and the continuation of SR-18 to the right. **Turn right (northeast) at stop sign and continue on SR-18.**
0.8	74.9	Hill on right at 3:00 is Gum Hill, consisting of basin-fill deposits capped by basalt of Gum Hill of Blank (1993), which has recently been dated with a minimum age of 5.7 Ma (Cornell and others, 2001). The basalt dips to the east into the southern extension of the Antelope Range fault (range-front fault) of Siders and others (1990).
1.8	76.7	Junction with paved road on right leading to the town of Newcastle with SR-18 bending left. **Turn right on Newcastle road.** View of southern extension of Antelope Range that is currently being mapped by Tom Butler and Don Cornell of Kent State University as part of their Masters theses (see Butler and others, 2001; Cornell and others, 2001).
3.4	80.1	Old Spanish Trail sign on right. Red and white rocks in the footwall block of the Antelope Range fault at 12:00 consist of basin-range faulted Iron Springs and Claron units capped by darker volcanics of the Isom Formation and Quichapa Group.
3.0	83.1	Greenhouses on left at 10:00 are heated by a blind geothermal resource associated with the range-front fault. The resource was delineated by geophysical surveys and drilling (Mabey and Budding, 1987; Blackett and others, 1990). Thickness of the basin west of the range-front fault is estimated to be ~ 3 km based on geophysical surveys (Pe and Cook, 1980).
2.3	85.4	Junction of Main Street of Newcastle with SR-56. **Turn right at stop sign and proceed east toward Cedar City.**
1.3	86.7	Hills on north side of the road at 10:00 consist of rhyolite lava domes (rhyolite of Silver Peak) dated at 8.4 ± 0.4 Ma (Shubat and Siders, 1988; Siders and others, 1990).
3.7	90.4	Gravel road to Desert Mound on left. Continue eastward on SR-56. View of iron mines on flank of Iron Mountain straight ahead. Stoddard Mountain is the tallest peak to the right of Iron Mountain just above the road in the distance.
1.6	92.0	The red hill north of the road on right (in the distance) consists of north-dipping, orange

clastics of the Iron Springs Formation with a cap of red Claron. The Claron wraps around the Iron Mountain intrusion. Iron Mountain is the tallest peak, with radio towers and a mine scar on top. Outcrops to right along the road also consist of Iron Springs and Claron dipping to the south. We are now traveling on the western extension of the up arched dome of the Iron Mountain intrusion.

2.7	94.7	Gravel road to old Irontown ruins on left. Continue eastward on SR-56. Irontown was an early iron ore-smelting site constructed and operated by pioneers in the late 1800s.
1.4	96.1	Gravel turnoff on left to Blowout pit. **Turn left on gravel drive for optional stop at iron workings at Blowout pit.** Keep to the right on gravel drive until small dirt trail on left.
0.2	96.3	**STOP 16.** OPTIONAL STOP AT BLOWOUT PIT. Stop and park by dirt trail on left. Walk a short distance north up trail to the rim of pit, now partially filled with water. Here hematite replacement ore deposits formed in the vertical to overturned Homestake Limestone Member (gray rocks in pit wall) of the Carmel Formation in the upper plate of the Sevier Iron Springs Gap thrust. Quartz monzonite porphyry is exposed in the opposite pit wall. Return to vehicles and return to SR-56.
0.3	96.6	Junction with SR-56. **Turn left and continue eastward to Cedar City.**
1.4	98.0	Junction with Pinto road on right. Continue eastward to Cedar City.
17.4	115.4	End of field trip at intersection of SR-56 (200 North) and Main Street.

REFERENCES

Adair, D.H., 1986, Structural setting of the Goldstrike district, Washington County, Utah: p. 129-135 *in* Griffin, D.T., and Phillips, W.R., editors, Thrusting and extensional structures and mineralization in the Beaver Dam Mountains, southwestern Utah: Utah Geological Association Publication 15, 217 p.

Anderson, J.J., 1985, Mid-Tertiary block faulting along west and northwest trends, southern High Plateaus, Utah [abs]: Geological Society of America, Abstracts with Programs, v. 20, no.3, p. 139.

_____ 1993, The Markagunt megabreccia--Large Miocene gravity slides mantling the northern Markagunt Plateau, southwestern Utah: Utah Geological Survey Miscellaneous Publication 93-2, 37 p.

Anderson, J.J., and Rowley, P.D., 1975, Cenozoic stratigraphy of the southwestern High Plateaus in Utah. *In* Anderson, J.J., Rowley, P.D., Fleck, R.J., and Nairn, A.E.M., editors, Cenozoic geology of southwest High Plateaus of Utah: Geological Society of America Special Paper 160, p. 1-52.

Anderson, R.E., 1971, Thin-skin distension in Tertiary rocks of southeastern Nevada: Geological Society of America Bulletin, v. 82, p. 43-58.

Anderson, R.E., and Barnhard, T.P., 1993, Heterogenous Neogene strain and its bearing on horizontal extension and horizontal and vertical contraction at the margin of the extensional orogen, Morman Mountains area, Nevada and Utah: U.S. Geological Survey Bulletin, 2011, 43 p.

Anderson, R.E., and Mehnert, H.H., 1979, Reinterpretation of the history of the Hurricane fault in Utah, *in* Newman, G.W., and Cook, H.D., editors, 1979 Basin and Range Symposium and Great Basin Field Conference: Denver and Salt Lake City, Rocky Mountain Association of Geologists and Utah Geological Association, p. 145-166.

Armstrong, R.L., 1972, Low-angle (denudation) faults, hinterland of the Sevier orogenic belt, eastern Nevada and western Utah: Geological Society of America Bulletin, v. 83, p. 1729-1753.

Barker, D.S., 1995, Crystallization and alteration of quartz monzonite, Iron Springs mining district, Utah – Relation to associated iron deposits: Economic Geology, v. 90, p. 2197-2217.

Best, M.G., Christiansen, E.H., and Blank, R.H., Jr., 1989, Oligocene caldera complex and calc-alkaline tuffs and lavas of the Indian Peak volcanic field, Nevada and Utah: Geological Society of America Bulletin, v. 101, p. 1076-1090.

Billings, M.P., 1972, Structural geology (third edition): Englewood Cliffs, Prentice-Hall, 606 p.

Blackett, R.E., Shubat, M.A., Chapman, D.S., Forster, C.B., Schlinger, C.M., and Bishop, C.E., 1990, The Newcastle geothermal system, Iron County, Utah - Geology, hydrology, and conceptual model: The U.S. Department of Energy Geothermal Division, p. 1-78.

Blank, H.R., 1959, Geology of the Bull Valley district, Washington County, Utah: Seattle, University of Washington, Ph.D. dissertation, 177 p.

_____ 1993, Preliminary geologic map of the Enterprise quadrangle, Washington and Iron Counties, Utah: U.S. Geological Survey Open-File Report 93-203, 55p., scale 1:24,000.

Blank, H.R., and Kucks, R.P., 1989, Preliminary aeromagnetic, gravity, and generalized geologic maps of the USGS Basin and Range - Colorado Plateau transition zone study area in southwestern Utah, southeastern Nevada, and northwestern Arizona (the "BARCO" project): U.S. Geological Survey Open-File Report 89-432, 16 p., scale 1:250,000.

Blank, H.R., and Mackin, J.H., 1967, Geologic interpretation of an aeromagnetic survey of the Iron Springs district, Utah: U.S. Geological Survey Professional Paper 516-B, 14 p., scale 1:48,000.

Blank, H.R., Rowley, P.D., and Hacker, D.B., 1992, Miocene monzonitic intrusions and associated megabreccias of the Iron Axis region, southwestern Utah, in Wilson, J.R., editor, Field guide to geologic excursions in Utah and adjacent areas of Nevada, Idaho, and Wyoming, Rocky Mountain section, Geological Society of America Guidebook: Utah Geological Survey Miscellaneous Publication 92-3, p. 399-420.

Bullock, K.C., 1973, Geology and iron deposits of Iron Springs district, Iron County, Utah: Brigham Young University Geology Studies, v. 20, part 1, p.27-63.

Butler, B.S., 1920, The ore deposits of Utah: U.S. Geological Survey Professional Paper 111, 672 p.

Butler, T., Cornell, D., Hacker, D., and Holm, D., 2001, Progress report of geologic mapping and remote sensing analysis of the Pinto quadrangle, Colorado Plateau transition zone, SW Utah, [abs], in Erskine, M.C., Faulds, J.E., Bartley, J.M., and Rowley, P.D., editors, The Geologic transition, High Plateaus to Great Basin - A symposium and field guide, the Mackin Volume: Utah Geological Association Publication 30 – Pacific Section American Association of Petroleum Geologists Publication GB78, p. 420.

Cook, E.F., 1954, Geology of the Pine Valley Mountains, Utah: Seattle, University of Washington unpublished Ph.D. dissertation, 236 p.

_____ 1957, Geology of the Pine Valley Mountains. Utah: Utah Geological and Mineralogical Survey Bulletin 58, 111 p.

_____ 1960, Geological atlas of Utah, Washington County: Utah Geological and Mineralogical Survey Bulletin 70, 119 p.

Cornell, D., Butler, T., Holm, D., Hacker, D., and Spell, T., 2001, Stratigraphy and Ar/Ar ages of volcanic rocks of the Pinto Quadrangle, Colorado Plateau transition zone, SW Utah, [abs], in Erskine, M.C., Faulds, J.E., Bartley, J.M., and Rowley, P.D., editors, The Geologic transition, High Plateaus to Great Basin - A symposium and field guide, the Mackin Volume: Utah Geological Association Publication 30 – Pacific Section American Association of Petroleum Geologists Publication GB78, p. 420.

Cory, C.E., 1988, Laccoliths - Mechanics of emplacement and growth: Geological Society of America Special Paper 220, 120 p.

Davis, G.H., 1999, Structural geology of the Colorado Plateau region of Southern Utah: Geological Society of America Special Paper 342, 157 p.

Dobbin, C.E., 1939, Geologic structure of the St. George district, Washington County, Utah: American Association of Petroleum Geologists Bulletin, v. 23, p.121-144.

Ekron, E.B., Orkild, P.P., Sargent, K.A., and Dixon, G.L., 1977, Geologic map of Tertiary rocks, Lincoln County, Nevada: U.S. Geological Survey Miscellaneous Investigations Series Map I-1041, scale 1:250,000.

Gardner, L.S., 1941, The Hurricane fault in southwestern Utah and northwestern Arizona: American Journal of Science, v. 239, p. 241-260.

Gilbert, G.K., 1877, Geology of the Henry Mountains, Utah: U.S. Geographical and Geological Survey of the Rocky Mountain Region, 170 p.

Gilluly, J., and Reeside, J.B., Jr., 1928, Sedimentary rocks of the San Rafael Swell and some adjacent areas in eastern Utah: U.S. Geological Survey Professional Paper 150-D, p. 61-110.

Goldstrand, P.M., 1994, Tectonic development of Upper Cretaceous to Eocene strata of southwestern Utah: Geological Society of America Bulletin, v. 106, p. 145-154.

Goldstrand, P.M., and Mullett, D.J., 1997, The Paleocene Grand Castle Formation - A new formation on the Markagunt Plateau of southwestern Utah, in Maldonado, F., and Nealey L.D., editors, Geologic studies in the Basin and Range-Colorado Plateau transition in southeastern Nevada, southwestern Utah, and northwestern Arizona, 1995: U.S. Geological Survey Bulletin 2153, p. 59-77.

Grant, S.K., 1991, Geologic map of the New Harmony quadrangle, Washington County, Utah: Utah Geological and Mineral Survey Open-File Report 206, 33 p., scale 1:24,000.

Hacker, D.B., 1995, Deformational structures related to the emplacement and growth of the Pine Valley laccolith, southern Iron Axis region, Washington County, Utah [abs]: Eos, Transactions, American Geophysical Union, v. 76, no. 46, p. 625.

———— 1998, Catastrophic gravity sliding and volcanism associated with the growth of laccoliths-examples from early Miocene hypabyssal intrusions of the Iron Axis magmatic province, Pine Valley Mountains, southwest Utah: Kent, Ohio, Kent State University, Ph.D. dissertation, 258 p.

Hacker, D.B., Rowley, P.D., Blank, H.R., and Snee, L.W., 1996, Early Miocene catastrophic gravity sliding and volcanism associated with intrusions of the southern Iron Axis region, southwest Utah [abs]: Geological Society of America Abstracts with Programs, v. 29, p. 511.

Hacker, D.B., Rowley, P.D., and Holm, D.K., 1999, Shallow intrusive, structural, and eruptive evolution of the gigantic Pine Valley laccolith, Pine Valley Mountains, southwest Utah [abs]: Geological Society of America Abstracts with Programs, v. 31, no.7.

Hatfield, S.C., Rowley, P.D., Sable, E.G., Maxwell, D.J., Cox, B.V., McKell, M.D., and Kiel, D.E., 2000, Geology of Cedar Breaks National Monument, Utah, *in* Sprinkel, D.A., Chidsey, T.C., Jr, and Anderson, P.B., editors, Geology of Utah's parks and monuments: Utah Geological Association Publication 28, p. 139-154.

Hauge, T., 1985, Gravity spreading origin of the Heart Mountain allochthon, northwestern Wyoming: Geological Society of America Bulletin, v. 96, p. 1440-1456.

Hauge, T., 1990, Kinematic model of a continuous Heart Mountain allochthon: Geological Society of America Bulletin, v. 102, p. 1174-1188.

Henry, C.D., Kunk, M.J., Muehlberger, W.R., and McIntosh, W.C., 1997, Igneous evolution of a complex laccolith-caldera, the Solitario, Trans-Pecos Texas: Implications for calderas and subjacent plutons: Geological Society of America Bulletin, v. 109, p. 1035-1054.

Hintze, L.F., 1980, Geologic map of Utah: Utah Geological and Mineral Survey, scale 1:500,000, Salt Lake City, Utah.

———— 1986, Stratigraphy and structure of the Beaver Dam Mountains, southwestern Utah, *in* Griffen, D.T., and Phillips, W.R., editors, Thrusting and extensional structure and mineralization in the Beaver Dam Mountains, southwestern Utah: Utah Geological Association Publication 15, p. 1-36.

Hunt, C.B., 1953, Geology and geography of the Henry Mountains region, Utah: U.S. Geological Survey Professional Paper 228, 234 p.

Jackson, M.D., and Pollard, D.D., 1988, The laccolith-stock controversy - New results from the southern Henry Mountains, Utah: Geological Society of America Bulletin, v. 100, p. 117-139.

Kurie, A.E., 1966, Recurrent structural disturbance of Colorado Plateau margin near Zion National Park, Utah: Geological Society of America Bulletin, v. 77, p. 867-872.

Leith, C.K., and Harder, E.C., 1908, The iron ores of the Iron Springs district, southern Utah: U.S. Geological Survey Bulletin 338, 102 p.

Lewis, A.E., 1958, Geology and mineralization connected withe the intrusion of a quartz monzonite porphyry, Iron Mountain, Iron Springs district, Utah: Pasadena, California Institute of Technology, Ph.D. dissertation, 75 p.

Lipman, P.W., and Mullineaux, editors, 1981, The 1980 eruptions of Mount St. Helens, Washington: U.S. Geological Survey Professional Paper 1250, 843 p.

Maybe, D.R., and Budding, K.E., 1987, High-temperture geothermal resources of Utah: Utah Geological and Mineral Survey Bulletin 123, 64 p.

Mackin, J.H., 1947, Some structural features of the intrusions in the Iron Springs district: Utah Geological Society, Guidebook to the geology of Utah. No.2, 62 p.

———— 1954, Geology and iron ore deposits of the Granite Mountain area, Iron County, Utah: U.S. Geological Survey Mineral Investigations Field Studies Map MF-14, scale 1:12,000.

———— 1960, Structural significance of Tertiary volcanic rocks in southwestern Utah: American Journal of Science, v. 258, no. 2, p. 81-131.

———— 1968, Iron ore deposits of the Iron Springs district, southwestern Utah, *in* Ridge. J.D., editor, Ore deposits of the United States, 1933-1967 (Graton-Sales volume): New York, American Institute of Mining and Metallurgical Petroleum Engineers, v. 2, p. 992-1019.

Mackin, J.H., and Ingerson, F.E., 1960, An hypothesis for the origin of ore-forming fluid: U.S. Geological Survey Professional Paper 400-B, p. B1-B2.

Mackin, J.H., and Rowley, P.D., 1976, Geologic map of The Three Peaks quadrangle, Iron County, Utah: U.S. Geological Survey Geologic Quadrangle Map GQ-1297, scale 1:24,000.

Mackin, J.H., Nelson, W.H., and Rowley, P.D., 1976, Geologic map of the Cedar City NW quadrangle, Iron County, Utah: U.S. Geological Survey Geologic Quadrangle Map GQ-1295, scale 1:24,000.

Maldonado, Florian, 1995, Decoupling of mid-Tertiary rocks, Red-Hills-western Markagunt Plateau, southwestern Utah, chapter I, *in* Scott, R.B., and Swadley, WC, editors, Geologic studies in the Basin and Range-Colorado Plateau transition in southeastern Nevada, southwestern Utah, and northwestern Arizona, 1992: U.S. Geological Survey Bulletin 2056, p. 233-254.

Maldonado, Florian, Sable, E.G., and Nealey, L.D., 1997, Cenozoic low-angle faults, western Markagunt Plateau, southwestern Utah, *in* Maldonado, F., and Nealey L.D., editors, Geologic studies in the Basin and Range-Colorado Plateau transition in southeastern Nevada, southwestern Utah, and northwestern Arizona, 1995: U.S. Geological Survey Bulletin 2153, p. 125-149.

Mattison, G.D., 1972, The chemistry, mineralogy, and petrography of the Pine Valley Mountains, southwestern Utah: College, PA, The Pennsylvania State University, Ph.D. dissertation, 141 p.

McDuffie, S., and Marsh, B.D., 1991, Pine Valley Mountain laccolith [abs.]: A thick, dacitic, phenocryst-rich body: American Geophysical Union-Minerological Society of America Spring Meeting 1991 Abstract Volume, p. 316.

McKee, E.H., Blank, H.R., and Rowley, P.D., 1997, Potassium-Argon ages of Tertiary igneous rocks in the eastern Bull Valley Mountains and Pine Valley Mountains, southwestern Utah, *in* Maldonado, F., and Nealey L.D., editors, Geologic studies in the Basin and Range-Colorado Plateau transition in southeastern Nevada, southwestern Utah, and northwestern Arizona, 1995: U.S. Geological Survey Bulletin 2153, p. 241-252.

Moores, E.M., Scott, R.B., and Lumsden, W.W., 1968, Tertiary tectonics of the White Pine-Grant Range region, east-central Nevada, and some regional implications: Geological Society of America Bulletin, v. 79, p.1703-1726.

Morris, S.K., 1980, Geology and ore deposits of Mineral Mountain, Washington County, Utah: Brigham Young University Studies in Geology, v. 27, pt. 2, p. 85-102.

Noble, D.C., and McKee, E.H., 1972, Description and K-Ar ages of volcanic units of the Caliente volcanic field, Lincoln County, Nevada, and Washington County, Utah: Isochron/West, no. 5, p. 17-24.

Pe, Win, and Cook, K.L., 1980, Gravity survey of the Escalante Desert and vicinity, Iron and Washington Counties, Utah: Earth Science Laboratory/University of Utah Research Institute Report No. DOE/ID/12079-14, 169 p.

Pierce, W., 1973, Principle features of the Heart Mountain fault and the mechanism problem, *in* DeJong, K.A., and Scholten, R., editors, Gravity and tectonics: New York, John Wiley & Sons, p.457-471.

———— 1991, Heart Mountain, Wyoming, detachment lineations - Are they in the microbreccia or in volcanic tuff?: Geological Society of America Bulletin, v. 103, p. 1133-1145.

Ratte, C.A., 1963, Rock alteration and ore genesis in the Iron Springs - Pinto mining district, Iron County, Utah: Tucson, University of Arizona, Ph.D. dissertation, 149 p.

Rowley, P.D., 1998, Cenozoic transverse zones and igneous belts in the Great Basin, western United States: their tectonic and economic implications, *in* Faulds, J.E., and Stewart, J.H., editors, Accomodation zones and transfer zones – The regional segmentation of the Basin and Range Province: Geological Society of America Special Paper 323, p. 195-228.

Rowley, P.D., and Barker, D.S., 1978, Geology of the Iron Springs mining district: Utah: Geological Association of Utah Publication 7, Guidebook to mineral deposits of southwestern Utah, p. 49-58.

Rowley, P.D., Cunningham, C.G., Steven, T.A., Mehnert, H.H., and Naeser, C.W., 1998, Cenozoic igneous and tectonic setting of the Marysvale volcanic field, and its relation to other igneous centers in Utah and Nevada, *in* Friedman, J.D., and Huffman, A.C., Jr. coordinators, Laccolith complexes of southeastern Utah – Time of emplacement and tectonic setting – Workshop proceedings: U.S. Geological Survey Bulletin 2158, p. 167-202.

Rowley, P.D., and Dixon, G.L., 2002, The Cenozoic evolution of the Great Basin are, U.S.A. – New interpretations based on regional geologic mapping, *in* Erskine, M.C., Faulds, J.E., Bartley, J.M., and Rowley, P.D., editors, The Geologic transition, High Plateaus to Great Basin - A symposium and field guide, the Mackin Volume: Utah Geological Association Publication 30 – Pacific Section American Association of Petroleum Geologists Publication GB78, p. 169-188.

Rowley, P.D., McKee, E.H., and Blank, H.R., Jr., 1989, Miocene gravity slides resulting from emplacement of the Iron Springs mining district, Iron County, Utah [abs]: Eos, Transactions, American Geophysical Union, v. 79, no. 43, p. 1309.

Rowley, P.D., Mehnert, H.H., Naeser, CW., Snee, L.W., Cunnigham, C.G., Steven, T.A., Anderson, J.J., Sable, E.G., and Anderson, R.E., 1994, Isotopic ages and stratigraphy of Cenozoic rocks of the Marysvale volcanic field and adjacent areas, west-central Utah: U.S. Geological Survey Bulletin 2071, 35 p.

Rowley, P.D., Nealy, L.D., Unruh, D.M., Snee, L.W., Mehnert, H.H., Anderson, R.E., and Gromme, C.S., 1995, Stratigraphy of Miocene ash-flow tuffs in and near the Caliente caldera complex, southeastern Nevada and southwestern Utah, *in* Scott, R.B., and Swadley, W.C., editors, Geologic studies in the Basin and Range-Colorado Plateau transition in southeastern Nevada, southwestern Utah, and northwestern Arizona, 1992: U.S. Geological Survey Bulletin 2056, p. 43-88.

Rowley, P.D., Snee, L.W., Anderson, R.E., Nealey, L.D., Unruh, D.M., and Ferris, D.E., 2001, Field trip to the Caliente caldera complex, east-striking transverse zones, and nearby mining districts in Nevada-Utah: implications for petroleum, ground-water, and mineral resources, *in* Erskine, M.C., Faulds, J.E., Bartley, J.M., and Rowley, P.D., editors, The Geologic transition, High Plateaus to Great Basin - A symposium and field guide, the Mackin Volume: Utah Geological Association Publication 30 – Pacific Section American Association of Petroleum Geologists Publication GB78, p. 401-418.

Rowley, P.D., Steven, T.A., Anderson, J.J., and Cunnigham, C.G., 1979, Cenozoic stratigraphic and structural framework of southwestern Utah: U.S. Geological Survey Professional Paper 1149, 22 p.

Rowley, P.D., Steven, T.A., and Menhert, H.H, 1981, Origin and structural implications of upper Miocene rhyolites in Kingston Canyon, Piute County, Utah: Geological Society of America Bulletin, pt. I, v. 92, p. 590-602.

Sable, E.G., and Anderson, J.J., 1985, Tertiary tectonic slide megabreccias, Markagunt Plateau, southwestern Utah [abs]: Geological Society of America Abstracts with Programs, v. 17, no. 4, p. 263.

Scott, R.B., and Swadley, W.C., 1995, Introduction, *in* Scott, R.B., and Swadley, W.C., editors, Geologic studies in the Basin and Range-Colorado Plateau transition in southeastern Nevada, southwestern Utah, and northwestern Arizona, 1992: U.S. Geological Survey Bulletin 2056, p. 1-4.

Shubat, M.A., and Siders, M.A., 1988, Geologic map of the Silver Peak quadrangle, Iron County, Utah: Utah Geological and Mineral Survey Map 108, 13 p., scale 1:24,000.

Siders, M.A., Rowley, P.D., Shubat, M.A., Christenson, G.E., and Galyardt, G.L., 1990, Geologic map of the Newcastle quadrangle, Iron County, Utah: U.S. Geological Survey Geologic Quadrangle Map GQ-1690, scale 1:24,000.

Spera, F.J., Yuen, D.A., Greer, J., and Sewell, G., 1985, Magma withdrawal from compositionally zoned magma chambers [abs]: Eos, Transactions, American Geophisical Union, v. 66, no. 18, p.397.

Spurney, J.C., 1984, Geology of the Iron Peak intrusion, Iron County, Utah: Kent, Ohio, Kent State University, M.S. thesis, 84 p.

Swadley, W.C., Page, W.R., Scott, R.B., and Pampeyan, E.H., 1994, Geologic map of the Delamar 3 SE quadrangle, Lincoln County, Nevada: U.S. Geological Survey Geologic Quadrangle Map GQ-1754, scale 1:24,000.

Threet, R.L., 1963, Geology of the Parowan Gap area, Iron County, Utah, *in* Heylum, E.B., editor, Geology of southwestern Utah: Intermountain Association of Petroleum Geologists Guidebook, 12th Annual Field Conference, p. 136-145.

Toby, E.F., 1976, Geology of the Bull Valley intrusive-extrusive complex and genesis of the associated iron deposits: Seattle, University of Washington, Ph.D. dissertation, 244 p.

Van Kooten, G.K., 1988, Structure and hydrocarbon potential beneath the Iron Springs laccolith, southwestern Utah: Geological Society of America Bulletin, v. 100, no. 11, p. 1533-1540.

Wernicke, Brian, 1981, Low-angle normal faults in the Basin and Range Province - Nappe tectonics in an extending ogogen: Nature, v. 291, p. 645-648.

Wernicke, Brian, Axen, G.J., and Snow, J.K., 1988, Basin and Range extensional tectonics at the latitude of Las Vegas, Nevada: Geological Society of America Bulletin, v. 100, p. 1738-1757.

Williams, P.L., 1967, Stratigraphy and petrography of the Quichapa Group, southwestern Utah and southeastern Nevada: Seattle, University of Washington, Ph.D. dissertation, 182 p.

HYDROLOGY AND GROUND-WATER CONDITIONS

OF THE TERTIARY MUDDY CREEK FORMATION IN THE

LOWER VIRGIN RIVER BASIN OF SOUTHEASTERN

NEVADA AND ADJACENT ARIZONA AND UTAH

Geological Society of America 2002 Rocky Mountain Section

Annual Meeting

Cedar City, Utah

May 10, 2002

FIELD TRIP LEADERS

By Michael Johnson, Virgin Valley Water District, Mesquite, NV 89027

500 Riverside Road (702) 346-5731

Gary L. Dixon, Southwest Geology, Inc., Blackfoot, ID 83221

Peter D. Rowley, Geologic Mapping, Inc., New Harmony, UT 84757

Terry C. Katzer, Cordilleran Hydrology, Inc., Reno, NV 89511

Michael Winters, Virgin Valley Water District, Mesquite, Nevada 89027

HYDROLOGY AND GROUND-WATER CONDITIONS OF THE TERTIARY MUDDY CREEK FORMATION IN THE LOWER VIRGIN RIVER BASIN OF SOUTHEASTERN NEVADA AND ADJACENT ARIZONA AND UTAH

FIELD TRIP LEADERS

By Michael Johnson, Virgin Valley Water District, Mesquite, NV 89027

Gary L. Dixon, Southwest Geology, Inc., Blackfoot, ID 83221

Peter D. Rowley, Geologic Mapping, Inc., New Harmony, UT 84757

Terry C. Katzer, Cordilleran Hydrology, Inc., Reno, NV 89511

Michael Winters, Virgin Valley Water District, Mesquite, NV 89027

ABSTRACT

The lower Virgin River Basin is a complex structural basin formed by Neogene extension in Nevada, Arizona, and Utah. There is a large volume of ground water in transient storage moving through the basin. Ongoing investigations to characterize the basin have determined that it is one of the deepest in the Basin and Range Province. The estimated depth to basement underlying the carbonate rock may be as great as 5 miles. Subsequent filling of the basin with the Muddy Creek Formation has created a deposit as thick as 6,000 feet. Many normal faults have modified the Miocene Muddy Creek Formation, enhancing the hydrologic properties of the formation. Several communities within the basin obtain municipal water supplies from the Muddy Creek Formation. Mesquite, Nevada, is the largest of these and one of the fast growing communities in the United States. The potable water supply is obtained solely from the Muddy Creek Formation. Prior to 1994, ground water production was generally less than 400 gallons per minute and exceeded Safe Drinking Water Act standards. Generally the Muddy Creek has a low transmissivity of 1,300 ft^2/day and is considered an aquitard. Where faulting has occurred, ground-water production is greatly enhanced with production averaging 1,500 gallons per minute and a transmissivity of 20,000 ft^2/day. Water quality is substantially better and in compliance with the Safe Drinking

Water Act with the exception of the new arsenic standard of 10 parts per billion. The most recent production wells constructed by the Virgin Valley Water District have been installed to a maximum depth of 3,300 feet and completed with 20-inch diameter casing. Depth to water within the basin varies from 1,200 feet below land surface to 2 feet above land surface.

INTRODUCTION

The lower Virgin River Valley (figure 1) is located largely in southern Nevada, in Clark and Lincoln Counties but also extends into Mohave County, Arizona, and Washington County, Utah. The amount of surface water and ground water that flows into the lower Virgin River Valley is substantial. The revised water resource budget for the basin includes an average of about 150,000 acre-feet/year of river water and 85,000 acre-feet/year of ground water (Dixon and Katzer, 2002). The available water resources from the lower Virgin River Valley that can reasonably be obtained for public use are estimated at approximately 130,000 acre-feet/year from the Virgin River, and 40,000 acre-feet/year from the ground-water system. Ground water is the primary source of water utilized in the basin, with current usage estimated at 12.000 acre-feet.

There is a large volume of ground water in transient storage that is moving through the basin to discharge points within and out of the basin. Based on earlier geophysical surveys the basin is one of the deepest in the Basin and Range Province. It is estimated that the depth to basement of the underlying carbonate rock is as great as 5 miles, averaging 1-3 miles in depth. The significance of the depth is that, while the volume of water is great within the basin-fill sediments, so is the distance to the carbonate aquifer underlying the sediments. Although the carbonate rocks are likely to be the most productive aquifer in the basin, they are untapped in the lower Virgin River Valley. While it is possible to drill to these depths, this is a considerable distance to drill for water.

The basin is bounded on the north and northeast by the Clover and the Beaver Dam Mountains respectively and on the east and south by the Virgin Mountains. Black Ridge extends from the east side of the junction of the Virgin River with Lake Mead in a northeasterly direction and merges into the Virgin Mountains. On the west and northwest side of the river are Mormon Mesa, Mormon Mountains, and the East Mormon Mountains. Additionally the basin receives surface and ground water from the Tule Desert, Basin 221 (Rush, 1968). This 190 square mile basin is located directly adjacent to the lower Virgin River, Basin 222 (Rush, 1968). Thus Tule Desert is considered part of the lower Virgin River flow system.

Much of the ground-water recharge to the lower Virgin Valley ground-water basin moves through the carbonate rocks to the Muddy Creek Formation, where the majority of the municipal and industrial wells derive their water. Geologic surface mapping, in concert with geophysics, has provided a better understanding of the subsurface structural configuration, which controls the movement of ground water through faults and fracture zones.

GEOLOGIC SETTING

The Mesquite basin is in the lower Virgin River Valley. It is a large structural depression that has been extensively deformed since its inception in Miocene time about 24 million years ago (mya). The basin is approximately 19 miles wide and over 62 miles long. It lies between the East Mormon Mountains to the west, Tule Springs Hills to the northwest, Beaver Dam Mountains to the northeast and east, and the basin is sharply truncated to the south by the Virgin Mountains. Bohannon and others (1993) described the Mesquite and Mormon Mesa basins as older basins with respect to the larger Virgin River depression, which extends west from the Colorado Plateau and Basin and Range transition zone to the Muddy Mountains near the towns of Logandale and Overton, Nevada.
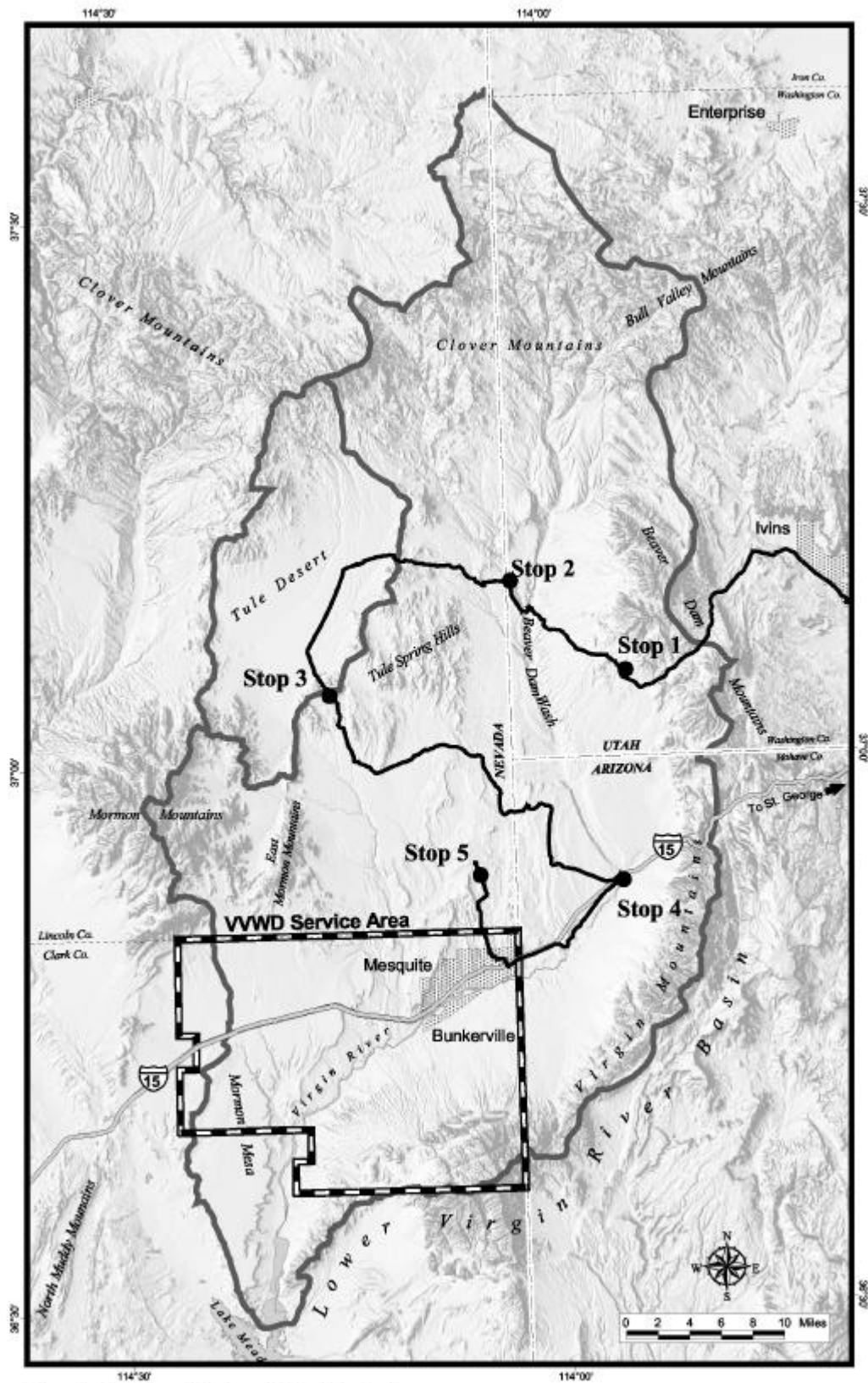
Figure 1.-- Location of the lower Virgin River Basin.

The period between 24 mya and 13 mya was marked by slow basin subsidence and accumulation of older sediments (including the Horse Springs Formation) in the Mesquite and Mormon basins. From 13 mya to 10 mya, a period of intense deformation separated the Mesquite basin from the Mormon Mesa basin to the southwest. Large displacement normal faults bounded both basins and the structural ridge that divided the two basins (Bohannon and others, 1993). Williams (1997) pointed out that, after the end of deposition of the Horse Springs Formation, the tectonic activity decreased. Bohannon and others (1993) showed that the upper part of these basin-fill deposits, the Muddy Creek Formation, is about 0.5 to 1 mile thick. Williams (1997, 1998) and Williams and others (1997) noted a similar thickness. Deposition of the Muddy Creek Formation into the Mesquite basin lasted about 6 million years, from 11.5 to 5.5 mya. The Muddy Creek Formation lies flat over most of its extent in this region, and is much less deformed than the underlying Horse Springs Formation. However, in the Mesquite basin, most of the Muddy Creek Formation and overlying calcrete deposits are moderately deformed, and dissected by modern-day washes.

At about 5.5 mya, the Colorado River, and most probably the Virgin River, were flowing into the Mesquite basin and formed Muddy Lake, an extensive body of water that extended from the base of the Clover Mountains southward into the Las Vegas basin. Subsequently, the Mesquite basin was breached and began draining into the Colorado River basin and eventually the Pacific Ocean. The subsequent lowering of base level after breaching caused a dramatic shift in deposition and erosion into and out of the Mesquite basin. Alluvial deposits record at least four cycles of incision and aggradation by the river and also record regrading of the surfaces between the river and the Virgin Mountains as their relative altitudes changed (Williams 1997). This rapid erosion of soft sediments in the basin provides modern day landforms.

Stratigraphically, rocks ranging from the Precambrian to Quaternary age sediments are observed in the Virgin River basin. A generalized synopsis is presented in Dixon and Katzer (2002).

HYDROLOGY

The lower Virgin River Valley is north trending and is about 80 miles long and about 35 miles at its widest point. It has a drainage area of about 1,723 mi^2, from the confluence of the Virgin River and Lake Mead on the Colorado River to the Virgin River gorge in the Beaver Dam Mountains (the U. S. Geological Survey (USGS) Narrows gage on the Virgin River near Littlefield, Arizona).

The climate of the lower Virgin River Valley varies from sub-alpine in the mountain blocks (precipitation exceeds 24 inches above an altitude of 8,000 feet), to a desert environment in the Mesquite area (precipitation is 6-7 inches at an altitude of about 1,500 feet). Daytime temperatures commonly exceed 100° F during summer months, with lows near freezing during the winter. Precipitation rates vary throughout the Virgin River drainage area. Higher rates of precipitation occur at higher elevations, mostly in the form of snow. On the Kolob Plateau (above 10,500 feet elevation) precipitation rates generally exceed 30 inches of water per year. St. George and Bloomington (about 3,000 feet elevation) receive about 10 inches of precipitation per year, mostly in the form of rain. Precipitation decreases to about 6 inches per year at Mesquite (about 1,600 feet elevation).

The Virgin River is the main surface-water feature in the lower Virgin River Valley there is only one other perennial stream, Beaver Dam Wash. The headwaters of the Beaver Dam Wash are in the Clover Mountains in Nevada, and the Beaver Dam and Bull Valley Mountains in Utah, all in the northeast part of the basin. The wash flows perennially into the basin and also into the Virgin River about 40 miles downstream from the headwaters at Schroeder Lake. Throughout its course, however, it is intermittent with several sections becoming dry after spring runoff.

Ephemeral drainages are evidence of surface-water runoff from the surrounding mountain blocks into the basin. Depending on storm patterns, flow often originates directly on the alluvial fans. Flash floods produce large debris loads, particularly from the Virgin Mountains south of the river.

The land-surface gradients from the mountains to the river are generally less north of the river, but large debris flows are still much in evidence.

There are several aquifers in the basin, and the main aquifer for municipal and industrial use is the unconsolidated sediments that make up the Muddy Creek Formation. The Muddy Creek Formation is a sequence of fine-grained sediments, mostly interbedded sand, silt, and clay that were deposited in a lake environment starting about 11.5 mya (Bohannon and others, 1993). The most successful wells tapping this aquifer system are drilled along fault zones identified by field observations, geologic mapping, aeromagnetic, gravity, and seismic surveys. (Johnson, 1995, Dixon and Katzer, 2002). The ground-water flow direction is generally from the northeast to the southwest toward the confluence of the Virgin River and Lake Mead. The ground-water flow system for the lower Virgin River Valley consists of source areas, generally in the surrounding mountain blocks and respective alluvial fans, and several aquifers that may or may not be in hydraulic continuity depending on location and extent. The deepest aquifer is the saturated Paleozoic carbonate rocks, which underlie the entire basin. The Muddy Creek Formation overlies the carbonate rocks and is several thousand feet thick

ACKNOWLEDGMENTS

William Lund reviewed the manuscript and provided information about the Hurricane fault zone. We are grateful for comments about the geology of the Beaver Dam Mountains from Lehi Hintze, on a field trip he led for the Dixie Geological Society. Dave Brickey manipulated the graphics for the field trip guidebook.

ROAD LOG

Increment Mileage	Cumulative Mileage	Description
0	0	BEGIN TRIP AT PARKING LOT at northwest corner of 200 South and 1150 West, Cedar City (west of Eccles Coliseum, at the western edge of the Southern Utah University campus). Head north on 1150 West. On the left, west of I-15, the Cross Hollow Hills consist of basin-fill and alluvial-fan deposits uplifted along faults and locally containing intertongued basalt lava flows of about 1 mya (Averitt, 1967; Anderson and Mehnert, 1979). According to gravity data, the major normal faults of the Hurricane fault zone are west of the Cross Hollow Hills (Cook and Hardman, 1967), but significant north-striking faults also are east of the Cross Hollow Hills. Here the Hurricane fault separates the Colorado Plateau on the east from the Great Basin on the west.
0.1	0.1	AT STOP SIGN, TURN LEFT (WEST) ONTO CENTER STREET AND CROSS I-15.
0.3	0.4	Stop sign at 1650 West. TURN RIGHT (NORTH).
0.3	0.7	Stop light at 200 North (US 56). TURN RIGHT (EAST).
0.3	1.0	Entrance ramp (Exit 59, the middle Cedar City exit) to I-15. TURN RIGHT (SOUTH) ONTO I-15.

0.5	1.5	Cross Hollow Hills on the right. At 9:00, Cedar Canyon, where Coal Creek enters Cedar Valley. Although a large stream draining the mountains, Coal Creek supplies Cedar City with none of its drinking water because it has been naturally polluted by gypsum contained the Jurassic Carmel Formation and in other Mesozoic sedimentary units in the canyon. The red ridge on the northern side of Cedar Canyon, just east of Cedar City, is the eastern flank (Triassic Moenkopi, Chinle, Moenave, and Kayenta Formations, with Jurassic Navajo Sandstone and Carmel Formation east of the ridge), of a Sevier-age anticline whose western flank has been cut off and downthrown along the Hurricane fault scarp (Averitt and Threet, 1973). The anticline can be looked upon as the leading edge above an eastward-verging blind Sevier thrust. Capping the Markagunt Plateau at the skyline is Brian Head, the highest point (about 11,300 ft, 3,446 m) on the Plateau and home of a ski resort and underlain by 26-mya ash-flow tuffs derived from the Great Basin. Cedar Breaks National Monument is just southwest of Brian Head (Hatfield and others, 2000).
1.0	2.5	Exit 57, the southern Cedar City exit. We will now travel along the north-striking Hurricane fault scarp. At this location, most of the wooded hills are landslides off the scarp.
2.4	4.9	Roadcuts of 1-mya basalt left and right, and continuing to the south. The basalts are sitting on red basin-fill deposits that fill the graben beneath us. This graben, with its basin-fill sediments, is at least 3 kilometers deep (Cook and Hardman, 1967). These sediments, and their tectonic setting, are comparable to the Muddy Creek Formation that will be one of the main focuses of this field trip. Movement on the Hurricane fault has taken place during the basin-range episode of deformation, which also created the topography we see in the Great Basin. This deformation has largely taken place in the past 10 million years, with at least 300 meters of it in the Quaternary (W.R. Lund, written communication, 2001).
1.2	6.1	The southern part of the Iron Springs Mining District, 10 kilometers to the west, at about 2:00. The Iron Springs District was formerly the largest U.S. iron district west of the Great Lakes region and the reason for the settlement of Cedar City. The district is defined by a north-northeast-trending string (the Iron Axis) of quartz monzonite porphyry laccoliths of about 22-20 mya (Mackin, 1947, 1960, 1968; Mackin and others, 1976; Mackin and Rowley, 1976; Barker, 1995). The iron deposits consist of huge hematite replacement bodies in the Homestake Limestone Member of the Jurassic Carmel Formation, which are virtually adjacent to the concordant intrusive contacts. The light-gray scar at 2:00 is the Mountain Lion pit, the largest in the district, adjacent to the Iron Mountain pluton. The southern part of the Iron Axis, especially the huge Pine Valley laccolith (Hacker, 1998), will be visited during a field trip today (Hacker and others, 2002) to see gravity slides that were shed off the flanks of the rising laccoliths and to see volcanic products that erupted following deroofing (Blank and others, 1992; Rowley and others, 2001).

|		
2.3	8.4	Exit 51, Kanarraville and Hamilton Fort. Hamilton Fort to the right, whereas Kanarraville is farther south and to the left. At about 2:00, the southern end of Quichapa Lake, in the center of the basin. It is dry most of the year. Just south of it is the well field for Cedar City's water supply, from ground water in basin-fill sediments. At 12:00 to 2:30 are the Harmony Mountains, made up of Tertiary ash-flow tuffs derived from calderas in the Great Basin (Anderson and Rowley, 1975). Most people consider the Harmony Mountains part of a Colorado Plateau transition zone, and that here the boundary between the Colorado Plateau and the Great Basin steps west. On the left, the North Hills, bounded by parts of the Hurricane fault zone east and west of it.
6.3	14.7	Exit ramp to Rest Area. To the left and right here and farther south, you will see several springs controlled by north-striking faults of the Hurricane fault zone. The road here starts to drop lower, as we head down the Colorado River drainage to St. George, which is 600 meters lower than our present elevation.
2.5	17.2	Exit 42, New Harmony. The high mountains to the right are the Pine Valley Mountains, underlain by apparently the world's largest laccolith, the 20-mya Pine Valley laccolith (Hacker, 1998). The Pine Valley Mountains are a Wilderness Area and a recharge area for the Navajo aquifer, the source of most of the water for Washington County, the fastest growing part of Utah (Heilweil and Freethey, 1992; Hurlow, 1998; Heilweil and others, 2000). This aquifer, in the Jurassic Navajo Sandstone, was the subject of a pre-meeting field trip (Heilweil and others, 2002) a few days ago. The Navajo forms massive red cliffs along the Hurricane scarp. To our left the Navajo Sandstone is carved into a series of beautiful ledges, known as the Five Fingers of the Kolob, although a much better view is afforded farther west of us. The valley to the right contains thin basin-fill deposits, a different ground-water basin from the one north of Hamilton Fort; this basin supplies much of the water for the New Harmony area (Heilweil and others, 2000).
2.0	19.2	Exit 40, Kolob section of Zion National Park. A road here climbs the Hurricane Cliffs to the left and goes several miles to the south, with hiking trails and great views of the Kolob Plateau and lower parts of Zion National Park.
2.9	22.1	On the right, Ash Creek Reservoir. At most times of the year, this is dry or nearly so because the dam on its south side is in Quaternary basalt flows and the dam leaks. Next pass through roadcuts in basalt flows and basaltic tephra.
0.6	22.7	Exit 36, Ranch Exit. Hills to the right belong to what local residents call Black Ridge, the highest part of a series of Quaternary basalt flows that were spread to the right and left of us, largely controlled by fractures from the Hurricane fault zone.
1.4	25.9	Exit 33, Ranch Exit.
1.6	27.5	Exit 31, Pintura. Pine Valley Mountains on our right.

1.1	28.6	Exit 30, Browse. On left, basalts dip east into the Hurricane fault zone.
3.2	31.8	Exit 27, Anderson Junction, with SR-17 to Toquerville and Hurricane. Basalts on left. west-dipping cuesta of Navajo Sandstone on right.
3.7	35.5	Exit 23, Leeds and Silver Reef. Silver Reef, to the right, was an important turn-of-the-century silver mining district (James and Newman, 1986; Proctor and Shirts, 1991). Navajo Sandstone on right.
3.9	39.4	As you go past Harrisburg on the left, note a water gap (Quail Creek) through a cuesta on the resistant Shinarump Conglomerate Member of the Triassic Chinle Formation, which here is part of the west flank of the Virgin anticline. To the west of the cuesta is the upper part of the Chinle Formation overlain by the Moenave, then the Kayenta Formations, whereas the overlying Navajo is west of I-15. Quail Creek Reservoir is east of the water gap.
4.0	43.4	Exit 16, Harrisburg Junction and SR-9 to Hurricane, which is east of the Virgin anticline.
4.6	48.0	Exit 10, Middleton Drive, Washington City. Red cuestas of Kayenta to the right and, farther on, Quaternary basalt flows sit on the Navajo and underlying Jurassic and Triassic units.
2.3	50.2	Exit 8, St. George Boulevard, St. George. Navajo Sandstone makes up the horizon on the right, on the northern side of St. George.
2.1	52.3	Exit 6, Bluff Street (SR-18), St. George. GO RIGHT, OFF I-15.
0.3	52.6	Stop sign on Bluff Street. TURN RIGHT (NORTH). The mesa west of Bluff Street is the home of St. George's airport, on Quaternary basalt flows. These flows rest on red, bentonitic shales of the upper member of the Kayenta and Chinle Formations. When buildings and roads are constructed in the east toe of this mesa, landslides are the result.
2.6	55.2	Stop light, intersection with Sunset Road. Get in the middle lane (that is, do not get in the far left lane) and TURN LEFT ONTO SUNSET.
2.2	57.4	Enter Santa Clara. The bluff above us on the right, with the houses on it, is the Petrified Forest Member of the Chinle Formation, infamous for its "blue clay" (bentonite) that is the bane of those homeowners who do not want their house sliding (Willis and Higgins, 1996).
1.2	58.6	Jacob Hamblin home on the right.
1.2	59.8	On the right, the road to Ivins. The high skyline on the right (Red Mountain) supported by Navajo Sandstone. Low on the flank of

this north-dipping cuesta is Kayenta, which intertongues upward with the Navajo.

2.5	62.3	On the right, the road to Kayenta development, a community of Santa Fe-style homes that are sitting, as you might expect, on the Kayenta Formation.
1.2	63.5	On the right, homes of the Shivwits Indian Reservation.
0.6	64.1	Cross the Santa Clara River, which drains the area to the north that contains the eastern Bull Valley Mountains and western Pine Valley Mountains. Shinarump Member of the Chinle Formation on the right.
0.7	64.8	Ghost town of Shivwits on left and right.
0.6	65.4	Road forks. BEAR LEFT. Shinarump Member above us to the right. The road to the right follows the Santa Clara River to Gunlock Reservoir, 8 kilometers to the north, then to Gunlock, just north of that. One of the main well fields utilized by St. George and Washington County Water Conservancy District is just south of the Gunlock Reservoir, sited in the Navajo Sandstone and just west of the Gunlock fault zone. The north-striking Gunlock fault zone, which is an oblique-slip fault (mostly normal and down on the west side, but locally left lateral) is considered by most people to mark the boundary between the Colorado Plateau transition zone to the east and the Great Basin to the west (Hintze and others, 1994). A major reason for the high water yield in the well field is fracture porosity due to the fault zone (Heilweil and others, 2000, 2002).
0.7	66.1	On the right, dirt road to Goldstrike, a former major disseminated gold deposit (Adair, 1986; Wilden and Adair, 1986), mined out and now reclaimed.
1.0	67.1	Start up into the northern Beaver Dam Mountains, an anticlinal uplift masterfully studied and analyzed by Hintze (1986), Hintze and others (1994), and Anderson and Barnhard (1993a, 1993b). On the left is the road to the mine and mill of the Apex rare-earths mine. Although the mill is just south of us, the mine is farther south and west, in replacement bodies in the Permian and Pennsylvanian Callville Limestone (Bernstein, 1986). Next start up through gray limestone of the Permian Toroweap and Kaibab Formations.
2.3	69.4	Light-yellow Permian Queantoweap Formation, as we continue down the stratigraphic section. The Queantoweap dips steeply east, part of a hogback capped to the east by the overlying Toroweap and Kaibab Formations (Hintze, 1986).
2.8	72.2	The road tops a low pass, Utah Hill, at the crest of the Beaver Dam Mountains. The road to the left goes to a relay tower. On the right and left, the rocks belong to the well-known carbonate aquifer of central and southern Nevada. This aquifer consists of the Mississippian Monte Cristo Limestone (Redwall equivalent) and other Paleozoic limestones. The streams to the west of this

drainage divide (the east side of the Beaver Dam Mountains) flow west into the lower Virgin River basin. But this current drainage follows an old (early Pleistocene or Pliocene) canyon that also drained west and cut through the Redwall and deposited a conglomerate in the old valley (L.F. Hintze, oral communication, 2001).

1.7	73.9	We are now in Precambrian basement gneiss and schist.

0.2   74.1   The sharp knob on the left with the tower on top of it is Castle Cliff, just east of a major high-angle, basin-range normal fault zone called the Piedmont fault zone. Most geologists consider this to be the boundary between the Colorado Plateau transition zone on the east and the Great Basin on the west. So the boundary has again jumped west. Castle Cliff consist of the Callville Limestone, which appears to be in the upper plate of a west-dipping, low-angle fault that has greatly attenuated the Redwall and underlying Devonian and Cambrian rocks in the footwall below (Hintze, 1986). The question is whether this fault is a Sevier thrust in which the hanging wall moved east, or a Tertiary detachment that moved west (L.F. Hintze, oral communication, 2001). On the right are the remains of a gas station that made a living supplying water and service to the cars formerly struggling eastward, and boiling over, up the long grade upward from Littlefield/Beaver Dam. Until construction of Interstate 15 through the Virgin River Gorge south of us, this road was the main highway from Las Vegas to St. George. Another gas station was at the summit of the road, Utah Hill (L.F. Hintze, oral communication, 2001).

2.3   76.4   Dirt road enters the blacktop we are on from the right. A sign at the intersection says "Big Cottonwood Game Ranch." TURN RIGHT (WEST) ONTO THE DIRT ROAD. Enter the Mesquite basin, downthrown in the past 10 million years along the Piedmont fault zone and filled with 10 kilometers of basin-fill sedimentary rocks of Miocene through Quaternary age (Blank and Kucks, 1989; Bohannon and others, 1993; Jachens and others, 1998; Langenheim and others, 2000a, b, 2001; Dixon and Katzer, 2002). The oldest of these basin-fill deposits belong to the Horse Spring Formation, well below us. Above this in the graben is the Muddy Creek Formation, overlain by Pliocene(?) and Quaternary surficial deposits. As we make the turn, the mountain mass in the far distance at 9:00 is the Virgin Mountains.

1.5   77.9   **STOP 1, BASIN OVERVIEW. PULL OFF ON THE SIDE OF THE ROAD.** Discuss the geologic framework of the lower Virgin River Hydrographic Basin, Basin 222, as defined by the Nevada State Engineer and the surface and ground-water hydrology of the area (Johnson, 1995; Dixon and Katzer, 2002). The resistant hills, mostly on our right, that we have been driving through consist of brecciated Mississippian Redwall Limestone that is resting on basin-fill sediments. Wernicke and his colleagues (Wernicke and others, 1985; Axen and others, 1990; Wernicke,
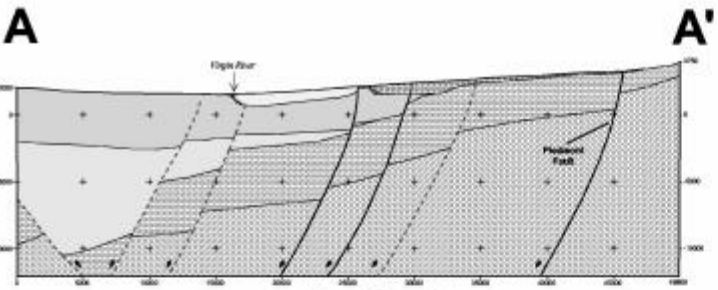
Figure 2.-- Generalized geological map of the lower Virgin River Basin
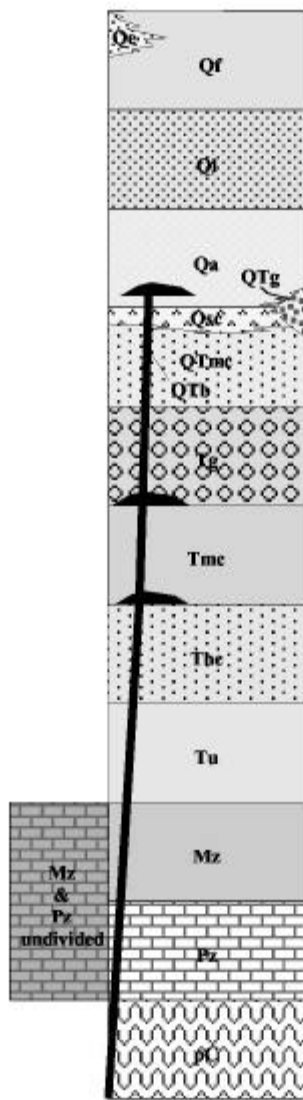
Qf Holocene Young Alluvium in washes and floodplains.

Qe Quaternary Evaporite discharge from fault zone in upper Toquop Wash.

Ql Quaternary Littlefield Formation. Sediments capped by spring-fed discharge deposits (1' - 2' thick).

Qa Quaternary Alluvium and colluvium.

QTg Quaternary to Tertiary gravel . In middle to upper Toquop Wash. Coarse-grained gravels, indurated, contains volcanic and sedimentary rocks.

Qsc Quaternary Spring fed carbonate overlying QTmc.

QTmc Mormon Mesa calcrete.

QTb Quaternary to Tertiary Basalt.

Tg Upper Tertiary Piedmont gravel. Mostly detritus of pC gneiss and schist detritus.

Tmc Middle Tertiary Muddy Creek Formation. Primarily fine to medium grained siltstone, sandstone, mudstone, and conglomerate.

Thc Middle Tertiary Red sandstone of Bohannon (1984) and Lovell Wash and Rainbow Garden members of the Horse Springs Formation of Bohannon (1984). Not exposed at surface.

Tu Lower Tertiary sediments. Probably includes some volcanic tuffs and lacustrine deposits.

Mz Mesozoic Rocks. Includes Baseline Sandstone, Aztec Sandstone, Moenave, Kayenta, Chinle, Moenkopi, Kaibab, and Toroweap Formations, undivided.

Mz & Pz Mesozoic and Paleozoic rocks, undivided. Not exposed at surface.

Pz Cambrian to Permian rocks, undivided. Principally carbonate rocks with some quartzite and sandstone. Structually complex.

pC Complex crystalline rocks of Proterozoic age. Primarily granite, gneiss, and schist.
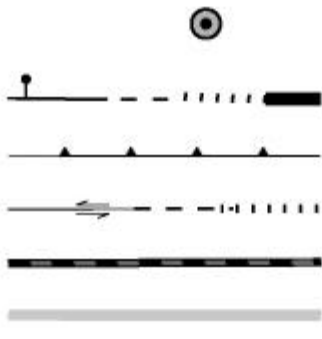
Virgin Valley Water District Well

Normal fault, bar and ball on downthrown side where known, dashed where inferred, dotted where concealed, thick solid line where intruded by basalt (QTb)

Thrust fault, teeth on upper plate, double arrows indicate sense of strike slip

Strike-slip fault, dashed where inferred, dotted where concealed

Geologic Cross-section Traverse

Structural Block Boundary

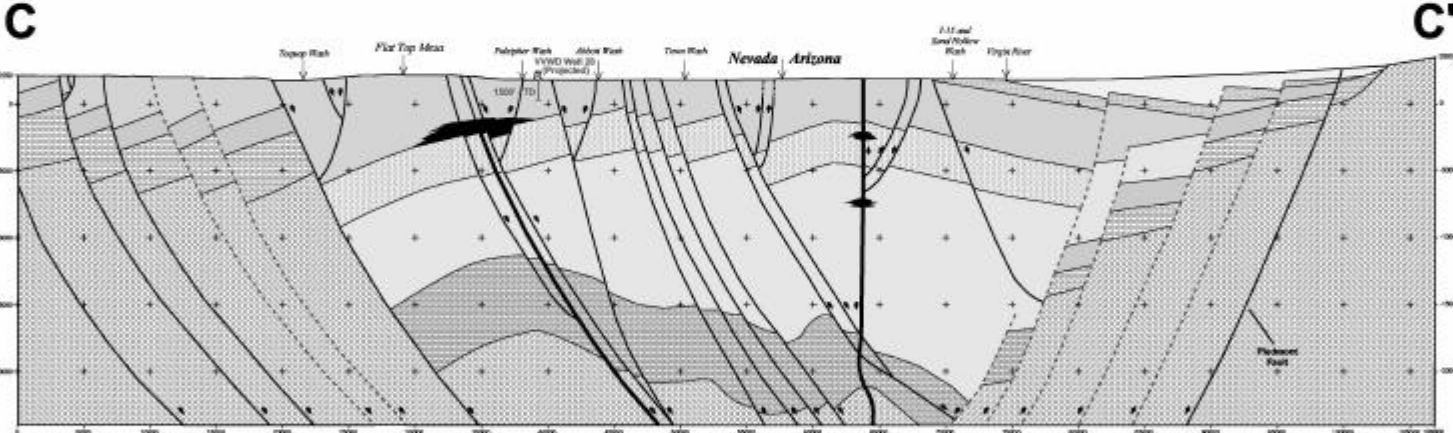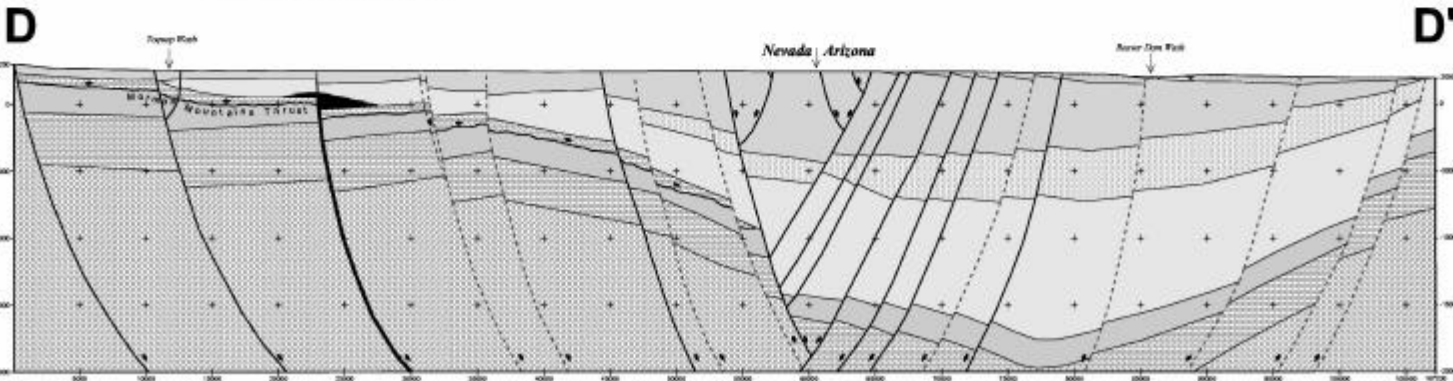Figure 3.-- Legend for the generalized geological map of the lower Virgin River Basin.
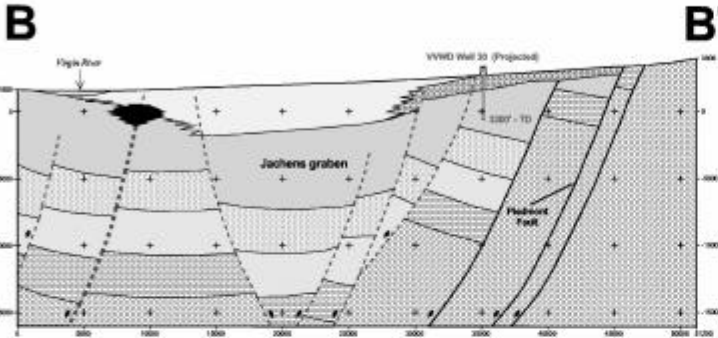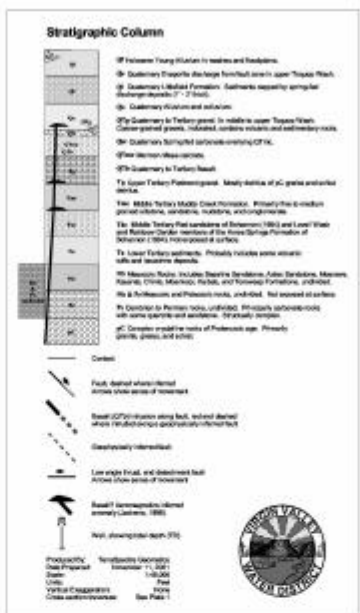
Figure 4.-- Cross-sections to accompany the generalized geological map of the lower Virgin River Basin.
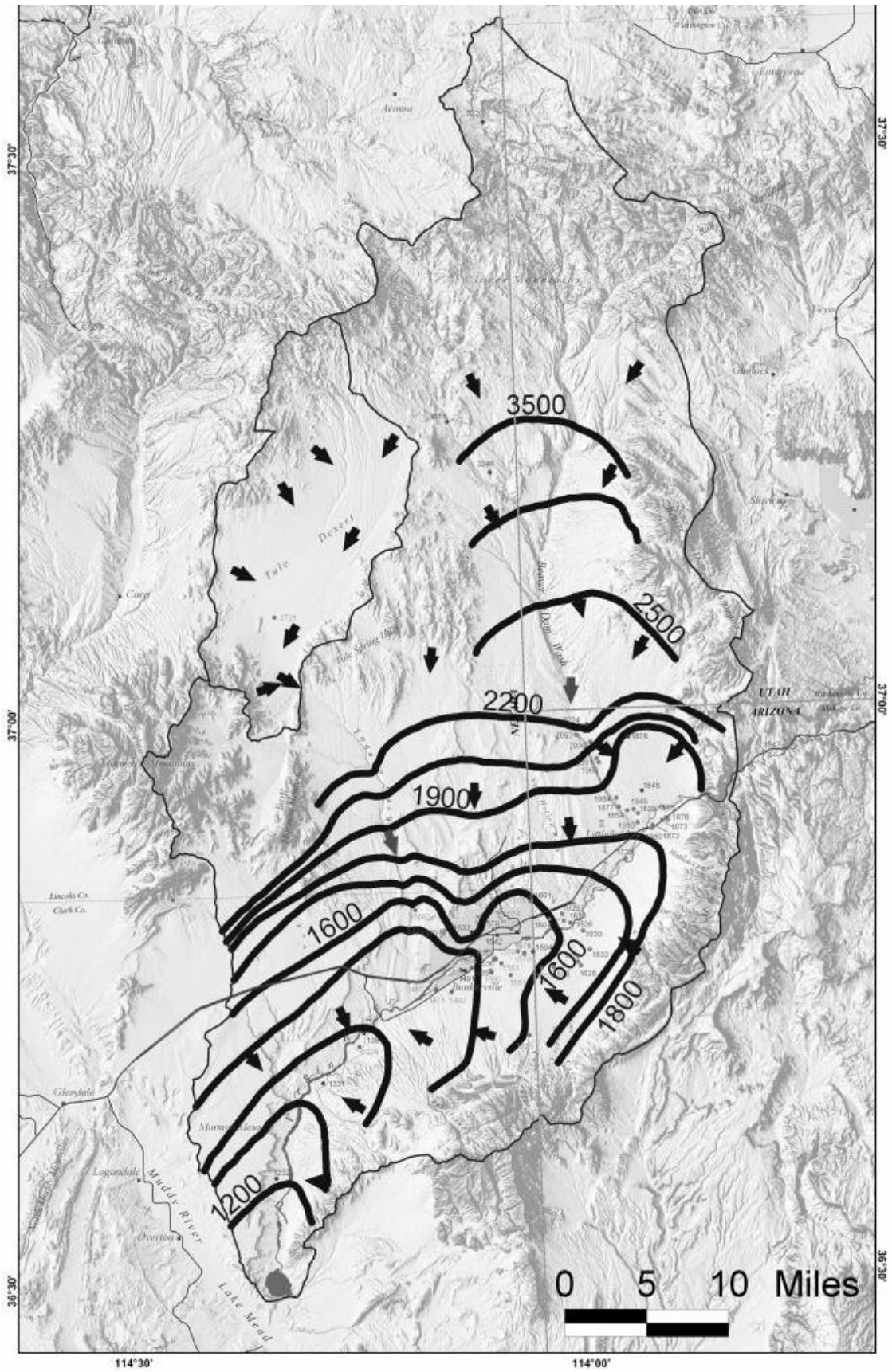
297

Figure 5. - - Potentiometric surface of the Lower Virgin River Basin.

1992; Hintze and Axen, 1995, 2001) argue that these rocks have moved out from the Beaver Dam Mountains along detachment 1992; Hintze and Axen, 1995, 2001) argue that these rocks have moved out from the Beaver Dam Mountains along detachment faults, the breakaway zone of which is the fault beneath Castle Cliff, whereas others (Carpenter and Carpenter, 1994; L.F. Hintze, oral communication, 2001; Katzer and Dixon, 2002) ascribe these Mississippian masses to landsliding off the steep mountain flank that had been raised along high-angle normal faults of the Piedmont fault zone. The Mormon and East Mormon Mountains are on our west horizon. We have passed through lots of roadcuts of Muddy Creek Formation, and there are more to come.

1.9	79.8	Hill of Mississippian breccia on the left. Terry Benches at 11:00 to 1:00. We are in a forest of Joshua trees.
3.9	83.7	Pass beneath power lines. The Kern River gas pipeline is just to the west, where it is marked. As many as a dozen gas-fired power plants (predominately air-cooled) are proposed for southern Nevada and adjacent Arizona, to be supplied by this pipeline.
0.7	84.4	Fork in the road. BEAR RIGHT ON THE MAIN ROAD.
1.5	85.9	Enter the canyon of Beaver Dam Wash. Lytle Ranch on the right, a Brigham Young University Agricultural Research Station.
0.2	86.1	Cross Beaver Dam Wash. Flow in the wash at this location is perennial with a base flow of 2 to 5 cubic feet per second (cfs). The conglomerate (fanglomerate) that makes up the canyon walls here is considered Muddy Creek Formation by some workers, but Hintze and Axen (1995) considered it more likely that it is Pleistocene and Pliocene, somewhat younger than the Muddy Creek. If we were to take a barely passable dirt road that will take off shortly to the right and travel about a kilometer up the canyon, we would see vertical, north-northwest-striking dikes of travertine limestone, as much as 3 meters wide, that parallel the wash for more than 1 kilometer and cut the conglomerate (Hintze and Axen, 1995). These are orifices of springs that probably date to the middle to Pleistocene (Dixon and Katzer, 2002).
0.8	86.9	**STOP 2; BEAVER DAM WASH OVERLOOK. PULL OVER AT THE FENCE LINE.** The road forks just south of the fence line Discussion on the hydrology of Beaver Dam Wash, which drains the Bull Valley Mountains and brings low-TDS water into the Mesquite basin (Holmes and others, 1997; Fogg and others, 1998), and the geology and significance of the conglomerate. A pediment caps this bench. Beaver Dam Wash is a major conduit for significant amounts of ground water and surface water moving into the basin from the north. The upper drainage area is in the Beaver Dam and Bull Valley Mountains in Utah and the Clover Mountains in Nevada. Numerous faults in the Central Mesquite structural basin define the present trace of the Beaver Dam Wash. The faults are not expressed at the surface, but have been

299

interpreted from gravity surveys (Baer, 1986; Blank and Kucks, 1989; Langenheim and others, 2000; and Jachens and others, written communication, 1998), seismic reflection data (Carpenter, 1989; Bohannon and others, 1993; and Carpenter and Carpenter, 1994), and resistivity soundings (Zohdy and others, 1994; Holmes and others, 1997). Gravity inferred faults are shown on cross sections as red dashed lines. Although we cannot find surface traces of these faults, in such an active wash, the fact that the wash is linear is reason to suspect that a fault zone controls the wash. In Bull Valley Wash, calcium carbonate veins 1 to 3 feet in diameter and up to several hundred feet long paralleling the wash. Hintze and Axen (1995) first recognized these veins while mapping the Scarecrow Peak quadrangle. The veins formed from ground-water discharge along existing faults that precipitated calcium carbonate as ground-water levels decreased.

RETURN TO THE VEHICLES AND TAKE THE RIGHT FORK.

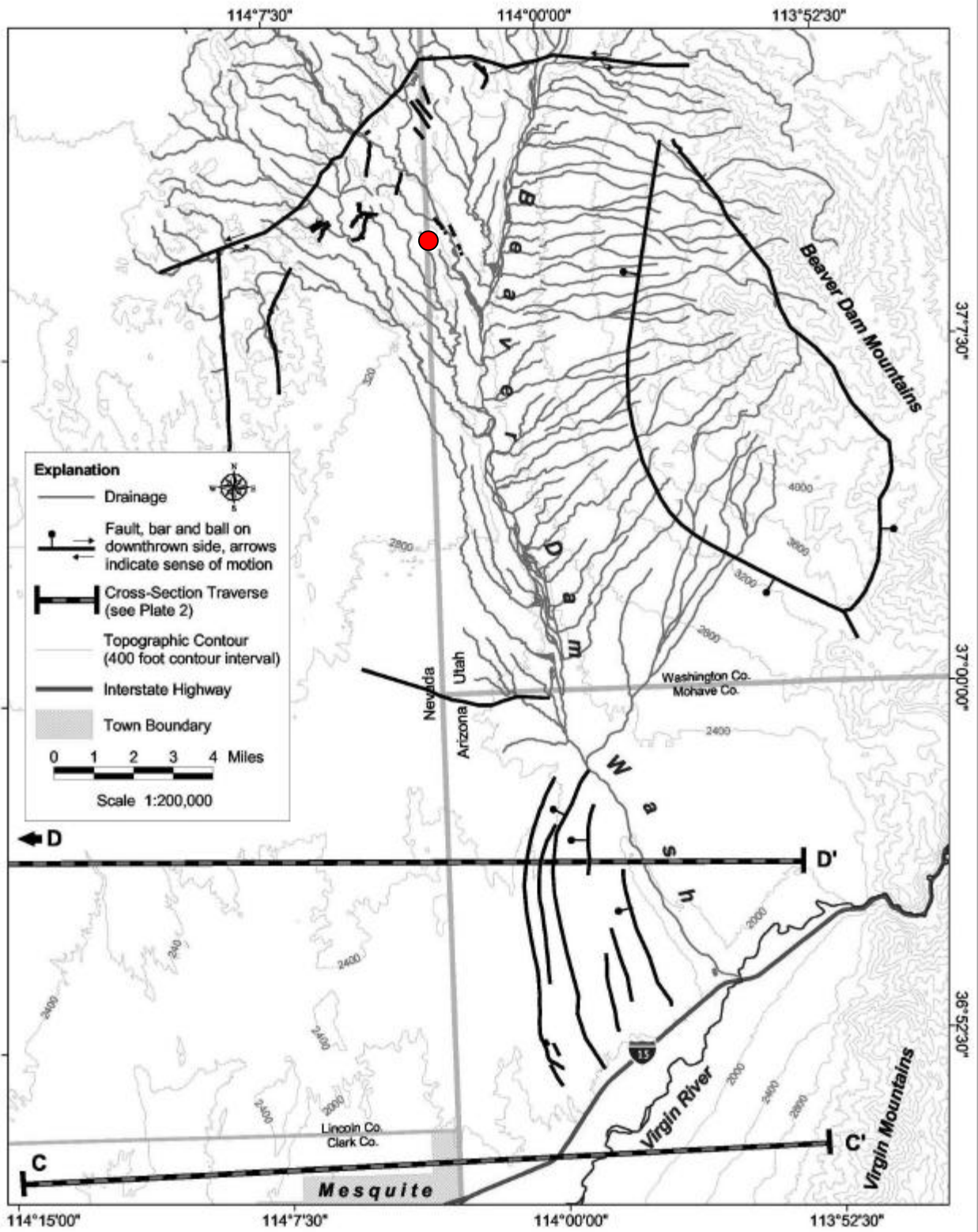|		
1.8	88.7	Road takes a sharp turn to the left.
1.2	89.9	Road forks. GO LEFT.
1.0	90.9	Road forks. GO LEFT Enter the Tule Springs Hills, mapped by Hintze and Axen (1995, 2001).
2.6	93.5	Snow Spring. Road forks. BEAR RIGHT. The red hills here are mostly the Moenkopi Formation and the Shinarump Member of the Chinle Formation (Hintze and Axen, 2001). The road here will go west for several miles along a major fault zone, which we consider to be a transverse zone. Such features, most of which strike east, are common in the Great Basin and serve as either barriers or conduits to ground-water flow (Ekren and others, 1976; Rowley, 1998; Rowley and Dixon, 2001).
1.5	95.0	Red Moenkopi on right faulted against Queantoweap Sandstone on the left. The higher ridge to the left is the Permian and Pennsylvanian Bird Spring Formation (Hintze and Axen, 2001).
1.4	96.4	Leave Tule Springs Hills and enter the Tule Desert, Hydrographic Basin 221. The hills are separated by the north-northeast-striking East Tule Desert fault zone, a normal fault down to the west (Hintze and Axen, 2001). The Tule Desert (Tule basin) is part of the Virgin Valley ground-water flow system (Dixon and Katzer, 2002). The basins to the west of the Tule Desert, are part of the carbonate aquifer of the White River ground-water flow system (Harrill and others, 1988; Dettinger, 1989; Dettinger and others, 1995; Prudic and others, 1995; Schmidt and Dixon, 1995; Brothers and others, 1996; Thomas and others, 1996; Burbey, 1997; Harrill and Prudic, 1998). Ground water travels south-southwest in both flow systems (Dixon and Katzer, 2002). Recharge for both systems is mostly central Nevada. The Clover Mountains include the high mountain to the west as well as the mountains at 12:00 to 2:00. The Clover Mountains to the north are underlain by a major Tertiary caldera complex that is faulted (Rowley and others,

300

Figure 6. --Stop 2, Structural geologic controls for Beaver Dam Wash.

1995). The Clover Mountains supply recharge to the local ground-water system.

2.1	98.5	Intersection with north-south road. Continue straight ahead.
0.4	98.9	Enter Sams Camp Wash.
0.7	99.6	Intersection with another north-south road. This one has a good deal of red flagging at the intersection, and the road to the left is as good as the one we are on. TURN LEFT (SOUTH). After we turn south, we are heading directly toward a jagged peak that is part of the East Mormon Mountains.
2.3	101.9	On the right is the well head for MW-2, a nested piezometer monitoring well installed by Vidler Water Company in 2001 to look for water in the Tule Basin. The Mormon Mountains are on the horizon at 12:00 to 2:30.
1.1	103.0	Cattle tank on the left, and another road comes in on the right. Continue straight ahead. Tule Springs Hills on the left.
2.0	105.0	Intersection with road to the left; this road goes southeast, out through the southern Tule Springs Hills. Continue straight.
0.5	105.5	On the right are the well heads for nested piezometer MW-1, monitoring wells MW-4 and MW-5, and VW-1, the first production well installed by Vidler Water Company last summer and last fall respectively (2001). The ground water is to be utilized primarily for the proposed Toquop Power plant and the Lincoln County Land Act. Toquop Power plant is a proposed 1,100 mega-watt, water-cooled power plant to be constructed along Toquop Wash about 15 kilometers south-southeast of here and powered by natural gas from the Kern River pipeline adjacent to the plant. Potentially over 7,000 acre-feet of ground water will be extracted and transferred into Basin 222. Some of the water production in the wells and MW-2 to the north are probably due to fracture porosity, perhaps caused by the East Tule Desert fault zone to the east. A west-northwest-trending seismic section runs very close to the wells (Carpenter and Carpenter, 1994; Hintze and Axen, 2001). Vidler Water has installed another monitoring well, MW-3, on the west side of the Tule Desert. Water levels from the three wells indicate that ground water flow in and near the Tule Desert (Basin 221) is to the south-southwest and drains through Toquop gap into the lower Virgin River Basin (Basin 222).
0.6	106.1	Intersect with an east-west road. GO LEFT.
0.9	107.0	Intersect with the southeast road of three stops ago, at a fence line. GO RIGHT. Enter the Tule Springs Hills.
0.8	107.8	Road enters on the left. STOP 3, SEVIER THRUST FAULT AT JUMBLED MOUNTAIN. On the high ridge (Jumbled Mountain) on the left, red rocks low on the slopes represent the Moenkopi Formation, over which is thrust gray Paleozoic carbonates that cap the ridge (Hintze and Axen, 2001).

2.9	110.7	Cabin and cattle tank on the left. Summit Spring, controlled by a fault. Just to the east, a north-striking normal fault that is down on the west side lifts up the high ridge of Mesozoic rocks to the east (Hintze and Axen, 2001). Discharge from the springs in Tule Hills and Tule Desert are small, ranging from 1 to 10 gallons per minute, and of poor water quality, (TDS greater than 1,000 mg/L).
0.3	111.0	Road enters on the right. STAY ON THE MAIN ROAD, BEARING LEFT.
3.6	114.6	Road comes in on the left. Continue straight ahead.
2.8	117.4	Cross a small wash, with caliche capping the pediment on the other side. Note small vertical calcium carbonate veins cutting this pediment cap, examples of probable orifices of spring discharge.
0.5	117.9	Road comes in on the left. Continue straight ahead.
1.6	119.5	Pass beneath a power line, where a road comes in sharply on the right. Continue straight ahead.
0.1	119.6	Cross the Kern River pipeline.
0.7	120.3	Road goes over the top of a caliche pediment and drops steeply down to the east.
0.1	120.4	Road enters on the left. Stay to the right.
1.3	121.7	Pop up on the top of a caliche mesa and bear right at the fence.
0.3	122.0	Road forks. Bear right and stay on the main road.
0.5	122.5	Road enters on the right. Bear left.
3.1	125.6	Come out of a soft (sandy) wash. On left is a corral.
0.9	126.5	Pass beneath electric transmission line. Cattle tank on right.
0.8	127.3	Well head of a USGS monitoring well on the left. Caliche outcrops in the Muddy Creek Formation.
8.0	135.3	Road enters on the left, then pass through a fence line.
1.0	136.3	Intersect with a blacktop road, Country Road 3454. GO RIGHT. Road runs parallel to I-15.
0.7	137.0	Stop sign at SR-91. GO RIGHT UNDER I-15.
0.3	137.3	Fence line crosses the road. TAKE A SHARP LEFT, HEADING TOWARD THE LITTLEFIELD, ARIZONA CEMETARY AND BACK TOWARD I-15.

0.2	137.5	**STOP 4, LITTLEFIELD RIVER GUAGE.** Go past the cemetery to an overlook above the Virgin River, below which is the green frame of the stream gauge. The gauge sits on a river terrace deposit that has indurated by caliche. One of the major orifices of Littlefield springs is on the opposite wall of the river (just right of the bridge abutment) (Trudeau, 1979; Trudeau and others, 1983). Littlefield Springs discharge 6,200 acre-feet of water per year, a significant part of the flow of the river in the winter. Littlefield gauge has been in continuous operation since 1933. Average annual flow of the Virgin River is 177,000 acre-feet per year (244 cfs) with an average TDS of 2,200 mg/L. Cliffs of Littlefield Formation on the left, an upper part of the basin-fill rocks. Spring flow is an important component of the water-resources budget because it provides a significant amount of water to the Virgin River Valley. Cole and Katzer (2000) defined a loss of river flow of about 30 cfs (22,000 afy) in the river reach from the junction of Black Rock Wash to the Narrows gage. Immediately below the Narrows gage the river flow begins to increase and continues to do so throughout the river reach downstream to the Littlefield gage and beyond. Additionally there is ground-water recharge and river flow loss to seepage that discharge to the river as spring flow. Thus, the average flow of the Virgin River at the Littlefield gage is about 177,000 acre-feet per year (Preissler and others, 1998, p. 56). According to Cole and Katzer (2000), about 142,000 acre-feet is direct surface-water runoff from the entire drainage area as measured at the Bloomington gage. There is also about 1.5 cfs (1,000 acre feet) of stream flow at the Beaver Dam gage (upstream about 1 mile from the mouth) according to Holmes and others (1997). Additionally, there are two bypasses around the Littlefield gage: (1) about 1 cfs in the Littlefield Irrigation Ditch diverted from Beaver Dam Wash (west side of the river), and (2) about 2-3 cfs from the Petrified Springs on the opposite bank (east side of the river). Both bypasses are used for irrigation downstream from the Littlefield gage. Early work by Moore (in Glancy and Van Denburgh, 1969, p.36) indicated that ground water or springs discharge into the river. In July 1968, Moore measured a 6 cfs increase in river flow between the Littlefield gage and the Mesquite diversion, about 8 miles down river. If 2 cfs for ET are added, the gain is about 8 cfs in 8 miles, or about 1 cfs/mile. If this same accretion occurs throughout the river length, then perhaps the spring flow to the river from ground water equals about 30 cubic feet per second (cfs) or ~ 22,000 acre-feet per year. Some of this may be accounted for by return flow from the Littlefield Canal which bypasses the gage on the west bank (about 1 cfs) and the flow from Petrified Springs which bypasses the gage on the east bank (about 2-3 cfs).

BOARD VANS AND RETURN TO THE BLACKTOP.

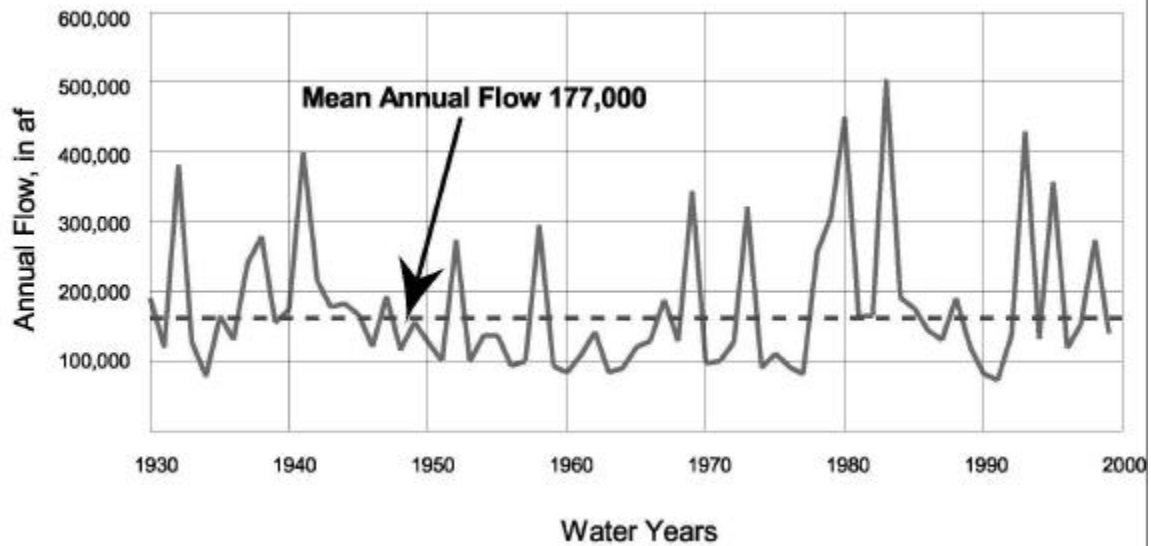|		
0.3	137.8	At SR-91, TURN LEFT (SOUTH, THEN WEST).
3.8	141.6	Cross a wash. Good outcrops of the Muddy Creek Formation on both sides of the road.
0.8	142.4	Roadcuts in Quaternary conglomerate.

Figure 7. - - Hydrograph of annual flows for the Virgin River at Littlefield, Arizona
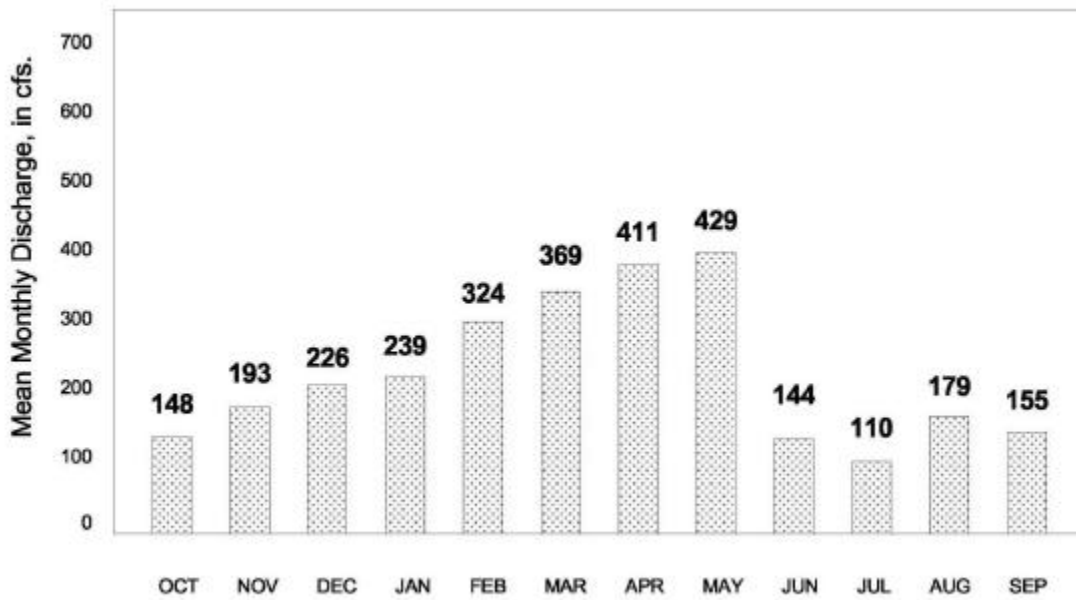

Figure 8. - - Mean monthly discharge for the Virgin River at Littlefield, Arizona

|		
2.9	145.3	Johnson Flat, faults bound the flat on both the east and west sides. Palms Golf Course on the left or south side of highway. North of I-15 but south of the bluff to the north small basalt outcrop occurs.
1.0	146.3	State line; enter Mesquite, Nevada.
0.7	147.0	Stop light at intersection with Sandhill Road. GO RIGHT, THEN UNDER I-15.
0.7	147.7	Near the buildings about 600 feet to the right, the Virgin Valley Water District (VVWD) production well, VVWD Well No. 27 adjacent to Town Wash (by palm trees and water hazard at Oasis Golf Course). The well is on the downthrown side of a normal fault cutting the Muddy Creek Formation (Johnson, 1995; Williams, 1997, Williams and others, 1997; Johnson and others, 2000; Dixon and Katzer, 2002) and produces about 1,700 gpm. Excellent exposures of the Muddy Creek are observed on the north side of the interstate.
0.3	148.0	Intersection with Turtleback Road. GO RIGHT.
0.7	148.7	At power lines, a sign reading "Landfill" points right. GO RIGHT. After making the turn, note Flat Top Mesa on the left. The Mesa consists of Muddy Creek Formation that is held up by caliche, which forms the Mormon Mesa surface to the east. But Flat Top Mesa is uplifted by faults east and west of it and stands higher than Mormon Mesa.
1.2	149.9	Clark County – Lincoln County line. Signs advertise the Bureau of Land Management land sale in Lincoln County, as authorized by the Lincoln County Land Act of 2000. The first sale (October, 2001) was to be for more than 6,000 acres, but only a small part (112 acres) of the Land Act was purchased by private interests. Continue on blacktop road.
2.4	152.3	Gravel road intersects on left. TURN LEFT. A yellow metal gate spans the road. Continue through the gate.
0.9	153.2	Fenced compound securing municipal facility operated by Virgin Valley Water District. Continue through the gate.
0.2	153.4	**STOP 5, VIRGIN VALLEY WATER DISTRICT RESERVOIRS AND PRODUCTION WELL.** PULL OVER AT THE RESERVOIR. Discussion on how production wells are sited along faults. View east of a newly drilled production well in a graben in the valley. From this vantage point, also look south on the slope of Quaternary fans and pediments that leads up to the Virgin Mountains. Facilities installed to provide municipal water supply for the service area of the Virgin Valley Water District in Clark County Nevada. Here the Muddy Creek Formation is covered by these deposits, geophysics must be used to locate faults beneath the Quaternary cover (Johnson, 1995; Jachens and others, 1998; Johnson and others, 2000; Langenheim and others, 2000a, b, 2001; Dixon and Katzer, 2002).
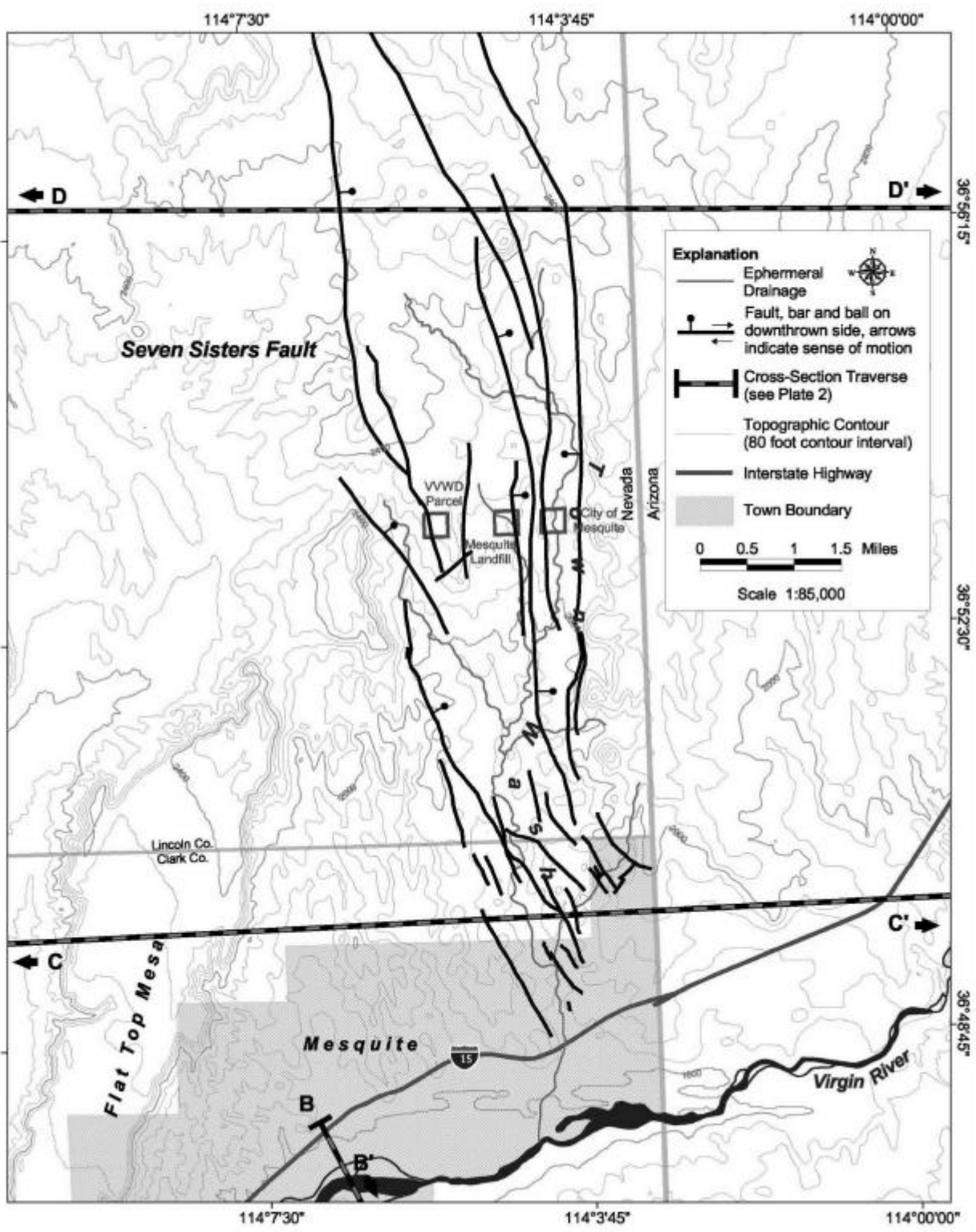
Figure 9. - - Structural geologic controls in the vicinity of Town Wash.

TURN AROUND AND RETURN TO I-15 EXIT NO. 122 IN MESQUITE, NV.

6.2	159.6	Entrance ramp to eastbound I-15. TURN LEFT AND ENTER I-15.
0.8	160.4	Nevada-Arizona state line. On left, excellent outcrops of subhorizontal Muddy Creek Formation. The mesa caps consist of caliche.
4.3	164.7	Muddy Creek outcrops continue to here on left. Virgin Mountains on the right, Beaver Dam Mountains ahead. Both are uplifted along the Piedmont fault zone along their northwest and west sides, respectively (Dixon and Katzer, 2002).
4.0	168.7	Exit 8, Littlefield and Beaver Dam. Beaver Dam Wash enters the Virgin River just north of the highway.
0.9	169.6	East side of the bridge crossing the Virgin River, with one of the major springs, with spring travertine, of the Littlefield spring complex just south of the east bridge abutment. Other springs of the complex continue east along the south side of the river. The conglomerates making up the bridge abutments have been informally called the Littlefield formation, but Billingsley and Workman (2000) map it as Muddy Creek Formation overlain by a Pleistocene calcrete.
0.4	170.0	Exit 9, Farm Road.
3.0	173.0	At entrance to The Narrows of the Virgin River, note well exposed fault on the right, one of the main faults of the Piedmont fault zone that here bounds the Beaver Dam Mountains. Movement on the Piedmont fault zone began in the Miocene and is as young as late Pleistocene, and possibly Holocene. The first rocks we see at the canyon entrance are gray and brown Mississippian Redwall Limestone, but several hundred meters south of the entrance, along the mountain front, the light-gray, well-bedded, Permian-Pennsylvanian Callville Limestone crops out (Billingsley and Workman, 2000). Bohannon and others (1991), however, correlated with rocks from the west and called these rocks the Mississippian Monte Cristo Limestone and the Permian-Pennsylvanian Bird Spring Formation, respectively. As we enter The Narrows, within a few hundred meters the rocks are dipping west more gently (15 to 25°) and the Callville rests on the Redwall above the inner gorge. From here until the Black Rock exit, the canyon generally goes by the name Virgin River Gorge. Constructing the interstate through it was one of the most expensive projects of the interstate highway system.
0.9	173.9	At about here, the Redwall is underlain by about 60 meters of light-gray and yellow-gray Devonian limestone, then in turn by Cambrian rocks down to river level. If you can see the Virgin River below you, you will notice that here near the west end of the gorge, it has water in the channel, but upstream in a few miles, it commonly does not. This water has high TDS, as does that of the Littlefield springs, because it has been naturally polluted by gypsiferous Mesozoic and upper Paleozoic rocks

(Trudeau, 1979; Trudeau and others, 1983; Dixon and Katzer, 2002).

2.8	176.7	As road bends to right, north-striking faults trend up the deep canyon to our left. They are downthrown on the east side (Bohannon and others, 1991).
0.4	177.1	The deep canyon entering on the right is Sullivan's Canyon, defined by a north-striking, oblique-slip fault (left-lateral and normal that is down on the east). This fault intersects another east-northeast striking, oblique-slip fault (left lateral and normal with the east side down) just south of the highway; this fault crosses the highway and continues parallel to us on our left (Bohannon and others, 1991). As the road bends left, Pleistocene river-terrace deposits are on our right.
0.6	177.7	On our left, Permian Toroweap Formation is dropped down along the north-northeast-striking fault, which is several hundred meters farther north of us; Redwall is north of this fault. More Pleistocene river terrace deposits on our right.
0.6	178.3	Exit 18, Cedar Pockets. More Pleistocene river terrace deposits on our right. The BLM plans to put an office at this exit. To our right is a lovely campground that is rarely used.
1.8	180.1	Start up out of the gorge at Cedar Pockets and cross the north-striking Grand Wash fault zone here. This is a major normal fault, with its west side downthrown, that to the south separates the Colorado Plateau to the east from the Basin and Range Province to the west (as, for example, where Grand Canyon ends and Lake Mead begins). To the north, this fault connects with the Gunlock fault. As we cross the fault the rocks are dipping gently east and consist of the Callville at road level and the Permian Queantoweap Sandstone just above us, and capping the hill just ahead and to our right. The Queantoweap is commonly red but generally yellow.
0.8	180.9	Pleistocene river terrace deposits to the left and right of us. At road level, the rocks still are Callville, but the Queantoweap is just above us. Just ahead of us, the road crosses an abandoned meander bend of the Virgin River; just to the right, the river is dry most of the time.
0.6	181.5	Small fault. Queantoweap on the east is downthrown against Callville on the west. Queantoweap dips gently to the east. The caprocks north and south of us, making the crest of the Beaver Dam Mountains, and likewise dipping east, are the Permian Toroweap and Kaibab Formations (Billingsley and Workman, 2000).
1.4	182.9	Here the Virgin River comes into the gorge from the north; from here, it generally parallels I-15 to the west.
4.3	187.2	Exit 22, Black Rock Road. To the north and south of us, the east-dipping Kaibab Formation goes below the surface and the Triassic Moenkopi Formation is exposed. The Virgin River is 3

kilometers north of us here, and by way of a rough jeep trail, a person may get down onto its flood plain. On and above the flood plain, sinkholes are abundant due to solution of gypsum and limestone in the Kaibab and Moenkopi Formations (Higgins, 1997; Katzer and others, 2000). Large parts of the river flow go into the sinkholes, to emerge at Littlefield springs (Katzer and others, 2000; Dixon and Katzer, in press).

1.9	189.1	Arizona-Utah State line.
0.9	190.0	Exit 1, Port of Entry.
3.6	193.6	Exit 4, Bloomington.
0.9	194.5	Cross the Virgin River.
1.0	195.5	Exit 6, Bluff Street, St. George. RETURN TO CEDAR CITY.
53.4	248.9	Eccles Coliseum.

END OF FIELD TRIP

REFERENCES

Adair, D.H., 1986, Structural setting of the Goldstrike district, Washington County, Utah, *in* Griffen, D.T., and Phillips, W.R., editors, Thrusting and extensional structures and mineralization in the Beaver Dam Mountains, southwestern Utah: Utah Geological Association Publication 15, p. 129-135.

Anderson, J.J., and Rowley, P.D., 1975, Cenozoic stratigraphy of the southwestern High Plateaus of Utah, *in* Anderson, J.J., Rowley, P.D., Fleck, R.J., and Nairn, A.E.M., editors, Cenozoic geology of southwestern High Plateaus of Utah: Geological Society of America Special Paper 160, p. 1-52.

Anderson, R.E., and Barnhard, T.P., 1993a, Aspects of three-dimensional strain at the margin of the extensional orogen, Virgin River depression area, Nevada, Utah, and Arizona: Geological Society of America Bulletin, v. 105, p. 1019-1052.

_____, 1993b, Heterogeneous Neogene strain and its bearing on horizontal extension and horizontal and vertical contraction at the margin of the extensional orogen, Mormon Mountains area, Nevada and Utah: U.S. Geological Survey Bulletin 2011, 43 p.

Anderson, R.E., and Mehnert, H.H., 1979, Reinterpretation of the history of the Hurricane fault in Utah, *in* Newman, G.W., and Goode, H.D., editors, Basin and Range Symposium: Rocky Mountain Association of Geologists and Utah Geological Association, p. 145-165.

Averitt, Paul, 1967, Geologic map of the Kanarraville quadrangle, Iron County, Utah: U.S. Geological Survey Geologic Quadrangle Map GQ-694, scale 1;24,000.

Averitt, Paul, and Threet, R.L., 1973, Geologic map of the Cedar City quadrangle, Iron County, Utah: U.S. Geological Survey Geologic Quadrangle Map GQ-1120, scale 1:24,000.

Axen, G.J., Wernicke, B.P., Skelly, M.F., and Taylor, W.J., 1990, Mesozoic and Cenozoic tectonics in the Sevier thrust belt of the Virgin River Valley area, southern Nevada, *in* Wernicke, Brian, editor, Basin and Range extensional tectonics near the latitude of Las Vegas, Nevada: Geological Society of America Memoir 176, p. 123-153.

Baer, J.L., 1986, Reconnaissance gravity and magnetic survey of the Northern Mesquite Basin, Nevada-Utah, in Griffen, D.T., and Phillips, W.R., editors, Thrusting and Extensional Structures and Mineralization in the Beaver Dam Mountains, Southwestern Utah: Utah Geological Association Publication 15, p. 109-118.

Barker, D.S., 1995, Crystallization and alteration of quartz monzonite, Iron Springs mining district, Utah—Relation to associated iron deposits: Economic Geology, v. 90, p. 2197-2217.

Bernstein, L.R., 1986, Geology and mineralogy of the Apex germanium-gallium mine, Washington County, Utah, *in* Griffen, D.T., and Phillips, W.R., editors, Thrusting and extensional structures and mineralization in the Beaver Dam Mountains, southwestern Utah: Utah Geological Association Publication 15, p. 119-128.

Billingsley, G.H., and Workman, J.B., 2000, Geologic map of the Littlefield 30' x 60' quadrangle, Mohave County, northwestern Arizona: U.S. Geological Survey Geologic Investigations Series Map I-2628, scale 1:100,000.

Blank, H.R., and Kucks, R.P., 1989, Preliminary aeromagnetic, gravity, and generalized geologic maps of the USGS Basin and Range-Colorado Plateau transition zone study area in southwestern Utah, southeastern Nevada, and northwestern Arizona (the "BARCO" project): U.S. Geological Survey Open-File Report 89-432, 16 p.

Blank, H.R., Rowley, P.D, and Hacker, D.B., 1992, Miocene monzonite intrusions and associated megabreccias of the Iron Axis region, southwestern Utah, *in* Wilson, J.R., editor, Field guide to geologic excursions in Utah and adjacent areas of Nevada, Idaho, and Wyoming: Geological Society of America, Rocky Mountain section meeting: Utah Geological Survey Miscellaneous Publication 92-3, p. 399-420.

Bohannon, R.G., Grow, J.A., Miller, J.J., and Blank, R.H., Jr., 1993, Seismic stratigraphy and tectonic development of Virgin River depression and associated basins, southeastern Nevada and northwestern Arizona: Geological Society of America Bulletin, v. 105, p. 501-520.

Bohannon, R.G., Lucchitta, Ivo, and Anderson, R.E., 1991, Geologic map of the Mountain Sheep Spring quadrangle, Mohave County, Arizona: U.S. Geological Survey Miscellaneous Investigations Series Map I-2165, scale 1:24,000.

Brothers, K., Katzer, T., and Johnson, M., 1996, Hydrology and steady state ground-water model of Dry Lake and Delamar Valleys, Lincoln County, Nevada: Las Vegas Valley Water District, Cooperative Water Project, Series Report No. 16, 48 p.

Burbey, T.J., 1997, Hydrogeology and potential for ground-water development, carbonate-rock aquifers, southern Nevada and southeastern California: U.S. Geological Survey Water-Resources Investigations Report 95-4168, 65 p.

Carpenter, J.A., and Carpenter, D.G., 1994, Analysis of basin-range and fold-thrust structure, and reinterpretation of the Mormon Peak detachment and similar features as gravity slide systems, southern Nevada, southwest Utah, and northwest Arizona, *in* Dobbs. S.W., and Taylor, W.J., editors, Structural and stratigraphic investigations and petroleum potential of Nevada, with special emphasis south of the Railroad Valley producing trend: Nevada Petroleum Society Conference Volume II, p. 15-52.

Cole, E., and Katzer, T., 2000, Analysis of gains and losses in Virgin River flow between Bloomington, Utah and Littlefield, Arizona: Southern Nevada Water Authority, Las Vegas, Nevada, 57 p.

Cook, K.L., and Hardman, Elwood, 1967, Regional gravity survey of the Hurricane fault area and Iron Springs district, Utah: Geological Society of America Bulletin, v. 78, p. 1063-1076.

Dettinger, M.D., 1989, Distribution of carbonate-rock aquifers in southern Nevada and the potential for their development—Summary of findings, 1985-88: Program for the study and testing of carbonate-rock aquifers in eastern and southern Nevada, Summary Report No. 1, 37 p.

Dettinger, M.D., Harrill, J.R., Schmidt, D.L., and Hess, J.W., 1995, Distribution of carbonate-rock aquifers and the potential for their development, southern Nevada and adjacent parts of California, Arizona, and Utah: U.S. Geological Survey Water-Resources Investigations Report 91-4146, 100 p.

Dixon, G.L., and Katzer, T.L., 2002, Geology and hydrology of the lower Virgin River valley in Nevada, Arizona, and Utah: Mesquite, Nevada, Virgin Valley Water District. Virgin Valley Water District Report, Report VVWD-01, 127 p.

Ekren, E.B., Bucknam, R.C., Carr, W.J., Dixon, G.L., and Quinlivan, W.D., 1976, East-trending structural lineaments in central Nevada: U.S. Geological Survey Professional Paper 986, 16 p.

Fogg, J.L., Muller, D.P., Summers, P.L., Simms, J.R., Ellingham, S.J., Renthal, J.S., and Dittberner, P.L., 1998, Beaver Dam Wash instream flow assessment: Bureau of Land Management, 109 p.

Hacker, D.B., 1998, Catastrophic gravity sliding and volcanism associated with the growth of laccoliths—examples from early Miocene hypabyssal intrusions of the Iron Axis magmatic province, Pine Valley Mountains, southwest Utah: Kent, Ohio, Kent State University, unpublished Ph.D. dissertation, 258 p.

Hacker, D.B., and Holm, D.K., 2002, Associated Miocene laccoliths, gravity slides, and volcanic rocks, Pine Valley Mountains and Iron Axis, southwestern Utah, in Lund, W.R., editor, Field excursions in southwestern Utah and adjacent areas of Arizona and Nevada: U.S. Geological Survey Open-Filer Report 02- , in press.

Harrill, J.R., and Prudic, D.E., 1998, Aquifer systems in the Great Basin region of Nevada, Utah, and adjacent states—Summary report: U.S. Geological Survey Professional Paper 1409-A, 66 p.

Harrill, J.R., Gates, J.S., and Thomas, J.M., 1988, Major ground-water flow systems in the Great Basin region of Nevada, Utah, and adjacent states: U.S. Geological Survey Hydrologic Investigations Atlas HA-694-C, scale 1:1,000,000.

Hatfield, S.C., Rowley, P.D., Sable, E.G., Maxwell, D.J., Cox, B.V., McKell, M.D., and Kiel, D.E., 2000, Geology of Cedar Breaks National Monument, Utah, in Sprinkel, D.A., Chidsey, T.C., Jr., and Anderson, P.B., editors, Geology of Utah's Parks and Monuments: Utah Geological Association Publication 28, p. 139-154.

Heilweil, V.M., and Freethey, G.W., 1992, Simulation of ground-water flow and water-level declines that could be caused by proposed withdrawals, Navajo Sandstone, southwestern Utah and northwestern Arizona: U.S. Geological Survey Water-Resources Investigations Report 90-4105, 51 p.

Heilweil, V.M., Freethey, G.W., Stolp, B.J., Wilkowske, C.D., and Wilberg, D.E., 2000, Geohydrology and numerical simulation of ground-water flow in the central Virgin River basin of Iron and Washington Counties, Utah: Utah Department of Natural Resources Technical Report No. 116, 139 p.

Heilweil, V.M., Goddard, K.E., Solomon, D.K., Watt, D.E., Thompson, R.W., and Hurlow, H.A., 2002, The Navajo aquifer system of southwestern Utah, in Lund, W.R., editor, Field excursions in southwestern Utah and adjacent areas of Arizona and Nevada: U.S. Geological Survey Open-Filer Report 02- , in press.

Higgins, J.M., 1997, Interim geologic map of the White Hills quadrangle, Washington County, Utah: Utah Geological Survey Open-File Report 352, scale 1:24,000.

Hintze, L.F., 1986, Stratigraphy and structure of the Beaver Dam Mountains, southwestern Utah, in Griffen, D.T., and Phillips, W.R., editors, Thrusting and extensional structures and mineralization in the Beaver Dam Mountains, southwestern Utah: Utah Geological Association Publication 15, p. 1-36.

Hintze, L.F., and Axen, G.J., 1995, Geologic map of the Scarecrow Peak quadrangle, Washington County, Utah, and Lincoln County, Nevada: U.S. Geological Survey Geologic Quadrangle Map GQ-1759, scale 1:24,000.

_____, 2001, Geologic map of the Lime Mountain quadrangle, Lincoln County, Nevada: Nevada Bureau of Mines and Geology Map 129, scale 1:24,000.

Hintze, L.F., Anderson, R.E., and Embree, G.F., 1994, Geologic map of the Motoqua and Gunlock quadrangles, Washington County, Utah: U.S. Geological Survey Miscellaneous Investigations Series Map I-2427, scale 1:24,000.

Holmes, W.F., Pyper, G.E., Gates, J.S., Schaefer, D.H., and Waddell, K.M., 1997, Hydrology and water quality of the Beaver Dam Wash area, Washington County, Utah, Lincoln County, Nevada, and Mohave County, Arizona: U.S. Geological Survey Water-Resources Investigations Report 97-4193, 71 p.

Hurlow, H.A., 1998, The geology of the central Virgin River basin, southwestern Utah, and its relation to ground-water conditions: Utah Geological Survey Water-Resources Bulletin 26, 53 p.

Jachens, R.C., Dixon, G.L., Langenheim, V.E., and Morin, R.L., 1998, Interpretation of an aeromagnetic survey over part of Virgin Valley, Tule Desert, and the valley surrounding

Meadow Valley Wash, southeastern Nevada: U.S. Geological Survey Open-File Report 98-804, 16 p.

James, L.P., and Newman, E.W., 1986, Surface character of mineralization at Silver Reef, Utah, and a possible model for ore genesis, *in* Griffen, D.T., and Phillips, W.R., editors, Thrusting and extensional structures and mineralization in the Beaver Dam Mountains, southwestern Utah: Utah Geological Association Publication 15, p. 149-158.

Johnson, M. E., 1995, Hydrogeology and ground-water production from Tertiary Muddy Creek Formation in the lower Virgin River basin of southeastern Nevada, northwestern Arizona, *in* Water in the 21st century—Conservation, demand, and supply: American Water Resources Association, p. 81-90.

Johnson, M.E., Dixon, G.L., and Katzer, Terry, 2000, Hydrogeology and ground-water conditions of the Tertiary Muddy Creek Formation in the lower Virgin River basin of southeastern Nevada, Arizona, and Utah [abs.]: Geological Society of America Abstracts with Programs, v. 32, no. 7, p. A-253.

Katzer, Terry, Cole, Erin, and Dixon, Gary, 2000, Geologic control solves hydrogeologic questions of gains and losses in the Virgin River in southwestern Utah [abs.]: Geological Society of America Abstracts with Programs, v. 32, no. 7, p. A-253.

Langenheim, V.E., Bohannon, R.G., Glen, J.M., Jachens, R.C., Grow, J.A., Miller, J.J., Dixon, G.L., and Katzer, T.C., 2001, Basin configuration of the Virgin River depression, Nevada, Utah, and Arizona—A geophysical view of deformation along the Colorado Plateau-Basin and Range transition, *in* Erskine, M.C., Faulds, J.E., Bartley, J.M., and Rowley, P.D., editors, The geologic transition, High Plateaus to Great Basin—A symposium and field guide (The Mackin Volume): Utah Geological Association and Pacific Section of the American Association of Petroleum Geologists: Utah Geological Association Publication no. 30, p. 205-225.

Langenheim, V.E., Dixon, G.L., and Glen, J.M., and Jachens, R.C., 2000a, Geologic and geophysical constraints on the hydrology of the lower Virgin River valley, Nevada-Arizona-Utah [abs.]: Geological Society of America Abstracts with Programs, v. 32, no. 7, p. A-253.

Langenheim, V.E., Glen, J.M., Jachens, R.C., Dixon, G.L., Katzer, T.C., and Morin, R.L., 2000b, Geophysical constraints on the Virgin River depression, Nevada, Utah, and Arizona: U.S. Geological Survey Open-File Report 00-407, 25 p.

Mackin, J.H., 1947, Some structural features of the intrusions in the Iron Springs district: Utah Geological Society Guidebook 2, 62 p.

_____, 1960, Structural significance of Tertiary volcanic rocks in southwestern Utah: American Journal of Science, v. 258, no. 2, p. 81-131.

_____, 1968, Iron ore deposits of the Iron Springs district, southwestern Utah, *in* Ridge, J.D., editor, Ore deposits of the United States, 1933-1967 (Graton-Sales volume): New York, American Institute of Mining and Metallurgical Petroleum Engineers, v. 2, p. 992-1019.

Mackin, J.H., and Rowley, P.D., 1976, Geologic map of The Three Peaks quadrangle, Iron County, Utah: U.S. Geological Survey Geologic Quadrangle Map GQ-1297, scale 1:24,000.

Mackin, J.H., Nelson, W.H., and Rowley, P.D., 1976, Geologic map of the Cedar City NW quadrangle, Iron County, Utah: U.S. Geological Survey Geologic Quadrangle Map GQ-1295, scale 1:24,000.

Proctor, P.D., and Shirts, M.A., 1991, Silver, sinners, and saints, a history of old Silver Reef, Utah: Paulmar, Inc., 224 p.

Prudic, D.E., Harrill, J.R., and Burbey, T.J., 1995, Conceptual evaluation of regional ground-water flow in the carbonate-rock province of the Great Basin, Nevada, Utah, and adjacent states: U.S. Geological Survey Professional Paper 1409-D, 102 p.

Rowley, P.D., 1998, Cenozoic transverse zones and igneous belts in the Great Basin, western United States--Their tectonic and economic implications, *in* Faulds, J.E., and Stewart, J.H., editors, Accommodation zones and transfer zones--The regional segmentation of the Basin and Range Province: Geological Society of America Special Paper 323, p. 195-228.

Rowley, P.D., and Dixon, G.L., 2001, The Cenozoic evolution of the Great Basin area, U.S.A.—New interpretations based on regional geologic mapping, *in* Erskine, M.C., Faulds, J.E., Bartley, J.M., and Rowley, P.D., editors, The geologic transition, High Plateaus to Great

Basin—A symposium and field guide (The Mackin Volume): Utah Geological Association and Pacific Section of the American Association of Petroleum Geologists: Utah Geological Association Publication no. 30, p. 169-188.

Rowley, P.D., Cunningham, C.G., Steven, T.A., Mehnert, H.H., and Naeser, C.W., 1998, Cenozoic igneous and tectonic setting of the Marysvale volcanic field, and its relation to other igneous centers in Utah and Nevada, *in* Friedman, J.D., and Huffman, A.C., Jr., coordinators, Laccolith complexes of southeastern Utah—Time of emplacement and tectonic setting—Workshop proceedings: U.S. Geological Survey Bulletin 2158, p. 167-202.

Rowley, P.D., Nealey, L.D., Unruh, D.M., Snee, L.W., Mehnert, H.H., Anderson, R.E., and Gromme, C.S., 1995, Stratigraphy of Miocene ash-flow tuffs in and near the Caliente caldera complex, southeastern Nevada and southwestern Utah, *in* Scott, R.B., and Swadley, W C, editors, Geologic studies in the Basin and Range—Colorado Plateau transition in southeastern Nevada, southwestern Utah, and northwestern Arizona, 1992: U.S. Geological Survey Bulletin 2056, p. 43-88.

Rowley, P.D., Snee, L.W., Anderson, R.E., Nealey, L.D., Unruh, D.M., and Ferris, D.E., 2001, Field trip to the Caliente caldera complex, east-striking transverse zones, and nearby mining districts in Nevada-Utah--Implications for petroleum, ground-water, and mineral resources: *in* Erskine, M.C., Faulds, J.E., Bartley, J.M., and Rowley, P.D., editors, The geologic transition, High Plateaus to Great Basin—A symposium and field guide (The Mackin Volume): Utah Geological Association and Pacific Section of the American Association of Petroleum Geologists: Utah Geological Association Publication no. 30, p. 401-418.

Rush, E.F. 1968, Index of hydrographic areas: Nevada Department of Conservation and Natural Resources, Division of Water Resources, Water Resource Information Series, Report 6, 38 p.

Schmidt, D.L., and Dixon, G.L., 1995, Geology and aquifer system of the Coyote Spring Valley area, southeastern Nevada: U.S. Geological Survey Open-File Report 95-579, 47 p.

Thomas, J.M., Welch, A.H., and Dettinger, M.D., 1996, Geochemistry and isotope hydrology of representative aquifers in the Great Basin region of Nevada, Utah, and adjacent states: U.S. Geological Survey Professional Paper 1409-C, 100 p.

Trudeau, D.A., 1979, Hydrogeologic investigations of the Littlefield Springs: Reno, Nevada, unpublished M.S. thesis, University of Nevada, 136 p.

Trudeau, D.A., Hess, J.W., and Jacobson, R.L., 1983, Hydrogeology of the Littlefield Springs, Arizona: Ground Water, v. 21, no. 3, p. 325-333.

Wernicke, Brian, 1992, Cenozoic extensional tectonics of the U.S. Cordillera, *in* Burchfiel, B.C., Lipman, P.W., and Zoback, M.L., editors, The Cordilleran orogen—Conterminous U.S., The geology of North America: Geological Society of America, Vol. G-3, p. 553-581.

Wernicke, B.P., Walker, J.D., and Beaufait, M.S., 1985, Structural discordance between Neogene detachments and frontal Sevier thrusts, central Mormon Mountains, southern Nevada: Tectonics, v. 4, p. 213-246.

Willden, Ronald, and Adair, D.H., 1986, Gold deposits at Goldstrike, Utah, *in* Griffen, D.T., and Phillips, W.R., editors, Thrusting and extensional structures and mineralization in the Beaver Dam Mountains, southwestern Utah: Utah Geological Association Publication 15, p. 137-147.

Williams, V.S., 1996, Preliminary geologic map of the Mesquite quadrangle, Clark and Lincoln Counties, Nevada, and Mohave County, Arizona: U.S. Geological Survey Open-File Report 96-676, scale 1:24,000.

_____, 1997, Preliminary geologic map of the Flat Top Mesa quadrangle, Clark and Lincoln Counties, Nevada: unpublished manuscript, 15 p., scale 1:24,000.

Williams, V.S., Bohannon, R.G., and Hoover, D.L., 1997, Geologic map of the Riverside quadrangle, Clark County, Nevada: U.S. Geological Survey Geological Quadrangle Map GQ-1770, scale 1:24,000.

Willis, G.C., and Higgins, J.M., 1996, Interim geologic map of the Santa Clara quadrangle, Washington County, Utah: Utah Geological Survey Open-File Report 339, scale 1:24,000.

Zohdy, A. A. R., Bisdorf, R.J., and Gates, J.S. 1994, A direct-current resistivity survey of the Beaver Dam Wash in southwest Utah, southeast Nevada, and northwest Arizona: U.S. Geological Survey Open File Report 94-676, 87 p.

GEOLOGICAL ENGINEERING FIELD CAMP EXERCISES

Geological Society of America 2002 Rocky Mountain Section Annual Meeting,
Cedar City, Utah
May 10, 2002

Home threatened by a small landslide that has formed on the headwall scarp of the much larger Green Hollow landslide near Cedar City, Utah.

Field Exercise Leaders

Santi, P.M., Department of Geology and Geological Engineering, Colorado School of Mines, Golden, CO 80401
Laudon, R.C. Department of Geology and Geophysics, University of Missouri-Rolla, Rolla, MO 65409

GEOLOGICAL ENGINEERING FIELD CAMP EXERCISES

Geological Society of America 2002 Rocky Mountain Section Annual Meeting, Cedar City, Utah
May 10, 2002

Santi, P.M., Department of Geology and Geological Engineering, Colorado School of Mines, Golden, CO 80401
Laudon, R.C. Department of Geology and Geophysics, University of Missouri-Rolla, Rolla, MO 65409

ABSTRACT

Over the past 29 years, the University of Missouri-Rolla (UMR) has conducted a geological engineering field camp near Cedar City, Utah, taken by undergraduate majors in geology and geological engineering. Part of the field camp is conducted as a traditional geology field camp, focusing on stratigraphy and rock identification, structural interpretation, and field mapping. Forty percent of the field camp focuses on field trips and exercises to give geological engineers practice in applying geological concepts to solve typical engineering problems. The exercises they complete require them to use geologic maps and field observations to identify geologic hazards, to estimate strength and other engineering properties of soil and rock, and to design structure layouts and hazard mitigation programs.

Field exercises in geological engineering provide students with a chance to use their geologic knowledge to identify and address a variety of engineering problems. By scheduling a variety of both short and long projects, students are exposed to a wide breadth of problems. They focus on individual hazards in projects of limited scope before they are expected to address these hazards on a large project, and the variety helps maintain their interest and enthusiasm levels. The students rely heavily on published geologic maps, just as they will in their careers, and they learn to discern the accuracy, precision, and reliability of maps prepared by others.

PURPOSE AND INTRODUCTION

Over the past 29 years, the University of Missouri-Rolla (UMR) has conducted a geology field camp in the vicinity of Cedar City, Utah. The field camp has always included a geological engineering component, taken by undergraduate majors in geological engineering. The purpose of the geological engineering component is to give geological engineers practice in applying the geologic concepts and mapping techniques they have been learning towards solving typical engineering problems. The exercises they complete require them to use geologic maps and field observations to identify geologic hazards, to estimate strength and other engineering properties of soil and rock, and to design structure layouts and hazard mitigation programs.

The Geological Engineering Field Camp Exercises short course for which this road log has been prepared has three goals. The first is to detail the pedagogical issues that a geological engineering field camp is intended to address. The second is to provide a set of example exercises for educators interested in conducting either short-term or long-term applied geology problems for their students. The third goal is to provide short course attendees with a broad overview of the complex geology and numerous geologic hazards in the Cedar City area.

FIELD CAMP STRUCTURE

The UMR field camp is typically five weeks in length. The first three weeks follow similar schedules, and are conducted like many other university field camps: students learn the stratigraphic column for the area, hear an overview of the geology of a particular location, and then develop geologic maps and cross-sections. During this time, they are expected to develop skills in rock and mineral identification, formation recognition, mapping techniques, and geologic drafting and presentation. At this point, the geology majors and the geological engineering majors generally split into two groups for focused instruction and problem solving in their respective areas during weeks four and five.

For the geological engineers, the fourth week of field camp has traditionally incorporated a trip to the Salt Lake City area for an overview of local engineering geology issues. Activities vary from year to year, but have

included tours of urban geologic hazards, tours of the Bingham Canyon open pit mine and environmental reclamation areas, visits to various underground coal mines, a visit to the Wasatch Drain Tunnel that supplies water to the Snowbird resort, and visits to the Thistle landslide complex and the nearby Schurtz Lake landslide and Joe's Canyon debris flow. The week is concluded with trips to Bryce Canyon and Grand Canyon National Parks for overviews of the geology.

The goal of the fourth week trip is to expose students to a wide variety of engineering problems that are affected or created by geology. The trip gives them a chance to contemplate how the same geologic units they have studied in detail for several weeks have influenced settlement, mining, and water supply, and have created hazards for transportation routes, businesses, and residential structures.

During the fifth week of the field camp, the students apply what they have learned to predict locations and severity of hazards, to suggest hazard mitigation methods, to prepare engineering geologic and engineering soils maps, and to interpret geologic maps for engineering use. The students rely heavily on published geologic maps during this week, just as they will in their careers, and they learn to discern the accuracy, precision, and reliability of maps prepared by others.

An overview of the regional geology in the vicinity of Cedar City is provided below, so that the reader may better understand the fifth-week exercises detailed afterwards in the road log.

REGIONAL GEOLOGY

Cedar City, Utah is an ideal location for a field camp for both geologists and geological engineers. It is located on two major geologic boundary lines, which gives access to varied types of geology. The Hurricane fault, which passes through the east side of Cedar City, is a major NNE-SSW trending, down-to-the-west, normal fault with a vertical displacement of at least 5,000 feet and possibly as much as 8,000 feet occurring over the past ten million years. The Hurricane fault is the structural boundary line between the Basin and Range geologic province to the west and the high Colorado Plateau to the east. Cedar City, located on the downthrown side, is at an elevation of 5,800 feet. Immediately across the fault to the east, Cedar Breaks National Monument is at over 10,000 feet and Brian Head Peak is just over 11,000 feet. Because of this topographic difference, deep erosional valleys have been cut into the upthrown side of the fault and large alluvial fans are deposited on the downthrown side. Also, because of the large topographic difference across the fault, unstable slope conditions have resulted in large landslides at several locations along the fault.

Regionally, the Hurricane fault is part of a much larger system. To the north it is equivalent to the Wasatch fault in Salt Lake City, and to the south, the fault continues to the Grand Canyon where associated basalt flows create Lava Falls, the largest cataract in the canyon. Also associated with the Hurricane fault are a series of basalt flows that flowed across the fault at various stages of its development. These basalt flows have been displaced, and are used to date and positively identify movement on the fault.

The Hurricane fault in the Cedar City area roughly coincides with the eastern (leading) edge of the western overthrust belt of North America (second major geologic boundary line). Valleys cutting the upthrown side of the fault expose spectacular cross section views of a number of different compressional structures. In one canyon, students develop a geologic map of a leading edge recumbant anticline, the single-most important structural trap for hydrocarbons in overthrust belts throughout the world. As students move up the valley they observe the progression of bedding plane attitudes from flat-lying, through increasing east dips, to overturned, then back through decreasing east dips, and finally back to flat lying, over a horizontal distance of about a mile and a half. This is an important exercise not only for developing their mapping skills, but also for the opportunity to observe firsthand the magnitude and complexities of such an important geologic structure. This is a structure that geological engineers in the petroleum industry are likely to be drilling, and there is no substitute for actually seeing such a structure in the field.

Table 1 shows a highly generalized summary of rocks units and tectonic events for the Cedar City area. The majority of rocks in the area consist either of valley-fill alluvium on the downthrown side of the Hurricane fault or Triassic and Jurassic (red colored) and Cretaceous (brown colored) rocks that crop out immediately across the Hurricane fault to the east. Paleozoic rocks are not exposed near Cedar City, but wells drilled in the area indicate thicknesses of 6,000 to 7,000 feet of Paleozoic rocks. The closest well-exposed thick section of Paleozoic rocks are in the Virgin River Gorge to the southwest of St. George (along I-15 to Las Vegas) and in the Grand Canyon.

The area is characterized by a series of major tectonic and erosional/depositional events. During Precambrian time (1.2-1.5 billion years ago) southern Utah and northern Arizona were probably the core of a major east-west trending mountain range. This range was topographically high and experienced erosion over the next 700 million years (this period is noted as "The Great Unconformity").

During early Paleozoic time (Cambrian through Mississippian), the western U.S. was relatively quiet and marine sediments were periodically deposited. During Pennsylvanian and Permian time, local uplifts throughout the western U.S. created a complex mosaic of highlands and basins resulting in highly varied geology for those two periods. At the end of Paleozoic time, the continents were linked together as Pangaea, and during Triassic and Jurassic time, redbeds and evaporites associated with the breakup of Pangaea were deposited. During Jurassic time the coastal plain where redbeds were being deposited dried up and a great desert was formed, which resulted in the spectacular eolian Navajo Sandstone so well exposed at Zion National Park. Immediately following deposition of the Navajo Sandstone, a small, north-south rift valley opened in central Utah and significant thicknesses of evaporites were deposited, resulting in the Carmel Formation exposed near Cedar City and Salina.

Early Cretaceous rocks are missing across all of Utah and Late Cretaceous time is marked by the climax of Sevier deformation. Sevier deformation is synonymous with thrusting in the western overthrust belt, and although thrusting is considered to have initiated during Jurassic time in Nevada, the effects in Utah are not seen until Late Cretaceous time. During the Late Cretaceous a major mountain range occupied all of western Utah, and it shed large volumes of sediment eastward into the Cretaceous interior seaway. The coals of Utah and Wyoming were deposited in coastal plain sediments associated with this seaway.

During early Tertiary time (Paleocene and Eocene), compression continued in the Laramide orogeny, but the structural style was much different. Laramide deformation is marked by Precambrian, granite-cored uplifts (such as the Uinta Mountains, the Black Hills, and the San Rafael Swell) which pushed up through overlying rocks creating typically asymmetrical uplifts with thrust faults along one flank. Between these uplifts, downdropped basins were developed and significant lacustrine sediments (such as the Green River, Flagstaff and Claron Formations) were deposited.

Table 1. Generalized stratigraphic column and tectonic events for the Cedar City area. Modified liberally from Hintze (1988).

System or Series	Tectonics	Formation	Thickness (feet)	Brief description and comments
Quaternary	Basin & Range tension faulting		0-300	Alluvium and basalt flows
Pliocene			0-6000	Valley fill, alluvial fans and basalt flows
Miocene		Intrusion		Quartz monzonite in Iron Springs area, 20 mya
Oligocene		Ash flow tuffs	300-4700	Numerous ash flow tuffs from west, 21-30 mya
Eocene Paleocene	Laramide Compression	Claron	700-1800	Lake deposits of Cedar Breaks and Bryce Canyon Laramide uplifts and lakes between uplifts
Cretaceous	Sevier Deformation (thrusting in Western Over-thrust belt)	Kaiparowits Iron Springs "Tropic" "Dakota"	1600-2500	Transition to Tertiary lacustrine deposits Sandstone and shale with some coal at the western edge of the Cretaceous interior seaway. Various names including Tropic, Dakota, Wahweap, and Straight Cliffs have been used with confusion
Jurassic		Carmel	1100-1250	Limestone, mudstone & evaporates (marine incursion)
		Navajo	1700	Eolian sandstone of Zion National Park
		Kayenta	700-1600	Redbeds, sandstones, and shales
		Moenave	350-550	Redbeds, sandstones, and shales
Triassic		Chinle	240-500	Shinarump Sandstone and Petrified Forest redbeds
		Moenkopi	1900	Redbeds, shales, siltstones, and evaporates
Permian		Kaibab	400	Limestone, very little seen in the Cedar City area
Paleozoic rocks below the Kaibab Formation are not exposed at the surface in the Cedar City area.				

319

During Oligocene time, approximately 20-30 million years ago, major volcanic activity occurred throughout the western U.S. and Mexico, resulting in the deposition of spectacular ash flow tuffs mainly to the west of Cedar City. At about 20 million years ago, quartz monzonite intrusions thought to be laccoliths were intruded in the Iron Springs area about ten miles west of Cedar City. Surrounding these intrusions significant iron ores were emplaced as veins and as replacement deposits in the Jurassic Carmel Formation. These iron ores have been mined discontinuously since 1851, and one of the abandoned mines now serves as a landfill.   During the Oligocene, the tectonic regime in the western U.S. changed from compressive to tensional, initiating Basin and Range normal faulting, which continues to the present.

TYPES OF EXERCISES

Because the students have spent several weeks in the field before starting their geological engineering exercises, and have waning motivation and enthusiasm, the authors' philosophy during the fifth week of the camp has been to challenge the students with a wide variety of exercises, both in terms of length and topic. The longer exercises allow them to spend parts of several days studying a site in detail, and the shorter problems allow them to think through a single engineering geology issue at one time. By careful scheduling, the short problems are sequenced to give the students some technical background for the aspect of the long project that they will tackle later that same day. Students start the day with a short quiz on several technical readings that cover the stops for that day.   An excellent overview of the engineering geology of southwestern Utah is presented in Mulvey (1992).

The short problems are considered "Hour Problems," and usually three of them are assigned each morning. Each problem deals with a different geologic hazard or issue, such as "debris flows," or "ground-water contamination." The students are taken to the problem site and use a geologic map and their knowledge of engineering geology, hydrogeology, and geomorphology to answer a series of questions regarding the engineering geology of the site. The Hour Problems are included below at Stops 1 through 9. They rely on the geologic map of the Cedar City quadrangle (Averitt and Threet, 1973), and several technical articles cited in the road log below.

The long problems are "Multi-Day Projects," and involve identification and mapping of geologic hazards, analysis and recommendation of mitigation methods, optimal siting of a number of facilities, and estimation of properties for foundation design. In all cases, four days are allotted for the Multi-Day Projects. Some years the students were required to prepare a typewritten report after they returned from field camp, and other years they prepared a more succinct report due on the last day of field camp. Four examples of Multi-Day Projects are included below at Stops 3, 7, 10, and 11. They rely on geologic maps of the Cedar City, Cedar City NW, and Three Peaks Quadrangles (Averitt and Threet, 1973; Mackin and others, 1976; and Mackin and Rowley, 1976; respectively).   A technical library is provided for the students covering engineering geology, southern Utah geology, rock engineering, and natural hazards mitigation.

"Single-Day Projects" help keep the students' attention levels and enthusiasm high by providing a break from the Hour Problems and Multi-Day Project work, while requiring them to maintain their focus on technical engineering geology topics. An example of a Single-Day Project is included below in Stop 12.

By mixing project length and topic, students typically are exposed to nine Hour Problems, a Multi-Day Project, and a Single-Day Project in a week. They receive instruction in a broad range of engineering geology topics, and the frequent transition of both topic and location helps maintain their interest.

ROAD LOG

The route progresses from Cedar City southward to Green Mountain, over Green Mountain to State Highway 14 (SR-14) in Cedar Canyon, down Cedar Canyon returning to Cedar City. Following several stops in Cedar City, the route heads westward for two stops in the Iron Springs area, and then northward for a final stop in the Parawon Gap area. Each stop illustrates a different geological engineering problem covered in the field camp. Stops near Cedar City are shown on figure 1 and stops away from the city are shown on figure 2.
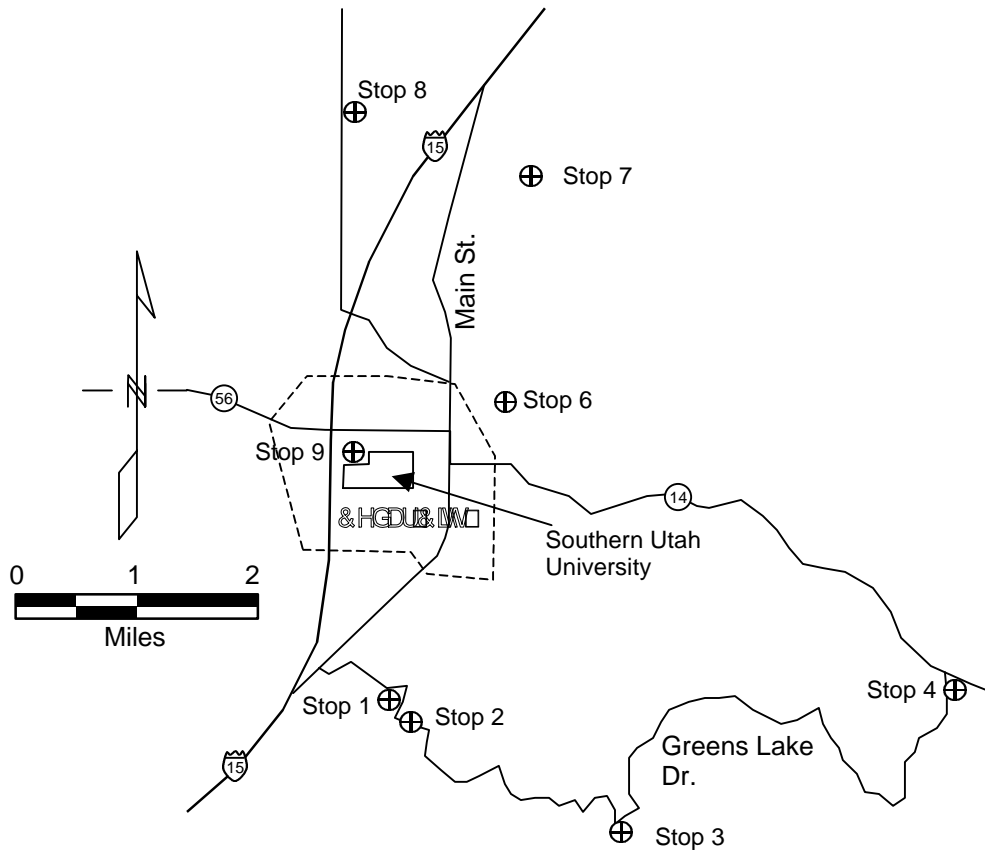
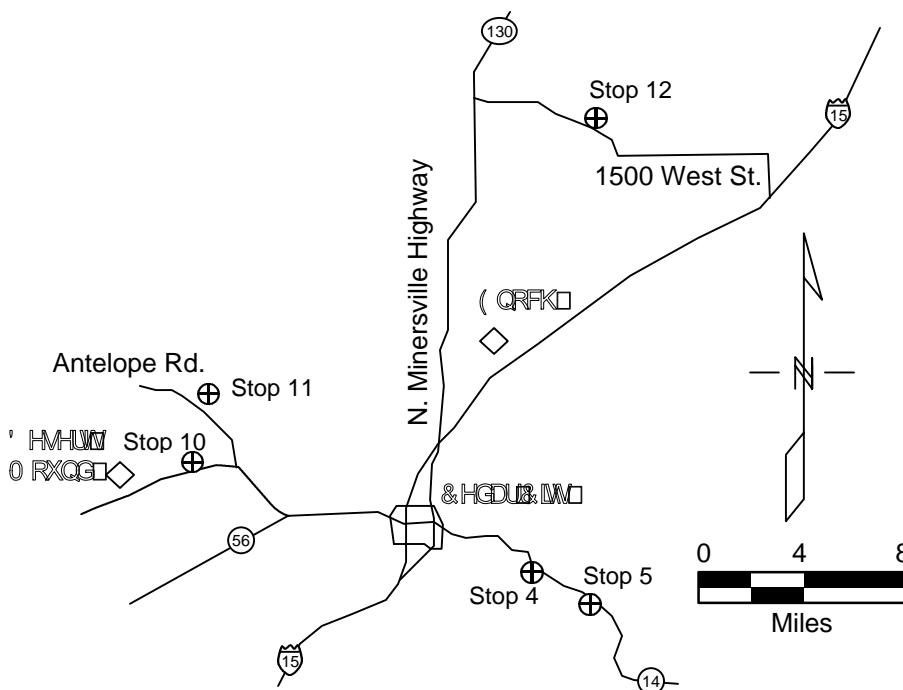*Figure 1. Local map of Cedar City showing road log stops.*

Figure 2. Regional map of the area surrounding Cedar City showing road log stops.

0.0	0.0	**START**. Begin at Southern Utah University, intersection of 200 S. Street and 1150 W. Street. Proceed East on Center Street.
0.9	0.9	Turn right (S) on Main Street.
1.7	2.6	Turn left (E) on Kolob Road.
0.2	2.8	Turn left on Greens Lake Drive.
1.0	3.8	Follow Greens Lake Drive up Green Mountain and park at the water tank.

STOP 1 – HOUR PROBLEM: LANDSLIDE. The purpose of this stop is to allow the students to consider construction on or near a large paleolandslide. They should learn how to recognize these features and how to evaluate the likelihood of renewed movement. The slide is referred to as the Green Hollow landslide, and it is a complex slide morphology mostly in the Cretaceous Tropic and Triassic Moenkopi Formations. The slide is estimated at 222 million cubic meters and is over 4 kilometers in length (Harty, 1992). Students are presented with the following questions:

1. Is the Green Hollow Landslide composed of material that traveled a short distance or a long distance? How do you know?
2. What is the most likely triggering event and why?
3. How can you tell?
4. Is it OK to build on it?
5. Beyond the toe of the landslide?
6. How would you decide?
7. Describe the sequence of materials you would expect in a drill hole placed near one of the vans.
8. Why do we not typically see landslides in the rock record?

Continue uphill (E) on Greens Lake Drive.

| 0.2 | 4.0 | Park on the second dirt road to the left. |

STOP 2 – HOUR PROBLEM: VOLCANIC / GEOMORPHOLOGY. At this stop, students use simple volcanic stratigraphy to judge relative ages and sequences of landscape-shaping events. The site of interest is the Cross Hollow Hills directly west of the stop, which are composed of Tertiary fanglomerates capped in places by Quaternary basalts. Basalt flow remnants can also be seen to the south, comprising the nearest ridge at the edge of Green Hollow. Background reading for this site is Bugden (1992). Students are presented with the following questions:

1. Where is the source of the basalt?
2. The fanglomerate?
3. What geologic hazards do these units present?
4. Outline a chronology of events leading to what you see across the valley.

Continue up Greens Lake Drive.

| 2.9 | 6.9 | Park at a broad meadow on a flat topographic bench, with a white picket fence on the right. |

STOP 3 – HOUR PROBLEM: HYDROGEOLOGY. At this location, students are introduced to geologic controls on spring location, and possible engineering modifications to spring flow. Green Lake and the surrounding marsh developed on the flat and back-tilted head of the Green Hollow landslide (figure 3). The spring, which appears to have been tapped to feed the water tank, issues from above a confining bed in the Tropic Formation. Students are presented with the following questions:

1. Why do the spring and Green Lake appear where they do?
2. What kind of water inflow would you expect in a horizontal adit above or below the spring?
3. What would happen if you stopped up the spring?
4. How would you keep a mine dry in the vicinity of the spring?
5. What sorts of depositional environments would favor development of springs millions of years later?

Figure 3. View from the top of Green Mountain across Green Lake (center) and the Green Hollow landslide (treeless area in center of photo, representing the down-dropped head of the landslide).

MULTI-DAY PROJECT: SUU RADIO TELESCOPE FACILITY. Students were asked to complete the following project in the vicinity:

Southern Utah University has recently received a large endowment from a grateful UMR field camp alum in order to construct a radio telescope array. The telescope will consist of the following structures:

1. A set of four 25-foot diameter dish antennas. The antennas will be installed in a line trending magnetic north, 2000 feet apart, and at the exact same elevation. You are to site the array somewhere between the elevations of 8000 and 9000 feet. Each antenna will require a 30x30 foot pad that should be able to support 2000 pounds per square foot.

2. A high-tension power line serving the array. The power line will extend from the center of section 22 to one end of the array. The line will be supported from towers 100 feet high and spaced every 1000 feet. Towers should be placed so that the aesthetic disruption will be minimal for Cedar Highlands residents. Each tower will require a 20x20 foot pad to support 4000 psf dead loads and 6000 psf transient (wind) loads.

3. A cooling water system for electrical equipment and transformers. The system requires a water supply and storage of 500,000 gallons.

4. A building to house a supercomputer and related electronic equipment. The equipment is very sensitive to movement and the building should be very stable. The building will be constructed in the southeast quarter of section 22, it will have a floor area of 1200 square feet, and impose loads of 2000 psf.

Here is what you are expected to do for this project:

Monday – Select locations for the antenna array, evaluate foundation materials and conditions, and evaluate the activity and impacts of the large landslide.

Tuesday – Develop a cooling water supply and storage plan (where will it come from and where will it be held). You need to decide if you can use Green Lake for this or if you need an alternate plan. Begin working your way down the hill to site power line towers. Pay particular attention to foundation materials, soil conditions, and geologic hazards.

Wednesday – Finish siting lower line towers. Select a site for the supercomputer building.

Thursday – Complete any remaining field work.

Due Thursday noon – Preliminary map showing locations of antennas, power line towers, cooling water storage, and supercomputer building. For each structure, include a list of geologic hazards and a short description of how you will address each hazard. For each structure list the expected foundation materials and comment on treatment needed.

You will work in groups on the project, but each student is expected to complete his or her own project report. Target length is about 10 to 15 pages of text, not including figures, tables, and appendices.

The goals of this project, as for the other Multi-Day Projects are to teach the students to interpret geologic maps and general technical references for engineering construction properties and geologic hazards, and to site various facilities. The general geologic issues impacting the project include the potential for reactivation of the Green Hollow Landslide, the thickness and foundation properties of landslide deposits, the impacts of increasing surface water storage (and infiltration) at the head of the landslide, and the practicality of large cuts and fills for the antenna sites.

Continue uphill to the end of Greens Lake Drive.

0.5	7.4	Turn left on Right Hand Creek Road and follow it around the north side of Green Mountain, and downhill to the intersection with Utah SR 14.
4.5	11.9	Park at the southeast corner of the intersection.

STOP 4 – HOUR PROBLEM: FLOODING. The two goals of this stop are to help the students to recognize the effects of long-term climate changes on river morphology and to help them identify proper uses of various features within a river basin. The students should recognize that the stream valley was cut much deeper than the current grade, that the terraces were deposited in a different post-glacial climatic period, and that the current stream is downcutting into the terraces. Background reading for the stop is Lund (1992). Students are presented with the following questions:
1. Is the stream channel here the size you would expect for this size floodplain? If not, why not?
2. Where would you build a structure to avoid the flooding hazard?
3. How could you protect the structure from flooding?
4. What are three constructive uses for the floodplain area?
5. Was this a depositional or erosional environment 10,000 years ago?
6. What will the current stream do to the floodplain in the next 10,000 years?

Turn right (E) and proceed on SR 14.

2.7	14.6	Park on the broad shoulder on the north side of the road.

STOP 5 – HOUR PROBLEM: LANDSLIDE. This site is the 1989 Cedar Canyon landslide, with a volume of approximately 1.5 million cubic meters (Harty, 1989). The slide is located in the Cretaceous Tropic / Dakota Formations, and the vertical cliffs above are the Cretaceous Straight Cliffs Formation (Harty, 1989). The goal of this stop is to help students identify and judge the effectiveness of various landslide remediation methods. Students are presented with the following questions:
1. List four remediation options to address the landslide hazard. Rank them from most desirable to least.
2. Explain why you felt the most desirable option was the most desirable.
3. Find two other geologic hazards in the vicinity and explain how they have been remediated (or how they could be).
4. How would this site be different if the climate suddenly had three times the current rainfall?

Proceed West on SR 14 back to Cedar City.

7.2	21.9	Upon entering town, turn right (N) on Highland Drive.
0.6	22.4	Follow Highland Drive to its dead end.
		Park in driveway of demolished house on left.

STOP 6 – HOUR PROBLEM: COLLAPSIBLE SOILS. At this location, the extent of damage caused by collapsible soils may be seen in the basement and foundation cracks in the demolished house. Background reading is from Rollins and others (1992). Students are presented with the following questions:

1. Looking at the crack patterns in this basement, describe the mode of settlement of the structure.
2. Describe briefly why some soils are collapsible.
3. If you were called in by the homeowner to diagnose the problem here, how would you distinguish the damage here from damage caused by expansive soils?
4. What would you do in order to rebuild at this location?
5. What other depositional environments and parent materials would produce similar problems?
6. What would happen to these materials if you buried and lithified them?
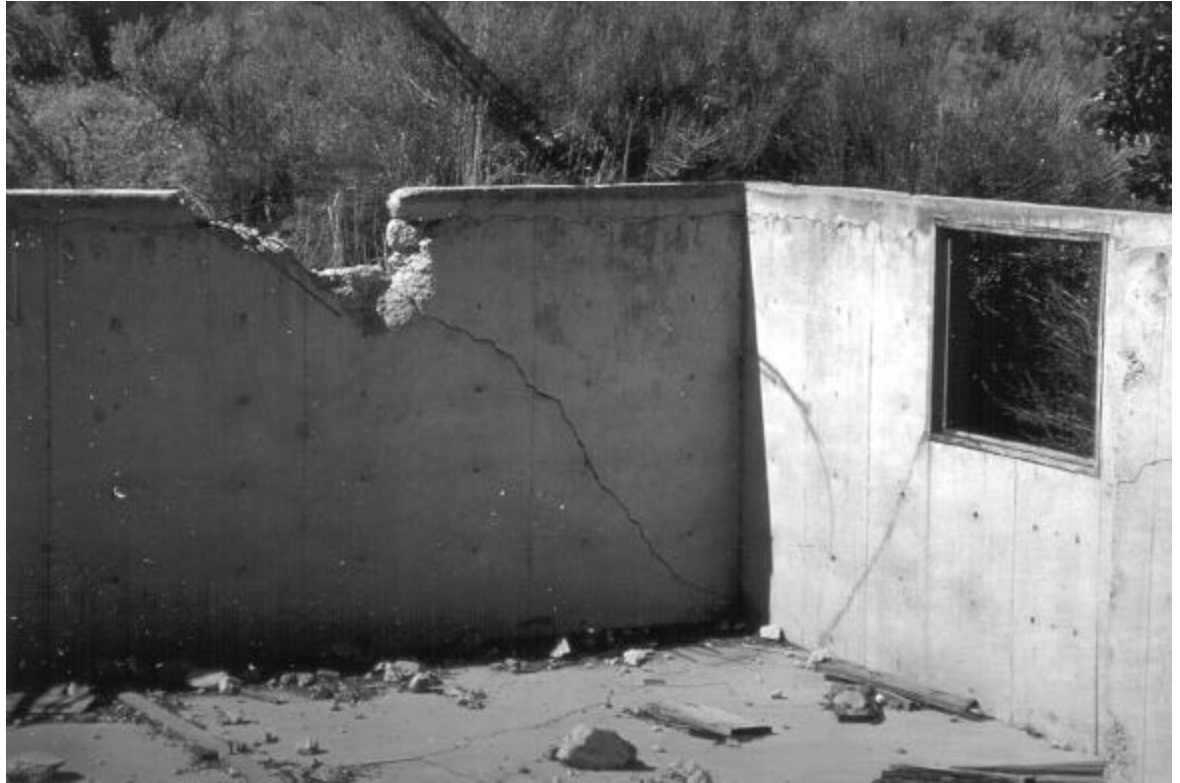

Figure 4. Basement of demolished house severely damaged by collapsible soils. Note the cracked walls and floor slab.

		Return to SR 14 (Center Street).
0.6	23.0	Turn right (W) on Center Street.
0.5	23.5	Turn right (N) on Main Street. On the left, note the berm protecting the high school from debris flows and flooding from Fiddlers Canyon.
2.4	25.9	Turn right (E) on Fiddlers Canyon Road.
0.6	26.4	Pass a school on the left and turn right on the dirt road leading across an open field to a debris basin.

STOP 7 – HOUR PROBLEM: DEBRIS FLOW. At this location, a large debris basin has been constructed to protect the structures downhill. Debris flow deposits are clearly exposed in the channel walls feeding into the basin. One of the goals of this stop is to help students distinguish between in-place residual soils (clast-supported, single rock type, exposed on the low ridge to the south) and debris flow deposits (matrix supported, multiple rock type). Additional goals are to introduce them to the ideas of debris flow morphology and debris flow hazard mapping and zonation. They are presented with the following tasks:
1. Draw a rough sketch of the geomorphology within ¼ mile of here.
2. Delineate different lobes of the debris fan and their sources.
3. Select a location for a building that minimizes debris flow hazards.
4. Explain how you selected this site.
5. Describe three ways to mitigate the debris flow hazard in this area.

6. Discuss three similarities between a debris flow fan and a delta.
7. Why does a delta have a better chance of becoming an oil reservoir?

MULTI-DAY PROJECT: CEDAR CITY MASTER PLAN. Students were asked to complete the following project in the vicinity:

In anticipation of northward expansion, Cedar City has hired you to delineate geologic hazards in an area north and northeast of town. For the region flanking the canyon mouths from Stephens Canyon to the canyon immediately north of Fiddlers Canyon, you are requested to do the following:
1. Prepare a GLQ map of the region.
2. Prepare a geologic hazards map of the region (anticipated hazards include the following, at a minimum: landslide breccia, landslide, rockfall, flooding, debris flow, collapsible soils, expansive soils, liquefaction, erosion, surface fault rupture, seismic amplification, aggregate resources, environmental contamination).
3. Zone hazards into low, medium, or high risk or other appropriate categorization. Provide descriptions of the characteristics of each category and cutoff values between categories.
4. Create five engineering geologic cross-sections (Dry, Stevens, Fiddlers, Fiddlers South and Fiddlers North Canyons).
5. Select the three best 1/16-section areas for your professors to buy.
   You should map all undeveloped areas that are not fenced.
   Here is your schedule for this project:
Monday – Map Dry Canyon (called Stephens on the topographic map).
Tuesday – Map Stephens (unnamed on the topographic map) and Fiddlers South.
Wednesday – Map Fiddlers Canyon and Fiddlers North Canyon.
Thursday – Complete any remaining field work.
Due Thursday noon – Drafts of maps and cross-sections.
   You will work in groups on this project, but each student is expected to complete his or her own project report. Target length is about 10 to 15 pages of text, not including figures, tables, and appendices.

While the project at Green Hollow focused on engineering properties and facility siting, this project focuses on engineering geologic mapping and hazard mapping and zonation. The Genesis-Lithology-Qualifier (GLQ) mapping method used for the project is described in Keaton (1984).

Return to Main Street.

0.6	27.0	Turn left (S).
1.8	28.8	Turn right (W) on Coal Creek Road. Cross over I-15 (the road is now called Bulldog Field Road). Cross a bridge over an intermittent stream that is part of the distributary network from Coal Creek. Pass several gravel pits.
2.7	31.5	Turn right onto dirt road parking just south of one of the pits.

STOP 8 – HOUR PROBLEM: GROUND-WATER CONTAMINATION. This site is on the broad outwash fan of Coal Creek. As one travels north from the I-15 crossing, the depth to ground water increases: Bulldog Field Road crosses an ephemeral stream, then a gravel pit with water in the bottom, then a pit containing trees but no standing water, then the current dry pit. The students should be able to use these observations to deduce that Coal Creek and its distributaries are losing streams, which explains the increasing depth to ground water as one moves away from the stream. They are presented with the following questions:
1. What is a reasonable estimate of the depth to ground water at this site?
2. What direction does ground water flow?
3. How well does this material transmit water?
4. Why is there no water in this gravel pit and there is water in the gravel pits to the south?
5. Where would you put 4 ground-water monitoring wells to detect contamination from the garbage left at the north end of this landfill?
6. If the canyon mouth of Coal Creek has boulders 1-2 feet in diameter, how far away from the mouth would you expect to run out of sand-sized particles (2mm)?

Proceed South on Bulldog Field Road.

1.5	33.0	Turn right (W) on Kittyhawk Drive.
0.5	33.4	Turn left (S) on Airport Road, cross over SR 56 (the road is now called College Way).
1.3	34.8	Turn left (E) on Center Street, cross over I-15.
0.4	35.2	Turn right into parking lot on the northeast end of the football stadium (at 1050 W. Street)

STOP 9 – HOUR PROBLEM: FAULT RUPTURE. At this location, the concealed North Hills fault shown on the geologic map (Averitt and Threet, 1973) abruptly ends. It provides an excellent opportunity to query the students on how they might try to locate the fault in an urban setting. The background reading for the site is Christenson and Nava (1992). Students are presented with the following problem:

> The "State Harm" Insurance Company has decided to begin selling earthquake insurance in the Cedar City area. They will charge two premiums: a higher one for houses within 150 feet of an active (Holocene movement) fault, and a lower one for houses more than 150 feet away. For the area bounded by Center Street and 200 North, develop an investigation plan to determine the location and activity of the North Hills fault. Draw a rough map to show your proposed work. What other factors should "State Harm" consider besides proximity and fault activity?
>
> Will the nearby surface expression of this fault (in the Qal) be preserved in the rock record? Why or why not?

Proceed back (E) on Center St. to College Way.

0.4	35.5	Turn right on College Way.
0.4	35.9	Turn left (W) on SR 56.
4.0	39.9	Turn right onto Antelope Road (SR 253).
2.9	42.8	Follow Antelope Road to left (toward Desert Mound) when it forks.
1.9	44.7	Park on right (northwest) side of road, near mine tailings piles to north.

STOP 10 – MULTI-DAY PROJECT: EIGHTMILE HILLS RETIREMENT COMMUNITY. Students were asked to complete the following project in the vicinity:

> You have been contracted by Gordo y Flaco Developers to assist them in laying out the Eightmile Hills Retirement Community development. In their tradition of riding down each successive wave of industry, Gordo y Flaco, Inc. have purchased approximately 2500 acres of useless land and intend to create yet another retirement community in southwest Utah. Having once been burned by geological problems in their "Thistle Canyon Emu Farm," they want you to pay particular attention to potential geologic hazards and help them design around such hazards.
>
> The housing development will consist of the following structures:
> 1. 1000 single family dwellings. Prices will range from $100,000 to $400,000, and lot size will vary from 10,000 to 60,000 square feet,
> 2. 4 multi-unit apartment buildings, similar to the ones you are staying in,
> 3. an 18 hole golf course,
> 4. a swimming / recreation center,
> 5. green space with hiking and mountain bike trails, and
> 6. road and utility infrastructure.
>
> Here is what you are expected to do for this project (specific deliverables are underlined):
>
> Monday – Begin preparing GLQ engineering geologic map for site (based on geologic map and your field observations).
>
> Tuesday – Finish GLQ map, prepare engineering soils map (based on soil survey of area) and geologic resource map (potential aggregate, future mining areas, etc. that construction should work around).
>
> Wednesday – Prepare geologic hazards map (include earthquake hazard zones based on soil amplification and proximity to active faults), provide recommendations for hazard mitigation, site zoning map for potential construction (where each structure would best be located), and map of water supply well locations and water storage facility location(s).
>
> Thursday – Complete any remaining field work.
>
> Due Thursday noon – Drafts of the 6 maps, including legends, and a one-page outline of your recommendations for hazard mitigation.

You will work in groups on this project, but each student is expected to complete his or her own project report. Target length is about 10 to 15 pages of text, not including figures, tables, and appendices.

This site offers three excellent conditions for an in-depth project. First, the students will find that although the geology is complicated, many of the rock units offer similar engineering properties and present similar hazards, so they may be conveniently grouped. Second, the students will find that subtleties in the topography of the valley area closely reflect geomorphic features such as alluvial fans, terrace deposits, and residual bedrock ridges. Third, the inactive mine and the mine tailings piles create substantial land-use problems for the students to plan around. The geologic map for the site is Mackin and others (1976).

Return to fork in road.

1.9	46.6	Turn left to proceed up other branch of road.
2.7	49.2	Turn right to cross railroad tracks and enter the Three Peaks area.
1.1	50.4	Park at a point where the Three Peaks are visible to the east and the outwash fans are visible to the west.

STOP 11 – MULTI-DAY PROJECT: THREE PEAKS ELECTRONICS RESEARCH AND DEVELOPMENT COMMUNITY. Students were asked to complete the following project in the vicinity:

A consortium of eight electronics industry companies has hired you to assist them in laying out the "Three Peaks Electronics Research and Development Community." The development is intended to provide living and working quarters, and infrastructure for approximately 2000 people who really want T3 internet access from their homes. The development area is outlined on the attached map and will consist of the following structures:

1. 1000 single family dwellings. Prices will range from $100,000 to $4,000,000, and lot size will vary from 10,000 to 100,000 square feet,
2. 8 multi-unit apartment buildings, similar to the ones you are staying in,
3. an 18 hole golf course,
4. a swimming / recreation center,
5. green space with hiking and mountain bike trails,
6. road and utility infrastructure,
7. a set of three 25-foot diameter geosynchronous satellite antennas. The antennas will be installed in a line trending magnetic north, 2000 feet apart, and at the exact same elevation. You are to site the array somewhere between elevations 5500 and 6000 feet. Each antenna will require a 20x20 foot pad which should be able to support 2000 pounds per square foot.
8. Four lab and research buildings with footprints of 300x1000 feet. The equipment in the buildings is very sensitive to movement and the buildings should be very stable. They will impose loads of 1000 psf.

Here is what you are expected to do for this project (specific deliverables are underlined):

Monday – Begin preparing GLQ engineering geologic map for site (based on geologic map and your field observations).

Tuesday – Finish GLQ map, prepare engineering soils map (based on soil survey of area) and geologic resource map (potential aggregate, future mining areas, etc. that construction should work around).

Wednesday – Field trip to Parowan Gap for Single-Day Project.

Thursday – Prepare geologic hazards map (include earthquake hazard zones based on soil amplification and proximity to active faults), provide recommendations for hazard mitigation, site zoning map for potential construction (where each structure would best be located), and map of water supply well locations and water storage facility location(s).

Friday – Complete any remaining field work.

Due Friday 3pm – Drafts of the 6 maps, including legends, and a three-page summary of your criteria for siting various facilities and your recommendations for hazard mitigation.

This project site is similar to the Eightmile Hills area to the south, except that the bedrock geology is more varied and the resulting engineering properties of the rock depend strongly on the specific underlying rock unit.

Return to the paved road.

1.1	51.5	Turn left and return to Cedar City.
10.0	61.5	Enter I-15 North.
3.0	64.5	Take exit 62 turn left under I-15, and proceed North on N. Minersville Highway (SR 130) towards Parawon.
13.1	77.6	Turn right (E) on paved road to Parawon Gap. Follow the road through the gap.
4.1	81.7	Park at the first sharp turn in the road.

STOP 12 – SINGLE-DAY PROJECT: PARAWON COAL MINE SLURRY POND.   Students were asked to complete the following project in the vicinity:

> Because of severe energy needs throughout the country, the Southern Utah Energy (SUE) Corporation is investigating the feasibility of renewing underground coal mining in the Parowan Gap area. You have been asked to assess the geology and site a dam to create a slurry pond for settlement of waste fines from initial coal washing. The dam and abutment foundation should be strong, impermeable, and resistant to dissolution. The reservoir should readily hold water or require only minor treatment to hold water.

> The mining engineer and company economist have selected 4 sites for you to consider, based on piping and power optimization. These sites are as follows:

> Proposed Site A – Lower Coal Canyon
>   Dam 100 feet high Crest at 5900' elevation
> Proposed Site B – Upper Coal Canyon
>   Dam 100 feet high Crest at 6100' elevation
> Proposed Site C – Section 26 Canyon
>   Dam 75 feet high   Crest at 6175' elevation
> Proposed Site D – Section 27 Canyon
>   Dam 100 feet high Crest at 6000' elevation

> At the end of the day, you should turn in a matrix table comparing the four sites and indicating your first choice. Items you may want to include in your table are geology and engineering stability of dam foundation and abutments, geology of reservoir pool, potential for leakage to ground water, topographic issues, proximity to borrow material, and geologic hazards and how they may be addressed.

> You are encouraged to survey the site and discuss options in groups, but each person will be responsible for producing their own assignment.

The complex structure of this area has produced faulting, dipping beds, and variable fracture density and weathering. The predominant geology consists of Cretaceous Iron Springs Formation sandstone at lower elevations (approximately 6000 feet) and Eocene Claron Formation conglomerates and siltstones at higher elevations. The authors' analysis concluded that Site D is the least desirable because of large, deep, open fractures in the vertically dipping Iron Springs Formation. Site C shows similar problems in the Claron Formation, but to a lesser degree. Site A has better rock conditions, but is very broad topographically. Site B was both narrow and flanked by thick, intact rock units and was considered the most ideal of the four sites.

SUMMARY

Field exercises in geological engineering provide students with a chance to use their geologic knowledge to identify and address a variety of engineering problems. By scheduling a variety of both short and long projects, students are exposed to a wide breadth of problems, they focus on individual hazards in projects of limited scope before they are expected to address these hazards on a large project, and the variety helps maintain their interest and enthusiasm levels. The students rely heavily on published geologic maps, just as they will in their careers, and they learn to discern the accuracy, precision, and reliability of maps prepared by others.

ACKNOWLEDGEMENTS

REFERENCES

Averitt, P., and Threet, R.L., 1973, Geologic map of the Cedar City quadrangle, Iron County, Utah: U.S. Geological Survey Geologic Quadrangle Map GQ-1120, scale 1:24,000.

Bugden, M., 1992, Volcanic hazards of southwestern Utah, *in* Harty, K.M., editor, Engineering and Environmental Geology of Southwestern Utah: Utah Geological Association Publication 21, p. 193-200.

Christenson, G.E., and Nava, S.J., 1992, Earthquake hazards of southwestern Utah, *in* Harty, K.M., editor, Engineering and Environmental Geology of Southwestern Utah: Utah Geological Association Publication 21, p. 123-137.

Harty, K.M., 1989, The Cedar Canyon landslide: Utah Geological and Mineral Survey, Survey Notes, v. 23, no. 2, p. 14.

Harty, K.M., 1992, Landslide distribution and hazards in southwestern Utah, *in* Harty, K.M., editor, Engineering and Environmental Geology of Southwestern Utah: Utah Geological Association Publication 21, p. 109-118.

Hintze, L, H., 1988 (revised 1993), Geologic history of Utah: Provo, Utah, Brigham Young University Press, 202,p.

Keaton, J.R., 1984, Genesis-Lithology-Qualifier (GLQ) System of engineering geology mapping symbols: Bulletin of the Association of Engineering Geologists, v. 21, no. 3, p. 355-364.

Lund, W.R., 1992, Flooding in southwestern Utah, *in* Harty, K.M., editor, Engineering and Environmental Geology of Southwestern Utah: Utah Geological Association Publication 21, p. 159-163.

Mackin, J.H., Nelson, W.H., and Rowley, P.D., 1976, Geologic map of the Cedar City NW quadrangle, Iron County, Utah: U.S. Geological Survey Geologic Quadrangle Map GQ-1295, scale 1:24,000.

Mackin, J.H. and Rowley, P.D., 1976, Geologic map of the Three Peaks quadrangle, Iron County, Utah: U.S. Geological Survey Geologic Quadrangle Map GQ-1297, scale 1:24,000.

Mulvey, W.E., 1992, Engineering geologic problems caused by soil and rock in southwestern Utah, *in* Harty, K.M., editor, Engineering and Environmental Geology of Southwestern Utah: Utah Geological Association Publication 21, p. 139-144.

Rollins, K.M., Williams, T., Bleazard, R., and Owens, R.L., 1992, Identification, characterization, and mapping of collapsible soils in southwestern Utah, *in* Harty, K.M., editor, Engineering and Environmental Geology of Southwestern Utah: Utah Geological Association Publication 21, p. 145-158.

Home destroyed by a rock fall on October 18, 2001 in Rockville, Utah near Zion National Park